NASA TT F-11,044

THEORETICAL PHOTOMETRY

E.Schoenberg

N 67-21261 (ACCESSION NUMBER)
333 (PAGES)
(NASA CR OR TMX OR AD NUMBER)
(THRU)
50 (CODE)
03 (CATEGORY)
FACILITY FORM 602

N71-70685 (ACCESSION NUMBER)
333 (PAGES)
(NASA CR OR TMX OR AD NUMBER)
(CODE)
(CATEGORY)
FACILITY FORM 602

Translation of "Theoretische Photometrie".
In: Handbuch der Astrophysik,
Vol.II/1, pp.1-280, 1929.

NOTICE
BECAUSE OF COPYRIGHT RESTRICTION THIS TRANSLATION HAS NOT BEEN PUBLISHED
ITS COPY IS FOR INTERNAL USE OF NASA PERSONNEL AND ANY REFERENCE TO THIS
PAPER MUST BE TO THE ORIGINAL GERMAN SOURCE.

NATIONAL AERONAUTICS AND SPACE ADMINISTRATION
WASHINGTON, D.C. 20546 SEPTEMBER 1967

PRINCIPLES OF ASTROPHYSICS

SECOND PART

I

F.Bottlinger, A.Brill, E.Schoenberg, H.Rosenberg

Berlin

Verlag Julius Springer

1929

TABLE OF CONTENTS

	Page
Introduction	1
I. DEFINITIONS, FUNDAMENTAL LAWS, AND PROBLEMS	4
1. Definition of Photometry	4
2. Basic Laws and Definitions in Radiology; Radiant Point	5
3. System of Radiant Points and Radiant Area	6
4. Irradiation of One Element by Another	7
5. Composite Radiation	8
6. Definitions of Visual Photometry	9
7. Sensitivity of the Eye for Brightness Differences of Individual Colors of the Spectrum	12
8. The Purkinje Phenomenon	12
9. Determination of the Factor K_λ; Sensitivity of the Eye to Radiation of Differing Wavelengths	13
10. The Fechner-Weber Psychophysical Law	14
11. Size Classes of Stars	16
12. Systematic Errors of Visual Photometry, due to Color of the Stars	18
13. Compensation of Photometric Observations	19
14. Illumination Problems; Illumination of a Plane Area by a Luminous Point	20
15. Illumination of an Arbitrary Closed Area	21
16. The Lambert Emanation Law	23
17. Illumination Density and Brightness of the Luminous Element	27
18. Some Problems in the Illumination of Areas by Areas	28
19. Several Problems of Diffuse Reflection	34
II. DIFFUSE REFLECTION	36
20. Lambert Formula and Lambert Albedo	36
21. Lommel-Seeliger Formula	37
22. New Formula for Diffuse Reflection and its Special Cases: Fessenkov and Lommel Formulas	42
23. Experimental Investigations of Diffuse Reflection	50
24. More Recent Studies	53
25. Light Scattering in the Air	56
26. Concept of Albedo	59
27. Seeliger's Albedo	60
28. Albedo of a Plane Area for Normal Irradiation and Reflection Coefficient in Direction of Irradiation	62
29. Determination of Albedo and Reflection Coefficient; Experimental Determination of Albedo	62
30. The Fessenkov Albedometer	65
31. Albedo of Magnesium Oxide and Clouds	68

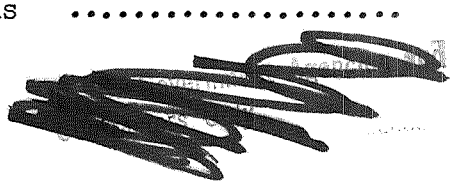

Page

III. ILLUMINATION OF THE PLANETS 69

32. Assumptions of the Theory 69
33. Calculation of the Quantity of Light Reflected by the Planet to the Earth at Different Phases 70
34. Determination of Albedo and Diameter of Planets 75
35. Bond's Definition of Albedo of a Planet 77
36. Light Distribution over a Planetary Disk 82
37. Influence of Surface Roughnesses on the Appearance and Phase Curve of a Planet 84
38. New Illumination Theory of the Moon 86
39. New Illumination Formulas for Large Planets 91
40. Relations between Linear Coordinates on a Planetary Disk and Angle of Incidence (i) and Angle of Reflection (ϵ) of Light 95

IV. ILLUMINATION OF PLANETARY SATELLITES 98

41. Illumination of a Satellite by its Planet 98
42. Calculation of the Ashen Light of the Moon 100
43. Influence of the Celestial Background 103
44. Eclipses of the Jovian Satellites 104
45. Influence of an Atmosphere on the Position of the Umbra of a Planet 110
46. Observations of Eclipses of Jupiter's Satellites by Harvard College Observatory 115
47. Seeliger's and v.Hepperger's Theories on Enlargement of the Earth's Shadow in Lunar Eclipses 118

V. INFLUENCE OF LIGHT DIFFRACTION IN THE TELESCOPE ON THE LIGHT DISTRIBUTION OVER A PLANETARY DISK; APPARENT DIAMETER OF THE DISK 125

48. Older Investigations on Diffraction 125
49. Investigations by H.Struve 126
50. Developments by Nagaoka 133
51. Visible Boundary of a Planetary Disk 145
52. Enlargement of a Planetary Disk by Ray Refraction 146

VI. ILLUMINATION OF DUSTLIKE MASSES 147

53. Hypotheses of the Theory 147
54. H.Seeliger Theory 148
55. Illumination of the Saturn Ring 153
56. Effect of Density of the Dust Formation 159
57. Influence of Transparency of the Dust Formation on the Light Variation 160
58. Variability of the Crêpe Ring 165
59. Formulas for Total Intensity of Ring and Saturn Disk 168

Page

60. Influence of Shadow-Casting on Brightness of the Saturn System 171
61. Shadow-Casting of the Ring 171
62. Shadow Cast by the Planet on the Ring 174
63. Observations of Brightness of the Saturn System 176
64. Observations of the Variability of the Ring 177
65. Consistency of the Saturn Ring; the Light-Scattering Haze 178
66. Zodiacal Light 179
67. Observations of Zodiacal Light Brightness 182
68. Illumination of Cosmic Dust Formations by Stars 186
69. Brightness of Comets 189
70. Schwarzschild's Theory on the Brightness of Halley's Comet 192

VII. EXTINCTION OF LIGHT IN THE EARTH'S ATMOSPHERE 195

71. Function of the Extinction Theory 195
72. Principles of the Theory and Lambert's Interpolation Formula 196
73. The Homogeneous Reduced Atmosphere 199
74. Determination of F(z) from the Refraction Curve 200
75. Bouguer's Extinction Theory 201
76. Laplace's Extinction Theory 204
77. Determination of the Transmission Coefficient and its Dependence on Altitude 207
78. Other Earlier Theories of Extinction 208
79. Bemporad's Investigations as to the Influence of Temperature Stratification of the Atmosphere on the Extinction 209
80. Bemporad's Extinction Theory 210
81. Analytical Development of the Extinction Integral, Based on Schmidt's Hypothesis 211
82. Determination of λ and H for Schmidt's Hypothesis 213
83. Integration of the Expression F(z) for Schmidt's Hypothesis 214
84. Influence of Geographical Location of Observation Site and Pressure and Temperature Fluctuations on the Extinction 218
85. Selective Extinction and Forbes' Phenomenon 220
86. Differential Extinction Determination from Observations at Stations of Various Height above Sea Level 222
87. Dependence of the Transmission Coefficient on Height above Sea Level 223
88. Direct Photometric Extinction Determinations 225
89. Transmittance of the Atmosphere for Radiation of Different Wavelengths 226
90. Influence of Water Vapor on Transmittance of Air for Radiation of Different Wavelengths; Nonselective Extinction by Water Vapor 230

Page

91. Energy Balance during Extinction of Radiation in the Atmosphere 233

VIII. THEORY OF DIFFUSION AND ABSORPTION OF LIGHT IN GASES AND ITS APPLICATION TO PLANETARY ATMOSPHERES 236

92. King's Theory; Definitions and Basic Principles 236
93. General Integral Diffusion Equation 237
94. Theorems from the Theory of Integral Logarithm and Derived Functions 243
95. Application to the Integral Equation of Diffusion (19) 245
96. Application of the Theory to the Terrestrial Atmosphere 251
97. Illumination of a Planet Surrounded by an Atmosphere .. 252
98. Comparison of the Illumination Theories of Planetary Atmospheres 257
99. Recent Investigations in this Field 258

Tables for the Photometry of Stars 260
Contents and Explanations 260
Table Ia Brightness Ratio I/I_o according to the Argument $m - m_o$ 270
Table Ib Brightness Ratio I_o/I according to the Argument $m - m_o$ 275
Table IIa Magnitude Classes in the Zöllner Photometer, Increasing with Brightness, according to the Argument: Reading of the Circle α in Degrees and Tenth Degrees 276
Table IIb Brightnesses in the Zöllner Photometer, in Units of Maximum Brightness on Reading the Circle = 90° 278
Table III For Determination of the Brightness m_{AB} of a Binary, if the Brightness of the Components m_A and m_B are Given 280
Table IVa Brightnesses of a Cloud Layer with Plane Boundaries, Calculated according to the Formula (see Table IVa) 281
Table IVb Coefficients a, b, c, d, e of Eq.(12) on p.48 283
Table Va Brightnesses of an Area with Plane Boundaries, Calculated according to Eq.(13) on p.48 284
Table Vb First Term of Eq.(13) on p.48 286
Table Vc Second Term of Eq.(13) on p.48 for the Maximum Value $\frac{3}{16}$ of the Coefficient $\frac{\pi\mu}{k}$ 288
Table VIa Phase Curves φ_1 and φ_2 in Eq.(7) on p.72 and Eq.(12) on p.73 290
Table VIb Auxiliary Quantities P and R of Seeliger's Formula [Eq.(22)], p.76 for Illumination of an Ellipsoid of Revolution 291

Page

Table VIc Reduction of the Brightness of the Planet Saturn (without Ring) at A = 0 and $\alpha = 0$ to the Brightness at A and $\alpha \neq 0$ 291

Table VIIa Seeliger's Density Function (see Table VIIa) of the Theory of the Saturn Ring [Eq.(15), p.159] 292

Table VIIb Function $\log M = \log \frac{\mathfrak{C}(\infty)}{\mathfrak{C}(\alpha)}$ according to the Arguments: Phase Angles α and $\xi = \frac{N\delta}{\sin \alpha} = \frac{D}{\sin \alpha}$ where D is the Volume Density of the Ring 292

Table VIIc Observed Phase Curve for the Mean Surface Brightness of the Ring, in Units of Brightness of the Planetary Center in Opposition 293

Table VIIIa Values for the Unocculted Portion X of the Ring and the Saturn Disk Portion Y Unocculted by the Ring, in Eq.(36) on p.170, in Units of the Unocculted Saturn Disk 294

Table VIIIb Reduction of Saturn Brightnesses to the Vanished Ring according to Eq.(36) on p.170, under Assumption of Lambert's Light Distribution over the Saturn Disk 295

Table IXa Auxiliary Quantities for Calculating the Shadow-Casting of the Ring onto Saturn and of the Planet onto the Ring 296

Table IXb Auxiliary Quantities for Calculating the Shadow-Casting of the Saturn Ring on the Planet, according to Eq.(40) on p.172 297

Table IXc Auxiliary Quantities $\lambda(a)$, $\lambda(b)$, and $\lambda(c)$ for Calculating the Shadow-Casting of Saturn on the Ring, according to Seeliger [Eq.(51), p.175] 298

Table Xa Mean Extinction Tables for Potsdam (Elevation, 100 m) and for the Summit of Säntis (2500 m); according to G.Müller 299

Table Xb Mean Extinction Tables for Potsdam, between 50° and 88° Zenith Distance, from Tenth to Tenth Degree in Brightness Logarithms (according to G.Müller) 300

Table XIa Bemporad's Mean Extinction Table (for 0°C, 760 mm, and Sea Level) 301

Table XIb Corrections of Extinction for Pressure and Temperature (according to Bemporad) 302

Table XIIa Traversed Air Masses according to Bemporad, for Various Apparent Zenith Distances of the Celestial Body 303

Table XIIb Corrections of the Air Masses $[F_1(z) - F(z)]$ for Pressure and Temperature, in Units of the Third Significant Figure (according to Bemporad) 308

Table XIIc $\frac{\log p_1}{\log p}$ for Various Values of Pressure and Temperature (in Celsius) according to Bemporad 308

Page

Table XIIIa The Function $Ce^{-C}G\{C(\sec\zeta - 1)\}$ according to L.V.King 309
Table XIIIb The Function $G(C \sec\zeta)$ according to L.V.King 309
Table XIIIc The Functions $f(C)$, $G(C)$, and $\Phi(C, 0)$ according to L.V.King 309
Table XIVa The Function $E(C, i)$ Corresponding to the Mean Solution of the Diffusion Integral Function [Eq.(29) on p.247] at an Absorption Coefficient $\gamma = 0$ and $C = c$ 310
Table XIVb The Function $\Phi(C,\varepsilon)=(1-e^{-C\sec\varepsilon})\cdot(1-f(C))+\cos\varepsilon[B(C)-B(C(1+\sec\varepsilon))+ +e^{-C\sec\varepsilon}\{B(C)-B(-C(\sec\varepsilon-1))\}]$ [Eq.(35) on p.249] 310
Table XIVc The Function $R'(C, \varepsilon, i) = C \sec\varepsilon\, G(C(\sec\varepsilon + \sec i))$ [Eq.(52) on p.177] for Various Values of C, ε, and i 311
Table XIVd The Function $\frac{1}{2}\Phi(C, \varepsilon)E(C, i)$ for Various Values of C, ε, and i 312
Table IVe The Function $R'(C, \varepsilon, i) + \frac{1}{2}\Phi(C, \varepsilon)E(C, i)$ for Various Values of C, ε, and i 313

References 316

THEORETICAL PHOTOMETRY

/1*

E.Schoenberg

ABSTRACT. Theoretical principles and fundamental laws of photometry, as they apply to planetary astronomy, are discussed with extensive mathematical treatment of luminescence and illumination of planets, satellites, interplanetary and interstellar dust, comets, etc. Effects of reflection and refraction on the light distribution and brightness variation of planetary disks, solar and lunar eclipses, zodiacal light are reviewed in detail. Various classical and modern theories on the extinction of light in the terrestrial atmosphere and scattering and diffusion of light in gases are critically compared. Extensive tables on stellar and planetary magnitudes and brightness ratios, density functions, extinction data, temperature and pressure corrections are included.

INTRODUCTION

The very first attempts to measure the luminous intensity of celestial bodies, so as to obtain data on their consistency, were made at a time of enormous progress in optics due to the work by Newton and Huygens, at the end of the Seventeenth and the beginning of the Eighteenth Century. Huygens himself (Ref.1) attempted to compare the brightness of Sirius with that of the sun, by attenuating the sunlight through a small aperture in the closed end of a long tube. The Swedish physicist Celsius (Ref.2) searched for a law on the light attenuation of illuminated areas but his conclusions, just as those by Huygens, were untenable because of the inadequacy of the methods used. Except for the formula for the fall-off of light with the square of the distance, physics had no tools of strict definitions and laws and no apparatus for measuring luminous intensities. Buffon (Ref.3) attempted to determine the loss suffered by sunlight on reflection from glass mirrors. However, it was not until the extensive work by Pierre Bouguer (Ref.4, 5) in 1698 - 1758 and by Johann Heinrich Lambert in 1728 - 1777 that the bases for photometry were created. In systematic experimental work, substantiated by logical theories, Bouguer treated the main problems involved: absorption of light on reflection and on passage through solid and liquid bodies as well as diffuse reflection from dull surfaces and on passage through turbid media. His measurements, which he extended also to celestial bodies especially to both sun and moon, were of a high degree of accuracy despite the simplicity of his measuring instruments. Bouguer discovered and defined the limb darkening of the sun, measured the brightness ratio of sun to moon, investigated the light attenuation of stars due to the extinction of light in the terrestrial atmosphere, and

---

* Numbers in the margin indicate pagination in the foreign text.

formulated the first theory of this phenomenon, basing it on the law of the dependence of absorption on the layer thickness (law of geometric progression) /2
discovered by him. In addition, Bouguer also made measurements on the light distribution in a clear sky. His theory of the extinction and the concepts on the process of diffuse reflection have become a permanent treasure of science.

Lambert's photometry (Ref.6) is a masterwork of logical acuity and systematic build-up. From the two basic laws of photometry, introduced and substantiated by Lambert, namely the cosine law for self-luminous body and the composite cosine law for dull surfaces, he systematically derived a number of highly important photometric theorems and definitions which, even today, form the basic principles of photometry. The theory of extinction and brightness of the sky was treated by Lambert independently of Bouguer; in addition, he was the first to successfully solve the problem of illumination of the planets by the sun. This had been done before Lambert - but less successfully and less completely - by Euler, Kies, and R.Smith (Ref.7, 8, 9). Here, Euler used the formula of diffuse reflection, named after him, as basis; however, this formula is in such great contradiction to the theory as well as to observations on dull-surface bodies that it can claim only historical interest. Lambert also has the merit of having defined the concept of albedo and of introducing it into astronomy. However, so far as the perspicacity of his observations is concerned, it lags behind that of Bouguer. Lambert's fame lies in the theoretical and logical build-up of modern science.

Near the turn of the Century, the eminent theoretician P.S.Laplace (Ref.10) developed a new theory of extinction, furnishing an important contribution to celestial photometry. Laplace demonstrated its correlation with the theory of ray refraction in the atmosphere and was the first to consider the curvature of the ray along its path.

After these fundamental works, the development of photometry, for a long period of time, proceeded mainly in practical application fields, in the perfection of astronomic photometers, and in the compilation of more accurate observations. F.Arago (Ref.11) and F.E.Neumann (Ref.12), in developing the theory of polarization, furnished a basis for construction of the polarization photometer which later found wide application under the name of Zöllner photometer. L.Seidel (Ref.13), around the middle of the Nineteenth Century, used a Steinheil photometer (Ref.14) for observing the brightness of planets and fixed stars. In this instrument, the extrafocal images of two celestial bodies are compared in the field of view of the eyepiece with respect to their area brightness, in which case this brightness can be measurably changed by varying the focal /3
length. Seidel's and Arago's (Ref.5) measurements of planets and their theoretical considerations of planets constitute valuable contributions to photometry, specifically since they were able to demonstrate the inadequacy of the Lambert reflection formula. Seidel himself set up a new table of extinction and derived a formula for the brightness of Saturn in dependence of the aperture of its rings.

The theory of diffraction of light in the telescope, which is of great importance for astronomic photometry, was treated by Schwerd (Ref.16) in a comprehensive work and, simultaneously, by Airy (Ref.17) under restriction to the phenomena in light points.

The middle of the same Century also saw a theoretical treatment by A.Beer (Ref.18) on the basic principles of photometric calculus as well as on other theoretical photometric papers, which gave a critical evaluation of Lambert's photometry, by G.Recknagel and J.Rheinauer (Ref.19, 20).

J.Herschel furnished a contribution to the theory of lunar phases by his measurements of the brightness of our satellite, using an ingenious astrometer (Ref.21).

Further considerable progress was produced by the highly intellectual work of Fr.Zöllner (Ref.22) which was published in the Sixties of the Nineteenth Century. Simultaneously with H.Wild (Ref.23), Zöllner constructed the Zöllner polarization photometer named after him which, essentially, was intended for observation of light points but also permitted the measurement of surface brightnesses; this instrument, without major changes, is still widely used in astronomy at present. Zöllner's measurements of fixed stars, the sun, and the planets with the new instrument yielded a high degree of accuracy and permitted a detailed critical evaluation of Lambert's theories on illumination of the planets. His own theory of illumination of the moon, however, is not too fortunate. Because of the multitude of theoretical considerations on the configuration of celestial bodies, which he attempted to substantiate by his own measurements, Zöllner's work has become of extreme importance for stellar photometry. Simultaneously with Zöllner, G.P.Bond (Ref.24), at Harvard College Observatory, /4 made photometric experiments on the brightness of the planets, the moon, and the sun, advancing theoretical photometry specifically by a new definition of the albedo of planets. However, his work was rescued from obscurity only after half a century by H.N.Russell.

The photometric phenomena exhibited by the Jupiter satellites during the eclipse were treated by A.Cornu and A.Obrecht (Ref.25, 26). The latter author developed a complete theory of these phenomena.

Considerable advance in theoretical photometry was registered through the investigations by Hugo v.Seeliger and his followers (Ref.27). Seeliger brought the theory of illumination of the planets, of the Saturn ring, and of the nebulae to such a high level in many respects that its confirmation by actual observations was not fully possible. This theory would require a sharpness of photometric measurements as it has not been attainable until now. The investigations by Seeliger and E.Lommel (Ref.28) on diffuse reflection, resulting in the laws named after these two researchers, are fundamental; Seeliger derived strict formulas for the illumination of an ellipsoid of revolution without, however, taking the effect of an ambient atmosphere into consideration. He was the first to develop the theory of illumination of dust-like masses, especially of the ring of Saturn, and drew conclusions as to the variability of the ring when close to opposition. Furthermore, he calculated the brightness of the zodiacal light and that of the nebulae in the neighborhood of luminous stars under the assumption that the former were produced from a cloud of meteorites. Just as fundamental is Seeliger's interpretation of the enlargement of the earth's shadow during lunar eclipses, based on a strict calculation of the refraction and absorption of light in the terrestrial atmosphere.

Of the work by pupils of Seeliger, we should mention that by E.Anding

(Ref.29) on the eclipse of the Jupiter moons and on the light distribution over a planetary disk. Another work on the above subject was published by V.Wellmann (Ref.30), while an investigation on the zodiacal light was performed by K.Schwend (Ref.31). G.Müller (Ref.32) has the great merit of giving, in his excellent handbook "Stellar Photometry", a compilation of more recent theoretical papers which mainly go back to Seeliger.

This should end our survey over the historical development of theoretical photometry. The literature references given here make no claim to completeness. /5 In essence, the bibliography refers to the development of problems treated in this book. Actual results of observations are given only if they are combined with theoretical considerations. More recent studies are discussed in this book with sufficient adequacy. In this volume, some results of the author's own work in the field of theoretical photometry are reported for the first time. This includes also a new formula for diffuse reflection and the theory of illumination of a planet surrounded by an atmosphere. The Appendix gives a number of auxiliary tables, partly taken from original papers and partly calculated anew. These tables are to facilitate tedious calculations and stimulate investigations of difficult new problems having to do with the illumination of planets.

I. DEFINITIONS, FUNDAMENTAL LAWS, AND PROBLEMS

1. Definition of Photometry

Stellar photometry is that part of astrophysics which investigates the radiation of celestial bodies as to their intensity.

This radiation manifests itself in astronomy in various manners; for example, astrophotometry is subdivided into various disciplines, depending on which of these effects forms the subject of study. Until now, it has been possible to measure the following effects of radiation emitted by stars:

1) Physiological effect on the human eye, forming the basis of the oldest field, namely that of visual photometry.
2) Chemical effect on a photographic plate, which at present is the most widespread basis of photographic photometry, convenient and highly suitable for statistical investigations on the brightness of objects of low luminous intensity.
3) Photoelectric effect, which can be measured with extreme accuracy and thus has become of great importance for detailed investigations of minor light fluctuations.
4) Thermal effect, which is measurable only for the brightest stars.

The first three effects of the radiation are selective.

The intensity of radiation of all effective wavelengths can be measured only by means of the thermal effect, since the receiver used for this (lampblack and platinum black) has the property of almost totally absorbing all wavelengths and to convert them into heat. Therefore, the bolometer, pyrheliometer, and any instrument that measures the intensity of the thermal effect of the ray on suitable black surfaces are the only ideal radiometers; with their help it has become

possible to define the limits of other radiation measuring methods. In this respect, the thermal effect of radiation belongs into the field of photometry and is mentioned already here, whereas the essential details are discussed in the Section on radiation theory. The term "photometry" (light measurement), strictly taken, is applicable only to the visual method since both photographic and photoelectric methods also cover radiations lying outside of the region perceived as light; nevertheless, this term is generally applied to these regions.

Consequently, the science of radiation represents the basis for various branches of photometry, all of which permit measuring only a portion of the total radiation; for this reason, the fundamental concepts and main laws of radiation, so far as they will be used in what follows, will have to be re- /6
viewed here before strictly formulating the definitions and fundamental laws of photometry which, in a certain sense, merely represent a translation of radiology into the older terminology of light phenomena.

2. Basic Laws and Definitions in Radiology; Radiant Point

In a homogeneous medium, radiation (energy) propagates rectilinearly in all directions starting from the radiant source. Thus, the rays originating from a radiant point represent the pathways of energy. If we form a conical surface, with its vertex at the radiant point, then the generatrices of the cone envelope represent the pathways of the radiation so that no radiation can pass through the lateral areas. Consequently, the same amount of radiation must pass through each section of the cone in unit time. This amount of radiation (amount of energy), denoted simply as radiation (energy), is then determined by the size of the solid angle ω. This angle has the surface of the section s formed by the cone with a sphere of radius 1 as dimension. Thus, if F denotes an arbitrary section of the cone at a distance r, we have

$$\omega = s = \frac{F}{r^2}. \tag{1}$$

Consequently, the amount of energy in the solid angle ω is identical with the energy or radiant flux through some section of the angle in unit time. We will denote this by G. The radiant intensity U in direction of the cone axis is the quotient of the energy flux and the size of the solid angle

$$U = \frac{G}{\omega}. \tag{2}$$

Thus, we also have the equation

$$G = U\omega = Us \tag{3}$$

for the radiant flux through some section of the solid angle in unit time.

If this energy flux is referred to unit area

$$B = \frac{G}{s} = \frac{G}{\omega} = U, \tag{4}$$

then B will be the irradiation which, according to eq.(4), is measured by the same factor as the radiant intensity U.

Let us now imagine the area ab = s shifted from the distance l to the distance r, with this area always remaining perpendicular to the axis of the cone; then, the flux on this area is reduced at the same ratio as the mutual position of the areas s = ab = $\alpha\beta$ and AB. For this reason, the energy flux on the area s, at a distance r, will be

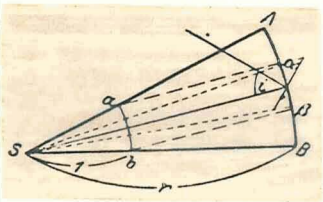

Fig.1 Fundamental Laws of Radiology.

$$G = \frac{Us}{r^2}. \tag{5}$$

If the area s is imagined as rotated about the angle i, then the energy flux on this area is just as large as on its perpendicular projection s cos i since both are located in the same solid angle. Consequently, if the angle of incidence of the ray on the area s is equal to i, then the energy flux on this area will be

$$G = \frac{Us\cos i}{r^2}. \tag{6}$$

The irradiation of the area correspondingly becomes /7

$$B = \frac{U\cos i}{r^2}. \tag{7}$$

3. System of Radiant Points and Radiant Area

If a number of radiant points are located at distances r_1, r_2, ... from the area s and if their radiant intensities are U_1, U_2, ..., with the angles of incidence of the radiation on the area s correspondingly being i_1, i_2, ..., then the total flux striking s must be equal to

$$G = \frac{U_1 s\cos i_1}{r_1^2} + \frac{U_2 s\cos i_2}{r_2^2} + \cdots. \tag{8}$$

If the mutual distance of the points is small with respect to the distance from s, so that we can set $i_1 = i_2 = i_3 = \ldots = i$ and also $r_1 = r_2 = r_3 = \ldots = r$, we obtain

$$G = \frac{s\cos i}{r^2}(U_1 + U_2 + U_3 + \cdots) = \frac{s\cos i}{r^2}U, \tag{9}$$

where

$$U = U_1 + U_2 + U_3 + \cdots. \tag{9'}$$

Consequently, under the mentioned conditions, a system of luminous points can be replaced by one point with a radiant intensity equal to the sum of the radiant intensities of the individual points.

Since a radiant area can be conceived as consisting of a number of closely

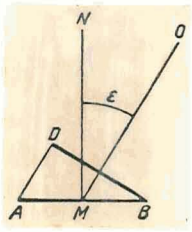

Fig.2 Radiant Area.

spaced radiant points, the above theorem is valid also for a radiant area.

If the radiant intensities of the individual points U_1, U_2 ... are mutually equal, then the radiant intensity of the area is proportional to the number of points or to the size σ of the radiant area

$$U = \eta\sigma. \tag{10}$$

In determining the intensity of radiation of a given area, however, a new element must be considered namely the direction of radiation. Let AB = σ be an element of the radiant area, MN the perpendicular to this area, MO an arbitrary direction making an angle ε with the normal, BD the vertical projection of AB equal to $\sigma \cos \varepsilon$ the so-called apparent size of AB in the direction MO. Denoting by U the radiant intensity in the direction ε, the theorem that this intensity, for a so-called black body, is proportional to the cosine of the emission angle ε is valid, so that

$$U = \eta\sigma\cos\varepsilon, \tag{11}$$

where η is a constant. We retain this equation also for arbitrary radiating bodies which do not strictly obey the cos ε law, by considering η in this case as no longer constant and, determined by the equation

$$\eta = \frac{U}{\sigma\cos\varepsilon} \tag{11'}$$

defining it instead as radiance or radiant emittance in the direction ε. Thus, for a black body, the radiance is the same under all angles.

4. Irradiation of One Element by Another

Let the radiant element σ emit radiation, under the emanation angle ε, toward an element s which it strikes under the angle of incidence i to the normal. Let r be the spacing of the elements. Then, the energy flux from σ to s, according to eq.(9), /8 will be

$$G = \frac{Us\cos i}{r^2},$$

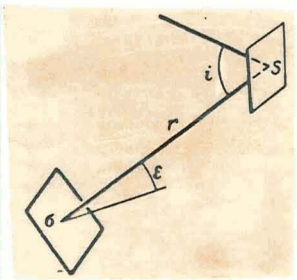

Fig.3 Irradiation of an Element of Area by Another.

where U denotes the radiant intensity under the angle ε, being determined from eq.(11). Hence,

$$G = \frac{\eta\sigma s\cos\varepsilon\cos i}{r^2}. \tag{12}$$

This represents the Lambert composite fundamental law of photometry. Lambert was of the opinion that this

law is generally valid at constant η; with the above restriction, we will retain his law in this particular form. Then, the irradiation will be

$$B = \frac{\eta \sigma \cos\varepsilon \cos i}{r^2}. \tag{13}$$

Since the area s, seen from σ, appears under the solid angle $\omega = \frac{s \cos i}{r^2}$, we can also write

$$G = \eta \sigma \omega \cos\varepsilon. \tag{14}$$

For a black body whose radiance is constant in all directions, it is easy to determine the radiation emitted into the solid angle 2π, i.e., the total radiation of a surface element toward one side. If we describe a sphere of radius 1 about the radiant element as center, the following amount of energy will fall on a segment of the sphere, between the parallels ε and $\varepsilon + d\varepsilon$:

$$dG = \eta \sigma \cos\varepsilon \, 2\pi \sin\varepsilon \, d\varepsilon$$

and, on the entire hemisphere,

$$G = 2\pi \eta \sigma \int_0^{\pi/2} \sin\varepsilon \cos\varepsilon \, d\varepsilon = \pi \eta \sigma. \tag{15}$$

5. Composite Radiation

In measuring radiant intensities, we generally have to do with mixed radiation of differing wavelengths, and measurement of monochromatic radiation intensity is possible only for the brighter stars. However, the radiance η differs for different wavelengths, a point which is explained in detail in radiology. Consequently, in applying the above formulas, this must be taken into consideration. If the radiation of a certain wavelength is meant, which will be denoted by the subscript λ, then the Lambert formula will apply in the following form:

$$G_\lambda = \frac{\eta_\lambda \sigma s \cos i \cos\varepsilon}{r^2}. \tag{12'}$$

If the composite energy flux is meant, this must be conceived as the sum of all energy fluxes for the individual wavelengths; since the total emissivity between the wavelengths λ_1 and λ_2 is represented by the sum

$$\eta_{12} = \sum_{\lambda_1}^{\lambda_2} \eta_\lambda \Delta\lambda$$

or, in a continuous spectrum, as

$$\eta_{12} = \int_{\lambda_1}^{\lambda_2} \eta_\lambda \, d\lambda$$

where each η_λ is multiplied by the region for which it can be considered as constant, then the total energy flux between the wavelengths λ_1 and λ_2 can be written in the form

$$G_{12} = \frac{\sigma s \cos\varepsilon \cos i}{r^2} \sum_{\lambda_1}^{\lambda_2} \eta_\lambda \Delta\lambda \quad \text{or} \quad = \frac{\sigma s \cos\varepsilon \cos i}{r^2} \int_{\lambda_1}^{\lambda_2} \eta_\lambda d\lambda. \tag{16}$$

Here, the radiance must be known from measurements of the energy distribution in the spectrum or must be calculated theoretically from the radiation laws. For visual radiation measurements, the limits of visibility are $\lambda_1 = 0.370\ \mu$ and $\lambda_2 = 0.760\ \mu$. Consequently, for visual measurements of a light source having a continuous spectrum, the above limits must be used.

In bolometric measurements of the total radiation, the total emissivity must be considered, denoted by the symbol

$$\eta = \int_0^\infty \eta_\lambda d\lambda. \tag{17}$$

6. Definitions of Visual Photometry

In visual photometry, the human eye together with the retina and the contiguous nervous apparatus over whose intermediary the radiant energy is transformed into a light sensation, represent the receiver of the radiation. Therefore, it is necessary to be entirely clear as to the transformation undergone by the radiation through this receiving apparatus, before it is converted into light sensation.

Ever since Helmholtz (Ref.33), it is known that, during penetration of the parts of the eye in front of the retina - namely cornea, crystalline lens, aqueous humor between these two, and vitreous humor beyond the lens - all rays having a wavelength longer than $0.812\ \mu$ are completely lost by absorption. According to other researchers, some of the infrared rays penetrate to the retina [according to Aschkinass (Ref.34) up to a wavelength of $1.4\ \mu$], but they definitely do not contribute to the light sensation. As lower limit of the visible wavelengths a value of $0.370\ \mu$ is generally assumed for the normal eye, which coincides with the limit of transmissivity of the crystalline lens for short-wave rays [Widmark (Ref.35)]. The normal limits of visibility are $0.760\ \mu$ in the extreme red and $0.370\ \mu$ in the extreme violet. Between these two, degrees of color perception are located at the following wavelengths:

Extreme red	$0.760\ \mu$	Blue-green (cyanogen)	$0.473\ \mu$
Red	$0.683\ \mu$	Blue	$0.439\ \mu$
Orange	$0.615\ \mu$	Violet	$0.410\ \mu$
Yellow	$0.559\ \mu$	Extreme violet	$0.370\ \mu$
Green	$0.512\ \mu$		

No accurate data exist on the process of conversion of the radiation striking the retina into the above-mentioned color perceptions. However, it is known (a point to be discussed in some detail here) that only a fraction of the radiant /10

energy of each wavelength striking the retina is converted into physiological energy Φ which produces the light sensation. Combining the absorption in front of the retina with that through the retina, we will denote the ratio of the physiological energy of the light sensation Φ for the wavelength λ to the external energy by K_λ and, for the composite radiation, by K_e; then, we can establish the following equations:

$$\Phi_\lambda = U_\lambda K_\lambda \quad \text{and} \quad \Phi_e = U_e K_e, \tag{18}$$

where U_λ and U_e denote the intensities of the external energy fluxes. The variability of the factor K_λ with the wavelength will be discussed in more detail. First, it is quite obvious that the definitions and fundamental laws of radiology can be translated by means of this factor into the basic concepts of visual photometry. Thus, the concepts of radiology will be replaced by the corresponding concepts of visual photometry, as follows:

G	energy flux, amount of energy	GK = Q	luminous flux, amount of light;
U	radiant strength, radiant intensity	UK = J	luminous strength, luminous intensity;
η	radiance	ηK = h	luminance or area brightness of a light source;
B	irradiation	BK = L	illumination.

Then, from the equations of radiology, this will yield the following corresponding relations:

Luminous point

$$Q = J\omega = \frac{Js\cos i}{r^2}. \tag{19}$$

The quantity of light in the solid angle ω is equal to the product of the luminous efficiency of the radiant point and the size of the angle ω. The quantity of light on the area s is directly proportional to the size of the area and to the cosine of the angle of incidence i, while it is inversely proportional to the square of the distance from the luminous point:

$$L = \frac{Q}{s} = \frac{J\cos i}{r^2}. \tag{20}$$

Illumination is the quantity of light per unit area and becomes equal to the luminous intensity J for a distance 1 from the luminous point and for i = 0:

$$J = h\sigma\cos\varepsilon. \tag{21}$$

The luminous intensity of the luminous area σ is proportional to the size of the area and to the cosine of the emanation angle. For a black body, the surface brightness h is constant:

Luminous area

$$Q = \frac{h\sigma s \cos\varepsilon \cos i}{r^2}. \qquad (22)$$

The quantity of light, striking the area s from the luminous area σ, is directly proportional to the cosine of the emanation angle ε and the cosine of the angle of incidence i, while it is inversely proportional to the square of the distance of the areas r.

The visual photometric quantities have no units of measurement in common with radiology, as it might appear from the above equations, since the factor K as the conversion factor of mechanical values into sensory quantities naturally cannot be determined in absolute amount despite the fact that its variability in relative units can be investigated. The units of visual photometry can only be compared with one another, and no direct transition to the units of radiology exists. Nevertheless, the eye itself can serve as relative radiometer, under the following conditions: If the luminous intensities of two light sources of equal color and size, whose images on the retina are closely adjacent, appear equal to each other, it can be concluded that the radiant intensity is also equal. This is true for two luminous points which are imaged on the retina as minute disks of equal diameter, as well as for adjacent areas in which the surface brightness is to be compared. If the two luminous points or the adjacent areas appear to the eye as having differing brightness, then the eye is unable to define the brightness difference. In that case, the usual comment is that the one point or the one area is brighter or darker than the other; with some training, a few degrees of brightness differences can be estimated but the eye is incapable of any strict measurement. This immediately leads to the principle to be used in building a visual photometer. Such an instrument must offer the possibility of varying, in a measurable manner, the intensity of one of the objects to be compared. In that case, equal luminous intensity of both objects can be obtained and reliably evaluated; this means also equal radiant intensity if the hue of the objects is the same. /11

The eye is highly sensitive to minor brightness differences. According to Bouguer (Ref.5, p.25), the eye can differentiate as little as 1/64 of the luminous intensity. Arago (Ref.36) observed that, during motion of a luminous object, up to 1/131 of the brightness is detectable, while Masson (Ref.37) found an average factor of 1/100, with almost the same value furnished in experiments by Fechner (Ref.38). Practical stellar photometry on point objects generally confirms that, under favorable conditions, 1% of brightness is differentiable. The eye perceives differences in surface brightness of adjacent equal-color areas more accurately than of point light sources, as demonstrated in observations of variable stars by means of surface photometers (Ref.39).

The sensitivity of different observers apparently differs widely, depending also on individual training, as any novice observer will confirm. In addition, this sensitivity differs for a light-adapted and a dark-adapted eye, being greater for the latter. Finally, the sensitivity decreases with increasing fatigue as is generally the case for the acuity of all human sensations. Naturally, the above figures presuppose optimum conditions, as they are usually realized in scientific measurements.

7. Sensitivity of the Eye for Brightness Differences of Individual Colors of the Spectrum

This sensitivity (Ref.40) differs widely, which is of great importance for spectrophotometric observations.

According to Lamansky, the differential threshold for green and yellow /12 is 1/286, for blue 1/212, for violet 1/109, for orange and red 1/78 resp. 1/70. Dobrowolsky gives figures for the individual colors that do not differ much from the above data. According to König and Brodhun, the sensitivity thresholds for the individual colors fluctuate much less and are in themselves larger: 1/40 to 1/51. This difference in data actually represents a confirmation of the temporal and individual difference in the sensitivity threshold; in addition, there may be some degree of partial color blindness of individual observers involved here.

For ordinary astrophotometric measurements of stars and planets, in which one has to do with mixed light rather than with pure spectral colors, these differences in sensitivity threshold are of less importance.

The principle of the visual photometer requires a matching of the artificial light to the color of the celestial object. This is generally reached only in first approximation. For point objects, the eye has only a negligible discriminative sensibility for various colors; in measurements with a surface photometer, a greater agreement of the colors is necessary. Unfortunately, more accurate figures on the differential threshold for mixed colors of celestial bodies are nonexistent. For the colors of the spectrum and for a normal color-trained eye, Uthoff (Ref.40) found a distinct difference in color hue on variation in wavelength by widely differing amounts. If these variations are measured in $\mu\mu$, the threshold in the extreme red is 4.7 $\mu\mu$, decreases rapidly in the orange, reaches a minimum of 0.9 $\mu\mu$ in the yellow, rises again to 1.9 $\mu\mu$ in the green, returns to a second minimum of 0.7 $\mu\mu$ in the blue-green, and finally rises again to 2.2 $\mu\mu$ toward the indigo. Thus, the eye is most sensitive to differences in wavelength in the orange-yellow and blue-green.

8. The Purkinje Phenomenon

Highly specific phenomena occur in colored objects of extremely low intensity. After some training, the eye is able to estimate brightness degrees even for fields of different color. Two fields of different color will appear equally bright at weak illumination, which no longer is the case as soon as the illumination for both fields is increased to the same degree; the field in the long-wave light will change in brightness to a greater extent. The originally equally bright fields (for example, red and blue) will then differ in that the red field will be brighter at increased illumination than the blue field while it will be darker at decreased illumination. Consequently, at weak illumination, the eye is more sensitive to blue light while at strong illumination it is more sensitive to red light.

This phenomenon is known as the Purkinje effect. It includes the familiar fact that, in a dark room, first the blue objects and then only the red ones are perceived.

Fortunately, as proved by Brodhun (Ref.41) in spectrophotometric experiments, the Purkinje phenomenon will no longer be present, or at least only to a negligible extent, as soon as the brightness exceeds a certain value, meaning that two different-color fields, appearing equally bright at this upper brightness limit, will remain equally bright on increasing the illumination at the same ratio.

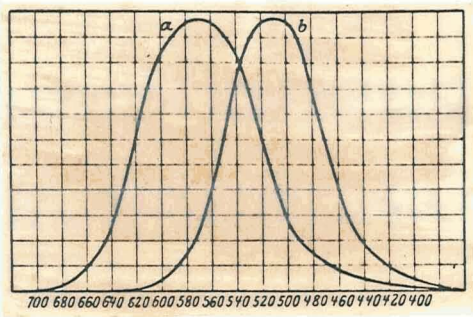

Fig.4 The Purkinje Phenomenon.

A.König (Ref.42), in collaboration with various other scientists, investigated the brightness distribution in the normal solar spectrum and plotted the results graphically. His curves are given in Fig.4. /13

In this diagram, the abscissas represent the wavelengths and the ordinates, the brightnesses. Curve a gives the brightness at an illumination at which the Purkinje effect no longer occurs, while curve b gives the brightness distribution at the lowest brightness gradation still usable in the measurement. In curve a, the maximum is located in the yellow-green near $\lambda = 570$ μμ. If the absolute brightness of the spectrum is gradually attenuated, for example by narrowing the slit, the maximum - due to the Purkinje effect - will gradually shift toward the violet end until it reaches the blue-green near $\lambda = 510$ μμ at the lowest brightness step.

For practical astrophotometry, the Purkinje effect constitutes a warning never to be satisfied with an approximately equal color in comparisons of artificial light with real starlight. This may lead to considerable errors in the case of faint stars if the observer connects these with much brighter stars by means of an attenuation device (Nicol prisms, optical wedge). Due to the Purkinje effect, the color of the artificial star changes in an entirely different manner when measuring the faint object than does the color of the real star, produced by the same phenomenon. However, this color difference is not perceived because of the low brightness. If the two stars to be compared are of exactly the same spectral type, i.e., of the same color, which differs from that of the artificial star, then the measured attenuation of the artificial star will not be a correct criterion for the brightness ratio of the stars.

9. Determination of the Factor K_λ; Sensitivity of the Eye to Radiation of Differing Wavelengths

Curve a in Fig.4 gives a picture as to the brightness distribution in the normal solar spectrum. This curve does not coincide with the curve for the intensity distribution of solar radiation, as it can be determined reliably by means of a bolometer. The reason for this difference lies in the above-mentioned difference of the factor K_λ for different wavelengths or, in other words, in the differing sensitivity of the human organ of sight for radiation of different wavelengths. A relative measure for the values of the factor K_λ can be obtained

by a comparison of bolometer and brightness measurements of the solar spectrum. In the accompanying table, we give the mean values derived by Langley from measurements made by three observers of the ratios of $J_\lambda : U_\lambda = K_\lambda$ where U_λ is the radiant intensity, J_λ the luminous intensity for the same wavelength, and $K_\lambda = 1$ for $\lambda = 0.75\ \mu$.

TABLE 1

	Wavelength λ in μ						
λ	0.40	0.47	0.53	0.58	0.60	0.65	0.75
K_λ	1600	62 000	100 000	28 000	14 000	1200	1

Accordingly, the sensitivity of the eye differs widely for the various wavelengths, being greatest for green rays. If, of two areas having equal /14 emissivity, the area a emits only rays of a wavelength 0.50 μ and the area b only rays of 0.65 μ, then a will appear 83 times brighter than b. It is conventional to say then that the surface brightness of a is 83 times that of b. If the areas are of equal size, their radiant intensities U_λ will be equal while their luminous intensities will be at the indicated ratio.

TABLE 2

STANDARD VALUES OF PHYSIOLOGICAL COEFFICIENTS

Wavelength in μ	K_λ	Wavelength in μ	K_λ	Wavelength in μ	K_λ
0.40	0.0004	0.53	0.862	0.65	0.107
0.41	0.0012	0.54	0.954	0.66	0.061
0.42	0.0040	0.55	0.995	0.67	0.032
0.43	0.0116	0.56	0.995	0.68	0.017
0.44	0.023	0.57	0.952	0.69	0.0082
0.45	0.038	0.58	0.870	0.70	0.0041
0.46	0.060	0.59	0.757	0.71	0.0021
0.47	0.091	0.60	0.631	0.72	0.00105
0.48	0.139	0.61	0.503	0.73	0.00052
0.49	0.208	0.62	0.381	0.74	0.00025
0.50	0.323	0.63	0.265	0.75	0.00012
0.51	0.503	0.64	0.175	0.76	0.00006
0.52	0.710				

Table 2 contains the standard values of physiological coefficients, in 1924 adopted by the Commission Internationale d'Éclairage in Geneva, which were derived as mean values from a total of 250 observers. Therefore, these are valid for a normal eye and have few if any of the individual differences which, for a given observer, may be considerable.

10. The Fechner-Weber Psychophysical Law

This law settles the question as to the dependence of the degree of per-

ception, for example, of the estimated luminous intensity of a given celestial body on the magnitude of the external stimulus, i.e., its radiant intensity. A simple concept of the nature of this law can be obtained from the phenomenon that the stars cannot be seen with the naked eye in daytime despite the fact that the absolute difference in intensity of a given star and of the surrounding sky against the celestial background is just as great in daytime as at night. In daytime, two absolutely strong intensities are compared while, at night, much weaker intensities are involved. This shows that the human eye evaluates the same difference of two light impressions as a function of their absolute magnitude in an entirely different manner. This can be demonstrated by a simple experiment: If a given plate is illuminated by one candle and another similar plate by two candles, the difference in brightness is immediately discernible; conversely, if one of the plates is illuminated by 150 candles and the other by 151, the difference cannot be perceived despite the fact that the intensity difference is naturally the same.

Entirely different results are obtained on varying two given light sources at the same ratio instead of by an equal plus. Fechner observed two cloud surfaces whose brightness difference was just about perceptible, first making his examination with the naked eye and then through absorbent glasses of differing density. The brightness difference remained just perceptible despite the fact that the absolute brightness was much lower. The glasses attenuated both luminous intensities at one and the same ratio. In general, these and numerous other experiments indicate that, at widely differing brightness degrees, the difference in intensities just about perceivable by the human eye constitutes almost the same fraction of the total intensity. Fechner was the first to /15 recognize and to formulate this law, observing and describing these particular phenomena. The lowest discrimination step, under optimum conditions, corresponds on the average to 1% of the total brightness. For a mathematical formulation of the law, the concept of estimated sensation E, in difference to the objective luminous intensity J which had been used before, must be introduced. The latter can be measured by means of photometers, under avoidance of the Purkinje effect, and objective ratios of luminous intensities, according to our fundamental equations, are equal to the intensity ratios of the radiation of equal color. The human eye, even without aid, is able to estimate degrees of brightness and thus has done great service to photometry. Before Zöllner gave the fundamentals of astrophotometry, estimating of brightness steps was the only method used; even today, such estimate methods are of considerable importance in the investigation of variable stars and in catalog work for astronomy. The objective brightnesses J are correlated, over the Fechner law, with the estimated brightnesses which will be denoted here as sensation factors E. Then, dE denotes the increase in degree of sensation corresponding to the increment dJ of objective brightness. According to Fechner, dE is thus proportional to the ratio dJ:J, namely

$$dE = c_1 \frac{dJ}{J}, \tag{23}$$

where c_1 is a constant. Integration will yield

$$E = c_1 \ln J + C = c \log J + C.$$

For a different pair of corresponding values E_0 and J_0, we then have

$$E_0 = c \log J_0 + C,$$

from which it follows that

$$E - E_0 = c \log \frac{J}{J_0}. \qquad (24)$$

Let us imagine two binaries in which the two stars subjectively differ by the same number of brightness steps (E - E_0 equal for both binaries); then the brightness ratio J/J_0 is the same for both binaries.

The Fechner law does not have unlimited validity. At very low brightnesses, this law becomes inaccurate, a fact already mentioned by Fechner himself. He attributed this deviation to the influence of the subjective idioretinal light of the eye itself which, even in complete darkness and with closed eyes, still produces a blurred irregular dim light. The optical nerves are stimulated not only by the external effect of light but there also exists a constant stimulation by internal influences which is the cause of the idioretinal light. This light is so faint that it becomes insignificant at increased light sensation. Denoting its intensity by J_e, the Fechner law would have the following form since this intensity is always added to the objective intensity:

$$dE = c \frac{dJ}{J + J_e}.$$

Thus, the increment in sensation is lower than in the case of $J_e = 0$; the deviation from the form of eq.(23) is greater the smaller J itself. As plausible /16 as this explanation appears, there is no reliable proof of its correctness and no accurate knowledge of the intensity of the idioretinal light; obviously, attempts by Fechner and Volkmann to determine this idioretinal light yielded too low a value. Similarly, the Fechner law fails at light impressions of such as intensity that the eye is blinded. Naturally, this needs no further explanation since such dazzling constitutes a damage to the visual apparatus which cannot withstand excessive stresses such as are produced, for example, by sunlight. The damage produced by directly looking into the sun is known to lead to blindness; however, even at lower luminous intensities that produce dazzling, the eye stops perceiving differences in intensity.

11. Size Classes of Stars

Starting in antiquity, celestial bodies have been grouped into certain brightness classes, so-called magnitudes, in accordance with the impression made by their light on the eye; six different classes were distinguished with the naked eye. The sensation differences between each two such classes are the same. Later, this brightness scale was extended also to fainter stars accessible only to the telescope, leading to an originally arbitrary classification of brightness in the sky. This raises the question whether this scale is substantiated by the Fechner law. The objective brightnesses of stars of magnitudes 1, 2, 3, ..., n are designated as J_1, J_2, J_3, ..., J_n while the corresponding sensation

factors are given the symbols E_1, E_2, ..., E_n. This leads to the equations

$$E_n = c \log J_n + C,$$
$$E_{n-1} = c \log J_{n-1} + C,$$

i.e.,

$$E_n - E_{n-1} = c \log \frac{J_n}{J_{n-1}}. \tag{25}$$

If the Fechner law is valid, it necessarily follows that

$$c \log \frac{J_n}{J_{n-1}} = k,$$

since the difference of two successive magnitude classes $E_n - E_{n-1}$ is constant. Denoting k:c by a new constant log $1/\rho$, we obtain

$$\frac{J_{n-1}}{J_n} = \varrho. \tag{26}$$

In fact, all previous investigations have shown that, within certain limits, the brightness ratio J_{n-1}/J_n can be considered as constant so that the size estimates of stars furnish a confirmation of the Fechner law. The proof is obtained by direct measurement of the intensity ratio J_{n-1}/J_n. Numerous special investigations, among others also the large Potsdam Catalog of Brightnesses (Potsdam Photometric Durchmusterung) which included all stars of the Bonner Durchmusterung of the Northern Sky up to magnitudes of 7.5 and was based on measurements with the Zöllner photometer, proved the constancy of ρ for one and the same observer. An exception in this respect are the estimated size classes of the brightest stars of the first and second magnitude. For fainter stars up to the sixth magnitude and also for telescopic stars, a rather constant value of ρ was obtained for each individual observer. The values all are close to $\rho = 2.5$, $\log \rho = 0.398$. By addition of the equations

$$\log J_1 - \log J_2 = \log J_2 - \log J_3 = \cdots = \log J_{n-1} - \log J_n = \log \varrho$$

we obtain

$$\log J_n - \log J_1 = -(n-1) \log \varrho.$$

This equation permits deriving the value of log ρ from such size estimates of /17
stars for which also photometric measurements of the intensities are available. Table 3, taken from Müller's "Photometry of Stars", contains a compilation of a number of determinations of log ρ for the estimates of the Bonner Durchmusterung from measurements by various observers. The first column gives the size classes of the stars used in the derivation.

An interesting fact in this table is the systematic course of Wolff's values of log ρ. However, according to Müller (Ref.43), this must be ascribed to systematic errors of measurement rather than to errors of estimate. The other rows of the table, except for deviations in the brighter stars of second to third magnitude, show no variation with the brightness. Nevertheless, as expected, the mean-square values differ for the individual observers.

TABLE 3

Bonn Estimates	Zöllner	Seidel	Peirce	Wolff	Harv. Phot.	Uranom. Oxon.	Potsd. Durchm.	Rosén	Lindemann
2nd - 3rd magnitude	0.406	0.487	—	0.368	0.396	0.424	0.329	—	—
3rd - 4th magnitude	0.283	0.362	0.391	0.328	0.368	0.368	0.329	—	0.291
4th - 5th magnitude	0.315	0.342	0.340	0.230	0.328	0.364	0.329	—	
5th - 6th magnitude	0.209	—	0.437	0.178	0.382	0.377	0.329	0.388	0.303
6th - 7th magnitude	—	—	—	—	—	—	0.400	0.388	0.394
7th - 8th magnitude	—	—	—	—	—	—	0.400	0.363	0.392
8th - 9th magnitude	—	—	—	—	—	—	—	0.379	0.437
Of all stars									
2nd - 6th magnitude	0.341	—	0.371	0.305	0.356	0.385	0.329	—	0.280
6th - 9th magnitude	—	—	—	—	—	—	0.400	0.380	0.402

According to a suggestion by Pogson, the more recent brightness catalogs assume a certain figure for log ρ, namely

$$\log \varrho = 0.4,$$

whence

$$\varrho = 2.512; \qquad \frac{J_n}{J_{n+1}} = 2.512.$$

This yields a strict definition of the size classes of the stars, and all brightness catalogs reduced by this figure will then differ only by the starting point of the numeration; actually, however, the measurements are subject to certain errors dependent on the color, which will be discussed later in the text. Naturally, the figure log ρ = 0.4 is arbitrary and was selected as a simple number for reasons of convenience. With their aid, the transition from stellar magnitudes to brightness ratios and vice versa mathematically proceeds as follows:

$$\frac{J_n}{J_{n_1}} = \operatorname{Num}\log[(n_1 - n)\,0{,}4] \qquad \text{and} \qquad n_1 - n = \frac{\log J_n - \log J_{n_1}}{0{,}4}. \tag{27}$$

The stellar magnitude can be given by eq.(27) with any desired accuracy, i.e., to an arbitrary number of significant figures, as they have become necessary because of the sharpness of modern photometric measurements. Conversion from magnitude differences to brightness ratios is facilitated by a table given in the Appenxix (Table I).

Equation (27) also permits any extension of the magnitude scale not only toward faint stars but also toward bright stars which now no longer, as had /18
been done originally, are designated merely as being of the first magnitude but, beyond zero, may also have negative size classes.

12. Systematic Errors of Visual Photometry, due to Color of the Stars

As mentioned already in Section 8, the differing sensitivity of the eye for

different colors must lead to errors in photometry, whenever the compared stars are not identical in color. These errors are especially pronounced in fainter stars and, in addition, are entirely individual since they depend on the color training of the eye. In fact, the various brightness catalogs of stars show systematic deviations, and an absolute brightness system for stars does not exist and, strictly taken, cannot exist. Nevertheless, any system extended by one and the same observer over a large number of stars of all spectral classes can be used as a standard system, and any similar system can then be reduced to the former system by systematic corrections for the stars of different spectral classes. The best known standard brightness systems at present are predominantly those of the Potsdam Photometric Durchmusterung and the Harvard Photometry. The former catalog comprises 14,200 stars of the Northern Hemisphere up to magnitude 7.5 while the latter catalog, covering the entire sky, contains 45,792 stars. A careful comparison of the brightnesses of the stars common to both catalogs, after subdividing them into groups by color and brightness, enabled the authors of the former of the above catalogs to derive a system of corrections known as "Potsd. Durchm. - Harv. Photom." which will be reproduced here. It is of some importance to state that the Potsdam observers differentiated 14 gradations of stellar color, ranging between white and red. Table 4 gives a compilation of these gradations, together with another frequently used stellar color system developed by Osthoff (Ref.44) who introduced a ten-step scale with subdivisions to one tenth for the colors of stars. The correction table combines the 14 Potsdam groups into four main groups.

TABLE 4

Color		Brightness of Stars	Potsdam — Harvard-Photometry				
Potsdam	Osthoff		W	GW	WG	G	All
W	2.4	$2^m.00 - 2^m.49$	+0.23	+0.20	+0.12	+0.07	+0.16
W+	2.5	2 .50 − 2 .99	+0.24	+0.21	+0.12	+0.05	+0.16
GW−	2.8	3 .00 − 3 .49	+0.25	+0.22	+0.11	+0.04	+0.16
GW	3.3	3 .50 − 3 .99	+0.27	+0.23	+0.11	+0.03	+0.16
GW+	3.8	4 .00 − 4 .49	+0.28	+0.23	+0.10	+0.02	+0.16
WG−	4.1	4 .50 − 4 .99	+0.29	+0.24	+0.10	+0.01	+0.16
WG	5.2	5 .00 − 5 .49	+0.30	+0.25	+0.10	−0.01	+0.16
WG+	5.5	5 .50 − 5 .99	+0.31	+0.26	+0.09	−0.02	+0.16
G−	6.1	6 .00 − 6 .49	+0.33	+0.27	+0.09	−0.03	+0.16
G	6.4	6 .50 − 6 .99	+0.34	+0.27	+0.09	−0.04	+0.16
G+	6.5	7 .00 − 7 .49	+0.35	+0.28	+0.08	−0.05	+0.16
RG−	6.7	7 .50 − 7 .99	+0.36	+0.29	+0.08	−0.07	+0.16
RG	6.9	8 .00 − 8 .49	+0.37	+0.30	+0.07	−0.08	+0.16
GR	8.8						

13. Compensation of Photometric Observations

The accuracy not only of the brightness estimates but also of the photometric measurements which, in the final analysis, reduces to estimating the equality of two light impressions, is subject to the Fechner law /19

$$E = c \log J + C,$$

according to which it is not the intensities themselves that are perceived but

their logarithms. This must be taken into consideration in balancing a series of observations whenever it is a question of determining the most probable brightness value. Let J_1, J_2, ..., J_n be the measured or estimated objective brightnesses to which the sensation intensities E_1, E_2, ..., E_n correspond, while the most probable values will be J and E. Then, the following equations are valid:

$$E_1 = c \log J_1 + C,$$
$$E = c \log J + C$$

or

$$E_1 - E = c \log \frac{J_1}{J}.$$

Similarly, we have

$$E_2 - E = c \log \frac{J_2}{J},$$
$$\cdots\cdots\cdots$$
$$E_n - E = c \log \frac{J_n}{J}.$$

Considering the quantities $E_1 - E$, $E_2 - E$, ..., $E_n - E$ as observation errors and basing the compensation on the Gauss error function, the sum of the mean-square errors must become a minimum, leading to the equation

$$\left(\log \frac{J_1}{J}\right)^2 + \left(\log \frac{J_2}{J}\right)^2 + \cdots + \left(\log \frac{J_n}{J}\right)^2 = \text{minimum.}$$

For determining the most probable brightness value J, this furnishes the equation

$$\log \frac{J_1}{J} + \log \frac{J_2}{J} + \cdots + \log \frac{J_n}{J} = 0$$

or

$$\log J = \frac{\log J_1 + \log J_2 + \cdots + \log J_n}{n}.$$

Consequently, in such compensations, the logarithms rather than the brightnesses themselves must be used as basis for the calculation, because of the fact that only the errors of the sensation factors or the brightness logarithms proportional to them have equal statistical weight.

Of course, an application of the Gauss error function presupposes that the quantities $E_n - E$ are pure observation errors, i.e., are due to imperfections of the human eye, whereas they actually are also influenced by external factors such as flicker of the images and variable transparency of the air during astronomic measurements. Seeliger (Ref.45) found that, if such external error sources predominate, a different compensation formula may be preferable.

14. Illumination Problems; Illumination of a Plane Area by a Luminous Point

We will now treat problems of the photometric calculus, of importance in

astronomy. Since the stars and planets, in most such problems, can be conceived as luminous points, it is suggested to treat this simple case of illumination problems separately.

As basis, we will use eqs.(19) - (22) and the definitions given in Section 6. /20

If the luminous point is at a finite distance from the area, the vertical distance between area and point will be denoted by c and the area itself will be decomposed into elements ds to which eq.(19) can be applied, i.e., for which the distance r and the angle of incidence of the light i have a definite value. The elementary quantities of light dQ must then be summed for all elements of the area, in which case the intensity J - since it is the same for a given luminous point in all directions - remains constant:

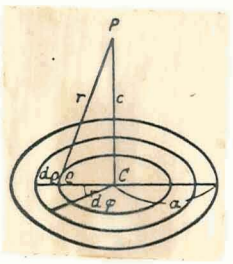

Fig.5 Illumination of a Circular Disk.

$$Q = J\int \frac{\cos i\, ds}{r^2},$$

where the integral must be extended over all elements of the area.

If the boundary of the area is a circle and if the luminous point is located perpendicularly above its center, then calculation of the integral is very simple. The area is resolved by polar coordinates into elements $ds = \rho d\varphi d\rho$ or, still simpler, into circular rings $2\pi\rho d\rho$ since r and i have the same value on all elements of such a circular ring. The total quantity of light, falling on the circular area of radius a, is then determined by a simple integral

$$Q = 2\pi J\int_0^a \frac{\varrho\, d\varrho \cos i}{r^2} = 2\pi J\int_0^a \frac{c\varrho\, d\varrho}{(\varrho^2 + c^2)^{\frac{3}{2}}} = 2\pi J\left\{1 - \frac{c}{\sqrt{a^2 + c^2}}\right\}. \qquad (28)$$

If the radius a is conceived as infinitely large, $Q = 2\pi J$ will be obtained. This is the quantity of light emitted by the luminous point toward one of the hemispheres.

15. Illumination of an Arbitrary Closed Area

Let us use here an equation for the elementary quantity of light, resulting from the fundamental equation (19) if a perpendicular is dropped from the radiant point P on the plane of an elementary area ds, denoted by p, is introduced. Then $p = r \cos i$, where r denotes the distance of the point P from ds while the elementary quantity of light is

$$dQ = J\, ds\, \frac{p}{r^3}. \qquad (29)$$

Let us imagine the closed area as being convex everywhere. If, from the radiant

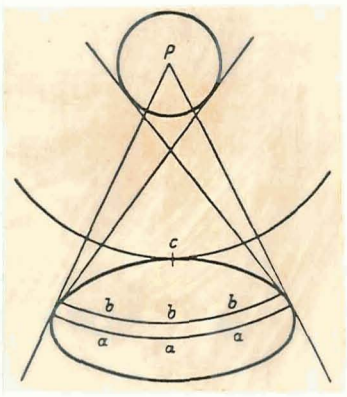

Fig.6 Illumination of a Closed Surface.

point, a tangent cone is drawn to the area, then a tangent curve aaa will be produced on this area which separates the illuminated from the shadowed portion. Describing a sphere about the radiant point P and laying all common tangential planes to this sphere and area, a conoidal enveloping surface will be formed whose tangent curve bbb with the area has the property that p will have the same value for all points on this surface, equal to the radius of the auxiliary sphere about P. The larger this radius is assumed, the shorter will be the tangent curves bbb until, as soon as the sphere osculates the area, they will coalesce into one point c. This is the point of strongest illumination which is also known as the "brilliant" point of the area. For this point, p reaches its maximum value while r becomes a minimum. If planes are laid through P and c, these will intersect the area along so-called illumination meridians on which the illumination decreases steadily from the point c. The intercepts of the area, perpendicular to Pc, are denoted as illumination parallels. On interconnecting the points of the area at which the illumination is the same, so-called isophots are obtained. It is easy to demonstrate that, if the area under consideration is a sphere, these isophots will coincide with the illumination parallels. This is so, even if the radiant point is located on the axis of rotation of a surface of revolution. /21

In calculating the total quantity of light coming from a luminous point and incident on a given area, it is only necessary to know the solid angle under which the area appears from the point P. This angle is measured by the area segment of a sphere of radius 1, cut out of the sphere starting from the tangent cone.

If the area is a sphere or a surface of revolution whose axis goes through the luminous point, then the tangent cone will be a right circular cone and the area segment which measures the solid angle will be a calotte on the sphere of radius 1. In the case of a sphere of radius a and distance c between the center and the luminous point, the area of the calotte becomes equal to the expression $2\pi\left\{1 - \frac{\sqrt{c^2 - a^2}}{c}\right\}$. Thus, the quantity of light incident on the sphere will be

$$2\pi J\left\{1 - \frac{\sqrt{c^2 - a^2}}{c}\right\}. \tag{30}$$

If the distance of the luminous point from the area is so large that it can be considered as equal for all its elements (r = const), then the elementary quantity of light, on introducing the symbol J_r for $J:r^2$, will become

$$dq = J_r\, ds \cos i, \tag{31}$$

where J_r thus denotes the intensity at a distance r. The enveloping cone is then transformed into a tangent cylinder whose axis lies in direction of the

rays. The equation of the isophots is now obtained from the condition that, for these, cos i = const. If the equation of the area is F(x, y, z) = 0 and if α, β, γ denote the angles of the incident rays made with the coordinate axes, then cos i - which is the cosine of the angle of the normal to the area made with the direction of the rays - is given for the isophots by the equation

$$\cos i = \frac{\frac{\partial F}{\partial x}\cos\alpha + \frac{\partial F}{\partial y}\cos\beta + \frac{\partial F}{\partial z}\cos\gamma}{\sqrt{\left(\frac{\partial F}{\partial x}\right)^2 + \left(\frac{\partial F}{\partial y}\right)^2 + \left(\frac{\partial F}{\partial z}\right)^2}} = \text{const}, \tag{32}$$

and this equation becomes the equation of the isophots.

For the sphere, the illumination limit is the great circle perpendicular to the direction of illumination, while the isophots are circles parallel to the great circles. In addition, the illumination at each point of the sphere is proportional to the sine of the width, counted as equator from the above illumination limit.

16. The Lambert Emanation Law

Equations (21) and (22), taken from the theory of radiation, constitute the basis for treating the problems of luminous areas. The equation for the quantity of light coming from the luminous area σ and striking the area s

$$Q = \frac{h\sigma s \cos\varepsilon \cos i}{r^2}$$

is based on the Lambert emanation law. This law follows for the so-called black body from its definition. However, the law also is valid in first approximation for any opaque incandescent body, which will be substantiated here by a proof because of the importance of this law for our problems. /22

Lambert himself (Ref.46) believed that his law was proved, among others, by the fact that the sun possesses uniform brightness. In reality, this is not so; the error can be ascribed to the fact that Lambert made no measurements on the light distribution over the solar disk or over any other self-luminous bodies such as incandescent plates or spheres. Nevertheless, the Lambert law is correct in its essential points. To furnish a proof of this law became possible only after Fourier's concept on the nature of emanation had been applied, according to which emanation takes place not only from the surface but also from a certain depth below this surface. As demonstrated by Zöllner (Ref.47), earlier attempts to prove the validity of the Lambert law, including the attempt by Lambert himself

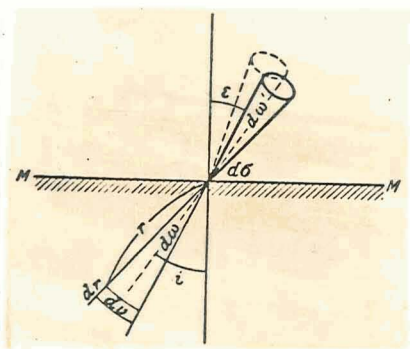

Fig.7 The Lambert Law for Self-Luminous Bodies.

as well as those by Beer and Rheinauer (Ref.48, 49), were inadequate. Zöllner was the first to use the Fourier concept for his proof, which was done also by other physicists such as Lommel (Ref.50). Even these proofs lack complete strictness in so far as they do not allow for the refraction of radiation at the periphery of the luminous body. If this is done, a minor deviation from Lambert's formula is obtained in astronomical practice; nevertheless, because of its basic interest, we will briefly discuss this deviation according to Smoluchowski de Smolan (Ref.51). The strict formula has the advantage of allowing also for the partial polarization of radiation, detected by actual observation.

Let us imagine the body as having a plane boundary and let us consider an element of area $d\sigma$ of the boundary surface MM as the vertex of the solid angle $d\omega$, extending under an angle i to the normal into the interior of the radiating body. Let us consider the radiation of an element of volume dv within this solid angle, at a distance r from $d\sigma$. Let dv be an element of the solid angle between the radii r and r + dr, and thus $dv = r^2 d\omega dr$. The luminosity of the body, which is supposed as equally large in all its parts, is assumed as equal to J_0 in all directions. Consequently, $J_0 dv$ is the quantity of light radiated by dv into the solid angle 1; thus, the quantity of light reaching the element $d\sigma$ from dv will be

$$q = \frac{J_0 dv\, d\sigma \cos i}{r^2} = J_0\, d\sigma \cos i\, dr\, d\omega,$$

provided that no absorption takes place along the path r. The reduction in quantity of light due to absorption over the path dr, is proportional to the original quantity of light q and to the segment dr, so that /23

$$dq = -kq\,dr$$

and, after integration over the entire segment r up to the surface,

$$\ln \frac{q_0}{q} = -kr; \qquad q_0 = qe^{-kr}.$$

Here, k is the absorption coefficient of the medium and q_0 the quantity of light reaching the surface. If the value of q is substituted into the last of the above equations, we obtain

$$q_0 = J_0\, d\omega\, d\sigma \cos i\, e^{-kr} dr.$$

From all elements of volume within the solid angle, the surface will receive the quantity of light obtained on integrating this expression from r = 0 to a distance r = ρ from which no more light will reach the surface:

$$Q = J_0\, d\omega\, d\sigma \cos i \int_0^{\rho} e^{-kr} dr = \frac{J_0}{k}\, d\sigma \cos i\, d\omega\, (1 - e^{-k\rho}). \qquad (33)$$

Since $e^{-k\rho}$ must be vanishingly small if the body is opaque, the following relation is obtained for such a body:

$$Q = \frac{J_0}{k} d\sigma \cos i \, d\omega . \tag{34}$$

If the refraction of rays on the surface can be neglected, the same energy flux will leave the element $d\sigma$ and reach the solid angle $d\omega$. Then, $i = \varepsilon$, and the Lambert emanation law will be obtained in the form

$$Q = J d\sigma \cos\varepsilon \, d\omega , \tag{35}$$

where we set

$$\frac{J_0}{k} = J .$$

In the case of vertical emanation ($\varepsilon = 0$), we would have $Q_0 = J d\sigma d\omega$ and

$$\frac{Q}{Q_0} = \cos\varepsilon .$$

Conversely, if the incandescent body is partly transparent, the integration must be carried out to the lower boundary. Imagining this body as bounded on both sides by parallel planes whose vertical distance is denoted by H, then $\rho = \frac{H}{\cos\varepsilon}$, which yields - assuming that $i = \varepsilon$ -

$$Q = \frac{J_0}{k} d\sigma \cos\varepsilon \, d\omega \left(1 - e^{-\frac{kH}{\cos\varepsilon}}\right), \tag{35'}$$

and also

$$Q_0 = \frac{J_0}{k} d\sigma \, d\omega \, (1 - e^{-kH})$$

so that

$$\frac{Q}{Q_0} = \cos\varepsilon \frac{1 - e^{-\frac{kH}{\cos\varepsilon}}}{1 - e^{-kH}} . \tag{36}$$

For $\varepsilon = 0^\circ$ and $\varepsilon = 90^\circ$, this expression becomes equal to 1 resp. 0, meaning that it will coincide with the Lambert law; however, for intermediate values, the expression shows deviations that are dependent on the product kH.

To investigate the case of a noticeable refraction and reflection of the /24 rays on emergence from the surface of the body, it is necessary to formulate a lemma on the refraction of a solid angle.

In Fig.7, we consider MM as the limit of two media I and II with the absolute refractive index n_1 and n_2. The radiation in the solid angle $d\omega$ with the inclination angle i to the normal, enters the solid angle $d\omega'$ with the inclination angle ε to the normal, into the upper medium. Then, according to Snellius' law, we have

$$n_1 \sin i = n_2 \sin\varepsilon . \tag{37}$$

The size of the solid angle is expressed in spherical coordinates by zenith distance and azimuth (A_1 and A_2) on the unit sphere so that

$$d\omega = \sin i\, dA_1\, di, \qquad d\omega' = \sin\varepsilon\, dA_2\, d\varepsilon.$$

Since, however, $A_1 = A_2$ and $dA_1 = dA_2$, it follows that

$$\frac{d\omega}{d\omega'} = \frac{\sin i\, di}{\sin\varepsilon\, d\varepsilon} = \frac{n_2}{n_1}\frac{di}{d\varepsilon}.$$

Differentiating eq.(37) will yield

$$n_1 \cos i\, di = n_2 \cos\varepsilon\, d\varepsilon$$

and thus

$$\frac{di}{d\varepsilon} = \frac{n_2 \cos\varepsilon}{n_1 \cos i},$$
$$\frac{d\omega}{d\omega'} = \left(\frac{n_2}{n_1}\right)^2 \frac{\cos\varepsilon}{\cos i}. \tag{38}$$

Consequently, we are assuming that the radiation, on its emergence from an opaque body, is refracted in $d\sigma$; then, the radiation is attenuated by reflection according to Fresnel's formula, at the following ratio:

$$p = 1 - \frac{1}{2}\left[\frac{\sin^2(i-\varepsilon)}{\sin^2(i+\varepsilon)} + \frac{\tan^2(i-\varepsilon)}{\tan^2(i+\varepsilon)}\right].$$

Therefore, the emerging energy flux will be

$$Q = p\frac{J_0}{k}\, d\sigma \cos i\, d\omega.$$

Substituting $d\omega$ by its expression [eq.(38)] yields

$$Q = p\frac{J_0}{k}\left(\frac{n_2}{n_1}\right)^2 d\omega'\, d\sigma \cos\varepsilon. \tag{34'}$$

Thus, the ratio $\frac{J_0}{k}$ which, in the simple Lambert law, represents the constant luminance of the surface or the constant area brightness of the luminous body, is replaced by the quantity

$$p\frac{J_0}{k}\cdot\frac{n_2^2}{n_1^2}$$

which no longer is constant since it varies with p and thus is dependent on i and ε. Therefore, the Lambert law is no longer strictly valid here. In addition, eq.(34') contains the Kirchhoff-Clausius theorem which expresses that the emissivity of a body I is proportional to the square of the refractive index of the medium II in which this body is located.

Because of the refraction, the obliquely radiated light must be partly /25

polarized. This had been found already by Arago as well as by Provostaye and Dessains; Magnus recognized refraction as being the basic cause. For partly transparent bodies, eqs.(34′) and (35′) are supplemented by the factor $(1 - e^{-kH\sec\varepsilon})$. This formula has been experimentally checked by various authors. For gases with a refractive index differing little from 1, the term $p\frac{n_2^2}{n_1^2}$ becomes almost equal to 1, and eq.(35′) - which is valid in this case - has been satisfactorily confirmed in experiments by Lummer and Reiche, Gross (Ref.52, 53) and others. In incandescent solid bodies such as quartz or metal plates, incandescent wires, etc., the deviations from the simple Lambert form [eq.(35)] in the sense of eq.(34′) are thus due to reflection and refraction. Consequently, the simple Lambert law [eq.(35)] must be considered as a limiting law which is strictly valid only for black radiation. Of the extensive literature on this subject, let us mention the theoretical papers by H.v.Helmholtz, Uljanin, and F.Jentzsch (Ref.53a, b, c). A complete survey over experimental work in this field was given by H.Cohn in his article on photometry in the Müller-Pouillet Textbook of Physics, Vol.II, 1929.

Since, in the astronomic applications of the emanation law of luminous bodies, only opaque radiators are in question, we will use this law in Lambert's form

$$Q = J d\sigma \cos\varepsilon d\omega,$$

where J denotes the luminance of the surface which, at strict validity of the Lambert law, must be a constant while it must vary with the emission angle in the case of deviations from this law.

17. Illumination Density and Brightness of the Luminous Element

If the quantity of light transferred from the element $d\sigma$ to an element ds of another body is to be determined, then the solid angle $d\omega$ must be replaced by the expression $ds \cos i/r^2$ since, at an angle of incidence i and a distance r, this represents the solid angle under which ds appears from $d\sigma$. This will yield

$$Q = J\frac{d\sigma\, ds \cos\varepsilon \cos i}{r^2}.$$

The illumination of the element ds is

$$L = J\frac{d\sigma \cos\varepsilon \cos i}{r^2}.$$

Setting here $i = 0$, the light will strike the surface vertically; this quantity of light $D = \frac{Jd\sigma \cos\varepsilon}{r^2}$, coming from the element $d\sigma$ and perpendicularly incident on unit area, is known also as illumination density. Replacing r by unit distance, the quantity of light $Jd\sigma \cos\varepsilon$ perpendicularly ariving from $d\sigma$ on the unit area at a distance 1 is obtained, which also is known as the quantity of

light emitted under the angle ε.

If the illuminated element ds is imagined as replaced by the human eye and if the effect of $d\sigma$ on the eye is taken as unit, then one speaks of the brightness of the luminous element, with a differentiation being made between real and apparent brightness. The former is equal to the illumination at vertical incidence, divided by the size of the element $d\sigma$, i.e., /26

$$H = \frac{D}{d\sigma} = J\frac{1}{r^2}\cos\varepsilon. \tag{39}$$

Conversely, the apparent brightness is equal to the illumination density, divided by the apparent size of the element $d\sigma$ which is equal to $\frac{d\sigma \cos \varepsilon}{r^2}$, i.e.,

$$h = \frac{Dr^2}{d\sigma\cos\varepsilon} = J. \tag{40}$$

For a luminous body obeying the Lambert law, the apparent surface brightness is the same at all points, independent of the body form, and is equal to the luminance. This means that it is also independent of the distance from the luminous body. The same definition of apparent surface brightness holds for illuminated bodies. If df denotes the reflecting area element, $\Gamma f(i, \varepsilon)$ the law of reflection, and $D = \frac{\Gamma f(i, \varepsilon)df}{r^2}$ the quantity of light perpendicularly reflected by unit area at a distance r, then the apparent brightness or the surface brightness of the element df

$$h = \frac{D}{d\omega} = \Gamma f(i,\varepsilon)\sec\varepsilon$$

will also be independent of the distance of the illuminated body.

18. Some Problems in the Illumination of Areas by Areas

If the quantity of light transmitted from a luminous body to an element of area ds is to be calculated, then the formula

$$dQ = \frac{J d\sigma\, ds\cos\varepsilon}{r^2}$$

must be summed over all elements $d\sigma$ of the body that are able to transmit light to ds, i.e., over all elements bounded by the tangent line to the tangent cone laid to the body from ds:

$$Q = ds\sum J\frac{d\sigma\cos\varepsilon}{r^2} = ds\int J\frac{d\sigma}{r^2}\cos\varepsilon. \tag{41}$$

At strict validity of the Lambert law, i.e., when the luminance of all elements

is the same, J can be moved in front of the summation or integral sign:

$$Q = J ds \int \frac{d\sigma \cos \varepsilon}{r^2}. \tag{42}$$

Since now $d\sigma \cos \varepsilon / r^2$ is equal to $d\omega$, which is the solid angle under which the element $d\sigma$ appears, we can also write

$$Q = ds \int J d\omega$$

and, at J = const,

$$Q = J ds \int d\omega = J ds \omega. \tag{43}$$

Consequently, the luminous area can be replaced by an area cut out by the tangent cone from the sphere of radius 1. Each point of this sector will then have the luminance of the corresponding element of the luminous body, and all points will have the same luminance.

1) Anding's theorem. Anding used the above lemma for drawing an important conclusion: "In all luminous areas that have a center, the illumination problem is reduced to determining the quantity of light transmitted by the pertaining area to a horizontal element, if the center of the area is vertically above this element." Let F be the luminous area with the center C and let df be the illuminated horizontal element. If, on the auxiliary sphere, $d\omega$ is the apparent size of an element dF and if, furthermore, M is the projection of the center and Z the projection of the zenith, then ZM will be the zenith distance z of the center and $Zd\omega$ will be the angle of incidence i. If the side $Md\omega$ is denoted by v and the angle between the sides v and z by φ, we obtain

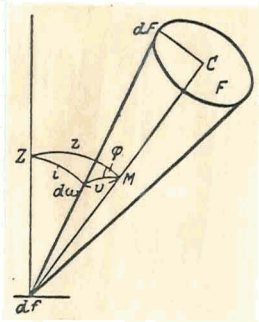

Fig.8 Anding's Theorem.

$$\cos i = \cos z \cos v + \sin z \sin v \cos \varphi.$$

The quantity of light, transferred from dF to df, is

$$dQ = J df \cos i d\omega$$

or, after substituting the value of cos i,

$$dQ = (J df \cos z \cos v + J df \sin z \sin v \cos \varphi) d\omega.$$

At a given center area, a second one exists for each element dF for which v has the same value while φ is transformed into the value $\varphi + \pi$. Therefore, on integrating over all elements dF, the second term is eliminated, yielding

$$Q = J df \int \cos z \cos v d\omega,$$

for the total quantity of light; since cos z is constant, we have

$$Q = J df \cos z \int \cos v d\omega.$$

It follows from this that the quantity of light thrown by a central area on a horizontal element is always proportional to the cosine of the zenith distance of the center. Until now, we had assumed equal luminance of the elements; however, the theorem is valid also if equal luminance corresponds to the elements v, φ and v, $\varphi + \pi$, in view of the fact that the second integral vanishes also in this case. Then, the total quantity of light becomes

$$Q = df \cos z \int J \cos v \, d\omega . \tag{44}$$

According to Anding's theorem, the illumination by a central area can thus be calculated simply for the case that the body is at the zenith, z = 0. However, in this case - since v = i - the integral of eq.(44) becomes equal to $\int J \cos i d\omega$. If a tangential plane is assumed as laid to the surface of the unit sphere at the zenith, then cos $id\omega$ becomes the projection of $d\omega$ onto this plane. Thus, the luminous area is replaced by its projection onto its tangential plane at the zenith, for example a sphere by a circle. If the sphere has the apparent radius s, then the radius of the circle will be sin s and the quantity of light, transmitted from a uniformly bright sphere to the element of area, will become simply proportional to the area of the circle:

$$Q = J df \pi \sin^2 s . \tag{45}$$

If the sphere is not at the zenith and if its center has the zenith distance z, then

$$Q = J df \pi \sin^2 s \cos z . \tag{46}$$

Similarly, the quantity of light of a uniformly bright ellipsoid, with the apparent semiaxes s_1 and s_2, will be found as /28

$$Q = J df \pi \sin s_1 \sin s_2 \cos z .$$

2) A quantity of light Q is to be calculated, coming from the sun and striking a horizontal element of area ds at the zenith distance z.

The intensity distribution over the sun, according to Emden (Ref.54) is assumed as

$$J = J_0 \tfrac{2}{5}(1 + \tfrac{3}{2} \cos i) . \tag{47}$$

Here, J_0 is the luminance of the center of the sun and i is the angle of reflection of the rays determined by the equation sin i = r:R, where R denotes the solar radius and r the distance from the solar center, assumed as expressed in radians. Let us shift the sun into the zenith and project it onto the tangential plane. This will give the sun as a circular disk which can be cut into rings $2\pi r dr$ of equal brightness decreasing toward the periphery. The quantity of light of the total disk will then become

$$Q_0 = 2\pi ds \int_0^R J r \, dr = \frac{4\pi J_0 ds}{5} \int_0^R \left(1 + \frac{3}{2}\sqrt{1 - \frac{r^2}{R^2}}\right) r \, dr .$$

After carrying out the integration, this yields

$$Q_0 = \tfrac{4}{5}\pi J_0 R^2 ds .$$

Consequently, at the zenith distance z, we obtain

$$Q = \tfrac{4}{5}\pi J_0 R^2 \cos z\, ds . \tag{48}$$

3) The quantity of light emanating from a partially eclipsed circular luminous disk of radius 1 (sun, star) having a limb darkening of

$$F(r) = A(1 + \mu \cos i) = A\left(1 + \mu\sqrt{1 - r^2}\right) \tag{49}$$

is to be calculated if the eclipse is produced by a circular disk of radius R.

The sought quantity of light, at $\mu = \frac{3}{2}$ (see previous problem) and at R equal to the lunar radius, corresponds to the illumination during solar eclipses since the above value of the constant μ corresponds to the limb darkening of the sun, according to visual measurements. At other values of μ, the formula is approximately valid also for different separate spectral regions, as demonstrated by Witting (Ref.55). So long as no accurate data are available on the limb darkening of stars of other spectral classes, this formula can be used as approximation also in this case.

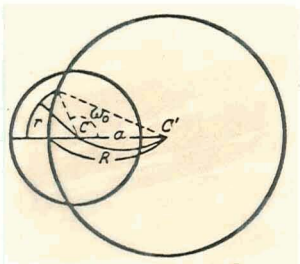

Fig.9 Eclipse of a Star.

Let us introduce polar coordinates (r, ω), with the origin at the center of the eclipsed disk, and let us calculate the angles ω from the connecting line between the centers of both disks. Let the center-to-center distance be a. Then, the sought quantity of light will be

$$Q = 2\int_{R-a}^{1} dr \int_{\omega_0}^{\pi} rF(r)\, d\omega = 2A\int_{R-a}^{1} dr \int_{\arccos\frac{r^2+a^2-R^2}{2ar}}^{\pi} r\left(1 + \mu\sqrt{1 - r^2}\right) dr\, d\omega , \tag{50}$$

where ω_0 represents the limiting value of ω corresponding to a certain r. On integrating to ω, we obtain /29

$$\begin{aligned} Q &= 2\pi\int_{R-a}^{1} rF(r)\, dr - 2\int_{R-a}^{1} rF(r) \arccos\frac{r^2 + a^2 - R^2}{2ar}\, dr \\ &= 2A\pi\int_{R-a}^{1} r\, dr + 2A\pi\mu\int_{R-a}^{1} r\sqrt{1 - r^2}\, dr - 2A\int_{R-a}^{1} r\left(1 + \mu\sqrt{1 - r^2}\right) \arccos\frac{r^2 + a^2 - R^2}{2ar}\, dr \\ &= 2A\pi\left(\frac{1}{2} - \frac{(R-a)^2}{2} + \frac{\mu}{3}\left[1 - (R-a)^2\right]^{\frac{3}{2}}\right) - 2A\left[\int_{R-a}^{1} r \arccos\frac{r^2 + a^2 - R^2}{2ar}\, dr\right] \end{aligned}$$

$$+\mu\int_{R-a}^{1} r(1-r^2)^{\frac{1}{2}}\arccos\frac{r^2+a^2-R^2}{2ar}\,dr\Bigg]. \qquad \text{II}$$

The first of the remaining integrals, after partial integration, will yield

$$I=\frac{1}{2}\left[\left(\arccos\frac{1+a^2-R^2}{2a}-(R-a)^2\pi\right)+\int r\,dr\,\frac{r^2-a^2+R^2}{\sqrt{2a^2r^2+2a^2R^2+2r^2R^2-r^4-a^4-R^4}}\right].$$

Setting, in the last integral,

$$x=r^2-a^2-R^2,$$

this integral is transformed into

$$=\frac{1}{2}\int_{-2aR}^{1-a^2-R^2}\frac{x+2R^2}{\sqrt{4a^2R^2-x^2}}\,dx=\left\{-\frac{1}{2}(4a^2R^2-x^2)^{\frac{1}{2}}\Big|_{-2aR}^{1-a^2-R^2}+\frac{R}{2a}\int_{-2aR}^{1-a^2-R^2}\frac{dx}{\sqrt{1-\frac{x^2}{4a^2R^2}}}\right\}$$
$$=-\frac{1}{2}\sqrt{4a^2R^2-(1-a^2-R^2)^2}-R^2\left(\arccos\frac{1-a^2-R^2}{2aR}-\pi\right).$$

Hence,

$$-2AI=-A\left[\arccos\frac{1+a^2-R^2}{2a}-\pi(R-a)^2-\frac{1}{2}\sqrt{4a^2R^2-(1-a^2-R^2)^2}\right.$$
$$\left.-R^2\arccos\frac{1-a^2-R^2}{2aR}+\pi R^2\right].$$

The integral II is left unchanged. It is true that this integral can be reduced to a function of two elliptical integrals of the first and second kind; however, this will make the numerical evaluation more difficult than that of the original integral. We then have

$$\begin{aligned}
Q&=A\left\{\pi+\frac{2\pi\mu}{3}[1-(R-a)^2]^{\frac{3}{2}}-\arccos\frac{1+a^2-R^2}{2a}+R^2\arccos\frac{1-a^2-R^2}{2aR}\right.\\
&\left.+\frac{1}{2}\sqrt{4a^2R^2-(1-a^2-R^2)^2}-\pi R^2-2\mu\int_{R-a}^{1}r(1-r^2)^{\frac{1}{2}}\arccos\frac{r^2+a^2-R^2}{2ar}\,dr\right\}\\
&=A\left\{\pi(1-R^2)-\arccos\frac{1+a^2-R^2}{2a}\right.\\
&\quad+R^2\arccos\frac{1-a^2-R^2}{2aR}+\frac{1}{2}\sqrt{4a^2R^2-(1-a^2-R^2)^2}\\
&\left.\quad+2\mu\left[\frac{\pi}{3}(1-(R-a)^2)^{\frac{3}{2}}-\int_{R-a}^{1}r(1-r^2)^{\frac{1}{2}}\arccos\frac{r^2+a^2-R^2}{2ar}\,dr\right]\right\}.
\end{aligned}\qquad (51b)$$

This formula has been derived for the case of a < R. It is easy to demonstrate that nothing is changed at a > R except that the term before the last is reduced to the form $\frac{2A\mu\pi}{3}$. Consequently, the formula

/30

$$Q = A\left\{\pi(1-R^2) - \arccos\frac{1+a^2-R^2}{2a} + R^2\arccos\frac{1-a^2-R^2}{2aR} + \frac{1}{2}\sqrt{4a^2R^2-(1-a^2-R^2)^2} + 2\mu\left[\frac{\pi}{3} - \int_{a-R}^{1} r(1-r^2)^{\frac{1}{2}}\arccos\frac{r^2+a^2-R^2}{2ar}\,dr\right]\right\} \tag{51a}$$

is valid for the beginning of the eclipse, both at R > 1 and R < 1; at R > 1, the formula is valid to within a = R, after which eq.(51b) becomes applicable until total eclipse has taken place. At $1 > R > \frac{1}{2}$, eq.(51a) is also valid to a = R while eq.(51b) is valid only to a = 1 - R which is the instant of internal osculation, to which the following, similarly derived formula must be applied:

$$Q = A\left\{\pi(1-R^2) + 2\mu\left[\frac{\pi}{3}(1-(R-a)^2)^{\frac{3}{2}} - \int_{R-a}^{a+R} r(1-r^2)^{\frac{1}{2}}\arccos\frac{r^2+a^2-R^2}{2ar}\,dr\right]\right\}. \tag{51c}$$

Finally, at $R < \frac{1}{2}$, eq.(51a) is valid to a = 1 - R. From a = 1 - R to a = R, the following formula is applicable:

$$Q = A\left\{\pi(1-R^2) + 2\mu\left[\frac{\pi}{3} - \int_{a-R}^{a+R} r^2(1-r^2)^{\frac{1}{2}}\arccos\frac{r^2+a^2-R^2}{2ar}\,dr\right]\right\}, \tag{51d}$$

while, from a = R to a = 0, eq.(51c) is in force.

Thus the quantity of light, emanated by a partially eclipsed disk, is brought to the form

$$Q = A(c + \mu d), \tag{52}$$

where c and d are functions of the distance and of the diameter of the disks, while μ is the constant characteristic for the limb darkening. The same problem was solved by H.N.Russell and H.Shapley (Ref.56) by a graphical method. The formula used as basis in their tables is identical with our formula (49) if our constants A and μ are replaced by the Russell constants

$$x = \frac{\mu}{1+\mu} \quad \text{and} \quad J_0 = \frac{A}{1-x}.$$

Here, J_0 is the brightness at the center while x, located between 0 and 1, is the criterion of limb darkening. The tables by P.Harzer (Ref.57) refer to a

formula obtained from eq.(49) by adding a term with cos 2i.

19. Several Problems of Diffuse Reflection

Let us now treat several problems in which the illumination is not produced by self-luminous bodies but by illuminated bodies which diffusely reflect the light. The laws of diffuse reflection will be discussed in more detail in the next Chapter. In the problems given here, we will apply the simple Lambert law for diffuse reflection, according to which the quantity of light, reflected by an area element ds under an angle ε, is expressed by

$$dq = \frac{AL}{\pi} \cos i \cos \varepsilon \, ds, \tag{49}$$

where A is a constant which, for a white body, is equal to 1 while i denotes the angle of incidence and L the illumination. /31

1) A circular white disk of radius R is exposed to vertical illumination from a very great distance. An element of area ds is located on the normal to the center of the disk in the path of the incident rays. At what distance x from the disk does the illumination of the area ds by the direct rays become twice as large as the illumination by the reflection from the disk?

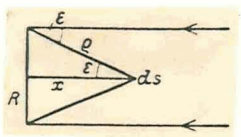

Fig.10 Reflection from a Wall to an Element of Area ds.

Let L be the illumination or the quantity of light falling on vertical unit area. Let the disk be imagined as cut into infinitely many narrow concentric rings struck by the quantities of light $2\pi L r dr$ and reflecting the quantities of light

$$2\pi L r dr \frac{A}{\pi} \cos \varepsilon \, d\omega = 2AL \cos \varepsilon \, r \frac{ds \cos \varepsilon}{\varrho^2} dr$$

on ds. Here, ρ is the distance of all elements of the ring from ds. Then, the total quantity of light, reflected on ds, will be

$$Q = 2AL \, ds \int_0^R \frac{\cos^2 \varepsilon}{\varrho^2} r \, dr.$$

Making use of the equations

$$\varrho \cos \varepsilon = x, \qquad d\varrho \cos \varepsilon = \varrho \sin \varepsilon \, d\varepsilon,$$
$$r = x \tan \varepsilon, \qquad dr = \frac{x}{\cos^2 \varepsilon} d\varepsilon,$$

for introducing ρ as the integration variable, we obtain

$$Q = 2ALds\,x^2 \int_x^{\sqrt{x^2+R^2}} \frac{d\varrho}{\varrho^3} = ALds\,x^2 \left(\frac{1}{\varrho^2}\right)_{\sqrt{x^2+R^2}}^{x} = ALds\left(1 - \frac{x^2}{x^2+R^2}\right).$$

The quantity of light, directly striking the other side of ds, is Lds. Consequently, setting A = 1, we obtain the following equation for x:

$$1 - \frac{x^2}{x^2+R^2} = \frac{1}{2},$$

from which it follows that x = R.

It is quite obvious that the illuminations can never become equal except for x = 0 and for R = ∞, in which case they also remain equal for all finite x.

2) Instead of for a circular disk, the above problem is to be solved for a parallel-irradiated sphere, with the difference that the fraction y of the direct illumination Lds at a distance R = 2ρ from the center of the sphere is sought (with ρ being the radius of the sphere).

For the reflection, only those elements of the sphere are in question that are bounded by the circle obtained as the tangent curve of the sphere to the tangent cone traced from ds. Let us subdivide the surface into zones $2\pi\rho^2 \sin i\, di$ which reflect the quantities of light

$$2\pi\varrho^2 \sin i\, di \frac{AL}{\pi} \cos i \cos\varepsilon\, d\omega = 2AL\varrho^2 \sin i \cos i \cos\varepsilon \frac{ds\cos(\varepsilon - i)}{r^2}$$

on ds. The total quantity of light, striking ds, will thus be

$$Q = 2AL\varrho^2 ds \int_0^{\arccos \varrho/R} \frac{\sin i \cos i \cos\varepsilon \cos(\varepsilon - i)}{r^2} di.$$

With the aid of the equations

/32

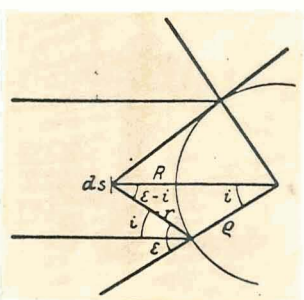

Fig.11 Reflection from a Sphere on an Element of Area ds in its Vicniity.

$$\cos i = \frac{R^2 + \varrho^2 - r^2}{2R\varrho}; \qquad \sin i\, di = \frac{r\, dr}{R\varrho};$$

$$\cos\varepsilon = \frac{R^2 - \varrho^2 - r^2}{2\varrho r};$$

$$\cos(\varepsilon - i) = \frac{R^2 - \varrho^2 + r^2}{2R\varrho}$$

we obtain

$$Q = \frac{AL\,ds}{4R^3\varrho} \int_{R-\varrho}^{\sqrt{R^2-\varrho^2}} \frac{[(R^2-\varrho^2)^2 - r^4][R^2 + \varrho^2 - r^2]}{r^3} dr.$$

After carrying out the equation, this yields

$$Q = \frac{AL}{4} ds \frac{\varrho^3}{R^3} \left\{ \frac{R^3}{\varrho^3} + \frac{R}{\varrho} + 2 - \left(\frac{R^2}{\varrho^2} - 1 \right)^2 \ln \sqrt{\frac{\frac{R}{\varrho} + 1}{\frac{R}{\varrho} - 1}} \right\},$$

and, if we set $\frac{\rho}{R} = x$,

$$Q = \frac{1}{4} ALds \left[1 + x^2 + 2x^3 - \frac{(1 - x^2)^2}{x} \ln \sqrt{\frac{1 + x}{1 - x}} \right].$$

Putting A = 1, the following equation is obtained for determining y:

$$\frac{Lds}{4} \left[1 + x^2 + 2x^3 - \frac{(1 - x^2)^2}{x} \ln \sqrt{\frac{1 + x}{1 - x}} \right] = yLds,$$

while, for $x = \frac{1}{2}$, we obtain

$$y = 0.283.$$

Consequently, the illumination in this case is much less than in the case of a reflecting disk. The increase in illumination up to a value Lds at the surface (x = 1) is considerably greater.

II. DIFFUSE REFLECTION

20. Lambert Formula and Lambert Albedo

Much more difficult than for the case of radiation of self-luminous bodies is the derivation of a theoretical formula for the quantity of light reflected from a dull surface. The laws of reflection are known only for smooth specular surfaces. For the problems of photometry of planets, comets, zodiacal light, and dark nebulae, however, the laws of the reflection from dull diffuse-reflecting bodies are of major importance. In pure physics, this problem is of no importance for the evaluation of the nature and consistency of given bodies and, in addition, had been little regarded because of its difficulty and the impossibility of ever obtaining generally valid laws. It is immediately obvious and confirmed in everyday experience that the quantity of light reflected by a dull body depends on its configuration. However, even in specially prepared dull substances with plane boundaries, the consistency of the dull surface, when viewed for example under a microscope, may be infinitely different and the amount of light reflected under various angles will depend on this consistency. Physics has available many other more effective methods for studying the nature of a given body. However, in astronomy, the amount of light reflected from the /33
illuminated comets, planets, etc. is one of the least accurately measurable quantities, but attempts to draw conclusions from this amount and from its variability at different illuminations as to the nature of the reflecting surface have actually been promising despite the lack of strict physical principles. Thus, it is understandable that the theory of diffuse reflection has mainly been

advanced from the astronomical side (Lambert, Zöllner, Seeliger).

The original formula for diffuse reflection was derived by Lambert (Ref.46, p.321ff) who greatly simplified his problem of determining the amount of light reflected from an illuminated dull surface with plane boundaries. Based on the observation that a wall, illuminated by the sun, appears as being of equal brightness from all viewing angles, he formulated the theorem that an illuminated dull surface behaves like a self-luminous surface, meaning that it reflects the light proportional to the cosine of the emanation angle. If ds denotes an element of the illuminated area on which a luminous flux is incident under the angle i and if L denotes the luminous flux on unit surface at vertical incidence, then the luminous flux striking ds will be Lds cos i. If the illuminated element now behaves like a self-luminous body, the quantity of light reflected by it under an angle ϵ will be

$$q = CL\cos i\cos\varepsilon\, ds,$$

where C is a proportionality factor, giving the fraction of the light reflected in vertical direction. Since the body absorbs a portion of the incident luminous flux, C < 1 is a constant determining the reflectivity. An element $d\omega$ of the hemisphere of radius 1, which we assume as being described about ds, will receive a luminous flux of

$$dQ = q\,d\omega = CL\,ds\cos i\cos\varepsilon\, d\omega,$$

meaning that the total hemisphere will receive the quantity of light Q = CLπds cos i [see the derivation of eq.(15) on p.7]. Since this luminous flux represents a certain portion A of the incident flux, we also have

$$Q = AL\,ds\cos i,$$

from which, by equating, we obtain

$$C = \frac{A}{\pi}. \tag{1}$$

The factor A, which indicates the portion of the incident luminous flux that is reflected into the solid angle π, is known as "albedo". This is always smaller than 1, since even for the whitest body a portion of the incident light will always be absorbed. Consequently, the Lambert formula can also be written in the form

$$q = \frac{A}{\pi} L\,ds\cos i\cos\varepsilon = \Gamma_1\cos i\cos\varepsilon\, ds, \tag{2}$$

where $\Gamma_1 = \frac{A}{\pi}$ L is a constant. This formula has no theoretical foundation but corresponds to observations on dull substances at least as well as other formulas to be discussed below, which are based on theoretical concepts as to the process of diffuse reflection.

21. Lommel-Seeliger Formula /34

Lommel (Ref.58), and after him Seeliger (Ref.59), started from the following

concept on the process of diffuse reflection: The light penetrates to a certain depth into the body during which time a certain portion is absorbed and then emerges again from the surface during which time it again undergoes absorption. In reality, the light suffers innumerous reflections on the molecules of the penetrated layer, and the attenuation of the light during its entire return trip is attributed to the light loss during reflection on the molecules. Lommel and Seeliger assumed that, as a result of these reflections, an element of volume dv scatters equal quantities of light in all directions, which undergo an attenuation (absorption) on their path within the substance, as in a homogeneous medium.

The surface of the dull body is assumed as having plane boundaries and the body itself is assumed as opaque; let dv be an element of volume within the body. The problem is to determine the amount of light emerging from the surface element of area ds under an angle ε to the normal if the angle of incidence of the light, assumed as being parallel, is i. Let L be the luminous flux incident on unit volume at the surface and let k be the absorption coefficient for the rays penetrating into the body. If dL denotes the variation of the luminous flux along the infinitely short path dx, then dL must be proportional to the luminous flux L, to the absorption coefficient k, and to the mean free path dx:

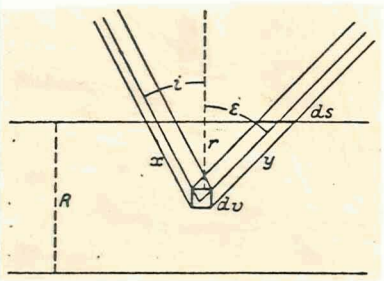

Fig.12 Reflection from the Interior of a Dull Plate.

$$dL = -kL\,dx.$$

From this, by integration from the surface to the distance x, the following expression is obtained for the quantity of light incident on dv:

$$L_x = Le^{-kx}dv.$$

If dv scatters a certain portion of the incident light, the diffusion coefficient will be denoted by μ; according to definition, this is the same for all directions, i.e., a constant, while the luminous flux in the direction ε to the normal is μL_x. On its return path y, this flux undergoes a second absorption which, according to Seeliger, will be characterized by another absorption coefficient k′. Thus, the following quantity of light reaches the surface from dv:

$$dq = \mu L_x e^{-k'y}dv = \mu L e^{-(kx+k'y)}dv,$$

or, since

$$x = r\sec i, \qquad y = r\sec\varepsilon \qquad \text{and} \qquad dv = dr\,ds,$$

$$dq = \mu L\,ds\,e^{-(k\sec i + k'\sec\varepsilon)r}dr.$$

To obtain the full luminous flux from the element ds, summation must be carried out over all elements dv up to a depth from which light just about can penetrate to the surface, i.e., from r = 0 to r = R where R denotes a depth below the surface for which $e^{-(kx+k'y)}$ becomes vanishingly small. Thus, we have /35

$$q = \mu L\, ds \int_0^R e^{-(k\sec i + k'\sec\varepsilon)r}\, dr$$

and, after carrying out the integration,

$$q = \mu L\, ds \frac{\cos i \cos\varepsilon}{k\cos\varepsilon + k'\cos i}\left[1 - e^{-R(k\sec i + k'\sec\varepsilon)}\right]. \tag{3}$$

The second term in parentheses is equal to zero for an opaque body, so that

$$q = \mu L\, ds \frac{\cos i \cos\varepsilon}{k\cos\varepsilon + k'\cos i}.$$

Setting also $\frac{k}{k'} = \lambda$ and $\frac{L\mu}{k'} = \Gamma_2$, we obtain

$$q = \Gamma_2\, ds \frac{\cos i \cos\varepsilon}{\cos i + \lambda\cos\varepsilon}. \tag{4}$$

The assumption of different absorption coefficients for the incident and reflected rays, according to modern concepts on the process of diffuse reflection, has no physical basis. If we actually have to do only with innumerous reflections of the light from molecule to molecule, which in their totality produce an attenuation (absorption) of the emitted light, then the Seeliger model does not constitute a picture of the true internal process. Different absorption coefficients for incident and reflected rays have their apparent reason in the experimental fact that colored powders show a lighter tint the finer they are ground. The light penetrates deeper into the surface layer of such powders the larger the pores between the individual grains. Thus, the selective absorption of light is greater the farther the light penetrates into the surface. On the return path of the rays from the depths to the surface, the light will already be colored and have undergone a less extensive loss by absorption. In this theory, diffraction phenomena which are the true cause of the coloration are disregarded and the grains of the powder are considered as diffusing particles. However, since according to modern concepts we have to do here with an intramolecular process, in which the reflections from molecule to molecule are connected with a slight and continuously varying absorption, the separation of the absorption coefficients into two different values seems unwarranted. Setting $k = k'$, the conventional form of the Seeliger equation will be obtained for the quantity of light emerging from the element ds:

$$q = \Gamma_2\, ds \frac{\cos i \cos\varepsilon}{\cos i + \cos\varepsilon}. \tag{5}$$

The apparent brightness of a dull substance with plane boundaries is $h_2 = \Gamma_2 \frac{\cos i}{\cos i + \cos\varepsilon}$ according to Seeliger and $h_1 = \Gamma_1 \cos i$ according to Lam-

bert. At vertical illumination, the value according to Seeliger will be $h_2 = \Gamma_2 \frac{1}{1 + \cos \varepsilon}$ and, according to Lambert, $h_1 = \Gamma_1$; at $\varepsilon = 0^\circ$ and $\varepsilon = 90^\circ$, the Seeliger values will be $h_2^0 = \frac{1}{2}\Gamma_2$ and $h_2^{90^\circ} = \Gamma_2$, i.e., the brightness according to Seeliger, in the vertical case, is half as large as in glancing illumination whereas, according to Lambert, the brightness depends exclusively on the angle of incidence and is independent of the emanation angle.

The Seeliger formula, also seen from the concept as to the process of diffuse reflection used here, can be considered only as a first approximation since the illumination of the element volume dv by the neighboring elements had been neglected in its derivation, which is not compatible with the concept of the diffusivity of each individual volume element. Each individual element of volume must be considered the center of a new light motion and thus must furnish a contribution to the illumination of the others. It is a priori obvious that the calculation of the effect of this mutual illumination of the elements leads to complex mathematical formulas. Lommel (Ref.28) rigorously followed his concepts and arrived at extremely complex expressions which he then attempted to simplify by introduction of empirical functions. The enormous mathematical apparatus used by Lommel for even approximately determining the effect of mutual interillumination of the volume elements is entirely unnecessary when opaque bodies are involved. /36

In an opaque body, the incident direct quantity of light near the surface will be much greater than the quantity due to self-illumination whereas, at a greater depth, both components may have the same order of magnitude. However, since from greater depths only a vanishing fraction of the total amount of light is able to reach the surface, it is obvious that the overall effect of diffusions of higher order cannot be very great. Therefore, it seems logical to calculate first the effect of reflections of second order. This is to mean the amount of light received by an element dv located at the interior from its neighboring elements, in which case it is assumed that these neighboring elements scatter only the directly received amount of light and that their illumination by the totality of the other elements is not taken into consideration.

The formula obtained from the Lommel concept, with this restriction, will be derived furthermore under consideration of the Rayleigh diffusion law. This law takes care of our concepts as to the light scattering on molecules in a more accurate manner than the assumption of uniform scattering in all directions. In other respects, however, the derivation is based on the same concepts as the Lommel theory.

Let us first discuss a special case of the simple Seeliger theory in which the body can be assumed as partly transparent. For such a body, the exponent $Rk(\sec i + \sec \varepsilon)$ can no longer be considered as large, and the second term in the parentheses in eq.(3) can no longer be assumed as vanishing. Thus, the following expression is obtained for the reflected quantity of light:

$$q = \Gamma_2 ds \frac{\cos i \cos \varepsilon}{\cos i + \cos \varepsilon} \left[1 - e^{-kR(\sec i + \sec \varepsilon)}\right]. \qquad (6)$$

In the case of a very small exponent, this expression, after expansion of the term in parentheses in a series and neglecting higher powers of the exponent, will assume the form

$$q = C ds,$$

where C is a constant.

The brightness of a body reflecting in this manner would be $h = \frac{C}{\cos \varepsilon}$ and thus would have to increase with increasing ε. A similar phenomenon can be observed on a dust-covered glass plate where the brightness actually increases at glancing observation. /37

For historical reasons, still another formula for diffuse reflection should be mentioned, known as the Euler formula since this mathematician had been most concerned with it; however, this formula possesses neither theoretical substantiation nor has it ever been even faintly confirmed by experiments. According to this formula, the quantity of light reflected by an element of area ds will be

$$q = \Gamma_3 \cos i \, ds, \qquad (7)$$

i.e., will be completely independent of the angle of reflection. According to this formula, the brightness of a plane plate, viewed under a large emanation angle, would have to increase and become infinitely great at glancing observation. In older astronomical papers, this formula has frequently been used for calculating the planetary brightness but will be abandoned by us.

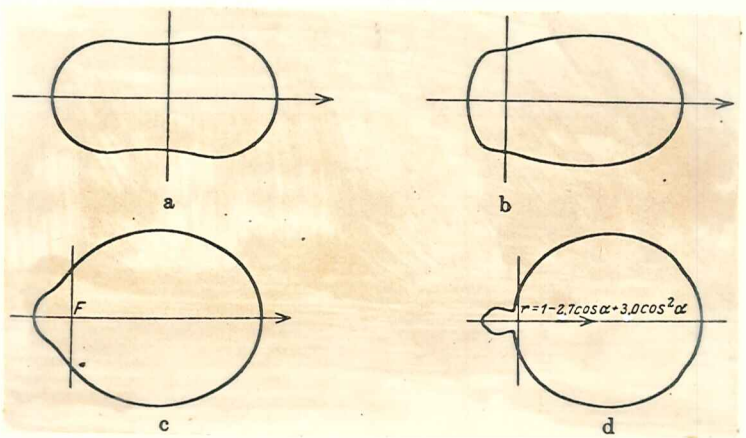

Fig.13 Diffusion Patterns.
a - According to Mie for infinitely small spheres;
b - According to Mie for gold spheres of 0.16 μ;
c - According to Senftleben for carbon particles of a gas flame; d - According to Schoenberg for water vapor spheres according to the formula $1 - 2.7 \cos \alpha + 3 \cos^2 \alpha$.

22. New Formula for Diffuse Reflection and its Special Cases: Fessenkov and Lommel Formulas

Lommel and Seeliger assumed that the internal diffusion of light takes place uniformly in all directions. However, Rayleigh (Ref.60), based on diffraction-theoretical considerations, was able to prove as early as 1871 that, in elements of volume that are smaller than $1/4\ \lambda$, the diffusion is dependent on the angle α between the incident and reflected ray and proceeds proportionally to $1 + \cos^2\alpha$. This result was confirmed by Kelvin and Schuster (Ref.61, 62). In 1908, Mie (Ref.63) investigated the case of coarser particles and, for small spheres of larger diameter, found widely differing diffusion patterns which were dependent on the material constant and on the size of the particles; these patterns all differed from the symmetrical Rayleigh pattern in that a much larger amount of radiation propagates in the direction of incident rays $\alpha = 180^\circ$ than in the opposite direction ($\alpha = 0^\circ$). The phenomenon occasionally is designated as /38 "Mie effect". This was mathematically investigated by H.Blumer (Ref.64), resulting in even more complex forms of which we show several in Fig.13. In practical experiments, the phenomenon was confirmed by various authors for the diffusion in air and by Senftleben and Benedikt for carbon particles of a gas flame, as shown in the diffusion pattern of Fig.13.

A satisfactory approximation to the general slope of these curves can be obtained by the function $1 - p\cos\alpha + q\cos^2\alpha$ with indeterminate coefficients p and q, whose special case, at $p = 0$ and $q = 1$, is the Rayleigh function. Consequently, if the diffusion, during penetration into a turbid medium, takes place on molecules and on relatively coarse particles, it is impermissible to assume a uniform scattering in all directions and a general diffusion theory would have to take the Mie effect into consideration.

Based on the above general formula, we will attempt to develop such a theory for an opaque body with plane boundaries, restricting the calculation to terms of the second order. This theory was developed during an investigation of the reflection of light on a cloud formation and was fully confirmed by measurements of the light distribution, as observed from high mountain tops above the clouds. A compact cloud cover, which can be assumed as opaque, offers ideal conditions for checking such a theory because of the fact that it is entirely certain here that the scattering particles are spheres of a definable size since a specular effect is excluded and since roughness of the boundaries and shadow-casting play only a subordinate role in view of the great transparency of the elevations.

Thus, we can assume that the scattering on the individual particles proceeds according to the formula

$$(1 - p\cos\alpha + q\cos^2\alpha).$$

Designating, as before, by L the amount of light incident on unit volume, by k the absorption coefficient of the light within the body, and by r and r′ the distance of the volume elements dv and dv′ from the upper boundary, it will be found that the element dv receives the quantity of light $Ldve^{-kr\sec i}$, so that the amount of light emerging from the body after reflection from dv and caused exclusively by dv will be

$$dq = \mu L dv e^{-kr(\sec i + \sec \varepsilon)}(1 - p\cos\alpha + q\cos^2\alpha), \tag{8}$$

where μ is a constant known as the diffusion coefficient. Let A_0 be the angle between the planes of the incident and the reflected ray, so that

$$\cos\alpha = \cos i \cos\varepsilon + \sin i \sin\varepsilon \cos A_0.$$

The quantity of light, emerging from the surface element of area $d\sigma$, is to be determined under consideration of reflections of the first order.

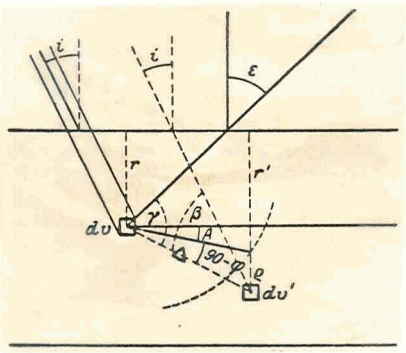

Fig.14 Internal Diffusion.

It is known that $dv = d\sigma dr$. Neglecting the illumination of dv by the neighboring elements and integrating eq.(8) between the limits of 0 and R, the following expression, as in eq.(3), is obtained for the emitted quantity of light:

$$q = \frac{\mu}{k} L d\sigma (1 - p\cos\alpha + q\cos^2\alpha)(1 - e^{-kR(\sec i + \sec\varepsilon)}) \frac{\cos i \cos\varepsilon}{\cos i + \cos\varepsilon},$$

which, for an opaque body ($R = \infty$), assumes the <u>/39</u> form

$$q = \frac{\mu}{k} L d\sigma (1 - p\cos\alpha + q\cos^2\alpha) \frac{\cos i \cos\varepsilon}{\cos i + \cos\varepsilon}. \tag{9}$$

This differs from the Seeliger formula [eq.(5)] only by the factor $(1 - p\cos\alpha + q\cos^2\alpha)$.

Let the cylindrical coordinates which determine the position of an element dv' with respect to dv, be $r - r' = \rho$, φ, and A. The meaning of these coordinates is shown in Fig.14; the azimuth A is counted from the plane of incidence of the light in dv. The element dv' directly receives the quantity of light $Ldv'e^{-kr'\sec i}$, of which the following quantity is reflected toward dv:

$$\mu L e^{-kr'\sec i}(1 - p\cos\beta + q\cos^2\beta)\frac{e^{-k\Delta}}{\Delta^2} dv\, dv',$$

where Δ is the spacing of the elements.

Consequently, of this portion the following amount of light will reach the surface:

$$\mu^2 L e^{-kr'\sec i - k\Delta - kr\sec\varepsilon} dv \frac{dv'}{\Delta^2}(1 - p\cos\beta + q\cos^2\beta)(1 - p\cos\gamma + q\cos^2\gamma),$$

where the meaning of the angles β and γ can be taken from Fig.14. After this, integration must be carried out over all dv' and over dv located in the direction of reflection, so as to obtain the total amount of diffusion of the second order. In this case, the elements dv' are assumed as only directly illuminated (quantity of light $Le^{-kr'\sec i}$), and their illumination by the neighboring elements is

neglected. Consequently, this means an integration of the last expression to four variables r, r′, φ, and A. The element of volume dv′, in our coordinates, reads

$$dv' = dr'(r'-r)\tan\varphi\, dA(r'-r)\sec^2\varphi\, d\varphi = (r'-r)^2\tan\varphi\sec^2\varphi\, d\varphi\, dA\, dr'.$$

If dv′ lies higher than dv, then

$$\Delta = (r-r')\sec\varphi.$$

If it lies below dv, then $\Delta = (r' - r)\sec\varphi$; in any case, we always have

$$\frac{dv'}{\Delta^2} = \tan\varphi\, d\varphi\, dr'\, dA.$$

In addition, we have

$$\cos\beta = \cos i\cos\varphi + \sin i\sin\varphi\cos A,$$
$$\cos\gamma = \cos\varepsilon\cos\varphi + \sin\varepsilon\sin\varphi\cos(A - A_0).$$

First, let us calculate the integral for the case that dv′ is located above dv, so that

$$\varrho = r - r', \qquad d\varrho = -dr'.$$

We then obtain

$$\mu^2 L\, d\sigma \iiint e^{-kr(\sec i+\sec\varepsilon)+k\varrho(\sec i-\sec\gamma)}\tan\varphi\, d\varphi\, d\varrho\, (\beta)\,(\gamma)\, dA\, dr, \tag{10}$$

where

/40

$$(\beta) = 1 - p\cos\beta + q\cos^2\beta,$$
$$(\gamma) = 1 - p\cos\gamma + q\cos^2\gamma.$$

It is suggested to integrate first to ρ, in which case we eliminate everything that is independent of ρ; we then have

$$\int_0^r\int_0^{\pi/2} e^{-kr(\sec i+\sec\varepsilon)+k\varrho(\sec i-\sec\varphi)}\tan\varphi\, d\varphi\, d\varrho$$
$$= e^{-kr(\sec i+\sec\varepsilon)}\frac{1}{k}\int_0^{\pi/2}\frac{\cos i\cos\varphi}{\cos i-\cos\varphi}\left[e^{kr(\sec i-\sec\varphi)}-1\right]\tan\varphi\, d\varphi.$$

Next, we integrate to r

$$\int_{r=0}^{\infty}\frac{1}{k}\int_0^{\pi/2}\frac{\cos i\cos\varphi}{\cos i-\cos\varphi}\tan\varphi\left(e^{kr(\sec i-\sec\varphi)}-1\right)e^{-kr(\sec i+\sec\varepsilon)}\, d\varphi\, dr$$

$$= \frac{1}{k}\int_0^{\infty}\int_0^{\pi/2} \frac{\cos i \cos\varphi}{\cos i - \cos\varphi} \tan\varphi\, e^{-kr(\sec\varphi + \sec\varepsilon)}\, d\varphi\, dr$$

$$- \frac{1}{k}\int_0^{\infty}\int_0^{\pi/2} \frac{\cos i \cos\varphi}{\cos i - \cos\varphi} \tan\varphi\, e^{-kr(\sec i + \sec\varepsilon)}\, d\varphi\, dr = \frac{1}{k^2}\frac{\cos i \cos^2\varepsilon}{\cos i + \cos\varepsilon}\int_0^{\pi/2} \frac{\sin\varphi}{\cos\varphi + \cos\varepsilon}\, d\varphi . \qquad (\alpha)$$

To carry out the integration to A, let us write the full expression of the integral:

$$\mu^2 L d\sigma \frac{1}{k^2}\frac{\cos i \cos^2\varepsilon}{\cos i + \cos\varepsilon}\int_0^{2\pi} dA \int_0^{\pi/2} \frac{\sin\varphi}{\cos\varphi + \cos\varepsilon}(1 - p\cos\beta + q\cos^2\beta)\times$$
$$\times (1 - p\cos\gamma + q\cos^2\gamma)\, d\varphi .$$

The functions cos β, cos γ that depend on A will be written in the form

$$\cos\beta = a + b\cos A,$$
$$\cos\gamma = m + n\cos(A - A_0),$$

where we set

$$a = \cos i \cos\varphi, \qquad m = \cos\varepsilon \cos\varphi,$$
$$b = \sin i \sin\varphi, \qquad n = \sin\varepsilon \sin\varphi .$$

Next, we take the integral

$$\int_0^{2\pi} [1 - p(a + b\cos A) + q(a + b\cos A)^2][1 - p(m + n\cos(A - A_0))$$
$$+ q(m + n\cos(A - A_0))^2]\, dA ,$$

which is decomposed into nine terms

$$(1) = \int_0^{2\pi} (1 - pa + qa^2)(1 - pm + qm^2)\, dA ;$$

$$(2) = \int_0^{2\pi} (1 - pa + qa^2)(2qmn - pn)\cos(A - A_0)\, dA ;$$

$$(3) = \int_0^{2\pi} (1 - pa + qa^2) qn^2 \cos^2(A - A_0)\, dA ;$$

$$(4) = \int_0^{2\pi} (2qab - pb)(1 - pm + qm^2)\cos A\, dA ;$$

$$(5) = \int_0^{2\pi} (2qab - pb)(2qmn - pn)\cos A \cos(A - A_0)\, dA ;$$

/41

$$(6) = \int_0^{2\pi} (2qab - pb)\, qn^2 \cos^2(A - A_0) \cos A\, dA;$$

$$(7) = \int_0^{2\pi} qb^2 (1 - pm + qm^2) \cos^2 A\, dA;$$

$$(8) = \int_0^{2\pi} (2qmn - pn)\, qb^2 \cos^2 A \cos(A - A_0)\, dA;$$

$$(9) = \int_0^{2\pi} q^2 b^2 n^2 \cos^2(A - A_0) \cos^2 A\, dA.$$

Carrying out the integration will yield

$$(1) = 2\pi(1 - pa + qa^2)(1 - pm + qm^2);$$

$$(2) = 0; \qquad (3) = \pi(1 - pa + qa^2) qn^2;$$

$$(4) = 0; \qquad (5) = \pi nb(2qa - p)(2qm - p) \cos A_0;$$

$$(6) = 0; \qquad (7) = \pi(1 - pm + qm^2) qb^2;$$

$$(8) = 0; \qquad (9) = \frac{qb^2 n^2 \pi}{4}(1 + 2\cos^2 A_0).$$

On introducing the designations

$$\left.\begin{aligned}
A_1 &= 2 + q(\sin^2 i + \sin^2 \varepsilon) + p^2 \sin i \sin\varepsilon \cos A_0 + \tfrac{q}{4} \sin^2 i \sin^2 \varepsilon (1 + 2\cos^2 A_0),\\
B_1 &= pq(\sin^2 i \cos\varepsilon + \cos i \sin^2 \varepsilon) + 2p(\cos i + \cos\varepsilon)\\
&\quad + 2pq(\sin i \sin\varepsilon \cos\varepsilon + \sin^2 \varepsilon \cos i) \cos A_0,\\
C_1 &= q^2(\sin^2 i \cos^2 \varepsilon + \cos^2 i \sin^2 \varepsilon) - q(\sin^2 i + \sin^2 \varepsilon) + 2q(\cos^2 i + \cos^2 \varepsilon)\\
&\quad - 2p^2 \cos i \cos\varepsilon - p^2 \sin i \sin\varepsilon \cos A_0 + 4q^2 \sin i \sin\varepsilon \cos i \cos\varepsilon \cos A_0\\
&\quad - \tfrac{1}{2} q \sin^2 i \sin^2 \varepsilon (1 + 2\cos^2 A_0),\\
D_1 &= pq(\sin^2 i \cos\varepsilon + \cos i \sin^2 \varepsilon) - 2pq(\cos i \cos^2 \varepsilon - \cos\varepsilon \cos^2 i)\\
&\quad + 2pq(\sin^2 \varepsilon \cos i + \sin i \sin\varepsilon \cos\varepsilon) \cos A_0,\\
E_1 &= 2q^2 \cos^2 \varepsilon \cos^2 i - q^2(\sin^2 i \cos^2 \varepsilon + \cos^2 i \sin^2 \varepsilon)\\
&\quad - 4q^2 \sin i \sin\varepsilon \cos i \cos\varepsilon \cos A_0 + \tfrac{1}{4} q \sin^2 i \sin^2 \varepsilon (1 + 2\cos^2 A_0),
\end{aligned}\right\} \qquad (11)$$

the integral (10) assumes the form /42

$$\left.\mu^2 L\, d\sigma \frac{\pi}{k^2} \frac{\cos i \cos^2 \varepsilon}{\cos i + \cos\varepsilon} \int_0^{\pi/2} \frac{\sin\varphi}{\cos\varphi + \cos\varepsilon} \times \right.$$
$$\left. \times (A_1 - B_1 \cos\varphi + C_1 \cos^2\varphi + D_1 \cos^3\varphi + E_1 \cos^4\varphi)\, d\varphi. \right\} \qquad (a)$$

In addition, the integration over the volume below dv must be carried out, i.e., for

$$r' > r.$$

If we set here

$$\varrho = r' - r,$$

we obtain, in the same manner as above, the following expression as a result of the integration to ρ:

$$\int_{\varrho=0}^{\infty}\int_{\varphi=0}^{\varphi=\pi/2} e^{-k(r+\varrho)\sec i - k\varrho\sec\varphi - kr\sec\varepsilon}\tan\varphi\, d\varphi\, d\varrho = \frac{1}{k}e^{-rk(\sec i+\sec\varepsilon)}\int_0^{\pi/2}\frac{\cos i\cos\varphi}{\cos i+\cos\varphi}\tan\varphi\, d\varphi.$$

On integrating further to r, we obtain an expression that results from the corresponding expression for the case r > r′ by permuting the angles i and ε:

$$\frac{1}{k}\int_{r=0}^{\infty} e^{-kr(\sec i+\sec\varepsilon)}dr\int_0^{\pi/2}\frac{\cos i\cos\varphi}{\cos i+\cos\varphi}\tan\varphi\, d\varphi = \frac{1}{k^2}\,\frac{\cos^2 i\cos\varepsilon}{\cos i+\cos\varepsilon}\int_0^{\pi/2}\frac{\sin\varphi}{\cos i+\cos\varphi}\,d\varphi. \qquad (\beta)$$

The integration to A is carried out exactly as before so that we have, as the second summand,

$$\left.\begin{aligned}\mu^2 L\, d\sigma\,\frac{\pi}{k^2}\,\frac{\cos^2 i\cos\varepsilon}{\cos i+\cos\varepsilon}\int_0^{\pi/2}\frac{\sin\varphi}{\cos i+\cos\varphi}\times\\ \times\,(A_1 - B_1\cos\varphi + C_1\cos^2\varphi + D_1\cos^3\varphi + E_1\cos^4\varphi)\,d\varphi.\end{aligned}\right\} \qquad (b)$$

Summation of eqs.(a) and (b) and performance of the simple integration to φ will then yield the following five values (except for the constant factor):

$$\mathrm{I} = \frac{\cos i\cos\varepsilon}{\cos i+\cos\varepsilon}\left(\cos i\ln\frac{1+\cos i}{\cos i} + \cos\varepsilon\ln\frac{1+\cos\varepsilon}{\cos\varepsilon}\right)A_1,$$

$$\mathrm{II} = \frac{\cos i\cos\varepsilon}{\cos i+\cos\varepsilon}\left(\cos i+\cos\varepsilon - \cos^2 i\ln\frac{1+\cos i}{\cos i} - \cos^2\varepsilon\ln\frac{1+\cos\varepsilon}{\cos\varepsilon}\right)B_1,$$

$$\mathrm{III} = \frac{\cos i\cos\varepsilon}{\cos i+\cos\varepsilon}\left(\frac{\cos i+\cos\varepsilon}{2} - \cos^2 i - \cos^2\varepsilon + \cos^3 i\ln\frac{1+\cos i}{\cos i} + \cos^3\varepsilon\ln\frac{1+\cos\varepsilon}{\cos\varepsilon}\right)C_1,$$

$$\mathrm{IV} = \frac{\cos i\cos\varepsilon}{\cos i+\cos\varepsilon}\left(\frac{\cos i+\cos\varepsilon}{3} - \frac{\cos^2 i+\cos^2\varepsilon}{2} + \cos^3 i + \cos^3\varepsilon - \cos^4 i\ln\frac{1+\cos i}{\cos i} - \cos^4\varepsilon\ln\frac{1+\cos\varepsilon}{\cos\varepsilon}\right)D_1,$$

$$\mathrm{V} = \frac{\cos i\cos\varepsilon}{\cos i+\cos\varepsilon}\left(\frac{\cos i+\cos\varepsilon}{4} - \frac{\cos^2 i+\cos^2\varepsilon}{3} + \frac{\cos^3 i+\cos^3\varepsilon}{2} - \cos^4 i - \cos^4\varepsilon + \cos^5 i\ln\frac{1+\cos i}{\cos i} + \cos^5\varepsilon\ln\frac{1+\cos\varepsilon}{\cos\varepsilon}\right).$$

The totality of these terms, multiplied by the coefficient $\frac{\mu^2}{k^2}$ $L\pi d\sigma$ will then be our integral (10) or the light quantity of second order. Combining this with the term of the first order [eq.(9)], we finally obtain /43

$$
\begin{aligned}
q = \frac{\mu}{k} L\, d\sigma \frac{\cos i \cos\varepsilon}{\cos i + \cos\varepsilon} \Bigg\{ & 1 - p\cos\alpha + q\cos^2\alpha \\
& + \frac{\pi\mu}{k}\Bigg[A_1 \left(\cos i \ln \frac{1+\cos i}{\cos i} + \cos\varepsilon \ln \frac{1+\cos\varepsilon}{\cos\varepsilon} \right) \\
& - B_1 \left(\cos i + \cos\varepsilon - \cos^2 i \ln \frac{1+\cos i}{\cos i} - \cos^2\varepsilon \ln \frac{1+\cos\varepsilon}{\cos\varepsilon} \right) \\
& + C_1 \left(\frac{\cos i + \cos\varepsilon}{2} - \cos^2 i - \cos^2\varepsilon + \cos^3 i \ln \frac{1+\cos i}{\cos i} + \cos^3\varepsilon \ln \frac{1+\cos\varepsilon}{\cos\varepsilon} \right) \\
& + D_1 \left(\frac{\cos i + \cos\varepsilon}{3} - \frac{\cos^2 i + \cos^2\varepsilon}{2} + \cos^3 i + \cos^3\varepsilon - \cos^4 i \ln \frac{1+\cos i}{\cos i} \right. \\
& \qquad \left. - \cos^4\varepsilon \ln \frac{1+\cos\varepsilon}{\cos\varepsilon} \right) \\
& + E_1 \left(\frac{\cos i + \cos\varepsilon}{4} - \frac{\cos^2 i + \cos^2\varepsilon}{3} + \frac{\cos^3 i + \cos^3\varepsilon}{2} - \cos^4 i - \cos^4\varepsilon \right. \\
& \qquad \left. + \cos^5 i \ln \frac{1+\cos i}{\cos i} + \cos^5\varepsilon \ln \frac{1+\cos\varepsilon}{\cos\varepsilon} \right) \Bigg] \Bigg\},
\end{aligned}
\tag{12}
$$

where the coefficients A_1 ... E_1 have the meaning defined by eqs.(11). As expected, the emitted amount of light depends not only on the angles of incidence and reflection but also on the azimuth; furthermore, it is dependent on the ratio of diffusion to absorption. This ratio has its maximum value for bodies that show no absorption and in which the light attenuation is thus due to pure diffusion. Furthermore, let us determine the maximum value of μ/k but let us first discuss the two special cases of the above-derived diffusion formula, namely the formulas by Fessenkov and Lommel.

Fessenkov (Ref.65) assumes Rayleigh diffusion at the interior of the body. Consequently, his formula must follow directly from the above expression at $p = 0$, $q = 1$. This immediately yields the following expression for the reflected quantity of light:

$$
\begin{aligned}
q = \frac{\mu L\, d\sigma}{k} \frac{\cos i \cos\varepsilon}{\cos i + \cos\varepsilon} \Bigg\{ & 1 + \cos^2\alpha + \frac{\pi\mu}{k}\Bigg[A_1' \left(\cos i \ln \frac{1+\cos i}{\cos i} + \cos\varepsilon \ln \frac{1+\cos\varepsilon}{\cos\varepsilon} \right) \\
& + C_1' \left(\frac{\cos i + \cos\varepsilon}{2} - (\cos^2 i + \cos^2\varepsilon) + \cos^3 i \ln \frac{1+\cos i}{\cos i} + \cos^3\varepsilon \ln \frac{1+\cos\varepsilon}{\cos\varepsilon} \right) \\
& + E_1' \left(\frac{\cos i + \cos\varepsilon}{4} - \frac{\cos^2 i + \cos^2\varepsilon}{3} + \frac{\cos^3 i + \cos^3\varepsilon}{2} - (\cos^4 i + \cos^4\varepsilon) \right. \\
& \qquad \left. + \cos^5 i \ln \frac{1+\cos i}{\cos i} + \cos^5\varepsilon \ln \frac{1+\cos\varepsilon}{\cos\varepsilon} \right) \Bigg] \Bigg\},
\end{aligned}
\tag{13}
$$

where the coefficients have the following meaning:

$$
A_1' = 2 + \sin^2\varepsilon + \sin^2 i + \frac{1 + 2\cos^2 A_0}{4} \sin^2 i \sin^2\varepsilon,
$$

$$
C_1' = 4 - 2\sin^2\varepsilon - 2\sin^2 i - 2\sin^2 i \sin^2\varepsilon + 4\sin i \sin\varepsilon \cos i \cos\varepsilon \cos A_0 -
$$

$$- \frac{1+2\cos^2 A_0}{2} \sin^2 i \sin^2 \varepsilon ,$$

$$E_1' = 2 - 3\sin^2 i - 3\sin^2 \varepsilon + 4\sin^2 i \sin^2 \varepsilon - 4\sin i \cos i \sin \varepsilon \cos \varepsilon \cos A_0$$

$$+ \frac{1+2\cos^2 A_0}{4} \sin^2 i \sin^2 \varepsilon .$$

Lommel (Ref.59), under the assumption of uniform diffusion in all directions, calculated the self-illumination of the particles up to higher orders and thus obtained highly complex formulas, which will not be given here. Nevertheless, his formula which he obtained under restriction to terms of the second order, follows directly from the above formula at p = q = 0. Then, the reflected quantity of light will be /44

$$q = \frac{\mu}{k} L d\sigma \frac{\cos i \cos \varepsilon}{\cos i + \cos \varepsilon} \left[1 + \frac{\mu}{k} 2\pi \cos \varepsilon \ln \frac{1+\cos \varepsilon}{\cos \varepsilon} + \frac{\mu}{k} 2\pi \cos i \ln \frac{1+\cos i}{\cos i} \right]. \qquad (14)$$

Let us now calculate the maximum value for the ratio μ/k which enters eqs.(12) and (13). Thus, we assume that the total loss of direct radiation, on passing an element of volume dv, is due to diffusion. The quantity of light, scattered by the element of volume dv into all directions, reads

$$2L dv \mu \int_0^{2\pi} dA \int_0^{\pi/2} (1 - p\cos\varphi + q\cos^2\varphi) \sin\varphi \, d\varphi = 4\pi L dv \mu \left(1 - \frac{p}{2} + \frac{q}{3}\right).$$

Conversely, the radiation absorbed along the path dr on passing the element of volume dv = drdσ, will be

$$L dv k .$$

Equating both expressions will yield

$$\frac{\mu}{k} = \frac{1}{4\pi \left(1 - \frac{p}{2} + \frac{q}{3}\right)}. \qquad (15)$$

In the case of Rayleigh scattering, this will change into

$$\frac{\mu}{k} = \frac{3}{16\pi}. \qquad (15a)$$

The table for brightnesses at various i, ε, A_0, calculated in the Appendix (Table Va) according to the Fessenkov formula (13), is valid under this assumption; however, the two terms of the first and second order of eq.(13) have been calculated also separately, thus giving the possibility of hypothetical calculations with different μ/k (Tables Vb and Vc). The Appendix also contains tables for the general formula (12), for pure diffusion and the values p = 2.7, q = = 3.0 (Table IVa); the quantities a_1, b_1, c_1, d_1, e_1 which are independent of the azimuth are compiled in special tables for the case that eq.(12) is to be

calculated for some given values of p and q (Table IVb). If the entire formula [eq.(12)] is to be tabulated in this case, it will be impossible to avoid a calculation of extensive tables for the quantities A_1, B_1, C_1, D_1, E_1 by means of eqs.(11). We were unable to tabulate the values of the two terms of eq.(12) separately for the case of

$$p = 2.7, \quad q = 3.0$$

and could give only the total expression for the brightness according to three arguments i, ϵ, and A (Table IVa). In this case, its maximum value [eq.(15)] was assumed for the coefficient μ/k. In representing the light distribution over a cloud surface, for which the formula had been derived, the latter assumption was more logical since water vapor, in the visible region of the spectrum, shows no noticeable absorption bands. However, these tables no doubt furnish a better basis for the reduction of brightness measurements of cloud formations on planets than any other of the known diffusion formulas despite the fact that, /45 strictly taken, the values p = 2.7, q = 3.0 are valid for representation of the brightnesses of a terrestrial cloud formation. Theoretically, eqs.(12) and (13) no doubt should be preferred over others, but one cannot expect that, for ordinary dull surfaces, they will give a much better representation of the observations than the simple Lambert formula. This is not so much due to its theoretical imperfection, such as the fact that higher terms of self-illumination are neglected, but to other reasons. For opaque bodies, neglecting these terms is of no significance in comparison with the other perturbing causes. This includes primarily the always unavoidable reflection on the surface elements themselves, whose influence is superposed to that of the internal diffusion.

A cloud cover with plane boundaries, built up of spherical droplets of known order of magnitude, offers, as no other body will, the ideal conditions for obtaining agreement of observation and theory. Here, reflection on its surface is out of the question and even the shadow-casting of small roughnesses plays no role in view of their almost complete transparency.

In fact, a practically complete confirmation of eq.(12) was obtained in actual observations.

23. Experimental Investigations of Diffuse Reflection

In all experimental investigations of diffuse reflection, it must be recalled that all possible transitions between diffuse and specular reflection exist in nature and that even one and the same material may not always show the same properties, since even minor changes in surface condition may lead to considerable differences in optical behavior. For example, Rayleigh (Ref.66) found that a difference exists between surfaces which had been freshly polished and those that had been left standing for some time, despite the fact that the naked eye was unable to discern any change in the polish. Surprisingly, this fact has been little regarded until very recently, and the literature contains designations of the various surfaces studied such as "paper", "white cardboard", "gray cardboard", "matte silver", "ground glass" which, naturally, are completely inadequate for defining the surface condition. Even Seeliger was satisfied with using designations such as "yellow rough paper", "brownish glass paper", "dried

loam". Thus, it is not surprising that the experimental investigations of the diffusion on dull surfaces led to the most contradictory results.

Almost all substances investigated to date show traces of regular reflection at the surface, which are cumulative with the effect of diffusion and render the results quite precarious. A survey over the various experimental data leads to the conviction that, the more complete the dullness of the investigated substances the better can the diffusion on these materials be represented by the simple Lambert formula or, expressed differently, of all simple formulas the Lambert version yields the best approximation. Regular reflection of which minute traces - as mentioned above - are present in most dull substances results in the fact that the emission curve becomes asymmetric and assumes an oval slope which is more pronounced the larger the angle of incidence. Let us assume a number of arbitrarily oriented specular elements on the surface. It is impossible to calculate the amount of light reflected by these elements in various /46 directions, since the relative number of elements having certain inclination angles to the normal are unknown; however, it is obvious that the light waves reflected by such a system of mirrors will produce mutual interference and that the transit differences of the light waves must decrease with increasing angle of incidence. This will lead to the consequence that the reflection from such an area increasingly approaches the regular reflection the larger the angle of incidence. Thus, if observations indicate greater quantities of light for the azimuth 180° than for 0° and if the oblateness of the emission curve becomes greater with increasing angle of incidence, then this can be considered as a direct proof for the presence of traces of regular reflection.

Let us give a brief survey over the most important experimental work published in this field.

Bouguer's (Ref.5) measurements on matte silver, gypsum, and Holland paper showed that, at almost coinciding direction of incidence and direction of viewing, i.e., at $i = e$, the surface brightness is not proportional to cos i but falls off rapidly. Lambert made measurements on Kremnitz white and on "crown paper" (presumably an especially high-quality writing paper) and considered the agreement with his law as adequate. Later, Lommel recalculated Lambert's values and found considerable discrepancies. After this, nothing was done for a long time in this particular field until science became interested in the nature of radiant heat and in the reflection of heat rays. The first to prove, in a purely qualitative manner, that also heat rays are diffusely reflected was Melloni (Ref.67). De la Prevostaye and Dessains (Ref.68) observed the reflection of heat rays of unknown wavelength and found the Lambert law fully confirmed for $i = 0^\circ$ in the case of a white-lead plate but only approximately substantiated for a cinnabar and lead-chromate plate and not at all for powdered silver.

Macquenne (Ref.69) also worked with heat rays and was able to confirm the Lambert law for low angles of incidence.

Knut Ångström (Ref.70) was the first to investigate the diffusion of heat rays after the Lommel law had become known; he also believed to have found a confirmation. This author studied the diffusion on cast gypsum, buffed gypsum, flowers of sulfur, writing paper, ground iron, and ground copper. L.Godard (Ref.71) always was able to demonstrate regular reflection in the substances

used by Ångström. He himself found that the cos ϵ law is strictly valid for $i = 0^\circ$, at least for sufficiently heavy layers.

Ångström later restricted his original statements and formulated the result as follows: At vertical irradiation, the diffusion surface represents an ellipsoid elongated in direction to the surface normal. At increasing i, the ellipsoid suffers less and less elongation, changes into a sphere at $i = 30^\circ$, and finally is transformed into an oblate ellipsoid. This demonstrates that also these observations, just as those by Bouguer, directly contradict the Seeliger law for low angles of incidence. The flattening of the diffusion surface for large angles of incidence might have its cause in regular reflection.

The observations by J.B.Messerschmitt (Ref.72), made with a Glan spectrophotometer agreed with the Lambert law for the case of porcelain but showed considerable deviations for other materials. Wiener (Ref.73) investigated gypsum at various azimuths and found that, up to $\epsilon = 60^\circ$, the diffusion is proportional to cos ϵ but generally decreases more rapidly than with cos i. /47

H.Wright (Ref.74) studied plates of colcothar, potassium chromate, zinc green, ultramarine, magnesium carbonate, and gypsum which were not cast but pressed in steel dies under high pressure. He thus was able to completely prevent regular reflection. His observations, which must be considered the most valuable contribution in this particular field, agreed well with the Lambert formula. He found the reflected quantity of light as being strictly proportional to cos ϵ, i.e., in complete contradiction to the Seeliger formula, but not entirely proportional to cos i; nevertheless, the deviations never exceeded 10%.

According to Pegram (Ref.75), fine gypsum powder, dusted freely on a suitable glass plate, accurately obeys the Lambert law.

Matthews (Ref.76), for one gypsum and two paper screens at constant ϵ, found the brightness to be proportional to cos i within the limits of $0^\circ - 50^\circ$, whereas the deviation was approximately 5% for $i = 75^\circ$.

Thaler (Ref.77) subjected Wright's measurements to a detailed critical evaluation, especially in view of the fact that this author did not sufficiently regard the azimuth. His own observations on gypsum plates, ground-glass plates, and plates of magnesium oxide were made by extensive expansions in spherical functions which, however, do not represent a general law of reflection. His materials, in contrast to those by Wright, still showed strong reflections as indicated by the increase in brightness at an azimuth of 180° and at $\epsilon = i$.

Of other investigations, we should mention those by Hutchins (Ref.78) who again confirmed the simple cos i law for low angles in studies on fine paper. For larger angles, he found considerable deviations.

H.Lehmann (Ref.79), in his attempt to find a suitable projection surface, investigated the diffusion for ordinary paper, silvered ground-glass plates, and aluminum bronze. Unfortunately, he gave no numerical data but merely a graphical representation. This investigation also yielded neither a confirmation nor a direct refutation of the Lambert law.

A special problem formed the topic of a series of investigations based on Wright's result, according to which, in the diffusion on absolutely dull surfaces, unpolarized incident rays are not polarized while polarized rays are completely depolarized.

24. More Recent Studies

N.Umow (Ref.80) made an attempt to prove that dull surfaces will only partly and quite nonuniformly depolarize the incident polarized light, with white bodies having a greater effect than black bodies since, in the ideal case, the white body completely depolarizes and the black one not at all even if its surface is completely dull. Colored bodies with a dull surface depolarize /48 mostly light rays of the wavelength characterizing the color of the respective body.

Umow's considerations were confirmed by various authors, specifically by D.Chmyrow and Slatowratzki (Ref.81), V.Návrat (Ref.82), and Woronkoff and Pokrowski (Ref.83).

It was especially the latter authors who further advanced the problem of diffuse reflection, in a large number of investigations based on Umow's concepts. They used a König-Martens spectrophotometer for studying a number of substances in various spectral regions and found that, in selectively absorbent bodies, the law of reflection is dependent on the wavelength.

1) In white bodies without selective absorption such as magnesium oxide, the Lambert law is almost fully obeyed at normal and quasi-normal incidence; however, the deviations in these bodies also increase with the angle of incidence of the light.

2) In selectively absorbing bodies, the deviations from the cosine law increase in the range of wavelengths that are most extensively absorbed, in such a manner that, for large reflection angles, the intensity of the scattered light increases.

For interpreting this deviation, Pokrowski (Ref.84) formulated an argument which was to allow for the reflection on the surface elements of the body. This returns us to Bouguer's concept of diffuse reflection, which was assumed as being due to reflections of elementary mirror surfaces inclined at various angles. E.M.Berry (Ref.85) recently developed formulas based on this particular concept; however, because of the uncertainty of all these experiments, due to the fact that, a priori, nothing is known on the distribution of the angles of inclination of the elementary mirrors, we are merely mentioning the fact here. Pokrowski calculated the amount of light J' reflected by the elementary mirrors in accordance with the Fresnel formula, under assumption of equal probability of all inclination angles. In that case, the intensity of the light reflected from the surface will be

$$J' = \frac{a}{2}\left[\frac{\sin^2(i'-d)}{\sin^2(i'+d)} + \frac{\tan^2(i'-d)}{\tan^2(i'+d)}\right] = \frac{a}{2}F(i',d), \qquad (16)$$

where

$$i' = \frac{i+\varepsilon}{2}, \qquad d = \arcsin\frac{\sin i'}{n}, \tag{16'}$$

while n is the refractive index and a is a constant; i′ is the angle of incidence on an elementary mirror and i that on the plane boundary of the surface.

The first equation in the system (16′) represents the condition that the reflected ray coincides with the direction of reflection ε.

TABLE 5

F(i′, d) for n = 1.5

i'	$\frac{F}{2}$	i'	$\frac{F}{2}$	i'	$\frac{F}{2}$	i'	$\frac{F}{2}$
0°	0.040	30°	0.042	60°	0.089		
5	0.040	35	0.043	65	0.121		
10	0.040	40	0.046	70	0.171	90°	1.000
15	0.040	45	0.050	75	0.253		
20	0.040	50	.0058	80	0.388		
25	0.041	55	0.066	85	0.613		

For the quantity of light, emerging from the interior of the body, Pokrowski assumed strict validity of the Lambert law, so that J″ = b cos ε; then, the total quantity of light from the surface will be

$$J = J' + J'' = b\cos\varepsilon + \frac{a}{2}F(i', d). \tag{17}$$

Since the function F(i′, d), as shown in Table 5, increases with the angle i′, this author was able to take into account a part of the above deviations from the Lambert law by means of eq.(17). However, as mentioned by H.Schulz /49
(Ref.86), the assumption of equal probability of all mirror inclinations presumably does not apply, at least for areas whose surface is ground or reinforced by a binder. For these, the low angles of inclination will have a greater probability than the large angles, so that introduction of a distribution function of the form

$$J = b\cos\varepsilon + \frac{a}{2}F(i', d)\{c + \cos\varepsilon e^{-K(i-\varepsilon)^2}\} \tag{18}$$

would be justified. Here, i and ε, as in eq.(16′), are always positive if they are located at opposite sides of the vertical. Pokrowski then added auxiliary terms to his formula in order to allow for the quantity of light escaping from greater depths below the surface through the voids between the particles of the body.

Of interest are also observations by Woronkoff and Pokrowski (Ref.87, 88) on the polarization phenomena in diffuse reflection. The arguments, already

established by Umow, that the partial polarization occurring on incidence of unpolarized light is greater the greater the absorption and that, conversely, polarized light is more extensively depolarized the lower the absorption, was checked by observations with a spectrophotometer and qualitatively confirmed. Pokrowski believed that the cause lay in the fact that the portion of the reflected light coming from the interior of the body and strictly obeying the Lambert law is unpolarized, even if it originated in polarized light, meaning that the polarization is produced exclusively on reflection at the surface. The polarization of natural light increases with the angles of incidence and reflection, reaching its maximum at $\frac{i + \epsilon}{2} = \varphi$ where φ denotes the angle of maximum polarization.

Pokrowski (Ref.89) also made studies of the diffusion of light on passage through turbid media, developing an elementary theory of the process. From the fact that the exponential formula

$$J_d = e^{-\beta L}$$

fails for the intensity of the transmitted light (with L being the layer thickness) in the case of very thin layers whereas it is well confirmed in the case of greater thicknesses, Pokrowski concluded that the transmitted light is composed of two parts: One part of the light penetrates unhindered through the voids between the particles of the medium, while another part is absorbed and scattered by these particles; the latter portion, as a fraction of the light /50
trapped by the particles, is added to the directly transmitted light. Denoting these two components of the intensity by J_d' and J_d'', we have

$$J_d = J_d' + J_d''. \tag{19}$$

The first part obeys the exponential function

$$J_d' = e^{-SL}. \tag{20}$$

The second part is represented as

$$J_d'' = K(1 - e^{SL})e^{-\beta L},$$

where S, K, and β are constants while L denotes the layer thickness. It is also possible to have L designate the concentration or the number of absorbing and scattering elements per unit volume.

The same argument is used in investigating the polarization phenomena in the transmitted light. Here, the Umow concept of these phenomena is confirmed. Even on passage through an optically inhomogeneous medium, linearly polarized light is depolarized in accordance with its scattering whereas the light passing through the voids between the scattering elements retains its polarization. The polarization of unpolarized light, on passage through turbid media, is found to be dependent on the concentration of the scattering elements and on the layer thickness as well as on the deflection angle (Ref.90).

For the brightness of a transilluminated layer, Pokrowski (Ref.91) derived

the following elementary argument:

$$H = H_0(1 - e^{-KL}),$$

where H_0 denotes the surface brightness of the light-scattering elements of the layer and L the layer thickness. This author found a satisfactory confirmation of the formula in measurements of the brightness of the sky at equal angular distance from the sun, where the layer thickness increases with the secant of the zenith distance of the observed point:

$$H = H_0(1 - e^{-KL_0 \sec Z}).$$

This formula neglects the mutual illumination of the elements and can be interpreted such that e^{-KL} is the portion of the voids between the elements per unit area through which the dark celestial vault shines through. Here, H_0 would be the brightness of a completely opaque layer and K the concentration of the luminous elements.

25. Light Scattering in the Air

Various observations have been made on this phenomenon. Two different possibilities for studying the diffusion law are in question. The first method is to study the light distribution in a clear sky at various angular distances from the sun; such measurements exist in large number (Ref.92 - 100). A second possibility for investigating the light scattering in the air is to measure the intensity of an air column, transilluminated by parallel rays and produced, at nighttime, for example by a searchlight or, in the darkened laboratory, by the sun or by a high-intensity artificial light (Ref.101, 102). /51

Both methods lead to the same result, namely that the light scattering in the air, although varying strongly with the atmospheric conditions and the dust content, shows a peculiar course obeying none of the simple diffusion laws; an extremely great increase in brightness, in direction of the incident rays, i.e., for low deflection angles Θ, is present. If the angle at the air particle, between the directions of the incident and reflected rays, is denoted as phase angle (α), a strong intensity rise takes place for phase angles close to 180°. This increase is much greater than required by the Rayleigh formula and, in addition, takes place for $\alpha = 180°$ but not for $\alpha = 0°$. Only at great altitudes above sea level does the light distribution in a clear sky approach the Rayleigh distribution; the blue color of the sky as well as the transmittance coefficients of the atmosphere for light of different wavelengths obey the Rayleigh theory quite accurately for higher altitudes. In the lower air layers, admixtures of coarser particles (which no longer are small with respect to the wavelength of the light) cause strong deviations

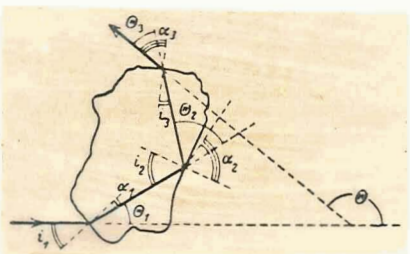

Fig.15 Influence of Refraction and Internal Reflection on Larger Particles, according to Pokrowski.

from the Rayleigh formula, since this formula takes account only of the diffraction phenomena on the air molecules. Mie (Ref.103) demonstrated that, at increasing particle size, the intensity maximum is shifted toward $\alpha = 180^\circ$ and that also the Rayleigh coloration falls off.

A similar effect of increase in intensity in the direction of incident radiation is observed for particles of arbitrary configuration, based on elementary considerations with the aid of the Fresnel formula, taking only the reflection and refraction on larger particles into consideration. We mention in this respect Pokrowski's studies on this subject.

Let i_1, d_1 be the angle of incidence and of refraction of the light on entering a particle and let Θ_1 be the angle of deflection (Fig.15). (In this diagram, we used α_1, α_2, α_3 instead of d_1, d_2, d_3.) The further ray path is shown in this sketch. The portion of light, reflected before entrance into the particle, has the following intensity according to Fresnel's formula:

$$J_r = \frac{a}{2}\left[\frac{\sin^2(i_1 - d_1)}{\sin^2(i_1 + d_1)} + \frac{\tan^2(i_1 - d_1)}{\tan^2(i_1 + d_1)}\right] = \frac{a}{2}F(i_1, d_1) = aM, \tag{21}$$

where i_1 must satisfy the condition

$$i_1 = \frac{\pi - \Theta}{2},$$

if the reflected ray is to reach the eye under the deflection angle Θ and if

$$\sin d_1 = \frac{\sin i_1}{n}.$$

Let us consider the ray which is deflected twice, once on entering the particle at an angle Θ_1 and once on leaving the particle at an angle Θ'' (not given in the diagram); this ray suffers the total deflection /52

$$\Theta = \Theta_1 + \Theta''.$$

The intensity after the first refraction is proportional to $1 - \frac{1}{2}F(i_1, d_1)$, where

$$i_1 - d_1 = \Theta_1.$$

In the first refraction, Θ_1 may be an arbitrary angle between $+\pi$ and $-\pi$ whereas in the second refraction, if the given direction Θ is to be established, it is always necessary that

$$\Theta'' = \Theta - \Theta_1.$$

Accordingly, the intensity of a twice refracted ray must be proportional to $[1 - \frac{1}{2}F(i_1, d_1)][1 - \frac{1}{2}F(i_2, d_2)]$, in which case we must have

$$i_2 - d_2 = \Theta'' = \Theta - \Theta_1$$

and

$$d_2 = \arcsin \frac{\sin i_2}{n}$$

Since Θ_1 may vary, which automatically will cause a change in Θ'', the intensity of the birefringent ray, at given Θ and at equal probability of all directions of the particles, must be represented as the sum of the elementary rays that correspond to different Θ_1:

$$J_d = b\int_{-\pi}^{+\pi} [1 - \tfrac{1}{2}F(i_1, d_1)][1 - \tfrac{1}{2}F(i_2, d_2)]d\Theta_1 = bN\,. \tag{22}$$

Here, b is a constant. The total brightness of the rays reflected in the given direction and refracted twice

$$J = J_r + J_d$$

can always be calculated as a function of Θ, provided that the refractive index n is given. If one wishes to define the amount corresponding to the ray which undergoes an internal reflection after a single refraction and then is refracted outward, then a quantity will be obtained for the intensity, after internal reflection, which is proportional to

$$[1 - \tfrac{1}{2}F(i_1, d_1)]\,\tfrac{1}{2}F(i_2, d_2)$$

in which case

$$i_2 = \frac{\pi - \Theta_2}{2} \qquad \text{and} \qquad d_2 = \arcsin \frac{\sin i_2}{n}.$$

After the second refraction, however, the intensity becomes proportional to

$$[1 - \tfrac{1}{2}F(i_1, d_1)]\,\tfrac{1}{2}F(i_2, d_2)\,[1 - \tfrac{1}{2}F(i_3, d_3)]\,,$$

where

$$d_3 - i_3 = \Theta_3 \qquad \text{and} \qquad d_3 = \arcsin \frac{\sin i_3}{n}.$$

In addition, the total deflection must be

$$\Theta = \Theta_1 + \Theta_2 + \Theta_3\,.$$

At given Θ, the quantities Θ_1 and Θ_2 may assume different values between $-\pi$ and $+\pi$, in which case Θ_3 is always determined by the last equation.

The sought intensity, at given Θ, will thus be

$$J_g = c\int_{-\pi}^{+\pi}\int_{-\pi}^{+\pi} [1 - \tfrac{1}{2}F(i_1, d_1)]\,\tfrac{1}{2}F(i_2, d_2)\,[1 - \tfrac{1}{2}F(i_3, d_3)]\,d\Theta_1\,d\Theta_2 = cP\,, \tag{23}$$

where c is a constant. In this calculation, only cases in which the rays within the particles move in a plane are taken into consideration. If also the other cases are to be considered, the calculation becomes highly complex. This calculation will not be made here, and the total intensity of the refracted and reflected rays, in accordance with eqs.(21), (22), and (23), will be formulated as /53

$$J = J_r + J_d + J_g = aM + bN + cP. \tag{24}$$

After numerical calculation of the integrals N and P for n = 1.56 and after determination of the coefficients a = 10, b = 8, c = 0.3 by compensation, a close approach to the observed reflection law of the air can be obtained already with this elementary theory, as shown in Fig.16. In this diagram, the solid curve has been calculated according to eq.(24). However, the observations based on various methods, compiled here and plotted by Pokrowski, show a still greater increase in intensity for low deflection angles than required by eq.(24).

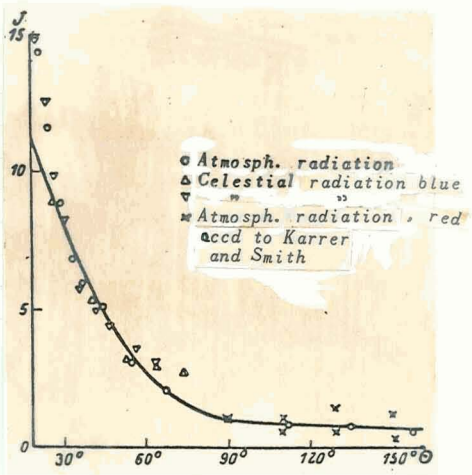

Fig.16 Intensity of Atmospheric Radiation according to Pokrowski (Ref.91).

Much more detailed investigations than in these elementary considerations have been made by Chr. Wiener (Ref.104) on the influence of larger particles (ice crystals, water droplets, and dust particles) on the light scattering in air, in his extensive work on brightness of the clear sky; his theory was confirmed by recent measurements of the sky brightness from high mountains (Teneriffa), which can be considered a proof for the existence of coarser particles even at such altitudes.

26. Concept of Albedo

The concept of albedo as obtained on the basis of the Lambert reflection law has been mentioned before (p.36); it was designated by Lambert as the ratio of the total quantity of light reflected from an element of area into the solid angle π to the incident quantity of light. Since, according to Lambert's law, the emitted amount of light depends exclusively on the emanation angle, the albedo will have the same value for all angles of incidence.

When using another illumination law as basis, such as the Seeliger law, in which the emitted quantity of light also depends on the angle of incidence, the albedo will have a different value for each individual angle of incidence of the light.

Seeliger (Ref.105) who drew attention to this fact suggested still another definition of the albedo, which would be valid for any illumination law.

Let an element of area $d\sigma$ be illuminated under the angle i and let L be the

amount of light vertically incident per unit area. Let the originally unknown illumination law be denoted by $f(i, \varepsilon)$; then, the amount of light reflected under the emanation angle ε and vertically striking an element ds at a distance l, will be

$$dq = CLd\sigma f(i,\varepsilon)ds,$$

where C is a constant which has a different value for each illumination law. /54
The quantity of light scattered on a hemisphere of radius l with $d\sigma$ as center, if the element of the sphere ds is expressed by the coordinates zenith distance (ε) and azimuth (ψ), will be equal to

$$q = CLd\sigma\int_0^{2\pi} d\psi\int_0^{\pi/2}\sin\varepsilon d\varepsilon f(i,\varepsilon) = 2\pi CLd\sigma\int_0^{\pi/2}\sin\varepsilon f(i,\varepsilon)d\varepsilon.$$

The albedo A is the ratio of this amount of light to the amount incident on $d\sigma$, so that

$$A = \frac{q}{L\cos i d\sigma} = 2\pi C\int_0^{\pi/2}\frac{f(i,\varepsilon)}{\cos i}\sin\varepsilon d\varepsilon. \qquad (25)$$

This proves our above statements as to the dependence of the albedo on the angle of incidence; at the same time, it is obvious that the albedo is independent of the angle of incidence only at $f(i, \varepsilon) = \cos i\varphi(\varepsilon)$, as for example in the Lambert law.

The simplest way of avoiding this uncertainty is to give the albedo the value possessed by A for a certain angle of incidence; for this reason, the albedo for normal incidence of light (i = 0) is a concept widely used at present.

27. Seeliger's Albedo

Conversely, Seeliger suggested to use the term albedo for the mean-square value of all A obtained for all values of the incidence angle. If this mean value is denoted by A_2, it would follow that

$$A_2 = \frac{1}{2\pi}\sum A,$$

where the summation must be carried out over all elements of the hemisphere of radius l and where A has the value defined by eq.(25). For a spherical zone, corresponding to the angles of incidence between i and i + di, the above sum is equal to $2\pi A \sin i\, di$ and, for the entire hemisphere,

$$2\pi\int_0^{\pi/2} A\sin i\, di,$$

so that

$$A_2 = \int_0^{\pi/2} A \sin i \, di$$

while, after introduction of the value of A,

$$A_2 = 2\pi C \int_0^{\pi/2} \tan i \, di \int_0^{\pi/2} f(i, \varepsilon) \sin \varepsilon \, d\varepsilon . \qquad (26)$$

This represents the definition of the Seeliger albedo. Substituting for f(i, ε) the Lambert law, eq.(25) will yield A = πC and eq.(26) will give $A_2 = \pi C$. Consequently, the two definitions of the albedo agree for the Lambert law.

Conversely, if the Seeliger illumination law is substituted for f(i, ε) in its general form

$$f(i, \varepsilon) = \frac{\cos i \cos \varepsilon}{\cos i + \lambda \cos \varepsilon},$$

then, the following value is obtained for A_2: /55

$$A_2 = 2\pi C_2 \int_0^{\pi/2} \sin i \, di \int_0^{\pi/2} \frac{\sin \varepsilon \cos \varepsilon}{\cos i + \lambda \cos \varepsilon} d\varepsilon .$$

Integration is carried out simplest by introducing a new variable x = cos i + + λ cos ε, from which it follows that

$$A_2 = \frac{2\pi C_2}{\lambda^2} \int_0^{\pi/2} \sin i \, di \{\lambda + \cos i \ln \cos i - \cos i \ln (\lambda + \cos i)\},$$

or, setting cos i = y,

$$A_2 = \frac{2\pi C_2}{\lambda^2} \left\{ \lambda - \int_1^0 y \, dy \ln y + \int_1^0 y \, dy \ln (\lambda + y) \right\}$$
$$= \frac{\pi C_2}{\lambda^2} \left\{ 1 - \lambda \ln \lambda + \frac{\lambda^2 - 1}{\lambda} \ln (1 + \lambda) \right\}. \qquad (27)$$

The Seeliger albedo has almost never been used in this general form. Setting here λ = 1, we obtain

$$A_2 = \pi C_2 , \qquad (27a)$$

i.e., the Seeliger albedo in this case is determined only by the proportionality factor of the Seeliger law. Let us furthermore use the subscript 2 for the Seeliger albedo defined by eq.(27a), while A_1 will always stand for the Lambert albedo.

In the Lambert albedo $A_1 = \pi C_1$, the quantity C_1 is the reflection coeffi-

cient (p.36) so that

$$C_1 = \frac{A_1}{\pi} = \frac{\Gamma_1}{L}. \tag{28}$$

In bodies obeying the Lambert law, both albedo and reflection coefficient are equivalent concepts. The latter, under omission of the factor $1/\pi$, is frequently assumed as 1 for a white body, i.e., used in the sense of albedo.

In the Seeliger albedo $A_2 = \pi C_2$, the quantity C_2 is the constant of the Seeliger law, i.e., [see p.39, eq.(5)]

$$C_2 = \frac{A_2}{\pi} = \frac{\Gamma_2}{L}. \tag{29}$$

28. Albedo of a Plane Area for Normal Irradiation and Reflection Coefficient in Direction of Irradiation

For practical application, the definition of albedo of a plane area for normal irradiation is the most suitable concept. If the reflection law is determined, in difference from the Lambert law, by a function $f(i, \varepsilon)$ then this albedo - according to eq.(25) - will be

$$A = 2\pi C \int_0^{\pi/2} f(0, \varepsilon) \sin\varepsilon \, d\varepsilon,$$

where C is a constant depending on the form of the function f.

For bodies with irregular boundaries, for minerals, and rocks in the native state, the reflection coefficient in the direction of irradiation is the most suitable constant for astronomic purposes. This coefficient represents the ratio of the amount of light reflected by the body in direction of the irradiation to the amount of light re-reflected in the direction of irradiation by a plane area of albedo 1 which obeys the Lambert law, if it receives the same amount of /56 light in a vertical direction as the irregularly shaped body. The albedo of such a body may depend largely on the accidental form, especially in view of the light losses produced by shadow-casting in oblique viewing, whereas the reflection coefficient for the direction of irradiation does depend on the form but not on the shadow effect. This coefficient* will be furthermore denoted by R.

29. Determination of Albedo and Reflection Coefficient; Experimental Determination of Albedo

Lambert (Ref.46, Sect.747) gave a method for determining the reflection

---

* The designation "reflection coefficient" is frequently used in the theory of diffusion for representing the fraction of the amount of light reflected in a certain direction to the incident quantity of light. In our problems, we will denote this coefficient by μ. If the scattering is uniform in all directions, then $4\pi\mu$ is the total scattered amount of light.

coefficient and made several experiments with an apparatus constructed by him. The principle of his instrument, which later was perfected by Zöllner (Ref.47, p.265), is as follows: Let (Fig.17) ab be the projection of a screen coated with a substance whose albedo is to be determined. This screen is illuminated by J as normally as possible, and its optical image s, projected through the lens L, is focused on another screen AB. In addition to ab, the light source J also illuminates AB; it is obvious that the farther this source is from ab the darker will be the optical image of ab in s, in comparison with the site at s′ illuminated by J. Lambert varied the position of the light source J until the image, formed in s, was exactly as bright as the portion of the screen directly illuminated in s′. Denoting the distance cJ by D, Js′ by D′, Ls by d, and the radius of the lens by d′, Lambert was able to demonstrate that, in close approximation, the reflection coefficient μ is given by the equation

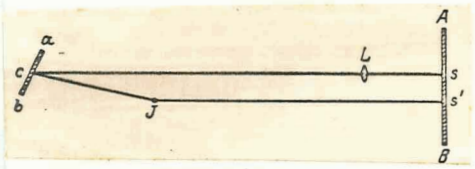

Fig.17 Lambert Albedometer.

$$\mu = \frac{1}{\varkappa}\left(\frac{dD}{d'D'}\right)^2.$$

Here, $\varkappa$ denotes the absorption coefficient of the lens which must be determined experimentally in each individual case.

Naturally, it is of importance that the areas to be compared not only have equal area brightness but also equal form; in addition, a point disregarded by Lambert, it is necessary to have the two areas to be compared receive light only as stipulated by the theory and no sidelight, which can be obtained by properly arranged dark screens.

Measurements of this type actually do not give the albedo but rather the reflection coefficient for normal or quasi-normal irradiation. In this manner, Zöllner obtained the reflection coefficients for various substances:

newly fallen snow	0.78
white paper	0.70
white sandstone	0.24
clay marl	0.16
quartz	0.11
moist arable soil	0.08

Measurements with instruments of this type are difficult, for which reason /57 the reflectivity of only one substance is determined in this manner, but with extreme care. Zöllner chose white paper. For the other substances, a conventional photometer is used, with which the materials, subjected to equal illumination conditions, are compared for brightness. This will yield relative reflection coefficients from which the absolute values can be calculated.

Using an instrument of the same design (Lambert-Zöllner type), J.Wilsing and J.Scheiner (Ref.106, 107) determined the reflection coefficients for the irradiation direction, on a large number of rocks and other materials. These

observations are of special value since, being made with a spectrophotometer, they refer to five different wavelengths separately and thus also characterize the color of the investigated body.

As comparison material, white chalk was selected whose absolute reflectivity was determined carefully by two different methods. The average value was 1.05, which was attributed by the observers to traces of regular reflection; in the calculations, this value had been assumed as 1.00. The reflection coefficients, derived from intensity comparisons of the spectrum of chalk and other minerals at different wavelengths, all refer to reflection in the direction of irradiation. The figures given in Table 6 in the albedo column thus represent albedo values only in Lambert's sense, for chalk as well as for the other materials.

TABLE 6

ALBEDO AND REFLECTION COEFFICIENTS OF MINERALS

	Albedo	0.448 μ	0.480 μ	0.513 μ	0.584 μ	0.638 μ	
Chalk	1.000	1.000	1.000	1.000	1.000	1.000	
Humus	0.564	0.548	0.550	0.568	0.565	0.592	bluish white
Rock salt	0.442	0.345	0.411	0.433	0.490	0.561	whitish brown
Crystalline limestone	0.418	0.373	0.449	0.405	0.407	0.463	white-gray
Sandstone	0.381	0.305	0.343	0.409	0.432	0.437	light yellowish
Granite	0.362	0.325	0.367	0.347	0.389	0.389	reddish gray
Gypsum	0.336	0.333	0.338	0.332	0.344	0.353	pure gray
Trachyte	0.303	0.267	0.286	0.289	0.325	0.360	light yellowish gray
Trass	0.260	0.193	0.234	0.271	0.293	0.332	light yellowish gray
Clay	0.237	0.193	0.213	0.272	0.256	0.263	yellowish gray
Mica schist	0.232	0.194	0.208	0.232	0.254	0.282	yellowish gray
Vesuvian ash, upper layer	0.192	0.158	0.175	0.198	0.213.	0.226	light bluish gray
Vesuvian ash, middle layer	0.179	0.125	0.160	0.166	0.220	0.251	light reddish gray
River sand	0.171	0.123	0.154	0.160	0.214	0.226	yellow-brown
Anhydrite	0.138	0.124	0.132	0.144	0.158	0.152	bluish gray
Syenite	0.132	0.111	0.113	0.142	0.143	0.156	reddish gray
Limestone	0.119	0.099	0.100	0.129	0.136	0.140	grayish brown
Biotite gneiss	0.116	0.100	0.100	0.125	0.131	0.132	reddish gray
Quartz porphyry	0.107	0.078	0.086	0.098	0.128	0.171	red-brown
Trachyte lava	0.098	0.082	0.091	0.105	0.100	0.115	pure gray
Gabbro	0.095	0.081	0.092	0.100	0.097	0.104	dark gray
Pitchstone porphyry	0.093	0.083	0.093	0.087	0.105	0.101	dark gray
Diabase	0.093	0.083	0.089	0.096	0.097	0.101	green-black
Obsidian	0.089	0.090	0.094	0.095	0.082	0.087	blue-black
Hekla lava	0.084	0.069	0.075	0.095	0.087	0.095	black-gray
Argillite	0.073	0.071	0.070	0.082	0.075	0.069	black-blue
Basalt	0.064	0.056	0.064	0.069	0.065	0.069	very dark gray
Vesuvian lava	0.050	0.010	0.043	0.051	0.058	0.061	" " "
Etna lava	0.048	0.039	0.048	0.054	0.046	0.053	dark gray
Brown coal	0.047	0.036	0.051	0.048	0.048	0.050	" "

Among these materials, there are four whose albedo was determined also /58
by Zöllner. The Zöllner values, except for one (quartz porphyry), are all lower than Wilsing's values which presumably is due to the uncertainty of the absolute reflection coefficient for white paper, which was used by Zöllner as comparison material.

30. The Fessenkov Albedometer

Strict albedo values were determined by Fessenkov (Ref.8) for normal irradiation of gypsum and snow. He used a novel albedometer in which the studied object was not directly illuminated by the light source but from the back of an illuminated paper.

The Fessenkov albedometer and his strict method of determining the albedo for normal incidence of the rays seem simple and instructive for investigations of this type; for this reason, they will be described here.

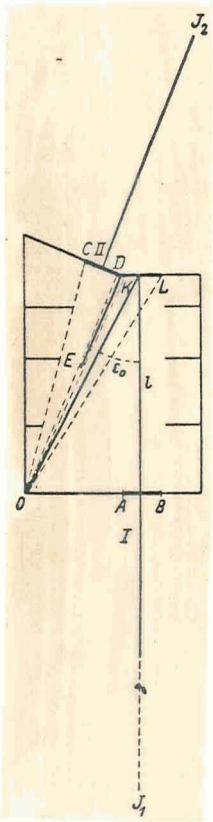

Fig.18 Fessenkov Albedometer.

Figure 18 shows the instrument with openings AB = I and CD = II on the front and rear wall, covered with translucent paper. The specimen to be studied is inserted at KL. For this specimen, the reflection law $f(0, \varepsilon)$ is determined in a separate investigation for which a few brightness measurements at different reflection angles are sufficient. The area AB, illuminated by J_1, in turn illuminates the object KL. Viewed from O, this object is compared with the area CD and, by varying the distance from the second light source J_2, equal brightness of both is adjusted. The opaque wall DE prevents an illumination of AB by CD and vice versa. Furthermore, it can be assumed that both light sources J_1 and J_2 are of equal brightness since their nonuniformity is eliminated on the average by interchanging and repeating the measurement. Let the radius of AB be ρ, and let the distance between AB and KL be l. The paper disk CD is accurately matched in dimension with the specimen to be studied.

The element ds of the disk I, with a distance ρ' from its center, transmits the following quantity of light to an element $d\sigma$ located in the central portion of KL:

$$\frac{L\,ds\cos^2 i}{r^2}\,d\sigma,$$

where

$$r^2 = l^2 + \varrho'^2 \qquad \text{and} \qquad \cos i = \frac{l}{\sqrt{l^2 + \varrho'^2}}.$$

The disk I is uniformly illuminated by J_1; since, according to Kononowitsch (Ref.109), paper obeys the Lambert law, the above expression takes account of the angle of incidence and of the emanation angle of the light (both equal to i). Here, L denotes the quantity of light emitted in a normal direction by unit surface of the back of AB. From the entire surface of the disk I, the following quantity of light is incident on $d\sigma$ /59

$$L_1 = L\,d\sigma \int_0^{2\pi} d\varphi \int_0^{\varrho} \varrho'\,d\varrho' \frac{\cos^2 i}{l^2 + \varrho'^2} = 2\pi L\,d\sigma\, l^2 \int_0^{\varrho} \frac{\varrho'\,d\varrho'}{(l^2 + \varrho'^2)^2},$$

since $ds = \rho' d\rho' d\varphi$.

Since ρ/l is a small quantity, an expansion in series and subsequent integration will yield

$$L_1 = \frac{\pi L d\sigma \varrho^2}{l^2}\left(1 - \frac{\varrho^2}{l^2} + \frac{\varrho^4}{l^4} \cdots\right).$$

The quantity of light, reflected from $d\sigma$ into the eye of the observer, is

$$\frac{CL_1 f(0, \varepsilon_0)}{l_1^2},$$

where C denotes the reflection constant, $l_1 = KO$, and the function $f(0, \varepsilon)$ is the reflection law valid for the specimen at $i = 0$. The apparent brightness of $d\sigma$ will be

$$\frac{CL_1 f(0, \varepsilon_0)}{l_1^2} \frac{l_1^2}{d\sigma \cos\varepsilon_0} = \frac{C\pi L \varrho^2}{l^2} \frac{f(0, \varepsilon_0)}{\cos\varepsilon_0}\left(1 - \frac{\varrho^2}{l^2} + \frac{\varrho^4}{l^4}\right).$$

Denoting by d_1 and d_2 the distances of the light sources J_1 and J_2 from I resp. II, the apparent brightnesses of II and I will be at a ratio of $\frac{d_1^2}{d_2^2} = n$. Since the apparent brightnesses of II and KL are identical, we thus also have obtained the brightness ratio of KL to I, if this were viewed from the inside out, yielding

$$\frac{C\pi\varrho^2}{l^2} \frac{f(0, \varepsilon_0)}{\cos\varepsilon_0}\left(1 - \frac{\varrho^2}{l^2} + \frac{\varrho^4}{l^4}\right) = n. \qquad (\alpha)$$

The next step is to calculate the albedo from the value $Cf(0, \varepsilon_0)$. The element $d\sigma$, under an angle ε, reflects the quantity of light

$$CLd\sigma f(0, \varepsilon) d\omega,$$

where the solid angle is $d\omega = \sin\varepsilon d\varepsilon dA$ (A = azimuth).

Consequently, the quantity of light reflected toward the hemisphere will be

$$CLd\sigma \int_0^{2\pi} dA \int_0^{\pi/2} f(0, \varepsilon) \sin\varepsilon d\varepsilon,$$

while the albedo is

$$A = 2\pi C \int_0^{\pi/2} f(0, \varepsilon) \sin\varepsilon d\varepsilon.$$

Here, it is only necessary to substitute the value of C from eq.(α). This yields

$$A = \frac{2\pi l^2}{\varrho^2} \frac{\cos\varepsilon_0}{f(0,\varepsilon)} \left(1 + \frac{\varrho^2}{l^2}\right) \int_0^{\pi/2} f(0,\varepsilon) \sin\varepsilon d\varepsilon . \qquad (\beta)$$

The albedo of bodies that cannot be investigated in this manner is then found by photometric comparison with another body (for example, gypsum) whose albedo is known. This comparison is made for normal incidence but different values of ε. If the apparent brightness of the two bodies is

$$\frac{CLf(0,\varepsilon)}{\cos\varepsilon} \quad \text{and} \quad \frac{C_1 L f_1(0,\varepsilon)}{\cos\varepsilon}$$

and if the brightness ratio of both is k, we obtain /60

$$k = \frac{Cf(0,\varepsilon)}{C_1 f_1(0,\varepsilon)},$$

or, expressing the constants C by the corresponding albedo,

$$\frac{A}{A_1} = \frac{k f_1(0,\varepsilon)}{f(0,\varepsilon)} \cdot \frac{\int_0^{\pi/2} f(0,\varepsilon)\sin\varepsilon d\varepsilon}{\int_0^{\pi/2} f_1(0,\varepsilon)\sin\varepsilon d\varepsilon} .$$

In this manner, the albedo of a plane gypsum plate was first determined with the albedometer. For the determination, Ångström's observations on diffuse reflection of gypsum were used for defining $f(0, \varepsilon)$. This yielded

$$A = 0.789 \pm 0.0046,$$

for gypsum whereas, when assuming that gypsum obeys the Lambert law and that the albedo is identical with the reflection coefficient, the result is as follows:

$$A = 0.866 \pm 0.0046.$$

In observations with a surface photometer, Fessenkov found that the function $f(0, \varepsilon)$ for snow was identical to that for gypsum within the accuracy of observation; a simple photometric comparison of gypsum and snow surfaces under equal illumination yielded the strict albedo for snow:

$$A = 0.705,$$

whereas the Lambert albedo, for the same observations, would be

$$A_1 = 0.775.$$

The latter figure agrees completely with that given by Zöllner of $A_1 = 0.78$ for

the Lambert albedo of snow. This investigation thus proves the necessity of strict indication as to which concept of albedo is meant.

31. Albedo of Magnesium Oxide and Clouds

F.Henning and W.Heuse (Ref.110) used a special method for investigating the reflectivity of magnesium oxide, which can be obtained in a simple manner by combustion of the metal and is suggested as standard white for relative measurements. They found the following figure for the total reflectivity or the albedo at normal incidence:

$$A = 0.953.$$

According to these authors, magnesium oxide - even at normal incidence - does not accurately obey the Lambert law. The brightness of a plane surface of magnesium oxide is somewhat less at large reflection angles than at vertical observation and obeys the formula $1 - 1.3 \sin^2 \frac{\varepsilon}{2}$, meaning that the function $f(0, \varepsilon) \sec \varepsilon$ will here be

$$f(0, \varepsilon) \sec \varepsilon = 1 - 1.3 \sin^2 \frac{\varepsilon}{2}.$$

Coblentz (Ref.111), for pulverized magnesium oxide mixed with traces of adhesive, found a value of $A = 0.863$ at $\lambda = 0.60\ \mu$. The same author obtained a slightly higher value for the albedo of lead carbonate, namely $A = 0.87 - 0.90$.

Of importance for astronomical purposes is a determination of the albedo /61 of clouds, since some planets are frequently - and others continuously - surrounded by cloud covers that reflect the sunlight to earth and hide the interior of the planet. In this case, it is of importance to observe a given cloud envelope from the top, for example from the peak of a high mountain or, preferably, from a dirigible.

The first method was used in observations at the Mt. Wilson Observatory by Abbot and Fowle (Ref.112) who used a bolometer in which the radiation of the sun was compared with that of an equally large cutout of the cloud cover below the mountain, at various azimuths and nadir distances. As a result of an approximate calculation of the incomplete observation series, the following value was obtained for the reflection coefficient of solar radiation within the limits from $0.3\ \mu$ to $3\ \mu$:

$$R = 0.65.$$

On suggestion by the same researchers, the albedo of an uninterrupted cloud cover extending to the horizon was measured from a dirigible close to Mt. Wilson by L.B.Aldrich (Ref.113), using a pyranometer. The receiver of this instrument, enclosed in a hemisphere, was directed downward and thus received the radiation of the clouds from all azimuths and nadir distances, from 0° to 90°. If the same receiver was pointed to the zenith, it received the radiation of the sun and of the diffuse celestial light. The value of this constant, expressed in

calories, was taken from simultaneous observations with the pyrheliometer. The value of the albedo was derived on the basis of the following theorem which presupposes validity of the Lambert formula*: The ratio of the re-radiation of a horizontal cloud layer, extending to infinity, on an area of 1 cm^2 above this layer to the amount of radiation incident on 1 cm^2 of the cloud surface is equal to the albedo since - except for the absorption - the horizontal area above the clouds receives as much radiation as an equally large parallel area of the clouds will scatter. The result of the measurements, for solar radiation from 0.3 μ to 3 μ, was

$$A = 0.78.$$

Photometric observations with a Martens polarization photometer of the reflectivity of clouds were made by K.Stuchtey and A.Wegener (Ref.114) from a balloon. They made a direct comparison of the brightnesses of various cloud formations with the brightness of a directly irradiated gypsum plate. The brightness ratios corresponded to the reflection coefficient for various angles of incidence and reflection, relative to the ratio of the reflection coefficient of the gypsum plate. This coefficient was assumed as 1, which - according to our above statements (p.67) - would imply a considerable error. The authors found the following mean value for all cloud types:

$$R = 0.73,$$

a value which should be further reduced.

M.Luckiesh (Ref.115), again from photometric measurements of various cloud types starting with thin semitransparent clouds and going to compact clouds of great depth, found values for the reflection coefficients of 0.36 to 0.78. /62
The accuracy of these values, because of the lack of data on the observation method, cannot be evaluated here.

III. ILLUMINATION OF THE PLANETS

32. Assumptions of the Theory

Let us now turn to application of the laws, derived in the previous Chapter or taken from results of physical practice, to the problems of the illumination of celestial bodies. Despite the fact that the laws for reflected radiation do not have the simplicity and uniqueness of those for self-luminous bodies, the observed brightnesses of the planets and the moon, thanks to the multiple illumination conditions under which they appear, permit many important conclusions as to the consistency of the reflecting surfaces. Celestial mechanics furnishes, with all desired accuracy, the distances of the planets and moons from the source of illumination, namely the sun, and from the observation point, namely the earth. Similarly, the dimensions and configuration of the illuminated bodies are mostly known. Consequently, there exists the possibility - assuming a

* The proof of this theorem is given in the first problem of Section 19.

certain ideal consistency of the surface - of calculating the quantities of light reflected under different illumination conditions and of comparing the calculation with actual observations. Of necessity, we can use only two simple illumination formulas as basis for the calculation, namely the Lambert and the Lommel-Seeliger formulas according to which the quantities of light, reflected from a surface element ds, can be represented by

$$dq = \Gamma_1 \cos i \cos\varepsilon\, ds \quad \text{accd. to Lambert,} \tag{1}$$

$$dq = \Gamma_2 \frac{\cos i \cos\varepsilon}{\cos i + \lambda \cos\varepsilon} ds \quad \text{accd. to Lommel-Seeliger.} \tag{2}$$

In addition, in cases in which considerable deviations between observation and calculation occur, theories can be developed that accurately allow for the real consistency of the surfaces.

It is obvious from the beginning that a planet with a solid surface and without atmospheric envelope will reflect the sunlight in an entirely different manner than a planet surrounded by an opaque cloud layer or having a semitransparent gaseous atmosphere. All these circumstances, rendering the theory more complicated, will be disregarded at first and only the following ideal case will be treated in this Chapter:

1) The planet is a sphere which diffusely reflects the light received by the sun, in accordance with the Lambert or Seeliger law.
2) The planet, at all points of its surface, has exactly the same consistency and exhibits no shadow-casting roughnesses.
3) The planet has no atmosphere, and the sunlight reaches its solid surface without undergoing any prior modification.

33. Calculation of the Quantity of Light Reflected by the Planet to the Earth at Different Phases

The phase angle α or the angle at the center of the planet, between the directions to sun and to earth, constitutes the fundamental variable for the theory since it defines the illuminated portion of the visible planet surface. Denoting the distances from the center of the planet to the sun by r and to the earth by Δ and designating the distance between earth and sun by R, these quantities - to be taken from the astronomical ephemerides - will determine the phase angle α according to the equation resulting from the triangle earth - sun - planet: /63

$$\cos\alpha = \frac{\Delta^2 + r^2 - R^2}{2r\Delta}.$$

For logarithmic calculations, the following form of the same equation is more convenient

$$\sin\frac{1}{2}\alpha = \frac{1}{2}\sqrt{\frac{(R+\Delta-r)(R+r-\Delta)}{r\Delta}}. \tag{3}$$

If the quantities r, as is the case for the moon, are not available in tabulated form, then the following simple equations whose derivation is entirely logical are suggested:

$$\left.\begin{aligned} \cos\gamma &= \cos(\lambda_\odot - \lambda)\cos\beta \\ \tan\alpha &= \frac{\sin\gamma}{\frac{\Delta}{R} - \cos\gamma} \end{aligned}\right\}, \tag{4}$$

where λ and β denote geocentric longitudes and latitudes.

Let us imagine a section laid through the center of the planet, perpendicular to the direction of the earth. Let this section be represented by the circle ABCD in Fig.19. The circle DESB is known in photometry as the "intensity equator" and is a great circle which contains the directions to the earth (E) and to the sun (S). Considering an element of surface ds whose spherical coordinates, with respect to the intensity equator and the center (E) of the visible planetary disk, are assumed as ψ for latitude and ω for longitude, then the size of the element ds, denoting the radius of the planet by ρ, will be

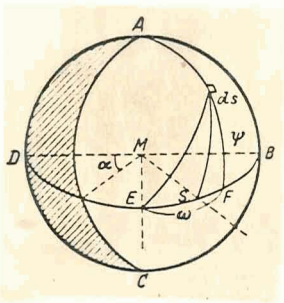

Fig.19 Illumination of a Sphere.

$$ds = \rho^2 \cos\psi\, d\omega\, d\psi .$$

The angle of incidence i of the light from the sun on the element ds and the reflection angle ε of this element toward the earth, both assumed as infinitely far, are determined from the rectangular spherical triangles FSds and FEds as follows:

$$\left.\begin{aligned} \cos i &= \cos\psi\cos(\omega - \alpha), \\ \cos\varepsilon &= \cos\psi\cos\omega . \end{aligned}\right\} \tag{5}$$

Substituting these values into eqs.(1) and (2) will yield expressions for the quantity of light radiated by the element ds at a phase angle α toward the earth, expressed in spherical coordinates:

$$\begin{aligned} dq_1 &= \Gamma_1 \rho^2 \cos^3\psi\, d\psi \cos(\omega - \alpha)\cos\omega\, d\omega , \\ dq_2 &= \Gamma_2 \rho^2 \cos^2\psi\, d\psi \frac{\cos\omega\cos(\omega - \alpha)}{\cos(\omega - \alpha) + \lambda\cos\omega}\, d\omega . \end{aligned}$$

If the amount of light, transmitted by the entire illuminated portions of the visible planetary disk to the earth, is to be calculated, the above expressions must be integrated for the surface of this portion. As shown in the diagram, the limits of integration for ψ are $-\pi/2$ and $+\pi/2$ while, for ω, they are $-\pi/2 + \alpha$ and $+\pi/2$. Therefore, we have the following expression for the total quantity of light in the case of Lambert's law:

$$q_1 = \Gamma_1 \varrho^2 \int_{-\pi/2}^{+\pi/2} \cos^3\psi \, d\psi \int_{\alpha-\pi/2}^{\pi/2} \cos(\omega - \alpha)\cos\omega \, d\omega .$$

Since, however, /64

$$\int_{-\pi/2}^{+\pi/2} \cos^3\psi \, d\psi = \tfrac{4}{3} \quad \text{and} \quad \int_{\alpha-\pi/2}^{\pi/2} \cos(\omega - \alpha)\cos\omega \, d\omega = \tfrac{1}{2}[(\pi - \alpha)\cos\alpha + \sin\alpha],$$

the integration will finally yield

$$q_1 = \Gamma_1 \varrho^2 \tfrac{2}{3} [\sin\alpha + (\pi - \alpha)\cos\alpha]. \tag{6}$$

For full illumination, when sun, planet, and earth are in one line and when $\alpha = 0$, this yields $q_1^0 = \frac{2}{3}\pi\Gamma_1\rho^2$. Consequently, we also have

$$q_1 = q_1^0 \frac{\sin\alpha + (\pi - \alpha)\cos\alpha}{\pi} = q_1^0 \varphi_1(\alpha). \tag{7}$$

In the case of the Lommel-Seeliger law, the integration proceeds as follows: We have

$$q_2 = \Gamma_2 \varrho^2 \int_{-\pi/2}^{\pi/2} \cos^2\psi \, d\psi \int_{\alpha-\pi/2}^{\pi/2} \frac{\cos\omega\cos(\omega - \alpha)}{\cos(\omega - \alpha) + \lambda\cos\omega} d\omega .$$

The first of the two integrals has the value $\pi/2$. For solving the second integral, Seeliger introduced new constants m and μ by means of the equations

$$m\sin\mu = \sin\alpha$$
$$m\cos\mu = \lambda + \cos\alpha .$$

We then obtain

$$q_2 = \frac{\Gamma_2\varrho^2\pi}{4m} \int_{\alpha-\pi/2}^{\pi/2} \frac{\cos\alpha + \cos(2\omega - \alpha)}{\cos(\omega - \mu)} d\omega ,$$

and, setting also $\omega - \mu = y$,

$$q_2 = \frac{\Gamma_2\varrho^2\pi}{4m} \int_{\alpha-\pi/2-\mu}^{\pi/2-\mu} \frac{\cos\alpha + \cos(2y + 2\mu - \alpha)}{\cos y} dy$$
$$= \frac{\Gamma_2\varrho^2\pi}{4m} \left\{ \int_{\alpha-\pi/2-\mu}^{\pi/2-\mu} \frac{\cos\alpha - \cos(2\mu - \alpha)}{\cos y} dy + 2\int_{\alpha-\pi/2-\mu}^{\pi/2-\mu} [\cos(2\mu - \alpha)\cos y - \sin(2\mu - \alpha)\sin y] \, dy \right\}.$$

Since

$$\int_{\alpha-\pi/2-\mu}^{\pi/2-\mu} \frac{dy}{\cos y} = \ln\left[\tan\left(\frac{\pi}{4} + \frac{y}{2}\right)\right]_{\alpha-\pi/2-\mu}^{\pi/2-\mu} = \ln\left[\cot\frac{\alpha - \mu}{2}\cot\frac{\mu}{2}\right],$$

we obtain

$$q_2 = \frac{\Gamma_2 \varrho^2 \pi}{2}\left\{\frac{2\cos\frac{\alpha}{2}\cdot\cos\left(\mu-\frac{\alpha}{2}\right)}{m} + \frac{\sin\mu\sin(\mu-\alpha)}{m}\ln\left[\cot\frac{\alpha-\mu}{2}\cot\frac{\mu}{2}\right]\right\}. \tag{8}$$

For full illumination, we have $\alpha = 0$ so that $\mu = 0$ and $m = 1 + \lambda$, whence

$$q_2^0 = \frac{\Gamma_2 \varrho^2 \pi}{1+\lambda}. \tag{9}$$

More important is the case $\lambda = 1$. Here, $m\cos\mu = 1 + \cos\alpha$; in addition, $\tan\mu = \frac{\sin\alpha}{1+\cos\alpha} = \tan\frac{\alpha}{2}$ or $\mu = \frac{\alpha}{2}$ and $m = 2\cos\frac{1}{2}\alpha$. Consequently, in this case we obtain, for the total reflected quantity of light /65

$$q_2 = \frac{\Gamma_2 \varrho^2 \pi}{2}\left\{1 - \sin\frac{\alpha}{2}\tan\frac{\alpha}{2}\ln\cot\frac{\alpha}{4}\right\} = \frac{\Gamma_2 \varrho^2 \pi}{2}\varphi_2(\alpha); \tag{10}$$

from which, at full illumination, it follows that

$$q_2^0 = \frac{\Gamma_2 \varrho^2 \pi}{2}. \tag{11}$$

Thus, we have

$$q_2 = q_2^0\left\{1 - \sin\frac{\alpha}{2}\tan\frac{\alpha}{2}\ln\cot\frac{\alpha}{4}\right\} = q_2^0\varphi_2(\alpha). \tag{12}$$

Consequently, eqs.(7) and (12) give the quantity of light reflected by the planet as a function of the phase angle alone. This function of the phase angle, which is of considerable importance in the photometry of planets, is known as the phase curve of the planet. The curve can be directly determined from observations, on expressing the brightnesses of the planets at different phase angles by the opposition brightness. However, to obtain a comparison of the observed with the theoretical phase curves $\varphi_1(\alpha)$ and $\varphi_2(\alpha)$ according to eqs.(7) and (12), the fact must be taken into consideration that the distance of the planets from the earth and sun is subject to variations. Since the quantities q_1 and q_2 resp. q_1^0 and q_2^0 generally express the amounts of light reflected in direction to the earth and thus are valid for a distance 1 and unit area at normal incidence, they would have to be multiplied by a factor of $1/\Delta^2$ resp. $1/\Delta_0^2$ to become comparable with the observations, if Δ_0 represents the distance of the planet from the earth in opposition. In addition, the variability of the constants Γ_1 and Γ_2 with the solar distance of the planet must be allowed for. We have

$$\Gamma_1 = \frac{A_1}{\pi}L \quad \text{and} \quad \Gamma_2 = \frac{A_2}{\pi}L,$$

where L denotes the quantity of light coming from the sun and vertically incident on unit surface of the planet. This is variable with the solar distance of the

planet and proportional to $1/r^2$. Denoting the value of r at the instant of opposition by r_0, the quantities of light Q_1, Q_2, Q_1^0, Q_2^0 actually striking the eye of the observer will be

$$\left.\begin{aligned} Q_1 &= q_1 \frac{1}{\Delta^2 r^2}; & Q_1^0 &= q_1^0 \frac{1}{\Delta_0^2 r_0^2}, \\ Q_2 &= q_2 \frac{1}{\Delta^2 r^2}; & Q_2^0 &= q_2^0 \frac{1}{\Delta_0^2 r_0^2}. \end{aligned}\right\} \tag{13}$$

Consequently, eqs.(7), (12), and (13) will yield the equations

$$\left.\begin{aligned} Q_1 &= Q_1^0 \frac{\Delta_0^2 r_0^2}{\Delta^2 r^2} \varphi_1(\alpha), \\ Q_2 &= Q_2^0 \frac{\Delta_0^2 r_0^2}{\Delta^2 r^2} \varphi_2(\alpha). \end{aligned}\right\} \tag{14}$$

The curves $\varphi_1(\alpha)$ and $\varphi_2(\alpha)$, calculated from these equations with the aid of observations, are directly comparable with the theoretical curves. The latter are tabulated in the Appendix for all phase angles from 0° to 180° (Table VIa).

Equations (6) and (10) can also be used for determining the albedo of the planets. For this, we first eliminate the quantity L not accessible to observation from the constants Γ_1 and Γ_2. According to eq.(45) (p.30), we have L = /66
$= \pi J \sin^2 s$ where J denotes the luminosity of the sun and s the apparent radius of the sun, viewed from the planet. Hence,

$$\Gamma_1 = JA_1 \sin^2 s \quad \text{and} \quad \Gamma_2 = JA_2 \sin^2 s. \tag{15}$$

In these expressions, the variability of the constants Γ_1 and Γ_2 with the distance r of the planet from the sun has already been allowed for. Thus, to pass again from q_1 and q_2 to the measurable quantities Q_1 and Q_2, the former quantities need be divided only by $1/\Delta^2$. On introducing the apparent radius σ of the planet, viewed from the earth, over the relation $\sin\sigma = \frac{\rho}{\Delta}$, we obtain instead of eqs.(6) and (10):

$$\left.\begin{aligned} Q_1 &= \tfrac{2}{3}\pi J A_1 \sin^2 s \sin^2\sigma \varphi_1(\alpha), \\ Q_2 &= \tfrac{1}{2}\pi J A_2 \sin^2 s \sin^2\sigma \varphi_2(\alpha). \end{aligned}\right\} \tag{16}$$

For full illumination,

$$\left.\begin{aligned} Q_1^0 &= \tfrac{2}{3} J A_1 \pi \sin^2 s_0 \sin^2\sigma_0, \\ Q_2^0 &= \tfrac{1}{2} J A_2 \pi \sin^2 s_0 \sin^2\sigma_0, \end{aligned}\right\} \tag{17}$$

where s_0 and σ_0 denote the apparent radii of sun and planet at the time of opposition.

34. Determination of Albedo and Diameter of Planets

The next step is to eliminate the quantity J in eqs.(16) and (17) for determining the albedo. Let L′ be the amount of light, coming from the sun and incident on unit area of the earth's surface; then

$$L' = J\pi \sin^2 S,$$

where S denotes the apparent radius of the sun, viewed from the earth. The ratio of the brightnesses of the planet to the sun or the quotient Q/L′ will be denoted by M. Then, eqs.(16) will yield the following albedo values:

$$\left.\begin{aligned} A_1 &= \tfrac{3}{2} M \frac{\sin^2 S}{\sin^2 s \sin^2 \sigma} \frac{1}{\varphi_1(\alpha)}, \\ A_2 &= 2M \frac{\sin^2 S}{\sin^2 s \sin^2 \sigma} \frac{1}{\varphi_2(\alpha)}. \end{aligned}\right\} \qquad (18)$$

If the brightness ratio M_0 is to be used for the moment of opposition, eq.(17) will furnish, in a similar manner,

$$\left.\begin{aligned} A_1 &= \tfrac{3}{2} M_0 \frac{\sin^2 S}{\sin^2 s_0 \sin^2 \sigma_0}, \\ A_2 &= 2M_0 \frac{\sin^2 S}{\sin^2 s_0 \sin^2 \sigma_0}. \end{aligned}\right\} \qquad (19)$$

It is obvious that $A_2 = \frac{4}{3} A_1$. According to the two definitions, the albedo values are derived from the opposition brightness of the planet, thus being at a constant ratio. The values calculated from eqs.(18) will then yield different values, depending on the value α; without knowing the real phase curve $\varphi(\alpha)$ it is impossible to decide which albedo value is closest to the real value. This uncertainty, for example, exists for small planets.

The same uncertainty is inherent to a method of determining the diameter of the planet from the systems of equations (18) and (19), if its albedo and apparent brightness are known. The problem is of great importance for asteroids and those planetary moons whose disks are too small for direct measurement. This /67 method has been used frequently and yielded rough estimates of the dimensions of these small celestial bodies.

A prerequisite here is to determine the brightness of the object H_0 in relation to that of one of the main planets in opposition. If the ratio of the albedo values according to both definitions of these values is denoted by a, the apparent radius of the sun viewed from both planets by $s_{1,0}$ resp. $s_{2,0}$, and the apparent radii of the planets viewed from the earth by $\sigma_{1,0}$ resp. $\sigma_{2,0}$, the following equation will be obtained from eqs.(19) for determining the unknown $\sigma_{1,0}$:

$$\sin^2 \sigma_{1,0} = \frac{H_0}{a} \frac{\sin^2 s_{2.0} \sin^2 \sigma_{2.0}}{\sin^2 s_{1.0}}, \qquad (20)$$

which means that we obtain one and the same value for both diffusion laws. Conversely, when replacing the opposition brightnesses by brightnesses at arbitrary phase angles α_1 resp. α_2 whose ratio is denoted by H, different values of the radii will be obtained under application of eqs.(18):

$$\left.\begin{aligned}\sin^2\sigma_1 &= \frac{H}{a}\,\frac{\sin^2 s_2 \sin^2\sigma_2}{\sin^2 s_1}\,\frac{\varphi_1(\alpha_2)}{\varphi_1(\alpha_1)}\,,\\ \sin^2\sigma_1 &= \frac{H}{a}\,\frac{\sin^2 s_2 \sin^2\sigma_2}{\sin^2 s_1}\,\frac{\varphi_2(\alpha_2)}{\varphi_2(\alpha_1)}\,.\end{aligned}\right\} \qquad (21)$$

In all preceding considerations, the planets were assumed as spherical. This raises the question whether it is necessary, in planets with extensive oblateness such as Jupiter and Saturn, to take this flattening into consideration. Whereas, for the older photometric methods, the conventional theory was entirely sufficient, it might be that, for reduction of the newest photoelectric measurements, a theory developed by Seeliger (Ref.116) on the illumination of ellipsoids of revolution may become necessary. This theory, on neglecting third powers of the oblateness, leads to simple formulas which will be given here together with auxiliary tables for their use; derivations of these formulas are cumbersome and, since they are of only specialized interest, can be omitted with full justification. Denoting by a and b the two semiaxes of the planets, by σ the apparent semimajor axis, and by A the quadrant angle of elevation of the earth above the equatorial plane of the planet, we obtain the following quantity of light reflected at the phase angle α, instead of eqs.(16)

$$\left.\begin{aligned}Q_1 &= 2\pi J A_1 \sin^2 s \sin^2\sigma \cos\alpha\,(P\cos^2 A + R\sin^2 A)\,,\\ Q_2 &= \frac{1}{2}\pi J A_2 \sin^2 s \sin^2\sigma\,\varphi_2(\alpha)\sqrt{1+\frac{a^2-b^2}{b^2}\sin^2 A}\,.\end{aligned}\right\} \qquad (22)$$

Here, P and R represent two quantities depending only on the oblateness of the planet and tabulated in Table VIb. For Saturn, Table VIc for various A contains the functions $Z = P\cos^2 A + R\sin^2 A$ and

$$\log\sqrt{1+\frac{a^2-b^2}{b^2}\sin^2 A}\,.$$

Thus, eqs.(22) differ from those for a sphere only by simple factors. With respect to their application, the following facts must be recalled:

The planets Mercury, Venus, and Mars, if at all, have only minor oblate- /68
ness. For these planets, eqs.(16) are fully sufficient. For Uranus and Neptune, it is completely superfluous to take the phase into consideration. Consequently, if the oblateness is to be considered, formulas must be used as they are obtained from the above formulas for $\alpha = 0$. These formulas, generally valid for the opposition at $A \neq 0$, are as follows:

$$\left.\begin{aligned}Q_1^0 &= 2\pi J A_1 \sin^2 s_0 \sin^2\sigma_0 (P\cos^2 A + R\sin^2 A),\\ Q_2^0 &= \frac{\pi}{2} J A_2 \sin^2 s_0 \sin^2\sigma_0 \sqrt{1+\frac{a^2-b^2}{b^2}\sin^2 A}\,.\end{aligned}\right\} \qquad (23)$$

In the case of Jupiter, the phase angle reaches $12^{\circ}.5'$ while the elevation of the earth above the equatorial plane of the planet is always less than 3° and $\frac{a^2 - b^2}{b^2} = 0.1$. Consequently, the entire reduction with respect to phase, for the case of Jupiter, will be P cos α resp. $\varphi_2(\alpha)$ and

$$Q_1 = Q_1^0 P \cos\alpha\,; \qquad Q_2 = Q_2^0 \varphi_2(\alpha)\,. \tag{24}$$

For Saturn, because of the strict reductions, it may be of importance to use eqs.(22) in a strict manner. In the theory of illumination of this planet, the reduction of its brightness to the instant A = 0 at which the earth enters the plane of its equator and the ring becomes invisible, plays a certain role. Denoting the value of Q for $\alpha = 0$ and A = 0 by $Q^0(0)$, we have

$$\left.\begin{aligned} Q_1 &= Q_1^0(0)\,\frac{\sin^2 s \sin^2\sigma}{\sin^2 s_0 \sin^2\sigma_0}\left(\cos^2 A + \frac{R}{P}\sin^2 A\right)\cos\alpha\,. \\ Q_2 &= Q_2^0(0)\,\frac{\sin^2 s \sin^2\sigma}{\sin^2 s_0 \sin^2\sigma_0}\sqrt{1 + \frac{a^2 - b^2}{b^2}\sin^2 A}\,\varphi_2(\alpha)\,. \end{aligned}\right\} \tag{25}$$

The quantity $\log Z = \log\left(\cos^2 A + \frac{R}{P}\sin^2 A\right)$ has been calculated for Saturn in a table by Seeliger, which is reproduced in our Table VIc.

35. Bond's Definition of Albedo of a Planet

Whereas both Lambert's and Seeliger's definition of albedo presupposed the validity of a certain reflection law, Bond (Ref.117) suggested as early as 1861 a definition of albedo which can be determined from photometric observations of a planet without making any assumption as to the reflection law valid on the surface. It is H.N.Russell's merit (Ref.118) of having drawn attention to the significance of Bond's albedo for astronomical purposes. The definition of Bond's or, as it is also called, spherical albedo is as follows: A sphere is exposed to illumination by parallel rays; the albedo of this sphere is the ratio of omnilaterally scattered light to incident light.

The quantity of light incident on a zone of the sphere of radius 1, between the angles of incidence i and i + di, is equal to $2\pi L \cos i \sin i\, di$. Of this, the fraction A determined by eq.(25) on p.60, is reflected. Consequently, since the total incident amount of light is equal to πL, we have for the above-defined albedo

$$A_B = 2\int_0^{\pi/2} A \sin i \cos i\, di = 4\pi C \int_0^{\pi/2} \sin i\, di \int_0^{\pi/2} f(i,\varepsilon)\sin\varepsilon\, d\varepsilon\,. \tag{26}$$

The advantage of this definition, compared to the others, lies in the possibility of determining its value even without knowing the function f(i, ε). /69

If $\varphi(\alpha)$ is the observed phase curve, reduced to constant distances of the

planet from the earth (Δ) and the sun (r), then we have $\varphi(\alpha) = 1$ for $\alpha = 0$. As before, let Q_0 be the amount of light coming from the planet and incident on unit area of the earth's surface, in opposition.

Let us imagine a sphere of radius Δ_0, with the planet at the center; then, the amount of light reflected from the planet on the spherical zone between the angles α and $\alpha + d\alpha$ will be equal to $2\pi\Delta_0^2 Q_0 \varphi(\alpha) \sin\alpha\, d\alpha$, and the quantity of light incident on the entire surface of the sphere will become

$$2\pi \Delta_0^2 Q_0 \int_0^\pi \varphi(\alpha) \sin\alpha \, d\alpha .$$

Let the apparent radius of the sun, for unit distance S, be s_0 at a distance r of the planet; let the amount of light coming from the sun and incident on unit area of the earth be L', and let J denote the intensity of solar radiation. If, furthermore, M_0 denotes the ratio of brightness of the planet in opposition (distances r_0 and Δ_0) to brightness of the sun at a distance 1, then $M_0 = \frac{Q_0}{L'}$, $Q_0 = M_0 J\pi \sin^2 S$; the quantity of light incident on the planet is $\pi\rho^2 J\pi \sin^2 s_0$. Consequently, the value of Bond's albedo is expressed by

$$A = \frac{2 M_0 \Delta_0^2 \sin^2 S \int_0^\pi \varphi(\alpha) \sin\alpha \, d\alpha}{\rho^2 \sin^2 s_0} = \frac{\sin^2 S \, M_0}{\sin^2\sigma_0 \sin^2 s_0} 2\int_0^\pi \varphi(\alpha) \sin\alpha \, d\alpha = pq, \qquad (27)$$

where σ_0 denotes the apparent radius of the planet in opposition, viewed from the earth. Let p be the product of the factors depending only on the geometric and photometric relations of the planet in opposition. Then, the second factor q will be the double integral determined exclusively by the phase curve.

The first factor, on introducing the distances and the radius of the planet, can be written in different form:

$$p = \frac{\sin^2 S}{\sin^2\sigma_0 \sin^2 s_0} M_0 = \frac{r_0^2 \Delta_0^2}{\rho^2} M_0 = \frac{r_0^2}{\sin^2\sigma_0} M_0 . \qquad (28)$$

Denoting by σ_0^1 the radius of the planet in seconds of arc, by g its stellar size in opposition (both referred to unit distance between sun and earth), and by G the brightness of the sun in magnitude classes again for the distance 1, then we have the following expression since ρ is measured in the same unit so that $\rho = \sin\sigma_0^1$:

$$\log p = 0.4(G - g) - 2\log\sin\sigma_0^1 . \qquad (29)$$

It is of interest that the factor p, defined in this manner, also represents the ratio of the brightness of the planet in opposition to that of a self-luminous body of the same size and position, which emits from each unit of its surface as much light as the planet receives from the sun at normal incidence.

The factor q under the integral sign contains the real phase curve of the planet. If this is replaced by the expressions $\varphi(\alpha)$ according to the Lambert and Seeliger laws, different values for q will be obtained. According to Lambert, we have /70

$$\left.\begin{aligned}\varphi_1(\alpha) &= \frac{1}{\pi}[\sin\alpha + (\pi-\alpha)\cos\alpha],\\ q &= 2\int_0^{\pi}\varphi_1(\alpha)\sin\alpha\, d\alpha = 1{,}5000.\end{aligned}\right\} \quad (30)$$

from which it follows that

According to the Lommel-Seeliger law, we have

$$\left.\begin{aligned}\varphi_2(\alpha) &= 1 - \sin\frac{\alpha}{2}\tan\frac{\alpha}{2}\ln\cot\frac{\alpha}{4};\\ q &= 2\int_0^{\pi}\varphi_2(\alpha)\sin\alpha\, d\alpha = (1-\ln 2)\tfrac{4}{3}\pi = 1.6366.\end{aligned}\right\} \quad (31)$$

In addition, we have the following relations for the latter law in accordance with the first definition of albedo [eq.(25) on p.60 and eq.(26) on p.77]:

$$\left.\begin{aligned}A &= 2\pi C\int_0^{\pi/2}\frac{\sin\varepsilon\cos\varepsilon}{\cos i+\cos\varepsilon}d\varepsilon = 2\pi C[1-\cos i\ln(1+\sec i)],\\ A_B &= \int_0^{\pi/2}A\sin i\cos i\, di = \tfrac{8}{3}\pi C(1-\ln 2) = 0.8183\,\pi C.\end{aligned}\right\} \quad (32)$$

The factor in parentheses in the first of these expressions fluctuates between values of 0.308 for $i = 0^\circ$ and unity for $i = 90^\circ$. Since, however, A can never be larger than 1 it follows that πC cannot be larger than 0.5 and A_B cannot be larger than 0.409. With consideration of the relation $A_B = pq$ and eq.(31), it can be concluded that a planet for which p is larger than 0.25 cannot obey the Lommel-Seeliger law.

If the integral from the actually observed phase curve can be calculated by mechanical quadrature, the Bond albedo will furnish an albedo value freed of all hypotheses which, in addition, characterizes the absorptivity of the planet surface in the strictest manner. If the concept is referred not only to the light radiation but also to the entire incident and reflected radiation, it will be useful for determining the temperature of a given planet.

Unfortunately, the phase curves for angles α from 0° to 180° can be observed only for the inferior planets. For the superior planets, Russell (Ref.119) was forced to use hypotheses and analogies in determining his albedo values. The great difference between Bond's albedo values and earlier values can be demonstrated on the example of Venus. Müller's observations of this planet yield a value of 1.194 for q and of 0.492 for p as well as, for the albedo, $A_B = pq = 0.59$, whereas Müller, from the same observations, derived values of 0.758 resp. 1.010 for the Lambert resp. for the Seeliger albedo. The value of the Seeliger albedo, which is greater than unity, constitutes a confirmation of the theorem

that, in planets for which p is larger than 0.25, the Seeliger reflection law can no longer be valid.

It is of some importance to note that p can be identified with the reflection coefficient in direction of the irradiation for irregularly shaped bodies; p can also be referred to the natural irregular forms of reflecting bodies and thus is most suitable for identifying the reflecting coefficients of individual lunar configurations, observed during opposition, with those of terrestrial substances. /71

Finally, it should be mentioned that Bond's albedo for a sphere is identical with the albedo of a plane area illuminated by parallel rays coming from all directions and uniformly striking this area, if the albedo of such an area is to mean the ratio of the total quantity of light reflected in all directions to the incident quantity. If L denotes the amount of light coming from unit solid angle and incident on the area, then the quantity of light received by the element $d\sigma$ under angles of incidence between i and i + di will be

$$2\pi L \cos i \sin i \, di \, d\sigma,$$

of which the fraction A is reflected. On integrating over the hemisphere and dividing by the total incident quantity of light $\pi L d\sigma$, the above-defined albedo will become

$$A_B = 2\int_0^{\pi/2} A \sin i \cos i \, di = 4\pi C \int_0^{\pi/2} \sin i \, di \int_0^{\pi/2} f(i, \varepsilon) \sin \varepsilon \, d\varepsilon. \qquad (33)$$

This expression is identical with that in eq.(26).

Determination of Bond's albedo is strictly possible only for the inferior planets, since the phase curves from $\alpha = 0^\circ$ to $\alpha = 180^\circ$ are known only for these. In calculating q for Mars and for the inferior planets, Russell used the following consideration: The theoretical curves for $\varphi(\alpha)$ calculated according to

TABLE 7

$q/\varphi(\alpha)$

α	Lambert	Seeliger	Venus	Moon	Mercury
0°	1.50	1.64	1.19	0.72	0.42
20	1.60	1.77	1.54	1.06	0.83
40	1.88	2.08	2.00	1.64	1.63
50	2.12	2.32	2.32	2.07	2.28
60	2.46	2.64	2.72	2.68	3.21
80	3.66	3.60	3.88	4.77	6.41

Lambert and Seeliger and the phase curves of Moon, Mercury, and Venus accurately known from observations, all show a widely differing slope. However, as indicated in Table 7, these curves give almost the same value for the quotient $q/\varphi(\alpha)$ at $\alpha = 50^\circ$, as it is obtained on the average, namely 2.20. Since the

albedo is determined also by the equation $A_B = p(\alpha) \frac{q}{\varphi(\alpha)}$, the following empirical equation can be written, provided that M_{50} is used for denoting the quotient of the brightness of the planet at a phase angle of 50° and the brightness of the sun:

$$A_B = 2.20\, M_{50} \frac{r^2 \Delta^2}{\varrho^2}. \qquad (34)$$

Here, the coefficient 2.20, considering the deviations of the individual values in the table as being of a random nature, is accurate to within a few percent; with the same accuracy, the albedo is obtained from the above formula under the assumption that also the curves of the other planets for $q/\varphi(\alpha)$ at $\alpha = 50°$ go through the corresponding point.

Since the phase curve of Mars is known to within $\alpha = 47°$, the value M_{50} can be found by minor extrapolation. In the case of asteroids, whose maximum /72
phase angle is between 20° and 30°, more extensive extrapolations are required.

The albedo values for Jupiter, Saturn, Uranus, and Neptune can only be estimated.

TABLE 8

BOND'S ALBEDO OF PLANETS AND SATELLITES

	p	q	Visual Albedo A_B	Photographic Albedo
Moon	0.105	0.694	0.073	0.051
Mercury	0.164	0.42	0.069	—
	0.077	0.72	0.055	—
Venus	0.492	0.20	0.59	0.60
Mars	0.139	1.11	0.154	0.090
Jupiter	0.375	1.5:	0.56:	0.73:
Saturn	0.420	1.5:	0.63:	0.47:
Uranus	0.42	1.5:	0.63:	—
Neptune	0.49	1.5:	0.73	—
Ceres	0.10	0.55	0.06:	—
Pallas	0.13	0.55:	0.07:	—
Juno	0.22	0.55:	0.12:	—
Vesta	0.48	0.55:	0.26:	—
Jupiter satellite I	0.46	1.5:	0.69:	—
" " II	0.51	1.5:	0.76:	—
" " III	0.30	1.5:	0.45:	—
" " IV	0.11	1.5:	0.16:	—
Titan	0.33	1.5:	0.50	—
Earth	0.37	1.20	0.45	—
	0.65	0.70	0.45	—

Of the two values for the earth's albedo, the first presupposes a phase curve of the earth equal to that of Venus and the second equal to that of the moon. The columns represent a value based on estimate. For the photographic albedo of the earth, according to Bond's definition, E.Öpik (Ref.120) derived a value of $A_B = 0.63 \pm 0.08$ in which he used the phase curve of Venus as basis.

36. Light Distribution over a Planetary Disk

Although, in view of the above statements, it cannot be expected that one of the two frequently mentioned reflection laws is valid for any planet, it is of importance to realize the manner in which a planet, meeting the ideal conditions listed in Section 32, would have to present itself to observation under various conditions. The study of light distribution over surfaces, using a surface photometer constructed specifically for this purpose, has recently been started by various authors and it can be expected that, with progressive perfection of planet photography, the study will be further expanded. For interpreting the observed brightness ratios, the theoretically calculated values represent a first criterion. For this reason, we will briefly review the simple considerations made by Anding (Ref.121) on this subject.

Equations (1) and (2) (p.70) for the quantities of light reflected by the element ds of the planet surface, after dividing by the apparent size of the element ds cos ε, yield the following expressions for the brightnesses on the planet surface:

$$\left.\begin{aligned} h_1 &= I'_1 \cos i, \\ h_2 &= I'_2 \frac{\cos i}{\cos i + \cos \varepsilon}. \end{aligned}\right\} \tag{35}$$

If, instead of the angles i and ε, the spherical coordinates ψ and ω defined by eq.(5) are introduced and if also Γ_1 and Γ_2 are substituted by their values of eq.(15) on p.74, we obtain /73

$$\left.\begin{aligned} h_1 &= JA_1 \sin^2 s \cos\psi \cos(\omega - \alpha), \\ h_2 &= JA_2 \sin^2 s \left[\frac{1}{2} + \frac{1}{2} \tan \frac{\alpha}{2} \tan \left(\omega - \frac{\alpha}{2}\right)\right]. \end{aligned}\right\} \tag{36}$$

From these formulas, the light distribution at full illumination, i.e., at α = = 0°, can be easily understood. According to the second equation of the system (36), this brightness is constant at all points of the disk. According to the first equation, the apparent brightness is proportional to cos ψ cos ω. Thus, it decreases from the center of the disk, where ω and ψ = 0, toward the limb and, in the direct vicinity of the limb where the angle of incidence of the light is almost 90°, becomes vanishingly small with cos i = cos ψ cos ω. The brightness at the center of the fully illuminated planetary disk, which will be denoted by h°, is

$$\left.\begin{aligned} h_1^\circ &= JA_1 \sin^2 s, \\ h_2^\circ &= \tfrac{1}{2} JA_2 \sin^2 s. \end{aligned}\right\} \tag{37}$$

If these values are substituted into eq.(36), the apparent brightnesses at an arbitrary point of the planetary disk will be obtained in units of the central brightness in opposition:

$$h_1 = h_1^\circ \cos\psi \cos(\omega - \alpha), \tag{38}$$

$$h_2 = h_2^0\left\{1 + \tan\frac{\alpha}{2}\tan\left(\omega - \frac{\alpha}{2}\right)\right\}.$$

To illustrate the curves of equal brightness for various phases, i.e., the isophots, we will introduce rectangular coordinates on the disk, counted from the intensity equator and the center of the visible disk. Let the intensity equator be the x-axis, positive on the side facing the sun. The radius of the planet is set as equal to 1. We then have

$$y = \sin\psi \quad \text{and} \quad x = \cos\psi\sin\omega. \tag{39}$$

Substituting these values into the first of the equations of the system (38) and denoting the quotient h_1/h_1^0 by a, we obtain

$$y^2\cos^2\alpha + x^2 - 2xa\sin\alpha + (a^2 - \cos^2\alpha) = 0. \tag{40}$$

This is the equation of the geometric locus of all points of the disk, having a brightness of a. It constitutes the equation of an ellipse whose minor axis is located along the x-axis; its center is by the segment a $\sin\alpha$ distant from the center of the disk; the semiaxes have the values $\sqrt{1 - a^2}$ and $\cos\alpha\sqrt{1 - a^2}$. Thus, the curves of equal brightness, according to Lambert, represent ellipses with different centers and different axes whose axial ratio, however, always remains equal to 1:cos α.

On a fully illuminated disk, the ellipses are transformed into circles with the radius $\sqrt{1 - a^2}$. The maximum of brightness is located at the center. For values of α between 0° and 90°, i.e., in the case of a more than half-illuminated disk, this maximum which always remains equal to h_1^0 is located at the point of the equator for which $\psi = 0$ and $\omega = \alpha$, i.e., at the point illuminated vertically by the sun. This point gradually migrates from the center of the disk to the positive limb which it reaches at $\alpha = 90°$. Consequently, the center of the positive limb, in quadrature, is just as bright as the center in opposition. If /74 α is accurately 90°, the ellipses of equal brightness - since their minor axes become zero - change into straight lines which are parallel to the terminator. If the phase increases further, the center of the positive limb will remain the brightest point of the disk. Its brightness is $h_1^0\sin\alpha$ and gradually decreases to a value of 0. Thus, this point has brightnesses, counted from the opposition, that first increase from 0 to h_1^0 and then, after quadrature, decrease from h_1^0 to 0. Toward the negative limb, the brightness at all phases decreases to zero. The positive limb is thus the limb which, because of its greater brightness, is always more sharply delimited which, after quadrature where the maximum of brightness is concentrated at this site, becomes especially pronounced.

The light distribution over a planetary disk is entirely different when applying the Lambert law than when applying the Lommel-Seeliger law. By exactly the same transformation [eq.(39)] of the second equation of the system (38), again denoting h_2/h_2^0 by a, the following formula is obtained for the geometric locus of points of equal brightness:

$$y^2 + x^2\frac{1 + 2b\cos\alpha + b^2}{(1 - b\cos\alpha)^2} = 1. \tag{41}$$

Here, $b = \frac{2 - a}{a}$ is used for abbreviation. This represents the equation of an ellipse whose center is located at the center of the disk and whose semimajor axis coincides with the connecting line between the poles whereas the value of the semiminor axis is $\frac{1 - b \cos \alpha}{\sqrt{1 - 2b \cos \alpha + b^2}}$. The curves of equal brightness are thus always semiellipses going through the poles. Equation (38) indicates that, at a fully illuminated disk, the brightness is the same for all points. In the case of a more than half-illuminated disk, ω may assume all values between $-\left(\frac{\pi}{2} - \alpha\right)$ and $+\frac{\pi}{2}$, and the brightness will increase continuously from zero at the negative limb to a value $h_2 = 2h_2^0$ at the positive limb. Even in the first or second quarter or in the crescent phase, the brightness at the positive limb will remain constant and equal to $2h_2^0$; the difference in appearance of the two limbs is even more pronounced here than in the case of Lambert's law.

37. Influence of Surface Roughnesses on the Appearance and Phase Curve of a Planet

Zöllner (Ref.47, p.38) made an attempt to calculate the influence of elevations at the lunar surface on the slope of the phase curve, obtaining a very simple expression which, however, as proved by both H.Seeliger and A.Searle (Ref.122, 123), was based on unjustified simplifications and, in addition, had been erroneously derived. As basis for his theory, Zöllner used the readily proved theorem that, under assumption of the Lambert law, the illumination of a smooth sphere is given at each phase angle by the same formula (except for the constant) as the illumination of the lateral area of a circular cylinder of definite size and position. Zöllner believed to be justified to apply this theorem, which in itself is correct, to the case in which both sphere and cylinder no longer have a uniformly rough surface but one covered with elevations; he believed furthermore that an irregular distribution of roughnesses can be replaced by a regular distribution so that, instead of arbitrarily distributed /75
mountains on the lunar surface, the illumination of a regularly grooved cylinder could be studied, whose grooves are formed by two planes each that intersect at a certain angle along an edge parallel to the cylinder axis. It is logical that the legitimacy of such a substitution would have to be proved; however, even if this assumption were admitted, the derivation of the illumination formula would still be erroneous and the fact that Zöllner was able to make this erroneous formula, containing only one constant (namely, the elevation angle of the mountains), agree with the observations of the luminance of the moon between $\alpha = 0^\circ$ and $\alpha = 70^\circ$ at a value of the elevation angle of $\beta = 52^\circ$, merely proves that it might serve as an interpolation formula for the phase curve in this particular region. Naturally, the constant β has no physical meaning.

It is obvious per se that the representation of the phase curve of the moon by a theoretical formula, which is to take account of the multiplicity of lunar formations by means of some reflection law, is an unsolvable problem. The reflectivity of various lunar sectors differs enormously, and the distribution of surface roughnesses is completely irregular. Similarly, the phase curve of the

various lunar formations, as a function of their configuration, must differ completely even if each plane element of their surface would obey one and the same reflection law. If it were possible to distribute the formations of the lunar surface over a number of types and to then define the percentual share of each type in the total surface, then the phase curves and the mean brightness values for the irradiation direction (in opposition) would have to be individually determined for each type. The phase curve of total brightness would then be obtained by summation of the individual phase curves. However, a representation of the lunar phase curve obtained in this manner would have only the usefulness of a check test on the correct classification into types but would have no independent physical meaning. The very first attempt at determining the phase curves of individual moon configurations from observations was made by W.F.Wislicenus (Ref.124). The same subject was treated by Wirtz, leading to phase curves for 20 different moon configurations which, however - partly because of excessive observation errors and partly because of choice of the argument for which Wirtz selected the "photometric factor" $\frac{\cos i \cos \epsilon}{\cos i + \cos \epsilon}$ merely indicated that the Seeliger law is not even halfway sufficient for representing the brightnesses and that most lunar configurations exhibit a distinct brightness maximum for the times of opposition, independent of their location on the lunar disk. The same phenomenon was observed and emphasized as being significant in observations by Barabaschew and Markow (Ref.125, 126) who also studied the brightnesses of individual lunar configurations at different phase angles. The brightness on the lunar surface thus is greatly influenced by the casting of shadows; at full moon, we have $i = \epsilon$ independent of the position of the disk, i.e., independent of the height of the sun over the horizon of the point, and where the shadows disappear for the eye of the observer, maximum brightness occurs. Barabaschew and Markow, in a number of papers, made an attempt at a /76
theoretical interpretation of this phenomenon; the former author assumed grooves and fissures as a characteristic form of the lunar surface, while Markow revealed the errors in the mathematical treatment of the problem. He attempted to represent the brightnesses, in Barabaschew's and his own observations, by means of the Fessenkov formula for diffuse reflection; this formula is eq.(13) on p.48, abbreviated to the first term:

$$f(i, \varepsilon) = (1 + \cos^2 \alpha) \frac{\cos i \cos \varepsilon}{\cos i + \cos \varepsilon}.$$

Since the factor $(1 + \cos^2\alpha)$ decreases from 2 to 1 between the phase angles of 0° and 90°, it is obvious that the steep drop of the phase curves in this region must be more accurately allowed for by the above formula than by the simple Seeliger formula. Since, until then, no observations on $\alpha = 90^\circ$ were available, the failure of the formula for larger phase angles could not be detected. It should also be noted that the decrease in brightness, for many lunar configurations, is greatest in the immediate neighborhood of opposition and frequently is as much as 20 - 30% of the opposition brightness. Naturally, the Fessenkov formula is inadequate for this. It is also known from a survey over observations on terrestrial substances, that the formula is just as inadequate as the Seeliger formula for the real conditions in the case of solid bodies.

In a later paper, Barabaschew (Ref.127) attempted to explain his own ob-

servations by making use of J.Wilsing's theory (Ref.128) of a porous consistency of the bright lunar rays as the cause of brightness; he then extended this theory over the entire lunar surface.

E.Öpik (Ref.129) used photographic means for studying the brightnesses of a large number of lunar configurations and derived also empirical illumination formulas for the lunar continents and maria. To represent the brightnesses as a function of i, ε, α, he selected the form

$$s = a + \Delta a - 2.5\, k \log \cos i - k'\varepsilon. \tag{42}$$

Here, s denotes the brightness in magnitude classes while a, k, and k′ are parameters that differ for the maria and continents; a and k are functions of the phase angle while k′ is constant between $\alpha = 28^\circ$ and $\alpha = 121^\circ$; Δa is the relative reflectivity for a given point referring to a mean reflectivity of the respective formation (continents or maria). The values of a and k are given in tables which indicate that their slope is quite similar. Öpik gave no theoretical explanation for his formula whose usefulness he saw in the fact that it might serve for determining the terrestrial albedo from the brightness of the earthlight. The functions a and k of the phase angle, according to statements by Öpik himself, must be considered as uncertain. For their derivation, extensive empirical diurnal corrections for the individual plates were necessary.

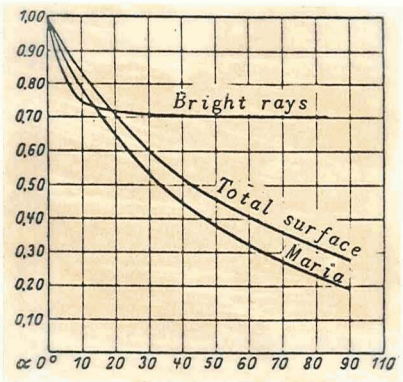

Fig.20 Slope of the Function $\psi(\alpha)$.

38. New Illumination Theory of the Moon

From the theoretical viewpoint, we had investigated the question as to the consistency of the lunar surface in some detail (Ref.130). These observations, taken with a surface photometer, refer to typical parts of the continents and maria. In addition to relative observations on the brightness of equivalent points on the disk, absolute observations of the brightness of the lunar limb /77 between the phase angles of 0° and 120° were made. This yielded the possibility of separating the influence of the phase. Various empirical formulas were tentatively derived for representing the relative brightnesses on the disk at different phase angles; the simplest, valid over a large portion of the phase, was found to be a formula of the Lommel-Seeliger form

$$f(i,\varepsilon) = \frac{\cos i \cos \varepsilon}{\cos i + \lambda \cos \varepsilon} \qquad \text{at} \qquad \lambda = \tfrac{1}{3}. \tag{43}$$

This formula fails only in the neighborhood of the terminator for angles of incidence larger than 75°. It is also possible to represent the brightnesses in the above form for all phase angles if the quantity λ is given values varying with the phase angle. However, it seems more advantageous to calculate with a constant value of λ and to investigate the dependence of the brightnesses on the phase angle in the form

$$dq = \Gamma f(i,\varepsilon)\psi(\alpha)\,ds. \qquad (44)$$

On making use of the observation by Barabaschew and Markow as to the brightness course of the bright rays, it was found that the function $\psi(\alpha)$ for these has a characteristic slope, steeply dropping in the neighborhood of opposition and, for the remaining surface, differing only little for continents and maria. Thus, three different types of lunar configurations are first differentiated, namely the continents, the maria, and the bright ray systems which differ in their reflectivity in direction of the irradiation as well as in the course of the "shadow function" $\psi(\alpha)$; further study of the variability of lunar configurations, for a more accurate classification according to the above principles, seems desirable. Figure 20 shows the slope of the shadow function $\psi(\alpha)$ under assumption of the Lambert law, for f(i, ε).

In the theoretical portion of his paper, the author used the Lambert reflection law for a plane element of area, which would best satisfy the observations on terrestrial substances. In fact, it was found that eq.(43), with the Seeliger form for f(i, ε), is useful only at variable λ and is a consequence of the special consistency of the lunar surface. Two striking features can be explained by the consistency of the lunar surface: on the one hand, the uniform brightness of the fully illuminated lunar disk, since a smooth surface, according to Lambert and also according to all experimental investigations on terrestrial substances, should show a decrease in brightness toward the limb; on the other hand, the steep drop in average brightness with the phase angle (Fig.21).

Whereas, for explaining the uniform brightness at full moon, the assumption of elevations on the surface is sufficient, the second finding of a substantial reduction in light cannot be explained in this manner.

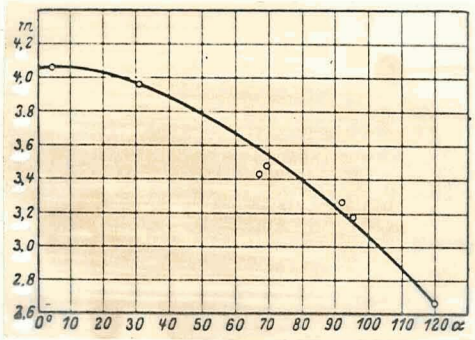

Fig.21 Reduction in Brightness of the Positive Lunar Limb with Increasing Phase Angle.

The author first formulated the hypothesis that the surface of the moon is uniformly covered with conical elevations of equal aperture angles, and then calculated the light distribution along the intensity equator at full moon. The greater the density of such elevations and the more acute the cones, the more would the brightness become equalized from the center toward the limb; although no uniform brightness can be reached, i.e., no complete agreement with the observation is obtained, this assumption possibly would be sufficient, in view of the uncertainty on the reflection law, for explaining the relative brightness at full moon and also at arbitrary phase angle. However, if the observed light reduction along the limb of the moon is to be explained by this hypothesis, one recognizes immediately its nonfeasibility since the brightness of the lunar limb, in the case of conical elevations, must increase after the opposition. This increase would continue up to the phase angle at which the sun enters the zenith of the visible cone envelopes. Furthermore, the bright-

ness decreases and rapidly drops to zero as soon as the sun illuminates only the rear faces of the cones. This is in complete contradiction to actual observations.

A similar result is obtained when assuming hemispherical and calotte-like elevations, for which the light distribution had been calculated under various assumptions as to the mutual distance of the elevations. Here again, it was found that the elevations produce an equilibration of the brightness from the center toward the limbs of the full-moon disk, despite the fact that complete equality cannot be reached under any of the assumptions as to their density; furthermore, it is demonstrated that the phase curve of the lunar limb originally results in a significant rise in brightness followed by a slow decrease. Of importance here is the auxiliary result that the reduction in brightness on the fully illuminated disk mainly is due to the illumination of the flat bottom area between such elevations whereas the visible calottes at the positive limb of the moon appear uniformly bright over a wide range of the phase angles. This is a consequence of their round shape.

An entirely different aspect is offered by the light distribution over a planetary disk if depressions of various shape in the plains are assumed. Starting from Wilsing's opinions on the developmental history and consistency of the lunar surface, the author calculated the illumination for hemispherical depressions for which various lava forms are highly characteristic. These hemispherical depressions on the free surface of the lava are produced by liberation of gases in the semimolten state and frequently are so closely spaced that the resultant roughness of the surface becomes extremely great. It is found that the brightnesses of such hemispherical depressions increase toward the limb of a fully illuminated planetary disk, so that it is possible, under assumption of a flat or slightly curved bottom between these depressions, to explain the uniform brightness of the full-moon disk. Even the observed light distribution at different phase angles up to 90° can be represented under the same assumptions, which is true also for the fall-off in brightness of the lunar limb within the same limits. For phase angles larger than 90°, all pores appear dark at all points of the intensity equator up to the limb, since no light can reach the eye from there. The light distribution and the light reduction of the lunar limb /79 are then dependent only on the form of the lava between the pores. Since this is entirely irregular, the question cannot be further pursued and only an /80 estimate calculation can be made for the reduction in brightness of the lunar limb between $\alpha = 90^\circ$ and $\alpha = 120^\circ$, under assumption of a curved ground between the pores; this agrees sufficiently well with actual observation. To illustrate the light losses, on lateral illumination of a porous surface, we are giving a photograph of pumice lava, taken from Schoenberg's treatise (Fig.22).

This theory refers to the typical surface of the moon on the continents. Since the maria, according to Öpik, exhibit almost the same reflection law, the theory would have to be valid also for these. To explain the special slope of the function $\psi(\alpha)$ in the ray systems, a different shape of depressions with still greater light losses in the immediate vicinity of the opposition had to be assumed. The author more or less observed the light losses in cylindrical pores and round apertures, produced in a perforated cover, and found that the second assumption can be used for explaining the phase curves of the ray systems.

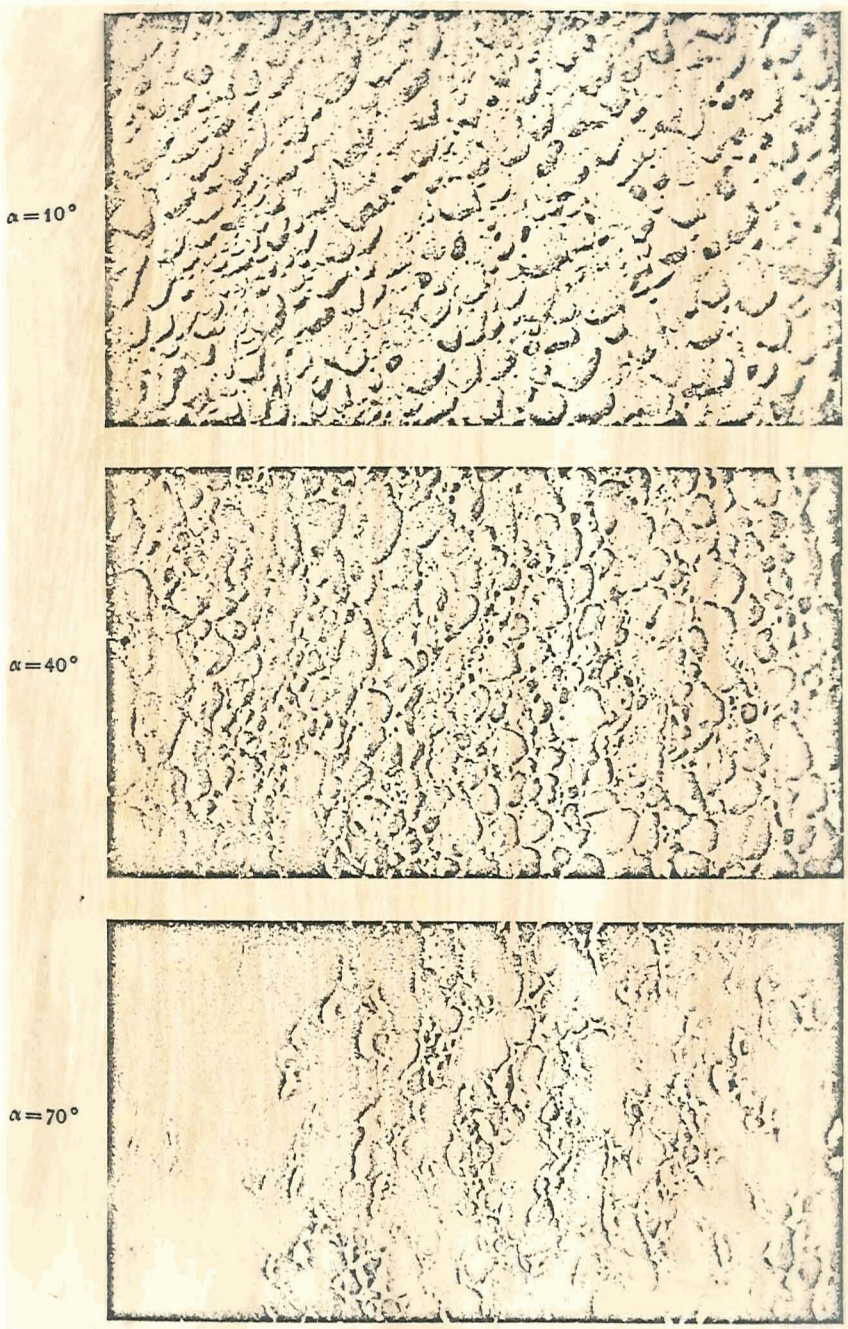

Fig.22 Pumice Lava Photographed under Various Angles (α) to the Direction of Illumination.

Thus, this illumination theory furnishes an adequate explanation for the photometric behavior of the moon and a substantiation of Wilsing's developmental history of our satellite. By introduction and analysis of the shadow function $\psi(\alpha)$ the author hoped to obtain an accurate classification of various lunar configurations, in accordance with their surface consistency which is no longer

detectable by telescope; this function seems of importance also for the illumination theory of other planets. For example, if planets with an opaque cloud cover such as Jupiter and Saturn, according to most recent measurements, exhibit phase coefficients varying from opposition, it would seem logical to look for the reason in shadow effects. However, in the case of elevations and depressions according to Schoenberg's investigations, these could never produce such a light loss as it must be assumed for explaining the phase coefficients. In fact, P.Guthnick and Schoenberg (Ref.131, 132) found phase coefficients of 0.m015 for 1° phase, in the case of Jupiter and Saturn, which - for Jupiter - at a maximum phase of 12° would constitute a reduction in quantity of light by 15%. If the shadow theory is to be retained as an explanation, only the model of a cloud cover interrupted by numerous openings can be applied. A slope of the function $\psi(\alpha)$, as that given for the ray systems in Fig.20, showing a steep drop in brightness close to opposition and constancy of $\psi(\alpha)$ at larger phase angles, would lead to an excessively large phase coefficient for the total brightness in the neighborhood of opposition. If the planet, in this case, is surrounded by a cloud envelope, the phenomenon can be explained only by assuming that this envelope has a porous structure, in which case the thickness of the cloud layer is vanishingly small in comparison to its height above the solid or liquid surface. If the openings in the clouds are assumed as circular, as indicated in Fig.23, and if their height above ground is denoted by h and their radius by r, then a decrease in light for the observer takes place as long as /81 the projections of the opening from the earth and from the sun still have a common portion. The maximum phase angle up to which such light reduction takes place thus represents a criterion for the ratio h/2r. In the case of circular openings, the course of the light reduction can be calculated. On overlapping, the common portion is a double segment whose area is equal to

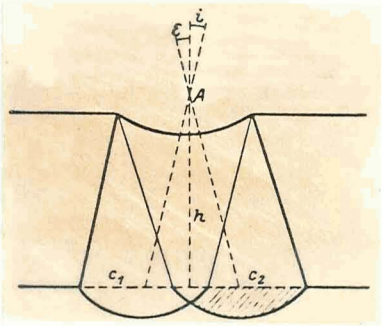

Fig.23 Light Losses in Circular Openings in a Cover.

$$F = r^2(2\beta - \sin 2\beta), \tag{45}$$

where 2β denotes the central angle between the intersection points of the circles. Setting $\cos\beta = \frac{C_1 C_2}{2r} = u$, we have $F = 2r^2(\text{arc cos } u - u\sqrt{1-u^2})$. This expression determines the amount of light from a circular cloud opening up to the instant at which u = 1.

However, there hardly ever is an occasion for following the process of light reduction of individual formations in a given planet to such an extent that the porous consistency of a surface could be determined with greater accuracy.

Instead, it might be possible to derive certain approximate values for h/2r. Since the center-to-center distance of both projections is given by the equation

$$C_1C_2 = \sqrt{h^2\sec^2 i + h^2\sec^2\varepsilon - 2h^2\cos^2\alpha\sec i\sec\varepsilon},$$

the following formula is obtained after introduction of the spherical coordinates ω and ψ on the planetary disk, by means of eq.(5) on p.71:

$$C_1C_2 = \frac{h\sin\alpha}{\cos\psi\cos\omega\cos(\omega-\alpha)}. \tag{46}$$

For $C_1C_2 = 2r$, no light escapes from the openings and the curve $\psi(\alpha)$ has a flex point. On substituting the coordinates of the observed point and of the value for α at the point of inflection, the value of h/2r can be calculated.

We would like to draw attention to one result of these investigations, which might be of importance for studying the light distribution over the disks of planets. A uniform or quasi-uniform brightness of the disk in opposition is no proof for the validity of the Seeliger law and is obtained also when assuming the Lambert law, as a consequence of elevations and depressions on the surface. In studies of the influence of atmospheres on the light distribution, the above assumption for the opposition must be considered the most probable first approximation for the appearance of a planet without atmosphere. The elevations and depressions on the surface attenuate the brightness of the center of the fully illuminated disk and intensify that of the limbs. As a result, the average surface brightness of a smooth sphere and that of a sphere covered with elevations and depressions will be almost the same. For planets which, like the moon, exhibit equal brightness on the fully illuminated disk because of roughnesses on their surface, the quantity p [Sect.35, eq.(28)], calculated from the opposition brightness, is directly comparable with the reflection coefficient in the direction of irradiation, as it has been determined in the laboratory. Conversely, for planets on which no complete equalization of the brightnesses on the fully illuminated disk takes place, the reflection coefficient in direction of the irradiation is comparable only with the quantity that had been determined during the opposition at the center of the disk by surface-photometric measurements.

39. New Illumination Formulas for Large Planets /82

According to the above statements, the light distribution over a planetary disk is a problem that can be treated theoretically only in exceptional cases, even in the absence of an atmosphere and at homogeneous consistency of the surfaces. The presence of an atmosphere which has a light-absorbing and light-scattering effect further complicates the problem. It will be demonstrated that the study of light distribution even of planets surrounded by atmospheres may nevertheless greatly advance our knowledge of their consistency. We will discuss only the actually observed light distribution on the planets Venus, Mars, Jupiter, and Saturn and will give its representation by empirical formulas which permit determining the photometric constants, defined in earlier Sections, for these planets based on photometric measurements and independent of all hypotheses on the reflection law.

The measurements of light distribution over the surfaces of large planets were made by the author (Ref.133) with the refractors of the Dorpat and Pulkova

Observatories. The studies consisted of intensity comparisons between the center of the visible disk or a topographically defined point and other points on the disk defined in the same manner, for which the angle of incidence and the angle of reflection of the light were calculated. The number of measurements which were extremely difficult because of the smallness of the planetary disk is not sufficient for deriving the constants of a complete illumination theory from the relative intensities. It was mainly a question of expressing the light distribution by convenient formulas; it was found that, for none of the planets, either the Lambert or the Seeliger law correspond even faintly to reality; instead, an influence of the atmosphere was distinctly noted as proved by the fact that the observations of all planets, for moderate phase angles, can be satisfactorily represented by the following formula for the quantity of light reflected from the element ds:

$$dq = kLe^{\varphi(i)}e^{\varphi(\varepsilon)}\cos\varepsilon\, ds\,\psi(\alpha), \tag{47}$$

where the function $\varphi(z)$ = A sec z + B sec z $\tan^2 z$ + ... characterizes the absorption of light, while k is a constant and L the amount of light perpendicularly incident on unit surface of the atmosphere; $\psi(\alpha)$ is a descending function, starting from a value of $\psi(0) = 1$. This formula presupposes that, aside from the absorbent effect of the atmosphere, the planetary disks would have to appear uniformly bright. Accordingly, representation by the formula

$$dq = kL(1 + \mu'\cos i + \nu'\cos 2i + \cdots)(1 + \mu'\cos\varepsilon + \nu'\cos 2\varepsilon + \cdots)\cos\varepsilon\, ds\,\psi(\alpha)$$

became possible, where the exponential function is replaced by Fourier series with identical coefficients. The brightnesses of two points on the surface, at identical α, thus are at a ratio of

$$\frac{h}{h_1} = \frac{(1 + \mu'\cos i + \nu'\cos 2i)(1 + \mu'\cos\varepsilon + \nu'\cos 2\varepsilon)}{(1 + \mu'\cos i_1 + \nu'\cos 2i_1)(1 + \mu'\cos\varepsilon_1 + \nu'\cos 2\varepsilon_1)}. \tag{48}$$

From such equations, the coefficients μ', ν' were determined for the four larger planets.

For the opposition, when i = ε at all points of the disk, a brightness uniformly decreasing from the center is obtained:

$$h_0 = kL(1 + \mu'\cos i + \nu'\cos 2i)^2 \tag{49}$$

while, for the center of the fully illuminated disk, we have /83

$$h_0' = kL(1 + \mu' + \nu')^2. \tag{49a}$$

If the total quantity of light, reflected from the planetary phase, is to be determined, then the expression

$$dq = kL(1 + \mu'\cos i + \nu'\cos 2i)(1 + \mu'\cos\varepsilon + \nu'\cos 2\varepsilon)\, ds\cos\varepsilon\,\psi(\alpha)$$

must be integrated over the visible disk which, again after the usual transformation of i and ε into spherical coordinates ψ and ω, will be carried out

here by means of the equations

$$\cos\varepsilon = \cos\psi\cos\omega,$$
$$\cos i = \cos\psi\cos(\omega - \alpha),$$
$$ds = \varrho^2\cos\psi\, d\psi\, d\omega.$$

It follows that

$$\begin{aligned}
q = kL\varrho^2\psi(\alpha)\Big\{&(1-\nu)^2\int_{-\pi/2}^{\pi/2}\cos^2\psi\, d\psi\int_{\alpha-\pi/2}^{\pi/2}\cos\omega\, d\omega\\
&+\mu(1-\nu)\int_{-\pi/2}^{\pi/2}\cos^3\psi\, d\psi\int_{\alpha-\pi/2}^{\pi/2}[\cos^2\omega(1+\cos\alpha)+\sin\alpha\sin\omega\cos\omega]\,d\omega\\
&+2\nu'(1-\nu')\int_{-\pi/2}^{\pi/2}\cos^4\psi\, d\psi\int_{\alpha-\pi/2}^{\pi/2}[\cos^3\omega(1+\cos^2\alpha)+\sin^2\alpha\sin^2\omega\cos\omega\\
&+2\sin\alpha\cos\alpha\cos^2\omega\sin\omega]\,d\omega\\
&+2\nu'\mu'\int_{-\pi/2}^{+\pi/2}\cos^5\psi\, d\psi\int_{\alpha-\pi/2}^{\pi/2}[\cos^4\omega(\cos\alpha+\cos^2\alpha)\\
&+\cos^3\omega\sin\omega(\sin\alpha+\sin 2\alpha)+\sin^2\alpha\sin^2\omega\cos^2\omega]\,d\omega\\
&+\mu'^2\int_{-\pi/2}^{+\pi/2}\cos^4\psi\, d\psi\int_{\alpha-\pi/2}^{\pi/2}[\cos^3\omega\cos\alpha+\cos^3\omega\sin\omega\sin\alpha]\,d\omega\\
&+4\nu'^2\int_{-\pi/2}^{+\pi/2}\cos^6\psi\, d\psi\int_{\alpha-\pi/2}^{\pi/2}[\cos^5\omega\cos^2\alpha+\cos^3\omega\sin^2\omega\sin^2\alpha\\
&+\sin 2\alpha\sin\omega\cos^4\omega]\,d\omega\Big\}.
\end{aligned} \tag{50}$$

Carrying out the simple integration, except for the constant factor $kL\varrho^2$ and the function $\psi(\alpha)$, yields six terms whose values are denoted by I to VI; for $\alpha = 0$, these are given on the right-hand side of the formulas:

$$\begin{aligned}
\mathrm{I} &= (1-\nu')^2\frac{\pi}{2}(1+\cos\alpha); & \mathrm{I}_0 &= (1-\nu')^2\pi;\\
\mathrm{II} &= \frac{2\mu'(1-\nu')}{3}(1+\cos\alpha)[(\pi-\alpha)+\sin\alpha]; & \mathrm{II}_0 &= \tfrac{4}{3}\mu'(1-\nu')\pi;\\
\mathrm{III} &= \tfrac{1}{4}\nu'(1-\nu')\pi[(1+\cos\alpha)(3+\cos^2\alpha)+\sin 2\alpha\sin\alpha]; & \mathrm{III}_0 &= 2\nu'(1-\nu')\pi;\\
\mathrm{IV} &= \tfrac{4}{15}\mu'\nu'[(\pi-\alpha+\sin\alpha)(3\cos\alpha+2\cos^2\alpha+1)+\sin^3\alpha]; & \mathrm{IV}_0 &= \tfrac{8}{5}\mu'\nu'\pi;\\
\mathrm{V} &= \frac{\pi\mu'^2}{8}(1+\cos\alpha)^2; & \mathrm{V}_0 &= \frac{\mu'^2}{2}\pi;\\
\mathrm{VI} &= \tfrac{1}{6}\nu'^2\pi(1+\cos\alpha)^3; & \mathrm{VI}_0 &= \tfrac{4}{3}\nu'^2\pi.
\end{aligned}$$

We determined the values of the constants μ', ν' for the large planets Venus, Mars, Jupiter, and Saturn, from observations of light distribution. Accordingly, the last formula can be used also for calculating the phase curve, except for the function $\psi(\alpha)$. However, this is of interest only for the two last planets, since a comparison of observed and calculated phase curves permits determining the function $\psi(\alpha)$. For the two closer planets with a greater vari- /84

ability of the phase angle, such a determination of $\psi(\alpha)$ has no physical interest since, for large α, the assumptions of the theory are no longer correct. Nevertheless, we will use the values of the coefficients μ', ν' and the total brightness q_0 of the planets in opposition for which instant the constants μ', ν' are defined, i.e., the total brightness and light distribution in opposition, for deriving the reflection coefficient in the direction of irradiation. For this quantity, which could also be determined by a direct comparison of the brightness of the sun with the measured brightness of the planetary centers in opposition, no data are in existence.

For the total brightness in opposition, at $\psi(\alpha) = 1$, we have

$$\left.\begin{aligned} q_0 &= kL\varrho^2\pi\left\{(1-\nu')^2 + \frac{4}{3}\mu'(1-\nu') + 2\nu'(1-\nu') + \frac{8}{5}\mu'\nu' + \frac{\mu'^2}{2} + \frac{4}{3}\nu'^2\right\} \\ &= kL\pi\varrho^2 f(\mu', \nu'). \end{aligned}\right\} \qquad (50')$$

On the other hand, according to Bond's definition of the albedo, the quantity p is equal to the ratio of this brightness to that of a sphere of the same size and position which, from each unit area of its surface, reflects as much light as the planet receives from the sun at normal incidence. Such a body thus has the brightness $L\pi\rho^2$, so that

$$p = \frac{q_0}{L\pi\varrho^2} = kf(\mu', \nu').$$

The brightness of the planetary center in opposition, denoting the reflection coefficient in direction of the irradiation by R, will be

$$h_0^{\circ} = kL(1 + \mu' + \nu')^2 = RL,$$

whence

$$R = k(1 + \mu' + \nu')^2 = \frac{p}{f(\mu', \nu')}(1 + \mu' + \nu')^2.$$

Substituting here the values p and μ', ν' for the four large planets, we obtain

	Russell	Schoenberg			$f(\mu', \nu')$	$(1+\mu'+\nu')^2$
Venus . .	$p = 0.492$	$R = 0.629$	$\mu' = -4.25$	$\nu' = 1.135$	+3.507	4.483
Mars . .	$p = 0.139$	$R = 0.244$	$\mu' = -2.56$	$\nu' = 0.54$	+0.592	1.040
Jupiter . .	$p = 0.375$	$R = 0.585$	$\mu' = 1.8$	$\nu' = 0$	+5.02	4.84
Saturn . .	$p = 0.420$	$R = 0.672$	$\mu' = 2.1$	$\nu' = 0$	+6.005	9.61 .

For R, the values shown in the second column are obtained. Consequently, these are considerably higher than the values p, a fact that must be ascribed to the brightness fall-off toward the limb which, according to Schoenberg's measurements, is considerable in all large planets due to absorption in the atmospheres. The manner of build-up of the obtained values R from the reflectivity of the surfaces and the atmospheres will not be investigated here. The negative values of μ', in the case of Venus and Mars, are a result of the calculation which had the purpose of representing the brightness fall-off toward the limb in the form of a Fourier series; obviously, these values have no physical

meaning. However, these two planets permit a much more detailed photometric /85
analysis, which might lead to important information on their atmospheres.

The principles of a strict theory on the absorptive and diffusive effect of an atmosphere surrounding a given planet will be discussed in a separate Section.

For the reduction of photometric measurements on the surface of the planets, we will give the formulas previously derived and used by us.

40. Relations between Linear Coordinates on a Planetary Disk and Angle of Incidence (i) and Angle of Reflection (ε) of Light

For facilitating the reduction of photometric data on the disks of Jupiter and Saturn, which have considerable oblateness, we will give here the formulas for transition from the linear coordinates of the points whose brightness is to be determined to the photometric variables i and ε. Since these angles are those made by the normal to the surface with the light rays, it is primarily a question of establishing a relation between the linear coordinates on the elliptical disk, measured with respect to the axes of the ellipse, and the planetographic coordinates on the surface of the ellipsoid.

Let

x, y, z = planetocentric rectangular coordinates of a point F of the surface, referred to the equator as a plane x, y;
ξ, η, ζ = geocentric coordinates of the same point, referred to a parallel system of axes at the center of the earth;
r, b, l and ρ, β, λ = corresponding planetocentric and geocentric spherical coordinates;
R, B, L = geocentric spherical coordinates of the center of the planet.

We then have

$$\left.\begin{aligned} \xi &= \varrho\cos\beta\cos\lambda = r\cos b\cos l + R\cos B\cos L,\\ \eta &= \varrho\cos\beta\sin\lambda = r\cos b\sin l + R\cos B\sin L,\\ \zeta &= \varrho\sin\beta \quad\;\; = r\sin b \quad\;\; + R\sin B. \end{aligned}\right\} \tag{51}$$

On aligning the axis x with the point of a length L, the above formulas will yield

$$\left.\begin{aligned} \varrho\cos\beta\cos(\lambda - L) &= r\cos b\cos(l - L) + R\cos B,\\ \varrho\cos\beta\sin(\lambda - L) &= r\cos b\sin(l - L),\\ \varrho\sin\beta \quad\;\; &= r\sin b \quad\;\; + R\sin B. \end{aligned}\right\} \tag{52}$$

On a geocentric sphere, let π and ζ be the poles of the terrestrial equator and of the planetary equator, while P is the planetary center. Let the planetocentric linear coordinates of the point F on the surface be

$$\left.\begin{aligned} u &= s\sin(p-P),\\ v &= s\cos(p-P), \end{aligned}\right\} \qquad (53)$$

where P and p denote the position angles of the minor axis of the ellipsoid and of the arc PF whose length is equal to s. From the spherical triangle ζFP in which

$$\begin{aligned} \zeta P &= 90^\circ - B, & \angle P\zeta F &= \lambda - L,\\ PF &= s, & \zeta F &= 90^\circ - \beta\\ \angle \zeta PF &= p - P, \end{aligned}$$

the following is obtained: /86

$$\begin{aligned} \sin s\sin(p-P) &= \cos\beta\sin(\lambda - L),\\ \sin s\cos(p-P) &= \sin\beta\cos B - \cos\beta\sin B\cos(\lambda - L),\\ \cos s &= \sin\beta\sin B + \cos\beta\cos B\cos(\lambda - L). \end{aligned}$$

On multiplying these equations by ρ and setting sin s = s, cos s = 1, using eqs.(53), we also obtain

$$\left.\begin{aligned} \varrho\sin s\sin(p-P) &= \varrho u = r\cos b\sin(l-L),\\ \varrho\sin s\cos(p-P) &= \varrho v = r\sin b\cos B - r\cos b\cos(l-L)\sin B,\\ \varrho\cos s &= \varrho = r\sin b\sin B + r\cos b\cos(l-L)\cos B + R. \end{aligned}\right\} \qquad (54)$$

Since, in addition,

$$\begin{aligned} x &= r\cos b\cos l,\\ y &= r\cos b\sin l,\\ z &= r\sin b, \end{aligned}$$

the last equations can be brought to the following form:

$$\left.\begin{aligned} \varrho u &= y\cos L - x\sin L,\\ \varrho v &= z\cos B - (x\cos L + y\sin L)\sin B,\\ \varrho &= z\sin B + (x\cos L + y\sin L)\cos B + R. \end{aligned}\right\} \qquad (55)$$

Introducing now the reduced width ν and the length μ by means of the equations

$$\begin{aligned} x &= a\cos\mu\cos\nu = r\cos b\cos l, & \frac{y}{x} &= \tan l = \tan\mu, \quad \mu = \lambda,\\ y &= a\sin\mu\cos\nu = r\cos b\sin l, & \frac{z}{y} &= \frac{c}{a}\tan\nu\operatorname{cosec}\mu = \tan b\operatorname{cosec} l,\\ z &= c\sin\nu = r\sin b, & \tan\nu &= \frac{a}{c}\tan b, \end{aligned}$$

where a and c are the semiaxes of the planets

the equations will assume the following form:

$$\left.\begin{aligned} \varrho u &= a\sin\mu\cos\nu\cos L - a\cos\mu\cos\nu\sin L = a\cos\nu\sin(\mu - L), \\ \varrho v &= c\sin\nu\cos B - a\cos(\mu - L)\sin B\cos\nu. \end{aligned}\right\} \tag{56}$$

Substituting ρ by R and retaining the denotations a and c for a/R and c/R, we obtain

$$\left.\begin{aligned} u &= a\cos\nu\sin(\mu - L), \\ v &= c\sin\nu\cos B - a\cos\nu\cos(\mu - L)\sin B. \end{aligned}\right\} \tag{57}$$

It is then necessary to solve these equations for the coordinates ν and μ - L. We have

$$u^2\sin^2 B + (v - c\sin\nu\cos B)^2 = a^2\sin^2 B\cos^2\nu = a^2\sin^2 B - a^2\sin^2 B\sin^2\nu$$

or

$$\sin^2\nu\,(a^2\sin^2 B + c^2\cos^2 B) - 2vc\sin\nu\cos B = (a^2 - u^2)\sin^2 B - v^2.$$

If

$$a^2\sin^2 B + c^2\cos^2 B = a^2(1 - e^2\cos^2 B) = k^2 \tag{α}$$

is introduced, where k is the perpendicular dropped from the center of the planet on a plane tangential to its surface going through the center of the earth and where e denotes the eccentricity, we obtain furthermore

$$k^2\sin^2\nu - 2vc\sin\nu\cos B = (a^2 - u^2)\sin^2 B - v^2,$$

or, after simple reductions /87

$$\left(k\sin\nu - \frac{vc\cos B}{k}\right)^2 = a^2\sin^2 B\left(1 - \frac{u^2}{a^2} - \frac{v^2}{k^2}\right)$$

and

$$\sin\nu = \frac{vc\cos B}{k^2} \pm \frac{a\sin B}{k}\sqrt{Q},$$

where

$$Q = 1 - \frac{u^2}{a^2} - \frac{v^2}{k^2}. \tag{β}$$

Substituting the value of sin ν into the second equation of the system (57), the following definite expressions for the reduced width ν and the length μ of the point F will be obtained:

$$\left.\begin{aligned} \cos\nu\sin(\mu - L) &= \frac{u}{a}, \\ \cos\nu\cos(\mu - L) &= \frac{a\sin B}{k^2}v - \frac{c\cos B}{k}\sqrt{Q}, \end{aligned}\right\} \tag{58}$$

where the plus sign has been omitted since it is valid for the invisible side of the planet. The planetographic width φ is then obtained from the equation

$$\tan\varphi = \frac{\tan\nu}{\sqrt{1-e^2}}. \tag{59}$$

The angles of incidence and reflection of the light at the point F are obtained from the triangles: sun, zenith of the point F, and planetary pole on the one hand and earth, zenith, and planetary pole on the other, in the following manner:

$$\left.\begin{aligned}\cos\varepsilon &= -\sin B\sin\varphi - \cos B\cos\varphi\cos(\mu - L),\\ \cos i &= -\sin B'\sin\varphi - \cos B'\cos\varphi\cos(\mu - L').\end{aligned}\right\} \tag{60}$$

Here, L′, B′ denote the heliocentric length and width of the planet. Consequently, we must solve eqs.(α), (β), (58), (59), and (60) in order to pass from u, v to i and ε.

IV. ILLUMINATION OF PLANETARY SATELLITES

41. Illumination of a Satellite by its Planet

The illumination formulas for planets naturally are valid also for their satellites except that, if maximum strictness of calculation is required, a calculation of the satellites also must take into consideration the amount of light received by them from the planet itself and re-reflected toward the earth. This portion, in comparison to the light coming from the sun itself, is extremely small but, in view of the extremely sharp modern photometric measurements, cannot be neglected in some cases. Nevertheless, the problem can be simplified by assuming the centers of the four celestial bodies in question as lying in the same plane and neglecting the dimensions of these with respect to their distances. For the total quantity of light, reflected by the satellite to the earth, we have Q = q′ + q″ where q′ is the light coming from the sun while q″ is that originating in the planet. Let

α = phase angle of the satellite,
$\varphi(\alpha)$ = phase curve of the satellite,
Δ_t = distance of the satellite from the earth,
r_t = distance of the satellite from the sun,
Δ_t^0, r_t^0 = the same distances, for the moment of opposition.

Then, according to Section 33, eq.(14), we have /88

$$q' = q_1^0\left(\frac{\Delta_t^0 r_t^0}{\Delta_t r_t}\right)^2\varphi(\alpha). \tag{1}$$

Let ds be an element of surface of the satellite, receiving light from the planet. Only a portion of the illuminated planetary surface contributes to its illumination, namely the portion visible from the satellite and shown as an unhatched segment in Fig.24. Let dq be the total quantity of light falling on ds at vertical incidence. This is expressed by an equation similar to eq.(1):

$$dq = dq^0\left(\frac{R^0 r_p^0}{R r_p}\right)^2\varphi'(\alpha')\,ds.$$

Here,

α' = phase angle of the planet with respect to the satellite,
$\varphi'(\alpha')$ = phase curve of the planet, viewed from the satellite,
R = distance between planet and satellite,
r_p = distance between sun and planet,
R^0, r_p^0, dq_0 = same distances and value of dq at $\alpha' = 0$.

However, the amount of light reflected from ds toward the earth and vertically striking the unit surface, is

$$dq'' = C\frac{dq}{\Delta_i^2}F(i, \varepsilon, \alpha),$$

where C denotes the reflection constant of the satellite surface, i the angle of incidence of the rays reaching the satellite element from the planet, and ε the reflection angle toward the earth.

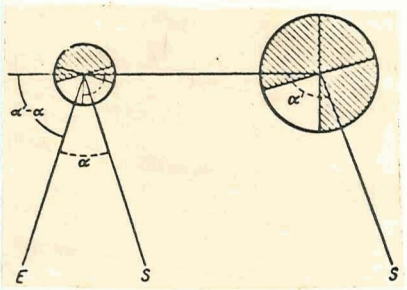

Fig.24 Illumination of the Satellites.

Nothing is known on the form of the reflection law for the satellite surface and also cannot be expected in view of the smallness of the satellite disk. Nevertheless, because of the smallness of the entire component q", it is permissible to use a known simple formula for $F(i, \varepsilon, \alpha)$, such as the Lambert formula $f(i, \varepsilon) = \cos i \cos \varepsilon$. In that case, denoting by A_1 the Lambert albedo, we obtain

$$dq'' = \frac{A_1}{\pi}\frac{dq_0}{\Delta_i^2}\left(\frac{R_0 r_p^0}{R r_p}\right)^2 \varphi'(\alpha')\cos i \cos\varepsilon\, ds = k\cos i\cos\varepsilon\, ds,$$

where k is a factor independent of i and ε. To obtain the total quantity of light q", integration must be carried out over the entire satellite surface illuminated by the planet visible from the earth. Again introducing the integration variables ψ and ω, calculated along the intensity equator of the satellite from the antiterrestrial point, as origins of the lengths ω, the following relations are obtained:

$$\begin{aligned}\cos\varepsilon &= \cos\psi\cos\omega,\\ \cos i &= \cos\psi\cos[\pi - (\alpha' - \alpha) - \omega],\\ ds &= \rho^2\cos\psi\, d\omega\, d\psi,\end{aligned}$$

where ρ is the radius of the satellite.

The integration limits for ψ are $-\frac{\pi}{2}$ and $\frac{\pi}{2}$ while, for ω, these limits /89 are $\frac{\pi}{2} - (\alpha' - \alpha)$ and $\frac{\pi}{2}$. Consequently, we have

$$\begin{aligned}q'' &= k\rho^2\int_{-\pi/2}^{+\pi/2}\cos^3\psi\, d\psi\int_{\pi/2-(\alpha'-\alpha)}^{\pi/2}\cos\omega\cos[\pi - (\alpha' - \alpha) - \omega]\, d\omega\\ &= \tfrac{2}{3}k\rho^2[\sin(\alpha' - \alpha) - (\alpha' - \alpha)\cos(\alpha' - \alpha)].\end{aligned}$$

Denoting $\frac{\rho^2}{\Delta_t^2}$ by $\sin^2\sigma_t$ where σ_t is the apparent radius of the satellite seen from the earth, and substituting dq_0 by the value $q_2^0 \frac{\Delta_p^{02}}{R_0^2}$ where q_2^0 denotes the amount of light coming from the planet in opposition and falling on unit area of the earth's surface, we finally have

$$q'' = \frac{2}{3}\frac{A_1}{\pi}\sin^2\sigma_t q_2^0 \left(\frac{\Delta_p^0 r_p^0}{R\, r_p}\right)^2 \varphi'(\alpha')\left[\sin(\alpha'-\alpha) - (\alpha'-\alpha)\cos(\alpha'-\alpha)\right]. \tag{2}$$

Because of the factor $\sin^2\sigma_t$, the value of q'' must be very small for all satellites; thus, the uncertainty as to the phase curve $\varphi'(\alpha')$ for which a value estimated from the known phase curves of Moon, Venus, and Mars must be substituted, will be of negligible importance. Furthermore, substituting in eqs.(1) and (2) the terms q_1^0 and q_2^0 (which are the light quantities of satellite and planet in opposition) by $q_1^0 = M_1^0 J\pi \sin^2 S$ and $q_2^0 = M_2^0 J\pi \sin^2 S$, where the meanings of M and S are the same as those given on p.78, and using eq.(28) on that same page for eliminating M_1^0 and M_2^0, we obtain

$$\left.\begin{aligned} q' &= p J \pi \sin^2\sigma_t \sin^2 s\, \varphi(\alpha), \\ q'' &= \tfrac{2}{3} A_1 p' J \frac{\Delta_p}{R^2} \sin^2\sigma_t \sin^2 s' \sin^2\sigma_p \varphi'(\alpha')\left[\sin(\alpha'-\alpha) - (\alpha'-\alpha)\cos(\alpha'-\alpha)\right] \\ Q &= q' + q''. \end{aligned}\right\} \tag{3}$$

Here, p and p' are Bond's reflection coefficients of the satellite and of the planet, J is the intensity of the solar radiation, σ_p the apparent radius of the planet seen from the earth, and s and s' the apparent radii of the sun viewed from the satellite and from the planet.

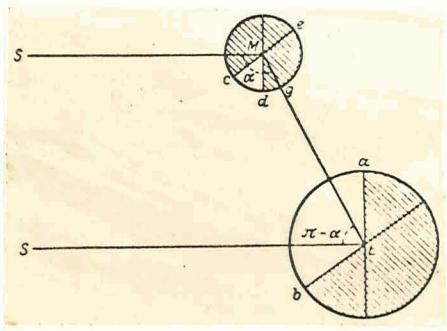

Fig.25 Illumination of the Earth's Moon.

42. Calculation of the Ashen Light of the Moon

It is known that the portion of the lunar disk not illuminated by the sun does not appear entirely dark at large phase angles but shines in a faint light which is known as "ashen light" of the moon. This light is due to illumination of the dark side of the moon by the earth which, at that time, appears almost fully illuminated when viewed from the moon. Observation of the brightness of this earthlight is of great importance since the albedo of the earth can be determined from it.

Let us again imagine the solar ray as striking both earth and moon in parallel direction. In Fig.25, α represents the phase angle of the moon and $\pi - \alpha$ the phase angle of the earth relative to the moon. The arc cd denotes the illuminated portion of the moon visible from the earth, while de is the portion of the lunar surface illuminated by the ashen light; this light originates in the portion of the illuminated earth, indicated by the arc ba. Furthermore, the

following notations are introduced here: /90

$\varphi'(\alpha)$ = phase curve of the earth seen from the moon,
σ' = radius of the earth seen from the moon,
S = radius of the sun seen from the earth,
p and p' = Bond's reflection coefficients of moon and earth,
Δ = distance between moon and earth,
R = distance between earth and sun.

If dq is the quantity of light vertically reflected by the total earth's phase on a surface element ds of the moon and if the opposition values are denoted by the subscript o, we obtain the equation

$$dq = dq_o \frac{R_0^2 \Delta_0^2}{R^2 \Delta^2} \varphi'(\pi - \alpha)\, ds$$

and, on using the relations given on p.78, as in the derivation of eq.(3) above,

$$dq = J\pi p' \sin^2 S \sin^2 \sigma' \varphi'(\pi - \alpha)\, ds\,. \qquad (4)$$

This equation assumes the form

$$dq_1 = \tfrac{2}{3} J A_1' \sin^2 S \sin^2 \sigma' (\sin\alpha - \alpha\cos\alpha)\, ds$$

for the Lambert law and

$$dq_2 = \frac{1}{2}\pi J A_2' \sin^2 S \sin^2 \sigma' \left\{1 - \cos\frac{\alpha}{2} \cot \frac{\alpha}{2} \ln \cot \left(45° - \frac{\alpha}{4}\right)\right\}$$

for the Seeliger law, if A_1' and A_2' denote the corresponding albedo values of the earth.

The quantity of light dq', reflected by this element ds earthward (perpendicular to unit area), is

$$dq' = \frac{\mu}{\Delta^2} F(i, \varepsilon, \alpha)\, dq\,,$$

where μ denotes a reflection constant or, according to Lambert,

$$dq_1' = \frac{A_1}{\Delta^2 \pi} \cos i \cos\varepsilon\, dq_1\,,$$

and, according to Seeliger,

$$dq_2' = \frac{A_2}{\Delta^2 \pi} \frac{\cos i \cos\varepsilon}{\cos i + \cos\varepsilon} dq_2\,,$$

where i and ϵ denote the angles of incidence and reflection of the light for the element ds, while A_1 and A_2 are Lambert's respectively Seeliger's albedo of the moon. For the ashen light, however, we have $i = \epsilon$ for all points, meaning that $\alpha = 0$; after introduction of the spherical coordinates ψ, ω, counted as usual from the intensity equator of the moon and the antiterrestrial point, the

following equations for dq′ are obtained:

$$\left.\begin{aligned} dq' &= J\mu\pi p' \frac{\varrho^2}{\Delta^2} \sin^2 S \sin^2\sigma' \varphi'(\pi-\alpha) F(i,i,o)\, d\omega\, d\psi \cos\psi, \\ dq'_1 &= \frac{2}{3\pi} J A_1 A'_1 \frac{\varrho^2}{\Delta^2} \sin^2 S \sin^2\sigma' (\sin\alpha - \alpha\cos\alpha)\cos^3\psi \cos^2\omega\, d\omega\, d\psi, \\ dq'_2 &= \frac{1}{4} J A_2 A'_2 \frac{\varrho^2}{\Delta^2} \sin^2 S \sin^2\sigma' \times \\ &\quad \times \left\{1 - \cos\frac{\alpha}{2}\cot\frac{\alpha}{2}\ln\cot\left(45^0 - \frac{\alpha}{4}\right)\right\}\cos^2\psi\cos\omega\, d\omega\, d\psi. \end{aligned}\right\} \quad (5)$$

To obtain the total amount of light, originating from the ashen light, these /91
expressions must be integrated over the dark portion of the visible lunar surface. The integration limits are $-\frac{\pi}{2}$ and $+\frac{\pi}{2}$ for ψ and $-\left(\alpha - \frac{\pi}{2}\right)$ and $+\frac{\pi}{2}$ for ω:

$$\left.\begin{aligned} q' &= J\mu\pi p' \sin^2\sigma \sin^2 S \sin^2\sigma' \varphi'(\pi-\alpha) \int_{-\pi/2}^{\pi/2} \int_{\pi/2-\alpha}^{\pi/2} F(i,i,o)\cos\psi\, d\psi\, d\omega, \\ &\text{accd. to Lambert:} \\ q'_1 &= \frac{4}{9\pi} J A_1 A'_1 \sin^2\sigma \sin^2 S \sin^2\sigma' (\sin\alpha - \alpha\cos\alpha)(\alpha - \sin\alpha\cos\alpha), \\ &\text{accd. to Seeliger:} \\ q'_2 &= \frac{\pi}{8} J A_2 A'_2 \sin^2\sigma \sin^2 S \sin^2\sigma' \\ &\quad \left\{1 - \cos\frac{\alpha}{2}\cot\frac{\alpha}{2}\ln\cot\left(45^\circ - \frac{\alpha}{4}\right)\right\}(1-\cos\alpha), \end{aligned}\right\} \quad (6)$$

where the apparent radius of the moon has been introduced over $\sin^2\sigma = \frac{\rho^2}{\Delta^2}$.

However, until now it has been impossible, in photometric observations of the luminous intensity of the lunar phases, to separate the minor component of the ashen light from that of the lunar crescent, for which reason no determination of the earth's albedo in this manner has been possible. Conversely, it is well possible to compare, by surface-photometric measurements, the luminous intensity of equivalent lunar configurations on the crescent moon and on the portion illuminated by the ashen light, and to then use the measured brightness ratios for determining the albedo. Such measurements were made already by Zöllner and have been repeated frequently in recent times. The area brightness of the element of surface ds is obtained after dividing the light quantity dq′ by the apparent size of the element $\frac{ds\cos\varepsilon}{\Delta^2}$. Therefore, for a point with the coordinates ψ and ω, we have the brightness

$$\left.\begin{aligned} h' &= \frac{dq'\Delta^2}{\varrho^2\cos^2\psi\cos\omega\, d\psi\, d\omega} = J\mu\pi p' \sin^2 S \sin^2\sigma' \varphi'(\pi-\alpha) F(i,i,o)\sec\psi\sec\omega, \\ h'_1 &= \qquad\qquad = \frac{2}{3\pi} J A_1 A'_1 \sin^2 S \sin^2\sigma' (\sin\alpha - \alpha\cos\alpha)\cos\psi\cos\omega, \end{aligned}\right\} \quad (7)$$

$$h_2' = \qquad = \frac{1}{4} J A_2 A_2' \sin^2 S \sin^2 \sigma' \times$$
$$\times \left\{1 - \cos\frac{\alpha}{2} \cot\frac{\alpha}{2} \ln\cot\left(45° - \frac{\alpha}{4}\right)\right\}.$$

Neither the Lambert nor the Seeliger law correspond to reality for the lunar surface, despite the fact that the stipulation of the latter law of uniform brightness of the full-moon disk and of the ashen light is satisfied; the function $F(i, \varepsilon, \alpha)$ sec ε, empirically determined for the typical lunar surface, is a constant [$F(i, i, o)$ sec $i = C$] for the full moon and thus also for the earth-light.

For this reason, only the general first form of the above equations can be used, but two different points must be taken into consideration here:

On the one hand, only portions of the lunar surface of equal reflection coefficients p can be compared, for example two points of the same mare separated by the terminator, or any similar points of the typical surface. On the other hand, it is of importance that the point measured on the bright crescent is properly reduced to its full-moon brightness. With either the Lambert or the Seeliger formula, this can be done only in an approximate manner; it is more realizable to use the empirical curve (Fig.21) for the typical points, and special reductions obtained from observations for the salient points. Let the angles i, ε, ψ, ω for the point measured on the dark portion of the moon be characterized by a prime. For the brightness on the crescent, equating the solar radius seen from the moon to S, we have $h = J\mu\pi \sin^2 S F(i, \varepsilon, \alpha)$ sec ε and eqs.(36) from p.82, so that

/92

$$\left.\begin{aligned}
\frac{h'}{h} &= \frac{p' \sin^2\sigma\, \varphi'(\pi - \alpha) C}{F(i, \varepsilon, \alpha) \sec\varepsilon}, \\
\frac{h_1'}{h_1} &= \frac{2A_1' \sin^2\sigma' (\sin\alpha - \alpha\cos\alpha)\cos\psi'\cos\omega'}{3\pi\cos\psi\cos(\omega - \alpha)}, \\
\frac{h_2'}{h_2} &= \frac{A_2' \sin^2\sigma' \left\{1 - \cos\frac{\alpha}{2}\cot\frac{\alpha}{2}\ln\cot\left(45° - \frac{\alpha}{4}\right)\right\}}{2\left[1 + \tan\frac{\alpha}{2}\tan\left(\omega - \frac{\alpha}{2}\right)\right]}.
\end{aligned}\right\} \qquad (8)$$

The constant C becomes 1 if $F(i, \varepsilon, \alpha)$ is equated to unity for $\alpha = 0$. For $\varphi'(\alpha)$ which is the phase curve of the earth, a mean value of the same function must be substituted for Venus and Mars or for Venus and Moon. In this manner, using the first equation, the Bond reflection coefficient p' can be determined while, using the other two equations, the Lambert or Seeliger albedo of the earth can be obtained. Extending the observations to a large number of points, the error produced by the uncertainty of the reflection coefficients and of the phase curves can be reduced at will.

43. Influence of the Celestial Background

In such measurements, another difficulty occurs which has a great influence

on the results; this is the brightness of the celestial background added to the brightness of the ashen light and produced by the closeness of the brightly illuminated crescent. Certain generally valid formulas for the brightness of the celestial background in the neighborhood of the luminescent lunar crescent cannot be established, since they are largely dependent on the atmospheric conditions and since they differ for each instrument used in the measurements. Therefore, it is preferable to supplement the measurements of the background in the neighborhood and outside of the dark limb, made with one and the same instrument, by studies of the light reduction of the celestial background at various distances from the limb at full moon and then, for the resultant curve, derive an analytical expression in the form of a function of the distance from the center of the disk f(r). The same form of the function can then be assumed for the illumination of an element of area dσ of the crescent by some other element, in which case r is replaced by the mutual distance of the two elements. Then, the total illumination at the point A by the entire crescent will be

$$J = \int\int_{S} f(r)\, d\sigma, \tag{9}$$

where the integral extends over all elements of the crescent. Here, one can either assume the brightnesses of the crescent to be constant or substitute them by their values obtained in special investigations. In the former case, a mean brightness of the crescent, readily obtainable from the phase curve of the moon, can be used in the calculation. Fessenkov (Ref.134), who used this method, /93 found the form $f(r) = \frac{1}{a + br^2}$ for f(r). After introduction of the polar coordinates ρ and φ for ds with the origin O at the center of the moon and counting φ from OA, a value of $r^2 = \rho^2 + \delta^2 - 2\rho\delta \cos\varphi$ will be obtained, where $\delta = OA$. With the calculated values of the integral

$$J = 2\int_0^R\int_0^\pi \frac{\varrho\, d\varrho\, d\varphi}{a + b(\varrho^2 + \delta^2 - 2\varrho\delta\cos\varphi)} \tag{10}$$

and the observed brightnesses of the celestial background at full moon, Fessenkov calculated the values of the constants $k = \frac{b}{a}$; after this, the brightnesses measured each evening outside the dark limb can be converted to brightnesses inside of the limb. For details, the reader is referred to the original paper.

This method is much more accurate than the conventional method of assuming the brightness of the celestial background, on the dark portion of the moon, as equal to that outside of this portion.

44. Eclipses of the Jovian Satellites

Observations on the eclipses of Jupiter's moons have always been of funda-

mental importance in astronomy. It is known that they offer an excellent means for determining the coordinates of the satellites, forming the basis of the Laplace and Delambre orbital constants. Based on the famous determination of the velocity of light by O.Roemer, such observations yielded a value of the solar parallax; in earlier times, they also served as light signals for longitude determinations at sea and in unexplored regions. The problem of the eclipse of a satellite is a task for theoretical photometry since the eclipse does not occur momentarily but requires the rather considerable length of time of 4 min up to 15 min, during which time the planetary shadow moves over the disk of the satellite. Fixing the instant of total eclipse depends greatly on the power of the telescope and on the atmospheric conditions, while the beginning of the eclipse depends on the acuity of observation. Therefore, it is of great importance to calculate the fall-off in brightness of the satellite during the eclipse and to extend the observations over as many periods of the eclipse as possible. This will facilitate calculating, from each of the observed brightnesses, the various states of totality, namely entry, mid-eclipse, and emergence, thus greatly increasing the accuracy. Pickering (Ref.135) was the one to pursue this idea in detail and to bring it to fruitition by a large series of observations made at Harvard Observatory and published as a report (Ref.136). Cornu (Ref.137) has the distinction of priority in this problem; he was the first to mention that the brightness of the satellite must change most rapidly at about mid-eclipse, for which reason the observations should be grouped as close as possible around this period of time. A simple photometer, built by him for this particular purpose, has not come into general use.

In calculating the eclipse curve, a certain assumption must be made as /94 to the brightness distribution over the satellite disk.

Obrecht (Ref.138) solved the problem for the case of equal brightness over the satellite disk, while V.Wellmann and E.Anding (Ref.139, 140) treated the case of the Lambert law. A strict solution of the problem leads to highly complex developments which cannot be given here in all details. Observations of the eclipse curves, with the use of modern photometric methods, will require a strict reduction as discussed in the above-mentioned papers. Presumably, the question will then be decided as to which assumptions on the reflection law should be preferred. The eclipse curves, observed until now, are not sufficiently accurate for this purpose. Therefore, we will be satisfied here with giving the theory in the form in which it suffices for our present observations, also giving the error limits involved.

The problem itself can be formulated as follows: A Jovian satellite enters the shadow of its planet; during this time, an ever greater portion of its disk is eclipsed until it becomes entirely invisible. The duration of the eclipse is as follows:

For the first satellite	$4^m 19^s$
for the second satellite	$5^m 32^s$
for the third satellite	$11^m 21^s$
for the fourth satellite	$16^m 27^s$.

The next step will be to determine the brightness fall-off of the satellite, as a function of time. The brightness will be expressed in units of brightness Q_o of the uneclipsed satellite.

Strictly taken, the conditions of motion in the Jovian system should be taken into consideration. However, in view of the short duration of the eclipse, no noticeable error is created if the motion of the shadow edge over the satellite is assumed as proportional to the time. In addition, the flattening of this edge, whose influence always is smaller than 0.0009 Q_0, can be neglected (Ref.139, p.11). As shown in Obrecht's tables, the influence of the curvature of the shadow edge is very slight. Only in the satellite IV does this influence reach a value in the limiting case of 0.022, but remains less than 0.007 for the other three satellites, so that it can be neglected here; consequently, the shadow boundary can be defined as going rectilinearly through the plane tangential to Jupiter's surface. At the low angular radius of the sun from a Jupiter distance (3'), the effect of the penumbra is extremely small, being - according to Obrecht - always less than 0.001; consequently, this effect can be disregarded. Thus, the sun is considered as a point source and the shadow limit is defined by the tangential plane going through this limit and through the planetary surface assumed as spherical at the point at which the satellite enters or leaves the shadow. It is of importance to mention here that such a simplified treatment of the problem, which is sufficient for the accuracy of observation if the satellites can be considered as spheres, leaves one question entirely open, namely the influence of Jupiter's atmosphere. This influence may be of great importance for the slope of the eclipse curve at the beginning and end, a point to be discussed later. Let us also disregard here the influence of the phase /95 which, in the case of Jupiter, does not exceed 12°, since the correction according to Obrecht, necessary in this case, will always be smaller than 0.01.

Under these conditions, the entire problem reduces to the following task: The reduction in brightness of an illuminated circular disk is to be determined, when this disk is occulted by a rectilinearly bounded dark screen, moving over the disk at uniform velocity.

Let the radius of the disk be equal to r and the shortest distance from the shadow edge to the center be denoted by a. Let us lay a rectangular coordinate system through the center of the disk, with the Y-axis parallel to the shadow edge. The apparent brightness of an element of area dxdy is a function of the distance from the center ρ. Thus, the quantity of light reaching the observer from the element dxdy will be

$$dq = kF(\varrho)\,dx\,dy,$$

where k is a constant and the function F, which is dependent on the illumination law, will be left indeterminate for the present. The total quantity of light, at a distance a of the shadow edge from the center, when more than half of the disk is illuminated, will be

$$Q = 2k\int_{-a}^{r}\int_{0}^{\sqrt{r^2-x^2}} F(\varrho)\,dx\,dy, \qquad (11)$$

where

$$\varrho = \sqrt{x^2 + y^2}.$$

Let us now assume that the light distribution over the fully illuminated disk

obeys the Lambert law. Then the apparent brightness is proportional to the cosine of the angle of incidence i on the surface of the sphere or, since sin i = $= \frac{\rho}{r}$, the amount of light reflected from the point x, y will be

$$dq = k \cos i \, dx \, dy = k \sqrt{1 - \frac{x^2 + y^2}{r^2}} \, dx \, dy$$

while the total amount of light becomes

$$Q = 2k \int_{-a}^{r} dx \int_{0}^{\sqrt{r^2 - x^2}} \sqrt{1 - \frac{x^2 + y^2}{r^2}} \, dy. \tag{12}$$

Setting $1 - \frac{x^2}{r^2} = b$ and $\frac{1}{r^2} = c$, we obtain

$$\int_{0}^{\sqrt{r^2 - x^2}} \sqrt{1 - \frac{x^2 + y^2}{r^2}} \, dy = \int_{0}^{\sqrt{r^2 - x^2}} \sqrt{b - cy^2} \, dy = \left[\frac{1}{2} y \sqrt{b - cy^2} + \frac{b}{2\sqrt{c}} \arcsin \sqrt{\frac{c}{b}} y \right]_{y=0}^{y = \sqrt{r^2 - x^2}}$$

$$= \frac{r\pi}{4} \left(1 - \frac{x^2}{r^2} \right).$$

Hence

$$Q = \frac{kr\pi}{2} \int_{-a}^{r} \left(1 - \frac{x^2}{r^2} \right) dx = \frac{k\pi}{2r} \left\{ r^2 (r + a) - \frac{1}{3} (r^3 + a^3) \right\}. \tag{13}$$

In an entirely uneclipsed disk, we have a = r so that the quantity of light will be /96

$$Q_0 = \frac{2}{3} k \pi r^2. \tag{14}$$

Finally, by division of eqs.(13) and (14), we obtain

$$\frac{Q}{Q_0} = \frac{1}{2} + \frac{3}{4} \frac{a}{r} - \frac{1}{4} \frac{a^3}{r^3}$$

or, introducing the denotation a:r = cos φ,

$$\frac{Q}{Q_0} = \frac{1}{2} + \frac{3}{4} \cos \varphi - \frac{1}{4} \cos^3 \varphi. \tag{15}$$

Thus, this equation furnishes the brightness in units of complete brightness before start of the eclipse, as a function of the distance a and, since the latter is proportional to the time, also as a function of time. It is obvious that, for a = 0, i.e., for the mid-eclipse, we have $\frac{Q}{Q_0} = \frac{1}{2}$ which means that the luminous intensity has dropped to half. In view of the concentric brightness distribution, this has to be expected per se.

If the shadow edge has moved beyond the center of the disk, the corresponding brightness values are obtained, if a in eqs.(13) and (15) is counted negative.

For the Lommel-Seeliger and the Euler reflection laws, both of which stipulate uniform brightness of the fully illuminated disk, the calculation of the eclipse curve is even less complicated. In that case, $F(\rho)$ in eq.(11) can be set equal to 1, directly yielding

$$Q = 2k\int_{-a}^{r} dx \int_{0}^{\sqrt{r^2-x^2}} dy = 2k\int_{-a}^{r} \sqrt{r^2-x^2}\,dx. \tag{16}$$

After carrying out the simple integration, we have

$$Q = k\left[x\sqrt{r^2-x^2} + r^2 \arcsin\frac{x}{r}\right]_{x=-a}^{x=r}$$

or, again setting $\frac{a}{r} = \cos\varphi$,

$$Q = kr^2\{\pi + \sin\varphi\cos\varphi - \varphi\}. \tag{17}$$

For the brightness of the uneclipsed disk, at a = r, we have

$$Q_0 = k\pi r^2,$$

so that, for the eclipse curve, we obtain

$$\frac{Q}{Q_0} = \frac{\pi - \varphi + \sin\varphi\cos\varphi}{\pi}. \tag{18}$$

The slope of the light curves according to eqs.(15) and (18) has been compiled in Table 9 based on the argument cos φ. Both curves have the characteristic

TABLE 9

a/r	Q/Q₀ Lambert	Q/Q₀ Seeliger	a/r	Q/Q₀ Lambert	Q/Q₀ Seeliger	a/r	Q/Q₀ Lambert	Q/Q₀ Seeliger	a/r	Q/Q₀ Lambert	Q/Q₀ Seeliger
1.0	1.000 7	1.000 19	0.5	0.844 60	0.804 56	0.0	0.500 75	0.500 64	−0.5	0.156 52	0.196 54
0.9	0.993 21	0.981 33	0.4	0.784 66	0.748 60	−0.1	0.425 73	0.436 63	−0.6	0.104 43	0.142 48
0.8	0.972 33	0.948 42	0.3	0.718 70	0.688 61	−0.2	0.352 70	0.373 61	−0.7	0.061 33	0.094 42
0.7	0.939 43	0.906 48	0.2	0.648 73	0.627 63	−0.3	0.282 66	0.312 60	−0.8	0.028 21	0.052 33
0.6	0.896 52	0.858 54	0.1	0.575 75	0.564 64	−0.4	0.216 60	0.252 56	−0.9	0.007 7	0.019 19
0.5	0.844	0.804	0.0	0.500	0.500	−0.5	0.156	0.196	−1.0	0.000	0.000

feature that their ordinates change most rapidly at mid-eclipse proportionally /97 to the time, since both curves have their flex point at a = 0. This follows directly from eqs.(13) and (17) if the second differential quotient 2a is formed. In fact, eq.(13) will yield

$$\frac{d^2Q}{da^2} = -\frac{ak\pi}{r}.$$

From eq.(17), we obtain in the same manner,

$$\frac{d^2Q}{da^2} = -\frac{2ak}{\sqrt{r^2 - a^2}},$$

and both values of $\frac{d^2Q}{da^2}$ become zero for a = 0.

Seeliger demonstrated generally that, for each form of the function $F(\sqrt{x^2 + y^2})$, the same property is retained. In fact, eq.(11) yields

$$\frac{dQ}{da} = 2k\int_0^{\sqrt{r^2 - a^2}} F(\sqrt{a^2 + y^2})\, dy$$

and, after a second differentiation,

$$\frac{d^2Q}{da^2} = 2k\left\{-\frac{aF(r)}{\sqrt{r^2 - a^2}} + \int_0^{\sqrt{r^2 - a^2}} \frac{\partial F(\sqrt{a^2 + y^2})}{\partial a}\, dy\right\}. \qquad (19)$$

Since, however

$$\frac{\partial F(\sqrt{a^2 + y^2})}{\partial a} = 2a\frac{\partial F(\sqrt{a^2 + y^2})}{\partial (a^2)} = 2a\frac{\partial F(\sqrt{a^2 + y^2})}{\partial (a^2 + y^2)},$$

introduction of the variable $a^2 + y^2 = \xi^2$ will furnish

$$dy = \frac{\xi\, d\xi}{\sqrt{\xi^2 - a^2}}$$

and, furthermore

$$\frac{\partial F(\sqrt{a^2 + y^2})}{\partial a}\, dy = 2a\frac{\partial F(\xi)}{\partial (\xi^2)}\frac{\xi}{\sqrt{\xi^2 - a^2}}\, d\xi = a\frac{\partial F(\xi)}{\partial \xi}\frac{d\xi}{\sqrt{\xi^2 - a^2}} = a\frac{F'(\xi)}{\sqrt{\xi^2 - a^2}}\, d\xi.$$

Substituting this value into eq.(19) and observing the integration limits for ξ which become r and a, we obtain

$$\frac{d^2Q}{da^2} = -2ak\left\{\frac{F(r)}{\sqrt{r^2 - a^2}} - \int_a^r \frac{F'(\xi)}{\sqrt{\xi^2 - a^2}}\, d\xi\right\}.$$

This expression vanishes for a = 0, for which reason this point will always be a flex point even if - as demonstrated by Seeliger - it might not always be the only point in the case of an arbitrary form of the function F.

This fact results in the logical requirement of reducing all observations of the eclipse process to the instant at which the satellite possesses half of

its luminous intensity, since this instant can be determined with greatest reliability and is also geometrically strictly defined.

The time between beginning and middle of the eclipse furnishes the value of the satellite radius. However, determining the exact instant of incipient eclipse is extremely difficult, and the slope of the eclipse curve is impossible to define theoretically.

Aside from the uncertainty as to the brightness of the limb, produced by /98 the fact that the reflection law is unknown, complications are created by all those phenomena that contribute, in lunar eclipses, to changes in the earth's shadow in either a positive or negative sense; these phenomena are due, on the one hand, to the influence of the atmosphere of the shadow-casting planet and, on the other hand, to physiological causes that will be discussed at the end of this Chapter (Sect.47).

Because of the basic importance of the influence of a planetary atmosphere on the position of its shadow edge for a correct interpretation of the photometric phenomena during eclipses, the considerations by Seeliger (Ref.141) on this subject will be discussed here. Despite the fact that these are more of a basic nature and offer no possibility for a strict calculation, they are suitable for giving some information on the uncertainties produced by observations of the Jovian satellites.

45. Influence of an Atmosphere on the Position of the Umbra of a Planet

Let us imagine a light ray, starting from the point S on the solar surface, passing the atmosphere of the planet whose radius is ρ and which has its center in P, being refracted there, and - after refraction - striking the point M on the satellite surface. This ray, at the point E, contacts an equidense layer of the atmosphere, concentric with the planetary surface. Let the radius of this

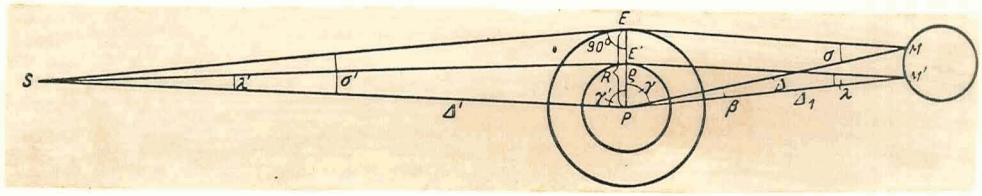

Fig.26 Influence of the Atmosphere on the Boundary of the Umbra.

atmospheric layer be R. Then, S as well as M will be at the apparent horizon of the point E. A ray, starting from S and touching the planetary surface at the point E' without refraction, is assumed to strike the satellite surface at M'. Let $SP = \Delta'$, $MP = \Delta$, and $M'P = \Delta_1$ and let the apparent angular distance of the point E from P, influenced by the refraction and seen from S resp. M be σ' resp. σ; furthermore, let the angles be $PSE' = \lambda'$, $PM'E' = \lambda$, $MPM' = \beta$, $SPE' =$

= γ', MPE′ = γ. Finally, let μ be the refractive index of the atmosphere at the point E and r the horizontal refraction at the same point*. Then, the following relations are valid, of which the first represents the fundamental equation of refraction:

$$\left.\begin{aligned} \Delta \sin\sigma &= \mu R, & \Delta' \sin\sigma' &= \mu R, \\ \gamma + \sigma &= 90^\circ + r, & \gamma' + \sigma' &= 90^\circ + r, \\ \Delta' \sin\lambda' &= \Delta_1 \sin\lambda = \varrho, \\ \beta &= 2r - \sigma - \sigma' + \lambda + \lambda'. \end{aligned}\right\} \tag{20}$$

Substituting the sine of the angles σ, σ', λ, λ' by the arc, we obtain

$$\beta = 2r - \mu R\left(\frac{1}{\Delta} + \frac{1}{\Delta'}\right) + \varrho\left(\frac{1}{\Delta'} + \frac{1}{\Delta_1}\right).$$

Let h be the height of the point E above the planetary surface so that R = /99
= ρ + h; then,

$$\beta = 2r + (1-\mu)\varrho\left(\frac{1}{\Delta} + \frac{1}{\Delta'}\right) - \mu h\left(\frac{1}{\Delta} + \frac{1}{\Delta'}\right) + \varrho\left(\frac{1}{\Delta_1} - \frac{1}{\Delta}\right). \tag{21}$$

The second term on the right-hand side can be omitted for the case of the earth; its value is smaller than 1″ for the earth's surface.

Similarly, in the third term, $1/\Delta'$ can be neglected for $1/\Delta$ and $\mu = 1$ can be set, so that we finally obtain

$$\beta = 2r - \frac{h}{\Delta} + \varrho\frac{\Delta - \Delta_1}{\Delta\Delta_1}. \tag{22}$$

The third term of this formula, over $\Delta - \Delta_1$, depends on the size of the angle β, i.e., on the point of the satellite surface where the investigated ray strikes this surface. For a given β, the difference $\Delta - \Delta_1$ will reach its maximum value at the apparent lunar limb. Denoting by ρ' the lunar radius and by Δ_0 the distance of the lunar center from the planetary center, this maximum value can be calculated in the following manner: This value, denoting the angle between Δ_1 and Δ_0 by x, will be

$$\varrho'^2 = \Delta^2 + \Delta_0^2 - 2\Delta\Delta_0\cos(x-\beta) = \Delta_0^2 - \Delta_1^2,$$
$$\Delta_0\cos(x-\beta) = \Delta_1\cos\beta + \varrho'\sin\beta,$$

whence

---

* The angle SE′M′ is equal to 180° whereas, at the point E, in addition to the tangent also the intercept of the uncurved rays above E must be assumed, making a mutual angle of 180 - 2r. The angle β determines the shift of the shadow edge. In Fig.26, this is negative.

$$\Delta^2 + \Delta_1^2 = 2\Delta\,(\Delta_1 \cos\beta + \varrho' \sin\beta) = 2\Delta\,\Delta_1 - 4\Delta\,\Delta_1 \sin^2\tfrac{1}{2}\beta + 4\Delta\,\varrho' \sin\tfrac{1}{2}\cos\tfrac{1}{2}\beta$$

and

$$\frac{\Delta - \Delta_1}{\Delta} = \pm 2\sqrt{\frac{\varrho'}{\Delta}\sin\frac{1}{2}\beta\cos\frac{1}{2}\beta - \frac{\Delta_1}{\Delta}\sin^2\frac{1}{2}\beta}\,.$$

Since an approximate calculation of the small term $\frac{\rho}{\Delta_1}\,\frac{\Delta - \Delta_1}{\Delta}$ is involved here, which may be of the order of seconds, the second term under the square root can be neglected as being of a higher order and Δ can be replaced by Δ_0; this will furnish

$$\frac{\Delta - \Delta_1}{\Delta} = \pm\sqrt{\frac{2\varrho'}{\Delta_0}\beta}$$

and

$$\sin 1''\left(\frac{\varrho}{\Delta_1}\,\frac{\Delta - \Delta_1}{\Delta}\right)'' = \pm\frac{\varrho}{\Delta_0}\sqrt{\frac{2\varrho'}{\Delta_0}\beta}\,.$$

Substituting here the values ρ and ρ', Δ_0 for the moon and denoting the value of β by β'' in seconds of arc, we obtain

$$\left(\frac{\varrho}{\Delta_1}\,\frac{\Delta - \Delta_1}{\Delta}\right)'' = \pm 0.72\sqrt{\beta''},$$

or, if γ is a positive or negative proper fraction, the result will finally be

$$\beta = 2r - \frac{h}{\Delta} + 0.72\gamma\,. \qquad (23)$$

This formula gives the angle by which the umbra radius of the planet, projected onto the satellite, would be changed by the refraction in comparison to that obtained without atmosphere, entirely disregarding the extinction. If β is positive, a reduction in the radius of the shadow will result. However, it might be that the lower layer of the atmosphere of the planet is opaque to horizontally incident solar rays, up to a height of h. This circumstance increases the radius of the umbra. The two effects cancel each other as soon as the angle becomes $\beta = 0$. This value of h is readily determined in first approximation. /100

Denoting by λ the ratio of the densities of two atmospheric layers at a height h and at the earth's surface

$$\lambda = \frac{\delta}{\delta_0}\,, \qquad (24)$$

and starting from Ivory's formula for the horizontal refraction r, the following equation will be obtained between the values of this quantity, for both atmospheric layers:

$$r = r_0(0.9121\lambda + 0.0879\lambda^2)\,. \qquad (25)$$

Substituting here the value of the horizontal refraction at the earth's surface according to Ivory $r_0 = 2037''.8$, we obtain

$$r = 1858''.7\lambda + 179''.1\lambda^2.$$

If for example, we take h = 36.5 km for which altitude - again according to Ivory - $\lambda = 0.006$, we obtain

$$r = 11''.15, \qquad \frac{h}{\Delta} = 19''.6$$

and thus

$$\beta = 2''.7 + 1''.4\gamma. \tag{26}$$

Consequently, this value definitely is still positive and will be even more so for deeper layers. It is obvious that an opaque atmospheric layer of 36.5 km would not be sufficient for enlarging the radius of the umbra. Just the opposite, the effect of the atmosphere reduces this radius further, so that the observed increase in the earth's shadow during lunar eclipses must be attributed to other causes.

Seeliger performed a calculation of light attenuation of the solar rays by the atmosphere at the above altitude; as expected, the amount of attenuation was negligible but, because of its basic importance, we will discuss it here.

The Laplace extinction theory of light (see Section on "Extinction") leads to the equation

$$\log \frac{J_z}{J} = -\frac{K}{\sin z} \times \text{refraction}, \tag{27}$$

where J is the brightness of the star outside the atmosphere and K is a constant; z is the apparent zenith distance of the star. In general, the refraction is calculated according to the formula $\alpha_z \tan z$, where α_z can be taken from the refraction table and is represented in the form

$$\alpha_z = \alpha_0\{1 + a\tan^2 z + b\tan^4 z + c\tan^6 z + \cdots\}.$$

Here, α_0 is the refraction constant which, according to Bessel, is $57''.76$, while a, b, c are constants.

This also furnishes the equation

$$\log \frac{J_z}{J} = -K\alpha_z \sec z, \tag{28}$$

and, for z = 0

$$\log \frac{J_0}{J} = -K\alpha_0 = A. \tag{29}$$

Here, A is the logarithm of the transmission coefficient which, according to Seeliger, has a value of 0.08874. After substitution of the Bessel constant, this yields for α_0 /101

$$\log K = 7.1258, \quad K = 0.001336.$$

Equation (27) is valid also for a given star in the horizon; substituting here the horizontal refraction r = 2094", it follows for the horizon

$$\log \frac{J_{90}}{J} = -K \times 2094 = -2.797 \quad \text{and} \quad \frac{J_{90}}{J} = 0.0016.$$

Presumably, this figure is still too low, as demonstrated by the discrepancies between theory and observation near the horizon. For an altitude of 36.5 km, we obtained a value of r = 11".15 for the horizontal refraction. The corresponding extinction in the horizon will thus be

$$\log \frac{J_{90}}{J} = -0.001336 \times 11''.15 = -0.0149,$$

and $J_{90}:J = 0.967$. Since the sunlight undergoes this attenuation twice, the total light attenuation will be less than 6%.

The limit of 36.5 km for an opaque atmosphere thus was taken by far too high.

For Jupiter, the value of the refraction constant is unknown. Observations of stellar occultations by the planet exhibit phenomena which definitely prove the existence of a dense atmosphere but are not suitable for determining the horizontal refraction.

Nevertheless, the values of the transmission coefficient of the Jovian atmosphere, derived by the author (Ref.142), indicate a strong horizontal refraction. For Jupiter, we have

$$\log \frac{J_0}{J} = -K\alpha_0 = -0.2009, \qquad \frac{J_0}{J} = 0.63, \qquad \text{absorption coefficient} = 0.37.$$

Here, K depends on the height of the homogeneous atmosphere and on its refractivity and absorptivity. A determination of K is impossible at present, since these quantities are entirely unknown. However, since the horizontal refraction is almost proportional to the density of the lower atmospheric layers, it is logical that, at equal composition of the terrestrial and the Jovian atmosphere, the horizontal refraction must first be increased at the ratio of the absorption coefficients $\frac{0.37}{0.17} = 2.2$ and then at the ratio of the mean free paths which are approximately given by the equation: mean free path $= \sqrt{2Rl + l_0^2}$; here, R is the radius of the planet and l_0 the height of its homogeneous atmosphere. Thus, when neglecting l_0^2, the refraction would have to be also increased at the ratio $\sqrt{\frac{(Rl_0)_{Jup.}}{(Rl_0)_{earth}}}$, which yields a factor of 3.3 already at equal height of the homogeneous atmospheres l_0 so that the total value will be 7.2. Accordingly, the horizontal refraction of Jupiter would be 4°, a value which is estimated rather too low than too high.

Nevertheless, the cooperation of refraction and extinction is not as easy to define for the Jovian atmosphere as is permitted by the Seeliger analysis for the terrestrial atmosphere. To calculate the refraction at various heights /102 above the surface, even in first approximation, is entirely out of the question for Jupiter since no data at all are available on the height of the atmosphere and the decrease in density. The shift of the shadow edge due to the above causes, however, most likely takes place on a much larger scale than in lunar eclipses. The duration of the eclipses of the Jupiter moons as well as the slope of the eclipse curves at the beginning and end of the eclipse are influenced by the Jovian atmosphere in an uncalculable manner; for this reason, only the mid-eclipse can be used theoretically.

46. Observations of Eclipses of Jupiter's Satellites by Harvard College Observatory

These theoretical objections to the usefulness of satellite eclipses for questions of a physical nature have been confirmed fully by observations made over many years at Harvard Observatory. These observations extended over 25 years (1878 - 1903) and were carried out with special photometers designed for this particular purpose, permitting a convenient and rapid measurement. As comparison object, another satellite was used in most cases while the planet itself was used in a few cases, in which the image of the planet was projected through a special telescope into the focal plane of the refractor. To increase the number of settings during the time of the eclipse, assistant observers were used which made it possible to perform 12 - 13 settings per minute. In all, 670 eclipses and emergences of the four satellites were observed, of which half refer to the satellite I. The eclipse curves are well substantiated by 40 - 60 individual measurements and distinctly show the slope of the light reduction.

This extensive material was worked up by R.A.Sampson (Ref.143) in a most excellent manner and used in the theory of the motion of Jupiter's satellites. As important as the results of this investigation are for the theory of motion of the satellites, they are disappointing in some respects because of the unexpectedly great deviations of the reduced individual moments.

The mean error of the occultation moment of the satellite I, which can best be defined from the occultation curve, is still $\pm 6^s$, which corresponds to an error in the time equation of $\pm 1^s.3$ while the error in the solar parallax is $\pm 0''.023$. It thus seems that, for determining these constants, the observation of eclipses is of only minor significance.

The reasons for the large random deviations of the occultation moments, which frequently exceed 30^s, are discussed in detail by the author. The derivation of the moment of mid-eclipse was performed under assumption of uniform brightness of the satellite disk, by estimating the moment of half-brightness with the aid of calculated eclipse curves that were fitted to the observed curves.

However, as shown in Fig.27 which gives several extreme cases of the Sampson curves, this slope is subject to considerable fluctuations which cannot be attributed to observation errors. As possible causes, Sampson discussed the

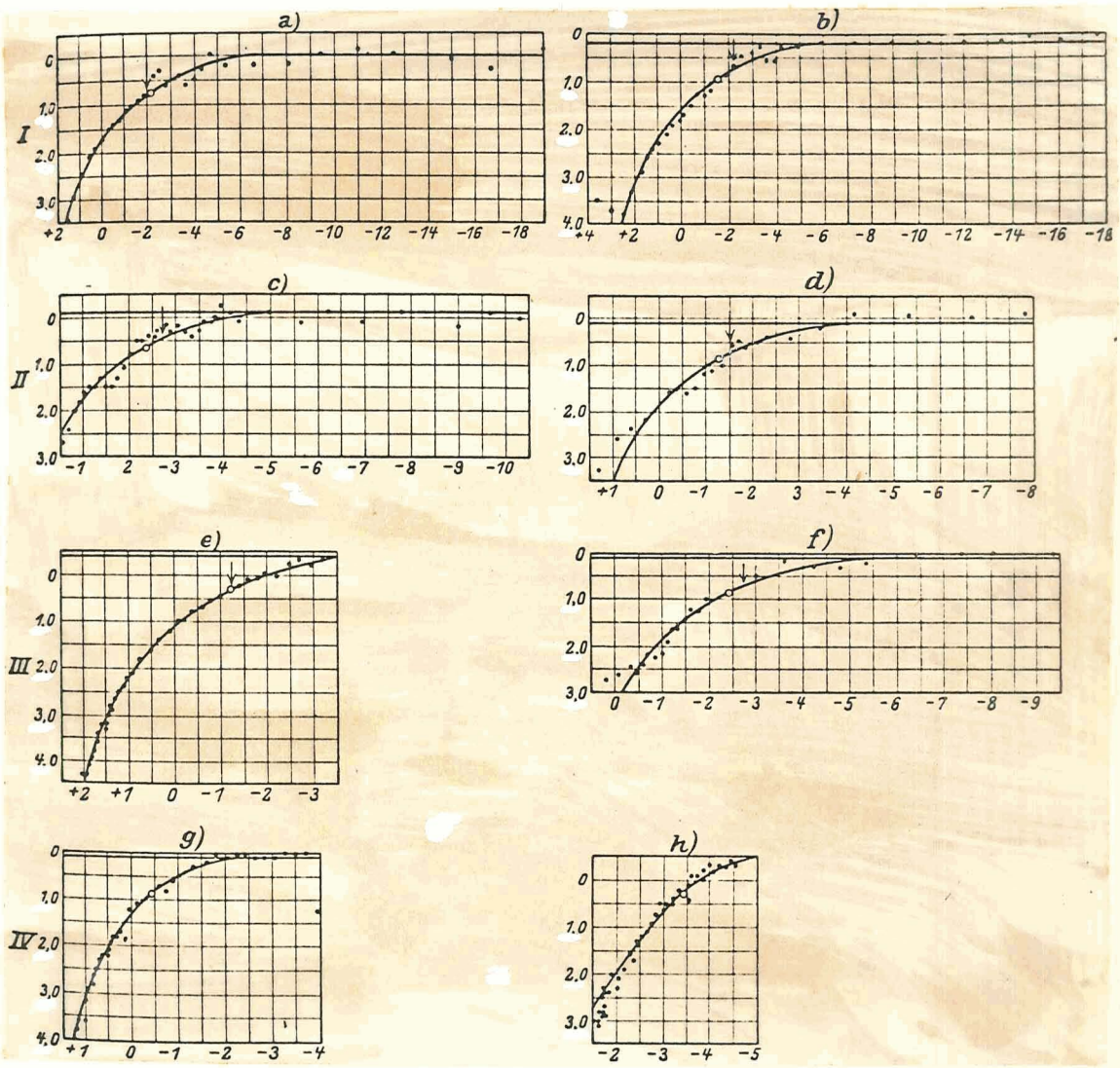

Fig.27 Eclipse Curves of Jupiter's Satellites, according to Observation at Harvard College Observatory.
a) Good agreement; b) Brightening at end of eclipse; c) Strong fluctuations; d) Shallow curve; e) Good agreement; f) Brightening at emergence; g) Good agreement; h) Observations at high latitudes. The small circles refer to points at which the brightness would have to be half of the uneclipsed value, according to the theory of motion; these points should have the ordinates $0^m.75$ since $0^m.0$ corresponds to full brightness; the abscissas are proportional to the time; no flex points are observed at the points which, in plotting the absolute values, should appear instead of the magnitude classes.

following:

1) errors in the assumed satellite diameters,
2) irregularities in the satellite motion,
3) irregular boundaries of the satellite disks,
4) phase of the satellites,
5) surface brightness of the disks, increasing or decreasing from the center,
6) light or dark spots on the disks,
7) equatorial streaks on the satellite disks,
8) influence of the Jovian atmosphere.

None of these causes, except for the last, can be made responsible for the extensive deviations, although the minor fluctuations in brightness may be due to the cause (6). This result is properly understood only when using the above /104 considerations on the cooperation of refraction and extinction of sunlight in the lower layers of the Jovian atmosphere. Various observers detected local disturbances in the atmospheric transparency of this planet, manifesting themselves in distortions of the satellite shadow during transit over the disk. Naturally, these disturbances are of a random nature since they occur at the limb of the planet and cause a noticeable shift of the shadow edge, as a function of its height. Nevertheless, a deviation of 30^s corresponds to an elevation of the cloud by 1/140 of the radius and a displacement of the Jupiter limb by $0''.13$. In view of the extensive upheavals constantly taking place on the surface of the planet, it seems entirely probable that the extended atmosphere of Jupiter undergoes extreme refraction and transmission disturbances due to ascending and descending currents. The physiological enlargement of the satellite shadow, discovered by Seeliger, presumably plays a certain role in the observed eclipse moments. This may be in part responsible for the fact that, due to the strong refraction, the expected reduction in the satellite shadow is not revealed in the observations and that the Jupiter diameter, derived from the duration of the eclipses, agrees well with micrometer measurements. Similarly, the satellite diameters, derived from the duration of the eclipses, agree well with the most recent measurements. Consequently, only the shape of the Jupiter shadow is subject to continuous fluctuations as they are occasionally observed even during the eclipse, thus distorting the eclipse curve and producing changes in this curve from case to case by the necessity of having to calculate each time with a different radius of the shadow, depending on the instantaneous atmospheric conditions along the Jupiter limb.

A confirmation of these results by means of a photoelectric photometer is highly desirable. Measurements of such a large brightness range (up to four magnitude classes) within a short period of time are no doubt influenced by systematic and personal errors which could easily be avoided by using a photoelectric photometer. In addition, a greater sharpness of the individual measurement will define the real slope of the eclipse curve in a much more reliable manner and separate the true deviations from observational error. It is impossible to decide at present whether a scrutiny of such deviations will permit conclusions as to the physical nature of the Jovian atmosphere.

Finally, we are giving here the results of Sampson's compensation of the Harvard observations, excluding the results referring to motion of the satellites. The column ΔT represents the corrections of Damoiseau's values (p.105) for the duration of the eclipses.

Satellite	Number of Observations	ΔT	Probable Error of One Observ.	Jupiter Radius	Satellite Radius
I	330	+ 67'	7".1	18".88	0".900
II	169	+ 76	11 .3	18 .95	0 .796
III	124	+170	11 .6	18 .90	1 .397
IV	47	+ 207	22 .1	18 .95	1 .341

47. Seeliger's and v.Hepperger's Theories on Enlargement of the Earth's Shadow in Lunar Eclipses

It has been known for long that, during lunar eclipses, the umbra of the earth is considerably larger than would be expected from the dimensions of the earth. Numerous experiments were made for determining this "enlargement factor" of the earth's umbra from observations; because of the inaccuracy of observations in earlier times, the experiments naturally furnished widely diverging values. The oldest of these determinations are given below: /105

LAHIRE	1:41	LEGENTIL.	1:61 to 1:25
J. CASSINI	1:123	LALANDE	1:69
LEMONNIER	1:82	LAMBERT	1:40 and 1:21
TOB. MAYER	1:60	MÄDLER and J. SCHMIDT	1:49

Around the turn of the Century, several authors published critical reviews over applicable observations and derived more reliable values of the enlargement factor; for example, A.Brosinsky (Ref.144), from 20 eclipses in which only the disappearance and the reappearance of the same craters were used, obtained a mean value of A = 1:55 with the individual values still fluctuating between 1:72.1 and 1:41.5. J.Hartmann (Ref.145) was not satisfied to determine the diameter of the umbra from the duration of the eclipse of individual craters. Since the charts for the moon and its libration are fully sufficient for the purpose in question, the occultation or the emergence of each individual lunar configuration can be used for calculating the umbra diameter, provided that the moments are sufficiently reliable. In this manner, a total of 28 eclipses with 4021 individual moments, from the beginning of the 19th Century to the year 1898, can be used for determining the enlargement factor. With respect to the type of compilation of these values, Hartmann and H.Seeliger (Ref.146) obtained greatly differing figures for the enlargement of the earth's shadow from these data. If the phenomenon is assumed as real and as caused by the terrestrial atmosphere, as had been done by almost all authors before Seeliger, it would be necessary to allow for the varying distance of the moon; this can be done by reduction to mean parallaxes (π_0) or with the aid of the factor π/π_0, with which the enlargement of the earth's shadow, expressed in seconds of arc, must be multiplied. Hartmann found the following values:

Period I	V = 53".07	V = 49".85
Period II	V = 48".62	V = 49".67

where two periods, in accordance with the accuracy of observation, are differentiated and also two different averagings: according to the accidental observation errors of all values without making a difference between observers and

according to the mean values of the individual observer. Seeliger who attributed the enlargement of the earth's shadow to physiological causes doubted the justification of a reduction to mean parallaxes and was convinced that the most reliable result from Hartmann's data would be a value of

$$V = 50''.6.$$

Seeliger (Ref.147) also drew attention to several peculiarities of the phenomenon, mentioned earlier by Hartmann and resulting from a closer study of Hartmann's individual values. Entry into and emergence from the shadow, /106 treated individually, lead to widely differing values:

	Period I	Period II
Entry	59".19	50".93
Emergence	49".30	47".46

In addition, individual better observation series show an apparent reduction in the shadow with increasing eclipse of the moon and a re-enlargement with decreasing eclipse. Thus, it can be expected that the entry and emergence of the lunar limb will also yield different values. In fact, Seeliger was able to confirm this finding since the values were as follows:

Limb I $V = 47''.0$
Limb II $V = 45''.4$.

A classification of the sizes V according to apparent distances of the individual craters from the center of the lunar disk seems of special interest but has never been made despite the abundant observational material available.

A refutation of the previously generally held view that the enlargement of the earth's shadow and its variability are due to the opaqueness of the lower atmospheric layers has already been given in Section 45, based on Seeliger's concept. Even if one assumes that the atmosphere has the effect of a nontransparent screen up to an altitude of 36.5 km, no enlargement of the umbra of the earth due to refraction of the solar rays will in reality occur. Rather, the unilluminated space at the distance of the moon would have to appear smaller than the earth's umbra calculated without allowance for the atmosphere.

However, if one admits the explanation of the phenomenon, given by Seeliger in the above-mentioned report, according to which a physiological cause is involved, then an accurate calculation will become necessary of the quantities of light reaching the lunar surface in the vicinity of the geometric shadow edge, with consideration of refraction and extinction. Such a calculation, as proved by Seeliger's extensive treatise on the subject, is quite complicated despite the fact that, in view of the uncertainty of present knowledge on the consistency of the upper atmospheric layers, it cannot be performed in an entirely strict form. Specifically, this is aggravated by the fact that, in addition to extinction and recraction, a noticeable dispersion of the solar rays takes place whose calculation would be extremely difficult and had also never been attempted by Seeliger himself. In all other respects, the Seeliger calculation is strict in so far as, under certain assumptions on the ray refraction and absorption and

under consideration of the nonuniform brightness of the solar disk, it develops the consequences of these assumptions with extreme accuracy. However, since in the final analysis a proof of a physiological cause of the enlargement of the earth's shadow must be brought by experiments with rotating disks which, obviously, are quite unreliable, it is permissible to give here the problem in a much simpler and only slightly less accurate form, which has the advantage of greater distinctness. Such a representation was made by J.v.Hepperger (Ref.148) who treated the problem a few years before Seeliger without consideration of the limb darkening of the solar disk. According to Seeliger, the influence of this limb darkening is negligible and the deviations of the calculated brightness course along the edge of the umbra, which were observed by both authors, must /107 be attributed mainly to the difference in the refraction and absorption theories used as basis.

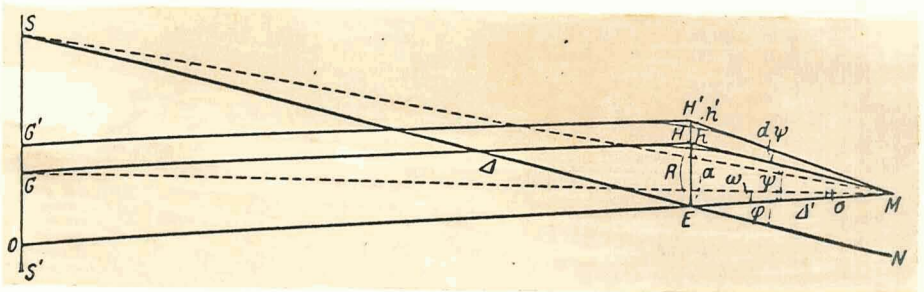

Fig.28 Enlargement of the Earth's Shadow during Lunar Eclipses.

In Fig.28, let S and E be the centers of the sun and earth, SN the axis of the umbra, M a point on the lunar surface, SS′ the solar radius, and O the point on the solar disk directed toward ME; G and G′ are two points on the sun which, over the terrestrial atmosphere (GhM and G′h′M), contribute to the illumination of M. Here, H and H′ are the intersection points of the ray directions before and after passage through the atmosphere. Furthermore, we are using the following notations:

$$\angle GMO = \omega \qquad HE = l$$
$$\angle HME = \psi \qquad hE = R = a + k, \text{ where a is the earth radius,}$$
$$\angle SME = \sigma \qquad SE = \Delta$$
$$\angle MEN = \varphi \qquad ME = \Delta'$$
$$\angle EHM = \angle EHG = 90° - r, \text{ where r is the horizontal refraction.}$$

Let the transmission coefficient for the ray GHM be A, and let the radius of the sun seen from M be $\angle SMS' = s$.

From the triangles HME and SEM, it follows that

$$l\cos r = \Delta' \sin\psi \qquad \text{and} \qquad \Delta' \sin\sigma = \Delta \sin(\varphi - \sigma)$$

or, with sufficient accuracy,

$$\varphi - \sigma = \frac{\Delta'}{\Delta}\sigma.$$

Denoting $\eta = \psi - \omega$, it follows from the triangle GHM that

$$GM \sin\eta = GH \sin 2r$$

or, with sufficient approximation on equating GH = SE and GM = $\Delta + \Delta'$,

$$\eta = 2r\frac{\Delta}{\Delta + \Delta'}.$$

From the point G′ on the solar disk, the path leads to M over the point H′ of the atmosphere, which corresponds to an increase in ψ and $d\psi$. On rotating the figure about OM as axis, H and H′ as well as G and G′ will describe circles about E and O. From all these points G, light will penetrate as far as M. So long as the circular ring described by GG′ is located entirely on the solar disk (at uniform brightness of the disk), the quantity of light corresponding to the angle $d\psi$ and reaching M will be equal to

$$dL = JA\,2\pi \sin\psi\, d\psi\,.$$

where J denotes the constant intensity of the rays while A is the transmitted fraction of the rays. Where the circular ring osculates the solar limb at the center angle λ (see Fig.29), the <u>/108</u>

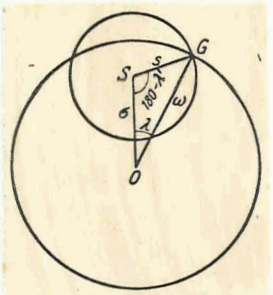

Fig.29 Portion of the Solar Disk Visible from the Moon.

quantity of light becomes smaller at the ratio $\frac{\lambda}{\pi}$, i.e.,

$$dL = 2JA\lambda \sin\psi\, d\psi\,.$$

On varying ψ from a to the limit of the atmosphere and integrating, the total quantity of light refracted by the atmosphere to M is obtained:

$$L = 2J\int_{a}^{\text{lim. atm.}} \lambda A \sin\psi\, d\psi\,.$$

If, above the atmospheric boundary, light reaches M without refraction, this can be expressed by the same integral since, in that case, A = 1, $\eta = \psi - \omega = 0$, i.e., $\psi = \omega$, and the quantity of light reaching M without interference by the earth will be $2J \int \lambda \sin\omega\, d\omega$.

Thus, for taking also the unrefracted light into consideration, it is only necessary to set the upper limit of the integral equal to $\psi = \sigma + s$. For calculating the angle λ, the following equations are used:

$$\sin^2\frac{\lambda}{2} = \frac{\sin\frac{s+\omega-\sigma}{2}\sin\frac{s-\omega+\sigma}{2}}{\sin\sigma\sin\omega}, \qquad \cos^2\frac{\lambda}{2} = \frac{\sin\frac{\omega+\sigma+s}{2}\sin\frac{\omega+\sigma-s}{2}}{\sin\sigma\sin\omega},$$

which, because of the smallness of the angles, can be written also in the form

$$\sin^2\frac{\lambda}{2}=\frac{(s+\omega-\sigma)(s-\omega+\sigma)}{4\sigma\omega};\qquad \cos^2\frac{\lambda}{2}=\frac{(\omega+\sigma+s)(\omega+\sigma-s)}{4\sigma\omega}.$$

If $\sigma < s$, the circles will intersect for

$$s-\sigma<\omega<s+\sigma,$$

resulting in $\pi > \lambda > 0$, whereas for

$$\omega\leqslant s-\sigma,\qquad \lambda=\pi,$$
$$\omega\geqslant s+\sigma,\qquad \lambda=0.$$

If $\sigma > s$, we obtain $\lambda > 0$ for $\sigma - s < \omega < \sigma + s$, while we obtain $\lambda = 0$ for this limit of ω and outside of the limit.

Let us make an elementary calculation of the quantity of light reaching M directly without refraction, which is simple at uniform brightness of the disk. Let Ψ be the value of ψ for which the effect of the atmosphere is vanishingly small. Then, $\omega = \Psi$ and, at $\Psi < \sigma + s$, a portion of the sun has a direct effect. The quantity of light of this element of area, bounded by two circular arcs, will be

$$J[\lambda_1' s^2-\lambda_1\Psi^2+\sigma\Psi\sin\lambda_1],$$

where λ_1' and λ_1 represent the values of λ' and λ belonging to the corresponding boundary.

The quantity of light, reaching M from the sun without intervention of the earth, is $L_0 = \pi J \sin^2 s$. Expressed in this unit, the quantity of light actually reaching M will be

$$H=\frac{2}{\sin^2 s}\int_{\psi_0}^{\Psi}\frac{\lambda}{\pi}A\sin\psi\,d\psi+\frac{\lambda_1'}{\pi}-\frac{\lambda_1}{\pi}\frac{\Psi^2}{s^2}+\frac{\sigma\Psi}{s^2}\frac{\sin\lambda_1}{\pi},$$

/109

if $\Psi < \sigma + s$. Here, ψ_0 is the lowest value that ψ is able to assume.

For $\Psi \geqslant \sigma + s$, all light reaching M passes through the atmosphere; then $\lambda_1 = \lambda_1' = 0$, and the upper limit of the integral will become equal to that value of ψ which corresponds to $\omega = \sigma + s$.

In view of the fact that the refraction r as well as the transmittance A are functions of the same variable, namely the height k above the earth's surface, this can be introduced as independent variable by setting

$$\xi=\frac{k}{a}=\frac{R-a}{a},$$
$$R=a(1+\xi).$$

However, we have

$$\Delta' \sin\psi = l \cos r,$$

and from the equation for the horizontal refraction, if μ denotes the refractive index at the height h, it follows that

$$\Delta' \sin\psi = \mu R = \mu a (1 + \xi),$$

whence

$$\frac{l}{a} \cos r = \mu (1 + \xi).$$

According to Bessel's refraction theory, v.Hepperger assumed the following expression for the correlation between the refractive index μ and the height ξ:

$$\mu^2 - 1 = c\delta_0 e^{-\varkappa_0 \xi},$$

where the air density δ_0 at the earth's surface and the constant c are in the following correlation with the refraction constant β_0:

$$\beta_0 = \frac{c\delta_0}{1 + c\delta_0}.$$

It is also possible, to write with sufficient accuracy:

$$\mu = 1 + \tfrac{1}{2}\beta_0 e^{-\varkappa_0 \xi}.$$

From this, it follows, again with sufficient accuracy, that

$$\frac{l}{a} \cos r = 1 + \xi + \frac{1}{2}\beta_0 e^{-\varkappa_0 \xi}$$

and

$$\sin\psi = \frac{a}{\Delta'}\left(1 + \xi + \frac{1}{2}\beta_0 e^{-\varkappa_0 \xi}\right) = \frac{l}{\Delta'} \cos r,$$

$$d\psi = \frac{a}{\Delta'} \frac{1 - \frac{1}{2}\beta_0 \varkappa_0 e^{-\varkappa_0 \xi}}{\cos\psi} d\xi.$$

Setting the parallax of the point M equal to that of the lunar center

$$\frac{a}{\Delta'} = \sin \Pi$$

and replacing cos ψ by cos Π, which does not constitute a loss of accuracy in five-place calculations, then the integral to be calculated in the equation for H will become

$$\int_{\psi_0}^{\psi_1} \frac{\lambda}{\pi} A \sin\psi \, d\psi = \frac{\sin^2 \Pi}{\cos \Pi} \int_{\xi_0}^{\xi_1} \frac{\lambda}{\pi} A \left(\frac{l}{a} \cos r\right)\left(1 - \frac{1}{2}\beta_0 \varkappa_0 e^{-\varkappa_0 \xi}\right) d\xi.$$

This integral can be determined by mechanical quadrature since it depends only /110 on ξ and on the elements of the eclipse. The values of horizontal transmit-

tance A and refraction r were calculated by Hepperger on the basis of Bessel's hypothesis as to the pressure drop with altitude; here, the former value is obtained from Müller's observations on extinction, while the constant $\varkappa_0$ is taken from Bessel's refraction theory. The lower limit ξ_0 of the integral is zero from $\sigma = 0$ to $\sigma = s + \omega_0$ where ω_0 represents the value of ω for $\xi = 0$. If $s < \sigma < s + \omega_0$, then only a portion of the lowest atmospheric layer will emit light toward M whereas the higher layers become effective on the opposite side of the earth. For $\sigma > s + \omega_0$, the quantity ξ_0 corresponds to a value $\omega = \sigma - s$. The upper limit ξ_1 refers throughout to $\omega = \Psi$ as long as $\Psi < \sigma + s$, and otherwise to $\omega = \sigma + s$.

Since the angles of incidence change only slightly, the calculated H are equal to the brightness ratios of the same lunar vicinity during eclipsed moon and during full moon. The geometric limit of the earth's umbra, since $s + \varphi_1 = \Pi = 57'2''.1$, is equal to the radius $\varphi_1 = 41'11''.2$.

TABLE 10

LOG H

φ_1	Accd. to v.Hepperger	Accd. to Seeliger I	Accd. to Seeliger II
2460″	7.576−10	7.347−10	7.180−10
2470	7.614^{38}	7.392^{45}	7.214^{34}
2480	7.656^{42}	7.445^{53}	7.250^{36}
2490	7.705^{49}	7.512^{67}	7.290^{40}
2500	7.765^{60}	7.604^{92}	7.338^{48}
2510	7.841^{76}	7.725^{121}	7.399^{61}
2520	7.930^{89}	7.850^{125}	7.478^{79}
2530	8.021^{91}	7.964^{114}	7.569^{91}
2540	8.106^{85}	8.064^{100}	7.667^{98}
2550	8.186^{80}	8.153^{89}	7.763^{96}
2560		8.232^{79}	7.855^{92}

Of considerable importance for the question as to the enlargement of the earth's shadow is the calculation of brightnesses along the edge of the umbra. This was done by v.Hepperger in accordance with the above-developed theory, while Seeliger used somewhat more accurate methods. The results are compiled in Table 10. In the column "Seeliger II", his results with consideration of the brightness fall-off along the solar limb are entered.

Assuming the enlargement of the earth's shadow V = 50″.6, derived by Seeliger the apparent terminator should be expected at 2521″.8. The slope of the Hepperger and the stricter Seeliger brightness curves do not let one expect such a terminator per se, despite the fact that the initial differences of the first curve show a small maximum at the point in question. Therefore, the problem could be checked only experimentally, which was attempted by Seeliger with the aid of rotating disks. On a circular disk (Fig.30), an area Oba was painted white and the remaining portion deep black, and the boundary Omb was calculated with consideration of the brightness curve during lunar eclipses. For this, the angle mOa = α must be assumed as proportional to the brightness at the distance in question. The center of the disk, whose radius was assumed as 15 cm, was given the brightness corresponding to $\varphi_1 = 2560''$ while the periphery received the brightness at $\varphi_1 = 2560''$. The brightnesses were those given in the second Seeliger table.

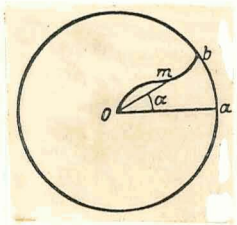

Fig.30 Rotating Disk for Representing the Light Reduction during Lunar Eclipses, according to Seeliger.

Consequently, in the case of a rapid rotation of

such a disk, a boundary line between light and dark would have to be expected at a distance of 9.13 cm from the center. The results of estimates of the apparent boundary were found to be dependent on the illumination intensity of the disk /111 as well as on the observers, of whom several participated in the experiments; however, all estimates gave values between 8.7 and 9.8 cm, which thus constitutes a satisfactory confirmation of the expected result.

It is of interest to note that the assumption that a terminator must appear whenever the differential quotient dH/dr shows a discontinuity, is by no means always true; only at greater abrupt changes in brightness will a terminator definitely be formed. The same is true for the differential quotient d log H/dr, and it seems that the second differential quotient d^2H/dr^2 or, within certain limits, even more so d^2 log H/dr^2 might play a substantial role for the phenomena in question. In any case, these are greatly influenced by the contrast phenomenon.

Of special interest are the conclusions drawn by both Hepperger and Seeliger on the effect of the lower atmospheric layers. The turbidity of this layer, due to cloud formation, is highly variable; this variability might be the cause of the differing brightnesses of the umbra during various lunar eclipses. An accurate analysis yields the following result:

The lower layers of the atmosphere send no light at all to the limit of the umbra, so that it is immaterial for the slope of the brightness curve near this limit whether the lower atmospheric layers are assumed as entirely transparent or entirely opaque. Thus, the variability of the enlargement factor V, if it is real and not due to observational errors, must be ascribed to other causes. Similarly, a reduction to the mean parallax is of subordinate importance for the edge of the umbra.

Conversely, the state of the troposphere is of great importance for the center of the umbra, in so far as the lower layers of the atmosphere exclusively transmit the sunlight to the internal portion of the umbra. Thus, the above suspicion is confirmed, but with the restriction that another factor - presumably to a much greater extent - influences the brightness of the umbra. This second cause is the variability of the parallax which has an unexpectedly great influence on the axis of the umbra. Seeliger calculated that the brightnesses at the center of the umbra, assuming equal transparency of the atmosphere, should be four times as large at apogee, i.e., at smallest lunar parallax, as at perigee. A more accurate investigation of these effects would be possible only under consideration of the dispersion of sunlight.

V. INFLUENCE OF LIGHT DIFFRACTION IN THE TELESCOPE ON THE LIGHT DISTRIBUTION OVER A PLANETARY DISK; APPARENT DIAMETER OF THE DISK

48. Older Investigations on Diffraction

The influence of diffraction on the focal images of luminous points in telescopes was investigated first by Airy (Ref.149). The well-known phenomena observed on fixed stars, namely the spreading of these stars into small disks

with encircling interference rings, was explained by Airy as a logical consequence of the diffraction at the lens aperture. He found the position of the rings in agreement with the theory and reduced the problem of determining the /112 intensity of the diffracted light at any point of the focal plane to an integral function which he represented by convergent series. The nature of this function, as a Bessel function of the first kind, was recognized only later. Almost simultaneously with Airy and independent of him, Schwerd (Ref.150) treated diffraction phenomena in telescopes and, in turn, completely solved the problem for luminous points. His tables of intensity maxima and minima, up to rings of the sixth order, agree with the measurements made by Fraunhofer on fictitious luminous points.

A generalization of the theory to light disks was never attempted by Airy, whereas Schwerd devoted several Chapters of his book to this subject matter and described the principle according to which one can pass from diffraction phenomena of luminous points to those of luminous lines and luminous disks. At the end, he gave several tables for the intensities at different distances from the geometric edge for a rectilinearly bounded disk as well as for a circular disk. These figures apparently were obtained by an approximation method which, however, is not sufficiently well explained. Because of the extreme complexity of Schwerd's method for the calculation of intensities, it is impossible to check on the accuracy.

Further progress in the theory of diffraction phenomena for luminous disks was made through the work of André (Ref.151) who extended Schwerd's tables and furnished also valuable experimental data on diffraction phenomena in telescopes. From a theoretical aspect, the first true advance over Airy's and Schwerd's work was constituted by H.Struve's investigations (Ref.152). In addition, independent authors in this particular field include Lommel (Ref.153) with two treatises and, more recently, H.Nagaoka (Ref.154).

49. Investigations by H.Struve

If we select the focal plane of the telescope to the principal plane xy and direct the z-axis along the optical axis of the objective and, in addition, if we denote the coordinates of a point N of the diffraction aperture by x, y, z and the focal length of the lens by f, then we obtain the following equations for the coordinates ξ_1, η_1 of a point M_1 of the focal plane, with the direction cosines of the refracted wave α_1, β_1:

$$x - \xi_1 = f\alpha_1; \quad y - \eta_1 = f\beta_1. \tag{1}$$

Let M_1 be the locus of the geometric image of a luminous point in the focal plane and let M, with the direction cosines α, β, be another point in the same plane toward which a certain portion of the light is diffracted; then, we also have

$$x - \xi = f\alpha; \quad y - \eta = f\beta. \tag{2}$$

The equation for the refracted wave, entering the telescope, will be

$$s_0 = \sin \frac{2\pi t}{T}, \tag{3}$$

if the amplitude is equated to 1. At the points M_1 and M, we have /113

$$s_1 = \sin 2\pi \left(\frac{t}{T} - \frac{q_1}{\lambda} \right),$$
$$s = \sin 2\pi \left(\frac{t}{T} - \frac{q}{\lambda} \right),$$

where T denotes the vibration period, λ the wavelength of the light, and q_1 and q the distances NM_1 and NM. Now, we have

$$q_1 = \sqrt{(x - \xi_1)^2 + (y - \eta_1)^2 + z^2}$$

and

$$q = \sqrt{(x - \xi)^2 + (y - \eta)^2 + z^2},$$
$$f^2 = x^2 + y^2 + z^2,$$

so that, if ξ/f, η/f are very small quantities and if we can set

we obtain the following expression on the basis of eqs.(1) and (2):

$$q = q_1 + \frac{x(\xi_1 - \xi) + y(\eta_1 - \eta)}{f} = a - \alpha x_1 - \alpha) - y(\beta_1 - \beta),$$
$$q = f - \frac{x\xi + y\eta}{f},$$

while the equation of the wave at $q_1 = f - \frac{x\xi_1 + y\eta_1}{f}$, point M will be

$$s = \sin \left[2\pi \left\{ \frac{t}{T} - \frac{}{\lambda} + \frac{x}{\lambda}(\alpha_1 - \alpha) + \frac{y}{\lambda}(\beta_1 - \beta) \right\} \right],$$

or else

$$s = \sin 2\pi \left(\frac{t}{T} - \frac{q_1}{\lambda} \right) \cos 2\pi \left[\frac{x}{\lambda}(\alpha_1 - \alpha) + \frac{y}{\lambda}(\beta_1 - \beta) \right]$$
$$+ \cos 2\pi \left(\frac{t}{T} - \frac{q_1}{\lambda} \right) \sin 2\pi \left[\frac{x}{\lambda}(\alpha_1 - \alpha) + \frac{y}{\lambda}(\beta_1 - \beta) \right].$$

The amplitude of this vibration can be imagined as resolved into two components C and S, so that

$$1 = C^2 + S^2, \tag{4}$$

where

$$C = \cos \frac{2\pi}{\lambda}((\alpha_1 - \alpha)x + (\beta_1 - \beta)y),$$
$$S = \sin \frac{2\pi}{\lambda}((\alpha_1 - \alpha)x + (\beta_1 - \beta)y). \tag{5}$$

This formula refers to a single element of area dxdy at the point N of the diffracting aperture, with the coordinates x, y, z. The vibration amplitude at the point M, produced by the total aperture, is given by the similar expression

$$A^2 = C^2 + S^2, \tag{6}$$

where

$$\left.\begin{aligned} C &= \iint \cos \tfrac{2\pi}{\lambda} ((\alpha_1 - \alpha)x + (\beta_1 - \beta)y)\, dx\, dy, \\ S &= \iint \sin \tfrac{2\pi}{\lambda} ((\alpha_1 - \alpha)x + (\beta_1 - \beta)y)\, dx\, dy \end{aligned}\right\} \tag{7}$$

and where the integrals must be taken over the entire diffracting aperture.

If this aperture is symmetric with respect to a rectangular system of axes in its plane, then the second integral must vanish. Consequently, in the case of a circular, elliptical, or other aperture, we have to do with two symmetry axes /114

$$S = 0,$$

in which case the brightness I at the point M, if k denotes a constant, becomes

$$I = kC^2, \tag{8}$$

where

$$C = \iint \cos \tfrac{2\pi}{\lambda} ((\alpha_1 - \alpha)x + (\beta_1 - \beta)y)\, dx\, dy.$$

Let us treat the case of a circular aperture and let us introduce polar coordinates over the equations

$$x = r\cos\omega, \qquad y = r\sin\omega. \tag{9}$$

Similarly, using the notations

$$\tfrac{2\pi}{\lambda}(\alpha_1 - \alpha) = r_1\cos\omega_1, \qquad \tfrac{2\pi}{\lambda}(\beta_1 - \beta) = r_1\sin\omega_1; \tag{10}$$

we obtain, for C,

$$C = \int_0^R \int_{\omega_1}^{\omega_1 + 2\pi} \cos(rr_1\cos(\omega - \omega_1))\, r\, d\omega\, dr,$$

where R denotes the radius of the diffracting aperture. Introducing the notations

$$rr_1 = \varrho \qquad \text{and} \qquad \omega - \omega_1 = v, \tag{11}$$

we obtain

$$C = \frac{1}{r_1^2} \int_0^{r_1 R} \int_0^{2\pi} \cos(\varrho\cos v)\, \varrho\, d\varrho\, dv.$$

It is known that, if the Bessel function of n-th kind of z is denoted by $J_n(z)$,

$$J_0(r) = \frac{1}{2\pi}\int_0^{2\pi} \cos(r\cos v)\, dv,$$

$$rJ_1(r) = \int_0^r J_0(r)\, r\, dr.$$

Consequently,

$$2\pi r_1 R J_1(r_1 R) = \int_0^{r_1 R}\int_0^{2\pi} \cos(r\cos v)\, r\, dv\, dr$$

and

$$C = \frac{2\pi}{r_1} R J_1(r_1 R). \tag{12}$$

Setting

$$r_1 R = z \tag{13}$$

we obtain

$$C = 2\pi R^2 \frac{J_1(z)}{z}. \tag{14}$$

Thus, the intensity at the point M will be /115

$$I = 4\pi^2 k R^4 \left(\frac{J_1(z)}{z}\right)^2, \tag{15}$$

while r_1 according to eq.(10) is defined by the equation

$$r_1 = \frac{2\pi}{\lambda}\sqrt{(\alpha_1-\alpha)^2 + (\beta_1-\beta)^2} = \frac{2\pi}{\lambda f}\sqrt{(\xi-\xi_1)^2 + (\eta-\eta_1)^2} = \frac{2\pi}{\lambda f} d. \tag{16}$$

Here, d denotes the linear mutual distance of the points M_1 and M, so that

$$d = f\zeta, \tag{17}$$

where ζ denotes their distance in radians. Consequently, eq.(13) is replaced by

$$z = \frac{2\pi}{\lambda} R\zeta. \tag{18}$$

Finally, referring the intensity to that of the geometric image point ($\alpha = \alpha_1$, $\beta = \beta_1$) as unit and taking into consideration that, for z = 0,

$$\frac{J_1(z)}{z} = \frac{1}{2},$$

then the intensity distribution in the focal plane is defined by

$$I = 4\left(\frac{J_1(z)}{z}\right)^2. \tag{19}$$

Accordingly, the curves of equal intensity are concentric circles about the geometric locus z = 0. On limiting the field of view to several minutes, this representation can be considered as completely exact. This constitutes the representation of diffraction phenomena for luminous points, as it has been known ever since Airy, in the elegant form given by H.Struve. With the aid of tables of the Bessel function J_1, it is easy to calculate the intensity. Practical experience has shown that two different luminous points of a spread-out light source cannot produce visible interference and that the intensity of any point, simultaneously illuminated by both luminous points, can be simply equated to the sum of the intensities which each luminous point would yield individually. This theorem makes it possible to extend the above-derived diffraction laws to luminous disks of arbitrary boundaries and reduces the determination of the luminous intensity of any point, located behind a diffracting aperture, to the evaluation of a double integral.

If the luminous disk is located at infinity and if the diffracting aperture is circular, the above formulas are valid for the intensity of a point M of the focal plane, where ζ is the angular distance from the geometric image of that point (α_1, β_1) of the disk whose diffracted light produces the illumination in $M(\alpha, \beta)$. Here, k is a constant depending on the specific intensity of the point on the disk and thus being a function of α_1 and β_1 alone.

Consequently, if we take the point M as the origin of a polar coordinate system (ζ, ψ) and if we imagine the projection of the luminous disk in the focal plane as resolved into the elements $\zeta d\zeta d\psi$, then the resultant intensity at M, which will be denoted by I, is equal to the sum of the intensities contributed by each of the elements of the disk, or equal to the expression

$$\int\int I(\zeta)\,\zeta\,d\zeta\,d\psi,$$

where the integration must be extended over all elements of the image of the luminous disk. For a point outside the boundary of the geometric image, denoted by the plus sign, we thus have /116

$$I(+) = \int_{\psi_1}^{\psi_2} d\psi \int_{\zeta_1}^{\zeta_2} I(\zeta)\,\zeta\,d\zeta,$$

where ζ_1 and ζ_2 are given as functions of ψ while ψ_1, ψ_2 denote the extreme values of the angle ψ corresponding to the tangents to the periphery of the disk. If, conversely, M is located within the boundary, then

$$I(-) = \int_0^{2\pi} d\psi \int_0^{\zeta_2} I(\zeta)\,\zeta\,d\zeta.$$

In the general case in which the intensity on the luminous disk varies from point to point, $I(\zeta)$ will be a function of ζ as well as of ψ, and the integration - even for simpler cases - becomes highly complex and can be performed only by mechanical quadrature. Struve treated only the case of uniformly bright disks for which k is a constant independent of ζ and ψ and in which the integration can be omitted. He substituted ζ by the variable z whose limiting values are as follows:

$$z_1 = \frac{2\pi}{\lambda} R\zeta_1, \qquad z_2 = \frac{2\pi}{\lambda} R\zeta_2.$$

Omitting the factor $\lambda^2 R^2$, eq.(15) will yield the expressions

$$I(+) = \int_{\psi_1}^{\psi_2} d\psi \int_{z_1}^{z_2} \frac{(J_1(z))^2}{z} dz, \qquad I(-) = \int_0^{2\pi} d\psi \int_0^{z_1} \frac{(J_1(z))^2}{z} dz, \tag{20}$$

which completely determine the relative intensity of the points in the focal plane. The geometric significance of these double integrals is extremely simple. "If a perpendicular to the focal plane is erected in the geometric image of a luminous point M_1, and if this perpendicular is used as the axis of rotation of a body of revolution whose generatrix has the equation $y = \left(\frac{J_1(z)}{z}\right)^2$, then the intensity produced by M_1, at a point M of the focal plane, can be measured by the ordinate y which the surface of revolution has at this point. However, the point M_1 has the same ordinate as soon as the axis of the body of revolution is shifted to M; if several luminous points M_1, M_2, M_3, ... of equal intensity are present, then the sum of all ordinates versus M_1, M_2, M_3, ... furnishes a criterion for the intensity at M. If, furthermore, the geometric images of the luminous points form a straight luminous line, then the intensity at M must be expressed by the content of the cross section of the body of revolution lying above the luminous line perpendicular to the focal plane; if this concept is extended to homogeneous luminous surfaces, then I can be conceived as a volume cut out by a right circular cylinder, whose perimeter represents the contour of the luminous disk, from the body of revolution whose axis - parallel to the cylinder axis - is located at M and whose generatrix has the equation $y = \left(\frac{J_1(z)}{z}\right)^2$."

TABLE 11

INTENSITY FOR DISKS WITH RECTILINEAR PERIMETER (ACCORDING TO STRUVE)

e	$I(+e)$	e	$I(+e)$	e	$I(+e)$	e	$I(+e)$
0.0	0.5000	1.5	0.1642	3.0	0.0630	6.0	0.0328
0.1	0.4730	1.6	0.1504	3.2	0.0602	6.2	0.0319
0.2	0.4461	1.7	0.1379	3.4	0.0581	6.4	0.0311
0.3	0.4195	1.8	0.1265	3.6	0.0564	6.6	0.0305
0.4	0.3934	1.9	0.1163	3.8	0.0547	6.8	0.0299
0.5	0.3678	2.0	0.1073	4.0	0.0528	7.0	0.0293
0.6	0.3428	2.1	0.0993	4.2	0.0506	7.4	0.0280
0.7	0.3187	2.2	0.0923	4.4	0.0484	7.8	0.0264
0.8	0.2955	2.3	0.0862	4.6	0.0459	8.2	0.0248
0.9	0.2732	2.4	0.0810	4.8	0.0434	8.6	0.0233
1.0	5.2521	2.5	0.0765	5.0	0.0410	9.0	0.0222
1.1	0.2321	2.6	0.0728	5.2	0.0389	9.8	0.0206
1.2	0.2132	2.7	0.0696	5.4	0.0369	10.6	0.0194
1.3	0.1956	2.8	0.0670	5.6	0.0353	11.4	0.0178
1.4	0.1793	2.9	0.0648	5.8	0.0339	12.2	0.0164
1.5	0.1642	3.0	0.0630	6.0	0.0328		

This theorem, which is quoted here from Struve, is due to Schwerd and was /117
given in a similar form by André. The theorem is applicable only to circular or annular apertures.

Struve gave a development of the above integral [eq.(20)] for the case of a rectilinear perimeter of the disk, which we will disregard here; this development resulted in a table for the intensity I(-e) and I(+e) where

$$e = \frac{2\pi}{\lambda} R\varepsilon \tag{21}$$

and where ε denotes the angular distance from the geometric rim of the disk. The table is given above (Table 11). As unit, the "full" intensity is assumed which would result if the luminous disk were to extend in all directions to infinity.

The values for I(-e) are obtained from this, by means of the relation

$$I(-e) = 1 - I(+e). \tag{22}$$

The brightness along the geometric rim thus is only half that obtainable without diffraction, increasing first rapidly and then decreasing slowly.

The table, in accordance with eq.(21), can be used for arbitrary apertures R, where R is measured in millimeters. At double the lens radius R, the same figures apply for a distance from the rim ε reduced by a factor of 2.

The intensity distribution in the case of circular luminous disks also depends on the angle bisector ρ of the disk and, as for the previous disk, on the radius R of the lens aperture and on the wavelength of light λ. We are giving here the two tables calculated by Struve for r = 50 and r = 10, where r = $= \frac{2\pi}{\lambda} R\rho$. These are expressed in units of full intensity which would correspond to an infinite extent of the luminous disk; if the figures are to be reduced to the intensity at the center, they must be divided by 0.9874 for r = 50 and by 0.9378 for r = 10. For a more convenient view, we referred the first of /118
Struve's tables to the central brightness as unit. Table 14 holds for the value of the product $R\rho'' = 950$ (with ρ'' being the radius of the disk in seconds of arc, and R in millimeter) and for green rays, $\lambda = 0.00058$ mm. The table indicates that, for an objective of 200 mm and a planetary disk of 5″ radius, the influence of diffraction becomes noticeable already at a distance of 0.2 radius from the limb. However, the table is approximately valid also for arbitrary products $R\rho''$ if a proportionally changed distance from the limb is introduced; this will show that, for Jupiter ($\rho = 20''$), at one and the same lens aperture, the influence of diffraction reaches its prior amount only at a distance of 0.05 ρ from the limb.

Despite the fact that, for the real conditions of the planets, the diffraction cannot be accurately determined with the means of modern theory (for this, the influence of the phase and of the respective intensity distribution would have to be taken into consideration), it can be concluded from the above investi-

TABLE 12

INTENSITY FOR CIRCULAR LUMINOUS DISKS (ACCORDING TO STRUVE)

$r = \frac{2\pi}{\lambda} R\varrho = 50; \quad \varepsilon = \frac{2\pi}{\lambda} R\varepsilon$

ε	$I(\varepsilon)$	ε	$I(\varepsilon)$	ε	$I(\varepsilon)$	ε	$I(\varepsilon)$	ε	$I(\varepsilon)$
−50.0	0.9874	−3.6	0.9325	−1.0	0.7348	+1.2	0.2010	+4.0	0.0430
—	—	−3.2	0.9292	−0.8	0.6909	+1.4	0.1675	+4.4	0.0398
−7.2	0.9629	−2.8	0.9227	−0.6	0.6436	+1.6	0.1391	+4.8	0.0354
−6.8	0.9612	−2.6	0.9166	−0.4	0.5930	+1.8	0.1159	+5.2	0.0312
−6.4	0.9592	−2.4	0.9086	−0.2	0.5404	+2.0	0.0971	+5.6	0.0275
−6.0	0.9574	−2.2	0.8972	−0.0	0.4859	+2.2	0.0825	+6.0	0.0247
−5.6	0.9555	−2.0	0.8822	+0.2	0.4322	+2.4	0.0715	+6.4	0.0229
−5.2	0.9525	−1.8	0.8622	+0.4	0.3799	+2.6	0.0635	+6.8	0.0217
−4.8	0.9481	−1.6	0.8379	+0.6	0.3298	+2.8	0.0577	+7.2	0.0206
−4.4	0.9426	−1.4	0.8096	+0.8	0.2828	+3.2	0.0509	—	—
−4.0	0.9360	−1.2	0.7742	+1.0	0.2395	+3.6	0.0467	+50.0	0.0011

TABLE 13

$r = 10$

ε	$I(\varepsilon)$	ε	$I(\varepsilon)$	ε	$I(\varepsilon)$	ε	$I(\varepsilon)$	ε	$I(\varepsilon)$
−10.0	0.938	−3.4	0.901	−0.4	0.550	+1.0	0.207	+4.0	0.026
−9.0	0.937	−3.0	0.892	−0.2	0.498	+1.4	0.140	+4.8	0.019
−8.0	0.935	−2.6	0.882	0.0	0.446	+1.8	0.091	+5.6	0.015
−7.2	0.933	−2.2	0.862			+2.2	0.060	+6.4	0.012
−6.4	0.930	−1.8	0.826	+0.2	0.393	+2.6	0.042	+7.2	0.010
−5.6	0.925	−1.4	0.772	+0.4	0.340	+3.0	0.034	+8.0	0.008
−4.8	0.919	−1.0	0.699	+0.6	0.293	+3.4	0.031	+9.0	0.007
−4.0	0.910	−0.8	0.656	+0.8	0.248	+3.8	0.028	+10.0	0.005
−3.8	0.907	−0.6	0.607	+1.0	0.207				

TABLE 14

Distances from the Disk Center	Brightness in Units of the Central	Distances from the Disk Center	Brightness in Units of the Central
0.00 of rad.	1.000	1.00 of rad.	0.492
—	—	1.02	0.243
0.80	0.987	1.04	0.098
0.90	0.962	1.06	0.055
0.92	0.948	1.08	0.044
0.94	0.938	1.10	0.034
0.96	0.893	1.20	0.012
0.98	0.744	—	—
1.00	0.492	2.00	0.001

gation that the peripheries of the planetary images must be excluded from the study of real brightness ratios.

50. Developments by Nagaoka /119

More recent investigations by Nagaoka (Ref.154) went beyond Struve's results. This author brought the problem of diffraction in uniformly bright disks with circular periphery to a concise form, going as far as a numerical evaluation and graphical representation. Because of the significance of the accompanying tables and diagrams, we will treat this paper in somewhat more detail.

Based on eq.(20), according to which the intensity of the diffracted light at a point with the direction cosine α, β is equal to

$$I = c \iint_z \frac{J_1^2(z)}{z}\, dz\, d\psi, \tag{23}$$

where, according to eqs.(18), (17), and (16),

$$z = \frac{2\pi}{\lambda} R\zeta = \frac{2\pi}{\lambda} \frac{R}{f} \sqrt{(\alpha_1 - \alpha)^2 + (\beta_1 - \beta)^2}, \tag{24}$$

the proportionality factor c is determined by referring I to the brightness of the center of an infinitely extended disk. Since

$$\frac{J_1^2(z)}{z} = -\frac{1}{2}\frac{d}{dz}(J_0^2(z) + J_1^2(z)),$$

it follows that

$$\int_0^z \int \frac{J_1^2(z)}{z}\, d\psi\, dz = \frac{1}{2}\int (1 - J_0^2(z) - J_1^2(z))\, d\psi.$$

For the brightness of the center of an infinitely extended disk, we obtain

$$\int_0^{2\pi} d\psi \int_0^{\infty} \frac{J_1^2(z)}{z}\, dz = \pi. \tag{25}$$

Consequently, $c = \frac{1}{\pi}$ and, in a general form,

$$I = \frac{1}{2\pi}\int (1 - J_0^2(z) - J_1^2(z))\, d\psi. \tag{26}$$

According to eq.(24), the variable z is proportional to the angular distance ζ in the focal plane of the imaged point up to the diffraction point.

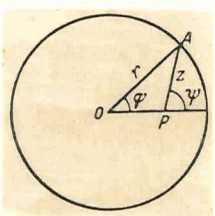

Fig.31 Diffraction of Light for Circular Disks, according to Nagaoka.

Let the circle of radius OA = r be an image of the disk at the corresponding scale and let P be the point for which the intensity of the diffracted light, produced by the total disk according to eq.(26), is sought. Then, AP = z for a point on the periphery and OP = νr, where OP:OA = $\nu \lesseqgtr 1$ depending on whether P is located inside or outside of the disk.

Since

$$z^2 = r^2(1 - 2\nu\cos\varphi + \nu^2)$$

and

$$r\cos\varphi = \nu r + z\cos\psi,$$

we have

$$d\psi = \frac{1 - \nu\cos\varphi}{1 - 2\nu\cos\varphi + \nu^2}\, d\varphi,$$

Consequently, the expression for the intensity [eq.(26)] can also be written in the form

$$I = \frac{1}{2\pi}\int_0^{2\pi}[1 - J_0^2(z) - J_1^2(z)]\,\frac{1 - \nu\cos\varphi}{1 - 2\nu\cos\varphi + \nu^2}\,d\varphi. \tag{27}$$

Setting

/120

$$\varphi = \pi - 2\Theta, \qquad \cos\varphi = 2\sin^2\Theta - 1,$$

we obtain

$$z = r(1+\nu)\sqrt{1 - k^2\sin^2\Theta} = \alpha\sqrt{1 - k^2\sin^2\Theta}, \tag{28}$$

where

$$k^2 = \frac{4\nu}{(1+\nu)^2} \qquad \text{and} \qquad \alpha = r(1+\nu).$$

We then still have

$$1 - k^2 = k'^2 = \left(\frac{1-\nu}{1+\nu}\right)^2.$$

For points inside the disk,

$$k' = \frac{1-\nu}{1+\nu}, \tag{29}$$

while for points outside the disk,

$$k' = \frac{\nu - 1}{\nu + 1}. \tag{30}$$

For points in the vicinity of the periphery, ν is almost equal to 1, so that we set

$$\nu = 1 \mp \varepsilon, \tag{30'}$$

where ε is a small quantity. For the peripheral points, neglecting higher powers of ε, we have

$$k = 1 \tag{31}$$

$$k' = \frac{\varepsilon}{2}. \tag{31'}$$

Furthermore,

$$\frac{1 - \nu\cos\varphi}{1 - 2\nu\cos\varphi + \nu^2} = -\left(1 \pm \frac{k'}{1 - k^2\sin^2\Theta}\right), \tag{32}$$

where the upper sign refers to internal points and the lower sign to external points. Denoting by u the elliptical integral

$$u = \int_0^{\Theta}\frac{d\Theta}{\sqrt{1 - k^2\sin^2\Theta}}$$

and by

$$K = \int_0^{\pi/2} \frac{d\Theta}{\sqrt{1 - k^2 \sin^2 \Theta}}$$

the complete elliptical integral of the first kind, and making use of the notations of elliptical functions

$$\sqrt{1 - k^2 \sin^2 \Theta} = dn\, u$$
$$\frac{k'}{dn\, u} = dn(u + K),$$

we finally obtain

$$z = \alpha \sqrt{1 - k^2 \sin^2 \Theta} = \alpha\, dn\, u$$
$$\frac{1 - \nu \cos\varphi}{1 - 2\nu \cos\varphi + \nu^2} d\varphi = [dn\, u \pm dn(u + K)]\, du.$$

Now, the intensity I [eq.(27)] is represented in the form

$$I = \frac{1}{\pi} \int_0^K \{1 - J_0^2(\alpha\, dn\, u) - J_1^2(\alpha\, dn\, u)\} [dn\, u \pm dn(u + K)]\, du. \qquad (33)$$

Let us individually treat the following four cases: 1) intensity at the center of the disk, 2) intensity at the periphery of the disk, 3) intensity at points within and without the disk, 4) intensity in the neighborhood of the periphery. /121

The intensity at the center of the disk is obtained from eq.(33) by setting $\nu = 0$, according to k = 0, dnu = 1 and dn(u + K) = 1, α = r and $K = \frac{\pi}{2}$. We then obtain

$$I_0 = 1 - J_0^2(r) - J_1^2(r). \qquad (34)$$

In calculating this expression, two cases must be differentiated. At low values of r, Nagaoka expanded

$$J_0^2(r) + J_1^2(r) = \frac{2}{\pi} \int_0^{\pi} J_0(2r \sin\omega) \cos^2\omega\, d\omega$$

in a power series

$$= \sum_0 A_n r^{2n} = 1 - \frac{1}{2} r^2 + \frac{5}{36} r^4 - \frac{7}{288} r^6 + \frac{7}{2400} r^8 - \frac{11}{43200} r^{10} + \cdots. \qquad (35)$$

For large values of r, the following semiconvergent series is valid:

$$J_0^2(r) + J_1^2(r) = \frac{2}{\pi r}\left(1 + \frac{1}{8r^2} - \frac{\cos 2r}{2r} - \frac{\sin 2r}{8r^2} + \cdots\right). \tag{36}$$

The derivation of these series is not given here; we merely wish to make the following statements as to the limits of applicability of the two series: According to eq.(24),

$$r = \frac{2\pi}{\lambda} R r'',$$

where r'' is the planetary radius in radians; at r'' = 10'' and R = radius of the objective = 6 cm, λ = 0.5 μ, we obtain r = 36.55; for cases astronomically in question at present, r always has rather high values. For these, the series (36) furnishes rapidly converging values. The slope of the function $J_0^2(r) + J_1^2(r)$ is characterized by flex points at the sites of the roots of the equation $J_1(r) = 0$; these flex points are located at $r_1 = 3.8317$, $r_2 = 7.0156$, $r_3 = 10.1735$, ... Except for these, the function $y = J_0^2(x) + J_1^2(x)$, which determines the brightness fall-off of the center of a finite round disk compared to a disk of infinite extent, has a course similar to that of a rectangular hyperbola

$$xy = \frac{2}{\pi},$$

which is obvious from the series (36).

Table 15, in the second column, gives the course of $I_0 = 1 - J_0^2(r) - J_1^2(r)$ for disks of different sizes; it is obvious that, for both sun and moon for which r > 2000 with an objective of 5 cm aperture, the influence of diffraction on the brightness of the center is only a few ten-thousandths.

Brightness at the limb. If, in eq.(33), we set $\nu = 1$ and correspondingly k = 1, k' = 0, dnu = cos Θ, dn(u + K) = 0, $\alpha = 2r$, and $z = 2r \cos \Theta$, then it follows that

$$I_p = \frac{1}{\pi}\int_0^{2r}[1 - J_0^2(z) - J_1^2(z)]\frac{dz}{\sqrt{4r^2 - z^2}} = \frac{1}{2} - \frac{1}{\pi}\int_0^{2r}[J_0^2(z) + J_1^2(z)]\frac{dz}{\sqrt{4r^2 - z^2}}. \tag{37}$$

In expanding this integral, it is again necessary to use the two series (35) and (36), with the first applicable for small values of r up to approximately the first root of $J_1(r) = 0$, i.e., r = 3.8317, after which the power series (36) is applied. According to Nagaoka, the results of relatively tedious expansions /122 and addition of the two partial integrals will be

$$I_p = \frac{1}{2} - \left(\frac{0.3093}{r} + \frac{0.2333}{r}\log r + \frac{0.0036}{r^3}\log r - \cdots\right). \tag{38}$$

It is clear that the intensity at the limb is closer to the value $\frac{1}{2}$ the larger the disk. The third column of Table 15 gives the values of this intensity, for various diameters of the disk.

TABLE 15

r	I_0	I_p	r	I_0	I_p	r	I_0	I_p
20	0.9676	0.4694	70	0.9909	0.4894	400	0.9984	0.4977
25	0.9750	0.4746	80	0.9920	0.4906	500	0.9987	0.4981
30	0.9784	0.4782	90	0.9929	0.4915	600	0.9989	0.4984
35	0.9820	0.4809	100	0.9936	0.4922	700	0.9991	0.4986
40	0.9841	0.4829	150	0.9958	0.4945	800	0.9992	0.4988
45	0.9858	0.4846	200	0.9968	0.4958	900	0.9993	0.4989
50	0.9874	0.4859	250	0.9975	0.4965	1000	0.9994	0.4990
60	0.9895	0.4879	300	0.9979	0.4970			

Brightness I_i inside and I_e outside the disk. For points located inside and outside the disk, not too close to the limb, the expansion (36) can be used for sufficiently large r since α is large and since dnu > 0; however, it is sufficient to use only one term:

$$J_0^2(\alpha\, dn\, u) + J_1^2(\alpha\, dn\, u) = \frac{2}{\pi\alpha\, dn\, u}.$$

Then, the integral (33) becomes equal to

$$I = \frac{1}{\pi}\int_0^K \left(1 - \frac{2}{\pi\alpha\, dn\, u}\right)[dn\, u \pm dn\,(u + K)]\, du. \tag{39}$$

Carrying out the integration yields I as a function of the complete elliptical integral of the first and second kind K and E:

$$\left.\begin{aligned} I_i &= 1 - \frac{1}{\pi^2\alpha}\left(\frac{E}{k'} + K\right) = 1 - \frac{2}{\pi^2(1+\nu)r}\left(\frac{E}{k'} + K\right), \\ I_e &= \frac{2}{\pi^2(1+\nu)r}\left(\frac{E}{k'} - K\right). \end{aligned}\right\} \tag{40}$$

These expressions are almost correct to within four significant figures, for values of αdnu that are larger than the first root of the equation $J_1(r) = 0$.

For small values of k′, approximate values of the elliptical integral can be used here:

$$\left.\begin{aligned} K &= \ln\frac{4}{k'} + \frac{1}{4}k'^2\left(\ln\frac{4}{k'} - 1\right) + \cdots, \\ \frac{E}{k'} &= \frac{1}{k'} + \frac{1}{2}k'\left(\ln\frac{4}{k'} - \frac{1}{1\cdot 2}\right) + \cdots, \end{aligned}\right.$$

which, substituted into eq.(40) and using eq.(29), will yield

$$I_i = 1 - \frac{2}{\pi^2(1+\nu)r}\left\{\left(1 + \frac{k'}{2}\right) + \ln\frac{4}{k'} - \frac{k'}{4}\right\} - \frac{2}{\pi^2(1-\nu)r}, \tag{41}$$

$$I_e = \frac{2}{\pi^2(1+\nu)\nu}\left\{\left(1-\frac{k'}{2}\right)+\ln\frac{4}{k'}+\frac{k'}{4}\right\}-\frac{2}{\pi^2(1-\nu)\nu}.$$

To find the intensity for values of k close to 1, the Landen transformation is used. Setting

/123

$$k_1 = \frac{1-k'}{1+k'} = \nu \quad \text{for interior points,}$$

$$k_1 = \frac{1}{\nu} \quad \text{for exterior points,}$$

$$k_2 = \frac{1-k'}{1+k_1'} = \left(\frac{\nu}{1+\sqrt{1-\nu^2}}\right)^2 \quad \text{for interior points,}$$

$$k_2 = \left(\frac{1}{\nu+\sqrt{\nu^2-1}}\right)^2 \quad \text{for exterior points,}$$

the following relations are valid:

$$K = \frac{\pi}{2}(1+k_1)(1+k_2)\cdots,$$

$$E = \{(1-k)^2 + \tfrac{1}{2}k^2(1-\tfrac{1}{2}k_1 - \tfrac{1}{4}k_1k_2+\cdots)\}K.$$

TABLE 16

(By Nagaoka)

ν	ε	$\frac{2}{\pi^2(1+\nu)}\left(\frac{E}{k'}+K\right)$
0.990	0.010	20.946
0.991	0.009	23.208
0.992	0.008	26.034
0.993	0.007	29.666
0.994	0.006	34.506
0.995	0.005	41.478
0.996	0.004	51.433
0.997	0.003	68.348
0.998	0.002	102.162
0.999	0.001	203.553
0.9999	0.0001	2027.6
ν	ε	$\frac{2}{\pi^2(1+\nu)}\left(\frac{E}{k'}-K\right)$
1.010	−0.010	19.591
1.009	−0.009	21.832
1.008	−0.008	24.634
1.007	−0.007	28.239
1.006	−0.006	33.018
1.005	−0.005	39.783
1.004	−0.004	49.893
1.003	−0.003	66.748
1.002	−0.002	100.482
1.001	−0.001	201.732
1.0001	−0.0001	2025.3

TABLE 17

(By Nagaoka)

ν	ε	$\frac{2}{\pi^2(1+\nu)}\left(\frac{E}{k'}+K\right)$	ν	ε	$\frac{2}{\pi^2(1+\nu)}\left(\frac{E}{k'}-K\right)$
0.05	0.95	0.6378	1.01	−0.01	19.591
0.10	0.90	0.6414	1.02	−0.02	9.533
0.15	0.85	0.6476	1.03	−0.03	6.199
0.20	0.80	0.6565	1.04	−0.04	4.542
0.25	0.75	0.6683	1.05	−0.05	3.554
0.30	0.70	0.6836	1.1	−0.1	1.6077
0.35	0.65	0.7027	1.2	−0.2	0.6779
0.40	0.60	0.7266	1.3	−0.3	0.3898
0.45	0.55	0.7562	1.4	−0.4	0.2560
0.50	0.50	0.7930	1.5	−0.5	0.1813
0.55	0.45	0.8392	1.6	−0.6	0.1349
0.60	0.40	0.8980	1.7	−0.7	0.1040
0.65	0.35	0.9746	1.8	−0.8	0.0824
0.70	0.30	1.0773	1.9	−0.9	0.0667
0.75	0.25	1.2214	2.0	−1.0	0.0549
0.80	0.20	1.4369	3.0	−2.0	0.0135
0.85	0.15	1.7936	4.0	−3.0	0.0053
0.90	0.10	2.4994	5.0	−4.0	0.0027
0.95	0.05	4.5834	10.0	−9.0	0.003
0.96	0.04	5.617	100.0	−99.0	0.0000
0.97	0.03	7.332			
0.98	0.02	10.747			
0.99	0.01	20.947			

Consequently, the expressions in parentheses in eq.(40) assume the approximate form

$$\left.\begin{aligned}\frac{E}{k'}+K&=\left(\frac{1+k'}{2k'}\right)^2\left\{1-\frac{k_1^2}{2}\left(1+\frac{1}{2}k_2\right)\right\}K,\\ \frac{E}{k'}-K&=\frac{(1-k')^2}{4k'}\left(1-\frac{k_2}{2}\right)K.\end{aligned}\right\} \qquad (42)$$

These formulas were used for calculating the intensities in the immediate vicinity of the limb.

In Tables 16 and 17, the expressions $\frac{2}{\pi^2(1+\nu)}\left(\frac{E}{k'}+K\right)$ and $\frac{2}{\pi^2(1+\nu)}\left(\frac{E}{k'}-K\right)$, entering eq.(40), are calculated for the interior and exterior points; in Table 16, they are given for points in the neighborhood of the limb [according to eq.(42)] and in Table 17 for points farther away from the limb [according to eq.(41)]. These figures must be multiplied by the missing factor 1/r to obtain the brightnesses for a given aperture and a given disk radius. Here, /124

$$r=\frac{2\pi R}{\lambda}r'',$$

where r″ denotes the radius of the disk in seconds of arc.

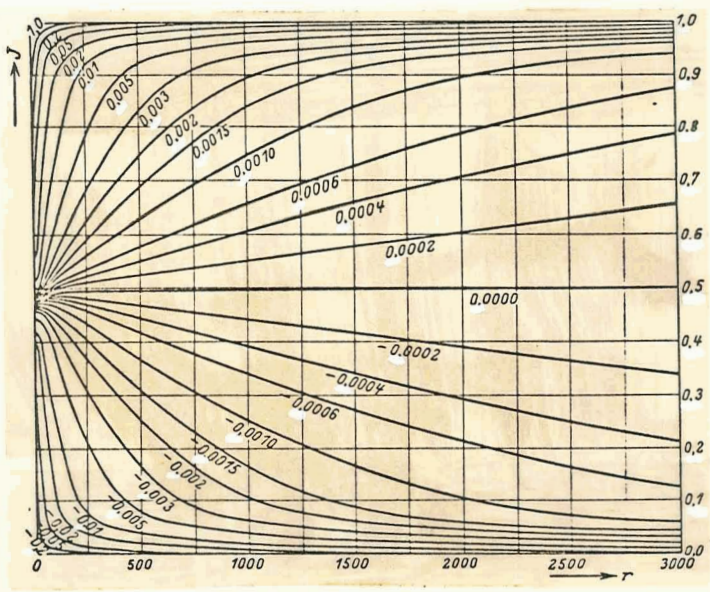

Fig.32 Slope of Limb Brightnesses for various Lens Apertures, according to Nagaoka.

The figures in Table 16 indicate a rapid fluctuation in brightness close to the limb, while the figures in Table 17 show a slow fluctuation within the disk at greater distances from the limb.

Figures 32 and 33 demonstrate the slope of the brightnesses; the first diagram, for various values of r, permits determining the brightness as the ordinate of the intercept with the curves of the various limb distances (ε). It is obvious that, for small ε, the decrease in brightness is greater the larger the aperture r. The brightness $\frac{1}{2}$ corresponds to the geometric limb. Conversely, Fig.33 illustrates the slope of brightnesses in the vicinity of the limb, for various values of $r\varepsilon$. This approximately confirms Struve's statement (p.133) on the sufficiency of one single table for the brightnesses of disks since, for equal products $r\varepsilon$, the slope of the intensity curves is practically the same. However, this is not strictly so, meaning that for low values of r the intensity curves are located farther downward than for high values.

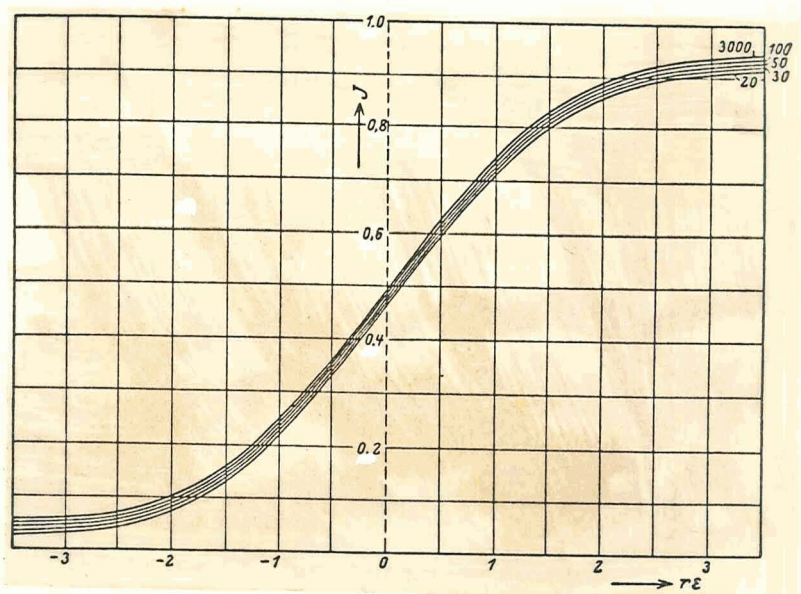

Fig.33 Limb Brightnesses for various Products $r\varepsilon$, according to Nagaoka.

The intensity in the immediate neighborhood of the geometric limb, which is of special importance and is approximately given in Table 16 and Fig.33, was calculated strictly by Nagaoka who used an artifice for overcoming most of the difficulties in the expansion. He decomposed the integral (33) into two components

$$I = \frac{1}{\pi}\int_0^K \{1 - J_0^2(\alpha\, dnu) - J_1^2(\alpha\, dnu)\}[dnu \pm dn(u+K)]\,du = I_1 \pm I_2,$$

whose meaning is obvious. Since, for values of k that are approximately equal to 1, $dnu = \sqrt{1 - k^2 \sin^2\Theta}$ becomes almost equal to $\cos\Theta$ (for $\varepsilon = 0.02$, we have /125 $k = 0.99995$), the first term will be

$$I_1 = \frac{1}{\pi}\int_0^{\pi/2}\{1 - J_0^2(\alpha\cos\Theta) - J_1^2(\alpha\cos\Theta)\}\,d\Theta. \tag{43}$$

This is the value for the limb brightness of the disk of radius $\frac{\alpha}{2} = \frac{r(1+\nu)}{2}$ [see eq.(37)] and can be taken from the tables as

$$I_1 = I_p\left(\frac{\alpha}{2}\right) = I_p\left(\frac{r(1+\nu)}{2}\right). \tag{44}$$

The deviation from the value of the limb brightness is determined by the second term, in which the plus sign applies to interior points and the minus sign to exterior points. This second integral is

$$I_2 = \frac{1}{\pi}\int_0^{\pi/2}\left\{1 - J_0^2\left(r(1+\nu)\sqrt{1-k^2\sin^2\Theta}\right) - J_1^2\left(r(1+\nu)\sqrt{1-k^2\sin^2\Theta}\right)\right\}\frac{k'd\Theta}{1-k^2\sin^2\Theta}. \tag{45}$$

Its calculation is obtained by decomposition into two parts and will be disregarded here. The result is given in Table 18, for various values of $r\varepsilon$.

TABLE 18

(By Nagaoka)

$$I_2 = \int_0^{\pi/2}\{1 - J_0^2[r(1+\nu)\sqrt{1-k^2\sin^2\Theta}] - J_1^2[r(1+\nu)\sqrt{1-k^2\sin^2\Theta}]\}\frac{k'd\Theta}{1-k^2\sin^2\Theta}.$$

$r\varepsilon$	I_2	$r\varepsilon$	I_2	$r\varepsilon$	I_2	$r\varepsilon$	I_2
0.1	0.0270	1.1	0.2679	2.1	0.4008	3.1	0.4393
0.2	0.0539	1.2	0.2868	2.2	0.4080	3.2	0.4406
0.3	0.0806	1.3	0.3044	2.3	0.4141	3.3	0.4419
0.4	0.1066	1.4	0.3208	2.4	0.4194	3.4	0.4430
0.5	0.1323	1.5	0.3357	2.5	0.4238	3.5	0.4439
0.6	0.1571	1.6	0.3496	2.6	0.4276	3.6	0.4450
0.7	0.1812	1.7	0.3623	2.7	0.4308	3.7	0.4458
0.8	0.2045	1.8	0.3736	2.8	0.4336	3.8	0.4469
0.9	0.2268	1.9	0.3839	2.9	0.4359	3.8317	0.4471
1.0	0.2479	2.0	0.3933	3.0	0.4378		

Some Applications of the Theory

/126

1. A luminous point at the limb of a bright disk. This is a case which is realized in astronomical practice during occultation of stars or satellites by the planets or by the moon. The intensity of the diffraction rings about a point source of light is given by the expression $\left(\frac{2J_1(z)}{z}\right)^2$ and can be taken,

for example, from Lommel's tables. The isophots thus are concentric circles to which the isophots of the disk are superposed. The result is a new system of isophots which is plotted in Fig.34 for the special case of equal brightness of the point and the center of the disk, which is set equal to 1. Here, r = 50 is assumed; e denotes the limb distance of the star. It is obvious that the intensity maximum of the star, i.e., its apparent locus, appears shifted toward the geometric limb with respect to the real locus denoted by an asterisk and that, at the instant of actual contact, the star is visible within the disk.

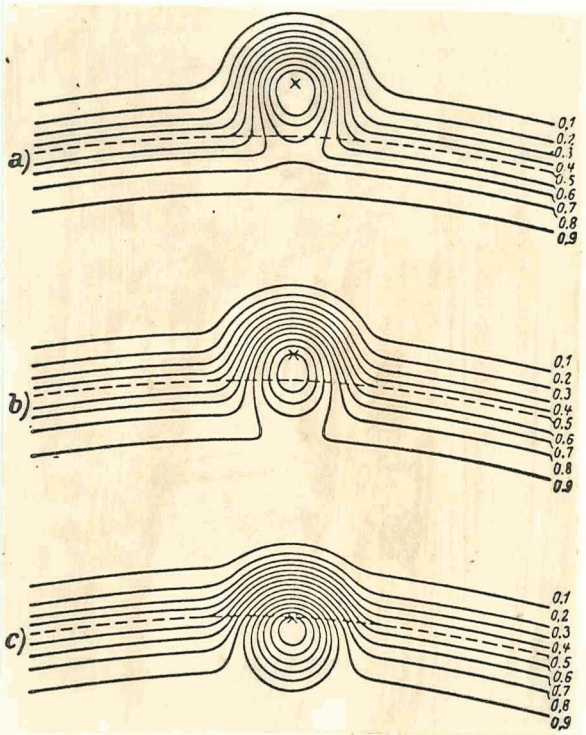

Fig.34 Luminous Point and Bright Disk (according to Nagaoka).
a) e = -2, b) e = -1, c) e = 0.

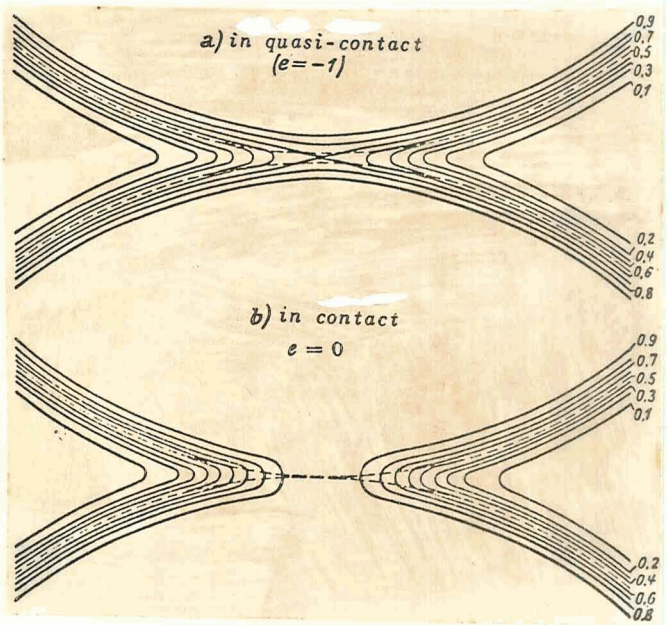

Fig.35 Two Bright Disks (according to Nagaoka).
$r = r_1 = 50$.

2. Two bright disks. Figure 35 shows the slope of the isophots on approach and contact of two bright disks of equal radius ($r = r_1 = 50$). Their brightnesses are also assumed as equal.

The broken curves indicate the position of the geometric limb. The distance of the limbs in Fig.35a is e = -1. Most likely, a premature coalescence of the limbs will occur in this case. /127

3. One bright and one dark disk. This case is realized during Venus and Mercury transits across the sun's face. Figure 36 shows the slope of the isophots at r = 50 and r_1 = 1000 in the neighborhood of the internal contact where the well-known "droplet phenomenon" occurs. At the point (a), the geometric limbs intersect while at (b) they osculate. Because of the bend of the isophots, the upper disk seems to have an apparent continuation toward the outside (bottom)

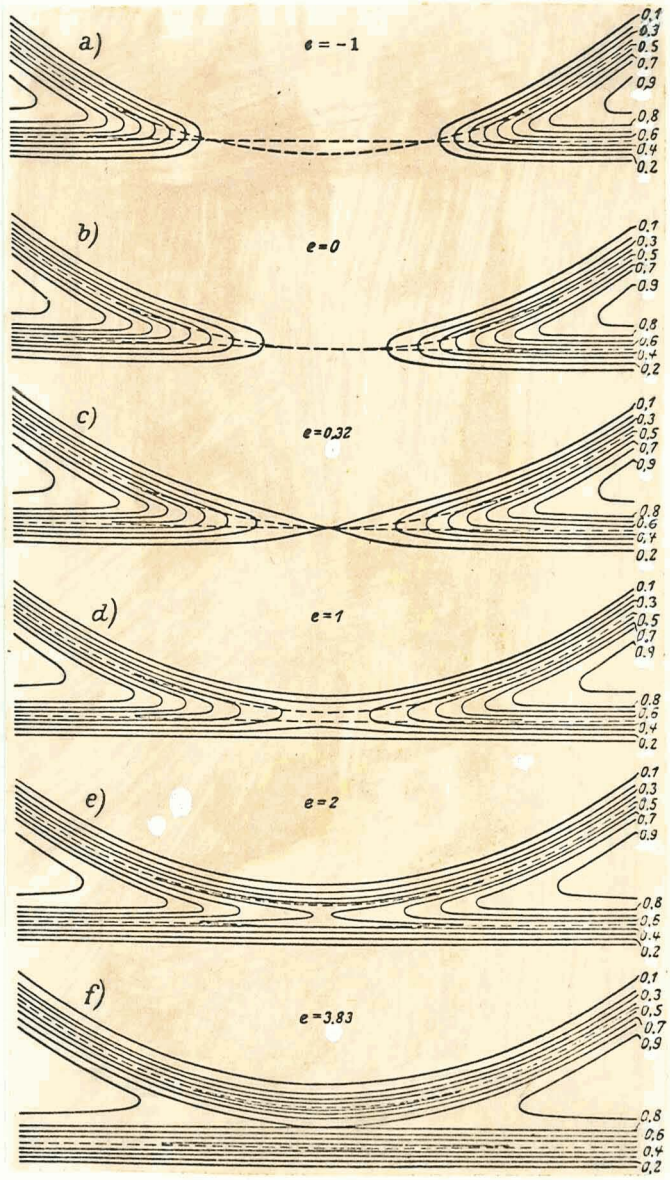

Fig.36 One Bright and One Smaller Dark Disk (according to Nagaoka). $r = 50$; $r_1 = 1000$.

and a dark bridge. At minor detachment of the geometric limbs (e = 0.32) in Fig.36c, the isophot 0.1 which envelops the dark disk comes into contact with an isophot of the same intensity outside the bright disk, which apparently produces an outward bulge of the dark disk. Only at greater distance of the limbs (Fig.36d, e, f) will the boundaries assume regular circular shapes.

4. Bright crescent. The light distribution about a uniformly bright crescent, bounded by two circular arcs of unlike radius, was investigated by Nagaoka with the aid of the above formulas and plotted for a few special cases. For small radii and a narrow crescent ($r = 50$, $r_1 = 100$, e = thickness of the crescent = 5), the slope of the isophots is given in Fig.37. For the eye, the result must be a rounding of the tips, which explains the observation that, in diameter determinations of the planet Venus, the values obtained close to the inferior conjunction are too low. At greater thickness of the crescent (Fig.37b), the influence is less noticeable; similarly, at very large radii (Fig.37c), the effect of the diffraction on the appearance of the tips is negligible. /128

In estimating the boundaries of disks by eye, physiological causes are involved which, however, will not be discussed here.

Since all mentioned investigations use the simplifying assumption of uniformly bright areas, they can give only a qualitative explanation of the phenomena produced by the diffraction. Fessenkov (Ref.155) investigated, in first approximation, a special case of diffraction phenomena at nonuniform brightness. He raised the question in how far the influence of the light and dark bands on Jupiter might affect the intensity distribution over the bright equatorial zone. To answer the question, he resolved the surface of the planet into alternately

bright and dark rectangles of uniform brightness, with a terminal dark polar calotte. The arrangement is assumed as symmetric with respect to the equator. Fessenkov used Struve's pattern for carrying out his expansions in Bessel functions; he came to the conclusion that the influence of the diffraction along the edge of the equatorial band is somewhat less than under assumption of uniform brightness of the entire disk.

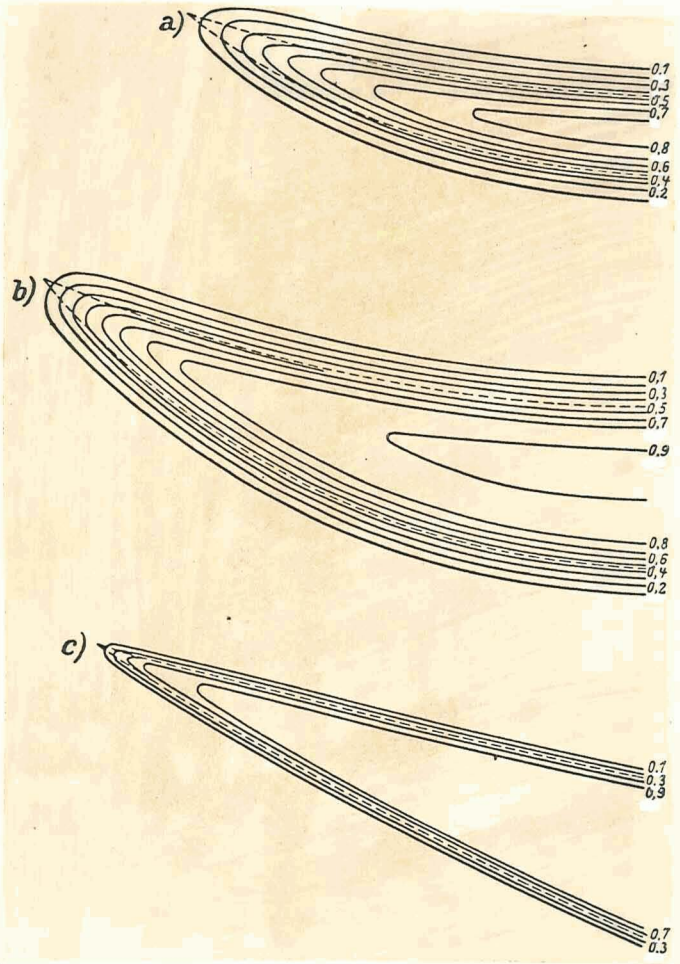

Fig.37 Bright Crescent (according to Nagaoka).

51. Visible Boundary of a Planetary Disk

As indicated in the tables, the brightness at the geometric limb of the disk is about one half of the central brightness; the fall-off is strongest here and anyhow quite extensive within 0.1 r in the neighborhood of the geometric /129 limb. Farther outside, the fall-off is more gradual and the intensity curve asymptotically approaches the zero value. However, the eye perceives a sharp boundary between light and dark, in accordance with physiological laws; this boundary need not - and generally does not - coincide with the geometric limb.

In general, it should be expected that, on decrease of the lens aperture, the measured diameters of the planets would be larger. However, this is by no means the case, as convincingly proved by H.Struve (Ref.152, p.58) in contrast to André (Ref.156). Thus, no confirmation of the diffraction theory for luminous disks by astronomic observations has as yet been obtained.

We will mention here an experiment according to which one could expect such a dependence. During his experiments with rotating disks, to check the theory of enlargement of the earth's shadow (see p.124), Seeliger also constructed a disk which, at rapid rotation, should give the brightness drop due to diffraction; thus, he actually produced an artificial large-scale planet. The radius of the disk was assumed as 7.2 cm and was observed from a distance of several meters. The disk had a highly instructive aspect. At the interior, it appeared almost uniformly bright and was surrounded by a narrow washed-out band which gradually passed over into almost uniform and practically complete darkness. This band disappeared at greater distance, and the measurement reliably gave a value of 7.93 cm as the boundary of the disk at a 4-m distance, as the mean value for three different observers whose individual values fluctuated between 7.6 and 8.6. This would mean an enlargement of the diameter by 10%. However, this figure must be largely dependent on the absolute brightness of the disk; this individual experiment is of significance only in so far as, in each case, an enlargement of the planetary disks had to be expected for physiological reasons.

We wish to mention still another cause of the apparent enlargement of planetary disks.

52. Enlargement of a Planetary Disk by Ray Refraction

If a sphere is surrounded by a refracting atmosphere, it must appear larger to an observer stationed outside of the sphere than it would be within its envelope, even if the gas envelope is completely transparent and thus invisible.

If one assumes concentric stratification of the atmosphere, becoming denser from the outside to the inside, then the fundamental equation of the theory of refraction can be applied to the refraction curve of the rays reaching the observer:

$$\mu r \sin i = \text{const}, \tag{46}$$

where μ is the refractive index at a distance r from the center, while i is the angle made by the outward-directed tangent to the refraction curve with r. If a point of the surface emits a light ray under an angle z to the normal and if this ray strikes the observer, then the following relation must exist:

$$\mu_0 R \sin z = \Delta \sin \sigma, \tag{47}$$

where μ_0 is the refractive index at the surface of the planet, R its radius, Δ the distance between observer and center, and σ the apparent distance of the mentioned point from the center of the planetary disk. Let σ_0 be the apparent /130 radius of the planet without atmosphere, so that

$$R = \Delta \sin\sigma_0 . \tag{48}$$

Consequently, eqs.(47) and (48) will yield

$$\sin\sigma = \mu_0 \sin\sigma_0 \sin z .$$

Since the maximum zenith distance for a ray, able to reach the observer, is $z = 90^\circ$, the apparent radius of the planet can be determined from the formula

$$\sin\sigma = \mu_0 \sin\sigma_0$$

or, with an accuracy sufficient for astronomical purposes,

$$\sigma = \mu_0 \sigma_0 . \tag{49}$$

This indicates that only the refractive index at the surface of the planet is of significance and that the law of density diminution in the atmosphere plays no role.

If the refractive indices differ for different wavelengths, the scattering will cause the apparent diameter in the more refractive rays to be greater than in the less refractive rays.

In reality, this increase never manifests itself in the pure form since, in addition to refraction, also a diffusion of the light takes place which may render the atmosphere itself visible. Since also the diffusion in the refractive rays will be dominant, an increase in the enlargement factor with decreasing wavelength should be expected. However, if the diffusion is insufficient and if the absorption is extensive, the atmosphere cannot become visible and the limb of the planet - because of the long light path - may even become invisible, so that the inverse result, namely a reduction of the diameter in certain ray classes, may occur.

VI. ILLUMINATION OF DUSTLIKE MASSES

53. Hypotheses of the Theory

In this Chapter, we will investigate the illumination of a system of small bodies, in which case the dimensions of the body can be considered as vanishingly small with respect to the dimensions of the entire system. However, the real dimensions of the body must be given a lower limit, which can be defined such that the laws of rectilinear propagation of light and of shadow-casting are still valid for the bodies of the system, since we will only treat the problem of mutual occultation and shadowing of the individual bodies. The phenomena of diffusion and diffraction of light in gaseous media and on minute solid particles, in which there can be no question of any shadow and in which the reflection proceeds according to laws different from the elementary laws, will be treated in a separate Chapter. A separation of these two problems is a necessity from the methodological viewpoint; if the two phenomena actually occur in the

combined state in nature, it is not difficult at all to correlate the separately developed theories for explaining the phenomena.

54. H.Seeliger Theory

The theory of illumination of dustlike masses has been recognized by H.Seeliger (Ref.157) as a problem important for astronomy and was developed with exceptional acumen, under application to the zodiacal light and the Saturn /131 rings. Since certain conclusions from this theory for the Saturn ring have been confirmed by actual observations, the Maxwell-Hirn opinion that the ring consists of a swarm of separate particles moving independently from one another along Kepplerian ellipses about the central body, has been largely substantiated and the theory of illumination of the ring has gained wide interest. For this reason, we will review this along general lines.

Let us first imagine a system of separate bodies of arbitrary form, which all are assumed as equally large and of spherical shape. These restrictions greatly facilitate the problem but are not necessary, as demonstrated by Seeliger, since the same conclusions can be drawn also for a system of spheres of arbitrarily unequal size. The dimensions of the body are assumed as small with respect to those of the cloud. The light source, i.e., the sun, is assumed as being a point source.

If such a cosmic cloud is illuminated by the sun, each mass particle will partly shadow others and, itself, will be partly occulted by other particles in front of it. The shadowed parts usually differ from the occulted parts. Only in the case of opposition, i.e., when the observer, seen from the dust cloud, appears in exactly the same direction as the sun, will both portions be completely identical. From this it follows that, in the vicinity of opposition, a more or less great increase in luminous intensity must take place. The mathematical problem involved here consists in calculating the magnitude of this luminosity increase. This has nothing to do with the investigation of the influence of the phase on the illumination of the individual mass particles. The latter problem has been treated in an earlier Section, and we will demonstrate here that the observations actually require a consideration of the phase effect on the illumination of individual particles. However, this must be separated from the problem of occultation and shadowing phenomena of the particles, of interest here.

The above-mentioned increase in light close to opposition, is practically independent of the form of the illumination law used as basis for the individual particles. A difference becomes noticeable only at larger phases.

Let dq' be the quantity of light transmitted by an infinitely small element of a sphere, located at the interior of the mass, to the eye of the observer when this element is neither shadowed nor occulted by any of the other spheres. However, both cases may occur separately, raising the question as to the average quantity of light dq of such an element, in the case that a large number of such elements are under consideration. Let the radius of all spheres be ρ. If ρ denotes the number of cases in which an element is completely free and unobstructed and if p' is the number of cases in which it is either occulted or shadowed,

then the element, in p cases, will send a quantity of light dq′ toward the earth and, in p′ cases, a quantity 0. The mean value of all these quantities of light is

$$dq = \frac{p}{p + p'} dq'.$$

At random distribution of the spheres, $w = \frac{p}{p + p'}$ will thus be the probability that an infinitely small element at the interior is neither shadowed nor occulted. In Fig.38 (p.153), R denotes the space of arbitrary configuration filled by the spheres, while df is an infinitesimal element. From df, we will draw two straight lines in direction to the sun and to the earth, and then describe two cylinder surfaces of radius ρ about these straight lines as axes, intersecting at the lower end. Let the space enclosed by the cylinders be denoted by V. If not one single sphere is positioned so that its center falls into the space V, then the element df is neither shadowed nor occulted. Thus, w also represents the probability that all sphere centers are located outside V. This probability is almost the same for all elements dv of one and the same sphere, disregarding the particles closest to the surface. Consequently, the quantity of light q reaching the earth from a single sphere will then be

/132

$$q = wq',$$

where q′ denotes the quantity of light at discrete location of the sphere. The value of q′, based on our earlier statements (see p.72) is a function of the phase angle

$$q' = \gamma\varphi(\alpha) = \Gamma\varrho^2\varphi(\alpha),$$

where γ and Γ depend on the reflectivity in the direction of irradiation, on the distance of the sphere from the light source, and on the form of the illumination law. Let the number of all spheres in R be N. Consequently, at uniform distribution of these spheres, a total of N/R spheres will be contained in unit volume. In one element of volume dv, this number is Ndv/R. The average quantity of light dQ, from the element dv toward the earth, will thus be

$$dQ = \frac{N}{R} dv\, wq'$$

or, after substituting the value of q′,

$$dQ = \gamma\varphi(\alpha) w \frac{N}{R} dv. \qquad (1)$$

Replacing dv by dxdσ, where dx is an element of the straight line dfE while dσ represents the apparent size of dv, we obtain

$$dQ = \gamma\varphi(\alpha) w \frac{N}{R} dx\, d\sigma,$$

and, for all spheres that furnish any contribution to the brightness of dσ, the following value is obtained:

$$Q = \gamma\varphi(\alpha)\frac{N}{R}d\sigma\int_0^X w\,dx, \tag{2}$$

where X denotes the length of the segment within the mass, from the outer periphery into the depth from where no light at all can penetrate outward. The apparent brightness of $d\sigma$ can be represented as follows:

$$J = \gamma\varphi(\alpha)\frac{N}{R}\int_0^X w\,dx. \tag{2'}$$

Generally, this formula contains the basis for a photometry of dustlike masses. Its generalization for the case of nonuniform density is automatically obtained. The function $\varphi(\alpha)$ is indeterminate for the time being. The first problem raised in this respect is the determination of w as a function of x, which is possible only under certain assumptions.

If we have only one sphere, then W_1 represents the probability of its center lying outside the space V; let W_2 be the probability that a second sphere satisfies the same condition after the first sphere has already satisfied the condition. Let W_3, W_4, ..., W_N be the corresponding probabilities for the 3rd, 4th, ..., and Nth sphere. Then, the probability w, as the probability of a composite event, will be /133

$$w = W_1 W_2 W_3 \ldots W_N.$$

However, the probability for the first sphere to lie within V is expressed by V/R; consequently, the probability that it lies outside of V will be

$$W_1' = 1 - \frac{V}{R}.$$

However, if a certain sphere is already located in the space R, then only the space R - k will remain for the center of a second sphere, where $k = \frac{32}{3}\rho^3\pi$. It is possible here that the first sphere is partly located in the space V. Thus, the probability W_2, provided that ε_1' is a positive (extremely small) proper fraction, will be

$$W_2 = \frac{R - V - k(1 - \varepsilon_1')}{R - k} = 1 - \frac{V - \varepsilon_1' k}{R - k}.$$

If this is supplemented by a third sphere, a space slightly larger than R - 2k will remain for its center, since k of the second and third sphere partly coincides with that of the first and second sphere. Thus, if ε_2 is designated as a proper fraction differing little from unity while ε_2' is an extremely small fraction, then - since, again, all the spheres may protrude into the space V - we will obtain

$$W_3 = 1 - \frac{V - 2\varepsilon_2' k}{R - 2\varepsilon_2 k}.$$

Expressed generally, the following relation is obtained for the N-th sphere:

$$W_N = 1 - \frac{V - (N-1)\,\varepsilon_{N-1}' k}{R - (N-1)\,\varepsilon_{N-1} k}.$$

Consequently,

$$w = \left(1 - \frac{V}{R}\right)\left(1 - \frac{V - \varepsilon_1' k}{R - k}\right)\cdots \qquad \cdots\left(1 - \frac{V - (N-1)\,\varepsilon_{N-1}' k}{R - (N-1)\,\varepsilon_{N-1} k}\right).$$

A strict calculation of the quantity V is impossible because of the great density of the spheres in the space R. Of the quantities ε_1, ε_2, ..., ε_{N-1} it is only known that they differ little from unity for small indices and that this difference must increase for large indices. The quantities ε_1', ε_2', ..., ε_{N-1}' are very small fractions that depend on the ratio V/R. Assuming that the density is low, a possibility exists to derive an approximate expression for w. In the case of thinly distributed matter, as it must be assumed for the zodiacal light as well as for the Saturn ring, the total content of all spheres must be considered as small with respect to the entire space R; thus, the error will not be excessive if we omit, in the last expression, all terms in which the small factor k/R or a power of this factor occur. This simply yields

$$w = \left(1 - \frac{V}{R}\right)^N.$$

In addition, in the expansion of the last expression, the higher powers of V/R can be neglected for the first power, so that

$$\ln w = N \ln\left(1 - \frac{V}{R}\right) = -N\frac{V}{R}$$

or

/134

$$w = e^{-N\frac{V}{R}}.$$

Substituting w into eq.(2'), we obtain

$$J = \gamma\varphi(\alpha)\frac{N}{R}\int_0^x e^{-N\frac{V}{R}}dx. \qquad (3)$$

This equation includes all cases of illumination of a system of small bodies that are not too densely distributed. In the general case of irregular delimitation of the mass, the solution becomes difficult since the function V of the phase angle assumes a complicated form.

However, also in the case of regular delimitation, a calculation of the volume V consisting of several segments is not too simple for low angles α.

Seeliger investigated the case of a spherically bounded dust cloud of uniform density and found that the brightness of this cloud, independent of the assumption as to the reflection law, will be nonuniform; as is logical, the side facing the light source is brighter and also contains a brightness maximum along the great circle going through the light source and the observer; this circle can be designated as intensity equator. Let us disregard the developments leading to these theorems and let us derive only the expression for the total quantity of light of such a sphere of radius a for the case $\alpha = 0$, since the result is of some interest. The total quantity of light Q is given by the integral

$$Q = \int J d\sigma,$$

where the integration must be extended over all volume elements dv of the sphere. For $\alpha = 0$, we have

$$Q = \gamma \varphi(0) \frac{N}{R} \int d\sigma \int_0^X e^{-\frac{N}{R} \varrho^2 \pi x} dx.$$

Let us then determine the position of the element of volume dv at the interior of the sphere by the angle ϑ made by the plane dv - observer - center of the sphere with the intensity equator of the sphere, by defining the apparent distance from the center and the depth of the element. If ε denotes the angle made by an element of surface ds with the direction toward the observer, then

$$d\sigma = ds \cos\varepsilon,$$

so that, for all points of a zone of the width $d\varepsilon$, having the observer as the pole, we obtain

$$d\sigma = a^2 \sin\varepsilon \cos\varepsilon \, d\varepsilon \, d\vartheta.$$

The integration must be extended over all values of ε between 0 and $\pi/2$ and, with respect to ϑ, also from 0 to 2π. Here, X is the length of the tangent going through dv in direction to the observer, so that $X = 2a \cos \varepsilon$; this yields

$$Q = \gamma a^2 \varphi(0) \frac{N}{R} \int_0^{2\pi} d\vartheta \int_0^{\pi/2} \sin\varepsilon \cos\varepsilon \int_0^{2a\cos\varepsilon} e^{-\frac{N}{R} \varrho^2 \pi x} dx$$

$$= 2a^2 \gamma \varphi(0) \frac{1}{\varrho^2} \int_0^{\pi/2} \sin\varepsilon \cos\varepsilon \left(1 - e^{-\frac{2aN}{R} \varrho^2 \pi \cos\varepsilon}\right) d\varepsilon.$$

Setting $\frac{2aN}{R} \rho^2 \pi = \nu$ and carrying out the integration, we obtain /135

$$Q = a^2 \gamma \varphi(0) \frac{1}{\varrho^2} \frac{\nu^2 - 2 + 2(1+\nu^2) e^{-\nu}}{\nu^2}.$$

Since R is the volume of the sphere

$$R = \tfrac{4}{3}\pi a^3,$$

it follows that

$$\nu = \frac{3}{2} N \left(\frac{\varrho}{a}\right)^2.$$

If the mass is opaque, then $N\pi\rho^2/\pi a^2$ becomes a large number and $e^{-\nu}$ becomes vanishingly small. Hence,

$$Q = \gamma a^2 \varphi(0) \frac{1}{\varrho^2}.$$

Since

$$\gamma = \Gamma \varrho^2,$$

it follows that

$$Q = \Gamma a^2 \varphi(0).$$

Consequently, the quantity of light of a spherical dust cloud is equal to the quantity which each of the small spheres forming this cloud would send toward the earth if it would have the diameter of the entire cloud. It is obvious that this result, valid only for the direction of irradiation, can be extrapolated to any form of the cloud. On varying the phase angle α, the conditions become less clear but, in any case, the quantity of light reflected by the dust cloud into various directions depends also on the slope of the phase curve of the individual components.

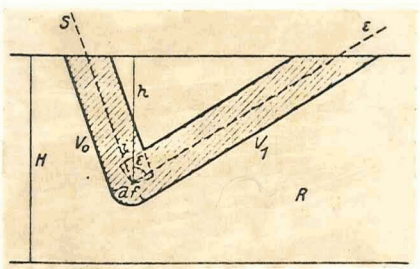

Fig.38 Illumination of the Saturn Ring, according to Seeliger.

55. Illumination of the Saturn Ring

Of special interest is the case in which the space R is bounded by two parallel planes, as is the case for the Saturn ring. Let H in Fig.38 be the total thickness of the layer, h the distance of the volume element dv from the upper boundary, i and ε the angles made by the normal to the boundary with the directions to sun and earth. Then, h = x cos ε and

$$J = \gamma \varphi(\alpha) \frac{N}{R \cos \varepsilon} \int_0^H e^{-N\frac{V}{R}} dh. \qquad (4)$$

The volume V consists of the two cylinders V_0 and V_1 and, in addition, of the small segment k bounded by a portion of the surface of the sphere, minus the segment common to the two cylinders which will be denoted by G. The ratio of the two latter segments to the sum $V_0 + V_1$ varies with the angle between the cylinder axes, in which case G strongly increases for small α while the portion k, in all cases, is so insignificant that it can definitely be neglected for the

volume of the two cylinders. If the phase angle is large, the same can be done for G. Let us first consider this case, in which

$$V = V_0 + V_1.$$

Since

$$V_0 = \varrho^2\pi \frac{h}{\cos i}, \qquad V_1 = \varrho^2\pi \frac{h}{\cos \varepsilon},$$

/136

it follows that

$$V = \varrho^2\pi h \frac{\cos i + \cos \varepsilon}{\cos i \cos \varepsilon}$$

and

$$J = \gamma\varphi(\alpha) \frac{N}{R \cos \varepsilon} \int_0^H e^{-\frac{N}{R}\varrho^2\pi h \frac{\cos i + \cos \varepsilon}{\cos i \cos \varepsilon}} dh.$$

Using the designation $y = \frac{N}{R} \rho^2\pi h \frac{\cos i + \cos \varepsilon}{\cos i \cos \varepsilon}$, this will yield

$$J = \frac{\gamma\varphi(\alpha)}{\varrho^2\pi} \frac{\cos i}{(\cos i + \cos \varepsilon)} \int_0^Y e^{-y} dy,$$

where the upper limit Y represents the value of y for h = H. From this, integration will yield

$$J = \frac{\gamma\varphi(\alpha)}{\varrho^2\pi} \frac{\cos i}{(\cos i + \cos \varepsilon)} (1 - e^{-Y}), \tag{5}$$

where the second term can be neglected, for the case that the space is opaque. Thus,

$$J = \frac{\gamma\varphi(\alpha)}{\varrho^2\pi} \frac{\cos i}{(\cos i + \cos \varepsilon)}. \tag{6}$$

This is an expression for the brightness of a solid body in accordance with the Lommel-Seeliger law, in which only the factor $\varphi(\alpha)$ or the phase curve of the individual bodies has been added. The mode of consideration, forming the basis of this derivation, is actually identical with the theory of absorption, on penetration of the light into the surface of the body. If this consideration is made for the case of low angles α, without considering the segment common to the two cylinders, and if one passes then to the limiting case $\alpha = 0$, an expression must be obtained of the form following from eq.(5) at $i = \varepsilon$. Let us denote the corresponding brightness by J_0' so that

$$J_0' = \frac{1}{2} \frac{\gamma\varphi(0)}{\varrho^2\pi} \left\{1 - e^{-2N\frac{H}{R}\frac{\varrho^2\pi}{\cos i}}\right\}. \tag{7}$$

Conversely, if the common segment G of the two cylinders were deducted from

the total volume V (in the limiting case at $\alpha = 0$), then V would consist of only one cylinder and we would have

$$V = \varrho^2 \pi \frac{h}{\cos i}.$$

Consequently, the brightness according to eq.(4) could be represented by the integral

$$J_0 = \gamma \varphi(0) \frac{N}{R \cos i} \int_0^H e^{-\frac{N}{R} \varrho^2 \pi \frac{h}{\cos i}} dh,$$

or, after carrying out the integration

$$J_0 = \frac{\gamma \varphi(0)}{\varrho^2 \pi} \left\{ 1 - e^{-N \frac{H}{R} \frac{\varrho^2 \pi}{\cos i}} \right\}. \tag{8}$$

On dividing this expression by eq.(7), we obtain /137

$$\frac{J_0}{J_0'} = 2 \frac{1 - e^{-\lambda}}{1 - e^{-2\lambda}}, \tag{8a}$$

where, for abbreviation, we have set $\lambda = N \frac{H}{R} \frac{\rho^2 \pi}{\cos i}$.

If the system is opaque, H and thus also λ must be considered as very large, so that $\frac{J_0}{J_0'} = 2$.

Consequently, the brightness of the system J_0 increases, at $\alpha = 0$, to about twice that at larger α. Since J_0', according to eq.(6), changes only little at low α, it follows that an opaque system of small bodies shows a behavior in the neighborhood of $\alpha = 0$ entirely different from that of a solid body. Simultaneously, the basic difference between a theory of absorption and a theory of illumination of dustlike masses is emphasized here.

Conversely, if the body is extremely transparent, then λ is very small so that, with decreasing α, we approach the limiting value

$$\frac{J_0}{J_0'} = 1,$$

where, finally, the entire mentioned brightness increase no longer is apparent. The Saturn ring is a formation, in which various stages intermediate between the mentioned two limiting cases occur. It is known that the ring consists of an internal dark so-called crêpe ring through which, during occultation, one can see the starlight shine with little attenuation so that this ring can be considered as quasi-transparent; the next is the bright B ring which must be considered as opaque, followed by the outermost fainter A ring which represents an intermediate stage between the two first rings and may be considered as slightly

transparent. Consequently, these three portions of the ring would have to exhibit the above-mentioned brightening phenomenon to various degrees during opposition.

Let us first investigate the case of an opaque ring in some detail. The essential point of the problem, according to the above statements, lies in considering the space G common to the two cylinders, whereas the lower hemispherical boundary can be neglected in each case as being vanishingly small. Thus,

$$V = V_0 + V_1 - G.$$

However, this equation is valid only for those volume elements of the ring at which the corresponding G is located entirely within the ring and is not intersected at all by the upper ring plane.

If the latter case is in question, a portion of G - which will be denoted here by Σ - remains outside the ring so that the following equation is valid:

$$V = V_0 + V_1 - G + \Sigma.$$

Denoting by h_1 the value of h for which Σ just about vanishes, the surface brightness will be composed of two parts:

$$J = \gamma q(\alpha) \frac{N}{R\cos\varepsilon}\left\{\int_0^{h_1} e^{-\frac{N}{R}(V_0+V_1-G+\Sigma)}\,dh + \int_{h_1}^{H} e^{-\frac{N}{R}(V_0+V_1-G)}\,dh\right\}. \tag{9}$$

Let us then designate the elevation angle of the earth and sun above the plane /138 of the ring by A and A′, so that $A = 90^\circ - \varepsilon$ and $A' = 90^\circ - i$; then,

$$V_0 = \varrho^2\pi\frac{h}{\sin A'}, \qquad V_1 = \varrho^2\pi\frac{h}{\sin A}.$$

A calculation of the spaces G and Σ is quite complicated and will be omitted here for greater clarity of the entire development. Therefore, we will write down the Seeliger expressions directly:

$$G = \frac{4}{3}\varrho^3\frac{1+\cos\alpha}{\sin\alpha}$$

and

$$\Sigma = \frac{(\sin A + \sin A')^2}{\sin\alpha\sin A\sin A'}\frac{\varrho^3}{\cos\mu}\left\{\cos\psi - \frac{1}{3}\cos^3\psi - \left(\frac{\pi}{2}-\psi\right)\sin\psi\right\},$$

where the quantities μ and ψ are determined by the equations

$$\tan\mu = \frac{\cos A\sin\beta}{\sin A + \sin A'}\sin\alpha, \tag{9'}$$

$$\varrho\sin\psi = \frac{h\cos\mu\sin\alpha}{\sin A + \sin A'}. \tag{9''}$$

Here, β is the angle between the plane going through Saturn, Sun, and Earth and a plane going through Saturn and Earth perpendicular to the plane of the ring.

According to Seeliger, the limiting value h_1 is determined by

(10)

Since also

$$V_0 + V_1 = \frac{\varrho^3 \pi}{\cos\mu} \frac{(\sin A + \sin A')^2}{\sin\alpha \sin A \sin A'} \sin\psi ,$$

then, for $h > h_1$, we have

$$V_0 + V_1 - G = \varrho^2 \pi h \frac{\sin A + \sin A'}{\sin A \sin A'} - \frac{4}{3} \varrho^3 \frac{1 + \cos\alpha}{\sin\alpha} ,$$

and, for $h < h_1$,

$$V_0 + V_1 - G + \Sigma = \frac{(\sin A + \sin A')^2}{\sin\alpha \sin A \sin A'} \frac{\varrho^3}{\cos\mu} \left\{ \cos\psi - \frac{1}{3}\cos^3\psi + \left(\frac{\pi}{2} + \psi\right)\sin\psi \right\} - \frac{4}{3}\varrho^3 \frac{1 + \cos\alpha}{\sin\alpha} .$$

In view of the smallness of the phase angle of Saturn (at the maximum, 6°.5) and the negligible differences between the angles A and A′ (at the maximum, 1°.5), the following simplifications of the above formula are permissible:

$$1 + \cos\alpha = 2 , \qquad \frac{(\sin A + \sin A')^2}{\sin A \sin A'} = 4 .$$

In addition, the angle μ which is of the same order as α can only be very small; therefore, we can also set cos μ = 1. Now, the expressions for V assume the following form:

$$V_0 + V_1 - G = \varrho^2 \pi h \frac{\sin A + \sin A'}{\sin A \sin A'} - \frac{8}{3} \frac{\varrho^3}{\sin\alpha} ,$$

$$V_0 + V_1 - G + \Sigma = \frac{4\varrho^3}{\sin\alpha} \left\{ \cos\psi - \frac{1}{3}\cos^3\psi + \left(\frac{\pi}{2} + \psi\right)\sin\psi - \frac{2}{3} \right\} .$$

Substituting these values into eq.(9), the second of the integrals becomes easy to calculate. We have /139

$$\int_{h_1}^{H} e^{-\frac{N}{R}(V_0 + V_1 - G)} dh = \frac{\sin A \sin A'}{\frac{N}{R}\varrho^2 \pi (\sin A + \sin A')} e^{\frac{8}{3}\frac{N}{R}\frac{\varrho^3}{\sin\alpha}} \left\{ e^{-mh_1} - e^{-mH} \right\} , \tag{11}$$

where, for abbreviation, we set

$$m = \frac{N}{R}\varrho^2\pi\frac{\sin A + \sin A'}{\sin A \sin A'}.$$

The second term in the parentheses can be neglected for an opaque ring. Consequently,

$$\int_{h_1}^{H} e^{-\frac{N}{R}(V_0+V_1-G)}\,dh = \frac{32}{3}\frac{\varrho}{\xi\sin\alpha}\frac{\sin A \sin A'}{(\sin A + \sin A')}\,e^{-\xi\frac{3\pi-2}{8\pi}},$$

where, again, for abbreviation, we introduce

$$\delta = \frac{32\varrho^3\pi}{3R} \qquad \text{and} \qquad \xi = \frac{N\delta}{\sin\alpha}. \tag{12}$$

Replacing now, in the first integral of eq.(9), the variable h by ψ with the aid of eq.(9″) (at $\cos\mu = 1$)

$$dh = \varrho\cos\psi\frac{\sin A + \sin A'}{\sin\alpha}d\psi,$$

we obtain, since $\psi = 0$ for $h = 0$ and since $\psi = \frac{\pi}{2}$ for $h = h_1$, the following expression

$$\int_0^{h_1} e^{-\frac{N}{R}(V_0+V_1-G+\Sigma)}\,dh = \varrho\frac{\sin A + \sin A'}{\sin\alpha}\int_0^{\pi/2} e^{-\frac{N}{R}(V_0+V_1-G+\Sigma)}\cos\psi\,d\psi.$$

Setting, in addition,

$$\Phi = \frac{3}{8\pi}\left\{\cos\psi - \frac{1}{3}\cos^3\psi + \left(\frac{\pi}{2}+\psi\right)\sin\psi - \frac{2}{3}\right\}, \tag{13}$$

we will have

$$\int_0^{h_1} e^{-\frac{N}{R}(V_0+V_1-G+\Sigma)}\,dh = \varrho\frac{\sin A + \sin A'}{\sin\alpha}\int_0^{\pi/2} e^{-\xi\Phi}\cos\psi\,d\psi.$$

Thus, for the brightness, the following expression is definitely obtained:

$$J = \gamma\varphi(\alpha)\frac{\varrho(\sin A + \sin A')}{R\delta\sin A}\left\{\xi\int_0^{\pi/2} e^{-\xi\Phi}\cos\psi\,d\psi + \frac{8}{3}e^{-\xi\frac{3\pi-2}{8\pi}}\right\}. \tag{14}$$

Here, $\varphi(\alpha)$ has been considered as constant throughout, so that $\frac{\gamma\varphi(\alpha)\rho}{R\delta} = \frac{3\gamma\varphi(\alpha)}{32\pi\rho^2}$ can be denoted by a single constant γ'. On introducing the notations

$$\left.\begin{aligned} \mathfrak{A} &= \xi \int_0^{\pi/2} e^{-\xi\Psi} \cos\psi \, d\psi , \\ \mathfrak{B} &= \frac{8}{3} e^{-\xi \frac{3\pi - 2}{8\pi}} \qquad \text{and} \qquad \mathfrak{C} = \mathfrak{A} + \mathfrak{B} \end{aligned}\right\} \tag{15}$$

the Seeliger final equation for the surface brightness of the ring is obtained:

/140

$$J = \gamma' \mathfrak{C}(\xi) \frac{\sin A + \sin A'}{\sin A} . \tag{16}$$

This formula, for an approximate calculation, can be brought to the form

$$J = \frac{3}{16\pi} \Gamma \varphi(\alpha) \mathfrak{C}(\xi), \tag{16'}$$

since

$$\frac{\gamma'}{\varrho^2} = \Gamma,$$

so that we can put

$$\frac{\sin A + \sin A'}{\sin A} = 2 .$$

For the function $\mathfrak{C}(\xi)$, Seeliger calculated a table which is compiled in the form $\mathfrak{C}(\infty)/\mathfrak{C}(\xi)$; here, as readily demonstrated, we have $\mathfrak{C}(\infty) = \mathfrak{A}(\infty) = \frac{3}{16}$. This will be given in the Appendix (Table VIIa).

Consequently, the last equation gives the brightness of the Saturn ring as a function of ξ and, since $\xi = \frac{N\delta}{\sin \alpha}$, also as a function of the phase angle and of the density. The fraction (sin A + sin A')/sin A differs only little from 2. Thus, it follows that the brightness of the Saturn ring is independent of the elevation angle of the earth and sun above its plane. This result of the theory has been confirmed by our observations (Ref.158), for the phase angles between 16° and 25°. For very small elevation angles, at the time of transit of both earth and sun through the plane of the ring, this result naturally is not applicable; in addition, the above theory requires a supplement in this case.

56. Effect of Density of the Dust Formation

Let us consider the dependence of the brightness on the phase angle in somewhat more detail. Seeliger calculated the function $\mathfrak{C}$ by numerical quadratures and compiled it in tables. The first table, mentioned above, gives the ratio $M = \frac{\mathfrak{C}(\xi)}{\mathfrak{C}(\infty)}$ according to the argument ξ, from 0 to 10,000; since ξ is also a function of δ, the slope of the brightnesses with the phase angle is dependent

also on the volume density. If the volume density or the fraction of the space filled by matter is denoted by D, we have

$$D = \frac{N \frac{4}{3}\pi \varrho^3}{R} = \frac{1}{8}\delta N. \tag{17}$$

Table 19 gives the course of $\mathfrak{C}(\xi)$ for several values of α and $N\delta$. This table is an extract of Seeliger's table which we are giving in Table VIIb of the Appendix, extended to lower and higher densities. If it should be possible to use the course of the surface brightness of the Saturn ring for determining a value of $N\delta$, we would obtain the volume density. Considering Table 19 for the values of $\mathfrak{C}(\xi)$, it is obvious that - for example, for $N\delta = 0.005$ - the brightness at $\alpha = 0^\circ.5$ has already dropped to almost half its value at $\alpha = 0^\circ$ and thereafter remains practically unchanged. Taking $N\delta = 0.00017$, the entire light variation will have taken place already between $\alpha = 0^\circ$ and $\alpha = 0^\circ.1$. At greater densities, the variability extends over a larger region, but its main portion is located between 0° and 1° face angle. Let us concentrate these considerations into a few theorems: /141

TABLE 19

$\mathfrak{C}(\xi)$

$N\delta$ =	0.1	0.05	0.01	0.005
$\alpha = 0.^{\circ}0$	0.533	0.533	0.533	0.533
0.1	0.485	0.453	0.352	0.317
0.2	0.453	0.411	0.318	0.294
0.3	0.430	0.385	0.302	0.286
0.4	0.411	0.366	0.291	0.281
0.5	0.396	0.352	0.289	0.279
1.0	0.352	0.317	0.279	0.273
2.0	0.317	0.294	0.273	0.270
3.0	0.302	0.286	0.270	0.269
4.0	0.294	0.281	0.270	0.268
5.0	0.289	0.279	0.269	0.268

A dustlike mass of such a thickness that it becomes entirely or practically opaque, exhibits a surface brightness which increases strongly with decreasing phase angle. For $\alpha = 0^\circ$, this might reach almost double the amount of brightness it had at low α. The light variation takes place at lower values of α the more the volume density of the dust formation decreases.

57. Influence of Transparency of the Dust Formation on the Light Variation

In the Saturn ring, the entire variability occurs within a few days close to opposition, which explains the fact that an actual observation of the phenomenon has become possible only very recently. Before making a comparison of theory and observation, we will treat the problem of semitransparent or translucent masses, which is of some importance for interpreting the phenomena on the Saturn ring. In the case of transparent masses, the second term in parentheses in eq.(11) cannot be neglected.

If, for clarity, the brightness equation is written in the form

$$J = \tfrac{3}{16}\Gamma'\left\{\mathfrak{A} + \tfrac{8}{3}e^{\frac{\xi}{4\pi}}\left(e^{-\frac{3}{2}\xi} - e^{-mH}\right)\right\}, \quad \left(\Gamma' = \frac{\Gamma\varphi(\alpha)}{\pi}\right),$$

then this term, which does not vanish for transparent bodies, will become

$$e^{-mH} = e^{-\frac{3}{32}\frac{N\delta}{\varrho}H\frac{\sin A+\sin A'}{\sin A\sin A'}} = e^{-\frac{3}{8}\frac{N\delta}{(\sin A+\sin A')}\frac{H}{\varrho}}.$$

Setting $\frac{N\delta}{(\sin A + \sin A')}\frac{H}{\rho} = \nu$, the quantity ν can be used as criterion for the transparency of the body. Then, the brightness of the transparent body will be

$$J = \tfrac{3}{16}I'\left\{\mathfrak{C}(\xi) - \tfrac{8}{3}e^{-\frac{3\pi\nu-2\xi}{8\pi}}\right\}, \tag{18}$$

a formula valid as long as $H > \rho\frac{\sin A + \sin A'}{\sin\alpha}$ or, which comes to the same, as long as

$$\frac{N\delta}{(\sin A+\sin A')}\frac{H}{\varrho} > \xi \quad \text{or} \quad \nu > \xi.$$

For bodies of lower density and smaller H, for which $\nu < \xi$, only the first term of the formula which corresponds to the volume $V = V_0 + V_1 + G - \Sigma$ alone need be used but with the difference that the integration must here be made from $h = 0$ to $h = h_1$, where

$$h_1 = \frac{\varrho(\sin A+\sin A')}{\sin\alpha},$$

i.e., to ψ up to the limit

$$\sin\psi = \frac{h}{\varrho}\frac{\sin\alpha}{(\sin A+\sin A')} = \frac{\nu}{\xi}.$$

In this case, the brightness reads /142

$$J = \tfrac{3}{16}I'\xi\int_0^{\psi} e^{-\xi\Phi}\cos\psi\, d\psi. \tag{19}$$

For $\xi = \nu$, both formulas lead to the same result, namely

$$J = \tfrac{3}{16}I'\nu\int_0^{\psi} e^{-\nu\Phi}\cos\psi\, d\psi = \tfrac{3}{16}I'\mathfrak{A}(\nu).$$

Setting, generally, $\nu = \xi + \sigma$ where σ is a positive quantity, eq.(18) is transformed into

$$J = \tfrac{3}{16}I'\{\mathfrak{A}(\xi) + \mathfrak{B}(\xi)(1 - e^{-\frac{3}{8}\sigma})\}. \tag{20}$$

Seeliger who tabulated the functions $\mathfrak{A}(\xi)$ and $\mathfrak{B}(\xi)$, concluded from this formula that, at greater values of $\nu(\nu > 14)$, the brightness will differ from that of an opaque body by only 1%. Setting, in addition, $\alpha = 0$, eq.(19) will yield

$$J_0 = I'(1 - e^{-\frac{3}{16}\nu}). \tag{21}$$

The magnitude of light variation at small α is then characterized by the quotient J_0/J where J must be calculated in accordance with eq.(18) or (19). The above equations indicate that the previously formulated law as to the dependence of the light variation on the density is valid, in both amount and interval, also for transparent masses.

As an approximate criterion for the light variation, the following expression can be used, as had been done in eq.(8a):

$$\frac{J_0}{J_1} = \frac{2(1 - e^{-\lambda})}{1 - e^{-2\lambda}}, \tag{22}$$

where we can set $\lambda = \frac{3}{16}\nu$, yielding for λ:

$$\frac{J_0}{J_1} = 1 + \frac{1}{2}\lambda - \frac{1}{24}\lambda^3 - \cdots$$

This indicates that noticeable light variations take place already for moderate values of λ. This is shown in the accompanying table.

Naturally, these variations are less pronounced than in an opaque body where J_0 may increase to almost twice the value of J_1.

λ	J_0/J_1
0.05	1.025
0.10	1.050
0.15	1.075
0.20	1.10
0.50	1.26
1.0	1.44

Consequently, for applying eqs.(18) and (19) to transparent dustlike bodies, the tables for $\mathfrak{A}$, $\mathfrak{B}$, and $\mathfrak{C}$ must be supplemented by a calculation of the integral in eq.(19), as required from case to case.

Whereas, for an opaque body at $\alpha = 0$, the brightness according to eq.(16′) can be reduced to the form

$$J_0 = \frac{3}{16\pi} I' \varphi(0) \mathfrak{C}(0) = \frac{I'}{\pi}, \tag{23}$$

it becomes, according to eq.(21), for the case of a transparent body

$$J_0 = \frac{I'}{\pi}\left\{1 - e^{-\frac{3}{32}\frac{N\delta H}{\varrho \sin A}}\right\}. \tag{24}$$

Thus, in the latter case the brightness depends largely on the angle A. For highly transparent bodies, J_0 is inversely proportional to sin A, in view of the fact that

$$J_0 = \frac{3}{32}\frac{I'}{\pi}\varphi(0)\frac{N\delta H}{\varrho}\frac{1}{\sin A}. \tag{25}$$

In the case of a nontransparent mass, the albedo of an individual particle can be determined if the surface brightness J_0 of the dust cloud in opposition /143

is known. As a typical example, let us calculate the reflection coefficient of the ring particles in both Saturn rings A and B. In this case, we will use the reflection coefficient of the Saturn center, derived previously (p.94), and also make use of several quantities that were contained in our earlier paper but were not applied to this particular problem. Here, let us assume the two rings as being nontransparent which is not true for the outer ring A. However, the magnitude of its transparency is still uncertain; for this, the value of the constant Γ will be needed. According to definition (p.149), the quantity of light reflected by an individual sphere at opposition [at $\varphi(0) = 1$]

$$q_0 = \Gamma \varrho^2 .$$

On the other hand, assuming Lambert's law, we have

$$q_0 = \frac{A_1}{\Delta^2 \pi} L \varrho^2 \frac{2}{3} \pi ,$$

where A_1 is the Lambert albedo, Δ the distance from the earth, and L the quantity of light per unit area.

Consequently,

$$\Gamma = \frac{2}{3} \frac{A_1 L}{\Delta^2} \quad \text{and} \quad J_0 = \frac{2}{3} \frac{A_1 L}{\Delta^2 \pi} . \tag{26}$$

However, the albedo A_1' of the Saturn center, which we have to use for comparison, is too uncertain a concept; therefore, let us introduce the reflection coefficient in direction of the irradiation. For an arbitrary reflection law, denoting by μ the reflection coefficient in direction of the irradiation for the entire sphere, we obtain

$$q_0 = \frac{\mu L \pi \varrho^2}{\Delta^2} \quad \text{and} \quad \Gamma = \frac{\mu L \pi}{\Delta^2} , \quad J_0 = \frac{\mu L}{\Delta^2} . \tag{27}$$

The brightness of the Saturn center in opposition, denoting the quantities referring to this by a prime, will be

$$J_0' = \frac{\mu' L}{\Delta^2} ,$$

whence

$$\frac{J_0}{J_0'} = \frac{\mu}{\mu'} . \tag{28}$$

Our own observations (Ref.158) yield a value of 0.891 for the mean brightness ratio of the two outer rings to the center in opposition and a value of $-0^m.593$ for the brightness difference of the ring B against the ring A, or the following brightness ratio:

$$\frac{J_A}{J_B} = 0.579 .$$

However, the surface dimensions of the two rings are not equal. Denoting the widths of the rings A and B by d_a and d_b and their mean radii by r_a, r_b, then the areas will be at a ratio of

$$\frac{A}{B} = \frac{r_a d_a}{r_b d_b},$$

whereas, using Barnard's values $d_a = 2''.53$, $d_b = 4''.17$, $r_a = 18''.76$, and $r_b = 14''.88$, we obtain /144

$$\frac{A}{B} = 0.765.$$

From this, the following brightness ratio of the two rings to the brightness of the center in opposition will be obtained:

$$J_A = 0.621, \qquad J_B = 1.073.$$

These ratios, according to our own observations, can be considered as constant within the limits of 16° to 25° of the elevation angle of the earth above the plane of the ring. Using the reflection coefficient $\mu = 0.672$ (see p.94) of the Saturn center in opposition, this yields the reflection coefficient of the ring particles for the rings A and B

$$\mu_A = 0.42, \qquad \mu_B = 0.72.$$

The quantity

$$\nu = \frac{N\delta}{(\sin A + \sin A')} \frac{H}{\varrho} = \frac{N\delta H}{2\varrho \sin A}, \tag{29}$$

which defines the transparency of the dust mass can be determined by observing the attenuation of the light of a given source, such as a fixed star, through the dustlike body. The light from a fixed star of a brightness J_0, after passing through a dust cloud of a thickness H/sin A, measured in direction of the light ray, will have a brightness of

$$J = J_0 e^{-\lambda}$$

where

$$\lambda = \frac{3}{16}\nu = \frac{3}{32}\frac{N\delta}{\varrho}\frac{H}{\sin A}.$$

Consequently, we have

$$\lambda = -\frac{1}{\log e}\log\left(\frac{J}{J_0}\right),$$

or, measured in stellar magnitudes, since $m - m_0 = -2.5 \log \frac{J}{J_0}$,

$$\lambda = 0.917(m - m_0), \tag{30}$$

where m and m_0 denote stellar magnitudes corresponding to the intensities J and J_0.

58. Variability of the Crêpe Ring

For interpreting certain phenomena, observed on the crêpe ring, it is of some importance to obtain a general concept as to the brightness of the Saturn surface visible through this ring. It is known that the dark ring can be observed either in its projection onto the dark celestial background or at points where it is projected onto the Saturn disk. Here, the ring gives the impression of a diaphanous veil over the disk. The dark ring was discovered rather late, in 1838 at the Berlin Observatory, and had previously escaped observation even through high-intensity telescopes. This fact as well as the uncertainty in descriptions of the ring and the veil at various times seem to suggest that changes take place in the dark ring which might have to do with the development of the entire configuration; on the other hand, the differing distinctness of the ring at various times might have to do with the illumination conditions.

Let us here give the Seeliger estimate calculations for the variability of a partly transparent ring. Let an element ds, if it is isolated, receive the quantity of light L cos i ds from the sun. Then, this element receives the /145 following amount of light through the dust mass:

$$L\,ds\cos i\,e^{-\lambda'}, \quad \text{where} \quad \lambda' = \frac{3}{32}\frac{N\delta}{\varrho}\frac{H'}{\sin A'}$$

and where H'/sin A' is the segment of the straight line drawn in direction to the sun and located within the dust formation. The earth, if it were standing completely free when viewed from ds, would receive a quantity of light of

$$\gamma' ds\,\frac{L}{\Delta^2}\,e^{-\lambda'} f(i,\varepsilon),$$

where $\gamma' f(i, \varepsilon)$ represents the reflection law. In reality, ds sends the following amount of light to the earth through the dust cloud:

$$dQ = \gamma' ds\,\frac{L}{\Delta^2} f(i,\varepsilon)\,e^{-(\lambda+\lambda')}, \qquad \lambda = \frac{3}{32}\frac{N\delta}{\varrho}\frac{H}{\sin A},$$

where H/sin A is the thickness of the dust formation in direction to the earth. Consequently, the apparent brightness will be

$$\frac{dQ}{ds\cos\varepsilon} = \frac{\gamma' L}{\Delta^2} f(i,\varepsilon)\sec\varepsilon\, e^{-(\lambda+\lambda')}.$$

To this must be added the light sent to the earth by the small spheres located on the above path; the resultant brightness is given by eqs.(18) and (19). Thus, the total brightness I of the element of area becomes

$$I = \frac{\gamma' L}{\Delta^2} f(i,\varepsilon)\sec\varepsilon\, e^{-(\lambda+\lambda')} + J.$$

In discussing this formula, we are assuming that the phase angle is very small and that J has the values given in eqs.(7) and (8). We will introduce the

additional notations of I_0 as the brightness of the surface element ds if it were entirely isolated and J_0 as the brightness of the ring if it were opaque. Then, the two limiting values

$$\left.\begin{aligned} J' &= J_0(1 - e^{-\lambda}), \\ J'' &= \tfrac{1}{2} J_0(1 - e^{-2\lambda}) \end{aligned}\right\} \qquad (31)$$

are obtained for J and, for the brightness of the surface,

$$I_0 e^{-(\lambda+\lambda')}.$$

Here, we can set $\lambda = \lambda'$ so that, for the total brightness, we obtain either

$$I = I_0\left(e^{-2\lambda} + \frac{J_0}{I_0}(1 - e^{-\lambda})\right)$$

or

$$I = I_0\left(e^{-2\lambda} + \frac{1}{2}\frac{J_0}{I_0}(1 - e^{-2\lambda})\right).$$

Here, in the first formula the term -2λ, for the moment $\alpha = 0$, must be substituted by $-\lambda$ since, at $\alpha = 0$, the absorption on the entire round trip takes place by the same spheres, i.e., is of the simple type. However, this coincidence, because of the great distance of the element ds from the ring, takes place only for extremely low values of α. Thus, it can be stated that the first formula no longer is valid for $\alpha = 0$, so that a third case must be differentiated in addition.

Thus, denoting J_0/I_0 by c, we obtain /146

$$\left.\begin{aligned} I/I_0 &= e^{-2\lambda} + c(1 - e^{-\lambda}), && 1) \\ &= e^{-2\lambda} + \tfrac{1}{2}c(1 - e^{-2\lambda}), && 2) \\ &= e^{-\lambda} + c(1 - e^{-\lambda}), && 3) \end{aligned}\right\} \qquad (32)$$

in which we have α very small for the case (1), α not very small for the case (2), and α strictly equal to zero for the case (3). For greater clarity, several values of I/I_0 have been calculated according to eq.(32), assuming c = 1; then, $(I/I_0)_3$ will always be equal to 1.

	$(I/I_0)_1$	$(I/I_0)_2$
$\lambda = 0.0$	1.00	1.00
0.1	0.91	0.91
0.2	0.85	0.84
0.3	0.81	0.77
0.4	0.78	0.72
0.5	0.76	0.68
0.6	0.75	0.65
0.7	0.75	0.62
0.8	0.75	0.60
0.9	0.76	0.58
1.0	0.77	0.57

This demonstrates that, also for moderate λ, i.e., at high transparency, brightness variations up to 25% at very low values of the angle α can take place. These variations occur so abruptly that they practically never are detectable. In fact, denoting by d the distance of the investigated element of the Saturn surface from the lower boundary of the ring, measured in direction to the sun, the total light variation can take place only if

$$\alpha < \frac{2\rho}{d}.$$

Obviously, d is larger than F where F is the shortest distance between the dark ring and the Saturn surface, which can be assumed as being about 15,000 km. It follows from this that $\alpha < (28\ \rho)''$ where ρ, expressed in kilometers, cannot be a very large number. Consequently, for values of α larger than the above-given value, the third case in eq.(32) is not in question.

As soon as α drops below the indicated limit, a distinct thinning of the veil takes place immediately and quite abruptly; this is more noticeable the larger c. This peculiar phenomenon lasts only a short time and is able to take place only if Saturn, at the time of opposition, is at one of the nodes of its orbit. Thus, there is very little hope that this will ever be observed. The striking aspect of the phenomenon is obliterated by the fact that the sun does not appear as a point source seen from Saturn (as was assumed here) but has a diameter of $3\frac{1}{2}'$.

However, in addition to the sudden thinning of the veil, other light variations must occur which have to do with the variation in the elevation angle A of the earth above the ring plane. To estimate the extent of this variation, a value must be defined for the quantity λ in eqs.(32). Seeliger derived such a value from Barnard's observation on the transit of the satellite Japetus through the shadow of the Saturn system. Barnard observed an attenuation of Japetus produced by the dark ring at its center, by 0.35 magnitude classes, indicating - since A at the time of observation was equal to 11°18' - the following values were obtained according to eq.(30):

$$\lambda = 0.32 \quad \text{and} \quad \lambda \sin A = 0.0627.$$

With these figures and for the values of c = 1 and c = $\frac{1}{2}$, Table 20 was compiled, giving the brightness values I of the crêpe ring under the three assumptions on the magnitude of α and for various values of the quadrant elevation angle A. This indicates that the crêpe ring shows considerable variations in light at low A. Even the free portion of the dark ring exhibits substantial variability, as can be demonstrated on hand of eqs.(31) where the first expression is valid for α = 0 and for α very small, while the second is valid for α not very small; however, we will not discuss this in more detail here. /147

TABLE 20

A	$c = 1$. $I:I_0$			$c = \frac{1}{2}$. $I:I_0$		
	1.	2.	3.	1.	2.	3.
1°	0.97	0.50	1.0	0.49	0.25	0.52
2	0.86	0.52	1.0	0.45	0.28	0.59
3	0.79	0.54	1.0	0.44	0.33	0.65
4	0.76	0.59	1.0	0.47	0.38	0.71
5	0.75	0.62	1.0	0.50	0.43	0.75
10	0.79	0.75	1.0	0.64	0.62	0.85
15	0.83	0.81	1.0	0.73	0.72	0.90
20	0.87	0.85	1.0	0.78	0.78	0.91
25	0.88	0.87	1.0	0.81	0.81	0.93
30	0.90	0.89	1.0	0.84	0.84	0.94

The above statements also are applicable to the outer A ring, since the partial transparency of this ring has been definitely established by two different observations. On the very clear photograph by Barnard of the Saturn system, Hepburn (Ref.159) observed a brightening at the point where the A ring passes over the Saturn disk. Ainslie (Ref.160) on February 9, 1917, followed the occultation of a star of the

seventh magnitude by the Saturn ring and was able to see the star through Cassini's division with very little attenuation of its light; he also saw the star through the A ring, in which case it had lost about 75% of its brightness. This indicates that the light variation of the three rings must differ and that they must be individually checked as to their variability if more detailed information is to be obtained on the density ratios in the ring system.

Prior developments presuppose that the particles, forming the ring system, are spheres of equal radius. However, Seeliger demonstrated that his theory is applicable also to the case where the radii of the spheres may, with equal probability, assume all possible values between two arbitrary limits. The tables of light variation are applicable also in this case, except than an argument modified by a constant factor must be used here. This factor differs so little from unity that for determining limiting values of the density which, at most, can be only a rough estimate the above-mentioned restriction to equal radii becomes meaningless.

Similarly, the assumption that the bodies are of spherical form constitutes no restriction of the theory, as proved by Seeliger, except that the function $\varphi(\alpha)$, representing the phase curve of the particles and previously assumed as constant, no longer can be considered as constant in the case of an arbitrary shape of the bodies; this function, as phase coefficient of the ring particles, can be entered into the condition equations in linear form relative to α and then defined.

Finally, the assumption of a point source of light or the neglecting of the solar dimensions become of entirely subordinate importance.

Seeliger's theory whose principles have been confirmed by actual observations thus constitutes a means of determining the limiting values for the volume density of the matter distributed over the various portions of the ring. There is no doubt that continued surface-photometric measurements of the intensity ratios will greatly advance our knowledge on this unique formation in the solar system. Seeliger voiced the suspicion that the density ratios in the rings are subject to variations. Therefore, a continued study of the system is even more desirable. /148

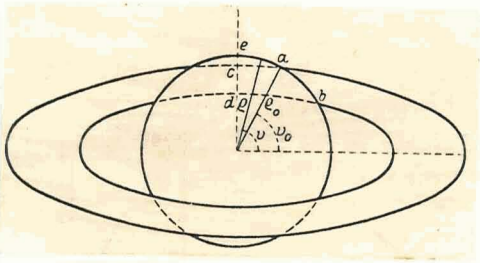

Fig.39 Occultation of the Ring by Saturn and Vice Versa.

59. Formulas for Total Intensity of Ring and Saturn Disk

Differential measurements of light distribution over the ring and the planetary disk are very difficult because of the smallness of the planetary image in the telescope. For a long period of time in the future, the total brightness of the system will have to remain the most often observed factor; therefore, it is necessary to give formulas for the total intensity of both Saturn and ring system, taking the light variation of the rings into consideration or permitting its determination.

The spheroid of Saturn presents itself to the observer as an elliptical disk whose semiaxes a and b′ are correlated with the semiaxes of the spheroid a, b, with the eccentricity e, and with the quadrant angle of elevation A of the earth over the equatorial plane, by the following equations:

$$b' = a\sqrt{1 - e^2\cos^2 A}, \qquad e^2 = \frac{a^2 - b^2}{a^2}.$$

The ring boundaries form ellipses concentric with the planetary disk whose semimajor axes are α and α' while the semiminor axes are

$$\beta = \alpha \sin A, \qquad \beta' = \alpha' \sin A.$$

If R denotes the area of the ring in the projection plane and Q_R the quantity of light transmitted from the ring to the earth, then

$$Q_R = RJ, \tag{33}$$

where J is the brightness of the ring. Denoting by Q_S the quantity of light which the unocculted Saturn disk would send toward the earth, with F being the area of the ring portions occulted by Saturn and Q_F the amount of light which the parts of Saturn occulted by the ring would send toward the earth and if, finally, Q_B is the amount of light actually sent by the entire system toward the earth, then

$$Q_B = (R - F)J + Q_S - Q_F, \tag{34}$$

where, at first, the mutual occultation of ring and sphere has been disregarded. With respect to calculating the individual quantities entering here, it should be stated that

$$R = \pi(\alpha^2 - \alpha'^2)\sin A. \tag{35}$$

In addition (see Fig.39), we have

$$\tfrac{1}{2}F = (abcd) = (bde) - (ace).$$

A calculation of the area R - F of the visible ring is simple and will be disregarded here, referring the reader to Seeliger's paper (Ref.161). The table by Seeliger for X = R - F is given in the Appendix (Table VIIIa). For calculating the quantity of light Q_S, an assumption must be made on the light distribution over the Saturn disk. Seeliger fully solved the problem for the case of uniform brightness of the disk and for the case of the Lambert law. It is known today that the first assumption must be rejected entirely, while the second deviates considerably from reality. However, photographs of Saturn through various ray filters prove that the formulas derived by us for the visually effective rays /149 are valid only for these. Since modern photometric methods, such as the photoelectric type, are effective for other ray classes and since, in measurements of the total brightness, further information on the Saturn system can be expected only by the high acuity of these methods, it is meaningless to convert the Seeliger theories for the visually observed light distribution over the disk. However, for the reduction of photoelectric data, a Lambert distribution of light

can be assumed in first approximation.

Therefore, we will compile here the formulas valid for the total brightness of the Saturn and ring system, valid for this assumption, as they are applicable to the reduction of photometric data under application of the Seeliger tables given in the Appendix.

Let

$Q_0(0)$ = brightness of the planet in middle opposition, reduced to the vanished ring;

Q_B = observed total brightness at median distance from earth and sun;

$X = R - F$ = unocculted area of the ring;

Y = unocculted portion of the Saturn disk;

$\frac{1}{M} = \mathfrak{C}(\alpha)$ = phase curve for the surface brightness of the ring;

$D = \cos\alpha$ = effect of the phase, neglecting the oblateness [eq.(25), p.77].

Then, according to eq.(16) the share of the rings in the total quantity of light Q_B will be

$$\gamma' X \frac{\sin A + \sin A'}{\sin A} \frac{1}{M},$$

while that of the planet becomes

$$Q_0(0)\, YD,$$

and, if $\gamma' : Q_0(0)$ as new constant is denoted by Γ, the total brightness will be

$$Q_B = Q_0(0)\left[\Gamma \frac{\sin A + \sin A'}{\sin A} \frac{X}{M} + YD\right]. \tag{36}$$

The quantities X and Y were tabulated by Seeliger (Table VIIIb), together with log M for various values of the density function (Table VIIb). Therefore, if the latter is used as argument here, then the factor at Γ and YD can be assumed as known so that the following equation can be derived:

$$Q_B = ax + by, \quad \text{where} \quad a = \frac{\sin A + \sin A'}{\sin A} \frac{X}{M}, \quad b = YD, \tag{37}$$

while the unknowns

$$x = \Gamma Q_0(0) \quad \text{and} \quad y = Q_0(0)$$

can be determined from observations. Their ratio will then yield the constant Γ. The manner in which the reflection coefficient of the ring particles can be obtained from this constant and from the known albedo of the Saturn center was

discussed on p.163 of this Chapter. These formulas disregard the influence of the phase coefficient of the ring particles $\varphi(\alpha)$ and of the Saturn disk $\psi(\alpha)$ which, according to our own investigations, should not be neglected. By introducing the corresponding factors $\varphi(\alpha) = 1 - \lambda\alpha$, $\psi(\alpha) = 1 - \lambda'\alpha$ into the condition equations, it is easy to take account of these influences and to determine also the phase coefficients. /150

60. Influence of Shadow-Casting on Brightness of the Saturn System

Until now, the shadow cast by the ring on the planet and, inversely, the shadow cast by the planet on the ring have not been considered in calculating the total brightness of ring + disk. Seeliger also investigated these influences and compiled the results of his theory in the form of tables available for general use. These influences, at the maximum, reach only a few percent of the total brightness and are in question exclusively for the reduction of highly accurate data. Since these effects increase with the phase angle, they can no longer be neglected in deriving the phase coefficient of the system, whenever a strict determination of this quantity is desired.

The highly complex derivations, in view of their specialized interest, will not be given in their entirety here; only the general sense and the use of the tables, which are given here in a somewhat abbreviated and slightly modified form (Appendix, Tables IXa, IXb, IXc), will be discussed.

61. Shadow-Casting of the Ring

The shadow cast by the ring reduces the unocculted portion Y of the Saturn disk. This correction ΔY was calculated by Seeliger for the case of a uniformly bright disk; however, here only the shadow of the outer ring boundary is in question since that of the inner boundary, already because of the semitransparent crêpe ring which adjoins the inner boundary, is no longer fully effective. The oblateness of the planet is considered only in part, which no doubt is completely legitimate.

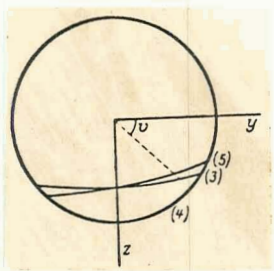

Fig.40 Shadow Cast by the Ring on Saturn (according to Seeliger).

Let A, A′ be the angle of elevation of the earth and sun above the plane of the Saturn equator while α is to denote the phase angle, i.e., the angle between earth (E) and sun (S) seen from the center of Saturn, with ι being the length difference of E and S at the Saturn equator; then, if

$$A' = A + \delta A$$

is set, we will have

$$\sin^2 \frac{\iota}{2} = \frac{\cos\delta A - \cos\alpha}{2\cos A \cos A'}. \qquad (38)$$

Figure 40 shows the visible disk of the planet, with a rectangular coordi-

nate system whose y-axis is located in the equator of the planet and whose z-axis is directed perpendicularly to this toward south; the x-axis is directed toward the earth, i.e., perpendicular to the plane of the paper. The curves (3) and (5) represent the projections of the shadow boundary of the ring and of the ring itself. The boundaries of the planet (4) were assumed here as being circular. Consequently, it is then a question of calculating the area S bounded by the curves (3), (4), and (5), for which the following argument is sufficient:

$$2S = \int_{v_0}^{v_1} dv\,(r'^2 - r^2),$$

where v_0 and v_1 are the bounding angles v, while r′ and r are the radius vectors corresponding to the shadow limit respectively to the ring limit.

Here, two cases must be differentiated: /151

Case 1: The curves (3) and (5) do not intersect on the planetary disk.

Denoting by a and b′ the major and minor axes of the planetary disk and by α and β the major and minor axes of the outer ring boundary, so that

$$b' = a\sqrt{1 - e^2\cos^2 A} \quad \text{and} \quad \beta = \alpha \sin A,$$

and denoting by φ an auxiliary angle determined by the equation

$$\tan\varphi = \frac{b'}{a}\sqrt{\frac{\alpha^2 - a^2}{b^2 - \beta^2}} \tag{39}$$

then the sought area is given by the simple formula

$$S = \delta A\,\Sigma \tag{40}$$

where $\Sigma = \Sigma_1 - \Sigma_0$, in which case

$$\Sigma_0 = \frac{\alpha^2}{2}\left(\varphi - \frac{1}{2}\sin 2\varphi\right)\cos A,$$
$$\Sigma_1 = \frac{\alpha^2}{2}\left[\pi - \left(\varphi - \frac{1}{2}\sin 2\varphi\right)\right]\cos A.$$

The quantities Σ_1, Σ_0, and Σ are given in Table IXb in the Appendix; Σ must always be positive.

Case 2: The ellipses (3) and (5) intersect on the planetary disk. For calculating this case, the intercept of the ellipses must be defined.

The corresponding angle v_2 is found from the equation

$$\tan v_2 = \frac{l\sin^2 A\cos A}{\delta A}, \tag{41}$$

whose solution decides whether Case 1 or 2 is in question. For this, the angle φ [eq.(39)] and v_0 are taken from Table IXa according to the argument A; here, v_0 and v_1 correspond to the equations

$$\tan v_0 = \sin A \tan\varphi, \qquad v_1 = \pi - v_0. \tag{42}$$

If v_2 is then located between v_0 and v_1, $v_0 < v_2 < v_1$, we have to do with Case 2 and the method to be applied is as follows: From Table IXb, the auxiliary quantity

$$V = \frac{\alpha^2}{2} \sin A \left(\frac{\cos\varphi}{\cos v_0}\right)^2 \tag{43}$$

is taken, forming

$$\left.\begin{aligned} S(v_1) &= \Sigma_1 \delta A + lV, \\ S(v_0) &= \Sigma_0 \delta A + lV, \\ S(v_2) &= \frac{\alpha^2}{2} \cos A \, \delta A \{\psi + \tan^2 A \tan\psi\}, \end{aligned}\right\} \tag{44}$$

and

where the angle ψ is given by the equation

$$\tan\psi = \frac{l \sin A \cos A}{\delta A} \tag{45}$$

and is assumed as $< 180^\circ$.

Then, the sought area will be

$$\left.\begin{aligned} S &= S(v_1) - S(v_2) \\ S &= S(v_2) - S(v_0), \end{aligned}\right\} \tag{46}$$

or

depending on which of the two values will be positive.

Thus, eqs.(38) and (41) must be solved in any case, while v_0 and v_1 must be calculated by means of the table so that one can decide whether Case 1 or 2 is involved. In Case 1, only Table IXb need be used, from which $\log \Sigma$ can be taken while S can be calculated according to eq.(40); in Case 2, a calculation of eqs.(44) and (44a) will be necessary in addition, so as to find the result from eq.(45). /152

The tables are so arranged that the angles A and A′ always must be taken with a positive sign and that l must always be calculated as a negative value.

The correction ΔY for the shadow-casting, at uniform brightness of the disk, apparently is

$$\Delta Y = \frac{S}{\pi a b}, \tag{47}$$

while, for the real light distribution, an easily estimated fraction of this quantity - which in itself is very small - can be assumed.

62. Shadow Cast by the Planet on the Ring

For calculating the brightness deficit due to the shadow cast by the planet on the ring, Seeliger derived strict formulas and tables. Figures 41a, b, c, d illustrate the various cases of shadow-casting involved. The shaded area is here bounded by four curves I, II, III, and IV, where I and II represent the visible boundary of the planet and of the shadow on the ring, while III and IV are the outer and inner boundaries of the ring. Denoting by ρ_1 and ρ_2 the radius vectors referring to I and II and corresponding to the same angle v, the sought area σ will be given by the integral

$$\sigma = \tfrac{1}{2}\int (\varrho_2^2 - \varrho_1^2)\, dv\,,$$

whose limits must be determined accordingly. In addition to the angle φ determined by eq.(39) and given in Table IXa, we also need the auxiliary angle f^* given by the equation

$$\tan f^* = -\frac{b'}{a}\cos A\,\frac{l}{\delta A} \qquad (48)$$

and in whose calculation eq.(38) for l and Table IXa for $b'(a = 1)$ can be used. /153

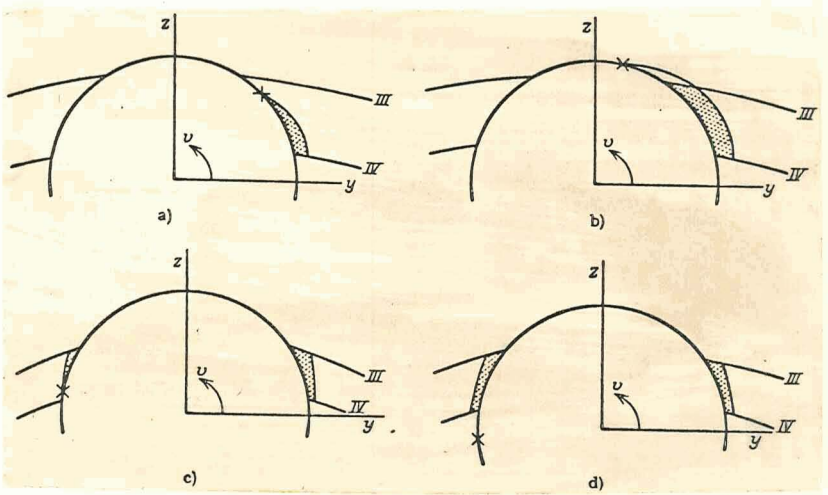

Fig.41 Shadow-Casting of the Planet on the Ring (according to Seeliger).

The value of the angle v, corresponding to the intercept of the curves I and II, is then obtained from

$$\tan v^* = +\frac{b'}{a\sin A}\tan f^*\,. \qquad (49)$$

This value facilitates the decision as to which of the four cases (a), (b), (c), and (d), illustrated in the diagrams, is involved. Naturally, the calculation

of σ differs in these four cases. In the cases sketched, A must be taken as positive and i as negative. The former mode represents a method of calculating the angle A exactly opposite to that generally used in the ephemerides. The symbols $A > 0$ and $i < 0$ can be assumed in all cases.

Denoting the values of v, corresponding to the intercepts of III and IV with I, by v_{III} and v_{IV}, the following four cases are possible:

a) v^* located between v_{IV} and v_{III}; in this case, the limits of our integral are given and the sought area is

$$\sigma = \sigma(v^*) - \sigma(v_{IV}),$$

b) v^* located between v_{III} and $180^\circ - v_{III}$; then

$$\sigma = \sigma(v_{III}) - \sigma(v_{IV}),$$

c) v^* located between $180^\circ - v_{III}$ and $180^\circ - v_{IV}$, i.e.,

$$\sigma = \sigma(v_{III}) - \sigma(v_{IV}) + \sigma(v^*) - \sigma(180^\circ - v_{III}),$$

d) $v^* > 180^\circ - v_{IV}$; then, as shown in the diagram, we have

$$\sigma = \sigma(v_{III}) - \sigma(v_{IV}) + \sigma(180^\circ - v_{IV}) - \sigma(180^\circ - v_{III}).$$

It should be mentioned that the ring boundary III may completely surround the planet (I). In that case, it will always be sufficient to set $v_{III} = 90^\circ$.

The values v_{III} and v_{IV} are obtained from Table IXa under φ and φ' because of the fact that

$$v_{III} = \varphi \quad \text{and} \quad v_{IV} = \varphi'. \tag{50}$$

The correction ΔX, for uniform brightness of the disk, and the correction ΔX_L for the Lambert light distribution are found from the shadowed area σ by means of the equations

$$\left.\begin{aligned} \Delta X &= +\frac{\sin A}{ab\pi}\sigma, \\ \Delta X_L &= \Delta X \frac{b}{2aP}, \end{aligned}\right\} \tag{50'}$$

with P being tabulated in Table VIb. The value of ΔX, in the four mentioned cases, is obtained from

$$\left.\begin{aligned} &\text{a)}\quad \Delta X = +l\frac{\alpha'^2 c}{2} - \delta A\,\lambda(a) + c\sigma(v^*), \\ &\text{b)}\quad \Delta X = -l\frac{\alpha^2 - \alpha'^2}{2}c + \delta A\,\lambda(b), \\ &\text{c)}\quad \Delta X = +l\frac{\alpha'^2 c}{2} + \delta A\,\lambda(c) + c\sigma(v^*), \\ &\text{d)}\quad \Delta X = +2\delta A\,\lambda(b), \end{aligned}\right\} \tag{51}$$

while $\lambda(a)$, $\lambda(b)$, $\lambda(c)$ is obtained from Table IXc; consequently, this leaves /154 only $\sigma(v^*)$ to be calculated, which is given by the equation

$$\sigma(v^*) = -l\frac{a^2}{2}\frac{\cos^2 f^*}{\cos^2 v^*} + \delta A M, \qquad (52)$$

where

$$M = \tfrac{1}{2}\left(\frac{a}{b'}\right)\frac{b^2\cos^2 A}{\sin^2 A}\{\sin f^* \cos f^* - f^*\}. \qquad (53)$$

All quantities, still required for calculating eqs.(51), (52), and (53), are compiled in Tables IXa and IXc.

The sequence of calculation for determining ΔX, after taking the angles A, A' from the ephemerides, would be as follows: Use eq.(38) for determining ι, and eqs.(48) and (49) for calculating v^*. After this, use eq.(50') for deciding whether the case (a), (b), (c), or (d) is involved, and then determine ΔX by means of the tables and eqs.(51), (53), (52), and finally (50).

Next, make the corrections ΔX, ΔY resp. ΔX_L, ΔY_L with negative signs on X, Y resp. X_L, Y_L. As mentioned above, the magnitudes of these corrections never exceed a few hundredths and thus are in question only for the reduction of highly accurate data of the total brightness of the Saturn system.

63. Observations of Brightness of the Saturn System

G.Müller (Ref.162) was the first to attempt a confirmation of Seeliger's theory of the Saturn ring, in a large series of observations of the total brightness of the Saturn system, extending over 11 years; he actually detected a fluctuation in Saturn's brightness with the phase, of about 20% of the total luminous intensity. He also found that his observations agreed satisfactorily with the Seeliger curve for the ring variability at $N\delta = 0.5$. The resultant mean volume density for the rings A and B is 0.06. However, it should be mentioned in this respect that, according to our own investigations (Ref.158, p.68), the deviations of the observations from the theory show a linear course, dependent on the phase angle, and that it is actually impossible to make a reliable choice for $N\delta$ between the values 0.3 and 0.8. Even the excellent and extensive series of 252 observations by Müller have just about been sufficient for proving the existence of a strong light fluctuation of the rings but were not even halfway adequate for determining a critical value of the density; this is more so the case for shorter observation series. From visual observation of the total brightness of the system, no progress whatever in this direction can be expected; much stricter methods will have to be used. This has been attempted by P.Guthnick who used photoelectric cells for measuring the planet brightnesses. He was able to follow the light reduction of the Saturn system, during the oppositions of 1918 and 1920, down to the lowest phase angles ($\alpha = 0^\circ.1$). A derivation of the variability of the ring from that of the system is made more difficult in the photoelectric method because of the fact that the brightness ratio of ring to disk differs for each type of rays and must be individually determined for the various photoelectric cells used. In any case, Guthnick's observations distinctly show that the Saturn system, in the immediate vicinity of the opposi-

tion between $\alpha = 0^{\circ}.0$ and $\alpha = 1^{\circ}.0$, undergoes a light increment of about $0^{m}.1$, an amount which cannot be attributed to the disk. Thus, Seeliger's theory again has been confirmed; however, the mean volume density of the ring matter is considerably less according to these observations. Under plausible assumptions on the brightness ratio of ring to disk, we derived a value of 0.01 from Guthnick's and Hertzsprung's observations (Ref.163). /155

64. Observations of the Variability of the Ring

Detailed investigations on the variability of the Saturn rings were published by us in a frequently cited paper. In observations of the brightness ratio of ring to disk with a focal-plane photometer, extending over 5 years, we were able to define accurately the relative brightness curve from the ring to the center of the disk, for all phase angles.

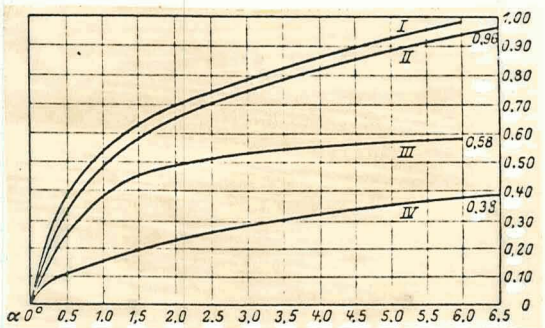

Fig.42 Brightness Difference between Saturn Center and Ring, in Magnitude Classes. I - Theoretical curve for the volume density D = 0.01; II - Calculated curve from Guthnick's measurements, 1918 (A = 18°); III - Calculated curve from Guthnick's measurements, 1920 (A = 6°); IV - Observed curve by Schoenberg (1913 - 1918); A between 16° and 27°.

This made it possible to reduce our own observations on the total brightness, as well as those by Müller, without the use of hypotheses, applying eq.(37) together with the observed brightness curve 1/M. It was found that the Saturn system, in addition to the variability of the ring of the specific Seeliger form as shown in the curves of Fig.42, with a sharp rise in brightness between $\alpha = 0^{\circ}$ and $\alpha = 1^{\circ}$, shows still another light decrement with the phase angle, progressing linearly with α. A more accurate analysis of this phenomenon leads to the conclusion that this variability must be ascribed in part to the Saturn disk and in part to the ring, so that the Saturn disk as well as the ring particles exhibit substantial phase coefficients (the former being $0^{m}.017$ and the latter $0^{m}.045$ per 1° phase). Although the former value for the disk, in view of the significant phase coefficients found by Guthnick and Schoenberg (Ref.164, 158, p.33) for the planet Jupiter, raises no doubt, the second value of the phase coefficient of the ring particles is excessively large and most likely is not real to its full amount. Instead, it must be assumed that this large value is a result of calculation and is actually due to the variability of the curve 1/M. Schoenberg's curve refers to the years 1913 - 1918. It was impossible to decide from the available data whether and in how far this curve varied from year to year.

Another important result of more recent investigations is the fact, derived by us from Guthnick's photoelectric measurements, that the variability of the ring shows a different course for the various ray classes. For the photo-

electrically effective rays, the curves II and III - as shown in Fig.42 - have a much steeper slope than for the visual rays, in which case the Seeliger phenomenon is even more pronounced. The slope of these curves, incidentally, depends also on the angle of elevation of the earth A, whereas no such dependence, in agreement with Seeliger's theory, exists.

We can give the following explanation for these peculiar conditions: The Seeliger theory does not figure at all with the scattering of light within the ring cloud. The resultant curves on the variability thus tacitly assume that /156 the mutual occultation of the ring bodies is complete. However, this cannot be so, since the ring particles must include such small particles that shadow-casting cannot be in question for them and that a scattering of the light must take place according to Rayleigh's or some other formula. However, a scattering of light in all directions takes place also at large dimensions of the bodies. Finally, the light reflected from the Saturn surface contributes to lightening of the shadows and, if these facts are taken into consideration, it is rather surprising that the Seeliger phenomenon is noticeable at all or, in the case of photoelectrically effective rays, is so pronounced.

65. Consistency of the Saturn Ring; the Light-Scattering Haze

A proof for the existence of a light-scattering nebulosity in the Saturn ring, which reflects selectively, is considered to be given by Wood's photographs of the Saturn system through various filters (Ref.165). These photographs show the following phenomena: The appearance of the body of Saturn itself and that of the rings differs completely on the various photographs taken through different color filters. On the one hand, the body of Saturn becomes increasingly darker when moving from the red to the violet end of the spectrum, during which process the absorption for violet rays steadily increases toward the limb of the disk. The ring, in comparison to the disk, becomes increasingly brighter which constitutes a proof for its lighter coloration; simultaneously, however, the difference in brightness between the brighter B ring and the fainter A ring disappears furthermore so that they are almost equally bright on the ultraviolet photograph whereas, for visually effective rays, the difference in brightness is $0^m.6$. In agreement with Wood himself, we conclude that the great brightness of the B ring is mainly explained by the haze spread over it; this haze, although of a lighter color than the surface of Saturn itself, predominantly reflects the yellow rays and thus is ineffective when photographing through blue and violet filters. The photoelectric measurements by Guthnick refer to the ring system freed of the effect of the yellow nebulosity and therefore emphasize the Seeliger occultation phenomenon with special distinctness whereas, for visual rays, the steep slope of the brightness curve is considerably flattened by illumination of the shadows. Based on this hypothesis, we attempted calculating the component of diffuse light from a comparison of the visually observed and photoelectrically obtained curve, which naturally is possible only in rough approximation. It is assumed that the component of the scattered light is independent of the phase angle. It was found that this component is 1.6 of that produced by the shadow-casting bodies, i.e., that visually observed, the light-scattering nebulosity is even brighter than the ring particles. Conversely, for the photoelectrically effective rays, the light of the haze is of almost no significance. The views stated here require a check by

direct brightness measurements of the variability of the two ring halves in different ray classes. Presumably, the share of the two ring halves in the variability of the system will differ, already because of the partial transparency of the A ring but also because of the differing attenuation by the diffuse light of the haze formation. L.Bell (Ref.166), and we ourselves in a later report /157 (Ref.167), formulated still another hypothesis for explaining the various colorations of the rings A and B. The A ring is covered by a haze formation of such small particles that they reflect only ultraviolet light and thus can be seen on the ultraviolet photographs by Wood. The alternating brightness difference of the two ring halves is due to this haze whereas the B ring, surrounded by a larger haze formation, shows no distinct brightness difference in the various ray classes. In that case, however, the above attenuation hypothesis would no longer be valid for the increased variability in the more refractory rays, so that even the confirmation of Seeliger's occultation hypothesis by previous measurements would become doubtful.

Without more detailed investigations on diffraction phenomena on minute particles, one cannot reject the possibility that the variability of the rings is due to a diffraction phenomenon. The differing slope of the brightness curve in rays of different color makes this assumption seem rather plausible.

66. Zodiacal Light

Based on the laws of illumination of dustlike masses, an attempt has been made to explain also the luminous intensity of the zodiacal light. Actually, spectroscopic observations prove that this low-intensity phenomenon, which can be conveniently observed only in tropical latitudes, has to do with reflected sunlight. The reflected particles, producing the zodiacal light, are assumed to be solid bodies whose dimensions are large in comparison with the wavelength of light; for this, Seeliger's theory of the illumination of dust formations is valid, except that the special phenomena occurring at the lowest phase angles and being of substantial importance for the Saturn rings lose their significance here. In the opinion of most researchers, the dust cloud producing the zodiacal light and spread over the plane of the ecliptic envelops the sun as well as the earth, while other authors believe that it envelops only the earth. The particles of this cloud, illuminated under extremely low phase angles, would have to be observed either in the immediate neighborhood of the sun (which, of course, is impossible) or at the antisolar point, the so-called gegenschein; however, this counterglow is so faint that no reliable measurements of its brightness have ever been made.

In calculating the reflected amount of light, the influence of mutual occultation and shadowing of the particles can be disregarded; in view of the very low volume density of the meteor swarm, as it must be assumed as primary cause of the zodiacal light, this represents no loss of accuracy. This statement can be substantiated by the following estimate calculation:

Let us consider the umbra of a sphere of radius ρ, located at a distance r from the sun and at a distance Δ from the earth; let us seek the probability that another sphere enters this umbra. Then, at a value $\rho = \frac{1}{2}$ meter and r:S = 300 (S = solar radius), the height of the shadow cone obviously will become

$\frac{r\rho}{S}$ = 150 m. The assumed values thus are rather too large than too small. If N spheres are located in the space Z, then the mean distance between these spheres - according to the expansions by Seeliger (Ref.168) - is given by the formula

$$2\left(\frac{Z}{N}\right)^{\frac{1}{3}} \frac{\Gamma(\frac{4}{3})}{(\frac{4}{3}\pi)^{\frac{1}{3}}}. \qquad (54)$$

Introducing here the radius ρ and assuming that the spheres occupy the 10^x-th portion of the space in which they are located, their mean distance will be /158

$$2\varrho\,\Gamma(\tfrac{4}{3})\,10^{\frac{x}{3}}.$$

This formula yields the following table:

Density	Mean Dist.	Density	Mean Dist.
10^{-6}	89 m	10^{-10}	1.9 km
10^{-7}	192	10^{-11}	4.1
10^{-8}	414	10^{-12}	8.9
10^{-9}	893	10^{-13}	19.2

This indicates that, at a density of 10^{-7}, less than one sphere will enter the shadow cone of the other sphere on the average. Since, actually, smaller spheres must also exist whose shadow cone would be correspondingly shorter, the probability becomes even less. In this case, the assumed density presumably is much too high for the meteor swarm of the zodiacal light.

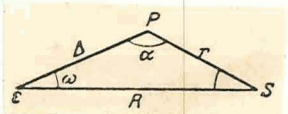

Fig.43
ε Earth, S sun, P a meteor.

Although this means that we can disregard the mutual occultation of meteors, the attenuations produced by the meteors within the two cones V_1 and V_2 would have to be considered in all strictness; the first of these cones has its apex in the meteor under consideration and its base in the sun, enveloping the latter, while the second has its apex in the eye of the observer and its base in the meteor itself. According to statements made in Section 54 [eq.(3)], the area brightness, if the sum of the two cone volumes is denoted by V so that $V_1 + V_2 = V$, will be

$$J = \gamma \int_0^{\Delta_0} \varphi(\alpha) \frac{N}{Z} e^{-N\frac{V}{Z}} \frac{\Delta^2}{\Delta^2 r^2}\, d\Delta = \gamma \int_0^{\Delta_0} \frac{\varphi(\alpha)}{r^2} \frac{N}{Z} e^{-N\frac{V}{Z}}\, d\Delta, \qquad (55)$$

where $\varphi(\alpha)$ denotes the phase curve and γ is a constant. Here, since sun and earth are within the cloud, allowance is made, in calculating the element dv, for the varying size of the volume element $\Delta^2 d\sigma d\Delta$, its varying distance from the sun and earth, and the variability of its phase angle. The exponential function under the integral sign, as demonstrated by K.Schwend (Ref.169) in his thesis, can be set equal to 1 whenever the volume density of the zodiacal space does not exceed 10^{-13}. At lower densities, the mutual occultation of the meteors can be neglected.

Consequently, in this case - introducing the denotation $\mu(r)$ for $\frac{4}{3}\pi\rho^3 N/Z$ - the brightness, in view of the fact that the density is a function of the solar distance, will be

$$J = \gamma_1 \int_0^{\Delta_0} \frac{\mu(r)}{r^2}\varphi(\alpha)\, d\Delta, \tag{56}$$

where

$$\gamma_1 = \gamma \frac{3}{4\pi\rho^3}.$$

Here, it is convenient to introduce α as integration variable, if the point is located in the ecliptic, using the following equations (Fig.43):

/159

$$\Delta = \frac{R\sin(\alpha+\omega)}{\sin\alpha} \quad \text{and} \quad r = \frac{R\sin\omega}{\sin\alpha}, \tag{57}$$

where R denotes the distance earth-sun and ω the elongation from the sun. We then have

$$d\Delta = -\frac{R\sin\omega}{\sin^2\alpha}\, d\alpha, \qquad \frac{d\Delta}{r^2} = -\frac{d\alpha}{R\sin\omega}$$

and

$$J = \gamma_1 \int_{\alpha_0}^{\pi-\omega} \frac{\mu(r)\,\varphi(\alpha)\, d\alpha}{R\sin\omega} = \frac{\gamma_1}{R\sin\omega}\int_{\alpha_0}^{\pi-\omega} \mu(r)\,\varphi(\alpha)\, d\alpha,$$

where

$$\alpha_0 = \arcsin\frac{R\sin\omega}{R_0},$$

if R_0 denotes the radius of the cloud spherically spreading around the sun, or else

$$J = \frac{C}{\sin\omega}\int_{\alpha_0}^{\pi-\omega} \mu(r)\,\varphi(\alpha)\, d\alpha, \tag{58}$$

where γ_1/R is replaced by a new constant C. This represents an integral equation of the first order, which would be useful for determining the function $\mu(r)$ if the function $\varphi(\alpha)$ were known. However, in view of the irregular shape of meteors this is not the case; in addition, both form and extent of the cloud are indeterminate. Furthermore, most likely the density μ is also a function of the height of the symmetry plane of the zodiacal light (ecliptic).

The first observer making an attempt at a theoretical discussion of his observations was Fessenkov (Ref.170). However, his observations, referring only to slight elongations from the sun, do not permit a check of the above assumptions. Therefore, he was satisfied with verifying the three illumination laws, by assuming the extent of the cloud as infinite and the density of the meteor swarm as inversely proportional to the solar distance $\mu = \frac{k}{r} = \frac{k\sin\alpha}{R\sin\omega}$.

Then, eq.(58) is simplified into

$$J = \frac{C_1}{\sin^2\omega}\int_0^{\pi-\omega} \varphi(\alpha)\sin\alpha\, d\alpha\,. \tag{59}$$

The first assumption, for the minor elongations from the sun to which the observations refer, constitutes no great restriction. The second assumption is a hypothesis whose justification cannot be checked. The phase curves according to

$$\left.\begin{aligned} &\text{LAMBERT} && \varphi(\alpha) = \frac{\sin\alpha + (\pi-\alpha)\cos\alpha}{\pi}, \\ &\text{SEELIGER} && \varphi(\alpha) = 1 - \sin\frac{\alpha}{2}\tan\frac{\alpha}{2}\ln\cot\frac{\alpha}{4}, \\ &\text{EULER} && \varphi(\alpha) = \cos^2\frac{\alpha}{2}, \end{aligned}\right\} \tag{60}$$

are substituted into the last integral and, after simple integrations, furnish /160 the following formulas for the brightness which, after determination of the constants C, can be compared from observations with the latter

$$\left.\begin{aligned} J_1 &= \frac{3C_1}{4\sin^2\omega}\left(\pi - \omega + \sin\omega\cos\omega + \frac{2}{3}\omega\sin^2\omega\right), \\ J_2 &= \frac{C_1}{\sin^2\omega}\left[\frac{20}{9} + \frac{16}{9}\left(\cos^6\beta + \sin^6\beta\right) - 4\cos^2 2\beta\right. \\ &\quad + \left(16\cos^4\beta - \frac{32}{3}\cos^6\beta\right)\log\cos\beta + \left(16\sin^4\beta\right. \\ &\quad \left.\left. - \frac{32}{3}\sin^4\beta\right)\log\sin\beta\right], \end{aligned}\right\} \tag{61}$$

where

$$\beta = \frac{\pi-\omega}{4},$$

and

$$J_3 = \frac{C_1}{\sin^2\omega}\left(1 + \cos\omega + \frac{\sin^2\omega}{2}\right).$$

The accompanying table illustrates the course of brightness along the center line of the zodiacal light, in accordance with these three formulas, within the region observed by Fessenkov (Ref.170) with a focal-plane photometer.

ω	LAMBERT	SEELIGER	EULER	Observed
34°	27.5	27.5	27.5	27.5
38	22.2	21.8	22.1	23.8
42	19.1	18.4	19.0	20.6
46	16.5	15.6	16.4	17.9
50	14.6	13.4	14.3	15.6

67. Observations of Zodiacal Light Brightness

These observations, made by van Rhijn (Ref.171) on Mt. Wilson in his investigations of the brightness distribution over the night sky, constitute at present the most abundant and most accurate material for solving problems as to the nature, extent, and mass distribution of the zodiacal-light matter. His observations extended over the entire

sky and had the purpose of determining the contribution of scattered stellar light to the brightness of the sky. The observations led to the remarkable result that the zodiacal light constitutes as much as 43% of the total amount of light in the night sky. Consequently, the investigations of this essential component of brightness form a major part of van Rhijn's work. Based on Seeliger's hypothesis of a spheroidally bounded meteor cloud, extending beyond the earth's orbit and having its center in the sun, van Rhijn attempted to determine the oblateness and density distribution of the cloud in such a manner that the observed brightness would be obtained automatically. The gegenschein, which is fully distinct in van Rhijn's measurements as brightness increment at the antisolar point, thus is considered as belonging to the zodiacal light and, in agreement with Seeliger (Ref.172), attributed to the increase in brightness of meteors near opposition. The conventional reflection laws do not give such an increase in brightness at opposition, as would be necessary for explaining the gegenschein; however, the phase curves of the inferior planets, of the moon, and of any irregularly bounded body leave no doubt that a brightening at low and lowest phase angles must be expected also for the meteors. In making hypotheses on the slope of the phase curve and the density law, as emphasized already by Seeliger, it is of importance to recall that, in direction of the gegenschein ($\lambda = 180^\circ$, $\beta = 0^\circ$), the form of the density law has no influence on the brightness whereas the slope of the phase curve, for small α, has a substantial influence; conversely, for the elongations $\lambda \leq 90^\circ$, the density distribution in the meteor cloud is of major influence. /161

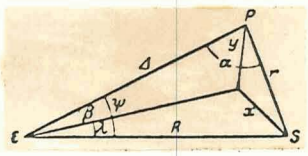

Fig.44 Relations between the Orthogonal Heliocentric (x, y) Coordinates of a Point P in the Zodiacal Light and the Geocentric Spherical Coordinates (β, λ) of this Light.

In this case, the formula for the brightness, on varying the density also with the height above this ecliptic (Fig.44), becomes

$$J = \gamma_1 \int_0^{\Delta_0} \frac{\mu(x, y)\,\varphi(\alpha)\,d\Delta}{r^2}. \tag{62}$$

Instead of eqs.(57), the following relations are now obtained from Fig.44:

$$\left.\begin{aligned} &r = R\frac{\sin\psi}{\sin\alpha}, \\ &\Delta = R\frac{\sin(\psi+\alpha)}{\sin\alpha} \quad \text{and} \quad d\Delta = -\frac{R\sin\psi}{\sin^2\alpha}\,d\alpha; \quad \frac{d\Delta}{r^2} = -\frac{d\alpha}{R\sin\psi}, \\ &y = \Delta\sin\beta = \frac{R\sin(\psi+\alpha)}{\sin\alpha}\sin\beta, \\ &x^2 = r^2 - y^2 = R^2\frac{\sin^2\psi - \sin^2\beta\sin^2(\psi+\alpha)}{\sin^2\alpha}, \quad \cos\psi = \cos\beta\cos\lambda, \end{aligned}\right\} \tag{63}$$

where β and λ denote the geocentric latitudes and longitudes of the point P.

Then, the brightness will be

$$J = \frac{\gamma_1}{R \sin \psi} \int_{\alpha_0}^{\pi - \psi} \mu(x, y)\, \varphi(\alpha)\, d\alpha . \tag{64}$$

The lower limit α_0 is the phase angle valid for the boundary of the cloud in the direction ψ.

A number of hypothetical calculations, with various formulas for the phase curve and various density laws, led van Rhijn, after successive corrections, to establish the form for $\varphi(\alpha)$ given in the accompanying table; up to $\alpha = 30^\circ$, this curve leads approximately to the formula $\varphi(\alpha) = \left(\frac{\pi - \alpha}{\pi}\right)^2$. The phase curve, obtained from the Seeliger law, is given for comparison.

α	Lommel-Seeliger	$\left(\frac{\pi - \alpha}{\pi}\right)^2$	$\varphi(\alpha)$ Assumed
0°	1.00	1.00	1.00
10	0.98	0.89	0.88
20	0.93	0.79	0.78
30	0.86	0.69	0.70
50	0.70	0.52	0.57
70	0.54	0.37	0.46
90	0.38	0.25	0.35
110	0.24	0.15	0.23
130	0.12	0.08	0.13
140	0.08	0.05	0.10

In the form of a Fourier series, the assumed phase curve will appear as follows (the formula is valid for $\alpha < 140^\circ$ but is adequate since no observations for larger phase angles are available):

$$\varphi(\alpha) = 0.655 - 0.711 \sin\alpha + 0.345 \cos\alpha + 0.406 \sin^2\alpha . \tag{65}$$

For the density distribution, van Rhijn assumed the following form: /162

$$\mu(x, y) = \mu_0 (1 - \lambda x^2 - \nu y^2), \tag{66}$$

which corresponds to the assumption that the areas of equal density are spheroids. The constants λ and ν must be determined from the observed brightness. This is then given by the equation

$$J = \frac{c}{\sin \psi} \int_{\alpha_0}^{\pi - \psi} (1 - \lambda x^2 - \nu y^2)(0.655 - 0.711 \sin\alpha + 0.345 \cos\alpha + 0.406 \sin^2\alpha)\, d\alpha , \tag{67}$$

where

$$c = \frac{\gamma_1 \mu_0}{R} = \frac{3 \mu_0 \gamma}{4 \pi \varrho^3 R} . \tag{68}$$

The lower boundary of the integral is given by the condition that the density becomes zero here, i.e., that

$$1 - \lambda x^2 - \nu y^2 = 0 ,$$

or, after substituting the values from eq.(63),

$$R^2 \sin^2 \alpha_0 - \lambda \sin^2 \psi - (\nu - \lambda) \sin^2 \beta \sin^2 (\psi + \alpha_0) = 0 .$$

Without going into details of a successive determination of the constants, we

will give here only their final values:

$$\lambda = 0.176$$
$$\nu = 1.406$$
$$c = 0.285 .$$

Thus, the equation of the generating ellipse of the spheroid will be

$$1 - 0.176 x^2 - 1.406 y^2 = \text{const} , \tag{69}$$

while the ratio of the major to the minor axis of this spheroid is $\sqrt{\frac{1.406}{0.176}} =$ $= 2.8$. These constants completely determine the averaged zodiacal light brightnesses, shown in the accompanying table and obtained from the totality of van Rhijn's observations, under consideration of Fessenkov's measurements.

Longitude from the Sun	Latitude					
	0°	10°	20°	30°	50°	70°
40°	0.32	0.26	0.19	0.13	0.07	0.05
50	0.25	0.21	0.16	0.11	0.07	0.05
60	0.18	0.17	0.14	0.11	0.07	0.05
70	0.15	0.14	0.12	0.10	0.07	0.05
80	0.13	0.12	0.10	0.09	0.06	0.05
90	0.11	0.10	0.09	0.08	0.06	0.05
110	0.09	0.08	0.08	0.07	0.06	0.05
130	0.08	0.08	0.07	0.07	0.06	0.05
150	0.08	0.08	0.07	0.07	0.06	0.05
170	0.09	0.08	0.07	0.07	0.06	0.05
180	0.10	0.09	0.08	0.07	0.06	0.05

The brightness unit in this table is that of a star of magnitude 1.0 of the Harvard magnitude scale, whose light is spread over an area of one square degree.

The value of the constants permits an approximate determination of the density of the meteor swarm.

In accordance with the meaning of eq.(1) on p.149, the constant γ represents the amount of light reflected by a meteor in the direction of illumination ($\varphi(0) = 1$), if sun and earth are at a distance 1. Consequently, if $L = J\pi \frac{S^2}{R^2}$ is the quantity of light incident on unit area at a distance R, with J being the surface brightness of the sun and S its radius, we obtain

$$\gamma = \frac{p}{\pi} L R^2 \pi \varrho^2 , \tag{69'}$$

if p represents the reflectivity (in the sense of albedo).

Substituting the value $\gamma = p J \pi S^2 \rho^2$ into eq.(68), it follows that /163

$$c = 0.285 = \frac{3}{4} p \mu_0 \frac{S^2}{R\varrho} J . \tag{70}$$

Introducing here the values $R = 149 \times 10^6$ km, S = 695,400 km, and $\rho = 0.0005$ km for the meteor radius and, in addition, using for J its value in the assumed unit calculated from the formula

$$J = \frac{\text{brightness of sun in units of a star of magnitude 1.0}}{\text{area of sun in square degrees}} = \frac{(2.512)^{27.7}}{0.224} = 54 \times 10^{10}$$

and, finally, using a value of p = 0.3 for the reflectivity of the meteors, then the following order of magnitude is obtained for the volume density μ_0 of the meteor swarm:

$$\mu_0 = 10^{-18}.$$

Thus, van Rhijn, under the assumption of Seeliger's theory, was able to represent his observations of the zodiacal light and furnish plausible values for the constants of the spheroid. A priori, the phase curve for the meteors, used as basis here, does not seem improbable. Nevertheless, in view of the large number of empirical constants introduced for representing the observations, the result cannot be considered a confirmation of Seeliger's theory; there is no doubt that the figures of the brightness table can just as well be interpreted by means of a different physical hypothesis, specifically if the slight brightness increase at the antisolar point, known as gegenschein, is considered as not belonging to the zodiacal light.

Of earlier authors who have made extensive studies on the theory of the zodiacal light, we should primarily mention A.Searle (Ref.173) who collected prior observations on the form and extent of the zodiacal light and whose theoretical considerations led to the same concept on the extent of the meteor cloud as that formulated by Seeliger and his followers. Among the latter, we should mention again K.Schwend (Ref.169) who, because of the lack of reliable brightness measurements, was unable to substantiate his theoretical conclusions, as was the case also for Searle.

68. Illumination of Cosmic Dust Formations by Stars

Seeliger (Ref.172) investigated the question whether cosmic dust formations, located in the neighborhood of stars, may appear as illuminated nebulous matter from earth so that one could assume that certain types of nebulae luminesce in reflected light. Because of the faintness of these objects and the difficulty of obtaining their spectrum independently of that of the neighboring stars, an experimental separation of self-luminous from illuminated nebulae is impossible at present; however, Seeliger's proof of the theoretical possibility that, under certain circumstances, illuminated cosmic dust clouds may enter the range of visibility, is at least of interest for future research.

Equation (55) refers to the case that both star and observer are within the cloud. Let us now investigate two other cases: 1) Star and observer are far outside the cloud so that its dimensions are small in comparison with these distances; 2) the star is located within the cloud and the observer far outside /164 it. In both cases, we assume uniform density of mass distribution. In the first case, $\varphi(\alpha)$ and the distance r can be assumed as constant for all parts of the cloud; the two cones V_1 and V_2 become cylinders and $V = V_1 + V_2 = \pi\rho^2(h_1 + h_2)$, where h_1 and h_2 are the lengths of the distances from the meteor to the earth

and sun within the cloud. Again denoting the volume density by $\mu = \frac{4}{3}\pi\rho^3 \frac{N}{Z}$ and, for abbreviation, introducing the notation

$$\frac{N}{Z}\pi\varrho^2 = \frac{3}{4}\frac{\mu}{\varrho} = \lambda, \tag{71}$$

eq.(55) becomes

$$J = \frac{\lambda}{\pi\varrho^2}\frac{\gamma\varphi(\alpha)}{r^2}\int_0^{\Delta_0} e^{-\lambda(h_1+h_2)}\,d\Delta = \frac{\gamma\varphi(\alpha)}{\pi\varrho^2}\frac{1}{r^2}\Phi(\lambda), \tag{72}$$

where

$$\Phi(\lambda) = \lambda\int_0^{\Delta_0} e^{-\lambda(h_1+h_2)}\,d\Delta. \tag{73}$$

Here, Δ_0 is the length of path covered by the earth-directed ray from the front to the rear boundary of the cloud.

Taking a dust layer, bounded by two parallel planes, and denoting the depth of the volume element below the frontal boundary by x and the thickness of the layer by X, we have

$$h_1 = \frac{x}{\cos i}, \qquad h_2 = \frac{x}{\cos\varepsilon}$$

and

$$\Phi(\lambda) = \lambda\int_0^{X} e^{-\lambda x\frac{\cos i+\cos\varepsilon}{\cos i\cos\varepsilon}}\frac{dx}{\cos\varepsilon} = \frac{\cos i}{\cos i+\cos\varepsilon}\left(1 - e^{-\lambda X\frac{\cos i+\cos\varepsilon}{\cos i\cos\varepsilon}}\right). \tag{74}$$

Furthermore, denoting the expression in parentheses by ψ, we have

$$J = \frac{\gamma}{\pi\varrho^2}\frac{\varphi(\alpha)}{r^2}\frac{\cos i}{\cos i+\cos\varepsilon}\psi.$$

This formula is valid only as long as $i < 90^\circ$. The maximum of brightness occurs at given i and e if $\psi = 1$ or if $\lambda = \infty$, i.e., $\rho = 0$. The greatest brightness is produced by a meteor cloud consisting of minute dust particles. For calculating a typical example, let us assume $\psi = 1$. Then,

$$J = \frac{\gamma}{\pi\varrho^2}\frac{\varphi(\alpha)}{r^2}\frac{\cos i}{\cos i+\cos\varepsilon}. \tag{75}$$

Substituting here the value of $\gamma = pLR^2\rho^2 = pJ_0\pi S^2\rho^2$ where S is the radius of the star and J_0 its surface brightness equated to that of the sun, we obtain

$$\frac{\gamma}{\pi\varrho^2} = pJ_0S^2 \qquad \text{and} \qquad J = \frac{pJ_0S^2}{r^2}\varphi(\alpha)\frac{\cos i}{\cos i+\cos\varepsilon}, \tag{76}$$

where S and r are expressed in units of the earth-sun distance. Assuming r = = 1000, i.e., about = 30 Neptune diameters, a value of 2.2×10^{-11} will be obtained for S^2/r^2. Substituting the above value $J_0 = 5.4 \times 10^{11}$ for J_0 and

taking into consideration that $\varphi(\alpha)\,\frac{\cos i}{\cos i + \cos \varepsilon}$ has a value of $\frac{1}{2}$ at $\alpha = 0$, /165 then

$$J_{max} = 6p,$$

where p denotes the reflectivity of the meteors which must be set at about $\frac{1}{3}$.

Let us imagine a dust cloud located at a distance of 30 Neptune diameters from a star of solar brightness. At a distance of the star corresponding to the parallax 0".01, this star would have the brightness of a star of magnitude 10.4 and would appear at a distance of 10" from the dust cloud. The cloud, however, would reach a surface brightness in the reflected light of the star that would by far exceed the brightness of the brightest spots of the zodiacal light (0.32).

Let us furthermore examine the case in which the star is located within the dust cloud while the observer is very far from it. In this case, we have $h_1 = r$ and both phase curve and distance r will become variable within the cloud, so that eq.(72) is replaced by

$$J = \frac{\lambda\gamma}{\pi\varrho^2}\int_0^X \frac{e^{-\lambda(h_2+r)}\varphi(\alpha)}{r^2}\,dx. \tag{77}$$

The further development depends on the form of $\varphi(\alpha)$.

On dropping a perpendicular s from the star onto the straight line drawn between the observer and the volume element under consideration, and denoting by m the distance of the foot of this perpendicular from the point of entry of the straight line into the dust cloud, we obtain

$$h_2 = m + s\cot\alpha, \qquad h_2 + r = m + s\cot\frac{\alpha}{2}, \qquad \frac{dx}{r^2} = -\frac{d\alpha}{s}$$

and

$$J = \frac{\lambda\gamma}{\pi\varrho^2}e^{-\lambda m}\int_0^X e^{-\lambda s\cot\frac{\alpha}{2}}\varphi(\alpha)\frac{dx}{r^2} = \frac{\lambda\gamma}{\pi\varrho^2}\frac{e^{-\lambda m}}{s}\int_{\alpha_1}^{\alpha_0} e^{-\lambda s\cot\frac{\alpha}{2}}\varphi(\alpha)\,d\alpha,$$

where α_0 and α_1 denote the values of α for the point of entry and point of emergence. Setting, in addition,

$$\nu = \lambda s, \qquad \psi_\nu(\alpha) = \nu\int_0^\alpha e^{-\nu\tan\frac{\alpha}{2}}\varphi(\pi-\alpha)\,d\alpha,$$

we will obtain, since $m = -s\cot\alpha_0$,

$$J = \frac{\gamma}{\pi\varrho^2 s^2}e^{\nu\cot\alpha_0}\{\psi_\nu(\pi-\alpha_1) - \psi_\nu(\pi-\alpha_0)\}. \tag{78}$$

For the function ψ_ν, Seeliger calculated a table on the basis of the Lambert law.

As before [eq.(76)], we substitute $\gamma/\pi\rho^2$ by $pJ_0S^2 = p\ 1.2 \times 10^7$. For the approximate values $\nu = 0.46$, $\alpha_1 = 0^\circ$, and $\alpha_0 = 130^\circ$, the calculation yields a value of 0.24 for $e^{\nu \cot \alpha_0} \{\psi_\nu(\pi - \alpha_1) - \psi_\nu(\pi - \alpha_0)\}$; accordingly, we have

$$J = \frac{0.29}{s^2} p\, 10^7.$$

If s = 1000 (earth's orbit radii), brightnesses will be obtained that exceed the greatest brightness of the zodiacal light and thus are measurable. This again corresponds to a distance of 10″ at a parallax of 0″.01. At greater proximity, the brightness increases with the square of the distance. In this case, one calculates with the brightness of a star of the magnitude and luminous intensity of the sun, appearing - at the mentioned distance - as having a magnitude 10.4. In absolutely brighter stars, the conditions for cosmic dust clouds to become visible are even more favorable. Consequently, it can be assumed as highly probable that cosmic dust, in the neighborhood of luminous masses, may appear as faint nebulous matter over considerable distances. If the individual dust particles are extremely small, being of the order of the wavelength of light, predominantly the short-wave rays of the incident light will be reflected, so that such a dust cloud will be even more distinct on a photograph than for the eye. /166

E.Hertzsprung (Ref.174), from measurements of the surface brightness of the Pleiades nebulae, attempted to obtain a criterion for their reflectivity and their mass. In his calculation, this author assumed that the central star over which the area of the nebula is spread would yield the same surface brightness as that produced at an albedo 1. Extrafocal stellar disks were used as comparison and their diameter and surface brightnesses were compared with those of the nebulae. In this case, two points were disregarded: first, the transparency of the nebulae through which the central stars shine and secondly the fact that the nebulae transmit only a portion of the received light in direction to the observer. A stricter photometric analysis of this phenomenon is entirely possible and would seem useful.

69. Brightness of Comets

The results of brightness determinations of comets have been of little use in obtaining data on the nature of these celestial bodies. Only recently had considerable progress been made by application of focal-plane photometric methods; further advance can be hoped from subjecting the excellent modern photographs to a photometric analysis. This will be demonstrated at the end of this Chapter, in discussing the first experiments by K.Schwarzschild on Halley's Comet.

The old methods of estimating the brightness of a comet either referred to the total brightness of the comet as it appears to the naked eye or in a low-power telescope or else to the brightness of the nucleus as a quasi-stellar formation, if the latter was discernible at all in the telescope.

The total brightness of a comet should obey the formula valid for the

planets $\frac{1}{r^2\Delta^2}$ where r is the distance from the sun and Δ that from the earth, provided that two prerequisites are met: The luminous mass of the comet would have to remain constant over its entire period of visibility and the comet would have to luminesce only in reflected sunlight.

As is known, none of these two conditions are satisfied since the comets, on approach to the sun, increase in extent and liberate gases which originally had been bound to the solid nucleus; in addition, spectral analysis shows that the comet not only emits the reflected sunlight but also its own light which again is not constant but depends on the distance from the sun and may extend far into the comet tail.

Despite this fact, it is conventional to use the above formula for a precalculation of the brightness development of a given comet from its brightness at discovery, since deviations from this formula which always take place in the sense of a greater brightness near the sun vary individually for each comet and may even differ for the various forms of one and the same comet; another reason for retention of this formula is the fact that no other physically substantiated formula exists as replacement. /167

Holetschek (Ref.175) who, in his highly valuable work on the brightness of comets, compiled and critically evaluated the historical data on the brightness of comets from antiquity to modern times, introduced as specific characteristic of the individual comets their brightness M_1 at a distance 1 from the earth and from the sun; for derivation, he also used the above quadratic formula. For other assumptions as to the origin of the cometary light, other reduction formulas for the total brightness would be in question.

If the comet would radiate only his proper light of constant intensity, its brightness would have to vary inversely proportional to the square of the earth distance Δ. Thus, in earlier times when the concepts as to the nature of comets were still controversial, this formula could be defended and applied.

Conversely, the surface brightness of the comet envelope most likely is independent of the earth distance and, for the case of reflected sunlight, will vary inversely proportional to the square of the solar distance r^2 or, for the case of self-luminance, be independent of this distance.

So far as the nucleus of the comet is concerned, it would have to follow the same laws as the total brightness.

Of the various attempts at defining the nature of the cometary light by photometric means, we will mention here only that made by Schmidt in Athens on the comet Coggia. Schmidt observed the brightness of the nucleus itself through a refractor with two different eyepieces, one strong and one weak type, and examined the total brightness of the head with the unaided eye. His measurements, in addition to the magnitude classes, calculated according to two formulas are compiled in the accompanying table.

This example is instructive in various respects. First, it shows the

Date 1874	Magnitude Estimates: With High Power Eyepiece Nucleus	With Low-Power Eyepiece Nucleus	With the Naked Eye, Total Brightness	Calculated Brightness: $\frac{1}{0.4}\log\frac{1}{r^n\Delta^2}+\text{const.}$	$\frac{1}{0.4}\log\frac{1}{r^2}+\text{const.}$
June 1	10m.0	8m.0	6m.5	10m.0	10m.0
11	10 .0	8 .0	5 .2	9 .3	9 .7
17	9 .0	7 .5	4 .6	8 .9	9 .5
18	9 .0	7 .7	4 .5	8 .8	9 .5
20	8 .0	7 .0	4 .5	8 .7	9 .4
22	8 .5	7 .2	4 .2	8 .5	9 .4
24	8 .0	6 .8	4 .0	8 .4	9 .3
27	9 .0	7 .0	4 .0	8 .1	9 .3
30	8 .5	7 .2	3 .5	7 .8	9 .2
July 2	7 .5	6 .7	3 .2	7 .7	9 .2
4	7 .5	6 .0	3 .0	7. 5	9 .2
6	7 .5	6 .7	2 .9	7 .3	9 .2
8	7 .0	6 .0	2 .5	7 .1	9 .1
10	7 .5	5 .5	1 .9	6 .9	9 .1
12	7 .0	5 .0	1 .5	6 .7	9 .2
13	6 .5	4 .7	1 .5	6 .6	9 .2

considerable deviation of the various brightness data, even for such a highly skilled observer as Schmidt; the influence of the eyepiece, in estimating the /168 brightness of the nucleus, is considerable - possibly because of the extent of the nucleus. Therefore, such estimates must emphasize the starlike consistency of the nucleus to prevent these estimates from becoming utterly useless. A comparison with the calculated brightnesses also shows that the formula $1/r^2$ does not even faintly agree with the observations, whereas the first formula more or less coincides with actual observations of the nucleus which would indicate that reflected sunlight is in question for this nucleus. Conversely, for the total light of the comet the formula valid for planets fails completely, since the light increment proceeds much more rapidly.

Naturally, it is possible to represent the observations of the total brightness of a comet by this formula in first approximation, on introducing an unknown power r^n; such attempts have been made repeatedly. The power of r thus becomes a criterion for the enlargement of the reflecting or self-luminous mass of the comet on its approach to the sun, so to say for the "evolution" of the comet. Together with the brightness M_1 at unit distance, this can be used as characteristic for individual comets and, in the case of periodic comets, can be compared from one apparition to the other. However, for the older apparitions, data for determining n were usually lacking. The detailed investigation by Holetschek, mentioned above, thus led only to a determination of M_1 for the older comet apparitions. Nevertheless, these results are highly valuable, specifically for periodic comets. In his second paper on this subject matter, Holetschek compiled the results for periodic comets as follows: Among the periodic comets, observed during at least two apparitions, only apparently constant or decreasing types exist; no increase in degree of brightness from one apparition to a later was detected in any of the comets. The older comets seem to be more permanent than the newer ones, but even they already carry the seed of decay. Just to mention the most important of the investigated comets, we should recall here that Halley's Comet showed no distinct change in brightness of the head nor in development of the tail. The same is true for the comets Pons-Brooks, Olbers, Tuttle, Finlay, and Winnecke. Faye's Comet seemed to decrease in brightness, although at an irregular rate. Encke's Comet, in the 33 appari-

tions observed to date, showed no distinct decrement.

Other authors drew somewhat more extensive conclusions from Holetschek's material and from more recent data. For example, Berberich (Ref.176) believed that the brightness of Encke's Comet had to do mainly with sunspot activity, since this comet in its various apparitions became brighter the greater the relative number of sunspots. This relation was confirmed later by Bosler (Ref.177).

S.V.Orlov (Ref.178) applied the formula $\frac{M_1}{\Delta^2 r^n}$, with the exponent n as characteristic of the evolution, to four comets and found a value of about 3.5 for n. Later, Kritzinger (Ref.179) made an attempt, based on the material by Holetschek and Orlov, to derive a correlation between the exponent n and the instant of formation of the tail. Finally, S.Vsechsviatsky (Ref.180) processed the brightness data of about 70 comets, for determining the exponent n. He found, as the mean for the strongly fluctuating values, a result of 4. For comets that had been observed over long periods of time, such as the comets 1914 V, 1905 I, 1912 II, 1899 I, the variability of n with the solar distance was investigated, showing throughout a decrease in n with approach to the sun. /169

Whereas Holetschek obtained his absolute values of the comet brightness M_1 (as mentioned before) by means of the quadratic formula, Vsechsviatsky calculated these brightnesses with the new formula $\frac{M_1}{\Delta^2 r^4}$ which he considered more reliable; by grouping the brightnesses M_1 according to the size of the semiaxis of the orbit and according to the inclination to the ecliptic, he confirmed the correlations that would have to be expected according to modern concepts on the nature of comets: The comets become absolutely weaker the more narrow their orbits and the greater the probability of their approach to a planet, meaning that, in the course of time, they lose their matter due to closeness of the sun and to perturbations by the planets.

This exhausts the main results of a rough photometry referring to the total brightness of the comets or of the nuclei; these results did not fulfill the hopes that they would permit a decision as to the nature of cometary light. This was made possible only by spectral analysis, which demonstrated that reflected sunlight as well as intrinsic luminescence are responsible for the brightness of a given comet.

Further progress in this respect can be expected with the use of microphotometers in the work-up of modern photographs.

70. Schwarzschild's Theory on the Brightness of Halley's Comet

In how far a skilled application of photometric analysis to brightness measurements may lead to important conclusions as to the nature of the comets will be demonstrated on the work done by Schwarzschild and Kron (Ref.181) who investigated the brightness distribution in the tail of Halley's Comet. On photographs of this comet, made with lenses of short focal length during an

expedition to Teneriffa, the brightness was photometrically rated and integrated in sections perpendicular to the apparent tail axis. This quantity J will be furthermore denoted as "cross-sectional brightness". This constitutes a criterion for the luminous mass of the tail which flows through cross sections perpendicular to the real tail axis. To demonstrate this, we must note the following: The various parts of the tail are located at unequal distances Δ' from the earth (ϵ), and the cross sections to the apparent axis make different angles ψ' with the real axis of the tail CC'. The variation in the distance Δ' causes no variation in surface brightness, while the linear extent of the cross section varies inversely proportional to Δ'. Consequently, the brightnesses J must be multiplied by Δ' to reduce them to equal distance. In addition, the area of the cross section is enlarged at a ratio $1/\sin\psi'$ (see Fig.45) with respect to the area of a section perpendicular to the real tail axis, if the tail is assumed as cylindrical over a short segment. Thus, the cross-sectional brightnesses must be reduced by a factor $\Delta' \sin\psi'$. A prerequisite here is that no occultation of the particles takes place and that they all contribute to the brightness, an assumption which is entirely legitimate in view of the extreme tenuity of the matter of the tail. /170

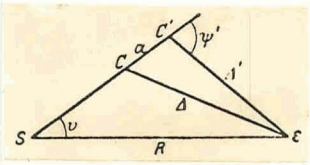

Fig.45
S Sun, ε earth, CC' axis of comet tail.

However, as shown in Fig.45, we have

$$\Delta' \sin\psi' = R \sin v = C,$$

where C is a constant for the same photograph; thus, the two reductions cancel out.

Since direct measurements of the velocity V of the tail matter of Halley's Comet had been made by Curtis, who derived them from the motion of compressed matter, Schwarzschild was able to make a direct check on the assumption that, for all cross sections of the tail,

$$JV = \text{const}, \tag{79}$$

and found a more or less complete confirmation. This led to the important conclusion that the luminous intensity of the tail sections of the comet is independent of the distance from the head. Consequently, this luminescence cannot be excited by processes taking place in the head of the comet since it would then decrease; rather, this luminescence is excited permanently and simultaneously in all parts of the tail, to which the reflected light must be added.

Considering the luminescence of the tail matter as resonance or reflection of solar radiation, the density of the matter can be defined from the surface brightness of the tail. Assuming that this matter consists of spherical particles of radius ρ, uniformly reflecting the sunlight toward all sides without absorption, and furthermore denoting their number per unit surface, seen from the earth, by n and denoting the radius of the sun by S, then the incident quantity of light will be $n\pi\rho^2 I\pi \frac{S^2}{r^2}$ where I is the surface brightness of the

sun. The quantity of light*, reflected from the tail matter in a definite direction, will be $n\pi\rho^2 I \frac{S^2}{2r^2}$, while the surface brightness of this matter, in units of solar brightness, will be

$$i = n\pi\varrho^2 \frac{S^2}{2r^2}.$$

If q represents the coordinate perpendicular to the radius vector and to the line of sight, then the cross-sectional intensity will be

$$J = \int i\,dq = \pi\varrho^2 \frac{S^2}{2r^2} \int n\,dq. \tag{80}$$

Let the real tail particles have a radius ρ_0 and a specific weight s; then the above formula will be valid for these particles, provided that ρ means a certain "effective" radius in which ρ^2/ρ_0^2 represents a sort of albedo. The total mass of the comet tail, projected onto unit surface, will then become

$$\frac{4}{3}\pi\varrho_0^3 s n = \frac{8}{3}\varrho_0\left(\frac{\varrho_0}{\varrho}\right)^2 s\frac{ir^2}{S^2}.$$

Imagining the tail compressed along the line of sight in such a manner that it assumes everywhere the maximum density of its central portion and denoting the resultant diameter in direction of the line of sight by p, then this maximum density becomes equal to

$$\delta = \frac{4}{3}\frac{\pi\varrho_0^3 s n}{p} = \frac{8}{3}\frac{\varrho_0}{p}\left(\frac{\varrho_0}{\varrho}\right)^2 s\frac{ir^2}{S^2}. \tag{81}$$

The total mass, passing through the cross section of the tail in unit time, /171
also known as the "yield" of the comet, denoting by V the velocity of the stream, will read

$$E = \frac{4\pi}{3}\varrho_0^3 V s \int n\,dq = \frac{8}{3}\varrho_0\left(\frac{\varrho_0}{\varrho}\right)^2 s V\frac{Jr^2}{S^2}. \tag{82}$$

When using eq.(80) for $\int$ ndq, the quantity J will mean the cross-sectional brightness multiplied by sin ψ which thus is referred to the cross section perpendicular to the comet axis.

Consequently, this equation, under a hypothesis for ρ_0 and $\frac{\rho}{\rho_0}$, permits calculating the yield of the comet if, as had been the case for Halley's Comet,

---

* In the denominator, the numeral 2 can be replaced by 4 in accordance with the conventional definition of the reflection coefficient of a uniformly scattering sphere (see note in Sect.29, p.62).

the stream velocity V is known. In addition, eq.(81) yields the maximum density if p is calculated from the measured width of the cross section and from the brightness distribution within this section. The brightness i, in units of solar surface brightness, must be determined from the photographic plates, for example, from extrafocal photographs of stars. Here, it is assumed that the tail has a cylindrical form which, over short segments, almost corresponds to reality.

Schwarzschild made two assumptions on the size of the particles ρ_o and calculated E and δ for these.

1) According to Arrhenius' theory on cometary tails, which attributes the motion of the tail matter to light pressure, it is necessary to assume $\rho_o = 10^{-4}$ cm at a specific weight of s = 1, so as to obtain the necessary compressive forces. In that case, we can also assume $\rho_o = \rho$. Of course, when assuming that the cometary light is reflected sunlight, the brightness of the band spectrum must be eliminated from the calculation.

2) The particles can be considered as fluorescent molecules whose radius would then be of the order of 10^{-8} cm. If the effective radius of such a molecule is assumed as having the same order of magnitude as the real radius $\rho_o = \rho$ and setting the molecular weight at s = 20, the values for E and δ of Halley's Comet listed under the hypothesis II will be obtained:

Hypothesis I	Hypothesis II
$E = 1500$ kg/sec	$E = 150$ gm/sec
$\delta = 2 \times 10^{-21}$	$\delta = 4 \times 10^{-24}$

At a density of 10^{-22} and a relative velocity of 100 km with respect to the streaming matter of the tail, the earth, on passage through the tail, would trap 10^{-10} gm per cm^2 during the course of one day, meaning that the total earth's surface would collect 250,000 kg in the same time. This gives an idea on the extreme tenuity of cometary tails.

VII. EXTINCTION OF LIGHT IN THE EARTH'S ATMOSPHERE

71. Function of the Extinction Theory

Under extinction of light, we mean the attenuation of light on passage through a medium, independent on whether this attenuation is due to scattering of the light within the medium or to absorption. The elementary law of attenuation can be assumed as identical for both processes, so that a theory of light extinction in the earth's atmosphere, whose task it is to calculate the intensity of the transmitted rays, can disregard the question as to the fate of the lost light.

The enormous significance of extinction for astrophysical research is /172
obvious, since the entire picture of the sky is quantitatively as well as qualitatively influenced by the fact that the sky must be observed through the turbid

medium of the atmosphere without any possibility of ever lifting this veil. The decrease in luminous intensity of the stars close to the horizon is several classes of magnitude; also qualitatively, the radiation of stars is considerably changed since the blue rays are absorbed most near the horizon.

Consequently, the theory of extinction is one of the fundamental aspects of astrophysics and has been treated repeatedly by eminent researchers. However, a complete solution of the problem encounters two insurmountable difficulties: One of these is of a theoretical nature and is due to our incomplete knowledge on the density and composition of the upper layers of the atmosphere; this difficulty interferes equally with all theories of astronomic refraction. The other difficulty in taking account of the extinction is the extremely rapid fluctuation in the lower layers of the earth's atmosphere, especially the varying component of water vapor which can be observed only at the surface of the earth. Naturally, a unified theory cannot possibly cover all these varying influences and must establish a certain average state of the air at clear sky. For this average state, the theory will have to furnish an answer to two different questions:

1) The mean free path of the light and thus its attenuation in the atmosphere are dependent on the zenith distance of the star and on the height at which the observer is stationed. It is here a question of finding the law according to which the luminous intensity of a given star varies as a function of its zenith distance, for various heights of the observer above sea level. A reduction of all photometric measurements to the brightness in the zenith at a certain elevation above sea level is a prime requisite for a useful comparison of measurements obtained at different times and different sites; consequently, an answer to the first question will result in tables of reduction to the zenith.

2) The brightnesses, reduced in this manner, are then still influenced by the attenuation of light on vertical passage through the atmosphere. This attenuation can be considered as identical for various geographic latitudes at equal elevation above sea level. The amount of this attenuation must be determined for calculating the brightnesses of stars outside the atmosphere.

Already the founders of photometry, Lambert (Ref.46, p.64) and Bouguer (Ref.5, p.315), created theories of extinction and made observations for checking on this theory. Both assumed the path of the ray in the atmosphere as rectilinear. The theories of Laplace and of more recent authors who allowed for the curvature of the ray due to diffraction are much more precise. However, Bouguer's extinction tables differ very little from the most recent types; therefore, the Bouguer theory will be discussed in some detail.

72. Principles of the Theory and Lambert's Interpolation Formula

The loss of light in a given medium over the elementary path ds, as in all theories of absorption, is assumed as proportional to the original intensity J /173 of the ray, the density of the medium ρ, and the mean free path:

$$dJ = -k\varrho J\,ds,$$

where k is a constant factor dependent on the nature of the medium. After integration over a layer of equal density, bounded by parallel planes, from s = 0 to s = s, we then obtain

$$\ln \frac{J_z}{J} = -k\varrho s, \qquad J_z = Je^{-k\varrho s}, \tag{1}$$

where J is the intensity outside of the layer, while J_z is the intensity at the end point of the layer at an inclination z to the normal. Denoting $e^{-k\rho}$ by a new constant p, the following equation is obtained:

$$J_z = Jp^s, \tag{2}$$

where p is the transmittance or transmission coefficient of the layer. If the density of the medium is not constant and varies over the path s, then eq.(1) will be replaced by

$$\ln J_z - \ln J = -k\int \varrho\, ds$$

or

$$J_z = Je^{-k\int \varrho\, ds}, \tag{3}$$

where the integral must be extended over the entire path of the light ray and where J denotes the intensity of the ray at the upper limit of the layer. A calculation of the integral in the exponent for the light path in the atmosphere at different zenith distances of a given star constitutes the main task of the extinction theory. This integral is an expression of the air mass penetrated by the ray.

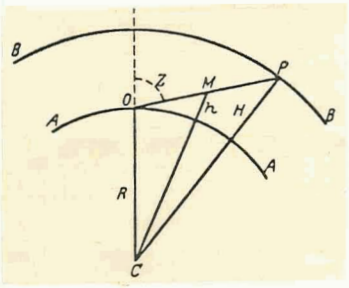

Fig.46 Rectilinear Light Path in the Atmosphere of the Earth.
AA earth's surface, BB limit of the atmosphere.

Because of refraction, the path s of the light ray is not rectilinear but curved, with this curvature being considerable in the lowest layers of the atmosphere. The curvature depends on the density ρ; this indicates the intimate connection of the extinction problem with that of refraction.

Lambert neglected the curvature of the light path in deriving his interpolation formula; therefore, his air masses or mean free paths are all too small and his extinction values must lag behind the true values; however, this becomes noticeable only at zenith distances above 80°.

In Fig.46, BB represents the limit of the atmosphere, AA the earth's surface, and PO a light ray incident under the zenith distance z. Let H be the height of the atmosphere and M a point on the ray path at a height h above the earth's surface. This will yield an expression for the mean free path OM = s, from the triangle MOC:

$$(R+h)^2 = R^2 + s^2 + 2Rs\cos z,$$

where only the positive sign is in question. Let us replace the variable height h of the point M by a new variable y, over the equation $y^2 = h^2 + 2Rh$, from which we obtain

$$s = -R\cos z + \sqrt{y^2 + R^2\cos^2 z}.$$

By differentiation, this yields /174

$$ds = \frac{y\,dy}{\sqrt{y^2 + R^2\cos^2 z}}.$$

Substituting this into eq.(3), it follows that

$$\ln\frac{J_z}{J} = k\int_S^0 \varrho\,ds = k\int_S^0 \varrho\,\frac{y\,dy}{\sqrt{y^2 + R^2\cos^2 z}},$$

where S denotes the entire length of the path OP; substituting here the limiting values of the new variables (at s = S, we have h = 0 and y = 0; at s = 0, we have $y = \sqrt{H^2 + 2RH} = Y$), we obtain

$$\ln\frac{J_z}{J} = k\int_0^Y \varrho\,\frac{y\,dy}{\sqrt{y^2 + R^2\cos^2 z}}. \tag{4}$$

Now,

$$(y^2 + R^2\cos^2 z)^{-\frac{1}{2}} = \sec z\,(R^2 + y^2\sec^2 z)^{-\frac{1}{2}} = \sec z\,(R^2 + y^2 + y^2\tan^2 z)^{-\frac{1}{2}},$$

and, on expanding this in a series in powers of y tan z, we have

$$\begin{aligned}(y^2 + R^2\cos^2 z)^{-\frac{1}{2}} = [&(R^2 + y^2)^{-\frac{1}{2}} - \tfrac{1}{2}(R^2 + y^2)^{-\frac{3}{2}}y^2\tan^2 z \\ &+ \tfrac{1}{2}\cdot\tfrac{3}{4}(R^2 + y^2)^{-\frac{5}{2}}y^4\tan^4 z + \cdots]\sec z,\end{aligned}$$

so that eq.(4) will yield the following series for the extinction

$$\ln J_z - \ln J = A\sec z - \tfrac{1}{2}B\sec z\tan^2 z + \tfrac{1}{2}\cdot\tfrac{3}{4}C\sec z\tan^4 z - \cdots, \tag{5}$$

where the coefficients A, B, C, ... have the values

$$A = k\int_0^Y \frac{\varrho\,y\,dy}{\sqrt{R^2 + y^2}},$$

$$B = k\int_0^Y \frac{\varrho\,y^3\,dy}{(R^2 + y^2)^{\frac{3}{2}}},$$

$$C = k\int_0^Y \frac{\varrho\,y^5\,dy}{(R^2 + y^2)^{\frac{5}{2}}}.$$

.....

These coefficients contain the law of density diminution in the atmosphere with the height h, while they are independent of the zenith distance. Lambert empirically determined A, B, C, ... from equations that can be obtained from eq.(5) in the following manner: On setting z = 0 in eq.(5), the attenuation of a vertically incident light ray will be

$$\ln \frac{J_0}{J} = A. \tag{6}$$

Subtracting eq.(5) from eq.(6), we obtain

$$\ln J_0 - \ln J_z = A(1 - \sec z) + \frac{1}{2} B \sec z \tan^2 z - \frac{1,3}{2,4} C \sec z \tan^4 z + \cdots, \tag{7}$$

which is an equation suitable for determining the coefficients A, B, C, ... from a series of observed zenith reductions. It is found that this formula, within /175 a large interval of zenith distances, satisfactorily fits the actual observations. On applying this formula to an observation series of several years, Müller found the following values for the coefficients:

$$A. \text{ Mod.} = -0.080441; \qquad B. \text{ Mod.} = -0.0000911.$$

From this, a transmission coefficient of the entire atmosphere of $\frac{J}{J_0} = 0.83$ is obtained for a vertical ray, meaning that a star at the zenith will lose 17% of its brightness due to extinction.

73. The Homogeneous Reduced Atmosphere

In eq.(3)

$$J_z = Je^{-k\int \varrho ds}$$

let us replace J which is the intensity of the ray outside of the atmosphere by the apparent intensity J_0 at the zenith, by making a suitable rearrangement; this has the advantage of being a directly observable or at least readily derivable quantity. Since the rays penetrating vertically through the atmosphere undergo no deflection, $\int \rho ds$ in the exponent is replaced by $\int_0^H \rho dh$ which is the integral of intensity of the air column perpendicular to the surface or the air mass m for unit cross section. If we set $m = \rho_0 \lambda$ where ρ_0 denotes the density of the air at the point of observation, then

$$\lambda = \int_0^H \frac{\varrho}{\varrho_0} dh \tag{8}$$

has the dimension of length and closely agrees with the so-called height of the homogeneous reduced atmosphere. This expression is to mean an atmosphere having the same density ρ_0 at all points as the real atmosphere at the point of observa-

tion and exerting the same pressure B_0. Obviously, the height of such an atmosphere is $l_0 = \frac{B_0}{g_0 \rho_0}$ since any variation in gravity can be neglected within the 8 km in question here. Using the mean values B_0, ρ_0, g_0 at a latitude of 45°, we obtain

$$l_0 = 7.990 \text{ km.}$$

Neglecting the temperature decrease with height, as is done in Bouguer's and Laplace's theories and assuming the simple Mariotte law as valid for the entire atmosphere, so that $B:B_0 = \rho:\rho_0$, we will obtain [as proved in eq.(23')]

$$\int \frac{\varrho}{\varrho_0} dh = \int \frac{B}{B_0} dh = l_0, \quad \text{i.e.,} \quad \lambda = l_0. \tag{9}$$

Thus, this assumption of the two theories, in calculating the quantity λ, corresponds to replacing the real atmosphere by an ideal atmosphere which does not have the same mass as the real atmosphere but only exerts the same pressure. If, in agreement with Bemporad, the temperature decrease is allowed for, a slightly larger value will be obtained for λ, namely $\lambda = 8.007$ km. Thus, the simple Mariotte law furnishes a satisfactory approximation for the mass of the total atmosphere.

On introducing the quantity λ, eq.(3) will have the form

$$J_0 = Je^{-k\lambda\varrho_0}. \tag{10}$$

On dividing eq.(3) by eq.(10), we obtain

$$J_z = J_0 e^{-k\int \varrho ds + k\lambda\varrho_0} = J_0 e^{-k\lambda\varrho_0\left[\frac{1}{\lambda}\int \frac{\varrho}{\varrho_0} ds - 1\right]} = J_0 p^{F(z)-1}, \tag{11}$$

where $p = e^{-k\lambda\rho_0}$ denotes the transmission coefficient of the total atmosphere /176 and where the function $F(z)$

$$F(z) = \frac{1}{\lambda}\int \frac{\varrho}{\varrho_0} ds \tag{12}$$

is designated as the mean free path of the light rays in the homogeneous reduced atmosphere. Obviously, a more correct definition for the function $F(z)$ is that in which it represents the air mass penetrated by the light rays if the air mass at the zenith is set equal to 1.

74. Determination of F(z) from the Refraction Curve

In the expression [eq.(12)] for $F(z)$, the term ds obviously represents an element of the refraction curve which is easy to derive from the fundamental formulas of the refraction theory. Denoting by i the angle of incidence of the

ray for an arbitrary concentric-spherical layer of the atmosphere with the refractive index μ and also denoting the corresponding values for the earth's surface by z and μ_0, it follows that

$$ds = \frac{dr}{\cos i} \tag{13}$$

and

$$r\mu \sin i = R\mu_0 \sin z. \tag{14}$$

Here, r = R + h is the radius of the layer in question. From the last equations, we obtain

$$ds = \frac{dr}{\sqrt{1 - \left(\frac{R\mu_0}{r\mu}\right)^2 \sin^2 z}}. \tag{15}$$

Substituting this expression into eq.(12), we have

$$F(z) = \frac{1}{\lambda} \int_R^{R+H} \frac{x\,dr}{\sqrt{1 - \left(\frac{R\mu_0}{r\mu}\right)^2 \sin^2 z}}, \tag{16}$$

where we also set

$$\frac{\varrho}{\varrho_0} = x \tag{17}$$

which denotes the relative density of the air with respect to the density at the point of observation; H is the height of the total atmosphere.

75. Bouguer's Extinction Theory

Just as Lambert, Bouguer (Ref.5) also assumed the path of the light ray in the atmosphere as rectilinear and thus neglects the phenomenon of refraction. This corresponds to the condition $\mu_0 = \mu$ so that, after introduction of r = R + + h and $\sin^2 z = 1 - \cos^2 z$, the following expression for F(z) is obtained:

$$F(z) = \frac{1}{\lambda} \int_0^H \frac{(R+h)\,x\,dh}{\sqrt{R^2\cos^2 z + 2Rh + h^2}},$$

$$F(z) = \frac{1}{R\cos z\,\lambda} \int_0^H (R+h)\,x \left(1 + \frac{2Rh + h^2}{R^2\cos^2 z}\right)^{-\frac{1}{2}} dh. \tag{18}$$

The condition for convergence of the binomial expansion of the radical in powers of h then is

$$\frac{2Rh + h^2}{R^2\cos^2 z} \leqq 1.$$

Let us designate the limiting value of h which just about satisfies this /177

condition or else the positive root of the equation

$$\chi^2 + 2R\chi - R^2\cos^2 z = 0 \tag{19}$$

by χ and let us resolve F(z) into the summands

$$F(z) = \frac{1}{\lambda}\left(\int_0^{\chi} + \int_{\chi}^{H}\right) = F_0(z) + F_1(z).$$

Then, the first integral is found by a series progressing in powers of h:

$$F_0(z) = \frac{1}{\lambda}\left\{\sec z \int_0^{\chi} x\,dh - \frac{\sec z \tan^2 z}{R}\int_0^{\chi} x h\,dh + \frac{3}{2}\frac{\sec^3 z \tan^2 z}{R^2}\int_0^{\chi} x h^2\,dh + \cdots\right\}. \tag{20}$$

The first term of the series, according to eq.(17), is practically nothing else but sec z; however, the other terms, just as in the Lambert series (5), require a hypothesis as to the dependence of the density x on the altitude. Whereas, however, Lambert empirically derived the coefficients of his series, Bouguer made a certain hypothesis as to that correlation, introducing the simple Mariotte law

$$\frac{B}{B_0} = \frac{\varrho}{\varrho_0} = x, \tag{21}$$

which is equivalent to neglecting the temperature decrease with altitude.

In addition, Bouguer also neglected the decrease in gravity with altitude, so that the differential equation of equilibrium of the atmosphere had the form

$$dB = -g_0\,\varrho\,dh = -g_0\,\varrho_0\,x\,dh. \tag{22}$$

From the two last equations, it then follows that

$$dx = \frac{dB}{B_0} = -\frac{g_0\varrho_0 x}{B_0}dh = -\frac{x}{l_0}dh \qquad \text{and} \qquad x = e^{-\frac{h}{l_0}}, \tag{23}$$

while an integration to the limit of the atmosphere will yield the above-mentioned relation

$$\int_0^H x\,dh = \lambda = -\int_{\varrho_0}^{0} l_0\,dx = l_0. \tag{23'}$$

This gives the relation between x and h for calculating the integrals in eq.(20). Taking also into consideration that $l_0 = \lambda$, we obtain

$$F_0(z) = \frac{1}{l_0}\left\{\sec z \int_0^{\chi} e^{-\frac{h}{l_0}}\,dh - \frac{\sec z \tan^2 z}{R}\int_0^{\chi} h e^{-\frac{h}{l_0}}\,dh + \frac{3}{2}\frac{\sec^3 z \tan^2 z}{R^2}\int_0^{\chi} h^2 e^{-\frac{h}{l_0}}\,dh - \cdots\right\}$$

while a successive integration will yield

$$F_0(z) = J_0 \sec z - \frac{J_1}{R} \sec z \tan^2 z + \frac{3}{2} \frac{J_2}{R^2} \sec^3 z \tan^2 z - \cdots , \tag{24}$$

where

$$J_0 = 1 - e^{-\frac{\chi}{l_0}}$$

$$J_1 = l_0 J_0 - \chi e^{-\frac{\chi}{l_0}}$$

$$J_2 = 2 l_0 J_1 - \chi^2 e^{-\frac{\chi}{l_0}}$$

$$\cdots\cdots\cdots\cdots$$

$$J_n = n l_0 J_{n-1} - \chi^n e^{-\frac{\chi}{l_0}} = \frac{\chi^{n+1}}{(n+1) l_0} e^{-\frac{\chi}{l_0}} \left\{ 1 + \frac{1}{n+2} \frac{\chi}{l_0} + \frac{1}{(n+2)(n+3)} \frac{\chi^2}{l_0^2} + \cdots \right\}.$$

This series was derived by Bemporad (Ref.182) at the occasion of a discussion of Bouguer's theory. This series is valid up to the limiting value χ which must be derived as a positive root of eq.(19) for a given z. If χ then results as the presumable limit of the atmosphere, the second term $F_1(z) = \int_{\chi}^{H} dF$ must be calculated in a different manner, for which Bemporad indicated a means. For $z = 82^\circ$, the value is $\chi = 64$ km which is sufficiently large for the height of the atmosphere at constant temperature. Therefore, $F_1(z)$ can be neglected up to this limit and all terms in the coefficients J dependent on χ can be eliminated; this yields the following expression for the mean free path corresponding to Bouguer's assumptions: /178

$$F(z) = \sec z - \frac{l_0}{R} \sec z \tan^2 z + \frac{3 l_0^2}{R^2} \sec^3 z \tan^2 z - \cdots . \tag{25}$$

Bouguer himself derived the following form:

$$F(z) = \sec z - \frac{l_0}{2R} \sec z \tan^2 z + \left(l_0 - \frac{1}{3} R \cos^2 z \right) \frac{l_0 \tan^2 z}{2 R^2 \cos^3 z} - \cdots . \tag{26}$$

Bemporad (Ref.183) proved that, in Bouguer's derivation which also is encountered in Müller's textbook (Ref.184), a very poor convergence is produced by substitution of the variable $u = 1 - x$ for h; this leads to a distortion of the coefficients, starting from the second term. For $z > 85^\circ$, the series (24) converges too slowly, so that Bemporad derived another series for greater zenith distances (Ref.185).

Bouguer's theory was derived by himself and also in other textbooks in a manner different from that used here in accordance with Bemporad; however, although that derivation is geometrically more illustrative it is also much more cumbersome. Apparently, expansion over the integral (16) which allows for the curvature of the light ray seems a detour since Bouguer's theory neglects this entirely. However, the advantage of proceeding in this manner lies in the fact that it leads to the formula corrected by Bemporad [eq.(25)] and permits a clearer view over the difference between Bouguer's and Laplace's theories.

76. Laplace's Extinction Theory

Laplace (Ref.186) derived his extinction formula mainly with consideration of its correlation with the formula on the refraction of light rays in the earth's atmosphere; his argument has been extremely fruitful for further development of the problem.

Based on eq.(16) for the air mass, the variability of the refractive index μ with altitude or with density of the atmosphere must be taken into consideration. For this relation, Newton's formula

$$\mu^2 - 1 = 2c\varrho \tag{27}$$

is assumed, where c is a specific constant known also as "specific refraction". This had been theoretically substantiated by Laplace on the basis of the emis- /179
sion theory of light, but withstands physical checks less well than the formulas

$$\mu - 1 = c'\varrho \quad \text{and} \quad \frac{\mu^2 - 1}{\mu^2 + 2} = c''\varrho,$$

of which the first has no theoretical substantiation while the second is preferable both from the theoretical and practical viewpoint. However, μ - 1 is so small for both air and gases in general that all three formulas are practically equivalent for the theory of refraction. This is even more so for extinction. The numerical value of c can be determined physically and astronomically. Let us mention a few of the more important determinations for the normal density of air at 0°C and 760 mm Hg:

Biot and Arago (physical)	$2c_0$ = 0.0005888
Bessel (from his own and Argelander's observations)	= 0.0005864
Bauschinger (from own observations, Munich 1891-1893)	= 0.0005830
Courvoisier (from own observations, Heidelberg 1900-1903) ...	= 0.0005836.

The constant c in eq.(27) is correlated with c_0 by the Mariotte-Gay-Lussac law

$$c = c_0 \frac{B}{760} \frac{1}{1 + \alpha t}, \tag{28}$$

where B denotes the pressure in millimeters and $\alpha = \frac{1}{273}$ is the expansion constant of the gases. Here, eq.(27) yields

$$\mu d\mu = c d\varrho = c\varrho_0 dx. \tag{29}$$

Laplace (just as Bouguer) made the assumption of equal temperature and equal gravity in all layers of the atmosphere, which leads to the validity of the Boyle-Mariotte law

$$\frac{B}{B_0} = \frac{\varrho}{\varrho_0} = x \quad \text{and} \quad dB = B_0 dx, \tag{30}$$

to the equilibrium condition (22)

$$dB = -g_0 \varrho_0 x\, dh \tag{22}$$

and to the equation (9)

$$l_0 = \frac{B_0}{g_0 \varrho_0} = \lambda. \tag{9}$$

From eqs.(22), (30), and (29) it then follows that

$$x\, dh = -\frac{dB}{g_0 \varrho_0} = -\frac{B_0\, dx}{g_0 \varrho_0} = -l_0\, dx = -\frac{\mu\, d\mu\, \lambda}{c \varrho_0}. \tag{31}$$

Substituting the above expression for xdr in eq.(16) and correspondingly varying and inverting the limiting values, we obtain

$$F(z) = \frac{1}{c \varrho_0} \int_1^{\mu_0} \frac{\mu\, d\mu}{\sqrt{1 - \left(\frac{R \mu_0}{r \mu}\right)^2 \sin^2 z}}. \tag{32}$$

Since the theory of refraction, at concentric spherical stratification of the level areas yields the strict expression

$$\text{Refr.} = \int_1^{\mu_0} \frac{\frac{R \mu_0}{r \mu} \sin z\, d\mu}{\mu \sqrt{1 - \left(\frac{R \mu_0}{r \mu}\right)^2 \sin^2 z}}, \tag{33}$$

a comparison between the differentials dF and dR of F and R will furnish the equation /180

$$dF = \frac{1}{c \varrho_0 \mu_0} \frac{d\ \text{refr.}}{\sin z} \mu^3 \frac{r}{R}.$$

Laplace neglected the factor $r\mu^3/R$ which differs little from unity. Then, integration will yield the Laplace extinction formula

$$F(z) = K \frac{\text{refr.}}{\sin z}, \tag{34}$$

where $K = \frac{1}{c \rho_0 \mu_0}$ is a constant.

Comparison of Bouguer's and Laplace's theories. The above statements indicate that Laplace neglects more than the decrease in gravity with altitude, which would correspond to the assumption $\frac{r^2}{R^2} = 1$ since the factor $\left(\frac{r\mu}{R}\right)^3$ is larger than the above factor. For this, the curvature of the light path has

been taken into consideration. According to Bemporad, the two neglections possibly cancel each other since representation of the observations by either theory is equally satisfactory.

Since the refraction usually is given by the expression $\alpha_z \tan z$ where α_z can be taken from the refraction tables, we have

$$F(z) = K\alpha_z \sec z. \tag{35}$$

Applying, for α_z, the conventional expansion of refraction in even powers of tan z,

$$\alpha_z = \alpha_0(1 + a\tan^2 z + b\tan^4 z + \cdots), \tag{36}$$

an expansion of the following form will be obtained for F(z):

$$F(z) = K\alpha_0 \sec z + K\alpha_0 a \sec z \tan^2 z + K\alpha_0 b \sec z \tan^4 z + \cdots, \tag{37}$$

which agrees with Bouguer's series (25) only in the two first terms. The influence of the third term becomes noticeable only at zenith distances above 80°. Anyhow, complete agreement of the series cannot be expected in view of the difference of the two theories. A comparison of the coefficients of the two first terms of F(z) is possible if the series (36) for the refraction is replaced by the two-term expression obtained from the refraction integral (33), on restricting the calculation to terms of the first order of the two quantities (Ref.187)

$$s = \frac{h}{R+h} \text{ and the so-called refraction constant } \alpha = \frac{c\varrho_0}{1 + 2c\varrho_0} \tag{38}$$

so that

$$R = \frac{\alpha}{1-\alpha}\tan z\left\{\left(1 + \frac{1}{2}\alpha - \frac{l_0}{R}\right) - \left(\frac{l_0}{R} - \frac{\alpha}{2}\right)\tan^2 z\right\}. \tag{39}$$

This expression gives the refraction up to 75° zenith distance in complete strictness and contains Oriani's theorem (Laplace) in which the refraction, up to this limit, can be strictly represented by eq.(39) independent of any hypotheses on the constitution of the atmosphere.

In fact, the coefficients contain only the refraction constant α and the height of the reduced atmosphere l_0 which depend exclusively on the state of the atmosphere at the point of observation. We have /181

$$\alpha_{t_0, B} = \bar{\alpha}\frac{B}{760}\frac{1}{1 + mt_0} \quad \text{and} \quad l_0 = \frac{B_0^*}{\varrho_0 g_0},$$

where $\bar{\alpha}$ denotes the normal value of the refraction constant (at t = 0 and B = = 760 mm).

Since, with sufficient accuracy, we can set here

$$\alpha = c\varrho_0 = \mu_0 - 1 = 0.00029 \quad \text{and} \quad \frac{l_0}{R} = 0.0013$$

the coefficient of the first term in the expression for F(z) obtained from eqs.(34) and (39)

$$F(z) = K\frac{\alpha}{1-\alpha}\sec z\left\{\left(1+\frac{1}{2}\alpha-\frac{l_0}{R}\right)-\left(\frac{l_0}{R}-\frac{\alpha}{2}\right)\tan^2 z\right\}$$

will be equal to 1, with an accuracy of 0.001 while that of the second term will be equal to $-\frac{l_0}{R}$ with an accuracy of 0.0001, thus confirming the agreement with the two first terms of Bouguer's formula (24).

In the fundamental formula (34) of Laplace's theory, the refraction taken from various tables can be given with arbitrary accuracy, except that the obtained extinction is limited by the accuracy of the formula itself. A calculation of the mean free paths F(z) according to eqs.(25) and (34) demonstrates that, up to z = 85°, both formulas yield exactly identical values and show noticeable deviations only at greater zenith distances; however, this is no proof for their correctness within such wide limits, since both formulas are in part based on exactly the same assumptions. At z = 87°, both formulas show a difference of 0^m.02 only if the zenith reduction

or

$$\left.\begin{aligned}\log J_0 - \log J_z &= -\log p\,[F(z)-1]\\ m_z - m_0 &= -\frac{\log p}{0.4}\,[F(z)-1]\end{aligned}\right\} \qquad (40)$$

is calculated according to eq.(11).

77. Determination of the Transmission Coefficient and its Dependence on Altitude

When observing the brightness of one and the same star at different altitudes, equations of the form of eq.(40) will yield the zenith brightness m_0 and the logarithm of the transmission coefficient. At present, the best value of p, determined by Müller in Potsdam in this manner, is p = 0.835. Since

$$p = e^{-k\lambda\varrho_0}, \qquad \ln p = -k\lambda\varrho_0, \qquad (41)$$

the logarithm of the transmission coefficient must be proportional to the barometer reading and must decrease with the elevation of the point of observation above sea level since the atmospheric density ρ_0 is proportional to the atmospheric pressure. Consequently, the transmission coefficient must be calculable from the coefficient determined once and for all at a given barometer reading for arbitrary elevations above sea level; however, because of the greater opacity of the lower atmospheric layers in comparison with the higher layers, this is possible only with very low accuracy.

78. Other Earlier Theories of Extinction

No major progress over Bouguer's and Laplace's theories was obtained in the past Century, in numerous investigations on the extinction theory. In 1841, Forbes (Ref.188) gave a uniform and concise presentation of the Lambert, Bouguer, and Laplace series; on the basis of his own actinometric observations of solar /182 radiation at various altitudes, he defended the concept that the intensity of radiation within the total atmosphere does not decrease in accordance with a geometric law as had been assumed previously; he stated that, at the beginning, the decrease in light is extensive since the selective absorption characteristic for the medium is greatest here and that this decrease subsequently becomes less. The intensity of the extra-atmospheric solar radiation, calculated under assumption of the photometric fundamental law, thus would be too low in value.

In 1867, Trépied (Ref.189) gave a modification of Laplace's theory, which, in the first two terms, agreed with the corrected formula by Bouguer [eq.(25)].

The theory by Maurer (Ref.190) developed in 1882 on the extinction of light was established with the intention of refining Laplace's theory by introduction of a more accurate formula for the refractive index of the air:

$$\mu = 1 + c\varrho .$$

He did not reach his goal since, because of introduction of a mean constant refractive index for the entire atmosphere, an entirely impermissible assumption was made. The mean free paths calculated according to Maurer deviate extensively from those given by Laplace and also agree much less with actual observations.

In 1891, Seeliger (Ref.191) derived the Laplace formula under assumption of the Bessel law on atmospheric density $\rho = \rho_0 \cdot e^{-\beta \frac{h}{r}}$ and then applied it to a selective list of Müller's observations, resulting in systematic differences of some extent.

In 1895, Hausdorff (Ref.192) made a detailed theoretical investigation to explain the mentioned differences but obtained no reliable interpretation. His result that the observed extinction cannot be represented by a physically useful absorption formula can be ascribed, as also distinctly proved by Kempf (Ref.193), to the fact that the observation material used was not homogeneous. This material (constituting the Potsdam empirical extinction table) consisted of two entirely different portions obtained under different transparency conditions. Whereas, for zenith distances of 0° to 80°, the table gives the mean values from a very large number of observations at widely differing atmospheric conditions, the table for low altitudes ($z = 80^\circ$ to $z = 88^\circ$) is based on observation of bright celestial bodies, usually planets during their rise and setting on extremely clear days on which such observations were at all possible. Other observational series by Müller (Ref.194) on the Säntis and by Müller and Kempf (Ref.195) on Mt. Etna and in Catania (1894) yielded highly satisfactory agreement up to zenith distances of 87° when based on Laplace's formula. A revision of the above observational material by Bemporad (Ref.196), based on his own /183 refined extinction theory (with consideration of the temperature gradient of the atmosphere), shows that this theory, up to zenith distances of 87°, permits a

practically complete representation of the observations. Naturally, a prerequisite here is that the transmission coefficient p remains constant during the observation. However, constancy of this coefficient, even during one single night, is extremely rare. If, as had been done by Bemporad in his observations on the Säntis, only the brightnesses of one and the same star are observed during a given night and if they are then used for deriving the two constants, namely the zenith brightness and the transmission coefficient, it will be found that wave-like variations occur and that a greater zenith brightness of the star does not always belong to a larger transmission coefficient, as it should have been expected here. The mentioned agreement with the theory is obtained only for mean values from a large number of nights. Consequently, despite the fact that one cannot agree with Hausdorff's concept, his investigation offers a certain interest from a theoretical viewpoint since he used a method suggested by Bruns (Ref.197) for the refraction; the two variables of integration, namely the refractive force and the altitude, were not correlated by him over an a priori hypothesis on the constitution of the atmosphere but, instead, their functional correlation was determined from the observations themselves by introducing the coefficients of a suitably selected function as indeterminate parameters and defining them by averaging the extinction observations. An obvious drawback of the Bruns-Hausdorff method lies in the practical impossibility of giving a physical interpretation of the obtained coefficients.

79. Bemporad's Investigations as to the Influence of Temperature Stratification of the Atmosphere on the Extinction

The fundamental formula by Laplace [eq.(34)] is based on the assumption of constant temperature in the atmosphere; even when introducing into his formula a strict value for the refraction, free of this assumption, the error due to the basic assumption is not eliminated. In addition, the other above-discussed neglects in Laplace's theory influence its accuracy to an extent impossible to predict in advance. In a critical evaluation, Bemporad (Ref.198) treated the degree of approximation of Laplace's formula by deriving strict values of the extinction for $z = 87^\circ$ under various assumptions as to the temperature gradient of the atmosphere and by comparing these with Laplace's value. In part, the calculations were made analytically under the assumption of Ivory's and Schmidt's formulas for the temperature gradient and, in part, by numerical integration under assumption of the temperature curve observed from 0 to 9 km altitude. Here, the starting point is the fundamental formula (16) for air masses, in which the densities are calculated with consideration of the Gay-Lussac law and the neglects of Laplace's theory are avoided. For all hypotheses, the result gives almost the same value of extinction at $z = 87^\circ$ which is by $0^m.1$ greater than the Laplace value. The accompanying table illustrates the results. The second row of the table contains the values of air masses $F(z)$ calculated for $z = 87^\circ$ under various hypotheses, while the third row gives the zenith reduction in magnitude classes, calculated according to the formula

$$m_z - m_0 = -\frac{\log p}{0.4}[F(z) - 1],$$

in which case the Müller value of $p = 0.835$ has been assumed for $\log p$. In /184

	Ivory $f=0.2$	Ivory $f=0.3$	Schmidt $\beta=6°.1$	Observed Temp. Decrease to 9 km Altitude	Laplace (Const. Temperature)
λ	8.0076	8.0070	8.0065	8.0067	7.9895
$F(87°)$ . . .	15.269	15.353	15.361	15.344	14.835
Ext. in magn. cl.	2.794	2.810	2.811	2.808	2.709
Ext.-Laplace	0.085	0.101	0.102	0.099	

accordance with eq.(8), λ here denotes the height of the reduced atmosphere, while f is the coefficient of Ivory's formula for the dependence of density on temperature:

$$\frac{1+mt}{1+mt_0} = 1 - f(1-x), \tag{42}$$

where β is the temperature gradient for 1 km altitude in Schmidt's formula:

$$t - t_0 = -\beta h. \tag{43}$$

Thus, the error of the Laplace theory is insignificant and is in question only for special investigations close to the horizon. Another result of Bemporad's calculations is the fact that the extinction is practically influenced only by the temperature in the lowermost layers of the atmosphere, up to 9 km.

Altitude in km	Observation $t-t_0$	Schmidt Observation	Ivory Observation
1	6°.1	0.0	− 0.6
2	11.5	+0.7	− 0.9
3	16.9	+1.4	− 1.5
4	22.3	+2.1	− 2.6
5	28.7	+1.8	− 5.0
6	35.6	+1.0	− 8.3
7	42.2	+0.5	−11.7
8	49.4	−0.6	−16.0
9	(58.4)	−3.5	−22.6

80. Bemporad's Extinction Theory

This theory (Ref.199) allows for the temperature decrease in the first 9 km of the atmosphere by the simple Schmidt formula

$$t - t_0 = -\beta h,$$

which satisfactorily represents the observations of scientific atmospheric soundings (Ref.200) within the mentioned limits. At a temperature gradient of $\beta = 6°.1$, an agreement with the observed mean-square values of temperature is obtained, as illustrated in the accompanying table. The last column of this table gives the deviation from Ivory's formula.

It should be mentioned at this point that it is of no practical significance which temperature law is used as basis for the higher atmospheric layers so long as an accuracy of $0^m.01$ up to 87° zenith distance is observed. Similarly, a still stricter consideration of the observed temperature drop within the first 9 km, than that obtained by Schmidt's formula, will have no substantial influence. To illustrate the point, we should first note that, based on the relation

$$m_z - m_0 = -\frac{\log p}{0.4}[F(z) - 1],$$

at p = 0.835, the value 0.051 in F(z) corresponds to an error of $0^m.01$ in $m_z - m_0$. Tentatively, Bemporad performed two strict calculations of the function F(z) for z = 87°, one for a constant temperature gradient of β = 6°.1 for the entire atmosphere and a second with strict adherence to the above-mentioned observations with the gradients 6.1, 5.4, 5.4, 5.4, 7.2, 7.2, 7.2, 7.2, 7.2 and a constant gradient 3.0 for altitudes above 9 km. The first assumption corresponds to a total height of the atmosphere of 45.1 km and the second, to a height of 81.6 km. Despite such widely differing assumptions, the values for the air masses F(z) differ only slightly: /185

$$\text{First Hypothesis} \begin{cases} F(z) = \int_0^9 = 11.844; \\ F(z) = \int_9^H = 3.517; \end{cases} \qquad \text{Second Hypothesis} \begin{cases} = 11.849. \\ = 3.495. \end{cases}$$

These show, on the one hand, that Schmidt's approximation is completely sufficient and that, on the other hand, the higher layers of the atmosphere, even at widely differing assumptions as to the temperature decrease, result in practically unnoticeable errors in the extinction. Conversely, the lower layers - to 9 km - have a noticeable influence, as demonstrated by a calculation of the extinction according to Ivory's hypothesis on the temperature decrease at f = 0.2. This hypothesis poorly represents the observed temperature decrease, as indicated in the last column of the table. The next table contains a compilation of the air masses, calculated by Bemporad, for the total atmosphere based on the three hypotheses and on Laplace's theory. This shows that the excessively low temperature gradient by Ivory (about 4° per km) causes an extinction error of $0^m.02$, while that by Laplace (0°) results in an error of $0^m.1$. In any case, the following theorem is applicable here: At given transparency ratios, the extinction exerted by the atmosphere in the case of oblique incidence of rays will be greater the greater the thermal gradient with height.

	Hypothesis I (Schmidt)	Hypothesis II	Hypothesis III (Ivory)	Laplace
$F(z), z = 87°$	15.361	15.344	15.269	14.835
Extinction	$2^m.811$	$2^m.808$	$2^m.794$	$2^m.709$

81. Analytical Development of the Extinction Integral, Based on Schmidt's Hypothesis

As starting point of Bemporad's expansions, eq.(16) for the air masses

$$F(z) = \frac{1}{\lambda}\int_0^H \frac{x\,dh}{\sqrt{1 - \left(\frac{R+h_0}{r+h}\right)^2 \sin^2 z}},$$

is used, into which the Laplace relation is substituted:

$$\mu^2 = 1 + 2c\varrho \qquad \text{or} \qquad \frac{\mu^2}{\mu_0^2} = 1 - 2\alpha(1 - x),$$

where $\alpha = \frac{c\rho_0}{1 + 2c\rho_0}$ is the refraction constant. In addition, the variable s is again introduced over the equations

$$s = \frac{h}{R + h} = \frac{r - R}{r}, \qquad \frac{R^2}{r^2} = (1 - s)^2 \quad \text{and} \quad dh = \frac{R\,ds}{(1 - s)^2}.$$

This will yield /186

$$F(z) = C_z R \int_0^S \frac{x\sqrt{1 - 2\alpha(1 - x)}\,ds}{(1 - s)^2\sqrt{Z^2 - \varepsilon_z(1 - x) + s - \frac{1}{2}s^2}}, \tag{44}$$

where, for abbreviation, we set

$$C_z = \frac{1}{\lambda\sqrt{2}\sin z}, \qquad Z^2 = \frac{1}{2}\cot^2 z, \qquad \varepsilon_z = \frac{\alpha}{\sin^2 z}. \tag{44'}$$

In this formula, as in the refraction theories, $\frac{1}{2}s^2$ in the denominator can be neglected and $\sqrt{1 - 2\alpha(1 - x)}$ can be set equal to unity. Instead of $ds/(1 - s)^2$, we can set $(1 + 2s)ds$ while neglecting a term of the second order in s. Then, we have

$$F(z) = RC_z \int_0^S \frac{x(1 + 2s)\,ds}{\sqrt{Z^2 - \varepsilon_z(1 - x) + s}}. \tag{45}$$

Here, we will substitute an expression for the relative density x as a function of the altitude s. We have the temperature law $t - t_0 = -\beta h$, which will be replaced by a very similar form

$$t - t_0 = -\beta\frac{R}{R + h}h = -\beta Rs. \tag{46}$$

This also results in an almost completely uniform temperature decrease but offers considerable analytical advantages over Schmidt's form. Furthermore, we have the boundary conditions at h = 0:

$$t = t_0, \qquad B = B_0, \qquad x = 1$$

and the equilibrium equation of the atmosphere: $dB = -g_0\left(\frac{R}{r}\right)^2\rho dh$. Introducing, as units for B and ρ, the normal values $\overline{B}$, $\overline{\rho}$ of these at t = 0, the equation can be written in the form

$$B\,dB = -g_0\left(\frac{R}{r}\right)^2\varrho\,\overline{\varrho}\,dr \qquad \text{or} \qquad dB = \frac{1}{l_0}\left(\frac{R}{r}\right)^2\varrho\,dr, \tag{47}$$

where $t_0 = \frac{\bar{B}}{g_0\bar{\rho}}$. Using the same units, the Gay-Lussac equation will become

$$B = \varrho(1 + mt). \tag{48}$$

On dividing eq.(48) by the equation for the earth's surface

$$B_0 = \varrho_0(1 + mt_0) \tag{49}$$

and introducing the variable s, we obtain

$$\frac{B}{B_0} = x(1 - \gamma s), \tag{50}$$

where

$$\gamma = \frac{m\beta R}{1 + mt_0}. \tag{50'}$$

In addition, eq.(47), after dividing by eq.(49), will yield the following expression by means of the equation

$$\begin{aligned} dr &= \frac{R\,ds}{(1-s)^2}; \\ \frac{dB}{B_0} &= -\frac{R}{l}x\,ds, \end{aligned} \tag{51}$$

where we set

$$l = l_0(1 + mt_0). \tag{52}$$

From eqs.(50) and (51), we then obtain the differential equation /187

$$(1 - \gamma s)\,dx = \left(\gamma - \frac{R}{l}\right)x\,ds, \tag{53}$$

whose integration, with consideration of the initial conditions s = 0, x = 1, yields

$$x = (1 - \gamma s)^k, \tag{54}$$

where

$$k = \frac{R}{\gamma l} - 1 = \frac{1}{m\beta l_0} - 1. \tag{54'}$$

Equation (54) constitutes the sought relation between x and s which must be substituted into the integral (45).

82. Determination of λ and H for Schmidt's Hypothesis

As shown in eq.(44'), the value of λ is needed in the factor C_z. This is determined by the equation

$$\lambda = \int_0^H \frac{\varrho}{\varrho_0}\,dh = R\int_0^S \frac{x\,ds}{(1-s)^2} = R\int_0^S \frac{(1-\gamma s)^k ds}{(1-s)^2}$$

where

$$S = \frac{H}{R+H}.$$

By expansion in series, we obtain

$$\lambda = R\int_0^S (1-\gamma s)^k \left(1 + 2s + \frac{2\cdot 3}{1\cdot 2}s^2 + \frac{2\cdot 3\cdot 4}{1\cdot 2\cdot 3}s^3 + \cdots\right) ds$$
$$= R\left(\frac{1}{\gamma(k+1)} + \frac{2}{\gamma^2(k+1)(k+2)} + \frac{6}{\gamma^3(k+1)(k+2)(k+3)} + \cdots\right),$$

taking into consideration that

$$1 - \gamma S = x_H^{1/k} = 0.$$

Under consideration of eq.(54′), we also obtain

$$\lambda = l_0(1+mt_0)\left(1 + \frac{2}{\gamma(k+2)} + \frac{6}{\gamma^2(k+2)(k+3)} + \cdots\right), \tag{55}$$

through which the earlier approximation $\lambda = l = l_0(1 + mt_0)$ is clarified.

Using the known values of l_0 and m, eq.(54′) at $\beta = 6^\circ.22$ furnishes

$$k = \tfrac{3}{2}$$

with which eq.(55) will give

$$\lambda = 8.0109\,\text{km}.$$

Then, the equation $S = \frac{1}{\gamma}$ yields S = 0.006894 and, from this,

$$H = 43\,\text{km}.$$

As demonstrated before, this obviously much too low value for the height of the atmosphere does not interfere much with the accuracy of the air masses F(z).

83. Integration of the Expression of F(z) for Schmidt's Hypothesis

Equation (45) for F(z) was resolved by Bemporad into two terms

$$\left.\begin{aligned} F(z) &= RC_z\int_0^S \frac{x\,ds}{\sqrt{Z^2 - \varepsilon_z(1-x)+s}} + RC_z\int_0^S \frac{2x\,s\,ds}{\sqrt{Z^2-\varepsilon_z(1-x)+s}} \\ &= \Phi(z) + \Psi(z), \end{aligned}\right\} \tag{56}$$

which were integrated separately.

After substituting eq.(54) /188

$$x = y^k, \quad \text{where} \quad y = (1 - \gamma s),$$

we obtain

$$\Phi(z) = \frac{R C_z}{\sqrt{\gamma}} \int_0^1 \frac{y^k \, dy}{\sqrt{\Gamma^2 - y - \Delta y}}, \tag{57}$$

where

$$\Gamma^2 = 1 + Z^2\gamma, \qquad \Delta y = \gamma \varepsilon_z (1 - y^k). \tag{57'}$$

Since ε_z, for larger zenith distances, is a small quantity (although in the zenith itself, not only ε_z but also C_z as well as Γ will become infinitely large), an expansion of the integral (57) in powers of Δy

$$\Phi(z) = \frac{R C_z}{\sqrt{\gamma}} \left\{ \int_0^1 \frac{y^k \, dy}{(\Gamma^2 - y)^{\frac{1}{2}}} + \frac{1}{2} \varepsilon_z \gamma \int_0^1 \frac{y^k (1 - y^k) \, dy}{(\Gamma^2 - y)^{\frac{3}{2}}} + \frac{1}{2} \cdot \frac{3}{4} \varepsilon_z^2 \gamma^2 \int_0^1 \frac{y^k (1 - y^k)^2 \, dy}{(\Gamma^2 - y)^{\frac{5}{2}}} + \cdots \right\} \tag{58}$$

will still be so convergent at Z = 89° that four terms are sufficient for calculating $\Phi(z)$ to within three significant figures.

However, Bemporad did not use the series (58) but another one which he obtained from the former by making the substitution

$$\frac{y}{\Gamma^2} = t, \qquad \frac{1}{\Gamma^2} = T. \tag{59}$$

We then have

$$\int_0^1 \frac{y^k \, dy}{(\Gamma^2 - y)^{\frac{1}{2}}} = \frac{1}{T^{k+\frac{1}{2}}} \int_0^T \frac{t^k \, dt}{(1 - t)^{\frac{1}{2}}},$$

$$\int_0^1 \frac{y^k (1 - y^k) \, dy}{(\Gamma^2 - y)^{\frac{3}{2}}} = \frac{1}{T^{k-\frac{1}{2}}} \int_0^T \frac{t^k \, dt}{(1 - t)^{\frac{3}{2}}} - \frac{1}{T^{2k-\frac{1}{2}}} \int_0^T \frac{t^{2k} \, dt}{(1 - t)^{\frac{3}{2}}}, \text{ etc.}$$

Now, the quantity T which is a function of the zenith distance and of the temperature has vanished from under the integral sign and occurs only as an upper limit. This has considerable advantages for the calculation which, essentially, is performed in numerical form. In this manner, Bemporad obtained the following expansion for $\Phi(z)$:

$$\Phi(z) = \frac{\sqrt{T}}{\sin z} \varphi_0(T) + \left(\frac{\sqrt{T}}{\sin z}\right)^3 \varphi_1(T) + \left(\frac{\sqrt{T}}{\sin z}\right)^5 \varphi_2(T) + \cdots, \tag{60}$$

where the functions φ have the values

$$\varphi_0(T) = \frac{C_0}{T^{k+1}} \int_0^T \frac{t^k\,dt}{(1-t)^{\frac{1}{2}}},$$

$$\varphi_1(T) = \frac{C_1}{T^{k+1}} \int_0^T \frac{t^k\,dt}{(1-t)^{\frac{1}{2}}} - \frac{C_1}{T^{2k+1}} \int_0^T \frac{t^{2k}\,dt}{(1-t)^{\frac{1}{2}}},$$

$$\varphi_2(T) = \frac{C_2}{T^{k+1}} \int_0^T \frac{t^k\,dt}{(1-t)^{\frac{1}{2}}} - \frac{2C_2}{T^{2k+1}} \int_0^T \frac{t^{2k}\,dt}{(1-t)^{\frac{1}{2}}} + \frac{C_2}{T^{3k+1}} \int_0^T \frac{t^{3k}\,dt}{(1-t)^{\frac{1}{2}}} \text{ etc.}$$

The coefficients C_0, C_1, C_2, and T have the following values: /189

$$\left.\begin{aligned} C_0 &= \frac{R}{\lambda\sqrt{2\gamma}}, \qquad C_1 = \frac{1}{2} C_0 \alpha\gamma, \qquad C_2 = \frac{1\cdot 3}{2\cdot 4} C_0 \alpha^2\gamma^2, \ldots \\ T &= \frac{1}{1+\gamma Z^2} = \frac{1}{1+\frac{1}{2}\gamma \cot^2 z}. \end{aligned}\right\} \qquad (61)$$

These depend on temperature and pressure at the site of observation; the integrals themselves, at the normal value k = 4.5, are readily reduced to trigonometric functions. The series is so convergent that five terms are sufficient, even for calculating the extinction in the horizon. Let us give here the values of the constants C_0 to C_3 for 0° and 760 mm:

$$\log C_0 = 1.6698048, \qquad \log C_1 = 9.995366 - 10,$$
$$\log C_2 = 8.49702 - 10, \qquad \log C_3 = 7.0444 - 10.$$

An expansion of the second term of the function F(z) in eq.(56) which, compared to the previous one, is of a lower order, is carried out in an entirely similar manner by introducing the same variables. Applying the same substitution, we obtain

$$\Psi(z) = 2RC_z \int_0^S \frac{x\,s\,ds}{\sqrt{Z^2 - \varepsilon_z(1-x) + s}} = \frac{2RC_z}{\gamma^{\frac{1}{2}}} \int_0^1 \frac{y^k(1-y)\,dy}{\sqrt{\Gamma^2 - y - \Delta y}}$$
$$= \frac{2}{\gamma}\Phi(z) - \frac{2RC_z}{\gamma^{\frac{1}{2}}} \int_0^1 \frac{y^{k+1}\,dy}{\sqrt{\Gamma^2 - y - \Delta y}}.$$

The Taylor expansion in powers of Δy yields

$$\Psi(z) = \frac{2}{\gamma}\Phi(z) - \frac{2RC_z}{\gamma^{\frac{1}{2}}} \left\{ \int_0^1 \frac{y^{k+1}\,dy}{(\Gamma^2 - y)^{\frac{1}{2}}} + \frac{1}{2}\varepsilon_z\gamma \int_0^1 \frac{y^{k+1}(1-y^k)\,dy}{(\Gamma^2 - y)^{\frac{3}{2}}} + \cdots \right\} \qquad (62)$$

Finally, the substitution $t = \frac{y}{\Gamma^2}$, $T = \frac{1}{\Gamma^2}$ will give

$$\left.\begin{aligned}\Psi(z) &= \frac{2}{\gamma}\Phi(z) - \left\{\frac{\sqrt{T}}{\sin z}\chi_0(T) + \left(\frac{\sqrt{T}}{\sin z}\right)^3\chi_1(T) + \cdots\right\}\\ &= \frac{\sqrt{T}}{\sin z}\psi_0(T) + \left(\frac{\sqrt{T}}{\sin z}\right)^3\psi_1(T) + \cdots,\end{aligned}\right\} \tag{63}$$

where we set

$$\chi_0(T) = K_0\frac{1}{T^{k+2}}\int_0^T \frac{t^{k+1}\,dt}{(1-t)^{\frac{1}{2}}}; \quad \chi_1(T) = K_1\left\{\frac{1}{T^{k+2}}\int_0^T\frac{t^{k+1}\,dt}{(1-t)^{\frac{1}{2}}} - \frac{1}{T^{2k+3}}\int_0^T\frac{t^{2k+1}\,dt}{(1-t)^{\frac{1}{2}}}\right\},$$

$$K_0 = \frac{2}{\gamma}C_0, \qquad K_1 = \frac{2}{\gamma}C_1,$$

$$\psi_0(T) = \frac{2}{\gamma}\varphi_0(T) - \chi_0(T),$$

$$\psi_1(T) = \frac{2}{\gamma}\varphi_1(T) - \chi_1(T).$$

Here, however, a calculation of the two first functions ψ_0 and ψ_1 is sufficient since, for the horizon, we have

$$\psi_0(1) = 0.0447,$$
$$\psi_1(1) = 0.0032,$$
$$\psi_2(1) = 0.0003.$$

Thus, the expansion of the function F(z) in odd powers of $\frac{\sqrt{T}}{\sin z}$ is as follows: /190

$$F(z) = F_0(T)\frac{\sqrt{T}}{\sin z} + F_1(T)\left(\frac{\sqrt{T}}{\sin z}\right)^3 + F_2(T)\left(\frac{\sqrt{T}}{\sin z}\right)^5 + \cdots, \tag{64}$$

where the functions F(T) represent the sums of the corresponding functions φ and ψ:

$$\left.\begin{aligned}T &= \frac{1}{1+\frac{1}{2}\gamma\cot^2 z}, \quad \log\frac{1}{2}\gamma = 1.8604900,\\ F_i(T) &= \varphi_i(T) + \psi_i(T), \text{ where } i = 0, 1, 2 \ldots.\end{aligned}\right\} \tag{64'}$$

For the value of the functions φ_i and ψ_i, Bemporad calculated tables which progress according to the argument T. These were then compiled in function tables for $F_i(z)$, yielding Table XIIa in the Appendix for the traversed air mass F(z). These progress as follows: between 0° and 60°, from degree to degree; between 60° and 84°, from tenth to tenth degree; from 84° to 89°, from minute to minute. The tables are in wide use at present for more refined investigations, despite the fact that - for ordinary photometric measurements in which a zenith distance of 75° is not exceeded - the Bouguer and Laplace tables are just as useful since they actually furnish the same extinction values as the new tables.

The value of Bemporad's tables thus is mainly of a theoretical nature, since they were the first that strictly considered the actual conditions in the troposphere relative to temperature and pressure. These tables, however, are based on the assumption that the absorptivity of the air layers is exclusively

dependent on the density, a hypothesis which cannot be strictly valid for the troposphere since the admixture of water vapor and dust particles greatly changes the absorptivity. However, a study of these influences becomes possible only by means of the strict tables.

The accompanying table gives a compilation of the air masses and the corresponding extinction values, calculated according to Bouguer, Laplace, and Bemporad.

z	Traversed Air Masses $F(z)$			Differences in Magnitude Classes	
	Bouguer	Laplace	Bemporad	Bouguer - Bemporad	Laplace - Bemporad
0°	1.000	1.000	1.000	0,00	0.00
70	2.897	2.899	2.904	0.00	0.00
75	3.800	3.803	3.816	0.00	0,00
80	5.551	5.563	5.600	−0.01	−0,01
81	6.113	6.129	6.177	−0.01	−0.01
82	6.798	6.818	6.884	−0,01	−0.01
83	7.649	7.676	7.768	−0.02	−0.02
84	8.730	8.768	8.900	−0.04	−0,03
85	10.142	10.196	10.395	−0.05	−0,04
86	12.047	12.125	12.439	−0.08	−0.06
87	14.724	14.835	15.364	−0,12	−0,10
88	18.677	18.835	19.787	−0,22	−0,19

It is obvious that the Bouguer and Laplace theories furnish almost the same values; they differ from the strict Bemporad values only at zenith distances above 80°.

84. Influence of Geographical Location of Observation Site and Pressure and Temperature Fluctuations on the Extinction

The mean extinction tables by Bemporad refer to the geographic latitude of 45°, a temperature of 0°C, and a barometer reading of 760 mm Hg. The functions φ and ψ depend on the gravity and the temperature gradient over the constant k which enters the integral as exponent, since we have /191

$$k = \frac{1}{m\beta l_0} - 1,$$

$$l_0 = g\frac{\overline{B}}{\varrho}.$$

The gravity at the point of observation is a function of latitude and elevation above sea level. Strictly speaking, a conversion of the tabular values of extinction to greater elevations of the observation site and to other latitudes would thus become necessary. However, a calculation for extreme cases shows that the correction for latitude is always negligibly small and that also the correction for altitude can be neglected up to 3000 m and 87° zenith distance, without resulting in an error of more than $0^m.01$ in the calculated extinction. For still more accurate investigations, Bemporad gave a method for taking the mentioned influences into consideration.

Since the function F(z) has an identical course for sea level and for 3000 m altitude, the difference in extinction can be due exclusively to the different values of the transmission coefficients p in the formula

$$\text{Extinction} = m_z - m_0 = -\frac{\log p}{0.4}[F(z) - 1].$$

The variations in extinction, produced by pressure and temperature at one and the same locus, are due to changes in the function F(z) as well as in the transmission coefficient p. Bemporad established small auxiliary tables for taking strict account of the variations in the coefficients of the functions φ_0, φ_1, ..., ψ_0, ψ_1, ... due to these influences.

Tables XIIb and XIIc in the Appendix permit a strict calculation of the variations of F(z) and log p for the zenith distances 87°, 88°, 89° at which they become first noticeable. This indicates that F(z) depends almost exclusively on the temperature whereas log p depends greatly on the pressure. This statement is substantiated by the equation used for calculating the table and following directly from the definition of $\ln p = -c\lambda\rho_0$. This is the equation

$$\log p = \log p_0 \frac{\lambda_t}{\lambda_0} \frac{B}{760} \frac{1}{1 + mt}.$$

Since λ_t is practically proportional to 1 + mt, only the influence of the pressure remains as the decisive factor. Here, p is the changed transmission coefficient, referring to the temperature t and the pressure B.

Table XIb is a compilation of the above-mentioned table and directly gives the corrections of the extinction values for pressure and temperature conditions that differ from normal.

The following formulas by Bemporad, obtained by strict calculation for a few extreme values and by interpolation of the intermediate values, illustrate the influence of temperature and pressure on the extinction (ΔE in magnitude classes):

/192

$$\begin{aligned}
z = 80^\circ \quad & \Delta E = +0.011\,\Delta\beta \\
z = 82 \quad & \Delta E = +0.015\,\Delta\beta \\
z = 84 \quad & \Delta E = -0.005\,\Delta\tau + 0.020\,\Delta\beta \\
z = 86 \quad & \Delta E = -0.012\,\Delta\tau + 0.030\,\Delta\beta \\
z = 87 \quad & \Delta E = -0.022\,\Delta\tau + 0.039\,\Delta\beta \\
z = 88 \quad & \Delta E = -0.040\,\Delta\tau + 0.050\,\Delta\beta \\
z = 89 \quad & \Delta E = -0.083\,\Delta\tau + 0.071\,\Delta\beta
\end{aligned}$$

where $\Delta\tau$ is expressed in 10 degrees, $\Delta\tau = 10t^\circ$, and $\Delta\beta$ in 10 mm:

$$\Delta\beta = \frac{B - 760}{10}.$$

This indicates that both corrections should be used only for special investigations of the extinction on the horizon.

85. Selective Extinction and Forbes' Phenomenon

In the preceding theoretical considerations, the atmosphere had been treated as a neutral medium which attenuates all wavelengths of the incident radiation to the same extent. In reality, the atmosphere does not have this property. On the one hand, the presence of water vapor and oxygen in the atmosphere is responsible for its opacity to certain ray species, which manifests itself in the occurrence of absorption lines and bands in the spectrum; these depend, in intensity and width, on the amount of water vapor or oxygen passed. The attenuating effect of this pure absorption is of the discontinuous type. Since this extends only over a narrow portion of the spectrum in the yellow and red region, its significance is negligible with respect to the continuous attenuation of the entire spectrum, produced by diffusion or light scattering on the molecules of the atmosphere. This increases continuously with decreasing wavelength and thus causes a greater attenuation of the blue and violet rays than of the red rays. A consequence of these phenomena is the fact that the transmission coefficient of the atmosphere must differ for different wavelengths. Thus, the derivation of Bouguer's fundamental formula (1) is correct only as long as radiation of a certain wavelength is involved. On restriction to a definite wavelength λ, the following relations can be used

$$J_{z,\lambda} = J_\lambda p_\lambda^{\sec z} \qquad \text{for a homogeneous layer}$$

and

$$J_{z,\lambda} = J_\lambda p_\lambda^{F(z)} \qquad \text{for the atmosphere ,}$$

where J_λ denotes the extra-atmospheric intensity of the radiation of wavelength λ. However, this raises the question whether the two following equations, of which each is correct in itself, exist side by side:

$$J p^{F(z)} = J_{\lambda_1} p_1^{F(z)} + J_{\lambda_2} p_2^{F(z)} + J_{\lambda_3} p_3^{F(z)} + \cdots$$
$$J = J_{\lambda_1} + J_{\lambda_2} + J_{\lambda_3} + \cdots ,$$

where J is the intensity of the total radiation of a celestial body outside the atmosphere, while p is a certain mean value of the transmission coefficients p_1, p_2, p_3, ... for the wavelengths λ_1, λ_2, λ_3, ... constituting the effective transmission coefficient of the total radiation as it is obtained from the measured brightness difference of a given celestial body at various elevations.

It can be demonstrated, which had been done by S.P.Langley (Ref.201) in all strictness, that the effective transmission coefficient determined by the conventional indirect method will be too high in value so that it will give too low an extra-atmospheric radiation J. The reason for this phenomenon is quite obvious. For selectively absorbing bodies, the phenomenon mentioned by Forbes and Crova (Ref.201, 202) must be accounted for, which states that the specific transmittance, or the transmittance referred to unit air mass, must increase with increasing layer thickness. After the transmitted spectral region has been narrowed by the front layers, the subsequent layers have a less absorbing effect. This phenomenon was already known to Lambert (1760); he noted that a set of equally thick colored glass plates does not attenuate the sunlight by constant amounts; the specific transmittance increases with the number of plates.

/193

It follows from this that at near-horizon position of the stars, certain effective transmission coefficients of the atmosphere will be larger in value than those determined at greater heights of the celestial bodies. The debate, started by this unrefutable theorem established by Langley, is still in progress. Langley himself believed that the extra-atmospheric radiation will be obtained by 40% too low because of the distorted transmission coefficient. Seeliger (Ref.204) mentioned that, in view of the narrowness of the visually effective spectral region, the influence of a continuous decrease in transmission coefficient with wavelength on the sought mean value can be only minor. Based on Langley's spectral transmission coefficients, he theoretically calculated the real value of p and found that it must be located between 0.75 and 0.82, meaning that it should give a light attenuation by at most 8% greater than ordinarily assumed. J.Wilsing (Ref.205) also found, especially for the visible portion of radiation between 0.45 and 0.68 μ, that the real total attenuation due to the effective transmission coefficient can be accurately represented by Bouguer's formula. The value obtained on the basis of the spectral-photometric measurements by G.Müller was p = 0.810, whereas Müller himself obtained a value of p = 0.835 from his measurements of the total radiation. The reason for this agreement lies in the fact that, within the limits of visual rays, the total intensities of sensation are proportional to the corresponding amounts of energy; in addition, the radiation curves, deformed by the extinction, agree sufficiently well with the curves of lower temperature. Thus, the visually observed total attenuation agrees with that calculated from the energy by means of the spectral transmission coefficients.

Despite this fact, traces of spectral extinction will always appear in the visual measurements of stars at various height, when sharper reduction is used. In 1891, Seeliger (Ref.204) found such traces in his Potsdam observations. In 1902, Bemporad (Ref.206), in his revision of Müller's measurements on the Säntis (Ref.207), demonstrated that, at greater transparency of the atmosphere, i.e., at a higher value of p, the formula /194

$$\log J_0 - \log J_z = -\log p\,[F(z) - 1]$$

does not always yield a greater zenith brightness J_0 of the star; in most cases, exactly the opposite is found. This again could be interpreted as due to an increase in transmission coefficient with the air mass, in the sense of spectral extinction.

H.G.Wolff (Ref.208) found that the Potsdam observations by Müller, when assuming a specific transmission coefficient increasing with the air mass, could be brought to better agreement. For p, he derived the empirical relation

$$p = p_0 + a \log F(z).$$

This was used also by Zipler (Ref.209) in 1921, in the work-up of his Babelsberg measurements. As values of the specific transmission coefficient p and the constant a, he found the following:

for Potsdam (by Wolff)	$p_0 = 0.750$,	$a = 0.034$,
for Babelsberg (by Zipler)	$p_0 = 0.723$,	$a = 0.062$.

We will give here some other more recent determinations of the transmission coefficient for the visually most effective region. The above-mentioned values by Wolff and Zipler refer to the effective wavelengths $\lambda = 0.575\ \mu$ resp. $0.571\ \mu$. Wilsing (Ref.210) determined a value of $p = 0.750$ for $\lambda = 0.570\ \mu$ from his bolometric measurements in Potsdam. Abbot and Fowle (Ref.211), in their bolometric measurements, found a value of $p = 0.701$ for Washington at the same wavelength. Finally, Bemporad (Ref.212) obtained a value of $p = 0.761$ from the pyrheliometric measurements by Ångström on Teneriffa.

86. Differential Extinction Determinations from Observations at Stations of Various Height above Sea Level

Simultaneous observations of one and the same celestial body from stations located at different elevations give the direct value of the extinction of the intermediate air masses. Of the same type were the actinometric and bolometric measurements by Langley (Ref.213) on Mt. Whitney and the visual-photometric observations by Müller and Kempf (Ref.214) in Catania and on Mt. Etna. A revision of the latter data by Bemporad (Ref.215) furnished the incentive for a number of publications that gave highly interesting results. At first, for a strict calculation of air masses steeply inclined to the horizon, it was found necessary to establish tables with respect to refraction, temperature, and pressure ratios, which are of a general scientific value. The tables cover elevations from 0 to 5000 m above sea level. An application of these tables to a strict reduction of Müller's observations resulted in an obvious rhythmic flow of the transmission coefficient with zenith distance, for the air layer Catania-Etna. Greater zenith distances produce higher values of the transmission coefficient in the sense of spectral extinction. Below, we give a compilation of the specific /195 transmission coefficients of air layers at various thicknesses and increasing inclination of the rays, as reduced by Bemporad. The first row of the compilation shows the transmission coefficients derived by H.G.Wolff from Müller's Potsdam observations, based on the Bouguer method. The second row contains the same data for the Catania-Etna stratum of about 3000 m thickness, derived from photometric measurements by Müller and Kempf; the third and fourth rows contain the transmission coefficients according to spectrophotometry measurements by Müller and Kron (Ref.216, 217) on Teneriffa, where the two strata obtained over the intermediate station (Pedrogil Pass) between Orotava and Alta Vista, are separately calculated; finally, the last row gives the results of pyrheliometric measurements by K.Ångström (Ref.218), again taken on Teneriffa, and by Bemporad in 1908 (loc. cit.) at Lincey.

	$z = 0°$	$50°$	$70°$	$80°$
Potsdam (97 m)	0.750	0.765	0.786	0.809
Catania-Etna (69 - 2942 m)	0.23	0.36	0.43	0.50
Orotava-Alta Vista (360 - 3260 m), $\lambda = 0.570\ \mu$	0.233	0.336	0.471	0.549
Pedrogil Pass-Alta Vista (1950 - 3260 m), $\lambda = 0.570\ \mu$	0.071	0.176	0.405	0.573
Guimar-Alta Vista (360 - 3252 m)	0.599	0.653	0.723	0.788

All rows show a distinct rhythmic flow with the zenith distance or with the thickness of the traversed air mass, which is more distinct the less this thickness. In addition, all specific transmission coefficients, valid for the total

atmosphere (8 km), are much lower than those derived from observations according to Bouguer's method (first row).

If the spectral extinction is to be responsible for the spectrophotometric results of the above tabulation, it must be assumed that it is effective also within a spectral region of 100 Å for the blue rays resp. of 30 Å for the red rays, since this was the width of the slit of Müller's spectrophotometer; at an infinitely narrow slit, no shift in the above figures should take place. However, Bemporad, for explaining this phenomenon, also took the possibility of a strong increase in extinction within the respective layer with height of the sun into consideration. The observations were all made on the sun and it is conceivable that, on gradual rise of the sun above the horizon, an ascent of the lower heated air masses with their haze content had taken place, which would result in a lower transmittance at greater solar height. Despite the fact that this phenomenon might have played a certain role in Müller's observations, the influence of spectral extinction cannot be doubted in view of other observations which, occasionally, were made at night.

87. Dependence of the Transmission Coefficient on Height above Sea Level

The above tabulation shows no influence of elevation above sea level on the transmission coefficient for the atmosphere above the site of observation. In 1917, Wilsing (Ref.219), derived the following empirical relation from determinations at seven stations, with barometer readings between 450 and 760 mm:

$$\log p_\lambda = -\frac{\varkappa(B)}{\lambda - 0.288}, \tag{65}$$

where the function dependent on the barometer reading B has the following form:

/196

$$\varkappa(B) = \frac{0.01826\,B}{1 - 1.703\,B^1}.$$

Thus, the transmission coefficient is not simply-proportional to the pressure, as required by Bouguer's theory. In Ångström's pyrheliometer measurements on Teneriffa, Bemporad (Ref.220) found a decrease in transparency of the air proportional to the fourth power of air density. Accordingly, the Bouguer theory cannot be applied to the lower layers of the atmosphere. Instead, in the fundamental equation for absorption

$$dJ = -k\varrho J\,ds$$

the quantity k must be considered as variable; accordingly, eq.(3), after integration, will be replaced by the generalized extinction equation in the form

$$J_z = Je^{-\int k\varrho\,ds}. \tag{66}$$

In accordance with Bemporad, the exponent $\int k\rho ds$, instead of the air mass of Bouguer's formula, would be more correctly designated as "optical air mass".

A strict theory of extinction should make it possible to calculate these optical air masses for different zenith distances and different elevations above sea level; however, this would be possible only if the variability of k with altitude were known. A special case of such a theory was treated by Bemporad (Ref.221), who assumed the empirically found relation

$$k = k_0 \varrho^4 \tag{67}$$

as valid for the entire atmosphere in one case and then only for the lower layers up to 5000 m altitude in the other case, whereas he presumed that constant transparency prevails at greater heights. Since the variability of k is caused by admixtures of water vapor and dust, the above assumption can be considered plausible.

In accordance with eqs.(10) - (18), the task of theory reduces to calculating the integrals

$$\lambda_1 = \int_0^H x^5 \, dh, \tag{68}$$

$$F_1(z) = \frac{1}{\lambda_1} \int_0^H \frac{x^5 \, dh}{\sqrt{1 - \left(\frac{R\mu_0}{r\mu}\right)^2 \sin^2 z}}, \tag{69}$$

where the first represents the optical mass of the atmosphere in vertical direction and the second, the optical masses for arbitrary zenith distances. It is easy to define λ_1 (as done in Sect.81) by series expansion of the expression

$dh = \frac{Rds}{(1 - s)^2}$ in the form

$$\lambda_1 = R \int_0^s (1 - \gamma s)^{\frac{5}{2}} (1 + 2s + 3s^2 + \cdots) \, ds.$$

A numerical calculation yields λ_1 = 1.872 km. Under assumption of eq.(67) for the transmittance, the total atmosphere absorbs somewhat less than 2 km normal air at sea level in horizontal direction. /197

The influence of the higher atmospheric layers is entirely insignificant. If the law given in eq.(67) is applied - as done above - to the entire atmosphere, then the values for the optical masses between 0 and 5 km and between 5 and 20 km will be as follows:

$$\int_0^5 x^5 \, dh = 1.76185 \quad \text{and} \quad \int_5^{20} x^5 \, dh = 0.11012.$$

Still greater heights, in calculating to five significant figures, furnish no contribution at all. Bemporad used mechanical quadrature for calculating the values of the function $F_1(z)$ corresponding to eq.(67), from 60° to 90° zenith

z	$\int_0^5$	$\int_5^{20}$	$F_1(z)$	$F(z)$
60°	1.8813	0.1174	1.9987	1.995
70	2.7478	0.1709	2.9187	2.904
75	3.6266	0.2246	3.8512	3.816
80	5.3867	0.3296	5.7163	5.600
85	10.5410	0.6090	11.1500	10.395
87	16.8950	0.8794	17.7744	15.365
89	38.4970	1.3098	39.8068	26.959
90	79.9776	1.4247	81.4023	39.651

distance. We are giving an excerpt from his table. The last column, for comparison, contains the values of the function F(z) corresponding to the old theory of equal transparency of equal air masses.

Up to a zenith distance of 60°, both theories yield the same values; at greater zenith distances, the difference increases steeply.

The same author also calculated a second hypothesis according to which the law of transparency [eq.(67)] would be valid only to a certain height H_0 whereas the old assumption $k = k_0 = \text{const}$ would apply to greater altitudes; in that case, the optical mass λ_0 in vertical direction would have the following form:

$$\lambda_0 = \int_0^{H_0} x^5\, dh + x_0^5 \int_{H_0}^{H} x\, dh. \tag{70}$$

The values for λ_0, with both assumptions as to the limit H_0, are as follows:

$$H_0 = 4 \text{ km}: \quad \lambda_0 = 2.5261,$$
$$H_0 = 5 \text{ km}: \quad \lambda_0 = 2.2330.$$

z	$H_0 = 4$ km		$H_0 = 5$ km		$F_1(z)$	$F_2(z)$	$F_3(z)$
	$\int_0^4$	$\int_4^H$	$\int_0^5$	$\int_5^H$			
60°	1.3235	0.6734	1.5771	0.4201	1.999	1.997	1.997
70	1.9332	0.9779	2.3035	0.6100	2.919	2.913	2.911
75	2.5518	1.2813	3.0401	0.7990	3.851	3.839	3.833
80	3.7918	1.8658	4.5157	1.1606	5.716	5.676	5.658
85	7.4333	3.3410	8.8367	2.0610	11.150	10.898	10.774
87	11.9544	4.6542	14.1633	2.8367	17.774	17.000	16.609
89	26.6070	6.5554	32.2726	3.8868	39.807	36.159	34.162
90	58.2326	7.0395	67.0465	4.1347	81.402	71.181	65.272

As shown in the accompanying excerpt from Bemporad's table, the difference between the two last assumptions, as well as the differences between these two assumptions and the first hypothesis, are negligible and are of practical importance only for zenith distances greater than 85°. For easier comparison, we entered the values of $F_1(z)$ of the preceding table.

88. Direct Photometric Extinction Determinations

On observing two disks of white paper of equal albedo, illuminated by the sun, at equal orientation but at greatly differing distances, the difference /198
in apparent brightness will directly yield the degree of extinction of a certain atmospheric layer. By this procedure, Wild (Ref.222), for the surface of the earth and, in a later paper (Ref.223), for air of differing purity enclosed in horizontal tubes, found extremely low values of transmittance. Haecker (Ref.224) found similar values for foggy air. Of other determinations made with this method, we will mention here only those by E.Oddone (Ref.225) who made photometric observations of snow fields in the Alps and the Apennines for determining the terrestrial extinction. The path covered by the investigated rays

through the atmosphere was 45 - 135 km. To obtain almost equal transparency conditions, the measurements were made only on days on which the visibility was about 100 km. Bemporad (Ref.226) strictly reduced Oddone's observations, under consideration of density variations along the line of sight, using the above-mentioned tables (Sect.86). The following table contains the results of this calculation:

Distance	Mt. Pernice (1.38 km) 45 km		Mt. Grigna (2.15 km) 85 km		Weissmies (3.5 km) 134 km	
Azimuth	S=O		N=O		NW	
	Feb. 16	Feb. 14	Jan. 1	March 4	March 4	
$F(z)$	2.959	4.114	6.502	7.353	11.173	11.282
p	0.656	0.719	0.876	0.871	0.953	0.943
p (ZIPLER)	0.790	0.811	0.839	0.847	0.873	0.873

If it can be assumed that the transmittance conditions were the same in the three different directions and that the values obtained on four different days are sufficiently reliable and comparable, it is striking here that the lower atmospheric layer (1.38 km) shows less transparency and that this increases with height and thickness of the air mass [F(z)]. For comparison, the bottom row gives the transmission coefficients of quantitatively equal air masses, as they were obtained with the conventional astronomic method by Zipler for Babelsberg. Qualitatively, the air masses differ in the two cases, since the former are closer to the surface of the earth. Whereas, in Zipler's figures, the influence of spectral extinction is manifest, the much greater cadence in Oddone's transmission coefficients can no longer be ascribed to this cause; instead, these coefficients express the influence of brightness of the hazy air itself. This effect, which counteracts the extinction (brightening more distant objects) and which is difficult to take into consideration, impairs the value of all transmission coefficients determined with this method.

89. Transmittance of the Atmosphere for Radiation of Different Wavelengths

We cannot list here all of the various determinations of the transmission coefficients p_λ for the individual wavelengths. To give a general view over the course of p_λ in the visible spectrum region, we are giving here the results obtained by Müller and Kron (Ref.227) with a Glan-Vogel spectrophotometer during their expedition to Teneriffa. They observed the solar spectrum for different /199 zenith distances of the sun, at three stations of different elevation. The data reduction was done according to Bouguer's formula $J_z = J_0 p_\lambda^{F(z)-1}$; the results, as mentioned above, show traces of spectral extinction because of the width of the slit.

Of the bolometric measurements by Abney, Langley, Wilsing, and Abbot (Ref.228 - 231), we will discuss only the latter since, being made at three different elevations with one and the same instrument, they extend over the longest observation time and thus can be considered as the most reliable mean values. For comparison purposes, the values for Potsdam are given (Ref.230).

MEAN VALUES OF TRANSMISSION COEFFICIENTS ACCORDING TO MÜLLER AND KRON

Wavelength μ	0.679	0.651	0.605	0.570	0.540	0.514	0.492	0.473	0.457	0.443	0.430
	Station Orotava (100 m)										
	0.818	0.833	0.780	0.784	0.768	0.763	0.749	0.721	0.708	0.693	0.656
	Station Pedrogil (1950 m)										
	0.907	0.899	0.878	0.866	0.859	0.852	0.842	0.821	0.808	0.791	0.769
	Station Alta Vista (3260 m)										
	0.950	0.937	0.912	0.894	0.895	0.887	0.877	0.866	0.863	0.840	0.818

TRANSMISSION COEFFICIENTS

Wavelength in μ	Washington 10 m	Mt. Wilson 1780 m	Mt. Whitney 4420 m	Potsdam 100 m	Wavelength in μ
0.30	—	—	0.510	0.706	0.44
0.325	—	(0.550)	0.584	0.740	0.46
0.35	—	0.612	0.660	0.764	0.48
0.375	—	0.662	0.738	0.781	0.50
0.39	0.445	0.694	0.763	0.795	0.52
0.42	0.586	0.764	0.806	0.808	0.54
0.43	0.600	0.778	0.822	0.819	0.56
0.45	0.640	0.800	0.851	0.830	0.58
0.47	0.671	0.827	0.880	0.840	0.60
0.50	0.705	0.858	0.900	0.850	0.62
0.55	0.739	0.876	0.918	0.861	0.64
0.60	0.760	0.890	0.934	0.871	0.66
0.70	0.839	0.942	0.956	0.881	0.68
0.80	0.865	0.964	0.972		
1.00	0.901	0.973	0.980		
1.30	0.916	0.972	0.980		
1.60	0.930	0.975	0.978		
2.00	0.909	0.957	0.940		
2.50	0.870	(0.900)	0.930		
3.00	—	—	0.910		

For a study of the individual causes of extinction - Rayleigh scattering on air molecules, scattering on larger particles, absorption in the permanent gases of the atmosphere and in water vapor - the above-mentioned results of Mt. Wilson Observatory are especially suitable. These were obtained during determination /200 of the solar constant over an observational series of several years, using the same highly sensitive instruments at all three stations; in addition, they cover the largest wavelength region, including even the broad water-vapor bands. They were subjected to a detailed theoretical analysis, first by L.V.King and then by F.E.Fowle (Ref.232).

According to Rayleigh and Schuster (Ref.233, 234), the effect of spectral extinction, in so far as it is caused by scattering on molecules, manifests itself in a decrease of the constant k of the absorption formula with the fourth power of the wavelength. If

$$J_z = Je^{-kF(z)},$$

then

$$k = \frac{32\pi^3(n-1)^2}{3N\lambda^4}. \tag{71}$$

Here, n denotes the refractive index of the air and N the number of molecules in unit volume. According to the theory of absorption and diffusion, developed by L.V.King (Ref.235), which will be discussed in detail in the next Section, the same constant k under consideration of diffusion, absorption (Fraunhofer lines), and scattering by coarse particles, is represented by

$$k_x = \frac{32}{3}\left\{\pi^3(n_0-1)^2\frac{H}{N_0}\lambda^{-4} + \alpha_0 H\right\}\frac{B}{B_0} + \text{a dust-dependent term,}$$

where B and B_0 denote the barometric pressure at the observation station (height x) and at sea level, while H is the height of the reduced atmosphere at 0° C and 760 mm Hg, with N_0 being the number of molecules in one cubic centimeter under the same conditions and k_x representing the constant k for the height x. Here, $\alpha_0 H$ is the term expressing the energy converted into heat during absorption.

The above equation, denoting λ^{-4} by z, has the form $k_x = mz + b$ so that the extinction coefficients k_x, when graphically represented, should form straight lines whose inclination tangent, depending on the elevation of the observation station, would have to differ. This tangent m yields the characteristic number N_0 over the equation

$$N_0 = \frac{32}{3}\pi^3(n_0-1)^2\frac{HB}{mB_0}. \tag{72}$$

We are reproducing here the graphical representation of k_x according to L.V.King (Fig.47), with the remark that the introduction of the two upper inclined straight lines, osculating the lower lines at one point, is arbitrary and is easily refuted by a stricter analysis of the observations. Nevertheless, the values obtained for Mt. Wilson and Mt. Whitney yield a satisfactory confirmation of Rayleigh's formula, since they are more or less accurately located on one straight line each. For the constants m and N_0, King found the following values:

	m	$m\frac{B_0}{B}$	N_0
Potsdam . .	0.00893	0.00904	$2.51 \cdot 10^{19}$
Washington.	0.01016	0.01011	$2.24 \cdot 10^{19}$
Mt. Wilson .	0.00806	0.00994	$2.28 \cdot 10^{19}$
Mt. Whitney	0.00592	0.01003	$2.26 \cdot 10^{19}$

in surprising agreement with the value obtained by Millikan who found 2.644×10^{19} for N_0 in laboratory experiments. /201

King also derived the value of the constant b from his plotting and believed that it constitutes a criterion for the heating of the atmosphere; however, the intercepts of the straight lines with the axes are too unreliable for permitting such a determination.

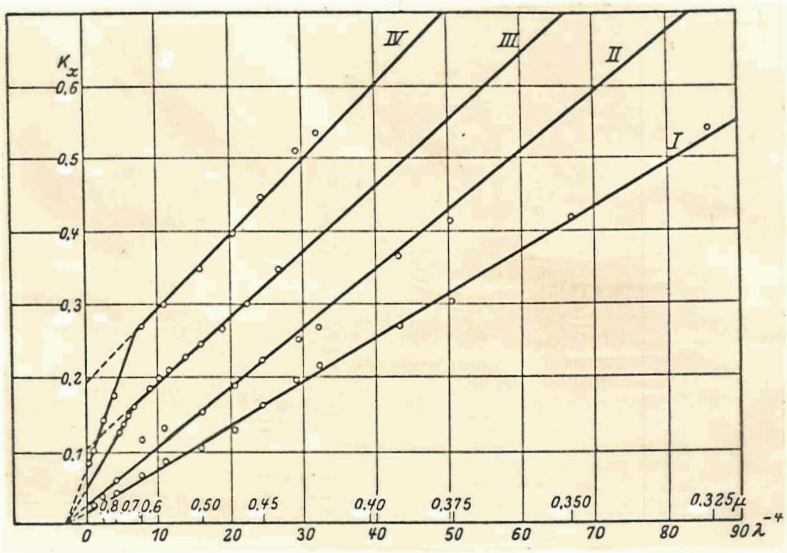

Fig.47 Extinction Coefficients of the Atmosphere on Mt. Whitney (I), on Mt. Wilson (II), in Potsdam (III), and in Washington (IV).
The abscissas are proportional to λ^{-4} (according to L.V.King).

The transmission coefficients used by King refer to humid air. Fowle (Ref.236), based on the same observations on Mt. Wilson, found the following value after correction for humidity:

$$N_0 = (2.70 \pm 0.02) \cdot 10^{19},$$

i.e., a still better agreement with Millikan's value.

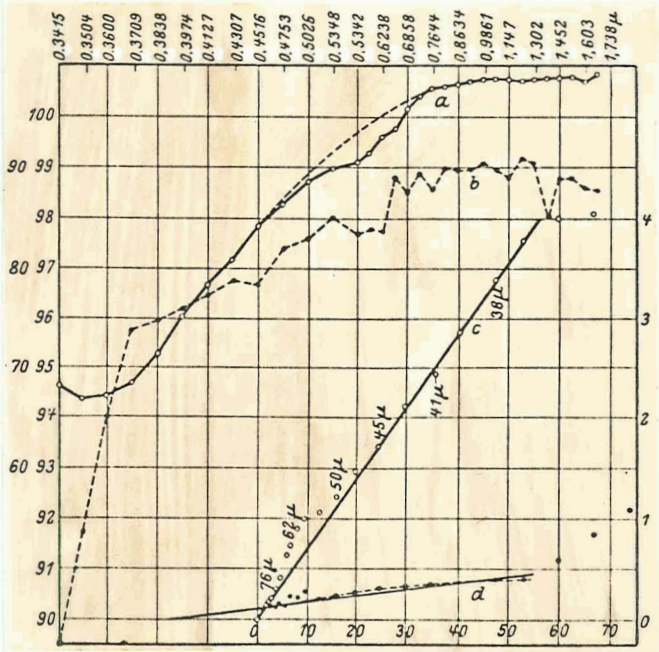

Fig.48 Extinction Coefficients for Mt. Wilson (according to Fowle).

In reality, the confirmation of Rayleigh's formula is by no means complete, even for high stations. The influence of absorption and scattering on coarser particles produces considerable deviations for longer wavelengths. Figure 48, taken from Fowle's paper, contains the extinction coefficients of dry air for Mt. Wilson in the lower straight lines c, which again are plotted in accordance with the argument λ^{-4}. In fact, these modified values distinctly show the deviations of observations in the region between 0.50 and 0.76 μ, which can be ascribed to selective

/202

absorption. For Washington and Potsdam, these deviations are still greater; for the visible spectrum region, as stated already by G.Müller, even the quadratic formula $k_x = k_0\lambda^{-2}$ represents the observations as accurately as the Rayleigh formula. However, the quadratic formula is not sufficient for the infrared region; A.Boutaric (Ref.237), for the exponent of the dispersion formula from Abbot's measurements, found values lower than 4, namely 2.1 for Washington, 3.1 for Mt. Wilson, and 3.3 for Mt. Whitney. Similar figures were obtained by Boutaric from absorption measurements in turbid media; he concluded from this that particles of the order of magnitude of the wavelengths of visible rays are suspended in the atmosphere.

Other empirical formulas, used by various authors for representing the decrease in transmittance of the atmosphere with wavelength, will be mentioned briefly. Wilsing (Ref.238) obtained a satisfactory representation of his bolometric observations by the above formula [eq.(65)].

In 1907, Bemporad (Ref.239) made use of the argument $J_z = Jp^{F(z)^n}$, where the second constant is the exponent n of the air mass F(z). K.Ångström (Ref.240) derived a formula in which the second empirically determined constant, namely the "density of the scattering layer" occurs as factor of the air mass. More recently, F.Linke (Ref.241) in 1922 introduced a "turbidity factor" T into the extinction formula for representing the mean transmission coefficient: $J_z = Jp^{TF(z)}$, where p denotes the mean transmission coefficient depending on the traversed air mass while T is a ratio of the total transmission coefficient of haze-filled masses to those of dry dust-free air, a ratio which is assumed as constant.

90. Influence of Water Vapor on Transmittance of Air for Radiation of Different Wavelengths; Non-selective Extinction by Water Vapor

It is known that the water vapor in the atmosphere produces a number of absorption bands of which the most important

$$\Phi(\lambda = 1.13\,\mu), \qquad \Psi(\lambda = 1.47\,\mu) \qquad \text{and} \qquad \Omega(\lambda = 1.89\,\mu)$$

lie in the infrared region of the spectrum. Figure 49 shows these bands in the intensity curve of the spectrum of a Nernst lamp. To quantitatively determine the influence of water vapor on the transmittance of the atmosphere and to take account of its varying content in calculating the values of the transmission coefficients, F.E.Fowle (Ref.242) made detailed investigations.

These investigations consisted of two parts. First, it was a question /203
of establishing, from laboratory experiments, a relation between the absorption within the water vapor bands and the amount of water vapor passed by the rays of a Nernst lamp. The former was determined from the energy curve (Fig.49) as the ratio of the ordinates of a certain wavelength within the bands Φ and Ψ of the lower curve and of the broken curve, in which case the latter represents the freehand-plotted course without absorption bands. The amount of water vapor, measured in centimeters of water column, which would produce the corresponding

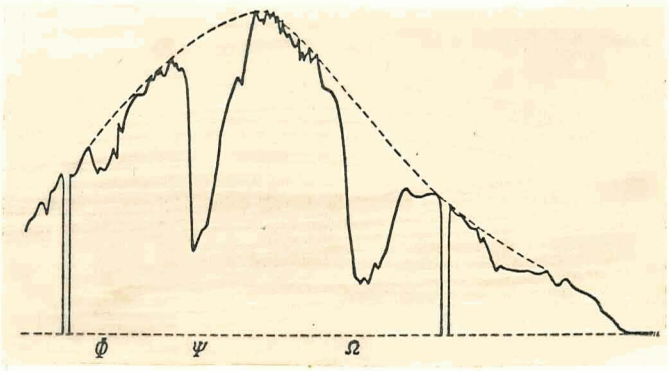

Fig.49 Absorption Bands of Water Vapor in the Spectrum of a Nernst Lamp (according to Fowle).

amount of water vapor after evaporation in a cylindrical vessel was accurately determined by conventional methods. The resultant relation would permit a determination of the amount of water vapor along the path of the light rays from a celestial body within the atmosphere, if the depth of its energy curve could be measured within the corresponding absorption bands. A prerequisite would be that the decreasing pressure, along the ray path in the atmosphere, has no influence on the obtained relation. A study by Eva von Bahr (Ref.243) on the transmittance of water vapor at various pressures indicates that this is largely dependent on the total pressure but is independent of the partial pressure. In view of this result and under application of Humphrey's tables (Ref.244) for the water vapor distribution at various heights of the atmosphere, Fowle concluded that an evaluation of the amount of water vapor contained in the atmosphere could be made from his curves obtained in the laboratory to within an accuracy of 2 - 3%.

In addition to the selective absorption in bands and lines, water vapor produces a general attenuation of the radiation, which has a substantial influence on the transmission coefficients p_λ as a function of atmospheric humidity. To define this effect and thus to obtain the transmittance of dry air, Fowle used the following method: If $a_{a\lambda}$ denotes the transmittance of dry air and $a_{w\lambda}$ that of the amount of water vapor of 1 cm water along the light path, then we have the relation

$$p_\lambda = a_{a\lambda} a_{w\lambda}^{w}, \tag{73}$$

where the exponent w denotes the true amount of water vapor measured in centimeters, or expressed logarithmically:

$$\log p_\lambda = \log a_{a\lambda} + w \log a_{w\lambda}. \tag{74}$$

From observations on Mt. Wilson, extending over many years, the amount of water vapor w was determined from the depths of the absorption bands. The logarithms /204 of the transmission coefficients p_λ, graphically plotted according to the quantity of water vapor w, resulted in straight lines for various regions of λ in accordance with the last equation in the system (74), whose inclination tangent represents the transmission coefficient for water vapor $\log a_{w\lambda}$. The curve b in Fig.48 represents the values $a_{w\lambda}$ and gives a possibility for converting the transmittance $a_{a\lambda}$ of dry air to humid air, in which the actual amount of water vapor w must be taken into consideration in accordance with eq.(73). The values of $\log a_{a\lambda}$ for dry air were graphically obtained as the ordinates of the straight lines (74) for w = 0. The values $a_{a\lambda}$ are represented in Fig.48 by the upper curve a, while the $-\log a_{a\lambda}$ values, according to the argument $\lambda^{-4} \cdot 10^{16}$, are

given in the lower straight line c. The depression in the region between 0.503 μ and 0.764 μ in the curve a as well as the corresponding bulge in the line c presumably are due to the selective absorption in the permanent gases of the atmosphere. According to Rowland's "A Preliminary Table of Solar Spectrum Wavelengths", the above-mentioned regions contain more than 440 absorption lines in addition to those belonging to water vapor. The influence of the broad water vapor bands is eliminated in the curve a by forming the p_λ values from fitted energy curves. Conversely, the minor depressions along the curve b must be ascribed to fine absorption lines of water vapor.

The accompanying table, for a number of wavelengths, gives the values of $a_{w\lambda}$ and $a_{a\lambda}$, in addition to the intensity $i_{o\lambda}$ of the solar energy curve outside the atmosphere, obtained with a bolometer on Mt. Wilson after correction for extinction.

SOLAR ENERGY IN ARBITRARY UNITS AND TRANSMISSION COEFFICIENTS FOR DRY AIR AND WATER VAPOR

λ in μ. .	0.342	0.350	0.360	0.371	0,384	0,397	0.413	0,431	0.452	0.475
$i_{o\lambda}$ . . .	102	130	160	198	227	322	437	518	681	807
$a_{a\lambda}$ . . .	(0.595)	0.626	0.655	0.686	0.713	0.752	0.783	0.808	0.840	0.863
$a_{w\lambda}$ . . .	0.920	0.926	0.934	0.940	0.945	0.949	0.953	0.957	0.961	0.964
λ in μ. .	0.503	0.535	0.574	0.624	0.686	0,764	0.864	0.987	1.146	1.302
$i_{o\lambda}$ . . .	907	1044	1197	1334	1416	1435	1431	1306	1025	775
$a_{a\lambda}$ . . .	0.885	0.898	0.905	0.929	0.959	0.979	0.987	0.992	0.996	0.997
$a_{w\lambda}$ . . .	0.968	0.972	0.970	0.975	0.981	0.984	0.986	0.987	0.987	0.987
λ in μ. .	1.452	1.603	1.738	1.870	2.000	2.123	2.242	2.348	—	—
$i_{o\lambda}$ . . .	586	435	343	262	187	123	88	74	—	—
$a_{a\lambda}$ . . .	0.998	0.999	0.999	0.999	0.999	0.999	0.999	0.999	—	—
$a_{w\lambda}$ . . .	0.987	0.987	0.987	0.987	0.986	0.985	0.984	0.983	—	—

The values $a_{a\lambda}$ refer to an elevation of 1730 m above sea level (barometer reading, 620 mm) while $a_{w\lambda}$ refers to 1 cm water vapor. This table was used as basis in the calculation of other tables for Mt. Whitney and Washington. For practical purposes, the following tables taken from the Smithsonian Physical Tables VII Edition, p.419, is sufficient:

λ in μ	0.360	0.384	0.413	0.452	0.503	0.535	0.574	0.624	0.653	0.720	0.986	1.74
$a_{a\lambda}$.	0.660	0.713	0.783	0.840	0.885	0.898	0.905	0.929	0.938	0.970	0.986	0.990
$a_{w\lambda}$.	0.950	0.960	0.965	0.967	0.977	0.980	0.974	0.978	0.985	0.988	0.990	0.990

This table refers to sea level.

From the table for Mt. Wilson, the transmission coefficient p_λ is obtained with the aid of the following formula for different elevations with a barometer reading B and an amount of water vapor w cm: /205

$$p_\lambda = a_{a\lambda}^{\frac{B}{620}} a_{w\lambda}^{w}. \tag{75}$$

Determination of the amount of water vapor is best done by spectroscopic means, as described above. If this is impossible, the formula derived by Hann can be used:

$$w = 2.3\, e_w\, 10^{-\frac{h}{22\,000}}, \tag{76}$$

where e_w denotes the pressure of water vapor at the observation site and h is the elevation of the station in meters. However, Fowle (Ref.245) demonstrated that this method does furnish values agreeing adequately with spectroscopic data in the yearly mean but is entirely unreliable for individual values.

Equation (75) does not allow for the extinction by dust and thus can be used only in the conversion of transmission coefficients for stations at high elevations (above 1000 m), for which the influence of dust can be considered as vanishingly small.

Fowle made an attempt to represent the obtained transmission coefficients $a_{w\lambda}$ of water vapor by Rayleigh's scattering formula, in a manner similar to that applied for $a_{a\lambda}$. The lowest straight line d in Fig.48 gives the graphical representation of $-\log a_{w\lambda}$ according to the argument $\lambda^{-4} \cdot 10^{-16}$. The deviations for short wavelengths and also for the depression zone near 0.6 μ are considerable, so that one cannot speak of a confirmation of the Rayleigh formula for atmospheric water vapor. Fowle also found that the observed attenuation of the rays by water vapor is much greater throughout than would be required by a diffusion through the molecules of this vapor. The attenuation is also greater than that resulting from a corresponding amount of liquid water. He concluded from this that the scattering by the water vapor may be effected by some aggregates larger than molecules.

Fowle's method of determining the amount of water vapor was excellently confirmed by direct humidity measurements with sounding balloons. By simultaneous spectroscopic observations of the solar radiation and measuring of the absorption band depths, a comparison became possible, showing the following agreement for three different observation days in the year 1913:

	July 23	Aug. 3	Aug. 8
Spectroscopic values . .	1.17 cm	2.06 cm	1.39 cm
Balloon values	1.07 „	2.09 „	1.41 „ .

91. Energy Balance during Extinction of Radiation in the Atmosphere

The calculated amounts of water vapor furnished the basis for investigating the energy balance during extinction of solar radiation or for separating the individual contributions of atmospheric extinction. Five such causes were differentiated: 1) general scattering by the molecules of the permanent gases in the atmosphere, discussed in the preceding Section; 2) diffusion by water vapor,

treated above ($a_{w\lambda}$); 3) selective absorption by water vapor; 4) selective absorption by the permanent gases in the atmosphere; 5) absorption by solid particles or dust. /206

Figure 50 gives the energy curve of the sun in the region of atmospheric absorption bands, whose significance had been investigated by Fowle. For radiators of lower temperature, absorption bands in the farther infrared would be in question; however, for solar radiation these play no role because of the drop of the energy curve in this region.

The tabulation below gives the designation of the various bands as well as their origin and the mean wavelength:

B	0.69 μ Oxygen,	Φ	1.13 μ Water vapor,
a	0.72 μ Water vapor,	Ψ	1.42 μ ,,
A	0.76 μ Oxygen,	Ω	1.89 μ ,,
—	0.81 μ Water vapor,	ω_1	2.01 μ ?
$\rho\sigma\tau$	0.93 μ ,,	ω_2	2.05 μ ?

The areas, formed by the depressions in the bands with an upper limit represented by the broken curve, yield a criterion for the energy loss by absorption; they were measured for the water vapor bands and plotted according to the argument of water vapor amounts, after which they were graphically fitted. These areas, when compared with the total area of the energy curve and converted by means of the total energy of the radiation simultaneously measured on the pyrheliometer into gram-calories, /207 will give the loss of radiation by selective absorption in the water vapor bands, as a function of the amount of water vapor. A measurement of the bands produced by oxygen will give the amount of oxygen absorption. On adding the amount of water vapor absorption to this, the total loss by absorption in the atmosphere will be obtained.

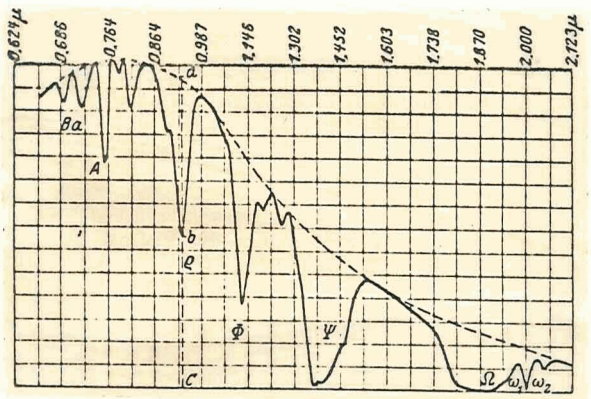

Fig.50 Energy Curve of the Sun in the Region of Atmospheric Absorption Bands (according to Fowle).

This made it possible to determine the percentual component of the energy loss by absorption, for various amounts of water vapor and various air masses. Of the tables, representing these losses and calculated for Mt. Whitney (4420 m), Mt. Wilson (1730 m) and Washington, only the first will be given in its entirety. This table, in the first row, contains the losses by diffusion while the second row gives the losses by absorption for completely dry air, i.e., absorption by the permanent gases of the atmosphere (B, A, ω_1, ω_2), and the third row gives the sum of the preceding figures. Furthermore, for various amounts of water vapor we are giving the losses by diffusion and absorption in the water vapor bands (a, $\rho\sigma\tau$, etc.) as well as the sum of these, increased by the total loss in dry air.

MT. WHITNEY ATMOSPHERE; EXTINCTION BY DRY AIR AND DRY AIR PLUS WATER VAPOR
Elevation 4420 m; Barometer Reading 44.7 cm;
Incident Solar Radiation, 1.93 gm-calorie

Air Mass	$m=1$		$m=2$		$m=3$		$m=4$		$m=5$		$m=7$	
Amount of Water Vapor	Gram-Calorie Loss	Percent. Loss	Gram-Calorie Loss	Percent. Loss	Gram-Calorie Loss	Percent. Loss	Gram-Calorie Loss	Percent. Loss	Gram-Calorie Loss	Percent. Loss	Gram-Calorie Loss	Percent. Loss
0.00 cm												
Air, scattered	0.14	7.3	0.23	11.9	0.31	16.1	0.38	19.7	0.44	22.8	0.55	28.5
Air, absorbed	0.01	0.5	0.01	0.5	0.01	0.5	0.01	0.5	0.01	0.5	0.02	1.0
Total loss	0.15	8.0	0.24	12.0	0.32	17.0	0.39	20.0	0.45	23.0	0.57	30.0
0.11 cm												
H_2O, scattered	0.01	0.5	0.01	0.5	0.01	0.5	0.01	0.5	0.02	1.0	0.02	1.2
H_2O, absorbed	0.08	4.1	0.10	5.2	0.11	5.7	0.12	6.2	0.12	6.2	0.13	6.7
Total loss	0.24	12.0	0.35	18.0	0.44	23.0	0.52	27.0	0.59	31.0	0.72	37.0
0.25 cm												
H_2O, scattered	0.01	0.5	0.02	1.0	0.03	1.6	0.04	2.1	0.04	2.1	0.05	2.7
H_2O, absorbed	0.10	5.2	0.12	6.2	0.13	6.7	0.14	7.3	0.15	7.8	0.16	8.3
Total loss	0.26	14.0	0.38	20.0	0.48	25.0	0.57	30.0	0.64	33.0	0.78	40.0
0.50 cm												
H_2O, scattered	0.02	1.0	0.04	2.1	0.06	3.1	0.07	3.6	0.08	4.1	0.10	5.2
H_2O, absorbed	0.12	6.2	0.15	7.8	0.16	8.3	0.17	8.8	0.18	9.4	0.20	10.4
Total loss	0.29	15.0	0.43	22.0	0.54	28.0	0.63	33.0	0.71	37.0	0.87	45.0

For the stations Mt. Wilson (mean amount of water vapor, 0.7 cm) and /207
Washington (for the driest day with 0.5 cm H_2O), two values for m = 1 and m = 3 are given below. The losses due to dry air, water vapor, and both together are as follows:

	Loss due to Dry Air	Due to H_2O	Together	
$m = 1$	8% (0.15 gm-cal.);	9% (0.17 gm-cal.);	17% (0.32 gm-cal.)	Mt. Wilson.
$m = 3$	20% (0.39 „);	13% (0.25 „);	33% (0.64 „)	
$m = 1$	10% (0.19 „);	10% (0.19 „);	20% (0.38 „)	Washington.
$m = 3$	23% (0.44 „);	19% (0.37 „);	42% (0.81 „)	

In the table for Mt. Whitney and Mt. Wilson, the loss of radiation due to dust could be neglected; in the table for Washington, the amount was not separately determined but included in the loss due to water vapor. The losses due to dust at m = 1 were 3, 5 and 14% respectively, at the three observation days in Washington.

The much greater transparency of the air over Mt. Whitney is due mainly to the low amount of water vapor present.

The tables indicate that, on the average, the energy loss is produced to about one half by scattering and absorption in the permanent gases and to one half by scattering and absorption in the water vapor.

Finally, we should mention an investigation by V.Fessenkov and Ye.Piaskovskiy (Ref.246); this paper refers to the Forbes phenomenon and was made possible by Fowle's absorption tables. From actinometric measurements of solar radiation at

the Pavlovsk Observatory, extending over many years, N.Kalitin found the following course of the transmission coefficient with the traversed air mass, in the sense of Forbes' phenomenon:

m	2–3	3–4	4–5	5–6	6–7	7–8	8–9	9–10
p	0.843	0.866	0.878	0.886	0.892	0.897	0.901	0.907

Fessenkov demonstrated that this course can be satisfactorily represented by Wilsing's formula (65) for p, as a function of two constants $\left[\log p_\lambda = \frac{a}{\lambda - b}\right]$, after integration over the real spectral region and under consideration of the absorption in the water vapor bands. For the visible region p is constant, in agreement with earlier work. /208

VIII. THEORY OF DIFFUSION AND ABSORPTION OF LIGHT IN GASES AND ITS APPLICATION TO PLANETARY ATMOSPHERES

92. King's Theory; Definitions and Basic Principles

The theory of diffusion of light by particles whose dimensions are small with respect to the wavelength of the incident light was originally developed by Lord Rayleigh (Ref.247). His diffusion formula is applicable to the molecules of a gas as well as to sufficiently small solid particles and thus offers the basis for treatment of the diffusion problem in the terrestrial atmosphere and in the atmosphere of other planets. An elegant application of the theory to the brightness distribution in the sky, at various distances from the sun, was given by L.V.King (Ref.248); the principles for treating this difficult task, of great importance for the physics of the atmosphere, had been given earlier by Schuster (Ref.249). King's analysis is of great importance also for the theory of extinction of light, since it brings proof that this is ascribable mainly to the diffusion on passage of the light through the atmosphere and depends only negligibly on absorption. King was successful in theoretically deriving the brightness of the celestial background from the observed extinction coefficients of solar radiation for various wavelengths and in obtaining a satisfactory agreement with the observations of brightness distribution over the clear sky. King's developments also permit an extension to the problem of brightness of a planet surrounded by an atmosphere, which is treated in our book; in fact, they might be of decisive importance for defining the nature of the light-reflecting surfaces of such planets. For this reason, the data will be presented here to the extent as required for application to our astronomical problems.

Let us denote the intensity of parallel-incident rays by E and that of diffuse radiation by J, where $J(r, \alpha)$ represents this intensity at the distance r and at the direction α to the incident rays. Let the elementary volume, receiving the radiation E and scattering it in all directions, be equal to dv. Then, the incident amount of radiation will be Edv, while that scattered in the direction α in the immediate neighborhood of dv will be $J(0, \alpha)dv$; conversely, at a distance r we have $J(r, \alpha)dv$ so that the amount of diffuse radiation, emitted by

dv into the solid angle dω, will become $J(r, \alpha)dvd\omega$.

The Rayleigh scattering formula furnishes a relation between incident and diffuse radiation

$$J(0, \alpha) = \mu(\alpha) E, \tag{1}$$

where the diffusion coefficient $\mu(\alpha)$ is a function of the angle α and of the density ρ, i.e., of the number N of the molecules in unit volume, depending also on the refractive index n of the gas and the wavelength λ of the light: /209

$$\mu(\alpha) = \frac{\frac{1}{2}\pi (n^2 - 1)^2 \lambda^{-4} (1 + \cos^2\alpha)}{N}. \tag{2}$$

This important formula has also been derived by Kelvin and Schuster (Ref.250, 251); the latter author obtained the formula from general considerations without special assumptions as to the nature of the particles.

Since n - 1 as well as N are proportional to the density of the gas, this will also be so for $\mu(\alpha)$. Consequently, we have the relation

$$\frac{\mu(\alpha)}{\mu_0(\alpha)} = \frac{N}{N_0} = \frac{\varrho}{\varrho_0}, \tag{3}$$

where the subscript 0 corresponds to a definite state of the gas.

This scattering of light attenuates the rays penetrating through the gas, without causing a loss in total radiation energy and without conversion of this energy into heat. However, the process of light absorption, which always accompanies diffusion and manifests itself in the occurrence of dark absorption lines in the spectrum, can be taken into consideration by using the conventional absorption equation for the loss dE of radiation over the short path dr:

$$dE = -\nu E\, dr, \tag{4}$$

where also ν is proportional to the number of molecules in unit volume, i.e., to the density ρ, so that the following equation will exist:

$$\frac{\nu}{\nu_0} = \frac{\varrho}{\varrho_0}.$$

In agreement with King, we will agree to have the coefficient ν mean the absorptive effect of the gas molecules and of other solid particles suspended in the atmosphere which, although at a different ratio from that of the first, will produce a diffusion effect according to eq.(2) as well as an absorption and thus contribute to heating of the atmosphere.

93. General Integral Diffusion Equation

Let us imagine a bounded mass of gas, in which each element of volume is

illuminated not only by direct radiation whose intensity is outside the gas mass E but also by all other elements that transmit diffuse rays to it. We treated a similar problem in deriving our own and Fessenkov's formulas for diffuse reflection but had restricted the calculation there to diffusion of the second order. We assumed that the other elements of the gas, contributing to the illumination of dv, receive only direct illumination. Here, we will treat the problem of mutual self-illumination of the gaseous elements in all strictness, i.e., without the above restrictions. The only exception is that, in the terms of higher order, we will calculate with a uniform diffusion in all directions. A mean diffusion coefficient $\bar{\mu}$ will be introduced by means of the equation

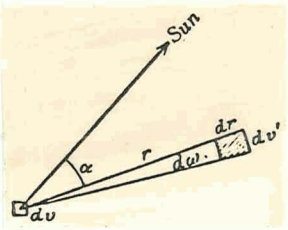

Fig.51 Scattering of Solar Radiation in the Atmosphere.

$$\bar{\mu} = \frac{1}{4\pi}\int \mu(\alpha)\, d\omega,$$

where the integral must be extended over the entire sphere or over the angle 4π: /210

$$\bar{\mu} = \frac{1}{4\pi}\frac{\pi^3}{2}\frac{(n^2-1)^2 2\pi}{N\lambda^4}\int_0^{\pi}(1+\cos^2\alpha)\sin\alpha\, d\alpha = \frac{2}{3}\frac{\pi^2(n^2-1)^2}{N\lambda^4}. \tag{5}$$

In that case, the diffusion coefficient

$$\bar{\mu}_0 = \frac{2}{3}\frac{\pi^2(n_0^2-1)^2}{N_0\lambda^4}, \tag{6}$$

will correspond to the normal conditions of pressure and temperature. In addition, we introduce the notations

$$4\pi\bar{\mu} = k \qquad \text{and} \qquad 4\pi\bar{\mu}_0 = k_0. \tag{7}$$

Let us consider the radiation emitted by an element of volume dv into the solid angle dω under an angle α, at a distance r and at a distance r + dr (Fig.51). Between this, let the elementary volume $dv' = r^2 d\omega dr$ be located. The radiation, originating in dv, thus undergoes two different attenuations within the element dv' (Fig.51):

$$-\frac{\partial}{\partial r}J(r,\alpha)\,dv\,d\omega\,dr = \nu\frac{J(r,\alpha)\,dv\,r^2\,d\omega\,dr}{r^2} + 4\pi\bar{\mu}\frac{J(r,\alpha)\,dv\,r^2\,d\omega\,dr}{r^2},$$

where the first term denotes the energy loss by absorption and the second term that by diffusion in the volume $r^2 d\omega dr$. From this it follows that

$$-\frac{\partial}{\partial r}J(r,\alpha) = (\nu + k)\,J(r,\alpha), \tag{8}$$

and, after introducing the designation

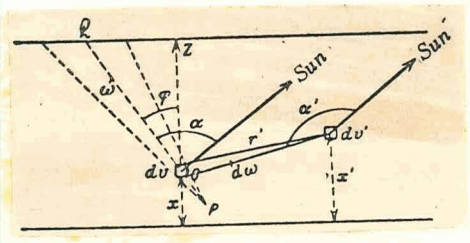

Fig.52 Scattering of Solar Radiation in a Plane-Parallel Bounded Atmosphere.

$$K = \nu + k \tag{9}$$

and integrating

$$J(r, \alpha) = J(0, \alpha)\, e^{-\int_0^r K\, dr}.$$

Let us imagine the gas as bounded by parallel planes (Fig.52) and let us assume the incident rays to be parallel. Then, the position of the volume element dv is defined by a coordinate x, representing the height above the earth's surface. We will write E(x)dv and J(x, r, α)dv if the dependence of the functions E and J on the height of the element dv is to be emphasized.

The radiation, incident on dv, consists of

1) the external amount of radiation E(x)dv of which an amount

$$\mu(\alpha)\, E(x)\, dv\, d\omega$$

is scattered into the solid angle dω;

2) the radiation transmitted by all other volume elements dv′ with the coordinates x′ and the distance r′ from dv, whose intensity is

$$\frac{J(x', r', \alpha')\, dv'}{r'^2}.$$

Of the latter radiation, a component

$$\mu(\widehat{r r'})\, \frac{J(x', r', \alpha')\, dv'\, dv}{r'^2}\, d\omega$$

is scattered into the solid angle dω. This component must be summed over all elements dv′. This yields /211

$$d\omega\, dv \int_{\Sigma} \frac{\mu(\widehat{r r'})\, J(x', r', \alpha')\, dv'}{r'^2},$$

where Σ denotes the total volume of the gas mass.

According to definition, the sum of the components 1) and 2) is equal to J(x, 0, α)dω which is the radiation in the immediate vicinity of dv in the solid angle dω under an angle α to the direction of the solar rays. Thus, we have the integral equation

$$J(x, 0, \alpha) = \mu(\alpha)\, E(x) + \int_{\Sigma} \mu(\widehat{r r'})\, \frac{J(x', 0, \alpha')\, e^{-\int_0^{r'} K\, dr'}}{r'^2}\, dv', \tag{11}$$

if J(x′, r′, α′) is determined by J(x′, 0, α′) according to eq.(10).

As soon as $J(x, 0, \alpha)$ as a function of x is known, which is possible by solving the integral equation (11), the radiation scattered in the solid angle ω toward a point P of the atmosphere can be obtained from the formula

$$T\omega = \omega \int_0^{r_0} J(x, 0, \alpha)\, e^{-\int_0^r K\, dr}\, dr, \tag{12}$$

where PO = r; the function under the integral sign, for a given x, depends on r and α and represents the intensity of the points O in the direction α. Consequently, the integral, extended to $r = r_0 = PQ$, will give the total intensity in the direction PQ while $T\omega$ gives the radiation in this direction contained in the solid angle ω. Thus, this is nothing else but the amount of light coming from a definite sector of the celestial background encompassing the solid angle ω and vertically incident on unit area at the point P.

In eq.(11), we will now substitute the constant mean diffusion constant, i.e., replace $\mu(\alpha)$ and $\mu(\widehat{r, r'})$ by the value $\bar{\mu}$ from eq.(5). In addition, dv' will be replaced by $r'^2 d\omega' dr'$, so that

$$J(x) = \bar{\mu} E(x) + \bar{\mu} \int_{\Sigma'} J(x')\, e^{-\int_0^{r'} K\, dr'}\, d\omega'\, dr'. \tag{13}$$

If we take into consideration that $\frac{\bar{\mu}}{\bar{\mu}_0} = \frac{k}{k_0} = \frac{\nu}{\nu_0} = \frac{K}{K_0} = \frac{\rho}{\rho_0}$ where the subscript 0 characterizes the values of the constants under normal conditions at the earth's surface, then the real atmosphere whose thickness must be imagined as decreasing in parallel layers to a value of zero at $x = \infty$ can be replaced by a homogeneous atmosphere of a density ρ_0. This density corresponds to that at the earth's surface under certain normal conditions. The height of such an atmosphere is given by the equation

$$H = \int_0^{\infty} \frac{\varrho}{\varrho_0}\, dx. \tag{14}$$

Instead of the variables r and x, new variables can be introduced over the transformation equations

$$R = \int_0^r \frac{\varrho}{\varrho_0}\, dr \qquad X = \int_0^x \frac{\varrho}{\varrho_0}\, dx \tag{15}$$

and a value of

/212

$$J(X) = \frac{\varrho_0}{\varrho} J(x), \tag{16}$$

can be used for the function J(x). Then, eq.(13) can be replaced by the following expression:

$$J(X) = \bar{\mu}_0 E(X) + \bar{\mu}_0 \int_{\Sigma} J(X') e^{-K_0 R'} dR' d\omega', \tag{17}$$

which refers to the homogeneous atmosphere having the properties of the lowermost layer of the real atmosphere and being also equivalent to the latter in its optical effect. The meaning of R′ and X′ is shown in Fig.53. The transformation is independent of the law of density decrease.

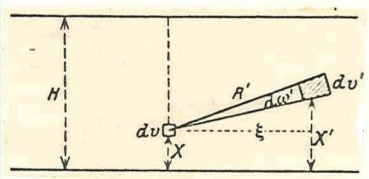

Fig.53 Scattering of Solar Radiation in the Reduced Homogeneous Atmosphere.

Equation (12), by means of the same transformation, changes into

$$T\omega = \omega \int_0^{R_0} J(X) e^{-K_0 R} dR, \tag{18}$$

where

$$R_0 = \int_0^{r_0} \frac{\varrho}{\varrho_0} dr.$$

The integral in eq.(17) must now be formed over all volume elements of a homogeneous atmosphere, extending to infinity as a plane-parallel layer of equal density ρ_0. The integration limits to X are X = 0 and X = H.

In cylindrical coordinates (ξ', ψ'), the expression for $d\omega'$ reads (Fig.53)

$$dR' d\omega' = \frac{dv'}{R'^2} = \frac{dX' \xi' d\xi' d\psi'}{\xi'^2 + (X' - X)^2},$$

where ψ' is the azimuth of the element dv′ with respect to a fixed direction. Now, the integral in eq.(17) assumes the form

$$\int_0^{2\pi} d\psi' \int_0^H J(X')\, dX' \int_0^{\infty} e^{-K_0[\xi'^2 + (X' - X)^2]^{\frac{1}{2}}} \frac{\xi' d\xi'}{\xi'^2 + (X' - X)^2}.$$

Designating

$$K_0[\xi'^2 + (X' - X)^2]^{\frac{1}{2}} = u,$$

so that

$$\frac{\xi' d\xi'}{\xi'^2 + (X' - X)^2} = \frac{du}{u},$$

the last integral will become equal to

$$\int_{K_0(X' - X)}^{\infty} e^{-u} \frac{du}{u} = -li\,(e^{-K_0(X' - X)}),$$

where li is the symbol for the integral logarithm. Since the lower limit of

this integral must be positive, the integration must be performed separately for the points located below the point X at which $X' - X < 0$. Then, eq.(17) will yield

$$J(X) = \bar{\mu}_0 E(X) - \\ -2\pi\bar{\mu}_0\left\{\int_0^X J(X')\,li\,e^{-K_0(X-X')}\,dX' + \int_X^H J(X')\,li\,e^{-K_0(X'-X)}\,dX'\right\}, \tag{19}$$

where the first integral vanishes for points at the earth's surface ($X = 0$).

The next step is to express, in the last equation, the intensity of direct /213 irradiation E(X) by the intensity S of the solar radiation outside the atmosphere. A consideration similar to that leading to eq.(10), when applied to the intensity E(X) and E(X + dX), again yields the exponential law

$$E(X) = Se^{K_0(X-H)\sec\zeta}, \tag{20}$$

where $(H - X)\sec\zeta$ denotes the mean free path in the homogeneous atmosphere. Here, S is the intensity of the solar radiation outside the atmosphere, for a given wavelength, while ζ is the zenith distance of the sun.

Approximate solution of the integral equation (19). Here, eq.(19) is of the Fredholm type of integral equations

$$u(x) = f(x) + \int_{x_1}^{x_2} u(\xi)\,K(x,\xi)\,d\xi, \tag{a}$$

which permits a convenient numerical calculation only for certain values of the kernel $K(x, \xi)$. King used an approximate method, which will be discussed here because of its elegance and usefulness for the diffusion problem.

If the function f(x), for all values of x between x_1 and x_2, is located between the limits of A and a ($A > a$), then in first approximation

$$u(x) \text{ is located between the limiting values } A + A\int_{x_1}^{x_2} K(x,\xi)\,d\xi \quad \text{and} \quad a + a\int_{x_1}^{x_2} K(x,\xi)\,d\xi,$$

assuming that $K(x, \xi)$ is positive everywhere. Using the notation

$$\varphi(x) = \int_{x_1}^{x_2} K(x,\xi)\,d\xi, \tag{b}$$

then, if $\varphi(x)$, for all values of x, is located between the limits B and b ($B > b$), we have $a + ab < u(x) < A + AB$ and, in second approximation,

$$a + (a + ab)b < u(x) < A + (A + AB)B$$

or

$$a(1 + b + b^2) < u(x) < A(1 + B + B^2).$$

On repeating this process as often as desired, it follows that

$$a(1 + b + b^2 + b^3 + \cdots) < u(x) < A(1 + B + B^2 + B^3 + \cdots).$$

If $|B| < 1$, both series will converge and

$$\varepsilon_1 < u(x) < \varepsilon_2, \quad \text{where} \quad \varepsilon_1 = \frac{a}{1-b} \quad \text{and} \quad \varepsilon_2 = \frac{A}{1-B}. \tag{c}$$

On substituting this into eq.(a), the following limits will be obtained for u(x):

$$u_1(x) = f(x) + \varepsilon_1 \varphi(x) \quad \text{and} \quad u_2(x) = f(x) + \varepsilon_2 \varphi(x), \tag{d}$$

where $u_1(x)$ and $u_2(x)$ can be designated as the extreme solutions of the integral equation.

If α denotes the mean value of the function f(x) between x_1 and x_2, i.e., if

$$\alpha = \frac{1}{x_2 - x_1} \int_{x_1}^{x_2} f(x)\,dx, \tag{e}$$

and if β is the mean value of $\varphi(x)$ between the same limits so that /214

$$\beta = \frac{1}{x_2 - x_1} \int_{x_1}^{x_2} \varphi(x)\,dx, \tag{f}$$

and if $\frac{\alpha}{1-\beta}$ is denoted by ε, then $\overline{u}(x) = f(x) + \varepsilon\varphi(x)$ can be called the mean solution of eq.(a). It is obvious that, if the value of $\overline{u}(x)$ differs little from $\frac{1}{2}[u_1(x) + u_2(x)]$ which is the mean value of the extreme solutions, it can be considered a good approximation for the strict solution of the integral equation. Below, we will use this value $\overline{u}(x)$ since the above condition is satisfied for the terrestrial atmosphere, according to King's calculations.

94. Theorems from the Theory of Integral Logarithm and Derived Functions

We have

$$li(e^{-x}) = -\int_x^\infty \frac{e^{-u}}{u}\,du; \tag{A}$$

$$D_x li(e^{-x}) = \frac{e^{-x}}{x}, \tag{B}$$

from which it follows, inversely, by partial integration:

$$\int_0^x li(e^{-\alpha x})\,dx = x\,li(e^{-\alpha x}) + \frac{e^{-\alpha x}-1}{\alpha}. \tag{C}$$

For real values of x, located within the limits $-17 \le x \le 17$, we can use the series

$$li(e^x) = \gamma + \frac{1}{4}\ln x^4 + x + \frac{1}{2}\frac{x^2}{2!} + \frac{1}{3}\frac{x^3}{3!} + \cdots, \tag{D}$$

$$li(e^{-x}) = \gamma + \frac{1}{4}\ln x^4 - x + \frac{1}{2}\frac{x^2}{2!} - \frac{1}{3}\frac{x^3}{3!} + \cdots, \tag{E}$$

where γ denotes the Eulerian constant = 0.577215665.

Let us denote, by f(x), the function

$$f(x) = e^{-x} + x\,li(e^{-x}). \tag{F}$$

After introducing the integration variables φ over the equations

$$u = x\sec\varphi, \qquad du = \frac{x\sin\varphi}{\cos^2\varphi}\,d\varphi$$

the integral $\int_x^\infty \frac{e^{-u}}{u^2}\,du$ will furnish

$$\int_x^\infty \frac{e^{-u}}{u^2}\,du = \frac{1}{x}\int_0^{\pi/2} e^{-x\sec\varphi}\sin\varphi\,d\varphi;$$

$$\int_0^{\pi/2} e^{-x\sec\varphi}\sin\varphi\,d\varphi = x\int_x^\infty \frac{e^{-u}}{u^2}\,du = e^{-x} + x\,li(e^{-x}) = f(x). \tag{G}$$

Hence,

$$f(0) = 1. \tag{H}$$

From eq.(B) it follows that /215

$$(ax)\,d[li(e^{-ax})] = e^{-ax}\,d(ax),$$

$$\int_\infty^c d[li(e^{-ax})]\,ax = \int_\infty^c e^{-ax}\,d(ax) = -e^{-ac}.$$

By partial integration, this yields

$$\int_\infty^c li(e^{-ax})\,dx = \frac{e^{-ac}}{a} + c\,li(e^{-ac}) = \frac{f(ac)}{a}; \tag{I}$$

$$\int_0^c f(u)\,du = \int_0^c e^{-u}\,du + \int_0^c u\,li(e^{-u})\,du = (1-e^{-c}) + \int_0^c u\,du\int_\infty^u \frac{e^{-x}}{x}\,dx =$$

$$= 1 - e^{-c} + \frac{1}{2}c^2 li(e^{-c}) - \frac{1}{2}\int_0^c ue^{-u}du = 1 - e^{-c} + \frac{1}{2}c^2 li(e^{-c})$$

$$+ \frac{1}{2}ce^{-c} - \frac{1}{2}(1 - e^{-c});$$

$$\int_0^c f(u)du = \frac{1}{2}[(1 - e^{-c}) + cf(c)].$$

$$\int_0^c f(ax)e^{-bx}dx = \int_0^c e^{-x(a+b)}dx + a\int_0^c xe^{-bx}li(e^{-ax})dx = \frac{1}{a+b}(1 - e^{-c(a+b)})$$

$$+ a\left\{\left[-\frac{1}{b}e^{-bx}xli(e^{-ax})\right]_0^c + \frac{1}{b}\int_0^c e^{-bx}D_x[xli(e^{-ax})]dx\right\}$$

$$= \frac{1}{a+b}(1 - e^{-c(a+b)}) - \frac{ac}{b}e^{-bc}li(e^{-ac}) + \frac{a}{b}\int_0^c e^{-bx}li(e^{-ax})dx$$

$$+ \frac{a}{b}\int_0^c e^{-x(a+b)}dx = \frac{1}{a+b}(1 - e^{-c(a+b)}) - \frac{ac}{b}e^{-bc}li(e^{-ac})$$

$$- \frac{a}{b^2}e^{-bc}li(e^{-ac}) - \frac{a}{b^2}\int_0^\infty \frac{e^{-ax}}{ax}dx + \frac{a}{b(a+b)}[1 - e^{-c(a+b)}]$$

$$+ \frac{a}{b^2}\int_0^\infty \frac{e^{-x(a+b)}}{x}dx - \frac{a}{b^2}\int_c^\infty \frac{e^{-x(a+b)}}{x}dx = \frac{1}{b}[1 - e^{-bc}f(ac)]$$

$$+ \frac{a}{b^2}\int_0^\infty \frac{e^{-x(a+b)} - e^{-ax}}{x}dx + \frac{a}{b^2}\left\{li[e^{-c(a+b)}] - e^{-bc}li(e^{-ac})\right\}. \qquad (J)$$

Since

$$\int_0^\infty \frac{e^{-\alpha x} - e^{-\beta x}}{x}dx = \ln\frac{\beta}{\alpha},$$

we finally have /216

$$\left.\begin{aligned}\int_0^c e^{-bx}f(ax)dx &= \frac{1}{b}[1 - e^{-bc}f(ac)]\\ &+ \frac{a}{b^2}\left[\ln\frac{a}{(a+b)} - e^{-bc}li(e^{-ac}) + li(e^{-(a+b)c})\right]\\ &= \frac{1}{b}[1 - e^{-bc}f(ac)]\\ &+ \frac{a}{b^2}\left[li(e^{-(a+b)c}) - e^{-bc}li(e^{-ac}) + \ln\frac{(ac)}{(a+b)c}\right].\end{aligned}\right\} \qquad (K)$$

95. Application to the Integral Equation of Diffusion (19)

In the first term of eq.(19), let us re-introduce the dependence of the diffusion on the phase angle α which had been eliminated because of replacement of $\mu_0(\alpha)$ by the coefficient $\bar{\mu}_0$; this will not lead to greater difficulty in

solving the integral equation but will account for the Rayleigh law in the main term. Then, eqs.(19) and (20) after division by $S\mu_0(\alpha)$ will yield

$$\frac{J(X)}{S\mu_0(\alpha)} = e^{-K_0(H-X)\sec\zeta} - \frac{2\pi\bar{\mu}_0}{S\mu_0(\alpha)}\left\{\int_0^X J(X')\,li(e^{-K_0(X-X')})\,dX' + \int_X^H J(X')\,(li\,e^{-K_0(X'-X)})\,dX'\right\}. \tag{21}$$

The sought function u will then be

$$u(X) = \frac{J(X)}{S\mu_0(\alpha)} \tag{22}$$

and

$$\varphi(X) = -2\pi\mu_0\left[\int_0^X li(e^{-K_0(X-X')})\,dX' + \int_X^H li(e^{-K_0(X'-X)})\,dX'\right].$$

According to eqs.(F) and (C) we have

$$-K_0\int_0^X li(e^{-K_0(X-X')})\,dX' = 1 - f(K_0X),$$

$$-K_0\int_X^H li(e^{-K_0(X'-X)})\,dX' = 1 - f[K_0(H-X)]$$

so that

$$\varphi(X) = \frac{1}{2}\frac{k_0}{K_0}\{2 - f(K_0X) - f[K_0(H-X)]\}. \tag{23}$$

The maximum value of $\varphi(X)$, at $X = \frac{H}{2}$, is

$$B = \left\{1 - f\left(\frac{1}{2}C\right)\right\}\frac{c}{C};$$

while the minimum value, at X = 0 and X = H, is

$$b = \frac{1}{2}\{1 - f(C)\}\frac{c}{C}, \tag{24}$$

where we set

$$C = K_0H, \qquad c = k_0H.$$

We have

$$K_0 = k_0 + \nu_0,$$

and denote

$$\gamma = \nu_0H,$$

so that

$$C = c + \gamma. \tag{25}$$

/217

The function f(x) of eq.(a) is $e^{-K_0(H-X)\sec\zeta}$ so that, according to eq.(e)

$$\alpha = \frac{1}{H}\int_0^H e^{-K_0(H-X)\sec\zeta}\,dX = \frac{\cos\zeta}{HK_0}\int_0^{K_0 H\sec\zeta} e^{-y}\,dy = \frac{1-e^{-C\sec\zeta}}{C\sec\zeta}. \tag{26}$$

Introducing the notation

$$G(x) = \frac{1-e^{-x}}{x}, \tag{27}$$

we obtain

$$\alpha = G(C\sec\zeta). \tag{27'}$$

Furthermore, for the mean value of the function $\varphi(X)$ according to eq.(f), we have

$$\beta = \frac{1}{2}\frac{k_0}{K_0}\frac{1}{H}\left[\int_0^H \{1-f(K_0X)\}\,dX + \int_0^H \{1-f[K_0(H-X)]\}\,dX\right] = \frac{1}{C}\frac{c}{C}\left[\int_0^C [1-f(u)]\,du\right].$$

By means of eqs.(J) and (27), we then readily obtain

$$\beta = \frac{c}{C}\left\{1-\frac{1}{2}f(C)-\frac{1}{2}G(C)\right\}. \tag{28}$$

Finally, we find

$$\left.\begin{aligned}
\varepsilon &= \frac{\alpha}{1-\beta} = \frac{G(C\sec\zeta)}{\frac{\gamma}{C}+\frac{1}{2}\frac{c}{C}\{f(C)+G(C)\}},\\
\varepsilon_1 &= \frac{a}{1-b} = \frac{e^{-C\sec\zeta}}{\frac{\gamma}{C}+\frac{1}{2}\left\{f(C)+1\right\}\frac{c}{C}},\\
\varepsilon_2 &= \frac{A}{1-B} = \frac{1}{\frac{\gamma}{C}+f\left(\frac{1}{2}C\right)\frac{c}{C}}.
\end{aligned}\right\} \tag{29}$$

Consequently, the approximate solution of eq.(19) has the form

$$\frac{J(X)}{\mu_0(\alpha)S} = e^{-K_0(H-X)\sec\zeta} + \varepsilon q(X), \tag{30}$$

where $\varphi(X)$ is determined by eq.(23) and where the average solution (29) must be substituted for ε, which always is located between the extreme solutions ε_1 and ε_2.

Then the radiation toward a point on the earth's surface in the direction φ to the vertical will be

$$T\omega = \omega\int_0^{R_0} J(X)\,e^{-K_0R}\,dR. \tag{31}$$

Since R = X sec φ and R_0 = H sec φ, we have

$$T(\varphi,\zeta)=\sec\varphi\int_0^H J(X)\,e^{-K_0X\sec\varphi}\,dX. \tag{32}$$

Conversely, for the radiation toward the outside or toward a point X = H at the boundary of the atmosphere, we obtain

$$R(\varphi,\zeta)=\sec\varphi\int_0^H J(X)\,e^{-K_0(H-X)\sec\varphi}\,dX. \tag{33}$$

Substituting J(X) from eq.(30), the following value is obtained for T(φ, ζ):

$$T(\varphi,\zeta)=\mu_0(\alpha)S\sec\varphi\left\{e^{-K_0H\sec\zeta}\int_0^H e^{-K_0X(\sec\varphi-\sec\zeta)}\,dX+\varepsilon\int_0^H e^{-K_0X\sec\varphi}\varphi(X)\,dX\right\}. \tag{34}$$

The first term assumes the form

$$=e^{-C\sec\zeta}G\left[(\sec\varphi-\sec\zeta)C\right]\frac{C}{K_0},\qquad \text{if}\qquad \varphi>\zeta,$$

and

$$=e^{-C\sec\varphi}G\left[(\sec\zeta-\sec\varphi)C\right]\frac{C}{K_0},\qquad \text{if}\qquad \zeta>\varphi.$$

The second term is transformed by means of eq.(K). First, after substitution of φ(X) from eq.(23), integration, and introduction of the variables K_0X = u, we have

$$\int_0^H e^{-K_0X\sec\varphi}\varphi(X)\,dX=\frac{1}{2}\frac{c}{C}\int_0^H e^{-K_0X\sec\varphi}[2-f(K_0X)-f\{K_0(H-X)\}]\,dX$$
$$=\frac{1}{2}\frac{1}{K_0}\frac{c}{C}\left[\frac{2(1-e^{-C\sec\varphi})}{\sec\varphi}-\int_0^C e^{-u\sec\varphi}f(u)\,du-e^{-C\sec\varphi}\int_0^C e^{u\sec\varphi}f(u)\,du\right].$$

The two integrals are substituted according to the auxiliary equation (K), yielding

$$=\frac{1}{2}\frac{1}{K_0}\frac{c}{C}\left\{\frac{1}{\sec\varphi}[(1-e^{-C\sec\varphi})(1-f(C))]-\frac{1}{\sec^2\varphi}\left[\ln\frac{C}{C(1+\sec\varphi)}\right.\right.$$
$$\left.-e^{-C\sec\varphi}li(e^{-C})+li(e^{-(1+\sec\varphi)C})\right]$$
$$\left.-\frac{e^{-C\sec\varphi}}{\sec^2\varphi}\left[\ln\frac{C}{C(1-\sec\varphi)}-e^{C\sec\varphi}li(e^{-C})+li(e^{-(1-\sec\varphi)C})\right]\right\}$$
$$=\frac{1}{2}\frac{c}{C}\frac{1}{K_0}\frac{1}{\sec\varphi}\Phi(C,\varphi),$$

where

$$\left.\begin{aligned}\Phi(C,\varphi) &= (1-e^{-C\sec\varphi})(1-f(C))\\ &\quad+\cos\varphi\{[li(e^{-C})-\ln C-li(e^{-C(1+\sec\varphi)})+\ln C(1+\sec\varphi)]\\ &\quad+e^{-C\sec\varphi}[li(e^{-C})-\ln(C)-li(e^{-C(1-\sec\varphi)})+\ln C(1-\sec\varphi)]\}\\ &= (1-e^{-C\sec\varphi})(1-f(C))+\cos\varphi\{B(C)-B[C(1+\sec\varphi)]\\ &\quad+e^{-C\sec\varphi}[B(C)-B[-C(\sec\varphi-1)]\},\end{aligned}\right\} \tag{35}$$

after the following notation has been introduced: /219

$$\left.\begin{aligned}B(x) &= li(e^{-x})-\ln x,\\ B(-x) &= li(e^{x})-\ln x.\end{aligned}\right\} \tag{36}$$

The series development for this function B, based on the series (D) and (E), is as follows:

$$\left.\begin{aligned}B(x) &= \gamma - x+\frac{1}{2}\frac{x^2}{2!}-\frac{1}{3}\frac{x^3}{3!}+\cdots,\\ B(-x) &= \gamma + x+\frac{1}{2}\frac{x^2}{2!}+\frac{1}{3}\frac{x^3}{3!}+\cdots.\end{aligned}\right\} \tag{37}$$

For $\varphi = 0$, we obtain

$$\Phi(C,0) = (1-e^{-C})(1-f(C))+B(C)-B(2C)+e^{-C}(B(C)-\gamma). \tag{38}$$

For $\varphi = \frac{\pi}{2}$, we obtain

$$\Phi\left(C,\frac{\pi}{2}\right) = 1-f(C). \tag{39}$$

This furnishes the following final expressions for the intensity of the celestial radiation, from the zenith distance φ at a zenith distance of the sun ζ:

$$\left.\begin{aligned}&\text{at } \zeta>\varphi:\\ &T(\varphi,\zeta) = \frac{\mu_0(\alpha)}{K_0}S\left\{C\sec\varphi\, e^{-C\sec\varphi}G[C(\sec\zeta-\sec\varphi)]+\frac{1}{2}\frac{c}{C}\varepsilon\,\Phi(C,\varphi)\right\},\\ &\text{at } \varphi>\zeta;\\ &T(\varphi,\zeta) = \frac{\mu_0(\alpha)}{K_0}S\left\{C\sec\varphi\, e^{-C\sec\zeta}G[C(\sec\varphi-\sec\zeta)]+\frac{1}{2}\frac{c}{C}\varepsilon\,\Phi(C,\varphi)\right\}.\end{aligned}\right\} \tag{40}$$

Calculation of the coefficient $\frac{\mu_0(\alpha)}{K_0}S$, based on eqs.(2), (6), and (7), will proceed as follows:

$$\left.\begin{aligned}\mu_0(\alpha) &= \frac{3}{4}(1+\cos^2\alpha)\bar{\mu}_0 = \frac{3}{4}(1+\cos^2\alpha)\frac{k_0}{4\pi},\\ \frac{S\mu_0(\alpha)}{K_0} &= \frac{S}{4\pi}\frac{3}{4}(1+\cos^2\alpha)\frac{c}{C}.\end{aligned}\right\} \tag{41}$$

The calculation of the first term of eq.(40) was facilitated by King through

establishing tables for the function G; for the second term, we calculated tables of the function $\Phi(C, \varphi)$ according to eq.(35) which, together with other tables on the theory of illumination of planetary atmospheres, will be discussed later in the text.

For the brightness of the zenith, eq.(40) yields

$$T(0,\zeta)=\frac{\mu_0(\zeta)}{K_0}S\left\{C\,e^{-C}G\left[C(\sec\zeta-1)\right]+\frac{1}{2}\frac{c}{C}\varepsilon\,\Phi(C,0)\right\}, \tag{42}$$

where $\Phi(C, 0)$ has been defined by eq.(38).

For the brightness in the horizon ($\varphi = \pi/2$), we find

$$T\left(\frac{\pi}{2},\zeta\right)=\frac{\mu_0(\alpha)\,S}{K_0}\left\{e^{-C\sec\zeta}+\frac{1}{2}\frac{c}{C}\varepsilon\,\Phi\left(C,\frac{\pi}{2}\right)\right\}, \tag{43}$$

where $\Phi(C, \pi/2)$ is determined by eq.(39).

It is easy to demonstrate on hand of eqs.(40) and (42) that, at low values of C, the approximate relation exists:

$$T(\varphi,\zeta)=\frac{\mu_0(\alpha)}{\mu_0(\zeta)}\sec\varphi\,T(0,\zeta)=\frac{1+\cos^2\alpha}{1+\cos^2\zeta}\sec\varphi\,T(0,\zeta). \tag{44}$$

This formula is sufficiently accurate for calculating the total intensity of /220 diffuse celestial radiation incident on the horizontal area. If this is denoted by $H(\zeta)$, we have

$$H(\zeta)=\int T(\varphi,\zeta)\cos\varphi\,d\omega,$$

where the integral must be extended over the hemisphere. Since $d\omega = \sin\varphi\, d\varphi d\psi$, we obtain

$$H(\zeta)=\int_0^{2\pi}d\psi\int_0^{\pi/2}T(\varphi,\zeta)\cos\varphi\sin\varphi\,d\varphi. \tag{45}$$

Using eq.(44), it follows that

$$H(\zeta)=\frac{T(0,\zeta)}{1+\cos^2\zeta}\int_0^{2\pi}d\psi\int_0^{\pi/2}(1+\cos^2\alpha)\sin\varphi\,d\varphi=\frac{8}{3}\frac{\pi}{1+\cos^2\zeta}T(0,\zeta),$$

and, for the total radiation of all wavelengths,

$$\int_0^{\infty}H(\zeta)\,d\lambda=\frac{8\pi}{3}\frac{1}{1+\cos^2\zeta}\int_0^{\infty}T(0,\zeta)\,d\lambda. \tag{46}$$

If tables for the zenith brightness $T(0, \zeta)$ are calculated according to eq.(42),

then the illumination of the horizontal area can be simply determined from the transmission coefficient according to eq.(46). The error produced by using eq.(44) for low altitudes is insignificant, because of the minor contribution of the radiation from such altitudes.

96. Application of the Theory to the Terrestrial Atmosphere

On hand of these developments, the light distribution in the clear sky as well as the illumination of the horizontal area can be calculated from the known transmission coefficients of the atmosphere. From the values of these quantities for various elements, determined on Mt. Wilson, Mt. Whitney, and in Washington by King, the above-mentioned elements were determined and compared with observations. The results of this extensive work were reported elsewhere (see p.231). Of special interest is the determination of atmospheric density or of the number of molecules per cubic centimeter, obtained in this analysis. This determination is based on the following relations:

The intensity of transmitted solar radiation, for an elevation x above sea level, is as follows:

$$E(X) = S e^{-K_0 (H-X) \sec \zeta}, \tag{47}$$

where

$$K_0 = \nu_0 + k_0.$$

This obeys the exponential law, independent of the cause of the radiation attenuation (absorption or diffusion, combined in the coefficient K). Here, H is the height of the "homogeneous" atmosphere while X is the "reduced height"

$$X = \int_0^x \frac{\varrho}{\varrho_0} dx \qquad \text{and} \qquad H = \int_0^\infty \frac{\varrho}{\varrho_0} dx,$$

i.e.,

$$H - X = \int_x^\infty \frac{\varrho}{\varrho_0} dx,$$

so that

$$\frac{H-X}{H} = \frac{\int_x^\infty \frac{\varrho}{\varrho_0} dx}{\int_0^\infty \frac{\varrho}{\varrho_0} dx} = \frac{B}{B_0},$$

/221

where B and B_0 denote the atmospheric pressure.

On introducing the designation

$$C_x = K_0 H \frac{B}{B_0} = C \frac{B}{B_0},$$

we have

$$E(x) = Se^{-C_x \sec z}. \tag{48}$$

Since, however,

$$C = (\nu_0 + k_0) H = \frac{32}{3} \frac{\pi^3 (n_0 - 1)^2 \lambda^{-4} H}{N_0} + \nu_0 H$$

it follows that

$$C = \beta \lambda^{-4} + \gamma, \quad \text{where} \quad \beta = \frac{\frac{32}{3} \pi^3 (n_0 - 1)^2 H}{N}, \quad \gamma = \nu_0 H. \tag{49}$$

The equation

$$C_x \frac{B_0}{B} = \beta \lambda^{-4} + \gamma \tag{50}$$

stipulates that the values C_x reduced to sea level for various wavelengths, when plotted as ordinates against the abscissa values λ^{-4}, will lie on a straight line with the inclination tangent β. From the value β, according to eq.(49), the number N of particles with Rayleigh scattering can be determined. This has been attempted by various authors and resulted in satisfactory agreement with the number of molecules per cm^3 (see p.233), which constitutes a proof for the fact that the diffusion actually is the predominant cause of extinction in the terrestrial atmosphere and that it mainly proceeds on the molecules of the air. However, a determination of the constant γ for the terrestrial atmosphere has been possible only with limited reliability. The transmission coefficients, suitable for such an investigation, must be freed of the influence of water vapor since the Rayleigh formula no longer applies to this. As shown in Fig.48, the straight line (50) then goes almost strictly through the origin of the coordinate system, which means that γ is very small.

97. Illumination of a Planet Surrounded by an Atmosphere

The statements in Sections 22, 39, 40, and 92 - 95 offer a means for making a photometric analysis of planets of our solar system surrounded by atmospheres. It can be hoped at present that, with respect to the planets Venus, Mars, Jupiter, and Saturn for which monochromatic photography has furnished excellent pictures in recent times, photometry will lift many more veils which, until now, have hidden the consistency of these planetary surfaces.

No systematic investigations of this type were available, so that we can only give a general outline of the possible procedure and facilitate such an investigation by tables given in the Appendix.

After determining the basis of the equations given in Section 40, from the linear coordinates on the planetary disk, the angles of incidence and reflection of the light (i and ε) for the points to be measured and after then determining the azimuths of the reflected ray against the plane of the incident ray with the aid of the phase angle α, it becomes finally possible to start determining the transmission coefficients of the atmosphere of the planets and the reflection law on its surface for individual wavelengths. The former, if the scattering of the light proceeds according to Rayleigh, would lead to a definition of the

/222

Avogadro number for the atmosphere. In the general case, three different causes must be differentiated for interpreting the measured brightnesses, all contributing to the brightness of the rated points:

1) their illumination by the sun, which decreases in accordance with the exponential law with the light path in the atmosphere;
2) attenuation of their brightness on return of the rays through the atmosphere, according to the new light path, and intensification by the brightness of the atmospheric column through which the surface portion is visible;
3) illumination of the measured portion of the surface by the total atmospheric light reaching this portion; this illumination is subject to the changes mentioned under 2) as is also true for direct illumination by the sun.

In Sections 93 - 95, under assumption of Rayleigh scattering, we derived formulas that permit taking also the two last contributions into consideration, provided that the scattering for the corresponding wavelength is not so great that the atmosphere will completely hide the planetary surface. In the latter case, we have to do with an opaque atmosphere scattering according to the Rayleigh law; here, the formula by Fessenkov [eq.(13)] derived for the brightness in Section 22 will be valid. A table of brightnesses according to eq.(13) is given in the Appendix (Table Va). This table is calculated for total scattering (without absorption). For the case of partial absorption, the coefficient of the second term $\pi\mu/k$ will have a lower value; to check on this possibility, tables were compiled that facilitate separate calculation of the second term (Tables Vb and Vc).

In the case of transparent atmospheres or atmospheres transparent only to certain ray classes, the reflection law is of importance for the amount of light reflected from the surface. Only for the case of a cloud surface, formed of droplets, does the law derived in Section 22 [eq.(12)] exist which can be used as basis for a photometric analysis of the surfaces of Venus, Jupiter, and Saturn. Otherwise, the Lambert law is primarily in question. The mentioned formula [eq.(12)] has been tabulated (Table IVa) and is valid for total diffusion; to facilitate the calculations for the case of absorption, Tables IVb can be used.

An element ds of the solid or cloudy plane surface receives direct solar radiation of a certain wavelength λ in an amount of

$$S\cos i\, e^{-K_\lambda H \sec i}\, ds = S\cos i\, e^{-C_\lambda \sec i}\, ds,$$

where i is the angle of incidence of the rays, S the amount of extra-atmospheric solar radiation striking unit surface, H the height of the homogeneous atmosphere and

$$K_\lambda = k_\lambda + \nu_\lambda, \qquad C_\lambda = K_\lambda H,$$

so that C_λ is the attenuation coefficient of the total atmosphere of the planet for the wavelength λ. The same element receives scattered light as the diffuse quantity of light according to eq.(46): /223

$$H_\lambda(i) = \frac{8}{3}\frac{\pi}{1+\cos^2 i}\,T_\lambda(0,i)\,, \tag{51}$$

where

$$T_\lambda(0,i) = \frac{3}{4}\frac{S}{4\pi}\frac{c}{C}(1+\cos^2 i)\left[Ce^{-C}G\{C(\sec i - 1)\} + \frac{1}{2}\frac{c}{C}E(C,i)\,\Phi(C,0)\right]$$

and where E has been substituted for the symbol ε, giving the averaged solution of the integral equation. Here, $T_\lambda(0, i)$ is easy to calculate, at given C_λ, by means of the tables for the functions $Ce^{-C}G[C(\sec\zeta - 1)]$ (Table XIIIa) and $\frac{1}{2}E(C, i)\Phi(C, 0)$ (Tables XIIIc and XIVa). The function $E(C, i)$ of eq.(29) has been calculated here for the case of complete diffusion ($\gamma = 0$; $c = C$), but the resultant error in the term of second order most likely is negligible also in cases in which absorption in the gases becomes noticeable. As argument for using the tables, we already require the quantity C_λ whose determination is primarily involved here. The diffuse illumination thus will be taken into consideration only if an approximate value for C_λ is available. However, this is true also for the brightness of the atmospheric column on the return path of the rays. For these, we have eq.(33); if we introduce, into this equation, the old symbol ε for the reflection angle φ, then we obtain

$$R(\varepsilon, i) = \sec\varepsilon\int_0^H J(X)\,e^{-K_0(H-X)\sec\varepsilon}\,dX\,,$$

where H - X must be substituted by X. This yields

$$R(\varepsilon, i) = \sec\varepsilon\int_0^H J(H-X)\,e^{-K_0 X\sec\varepsilon}\,dX\,.$$

Since, however, according to eq.(23) we have $\varphi(H - X) = \varphi(X)$, the following expression is obtained by means of eq.(30):

$$R(\varepsilon, i) = \mu_0(\alpha)\,S\sec\varepsilon\left[\int_0^H e^{-K_0 X(\sec\varepsilon+\sec i)}\,dX + E\int_0^H e^{-K_0 X\sec\varepsilon}\,\varphi(X)\,dX\right].$$

After integration of the first term and using the integral (35), we have

$$R_\lambda(\varepsilon, i) = \frac{\mu_0(\alpha)S}{K_\lambda}\left[C_\lambda\sec\varepsilon\,G(C_\lambda(\sec\varepsilon+\sec i)) + \frac{1}{2}\frac{c_\lambda}{C_\lambda}E(C_\lambda, i)\,\Phi(C_\lambda, \varepsilon)\right].$$

The two summands in the brackets as well as their sum are given in tables (Tables XIVc, XIVd, and XIVe), again for the case $c_\lambda = C_\lambda$, i.e., for the case of total diffusion. The only unknown in using these tables is the attenuation coefficient C_λ, since even C_λ is eliminated with the aid of the second equation in the system (41) and, for $c_\lambda = C_\lambda$, we obtain

(52)

Thus, for calculating the third component of the brightness, only the value of the attenuation coefficient of the atmosphere for the corresponding wavelength is required. An approximate value for this coefficient can be obtained as follows: Denoting the reflection law on the surface by $\Gamma f(i, \epsilon, A)$ and the attenuation coefficient on the return path of the rays by C'_λ, the quantity of light coming from unit area ds and leaving the atmosphere can be written as /224

$$dq = \Gamma f(i, \varepsilon, A)\, e^{-(C_\lambda \sec i + C'_\lambda \sec \varepsilon)}\, ds$$

while, for the apparent brightness of the corresponding point, we can set

$$h = \Gamma f(i, \varepsilon, A)\, e^{-(C_\lambda \sec i + C'_\lambda \sec \varepsilon)} \sec \varepsilon\,. \tag{53}$$

From the relative brightnesses of two points of the surface compared to a third reference point with the coordinates i_0, ϵ_0, A_0, it is then possible to obtain C_λ and C'_λ by means of equations of the form

$$\ln \frac{h_n}{h_0} - \ln \frac{f(i_n, \varepsilon_n, A_n)}{f(i_0, \varepsilon_0, A_0)} \frac{\sec i_n}{\sec i_0} = -C_\lambda(\sec i_n - \sec i_0) - C'_\lambda(\sec \varepsilon_n - \sec \varepsilon_0)\,, \tag{54}$$

where the number n of the equations must be increased as far as possible by addition of several points. The coefficient C'_λ must be smaller than C_λ since, otherwise, sighting of the surface through the atmosphere would become impossible for a wavelength λ.

With the approximate value C_λ, the second approximation in which complete diffusion for the respective wavelength is assumed, can be calculated as follows: The quantity of light, coming from one point of the surface, is composed of two portions:

$$dq = dq_1 + dq_2,$$

where dq_1 originates in the element ds itself while dq_2 is due to the atmospheric column on the path of the rays. Here, dq_1 has its source, on the one hand, in the direct illumination by solar rays and, on the other hand, in the diffuse illumination of the element

$$dq_1 = dq'_1 + dq''_1.$$

If A_λ denotes the albedo of the surface element for the given wavelength, then $\Gamma = \frac{A_\lambda S}{\pi}$ and

(55)

$$\left.\begin{aligned} dq'_1 &= S\frac{A_\lambda}{\pi} f(i, \varepsilon, A)\, e^{-C_\lambda(\sec i + \sec \varepsilon)}\, ds; \\ dq''_1 &= \frac{A_\lambda}{\pi} H_\lambda(C_\lambda, i)\, e^{-C_\lambda \sec \varepsilon}\, ds = \frac{8}{3}\frac{A_\lambda e^{-C_\lambda \sec \varepsilon}}{1 + \cos^2 i} T_\lambda(0, i)\, ds \\ &= \frac{SA_\lambda}{2\pi} e^{-C_\lambda \sec \varepsilon}\left\{C_\lambda e^{-C_\lambda} G[C_\lambda(\sec i - 1)] + \frac{1}{2} E(C_\lambda, i)\, \Phi(C_\lambda, 0)\right\} ds\,. \end{aligned}\right\} \tag{56}$$

Hence,

$$dq_1 = \frac{SA_\lambda}{\pi} e^{-c_\lambda \sec\varepsilon} \times \left[f(i, \varepsilon, A)\, e^{-c_\lambda \sec i} + \frac{1}{2}\left\{ C_\lambda e^{-c_\lambda} G(C_\lambda(\sec i - 1)) + \frac{1}{2} E(C_\lambda, i)\, \Phi(C_\lambda, 0) \right\} \right]. \tag{57}$$

The quantity of light dq_2 is obtained from the intensity $R(\varepsilon, i)$ according to eq.(52):

$$dq_2 = \frac{3}{16\pi} S(1 + \cos^2\alpha) \left[C_\lambda \sec\varepsilon\, G(C_\lambda(\sec\varepsilon + \sec i)) + \frac{1}{2} E(C_\lambda, i)\, \Phi(C_\lambda, \varepsilon) \right] ds. \tag{58}$$

The measured brightnesses are then obtained from the equation

$$h = \frac{dq_1 + dq_2}{ds} \sec\varepsilon. \tag{59}$$

This calculation, since it assumes complete scattering of the light, can lead to a useful result only in the case of ray classes for which this assumption is valid. This leads to a more accurate value of C_λ, in which case also the albedo A_λ of the surface for the wavelength λ must be obtained. Photographs in the region of wavelengths which show an absorption in addition to the scattering must be reduced according to the general formula for dq_1'' and dq_2. In this case, we have /225

$$\left.\begin{aligned} T_\lambda(0, i) &= S \frac{3}{16\pi}(1 + \cos^2 i) \frac{c_\lambda}{C_\lambda} \left[C_\lambda e^{-c_\lambda} G\{C_\lambda(\sec i - 1)\} + \frac{1}{2} \frac{c_\lambda}{C_\lambda} E\, \Phi(C_\lambda, 0) \right] \\ &= \frac{3}{16\pi} S(1 + \cos^2 i) c_\lambda \left[e^{-c_\lambda} G\{C_\lambda(\sec i - 1)\} + \frac{c_\lambda}{C_\lambda^2} E\, \Phi(C_\lambda, 0) \right] \end{aligned}\right\} \tag{60}$$

and

$$dq_1'' = \frac{S}{2\pi} A_\lambda e^{-c_\lambda \sec\varepsilon} c_\lambda \left[e^{-c_\lambda} G\{C_\lambda(\sec i - 1)\} + \frac{c_\lambda}{C_\lambda^2} E(C_\lambda, i)\, \Phi(C_\lambda, 0) \right] ds. \tag{61}$$

Similarly, we obtain for dq_2,

$$dq_2 = \frac{3}{16\pi} S(1 + \cos^2\alpha) c_\lambda \left[\sec\varepsilon\, G\{C_\lambda(\sec\varepsilon + \sec i)\} + \frac{1}{2} \frac{c_\lambda}{C_\lambda^2} E(C_\lambda, i)\, \Phi(C_\lambda, \varepsilon) \right] ds. \tag{62}$$

Here, not only A_λ, C_λ but also c_λ are determined by successive approximations, in which case the fraction $\frac{c_\lambda}{C_\lambda^2}$, in calculating dq_1'' and dq_2, can be set equal to 1.

After the values C_λ have been determined in this manner for several values of λ, they must satisfy the following equation, which is linear with respect to λ^{-4}:

$$C_\lambda = \beta \lambda^{-4} + \gamma_\lambda \tag{63}$$

where

$$\beta = \frac{\frac{32}{3}\pi^3 (n_0 - 1)^2 H}{N} \tag{64}$$

and

$$\gamma_\lambda = r_\lambda H = C_\lambda - c_\lambda . \tag{65}$$

From this, $\frac{(n_0 - 1)^2 H}{N}$ and c_λ are determined. A value for the height of the homogeneous atmosphere is impossible to obtain from this theory since it neglects the curvature of the atmospheric layers. One possibility is to use the Bouguer extinction formula [eq.(25)] from p.203. If, in eq.(53), the second term of Bouguer's formula for the light path is used and if we write

$$h = \Gamma f(i, \varepsilon, A)\, e^{-C_\lambda (\sec i - b \sec i \tan^2 i) - C'_\lambda (\sec \varepsilon - b \sec \varepsilon \tan^2 \varepsilon)} \sec \varepsilon ,$$

one could attempt to use the relative brightnesses of points with widely differing i and ε, with the aid of the equations

$$\left.\begin{aligned} \ln \frac{h_n}{h_0} - \ln \frac{f(i_n, \varepsilon_n, A_n)}{f(i_0, \varepsilon_0, A_0)} \frac{\sec i_n}{\sec i_0} &= -C_\lambda (\sec i_n - \sec i_0) - C'_\lambda (\sec \varepsilon_n - \sec \varepsilon_0) \\ &+ C_\lambda b (\sec i_n \tan^2 i_n - \sec i_0 \tan^2 i_0) + C'_\lambda b' (\sec \varepsilon_n \tan^2 \varepsilon_n - \sec \varepsilon_0 \tan^2 \varepsilon_0) \end{aligned}\right\} \tag{66}$$

for determining also the coefficients b and b′, of which the former has a value of

$$b = \frac{H}{R} ,$$

where R denotes the radius of the planet. If it should be possible to find a value for H in this manner, only the value of the refractive index would have to be determined for obtaining the Avogadro number N, which is of great importance for the physics of planetary atmospheres.

98. Comparison of the Illumination Theories of Planetary Atmospheres

/226

A comparison of eqs.(12) and (13) for diffuse reflections with eq.(52) of this Section readily shows their close relationship. The latter formula has the Rayleigh diffusion formula as a basis in common with eq.(13) but refers to the case of a transparent layer, whereas eq.(12) is valid for an opaque body with plane boundaries, especially for an opaque gas atmosphere whose curvature can be neglected. However, when converted to the case of opacity, eq.(52) would not lead to the form of eq.(12) since the diffusion in the terms of higher order had been assumed as uniform in all directions. Rather, an extension of eq.(13)

$$\left.\begin{aligned} q &= L\, d\sigma \frac{\cos i \cos \varepsilon}{\cos i + \cos \varepsilon} \frac{\mu}{k} \times \\ &\times \left\{ 1 + \cos^2 \alpha + \frac{\pi \mu}{k} \left[A'_1 a_1 + C'_1 c_1 + E'_1 e_1 + \frac{\pi \mu}{k} (\text{third term}) \right] \right\} \end{aligned}\right\} \tag{67}$$

to terms of the third and higher order would lead to an entirely strict Rayleigh reflection theory for opaque bodies. That a consideration of terms of higher order of diffusion is of great importance is demonstrated by a comparison of the

two first terms in our tables. In the case of total diffusion, the second term is not less than 45% of the first term, and only at lower values of the coefficient $\pi\mu/k$, i.e., in the presence of absorption, will the convergence of the series (66) become more rapid. However, the value of the coefficient $\pi\mu/k$ and that of the higher terms has a considerable influence on the limb darkening of a planet surrounded by an atmosphere. In this respect, our tables are highly instructive. Let us consider the numerals along the diagonal in Table Va, corresponding to the brightnesses in opposition ($i = \epsilon$, $A = 0$); it will be found that the uniform brightness of the fully illuminated planetary disk, which would be obtained when considering only the first term of the diffusion (see Table Vb), vanishes on carrying the second term and that a slight fall-off of light along the limb occurs. Consideration of the third term, which necessarily must be positive, would further increase this limb darkening. This leads to the important theorem: An atmosphere, scattering light in Rayleigh's sense, at total diffusion and full illumination, will lead to a limb darkening at the outermost edge of about 20%. However, in practical application such darkening will not be noticeable since it starts only at a distance of 0.01 R to 0.02 R from the limb.

The conditions change rapidly in the direct neighborhood of opposition. The intensity ratios are especially complex in the case of an atmosphere surrounded by clouds, in accordance with eq.(12) (Table IVa). Here, where the diffusion diagram is asymmetric for the individual droplet with preponderance of the radiation in the direction $\alpha = 180^{\circ}$, an extreme dependence of the luminous intensity on the azimuth occurs which, at greater angles of incidence, becomes increasingly stronger. The brightness contrasts on reflection from a cloud surface built up of larger particles are so extensive that it should not be difficult to differentiate and separate them from the Rayleigh scattering in the gases of the atmosphere, during photometric analysis.

99. Recent Investigations in this Field

The last decades and especially the last oppositions of the planet Mars have furnished abundant and frequently excellent observational material for a photometric analysis of the planet surfaces. We merely mention here the photographs taken of Mars and Jupiter by W.H.Wright (Ref.252) with a Crossley re- /227
flector, the photographs taken by R.J.Trümpler (Ref.253) with the large reflector of Lick Observatory, the photographs of the planet Venus by Frank E.Ross (Ref.254), and the older photographs of Jupiter and Saturn by R.Wood (Ref.255). In all these photographs, light filters were used. The photographs show a number of surprising and instructive phenomena which would never have been discovered in visual observations of the planets. These entirely new phenomena have greatly increased the interest in research on the physical nature of planets. In addition, numerous attempts were made at a theoretical interpretation of the phenomena, despite the fact that the difficulty of such an interpretation was generally recognized. Let us mention here only the most important of these newly discovered facts.

1) The limb darkening, in all of the above-mentioned planets, differs for different filters; the degree and dependence of this darkening on the wavelength of the filters is individual for each planet.

2) The structure of the surface is more distinct for long-wave rays in the case of Mars, Jupiter, and Saturn whereas surface configurations are recognizable only on violet photographs for Venus while a uniform light fall-off without any structure can be seen on red photographs.

3) The diameter of Mars and Venus* appears larger for the violet rays than for the red rays, with the difference for Mars being 3% of the diameter between the wavelengths 440 and 760 μμ. The increase in diameter was confirmed also for smaller wavelength differences by Trümpler who found a difference of 0.86% between 560 and 600 μμ.

4) The two Saturn-ring halves A and B show entirely different brightness ratios that depend on the wavelength; in ultraviolet rays, they are uniformly bright, with Cassini's division disappearing completely.

Especially the phenomenon, mentioned under 3), which would give a height of more than 100 km for the light-scattering atmosphere of Mars, started a theoretical debate on the atmosphere problem. V.Fessenkov and D.H.Menzel (Ref.256, 257) found that such an extent of a gaseous atmosphere over the surface of Mars contradicts the conditions of aerostatic equilibrium; they were inclined to believe that the luminescence of the atmosphere at this height is due to a layer of extremely thin haze which reflects only ultraviolet light. The ultraviolet photographs of Mars, except for the polar cap of the planet, mostly show no structure and thus represent pictures of its atmosphere that are especially suitable for a photometric analysis according to our formulas. The considerations by V.Fessenkov and those by D.H.Menzel on the intensity of atmospheric radiation, in view of the neglections made by both authors and in view of the hypotheses they were forced to introduce, are not suitable for solving the problem as to the extent of the Martian atmosphere. A detailed study of photographs in as monochromatic as possible a light will constitute a task for the future which will not be discouraged by the difficulties of the problem; after all, it is of extreme importance to explore the nature of our nearest neighbors in the sky about which we know less at present than about distant fixed stars.

---

* For the latter planet, the phenomenon has been confirmed in unpublished visual measurements at the Breslau Observatory.

Contents and Explanations

TABLE Ia(p.270- 274)

This table is used for converting from magnitude class differences $m - m_0$ to brightness ratios I/I_0 and vice versa, according to the formula

$$\frac{I}{I_0} = 2.512^{m_0 - m} \quad \text{or} \quad \frac{I}{I_0} = \text{Numlog}\,[(m_0 - m)\ 0.4].$$

The table extends to $m - m_0 = 5^m.0$.

TABLE Ib (p.275)

This table gives I_0/I according to the same argument $m - m_0$ for the values of $m - m_0 = 5^m.0$ to $10^m.0$.

TABLE IIa (p.276)

This table is used for converting the readings of the Zöllner photometer circle in magnitude classes, where it is assumed that a reading of $5^\circ.0$ on the circle corresponds to a brightness of $0^m.0$ and that the magnitude classes increase with the brightnesses. If the index error of the circle is zero or eliminated, it follows from Malus' law that $\frac{I_1}{I_2} = \frac{\sin^2\alpha_1}{\sin^2\alpha_2}$, where I_1 and I_2 are the brightnesses corresponding to the readings α_1 and α_2 of the circle. Therefore, the table was calculated according to the formula

$$m = 5(\log\sin\alpha - \log\sin 5^\circ.0).$$

TABLE IIb (p.278)

This table gives the brightnesses I in the Zöllner photometer according to the argument α (reading of the circle) on the absolute scale, in units of maximum brightness occurring at a reading of $\alpha = 90^\circ.0$ (index error of the circle, equal to 0).

TABLE III (according to E.Hertzsprung, NAT 2, No.1) (p.280)

This table is used for determining the magnitude class of a binary m_{AB} if the values of the components m_A and m_B of this star are given. Conversely, the table can be used also for determining the magnitude classes m_A and m_B from the total brightness m_{AB} and the difference $m_A - m_B$. The table was calculated according to the equation

$$m_A - m_{AB} = 2.5 \log \{1 + \mathrm{Numlog}\,[0.4\,(m_A - m_B)]\}$$

directly obtained from an addition of the absolute brightness values according to eq.(27) on p.18. Example: The brightnesses of the components of Castor are $m_A = 1.99$; $m_B = 2.85$; $m_B - m_A = 0.86$. This value lies between 0.862 and 0.830 of the table so that $m_A - m_{AB} = 0.41$ corresponds to it. Consequently, $m_{AB} = 1.99 - 0.41 = 1.58$. Conversely, if $m_{AB} = 1.58$ and $m_A - m_B = 0.86$ are given, we can find $m_A - m_{AB} = 0.41$ and $m_A = (m_A - m_{AB}) + m_{AB} = 1.99$, $m_B = m_A + (m_B - m_A) = 1.99 + 0.86 = 2.85$.

TABLE IVa (p.281) /229

This table is used for calculating the brightnesses according to eq.(12) on p.48 for diffuse reflection which, at the values of the constants $p = 2.7$, $q = 3.0$, corresponds to the reflection on a cloud layer with plane boundaries. These brightnesses, except for the constant $\mu L/k$, are equal to

$$h = \frac{\cos i}{\cos i + \cos \varepsilon}\left\{1 - p\cos\alpha + q\cos^2\alpha + \frac{\pi\mu}{k}[A_1 a_1 - B_1 b_1 + C_1 c_1 + D_1 d_1 + E_1 e_1]\right\}$$

and were calculated for $p = 2.7$, $q = 3.0$ and complete diffusion, to which the maximum value

$$\frac{\pi\mu}{k} = \frac{1}{2.6}$$

corresponds.

TABLE IVb (p.283)

This table gives the values of the coefficients a_1, b_1, c_1, d_1, e_1 of the same formula [eq.(12)] on p.48

$$a_1 = [\cos i \ln(1 + \sec i) + \cos\varepsilon \ln(1 + \sec\varepsilon)],$$
$$b_1 = [\cos i + \cos\varepsilon - \cos^2 i \ln(1 + \sec i) - \cos^2\varepsilon \ln(1 + \sec\varepsilon)],$$
$$c_1 = [\tfrac{1}{2}(\cos i + \cos\varepsilon) - (\cos^2 i + \cos^2\varepsilon) + \cos^3 i \ln(1 + \sec i) + \cos^3\varepsilon \ln(1 + \sec\varepsilon)],$$
$$d_1 = [\tfrac{1}{3}(\cos i + \cos\varepsilon) - \tfrac{1}{2}(\cos^2 i + \cos^2\varepsilon) + \cos^3 i + \cos^3\varepsilon - \cos^4 i \ln(1 + \sec i) - \cos^4\varepsilon \ln(1 + \sec\varepsilon)],$$
$$e_1 = [\tfrac{1}{4}(\cos i + \cos\varepsilon) - \tfrac{1}{3}(\cos^2 i + \cos^2\varepsilon) + \tfrac{1}{2}(\cos^3 i + \cos^3\varepsilon) - \cos^4 i - \cos^4\varepsilon + \cos^5 i \ln(1 + \sec i) + \cos^5\varepsilon \ln(1 + \sec\varepsilon)].$$

TABLE Va (p.284)

This table is used for calculating the brightnesses according to eq.(13) on p.48 for diffuse reflection. These brightnesses, except for the constant factor $\mu L/k$, are equal to

$$h = \frac{\cos i}{\cos i + \cos\varepsilon}\left[1 + \cos^2\alpha + \frac{\pi\mu}{k}(A_1' a_1 + C_1' c_1 + E_1' e_1)\right]$$

and were calculated with the maximum value $\frac{\pi\mu}{k} = \frac{3}{16}$ for complete diffusion.

The coefficients a_1, c_1, and e_1 have the same value as in eq.(12) on p.48 and are tabulated in Table IVb.

TABLE Vb (p.286)

This table contains the value of the first term of eq.(13) on p.48, according to the arguments of i as angle of incidence, ε as angle of reflection, and A_0 as azimuth. The first term in parentheses in eq.(13) reads

$$1 + \cos^2\alpha = 1 + (\cos i \cos\varepsilon + \sin i \sin\varepsilon \cos A_0)^2,$$

and the table was calculated according to this formula.

TABLE Vc (p.288)

This table contains the second term of eq.(13) on p.48, multiplied by the maximum value of the coefficient $\frac{\pi\mu}{k} = \frac{3}{16}$ (total diffusion). The table can be converted for smaller values of the coefficient on multiplying by a corresponding factor and, together with the preceding table, can serve for forming eq.(13) in the presence of absorption. Thus, the table contains the values

$$\frac{3}{16}[A'_1 a_1 + C'_1 c_1 + E'_1 e_1],$$

where A'_1, B'_1, C'_1 have the values given on p.48 while the coefficients a_1, c_1, and e_1 are tabulated in Table IVb.

TABLE VIa (p.290) /230

This table contains the phase curves $\varphi_1(\alpha)$ and $\varphi_2(\alpha)$ according to Lambert and Seeliger in eq.(7) on p.72 and eq.(12) on p.73 for reduction of the opposition brightness q_1° and q_2° of a planet to the brightness at a phase angle α

$$q_1 = q_1^\circ \frac{\sin\alpha + (\pi - \alpha)\cos\alpha}{\pi} = q_1^\circ \varphi_1(\alpha) \text{ accd. to Lambert,}$$

$$q_2 = q_2^\circ \left(1 - \sin\frac{\alpha}{2} \tan\frac{\alpha}{2} \ln\cot\frac{\alpha}{4}\right) = q_2^\circ \varphi_2(\alpha) \text{ accd. to Seeliger,}$$

where q_1, q_2, q_1°, q_2° are brightnesses reduced to a constant distance from both earth and sun.

TABLE VIb and TABLE VIc (p.291)

These tables contain auxiliary quantities for the amount of light reflected from an ellipsoid of revolution, according to Seeliger and calculated from eq.(22) on p.75:

$$Q_1 = 2\pi J A_1 \sin^2 s \sin^2\sigma \cos\alpha \,(P\cos^2 A + R\sin^2 A) \quad \text{on assumption of Lambert's law,}$$

$$Q_2 = \frac{\pi}{2} J A_2 \sin^2 s \sin^2\sigma \,\varphi_2(\alpha) \sqrt{1 + \frac{a^2 - b^2}{b^2}\sin^2 A} \quad \text{" " " Seeliger's "}$$

where A is the quadrant angle of elevation of the earth above the plane of the planetary equator. Table VIb gives the quantities P and R which are exclusively dependent on the axial ratio $\frac{a}{b}$. Table VIc is used for reducing the brightness of Saturn at A = 0 and α = 0 to the brightness at α and A $\neq$ 0. The table is based on the axial ratio $\frac{a}{b}$ = 1.1222 and gives the following quantities, dependent on the elevation angle A:

$$Z = P\cos^2 A + R\sin^2 A, \qquad Z(A) = \frac{Z}{P} = \cos^2 A + \frac{R}{P}\sin^2 A$$

and

$$X(A) = \sqrt{1 + \frac{a^2 - b^2}{b^2}\sin^2 A}$$

in eqs.(25) on p.77):

$$Q_1 = Q_1^0(0)\,\frac{\sin^2 s \sin^2\sigma}{\sin^2 s_0 \sin^2\sigma_0}\,Z(A)\cos\alpha$$

and

$$Q_2 = Q_2^0(0)\,\frac{\sin^2 s \sin^2\sigma}{\sin^2 s_0 \sin^2\sigma_0}\,\varphi_2(\alpha)\,X(A).$$

TABLE VIIa (p.292)

This table gives the values of the function $\mathfrak{G}(\xi) = \xi \int_0^{\pi/2} e^{-\xi\varphi}\cos\varphi\, d\varphi + \frac{8}{3} e^{-\xi\frac{3\pi-2}{8\pi}}$ (eq.15) p.168 where $\xi = \frac{N\delta}{\sin\alpha} = \frac{8D}{\sin\alpha}$ is a function of the volume density D and of the phase angle α. This function $\mathfrak{G}(\xi)$ is used for reducing the surface brightness of the ring to the moment α = 0 in eq.(16) on p.169. The function is given in the table in the form $M = \frac{\mathfrak{G}(\infty)}{\mathfrak{G}(\xi)}$ according to the argument ξ, where $\mathfrak{G}(\infty) = \frac{16}{3}$.

TABLE VIIb (p.293)

This table gives the logarithm of the same function $\log M = \log \frac{\mathfrak{G}(\infty)}{\mathfrak{G}(\alpha)}$ according to the two arguments ξ and α and is used for determining the volume density from the brightness of the ring measured at different values of the phase angle.

TABLE VIIc (p.293) /231

This table contains the measured mean brightnesses of the rings B and A of Saturn, obtained from observations during 1914 - 1918 (see Fig.42, p.177). These brightnesses are expressed in unit brightness of the center of the Saturn disk and can be used for reducing the total brightness of the Saturn system to the vanished ring as phase curve of the surface brightness of the ring $\frac{1}{M} = \mathfrak{C}(\alpha)$. In this case, the formula $Q_B = Q_0(0)\left[\Gamma \frac{\sin A + \sin A'}{\sin A} X\mathfrak{C}(\alpha) + YD\right]$ for total brightness must be used in eq.(36) on p.170, while the constant Γ, which is the ratio of the surface brightness of the ring to the Saturn center at $\alpha = 0$, must be given the value $\Gamma = 0.891$ (see p.163).

TABLE VIIIa (p.294)

This table contains the values for the visible (unocculted) portion of the ring X and the Saturn disk Y, necessary for reducing the Saturn brightnesses to the vanished ring according to eq.(36) on p.170, both expressed in units of the full Saturn disk. A small table gives the values of the phase curve $D = \varphi_2(\alpha)$ for the case of Seeliger's law.

TABLE VIIIb (p.295)

This table contains the quantities X_L and Y_L which are equivalent to the quantities X and Y given in the preceding table; however, here they are valid for the assumption of a Lambert light distribution over the Saturn disk. In addition, the phase curve $\varphi_1(\alpha)$ for the Lambert law, which reduces to a value $\cos\alpha$ because of the smallness of the phase angle, is given in a table.

TABLE IXa (p.296)

This table contains auxiliary quantities for calculating the shadow-casting of the ring on the visible Saturn disk and of the planet on the visible portion of the ring. According to the argument A, which is the elevation angle of the earth above the plane of the ring, this table gives the value of the minor axis of the visible planetary ellipse

$$b' = a\sqrt{1 - e^2\cos^2 A}$$

and the auxiliary angle φ which is determined by eq.(39) on p.172: $\tan\varphi = \frac{b'}{a}\sqrt{\frac{\alpha^2 - a^2}{b^2 - \beta^2}}$ where α and β denote the major and minor axes of the outer ring boundary. The fourth column gives the angle v_0 determined from eq.(42) on p.172: $\tan v_0 = \sin A \tan\varphi$. The fifth column gives the auxiliary angle $\varphi' = v_{1V}$ (see p.175), calculated according to the formula

$$\tan\varphi' = \frac{b'}{a}\sqrt{\frac{\alpha'^2 - a^2}{b'^2 - \beta^2}}$$

where α' is the major axis of the internal boundary of the ring. The angle v_0' corresponds to the angle v_0 but refers to the inner boundary of the ring and is not needed here. The last column contains the auxiliary quantity $c = \frac{\sin A}{ab \cdot 180}$ which is used for calculating the shadow-casting of the planet on the ring.

TABLE IXb (p.297)

This table contains the auxiliary quantities $\log \Sigma_0$, $\log \Sigma_1$, $\log \Sigma$, and $\log V$ for calculating the shadow-casting of the Saturn ring on the planet, according to the argument A = elevation angle of the earth above the ring plane. If A′ denotes the elevation of the sun above the same plane, then

$$\delta A = A' - A,$$

and the occulted area S will be:

in the case I [eq.(40), p.172] $S = \delta A\,(\Sigma_1 - \Sigma_0) = \delta A\,\Sigma,$

in the case II [eqs.(44) and (45), p.173] $S = S(v_1) - S(v_2)$ resp. $= S(v_2) - S(v_0),$

depending on which value will be positive. The values S(v) must be calculated according to the formulas

$$\begin{aligned} S(v_1) &= \Sigma_1\,\delta A + lV, \\ S(v_0) &= \Sigma_0\,\delta A + lV, \\ S(v_2) &= \frac{\alpha^2}{2}\cos A\,\delta A\,(\psi + \tan^2 A \tan\psi), \end{aligned}$$

where

$$\tan\psi = \frac{l \sin A \cos A}{\delta A}.$$

/232

The area S, determined in this manner and after referring it to the total area πab as unit, is subtracted as

$$\Delta Y = \frac{S}{\pi\, a b}$$

from the visible area Y.

TABLE IXc (according to Seeliger, p.298)

This table contains the auxiliary quantities for calculating the shadow-casting of Saturn on the ring, according to eqs.(51) on p.175, for the four different cases:

$$\begin{aligned} \text{a)}\quad \Delta X &= \frac{l\,\alpha'^2\,c}{2} - \delta A\,\lambda(a) + c\sigma(v^*). \\ \text{b)}\quad \Delta X &= -\frac{l(\alpha^2 - \alpha'^2)}{2}\,c + \delta A\,\lambda(b). \\ \text{c)}\quad \Delta X &= \frac{l\,\alpha'^2\,c}{2} + \delta A\,\lambda(c) + c\sigma(v^*). \\ \text{d)}\quad \Delta X &= 2\,\delta A\,\lambda(b). \end{aligned}$$

The quantities c are contained in Table IXa, while $\lambda(a)$, $\lambda(b)$, and $\lambda(c)$ are given in Table IXc. The tables are so arranged that i and δA are expressed in straight lines and their fractions, with the former always assumed as negative. With respect to calculating $\sigma(v^*)$ and for sequence of the calculations, see p.176.

TABLE Xa (according to G.Müller, p.299)

This table contains the values of the mean extinction for the visual brightnesses of the stars for Potsdam (elevation 100 m) and the summit of Säntis (2500 m). The tabular data are purely empirical, in view of the fact that the compensation of the observed brightnesses was done graphically, without the use of any theory. The Potsdam values, however, correspond to Bouguer's formula up to a zenith distance of 80° at a mean transmission coefficient p = 0.835; for greater zenith distances they are based on observations on especially clear evenings and thus correspond to a higher value of the transmission coefficient. The values obtained for the Säntis are based on observations of one and the same stars down to the horizon and thus can be considered as homogeneous in themselves.

TABLE Xb (according to Müller, p.300)

This table contains the same extinction values for Potsdam as the preceding table, but for greater zenith distances between 50° and 88°, in steps of tenth to tenth degree.

TABLE XIa (p.301)

The table is a mean extinction table established by Bemporad for 0°C and 760 mm pressure at sea level, calculated with the transmission coefficient p = = 0.835 according to the formula

$$\text{Ext.} = m_z - m_0 = -\frac{\log p}{0.4}\{F(z) - 1\},$$

where F(z), representing the traversed air mass, has been assumed according to Bemporad's expansion of this function (see p.217).

TABLE XIb (according to Bemporad, p.302)

This table contains the corrections of the extinction for pressure and temperature, at zenith distances of 87°, 88°, and 89° for which these corrections become noticeable. The values of the tables were calculated by means of Tables XIIb and XIIc which contain corrections for the transmission coefficient p and for the air masses F(z) as a function of pressure and temperature, and correct the values of Table XIa.

TABLE XIIa (p.303) /233

This table, just like Table XIa, refers to normal conditions of pressure and temperature at sea level (760 mm and 0°C) and contains the values of the function F(z) calculated by Bemporad on the basis of his own theory (see

pp.209ff), which expresses the air mass traversed by the ray with the apparent zenith distance z. The height of the homogeneous atmosphere or the unit force F(z), in this theory, is

$$\lambda = \int_0^H \frac{\varrho}{\varrho_0}\, dh = 8.0109 \text{ km}$$

while the height of the total atmosphere is H = 43 km, with the constant temperature gradient of 6°.22 (Schmidt's hypotheses); see also Sections 80 and 81, pp.209ff.

TABLE XIIb (according to Bemporad, p.308)

This table contains the corrections of the air masses F(z) of the preceding table for pressure and temperature at zenith distances of 87°, 88°, and 89° in which they become first noticeable.

TABLE XIIc (according to Bemporad, p.308)

This table gives the variations of log p with temperature and pressure, according to the formula

$$\log p = \frac{\lambda_t}{\lambda_0} \frac{B}{760} \frac{1}{1 + mt} \log p_0 ,$$

where log p represents the value referring to the changed temperature and pressure conditions (t and B).

TABLE XIIIa (according to L.V.King, p.309)

This table contains the auxiliary quantity

$$C e^{-c} G\{C(\sec\zeta - 1)\},$$

where the function G(x) is defined by the equation

$$G(x) = \frac{1 - e^{-x}}{x} .$$

This occurs in King's diffusion theory and has been tabulated by him in the form given here. Its accuracy is 1 - 2 units of the third significant figure.

TABLE XIIIb (according to L.V.King, p.309)

This table contains the function G(C sec ζ) which occurs in the mean solution of the integral equation of diffusion (ε) in eq.(29) on p.247 and is given after elimination of a few minor computational errors and addition of the column for ζ = 85°, according to L.V.King.

TABLE XIIIc (according to L.V.King, p.309)

This table, according to the argument C (attenuation coefficient), contains the functions

$$f(C) = C\int_C^\infty u^{-2}e^{-u}\,du = e^{-C} + C\,li(e^{-C}),$$ see eq. (G) on p.244,

$$G(C) = \frac{1 - e^{-C}}{C}$$

and

$$\Phi(C, 0) = (1 - e^{-C})\{1 - f(C)\} + B(C) - B(2C) + e^{-C}[B(C) - \gamma],$$ eq. (38) on p.249 ($\gamma = 0.5772$).

TABLES XIV /234

These tables, referring to the theory of illumination of planetary atmospheres, were calculated here for the first time, based on Tables XIII. They refer to the equations given in Sections 97 and 98. In these tables, the conventional notation for the angle of incidence and angle of reflection of the light i and ε are used instead of the angles ζ and φ in King's theory; in addition E(C, i) is used for the mean solution of the integral equation of diffusion, instead of ε in eq.(29).

TABLE XIVa (p.310)

This table gives the values of the function

$$E(C, i) = \frac{G(C\sec i)}{\frac{1}{2}\{f(C) + G(C)\}},$$

corresponding to the function ε in eq.(29) at $\gamma = 0$, $C = c$. The table permits calculating the functions T(0, i) and R(ε, i) into which E(C, i) enters.

TABLE XIVb (p.310)

This table contains the values of the function $\Phi(C, \varepsilon)$ in eq.(35) on p.248

$$\Phi(C, \varepsilon) = (1 - e^{-C\sec\varepsilon})(1 - f(C)) + \cos\varepsilon\{B(C) - B(C(1 + \sec\varepsilon)) + e^{-C\sec\varepsilon}[B(C) - B(-C(\sec\varepsilon - 1))]\},$$

according to the arguments C and ε, and serves for calculating the function $R_\lambda(\varepsilon, i)$ according to eq.(52) on p.254.

TABLE XIVc (p.311)

This table gives the first summands in the brackets of the function $R_\lambda(\varepsilon, i)$ according to eq.(52) on p.254, which here is designated by

$$R'(C, \varepsilon, i) = C\sec\varepsilon\, G(C(\sec\varepsilon + \sec i)).$$

The arguments are C, ϵ, and i. The table is to serve for calculating the function $R_\lambda(\epsilon, i)$ in the case of absorption since, in this case, the second term of $R_\lambda(\epsilon, i)$ contained in the following table undergoes a change.

TABLE XIVd (p.312)

This table gives the values of the function

$$\tfrac{1}{2}\Phi(C, \varepsilon)\, E(C, i),$$

according to three arguments C, ϵ, and i where E(C, i) is taken from Table XIVa and is valid for the case of total diffusion [eq.(52) on p.254].

TABLE XIVe (p.313)

This table contains the sums of the corresponding values of the two preceding tables and, to within the factor $\frac{3S}{16\pi}(1 + \cos^2\alpha)$, offers the values of the function

$$R(\varepsilon, i) = \frac{3S}{16\pi}(1 + \cos^2\alpha)\left[R'(C, \varepsilon, i) + \frac{1}{2}\Phi(C, \varepsilon)\, E(C, i)\right]$$

for various values of C, ϵ, and i and for the case of total diffusion.

TABLE Ia

BRIGHTNESS RATIO I/I_0 ACCORDING TO THE ARGUMENT $m - m_0$

$m-m_0$	0	1	2	3	4	5	6	7	8	9
0.00	1.0000	*991	*982	*972	*963	*954	*945	*936	*927	*918
1	0.9908	899	890	881	872	863	854	845	836	827
2	.9818	809	800	791	782	773	764	755	746	737
3	.9728	719	710	701	692	683	674	665	656	647
4	0.9638	629	620	612	603	594	585	577	568	559
5	.9550	541	532	524	515	506	497	489	480	471
6	.9462	453	445	436	428	419	411	402	393	385
7	0.9376	367	359	350	342	333	325	316	308	299
8	.9290	281	273	264	256	247	239	230	222	213
9	.9204	196	188	180	171	163	154	146	137	129
0.10	0.9120	112	104	096	087	079	070	062	053	045
1	.9036	028	020	012	003	*995	*987	*978	*970	*962
2	.8954	945	937	929	921	912	904	896	888	880
3	.8872	863	855	847	839	831	823	815	806	798
4	0.8790	782	774	766	758	750	742	734	726	718
5	.8710	702	694	686	678	670	662	654	646	638
6	.8630	622	614	606	598	590	582	574	566	559
7	0.8551	543	535	527	513	511	504	496	488	480
8	.8472	464	457	449	441	433	426	418	410	402
9	.8395	387	379	371	364	356	348	341	333	325
0.20	0.8318	310	302	295	287	279	272	264	257	249
1	.8241	234	226	219	211	204	196	188	181	173
2	8166	158	151	143	136	128	121	113	106	098
3	.8091	084	076	069	061	054	046	039	032	024
4	0.8017	009	002	*995	*987	*980	*973	*965	*958	*951
5	7943	936	929	921	914	907	900	892	885	878
6	7871	863	856	849	841	834	827	820	813	806
7	0.7798	791	784	777	770	762	755	748	741	734
8	.7727	720	713	706	698	691	684	677	670	663
9	.7656	649	642	635	628	621	614	607	600	593
0.30	0.7586	579	572	565	558	551	544	537	530	523
1	.7516	509	502	496	489	482	475	468	461	454
2	7447	440	434	427	420	413	406	400	393	386
3	.7379	372	366	359	352	345	338	332	325	318
4	0.7311	305	298	291	284	278	271	264	258	251
5	.7244	238	231	224	218	211	204	198	191	184
6	.7178	171	165	158	152	145	138	132	125	119
7	0.7112	106	099	092	086	080	073	066	060	053
8	.7047	040	034	028	021	014	008	002	*995	*989
9	.6982	976	970	963	957	950	944	938	931	925
0.40	0.6918	912	906	899	893	886	880	874	868	861
1	.6855	849	842	836	830	823	817	811	805	798
2	.6792	786	780	773	767	761	755	748	742	736
3	.6730	724	717	711	705	699	693	686	680	674
4	0.6668	662	656	650	644	637	631	625	619	613
5	.6607	601	595	589	583	577	570	564	558	552
6	.6546	540	534	528	522	516	510	504	498	492
7	0.6486	480	474	468	462	457	451	445	439	433
8	.6427	421	415	409	403	397	391	386	380	374
9	.6368	362	356	350	345	339	333	327	321	315
0.50	0.6310	304	298	292	286	281	275	269	263	257
$m-m_0$	0	1	2	3	4	5	6	7	8	9

TABLE Ia (continued)

BRIGHTNESS RATIO I/I_0 ACCORDING TO THE ARGUMENT $m - m_0$

$m-m_0$	0	1	2	3	4	5	6	7	8	9
0.50	0.6310	304	298	292	286	281	275	269	263	257
1	.6252	246	240	234	229	223	217	212	206	200
2	.6194	189	183	177	172	166	160	155	149	143
3	.6138	132	126	121	115	109	104	098	093	087
4	0.6081	076	070	065	059	053	048	042	037	031
5	.6026	020	014	009	003	*998	*992	*987	*981	*976
6	.5970	965	959	954	948	943	937	932	927	921
7	0.5916	910	905	899	894	888	883	878	872	867
8	.5861	856	850	845	840	834	829	824	818	813
9	.5808	802	797	792	786	781	776	770	765	760
0.60	0.5754	749	744	738	733	728	723	717	712	707
1	.5702	696	691	686	681	675	670	665	660	655
2	.5649	644	639	634	629	623	618	613	608	603
3	.5598	592	587	582	577	572	567	562	556	551
4	0.5546	541	536	531	526	521	516	511	506	500
5	.5495	490	485	480	475	470	465	460	455	450
6	.5445	440	435	430	425	420	415	410	405	400
7	0.5395	390	385	380	375	370	365	360	355	350
8	.5346	341	336	331	326	321	316	311	306	301
9	.5297	292	287	282	277	272	267	262	257	252
0.70	0.5248	243	238	234	229	224	219	214	210	205
1	.5200	195	190	186	181	176	171	166	162	157
2	.5152	147	143	138	133	129	124	119	115	110
3	.5105	100	096	091	086	082	077	072	068	063
4	0.5058	053	049	044	040	035	031	026	022	017
5	.5012	007	003	*998	*993	*989	*984	*980	*975	*970
6	.4966	961	957	952	948	943	939	934	929	925
7	0.4920	916	911	907	902	898	893	889	884	880
8	.4875	871	866	862	857	853	848	844	839	835
9	.4831	826	822	817	813	808	804	800	795	791
0.80	0.4786	782	777	773	769	764	760	756	751	747
1	.4742	738	734	729	725	721	716	712	708	703
2	.4699	695	690	686	682	677	673	669	664	660
3	.4656	652	647	643	639	634	630	626	622	617
4	0.4613	609	605	600	596	592	588	584	579	575
5	.4571	567	562	558	554	550	546	542	537	533
6	.4529	525	521	516	512	508	504	500	496	492
7	0.4487	483	479	475	471	467	463	459	454	450
8	.4446	442	438	434	430	426	422	418	414	410
9	.4406	402	398	394	390	385	381	377	373	369
0.90	0.4365	361	357	353	349	345	341	337	333	329
1	.4325	321	317	313	309	305	301	297	293	289
2	.4285	281	277	273	270	266	262	258	254	250
3	.4246	242	238	234	230	227	223	219	215	211
4	0.4207	203	200	196	192	188	184	180	176	172
5	.4169	165	161	157	153	150	146	142	138	134
6	.4130	127	123	119	115	112	108	104	100	096
7	0.4093	089	085	081	078	074	070	066	063	059
8	.4055	051	048	044	040	036	033	029	025	022
9	.4018	014	011	007	003	*999	*996	*992	*988	*985
1.00	0.3981	977	947	970	966	963	959	955	952	948
$m-m_0$	0	1	2	3	4	5	6	7	8	9

TABLE Ia (continued)

BRIGHTNESS RATIO I/I_0 ACCORDING TO THE ARGUMENT $m - m_0$

$m-m_0$	0	1	2	3	4	5	6	7	8	9
1.00	0.3981	977	974	970	966	963	959	955	952	948
1	.3945	941	937	934	930	926	923	919	916	912
2	.3908	905	901	898	894	890	887	883	880	876
3	.3873	869	865	862	858	855	851	848	844	841
4	0.3837	834	830	826	823	819	816	812	809	805
5	.3802	798	795	791	788	784	781	777	774	770
6	.3767	764	760	757	753	750	746	743	739	736
7	0.3732	729	726	722	719	715	712	708	705	702
8	.3698	695	692	688	685	681	678	674	671	668
9	.3664	661	658	654	651	648	644	641	638	634
1.10	0.3631	627	624	621	617	614	611	607	604	601
1	.3598	594	591	588	584	581	578	574	571	568
2	.3564	561	558	555	551	548	545	542	538	535
3	.3532	529	525	522	519	516	512	509	506	503
4	0.3499	496	493	490	487	483	480	477	474	471
5	.3467	464	461	458	455	451	448	445	442	439
6	.3436	432	429	426	423	420	417	414	410	407
7	0.3404	401	398	395	392	388	385	382	379	376
8	.3373	370	367	364	360	357	354	351	348	345
9	.3342	339	336	333	330	327	324	320	317	314
1,20	0.3311	308	305	302	299	296	293	290	287	284
1	.3281	278	275	272	269	266	263	260	257	254
2	.3251	248	245	242	239	236	233	230	227	224
3	.3221	218	215	212	209	206	203	200	197	194
4	0.3192	189	186	183	180	177	174	171	168	165
5	.3162	159	156	154	151	148	145	142	139	136
6	.3133	130	128	125	122	119	116	113	110	107
7	0.3105	102	099	096	093	090	087	085	082	079
8	.3076	073	070	068	065	062	059	056	054	051
9	.3048	045	042	040	037	034	031	028	026	023
1.30	0.3020	017	014	012	009	006	003	001	*998	*995
1	.2992	990	987	984	981	979	976	973	970	968
2	.2965	962	959	957	954	951	948	946	943	940
3	.2938	935	932	930	927	924	921	919	916	913
4	0.2911	908	905	903	900	897	895	892	889	887
5	.2884	881	879	876	873	871	868	866	863	860
6	.2858	855	852	850	847	844	842	839	837	834
7	0.2831	829	826	824	821	818	816	813	811	808
8	.2805	803	800	798	795	793	790	787	785	782
9	.2780	777	775	772	770	767	764	762	759	757
1,40	0.2754	752	749	747	744	742	739	737	734	732
1	.2729	726	724	721	719	716	714	711	709	706
2	.2704	701	699	696	694	692	689	687	684	682
3	.2679	677	674	672	669	667	664	662	660	657
4	0.2655	652	650	647	645	642	640	638	635	633
5	.2630	628	625	623	621	618	616	613	611	609
6	.2606	604	601	599	597	594	592	589	587	585
7	0.2582	580	578	575	573	570	568	566	563	561
8	.2559	556	554	552	549	547	544	542	540	537
9	.2535	533	530	528	526	523	521	519	517	514
1,50	0.2512	510	507	505	503	500	498	496	493	491
$m-m_0$	0	1	2	3	4	5	6	7	8	9

TABLE Ia (continued)

BRIGHTNESS RATIO I/I_0 ACCORDING TO THE ARGUMENT $m - m_0$

$m-m_0$	0	1	2	3	4	5	6	7	8	9
1.50	0.2512	510	507	505	503	500	498	496	493	491
1	.2489	487	484	482	480	477	475	473	471	468
2	.2466	464	462	459	457	455	452	450	448	446
3	.2443	441	439	437	434	432	430	428	426	423
4	0.2421	419	417	414	412	410	408	405	403	401
5	.2399	397	394	392	390	388	386	383	381	379
6	.2377	375	372	370	368	366	364	362	359	357
7	0.2355	353	351	349	346	344	342	340	338	336
8	.2333	331	329	327	325	323	321	318	316	314
9	.2312	310	308	306	304	301	299	297	295	293
1.60	0.2291	289	287	285	282	280	278	276	274	272
1	.2270	268	266	264	262	259	257	255	253	251
2	.2249	247	245	243	241	239	237	235	233	231
3	.2228	226	224	222	220	218	216	214	212	210
4	0.2208	206	204	202	200	198	196	194	192	190
5	.2188	186	184	182	180	178	176	174	172	170
6	.2168	166	164	162	160	158	156	154	152	150
7	0.2148	146	144	142	140	138	136	134	132	130
8	.2128	126	124	122	120	118	116	114	113	111
9	.2109	107	105	103	101	099	097	095	093	091
1.70	0.2089	087	085	084	082	080	078	076	074	072
1	.2070	068	066	064	063	061	059	057	055	053
2	.2051	049	047	045	044	042	040	038	036	034
3	.2032	030	029	027	025	023	021	019	017	016
4	0.2014	012	010	008	007	005	003	001	*999	*997
5	.1995	993	992	990	988	986	984	982	980	979
6	.1977	975	974	972	970	968	966	964	962	961
7	0.1959	957	956	954	952	950	948	946	944	943
8	.1941	939	938	936	934	932	930	928	926	925
9	.1923	921	920	918	916	914	912	910	908	907
1.80	0.1905	904	902	900	898	897	895	893	891	890
1	.1888	887	885	883	881	880	878	876	874	873
2	.1871	870	868	866	864	863	861	859	857	856
3	.1854	853	851	849	847	846	844	842	840	839
4	0.1837	836	834	832	830	829	827	825	823	822
5	.1820	819	817	815	813	812	810	808	806	805
6	.1803	802	800	798	796	795	793	791	789	788
7	0.1786	785	783	782	780	778	777	775	773	772
8	.1770	769	767	766	764	762	761	759	757	756
9	.1754	753	751	750	748	746	745	743	741	740
1.90	0.1738	737	735	734	732	730	729	727	725	724
1	.1722	721	719	718	716	714	713	711	709	708
2	.1706	705	703	702	700	698	697	695	693	692
3	.1690	688	687	685	684	682	681	679	678	676
4	0.1675	673	672	670	669	667	666	664	663	661
5	.1660	659	657	656	654	652	651	649	647	646
6	.1644	642	641	639	638	636	635	633	632	630
7	0.1629	627	626	624	623	621	620	618	617	615
8	.1614	613	611	610	608	607	605	604	603	601
9	.1600	598	597	595	594	592	591	589	588	586
2.00	0.1585	583	582	580	579	577	576	574	573	572
$m-m_0$	0	1	2	3	4	5	6	7	8	9

TABLE Ia (continued)

BRIGHTNESS RATIO I/I_0 ACCORDING TO THE ARGUMENT $m - m_0$

$m-m_0$	0	1	2	3	4	5	6	7	8	9
2.0.	0.1585	0.1570	0.1556	0.1542	0.1528	0.1514	0.1500	0.1486	0.1472	0.1459
1	.1445	.1432	.1419	.1406	.1393	.1380	.1368	.1355	.1342	.1330
2	.1318	.1306	.1294	.1282	.1271	.1259	.1247	.1236	.1225	.1213
3	.1202	.1191	.1180	.1170	.1159	.1148	.1137	.1127	.1117	.1107
4	0.1096	0.1086	0.1076	0.1067	0.1057	0.1047	0.1038	0.1028	0.1019	0.1009
5	.1000	.0991	.0982	.0973	.0964	.0955	.0946	.0938	.0929	.0920
6	.0912	.0904	.0895	.0887	.0879	.0871	.0863	.0855	.0847	.0839
7	0.0832	0.0824	0.0817	0.0809	0.0802	0.0794	0.0787	0.0780	0.0773	0.0766
8	.0759	.0752	.0745	.0738	.0731	.0724	.0718	.0711	.0705	.0698
9	.0692	.0685	.0679	.0673	.0667	.0661	.0656	.0649	.0643	.0637
3.0	0.0631	0.0625	0.0619	0.0614	0.0608	0.0603	0.0597	0.0592	0.0586	0.0581
1	.0575	.0570	.0565	.0560	.0555	.0550	.0545	.0540	.0535	.0530
2	.0525	.0520	.0515	.0511	.0506	.0501	.0497	.0492	.0488	.0483
3	.0479	.0474	.0470	.0466	.0461	.0457	.0453	.0449	.0445	.0441
4	0.0437	0.0433	0.0429	0.0425	0.0421	0.0417	0.0413	0.0409	0.0406	0.0402
5	.0398	.0394	.0391	.0387	.0384	.0380	.0377	.0373	.0370	.0366
6	.0363	.0360	.0356	.0353	.0350	.0347	.0344	.0340	.0337	.0334
7	0.0331	0.0328	0.0325	0.0322	0.0319	0.0316	0.0313	0.0310	0.0308	0.0305
8	.0302	.0299	.0296	.0294	.0291	.0288	.0286	.0283	.0281	.0278
9	.0275	.0273	.0270	.0268	.0265	.0263	.0261	.0258	.0256	.0254
4.0	0.0251	0.0249	0.0247	0.0244	0.0242	0.0240	0.0238	0.0236	0.0233	0.0231
1	.0229	.0227	.0225	.0223	.0221	.0219	.0217	.0215	.0213	.0211
2	.0209	.0207	.0205	.0203	.0201	.0200	.0198	.0196	.0194	.0192
3	.0191	.0189	.0187	.0185	.0184	.0182	.0180	.0179	.0177	.0175
4	0.0174	0.0172	0.0171	0.0169	0.0167	0.0166	0.0164	0.0163	0.0161	0.0160
5	.0158	.0157	.0156	.0154	.0153	.0151	.0150	.0149	.0147	.0146
6	.0145	.0143	.0142	.0141	.0139	.0138	.0137	.0136	.0134	.0133
7	0.0132	0.0131	0.0129	0.0128	0.0127	0.0126	0.0125	0.0124	0.0122	0.0121
8	.0120	.0119	.0118	.0117	.0116	.0115	.0114	.0113	.0112	.0111
9	.0110	.0109	.0108	.0107	.0106	.0105	.0104	.0103	.0102	.0101
5.0	0.0100	.0099	.0098	.0097	.0096	.0095	.0095	.0094	.0093	.0092

TABLE Ib

/240

BRIGHTNESS RATIO I_o/I ACCORDING TO THE ARGUMENT $m - m_o$

$m-m_o$	0	1	2	3	4	5	6	7	8	9
5.0	100.00	100.93	101.86	102.80	103.75	104.71	105.68	106.66	107.65	108.64
5.1	109.65	110.66	111.69	112.72	113.76	114.82	115.88	116.95	118.03	119.12
5.2	120.23	121.34	122.46	123.60	124.74	125.89	127.06	128.23	129.42	130.62
5.3	131.83	133.05	134.28	135.52	136.77	138.04	139.32	140.61	141.91	143.22
5.4	144.54	145.88	147.23	148.59	149.97	151.36	152.76	154.17	155.60	157.04
5.5	158.49	159.96	161.44	162.93	164.44	165.96	167.49	169.04	170.61	172.19
5.6	173.78	175.39	177.01	178.65	180.30	181.97	183.65	185.35	187.07	188.80
5.7	190.55	192.31	194.09	195.88	197.70	199.53	201.37	203.24	205.12	207.01
5.8	208.93	210.86	212.81	214.78	216.77	218.78	220.80	222.84	224.91	226.99
5.9	229.09	231.21	233.35	235.51	237.68	239.88	242.10	244.34	246.60	248.89
6.0	251.19	253.51	255.86	258.23	260.62	263.03	265.46	267.92	270.40	272.90
6.1	275.42	277.97	280.54	283.14	285.76	288.40	291.07	293.77	296.48	299.23
6.2	302.00	304.79	307.61	310.46	313.33	316.23	319.15	322.11	325.09	328.10
6.3	331.13	334.20	337.29	340.41	343.56	346.74	349.95	353.18	356.45	359.75
6.4	363.08	366.44	369.83	373.25	376.70	380.19	383.71	387.26	390.84	394.46
6.5	398.11	401.79	405.51	409.26	413.05	416.87	420.73	424.62	428.55	432.51
6.6	436.52	440.56	444.63							
6.7	478.63	483.06	487.53	492.04	496.59	501.19	505.83	510.51	515.23	520.00
6.8	524.81	529.66	534.56	539.51	544.50	549.54	554.63	559.76	564.94	570.16
6.9	575.44	580.76	586.14	591.56	597.04	602.56	608.14	613.76	619.44	625.17
7.0	630.96	636.80	642.69	648.63	654.64	660.69	666.81	672.98	679.20	685.49
7.1	691.83	698.23	704.69	711.21	717.79	724.44	731.14	737.90	744.73	751.62
7.2	758.58	765.60	772.68	779.83	787.05	794.33	801.68	809.10	816.58	824.14
7.3	831.76	839.46	847.23	855.07	862.98	870.96	879.02	887.16	895.37	903.65
7.4	912.01	920.45	928.97	937.56	946.24	954.99	963.83	972.75	981.75	990.83
7.5	1000.0	1009.3	1018.6	1028.0	1037.5	1047.1	1056.8	1066.6	1076.5	1086.4
7.6	1096.5	1106.6	1116.9	1127.2	1137.6	1148.2	1158.8	1169.5	1180.3	1191.2
7.7	1202.3	1213.4	1224.6	1236.0	1247.4	1258.9	1270.6	1282.3	1294.2	1306.2
7.8	1318.3	1330.5	1342.8	1355.2	1367.7	1380.4	1393.2	1406.1	1419.1	1432.2
7.9	1445.4	1458.8	1472.3	1485.9	1499.7	1513.6	1527.6	1541.7	1556.0	1570.4
8.0	1584.9	1599.6	1614.4	1629.3	1644.4	1659.6	1674.9	1690.4	1706.1	1721.9
8.1	1737.8	1753.9	1770.1	1786.5	1803.0	1819.7	1836.5	1853.5	1870.7	1888.0
8.2	1905.5	1923.1	1940.9	1958.8	1977.0	1995.3	2013.7	2032.4	2051.2	2070.1
8.3	2089.3	2108.6	2128.1	2147.8	2167.7	2187.8	2208.0	2228.4	2249.1	2269.9
8.4	2290.9	2312.1	2333.5	2355.1	2376.8	2398.8	2421.0	2443.4	2466.0	2488.9
8.5	2511.9	2535.1	2558.6	2582.3	2606.2	2630.3	2654.6	2679.2	2704.0	2729.0
8.6	2754.2	2779.7	2805.4	2831.4	2857.6	2884.0	2910.7	2937.7	2964.8	2992.3
8.7	3020.0	3047.9	3076.1	3104.6	3133.3	3162.3	3191.5	3221.1	3250.9	3281.0
8.8	3311.3	3342.0	3372.9	3404.1	3435.6	3467.4	3499.5	3531.8	3564.5	3597.5
8.9	3630.8	3664.4	3698.3	3732.5	3767.0	3801.9	3837.1	3892.6	3908.4	3944.6
9.0	3981.1	4017.9	4055.1	4092.6	4130.5	4168.7	4207.3	4246.2	4285.5	4325.1
9.1	4365.2	4405.6	4446.3	4487.5	4529.0	4570.9	4613.2	4655.9	4698.9	4742.4
9.2	4786.3	4830.6	4875.3	4920.4	4965.9	5011.9	5058.3	5105.1	5152.3	5200.0
9.3	5248.1	5296.6	5345.6	5395.1	5445.0	5495.4	5546.3	5597.6	5649.4	5701.6
9.4	5754.4	5807.6	5861.4	5915.6	5970.4	6025.6	6081.4	6137.6	6194.4	6251.7
9.5	6309.6	6368.0	6426.9	6486.3	6546.4	6606.9	6668.1	6729.8	6792.0	6854.9
9.6	6918.3	6982.3	7046.9	7112.1	7177.9	7244.4	7311.4	7379.0	7447.3	7516.2
9.7	7585.8	7656.0	7726.8	7798.3	7870.5	7943.3	8016.8	8091.0	8165.8	8241.4
9.8	8317.6	8394.6	8472.3	8550.7	8629.8	8709.6	8790.2	8871.6	8953.7	9036.5
9.9	9120.1	9204.5	9289.7	9375.6	9462.4	9549.9	9638.3	9727.5	9817.5	9908.3
10.0	10000									
$m-m_o$	0	1	2	3	4	5	6	7	8	9

TABLE IIa

MAGNITUDE CLASSES IN THE ZÖLLNER PHOTOMETER, INCREASING WITH BRIGHTNESS, ACCORDING TO THE ARGUMENT: READING OF THE CIRCLE α IN DEGREES AND TENTH DEGREES

(The magnitude class $0^m.000$ has been assumed at the reading $5^\circ.0$)

α°	.0	.1	.2	.3	.4	.5	.6	.7	.8	.9	1.0	α°
4	−0.484	−0.430	−0.378	−0.327	−0.277	−0.228	−0.180	−0.134	−0.088	−0.044	∓0.000	4
5	∓0.000	+0.043	.085	.126	.166	.206	.246	.284	.321	.358	.394	5
6	.394	.430	.466	.500	.534	.568	.601	.634	.666	.697	.728	6
7	.728	.759	.789	.818	.848	.877	.906	.934	.962	.989	1.016	7
8	1.016	1.043	1.070	1.096	1.122	1.147	1.172	1.197	1.222	1.246	.270	8
9	.270	.294	.317	.341	.364	.386	.409	.432	.454	.476	.497	9
10	1.497	1.518	1.539	1.560	1.581	1.602	1.622	1.642	1.662	1.682	1.702	10
11	.702	.721	.740	.759	.778	.797	.816	.834	.852	.870	.888	11
12	.888	.906	.923	.940	.958	.975	.992	2.009	2.026	2.042	2.059	12
13	2.059	2.076	2.092	2.108	2.124	2.140	2.155	1.70	.186	.202	.217	13
14	.217	.232	.247	.262	.277	.292	.306	.322	.337	.351	.364	14
15	.364	.377	.391	.405	.418	.432	.446	.460	.473	.487	.501	15
16	.501	.513	.526	.539	.552	.564	.577	.590	.603	.616	.629	16
17	.629	.641	.653	.665	.677	.689	.701	.713	.725	.737	.749	17
18	.749	.760	.771	.783	.794	.805	.817	.828	.839	.851	.862	18
19	.862	.872	.883	.894	2.904	2.915	2.926	2.936	2.947	2.958	2.969	19
20	2.969	2.979	2.989	2.999	3.009	3.019	3.029	3.039	3.049	3.059	3.070	20
21	3.070	3.080	3.090	3.099	.109	.118	.128	.138	.147	.157	.167	21
22	.167	.177	.186	.195	.204	.213	.222	.231	.240	.249	.258	22
23	.258	.266	.275	.284	.292	.301	.310	.318	.327	.336	.345	23
24	.345	.353	.361	.370	.378	.386	.395	.403	.411	.420	.428	24
25	.428	.436	.444	.452	.460	.468	.476	.484	.492	.500	.508	25
26	.508	.516	.524	.532	.539	.547	.554	.562	.569	.577	.584	26
27	.584	.591	.598	.605	.613	.620	.627	.634	.642	.649	.657	27
28	.657	.664	.671	.678	.685	.692	.699	.706	.713	.720	.727	28
29	.727	.733	.740	.747	.753	.760	.767	.773	.780	.787	.793	29
30	3.793	3.800	3.806	3.813	3.819	3.825	3.832	3.838	3.844	3.851	3.858	30
31	.858	.864	.870	.876	.883	.889	.895	.901	.907	.914	.920	31
32	.920	.926	.932	.938	.944	.950	.956	.962	.968	.974	.979	32
33	.979	.984	.990	.996	4.002	4.007	4.013	4.019	4.025	4.031	4.037	33
34	4.037	4.043	4.048	4.054	.059	.065	.070	.076	.081	.087	.092	34
35	.092	.097	.102	.108	.113	.118	.124	.129	.135	.140	.145	35
36	.145	.151	.156	.161	.166	.171	.176	.181	.186	.191	.196	36
37	.196	.200	.205	.210	.215	.220	.225	.230	.235	.240	.245	37
38	.245	.250	.254	.259	.164	.269	.274	.278	.283	.288	.293	38
39	.293	.297	.302	.306	.311	.315	.320	.324	.329	.334	.339	39
40	4.339	4.343	4.348	4.352	4.357	4.361	4.366	4.370	4.374	4.378	4.383	40
41	.383	.387	.392	.396	.401	.405	.409	.413	.418	.422	.426	41
42	.426	.430	.435	.439	.443	.447	.451	.455	.459	.463	.467	42
43	.467	.471	.475	.479	.483	.487	.491	.495	.499	.503	.507	43
44	.507	.511	.515	.519	.523	.527	.531	.534	.538	.542	.546	44
45	.546	.550	.554	.557	.561	.565	.569	.572	.576	.579	.583	45
46	.583	.586	.590	.594	.598	.601	.605	.608	.612	.615	.619	46
47	.619	.622	.626	.629	.633	.636	.640	.643	.647	.650	.654	47
48	.654	.657	.661	.664	.667	.670	.674	.677	.681	.684	.687	48
49	.687	.690	.694	.697	.700	.703	.707	.710	.714	.717	.720	49
50	4.720	4.723	4.726	4.729	4.732	4.735	4.739	4.742	4.745	4.748	4.751	50
51	.751	.754	.757	.760	.763	.766	.769	.772	.775	.778	.781	51
52	.781	.784	.787	.790	.793	.796	.799	.801	.804	.807	.810	52
53	.810	.813	.816	.819	.822	.824	.827	.830	.833	.835	.838	53

TABLE IIa (continued)

α°	.0	.1	.2	.3	.4	.5	.6	.7	.8	.9	1.0	α°
54	.838	.841	.844	.846	.849	.852	.855	.857	.860	.862	.865	54
55	.865	.868	.871	.873	.876	.878	.881	.883	.886	.888	.891	55
56	.891	.893	.896	.898	.901	.903	.906	.908	.911	.913	.916	56
57	.916	.918	.921	.923	.926	.928	.931	.933	.936	.938	.941	57
58	.941	.943	.945	.947	.950	.952	.954	.956	.959	.961	.964	58
59	.964	.966	.968	.970	.973	.975	.977	.979	.982	.984	.986	59
60	4.986	4.988	4.990	4.992	4.995	4.997	4.999	5.001	5.003	5.005	5.007	60
61	5.007	5.009	5.012	5.014	5.016	5.018	5.020	.022	.024	.026	.028	61
62	.028	.030	.032	.034	.036	.038	.040	.042	.044	.046	.048	62
63	.048	.050	.052	.053	.055	.057	.059	.061	.063	.065	.067	63
64	.067	.068	.070	.072	.074	.076	.078	.080	.081	.083	.085	64
65	.085	.087	.088	.090	.092	.094	.095	.097	.099	.101	.102	65
66	.102	.104	.105	.107	.109	.111	.112	.114	.115	.117	.118	66
67	.118	.120	.122	.123	.125	.127	.128	.130	.131	.133	.134	67
68	.134	.136	.137	.139	.140	.142	.143	.145	.146	.148	.149	68
69	.149	.151	.152	.154	.155	.156	.158	.159	.160	.162	.163	96
70	5.163	5.165	5.166	5.167	5.169	5.170	5.171	5.173	5.174	5.175	5.176	70
71	.176	.178	.179	.180	.182	.183	.184	.186	.187	.188	.189	71
72	.189	.191	.192	.193	.194	.196	.197	.198	.199	.200	.201	72
73	.201	.203	.204	.205	.206	.207	.208	.209	.211	.212	.213	73
74	.213	.214	.215	.216	.217	.218	.219	.220	.221	.222	.223	74
75	.223	.224	.225	.226	.227	.228	.229	.230	.231	.232	.233	75
76	.233	.234	.235	.236	.236	.237	.238	.239	.240	.241	.242	76
77	.242	.243	.244	.245	.245	.246	.247	.248	.249	.250	.250	77
78	.250	.251	.252	.253	.253	.254	.255	.256	.256	.257	.258	78
79	.258	.259	.259	.260	.261	.262	.262	.263	.264	.265	.265	79

TABLE IIb

BRIGHTNESSES IN THE ZÖLLNER PHOTOMETER, IN UNITS OF MAXIMUM BRIGHTNESS ON READING THE CIRCLE = 90°

Argument: reading of circle

°	,0		,1		,2		,3		,4		,5		,6		,7		,8		,9		1,0	°
3	0.0027	2	0.0029	2	0,0031	2	0,0033	2	0.0035	2	0,0037	2	0.0039	3	0.0042	2	0,0044	2	0,0046	3	0,0049	3
4	,0049	2	,0051	3	,0054	2	,0056	3	,0059	3	,0062	2	,0064	3	,0067	3	,0070	3	,0073	3	,0076	4
5	0.0076	3	0,0079	3	0,0082	3	0,0085	4	0.0089	3	0,0092	3	0.0095	4	0.0099	3	0.0102	4	0.0106	3	0,0109	5
6	.0109	4	,0113	4	.0117	3	.0120	4	,0124	4	.0128	4	,0132	4	.0136	4	,0140	4	,0144	5	.0149	6
7	,0149	4	,0153	4	,0157	4	,0161	5	.0166	4	,0170	5	,0175	5	.0180	4	,0184	5	,0189	5	,0194	7
8	,0194	5	.0199	4	,0203	5	,0208	5	,0213	5	,0218	6	.0224	5	,0229	5	.0234	5	.0239	6	.0245	8
9	.0245	5	.0250	6	.0256	5	.0261	6	.0267	5	,0272	6	.0278	6	.0284	6	.0290	6	.0296	6	.0302	9
10	0.0302	6	0.0308	6	0,0314	6	0.0320	6	0,0326	6	0,0332	6	0 0338	7	0.0345	6	0.0351	7	0,0358	6	0,0364	10
11	.0364	7	.0371	6	.0377	7	.0384	6	.0390	7	.0397	7	.0404	7	.0411	7	.0418	7	.0425	7	.0432	11
12	.0432	7	.0439	8	.0447	7	.0454	7	.0461	7	.0468	8	.0476	7	.0483	8	.0491	7	.0498	8	.0506	12
13	.0506	8	.0514	7	.0521	8	.0529	8	.0537	8	.0545	8	.0553	8	.0561	8	.0569	8	.0577	8	.0585	13
14	.0585	9	.0594	8	.0602	8	.0610	8	.0618	9	.0627	8	.0635	9	.0644	9	.0653	8	.0661	9	.0670	14
15	0.0670	9	0.0679	8	0.0687	9	0.0696	9	0.0705	9	0.0714	9	0.0723	9	0.0732	9	0.0741	9	0.0750	10	0,0760	15
16	.0760	9	.0769	9	.0778	10	.0788	9	.0797	10	.0807	9	.0816	10	.0826	9	.0835	10	0,845	10	.0855	16
17	.0855	10	.0865	9	.0874	10	.0884	10	.0894	10	.0904	10	.0914	10	.0924	10	.0934	11	.0945	10	.0955	17
18	.0955	10	.0965	11	.0976	10	.0986	10	.0996	11	.1007	10	.1017	11	.1028	11	.1039	10	.1049	11	.1060	18
19	.1060	11	.1071	11	.1082	10	.1092	11	.1103	11	.1114	11	.1125	11	.1136	11	.1147	12	.1159	11	.1170	19
20	0.1170	11	0.1181	11	0,1192	12	0,1204	11	0.1215	12	0.1227	11	0,1238	11	0.1249	12	0.1261	12	0.1273	11	0,1284	20
21	.1284	12	.1296	12	,1308	12	,1320	11	,1331	12	,1343	12	.1355	12	,1367	12	.1379	12	,1391	12	,1403	21
22	.1403	12	,1415	13	,1428	12	,1440	12	.1452	12	.1464	13	.1477	12	,1489	13	.1502	12	.1514	13	,1527	22
23	.1527	12	.1539	13	.1552	13	,1565	12	.1577	13	,1590	13	.1603	13	,1616	12	,1628	13	.1641	13	.1654	23
24	,1654	13	,1667	13	.1680	13	.1693	13	,1706	14	,1720	13	.1733	13	.1746	13	,1759	14	,1773	13	.1786	24
25	0.1786	14	0.1800	13	0.1813	13	0.1826	14	0.1840	13	0,1853	14	0.1867	14	0.1881	13	0.1894	14	0.1908	14	0,1922	25
26	.1922	14	.1936	13	.1949	14	.1963	14	.1977	14	.1991	14	.2005	14	.2019	14	.2033	14	,2047	14	,2061	26
27	.2061	14	,2075	14	,2089	15	,2104	14	,2118	14	,2132	14	,2146	15	.2161	14	.2175	15	.2190	14	,2204	27
28	.2204	14	.2218	15	.2233	15	.2248	14	,2262	15	.2277	14	.2291	15	.2306	15	.2321	15	,2336	14	.2350	28
29	.2350	15	.2365	15	,2380	15	.2395	15	,2410	15	,2425	15	.2440	15	.2455	15	.2470	15	,2485	15	,2500	29
30	0,2500	15	0.2515	15	0,2530	16	0.2546	15	0,2561	15	0.2576	15	0.2591	15	0.2606	16	0.2622	15	0.2637	16	0.2653	30
31	.2653	15	,2668	16	.2684	15	,2699	15	.2714	16	,2730	16	.2746	15	.2761	16	.2777	15	,2792	16	.2808	31
32	.2808	16	.2824	16	.2840	15	,2855	16	.2871	16	.2887	16	.2903	16	.2919	15	,2934	16	,2950	16	.2966	32
33	,2966	16	.2982	16	.2998	16	,3014	16	,3030	16	,3046	16	.3062	16	,3078	17	.3095	16	.3111	16	,3127	33
34	.3127	16	.3143	16	.3159	17	.3176	16	,3192	16	.3208	16	.3224	17	,3241	16	.3257	17	.3274	16	.3290	34
35	0,3290	16	0.3306	17	0.3323	16	0.3339	17	0.3356	16	0,3372	17	0.3389	16	0.3405	17	0,3422	16	0.3438	17	0.3455	35
36	.3455	17	.3472	16	,3488	17	,3505	17	.3522	16	.3538	17	.3555	17	.3572	16	.3588	17	,3605	17	,3622	36
37	.3622	17	.3639	16	.3655	17	.3672	17	.3689	17	.3706	17	.3723	17	.3740	17	.3757	17	.3774	16	.3790	37
38	.3790	17	.3807	17	.3824	17	.3841	17	.3858	17	.3875	17	.3892	17	.3909	17	.3926	17	.3943	17	.3960	38
39	.3960	18	.3978	17	.3995	17	.4012	17	.4029	17	.4046	17	.4063	17	.4080	17	.4097	18	.4115	17	.4132	39

TABLE IIb (continued)

°	.0		.1		.2		.3		.4		.5		.6		.7		.8		.9		1.0	°
40	0.4132	17	0.4149	17	0.4166	17	0.4183	18	0.4201	17	0.4218	17	0.4235	17	0.4252	18	0.4270	17	0.4287	17	0.4304	40
41	.4304	17	.4321	18	.4339	17	.4356	17	.4373	18	.4391	17	.4408	17	.4425	18	.4443	17	.4460	17	.4477	41
42	.4477	18	.4495	17	.4512	17	.4529	18	.4547	17	.4564	18	.4582	17	.4599	17	.4616	18	.4634	17	.4651	42
43	.4651	18	.4669	17	.4686	18	.4704	17	.4721	17	.4738	18	.4756	17	.4773	18	.4791	17	.4808	18	.4826	43
44	.4826	17	.4843	17	.4860	18	.4878	17	.4895	18	.4913	17	.4930	18	.4948	17	.4965	17	.4982	18	.5000	44
45	0.5000	18	0.5018	17	0.5035	17	0.5052	18	0.5070	17	0.5087	18	0.5105	17	0.5122	18	0.5140	17	0.5157	17	0.5174	45
46	.5175	18	.5192	17	.5209	18	.5227	17	.5244	18	.5262	17	.5279	17	.5296	18	.5314	17	.5331	18	.5349	46
47	.5349	17	.5366	18	.5384	17	.5401	17	.5418	18	.5436	17	.5453	17	.5470	18	.5488	17	.5505	18	.5523	47
48	.5523	17	.5540	17	.5557	18	.5575	17	.5592	17	.5609	18	.5627	17	.5644	17	.5661	17	.5678	18	.5696	48
49	.5696	17	.5713	18	.5731	17	.5748	17	.5765	17	.5782	17	.5799	18	.5817	17	.5834	17	.5851	17	.5868	49
50	0.5868	18	0.5886	17	0.5903	17	0.5920	17	0.5937	17	0.5954	17	0.5971	17	0.5988	17	0.6005	17	0.6022	18	0.6040	50
51	.6040	17	.6057	17	.6074	17	.6091	17	.6108	17	.6125	17	.6142	17	.6159	17	.6176	17	.6193	17	.6210	51
52	.6210	16	.6226	18	.6244	16	.6260	17	.6277	17	.6294	17	.6311	17	.6328	17	.6345	16	.6361	17	.6378	52
53	.6378	17	.6395	17	.6412	16	.6428	17	.6445	17	.6462	16	.6478	17	.6495	17	.6512	16	.6528	17	.6545	53
54	.6545	17	.6562	16	.6578	17	.6595	16	.6611	17	.6628	16	.6644	17	.6661	16	.6677	17	.6694	16	.6710	54
55	0.6710	16	0.6726	17	0.6743	16	0.6759	17	0.6776	16	0.6792	16	0.6808	16	0.6824	17	0.6841	16	0.6857	16	0.6873	55
56	.6873	16	.6889	16	.6905	16	.6921	17	.6938	16	.6954	16	.6970	16	.6986	16	.7002	16	.7018	16	.7034	56
57	.7034	16	.7050	16	.7066	15	.7081	16	.7097	16	.7113	16	.7129	16	.7145	15	.7160	16	.7176	16	.7192	57
58	.7192	16	.7208	15	.7223	16	.7239	15	.7254	16	.7270	16	.7286	15	.7301	15	.7316	16	.7332	15	.7347	58
59	.7347	16	.7363	15	.7378	15	.7393	16	.7409	15	.7424	15	.7439	16	.7455	15	.7470	15	.7485	15	.7500	59
60	0.7500	15	0.7515	15	0.7530	15	0.7545	15	0.7560	15	0.7575	15	0.7590	15	0.7605	15	0.7620	15	0.7635	15	0.7650	60
61	.7650	14	.7664	15	.7679	15	.7694	14	.7708	15	.7723	15	.7738	14	.7752	15	.7767	15	.7782	14	.7796	61
62	.7796	14	.7810	15	.7825	14	.7839	15	.7854	14	.7868	14	.7882	14	.7896	15	.7911	14	.7925	14	.7939	62
63	.7939	14	.7953	14	.7967	14	.7981	14	.7995	14	.8009	14	.8023	14	.8037	14	.8051	14	.8065	13	.8078	63
64	.8078	14	.8092	14	.8106	14	.8120	13	.8133	14	.8147	13	.8160	14	.8174	13	.8187	14	.8201	13	.8214	64
65	0.8214	13	0.8227	14	0.8241	13	0.8254	13	0.8267	13	0.8280	13	0.8293	14	0.8307	13	0.8320	13	0.8333	13	0.8346	65
66	.8346	13	.8359	13	.8372	12	.8384	13	.8397	13	.8410	13	.8423	13	.8436	12	.8448	13	.8461	12	.8473	66
67	.8473	13	.8486	12	.8498	13	.8511	12	.8523	13	.8536	12	.8548	12	.8560	12	.8572	13	.8585	12	.8597	67
68	.8597	12	.8609	12	.8621	12	.8633	12	.8645	12	.8657	12	.8669	11	.8680	12	.8692	12	.8704	12	.8716	68
69	.8716	11	.8727	12	.8739	12	.8751	11	.8762	12	.8774	11	.8785	11	.8796	12	.8808	11	.8819	11	.8830	69
70	0.8830	12	0.8842	11	0.8853	11	0.8864	11	0.8875	11	0.8886	11	0.8897	11	0.8908	10	0.8918	11	0.8929	11	0.8940	70
71	.8940	11	.8951	11	.8962	10	.8972	11	.8983	10	.8993	11	.9004	10	.9014	10	.9024	11	.9035	10	.9045	71
72	.9045	10	.9055	11	.9066	10	.9076	10	.9086	10	.9096	10	.9106	10	.9116	10	.9126	9	.9135	10	.9145	72
73	.9145	10	.9155	10	.9165	9	.9174	10	.9184	9	.9193	10	.9203	9	.9212	10	.9222	9	.9231	9	.9240	73
74	.9240	9	.9249	10	.9259	9	.9268	9	.9277	9	.9286	9	.9295	9	.9304	9	.9313	8	.9321	9	.9330	74
75	0.9330	9	0.9339	8	0.9347	9	0.9356	9	0.9365	8	0.9373	9	0.9382	8	0.9390	8	0.9398	8	0.9406	9	0.9415	75
76	.9415	8	.9423	8	.9431	8	.9439	8	.9447	8	.9455	8	.9463	8	.9471	8	.9479	7	.9486	8	.9494	76
77	.9494	8	.9502	7	.9509	8	.9517	7	.9524	8	.9532	7	.9539	7	.9546	8	.9554	6	.9560	8	.9568	77
78	.9568	7	.9575	7	.9582	7	.9589	7	.9596	6	.9602	7	.9609	7	.9616	7	.9623	6	.9629	7	.9636	78
79	.9636	6	.9642	7	.9649	6	.9655	7	.9662	6	.9668	6	.9674	6	.9680	6	.9686	6	.9692	6	.9698	79
80	0.9699	5	0.9704	6	0.9710	6	0.9716	6	0.9722	6	0.9728	5	0.9733	6	0.9739	5	0.9744	6	0.9750	5	0.9755	80

TABLE III

FOR DETERMINATION OF THE BRIGHTNESS m_{AB} OF A BINARY, IF THE BRIGHTNESS OF THE COMPONENTS m_A AND m_B ARE GIVEN

$m_B - m_A$	$m_A - m_{AB}$	$m_B - m_A$	$m_A - m_{AB}$	$m_B - m_A$	$m_A - m_{AB}$	$m_B - m_A$	$m_A - m_{AB}$
$+\infty$	$0^m.00$	$+1^m.828$	$0^m.19$	$+0^m.961$	$0^m.38$	$+0^m.415$	$0^m.57$
$5^m.84$	.01	1.765	.20	.928	.39	.390	.58
4.641	.02	1.706	.21	.894	.40	.367	.59
4.082	.03	1.649	.22	.862	.41	.341	.60
3.712	.04	1.594	.23	.830	.42	.319	.61
3.434	.05	1.542	.24	.799	.43	.295	.62
3.211	.06	1.492	.25	.768	.44	.272	.63
3.025	.07	1.443	.26	.738	.45	.250	.64
2.864	.08	1.396	.27	.709	.46	.227	.65
2.723	.09	1.351	.28	.680	.47	.205	.66
2.597	.10	1.307	.29	.652	.48	.183	.67
2.483	.11	1.264	.30	.624	.49	.161	.68
2.379	.12	1.223	.31	.596	.50	.140	.69
2.284	.13	1.182	.32	.569	.51	.119	.70
2.195	.14	1.143	.33	.542	.52	.097	.71
2.113	.15	1.105	.34	.516	.53	0.77	.72
2.035	.16	1.068	.35	.490	.54	.056	.73
1.962	.17	1.031	.36	.465	.55	.036	.74
1.893	0.18	0.996	0.37	.439	0,56	$+0.015$	0.75
$+1.828$		$+0.961$		$+0.415$		-0.005	

TABLE IVa

BRIGHTNESSES OF A CLOUD LAYER WITH PLANE BOUNDARIES, CALCULATED ACCORDING TO THE FORMULA

$$h = \left(1 - 2.7\cos\alpha + 3.0\cos^2\alpha + \frac{1}{2.6}Az\right) \cdot \frac{\cos i}{\cos i + \cos\varepsilon},$$

where $Az = A_1a_1 - B_1b_1 + C_1c_1 + D_1d_1 + E_1e_1$ [see eq. (12) on p. 48]

ε	A \ i	0	10	20	30	40	50	60	70	80	85	90
	0	0.895	0.883	0.799	0.703	0.596	0.499	0.421	0.347	0.231	0.135	0.000
	45	0.895	0.883	0.799	0.703	0.596	0.499	0.421	0.347	0.231	0.135	0.000
	60	0.895	0.883	0.799	0.703	0.596	0.499	0.421	0.347	0.231	0.135	0.000
0	75	0.895	0.883	0.799	0.703	0.596	0.499	0.421	0.347	0.231	0.135	0.000
	90	0.895	0.883	0.799	0.703	0.596	0.499	0.421	0.347	0.231	0.135	0.000
	105	0.895	0.883	0.799	0.703	0.596	0.499	0.421	0.347	0.231	0.135	0.000
	120	0.895	0.883	0.799	0.703	0.596	0.499	0.421	0.347	0.231	0.135	0.000
	135	0.895	0.883	0.799	0.703	0.596	0.499	0.421	0.347	0.231	0.135	0.000
	180	0.895	0.883	0.799	0.703	0.596	0.499	0.421	0.347	0.231	0.135	0.000
	0	0.897	0.920	0.866	0.784	0.672	0.548	0.432	0.321	0.192	0.107	0.000
	45	0.897	0.908	0.850	0.761	0.649	0.532	0.427	0.327	0.202	0.115	0.000
	60	0.897	0.902	0.834	0.744	0.634	0.523	0.426	0.334	0.213	0.122	0.000
10	75	0.897	0.893	0.819	0.727	0.620	0.516	0.428	0.344	0.223	0.128	0.000
	90	0.897	0.885	0.804	0.710	0.606	0.511	0.433	0.359	0.238	0.139	0.000
	105	0.897	0.877	0.790	0.695	0.596	0.509	0.443	0.376	0.254	0.150	0.000
	120	0.897	0.868	0.778	0.682	0.588	0.510	0.454	0.395	0.273	0.162	0.000
	135	0.897	0.863	0.765	0.674	0.583	0.514	0.467	0.415	0.289	0.171	0.000
	180	0.897	0.853	0.754	0.698	0.579	0.522	0.488	0.443	0.313	0.185	0.000
	0	0.850	0.908	0.895	0.849	0.765	0.634	0.495	0.349	0.185	0.095	0.000
	45	0.850	0.891	0.795	0.794	0.700	0.585	0.465	0.340	0.197	0.109	0.000
	60	0.850	0.874	0.854	0.760	0.666	0.540	0.428	0.347	0.206	0.108	0.000
20	75	0.850	0.858	0.800	0.726	0.635	0.541	0.453	0.363	0.227	0.128	0.000
	90	0.850	0.843	0.774	0.696	0.612	0.534	0.466	0.392	0.256	0.146	0.000
	105	0.850	0.828	0.750	0.673	0.598	0.539	0.496	0.429	0.299	0.180	0.000
	120	0.850	0.815	0.731	0.657	0.595	0.555	0.530	0.489	0.335	0.195	0.000
	135	0.850	0.801	0.776	0.646	0.599	0.579	0.572	0.536	0.376	0.220	0.000
	180	0.850	0.790	0.700	0.641	0.623	0.625	0.647	0.623	0.442	0.256	0.000
	0	0.812	0.892	0.921	0.920	0.864	0.755	0.605	0.424	0.220	0.111	0.000
	45	0.812	0.866	0.862	0.834	0.768	0.661	0.534	0.388	0.215	0.114	0.000
	60	0.812	0.846	0.825	0.784	0.711	0.616	0.521	0.385	0.226	0.126	0.000
30	75	0.812	0.826	0.788	0.738	0.667	0.588	0.504	0.405	0.254	0.143	0.000
	90	0.812	0.807	0.756	0.702	0.642	0.585	0.530	0.455	0.300	0.173	0.000
	105	0.812	0.790	0.730	0.681	0.640	0.612	0.570	0.530	0.365	0.214	0.000
	120	0.812	0.776	0.713	0.674	0.657	0.662	0.657	0.628	0.443	0.259	0.000
	135	0.812	0.766	0.701	0.671	0.688	0.725	0.762	0.731	0.517	0.304	0.000
	180	0.812	0.794	0.696	0.700	0.756	0.847	0.927	0.909	0.654	0.425	0.000
	0	0.778	0.864	0.938	0.976	0.984	0.894	0.743	0.536	0.279	0.140	0.000
	45	0.778	0.834	0.858	0.865	0.845	0.751	0.623	0.460	0.253	0.132	0.000
	60	0.778	0.816	0.817	0.804	0.776	0.689	0.583	0.446	0.259	0.140	0.000
	75	0.778	0.797	0.779	0.754	0.728	0.658	0.578	0.471	0.296	0.167	0.000
40	90	0.778	0.780	0.750	0.726	0.715	0.673	0.624	0.548	0.363	0.208	0.000
	105	0.778	0.766	0.734	0.723	0.741	0.740	0.736	0.676	0.464	0.270	0.000
	120	0.778	0.755	0.730	0.742	0.801	0.848	0.887	0.842	0.592	0.348	0.000
	135	0.778	0.749	0.734	0.777	0.880	0.977	1.055	1.020	0.691	0.391	0.000
	180	0.778	0.744	0.765	0.854	1.035	1.215	1.354	1.327	0.946	0.548	0.000
	0	0.776	0.839	0.927	1.018	1.066	1.027	0.904	0.679	0.354	0.174	0.000
	45	0.776	0.815	0.855	0.885	0.894	0.838	0.732	0.555	0.310	0.163	0.000
	60	0.776	0.802	0.789	0.830	0.820	0.765	0.677	0.530	0.313	0.170	0.000
	75	0.776	0.790	0.791	0.792	0.784	0.745	0.685	0.568	0.357	0.205	0.000
50	90	0.776	0.783	0.780	0.789	0.802	0.799	0.780	0.688	0.461	0.274	0.000
	105	0.776	0.780	0.788	0.824	0.882	0.908	0.962	0.890	0.614	0.362	0.000
	120	0.776	0.782	0.812	0.892	1.011	1.155	1.211	1.151	0.810	0.476	0.000
	135	0.776	0.787	0.846	0.977	1.164	1.352	1.487	1.445	1.013	0.590	0.000
	180	0.776	0.809	0.914	1.140	1.448	1.755	1.972	1.928	1.362	0.795	0.000

TABLE IVa (continued)

ε	A \ ι	0	10	20	30	40	50	60	70	80	85	90
60	0	0.842	0.852	0.931	1.047	1.139	1.162	1.070	0.852	0.492	0.255	0.000
	45	0.842	0.842	0.874	0.925	0.954	0.941	0.849	0.676	0.395	0.205	0.000
	60	0.842	0.840	0.865	0.902	0.893	0.871	0.793	0.648	0.392	0.206	0.000
	75	0.842	0.844	0.852	0.873	0.886	0.882	0.830	0.710	0.453	0.248	0.000
	90	0.842	0.854	0.876	0.918	0.957	1.003	0.994	0.894	0.604	0.339	0.000
	105	0.842	0.873	0.932	1.018	1.128	1.237	1.286	1.201	0.816	0.479	0.000
	120	0.842	0.895	0.997	1.138	1.359	1.557	1.644	1.594	1.130	0.654	0.000
	135	0.842	0.920	1.075	1.319	1.616	1.912	2.096	2.021	1.453	0.837	0.000
	180	0.842	0.961	1.216	1.605	2.075	2.536	2.833	2.755	1.969	1.150	0.000
70	0	1.016	0.925	0.959	1.075	1.199	1.275	1.246	1.046	0.672	0.372	0.000
	45	1.016	0.943	0.934	0.984	1.030	1.042	0.989	0.831	0.524	0.283	0.000
	60	1.016	0.962	0.953	0.976	0.999	0.997	0.948	0.804	0.516	0.281	0.000
	75	1.016	0.992	0.997	1.025	1.055	1.068	1.039	0.913	0.611	0.341	0.000
	90	1.016	1.032	1.077	1.111	1.227	1.293	1.307	1.220	0.837	0.481	0.000
	105	1.016	1.082	1.179	1.343	1.514	1.672	1.756	1.660	1.191	0.699	0.000
	120	1.016	1.137	1.342	1.590	1.885	2.163	2.331	2.249	1.634	0.972	0.000
	135	1.016	1.194	1.472	1.851	2.283	2.716	2.955	2.877	2.107	1.260	0.000
	180	1.016	1.274	1.711	2.302	2.972	3.624	4.027	3.953	2.913	1.753	0.000
80	0	1.329	1.088	1.018	1.096	1.230	1.311	1.417	1.324	0.972	0.607	0.000
	45	1.329	1.146	1.072	1.073	1.115	1.148	1.138	1.031	0.747	0.439	0.000
	60	1.329	1.206	1.136	1.127	1.142	1.158	1.128	1.015	0.721	0.427	0.000
	75	1.329	1.264	1.247	1.264	1.307	1.322	1.305	1.203	0.875	0.526	0.000
	90	1.329	1.347	1.408	1.498	1.602	1.708	1.740	1.648	1.240	0.766	0.000
	105	1.329	1.442	1.644	1.819	2.046	2.274	2.434	2.345	1.811	1.146	0.000
	120	1.329	1.549	1.843	2.209	2.612	2.998	3.253	3.218	2.528	1.624	0.000
	135	1.329	1.638	2.067	2.576	3.048	3.751	4.182	4.149	3.287	2.132	0.000
	180	1.329	1.775	2.435	3.260	4.172	5.040	5.667	5.736	4.586	3.001	0.000
85	0	1.514	1.183	1.044	1.078	1.200	1.297	1.464	1.460	1.209	0.854	0.000
	45	1.514	1.264	1.154	1.098	1.120	1.159	1.173	1.111	0.874	0.581	0.000
	60	1.514	1.343	1.223	1.194	1.184	1.196	1.183	1.102	0.850	0.550	0.000
	75	1.514	1.412	1.381	1.378	1.406	1.416	1.420	1.338	1.048	0.684	0.000
	90	1.514	1.524	1.588	1.694	1.774	1.887	1.945	1.886	1.526	1.029	0.000
	105	1.514	1.649	1.881	2.067	2.312	2.589	2.748	2.740	2.282	1.583	0.000
	120	1.514	1.781	2.116	2.528	2.980	3.412	3.748	3.810	3.235	2.289	0.000
	135	1.514	1.891	2.393	2.970	3.499	4.261	4.800	4.941	4.245	3.040	0.000
	180	1.514	2.060	2.805	3.766	4.794	5.779	6.595	6.874	5.978	4.331	0.000
90	0	1.687	1.261	1.051	1.014	1.105	1.268	1.437	1.560	1.580	1.492	0.650
	45	1.687	1.368	1.227	1.079	1.059	1.081	1.113	1.116	1.028	0.878	0.295
	60	1.687	1.454	1.301	1.209	1.163	1.145	1.133	1.092	0.961	0.761	0.200
	75	1.687	1.530	1.488	1.446	1.428	1.424	1.416	1.367	1.207	0.956	0.251
	90	1.687	1.696	1.741	1.806	1.880	1.968	2.030	2.044	1.864	1.562	0.500
	105	1.687	1.840	2.043	2.274	2.522	2.852	2.966	3.060	2.931	2.578	0.950
	120	1.687	1.987	2.370	2.808	3.276	3.735	4.128	4.364	4.291	3.894	1.550
	135	1.687	2.129	2.686	3.345	4.047	4.743	5.348	5.743	5.743	5.309	2.205
	180	1.687	2.326	3.189	4.213	5.332	6.446	7.427	8.126	8.241	7.759	3.350

TABLE IVb Coefficients $a_1 = [\cos i \ln(1 + \sec i) + \cos\varepsilon \ln(1 + \sec\varepsilon)]$ of eq. (12) on p. 48

ε \ i	0°	10°	20°	30°	40°	50°	60°	70°	80°	90°
0°	1.3862	1.3833	1.3740	1.3579	1.3330	1.2962	1.2424	1.1696	1.0248	0.6931
10°	1.3833	1.3804	1.3711	1.3550	1.3301	1.2932	1.2395	1.1577	1.0219	0.6902
20°	1.3740	1.3711	1.3618	1.3457	1.3208	1.2840	1.2302	1.1484	1.0126	0.6809
30°	1.3579	1.3550	1.3457	1.3296	1.3047	1.2679	1.2141	1.1323	0.9965	0.6648
40°	1.3330	1.3301	1.3208	1.3047	1.2798	1.2430	1.1892	1.1074	0.9716	0.6399
50°	1.2962	1.2932	1.2840	1.2679	1.2430	1.2062	1.1524	1.0706	0.9348	0.6031
60°	1.2424	1.2395	1.2302	1.2141	1.1892	1.1524	1.0986	1.0168	0.8810	0.5493
70°	1.1606	1.1577	1.1484	1.1323	1.1074	1.0706	1.0168	0.9350	0.7992	0.4675
80°	1.0248	1.0219	1.0126	0.9965	0.9716	0.9348	0.8810	0.7992	0.6634	0.3317
90°	0.6931	0.6902	0.6809	0.6648	0.6399	0.6031	0.5493	0.4675	0.3317	0.0000

TABLE IVb Coefficients $b_1 = [\cos i + \cos\varepsilon - \cos^2 i \ln(1 + \sec i) - \cos^2\varepsilon \ln(1 + \sec\varepsilon)]$ of eq. (12) on p. 48

0°	−0.6138	−0.6120	−0.6068	−0.5971	−0.5827	−0.5620	−0.5323	−0.4890	−0.4230	−0.3069
10°	− .6120	− .6102	− .6050	− .5953	− .5809	− .5602	− .5305	− .4872	− .4212	− .3051
20°	− .6068	− .6050	− .5998	− .5901	− .5757	− .5550	− .5253	− .4820	− .4160	− .2999
30°	− .5971	− .5953	− .5901	− .5804	− .5660	− .5453	− .5156	− .4723	− .4063	− .2902
40°	− .5827	− .5809	− .5757	− .5660	− .5516	− .5309	− .5012	− .4579	− .3919	− .2758
50°	− .5620	− .5602	− .5550	− .5453	− .5309	− .5102	− .4805	− .4372	− .3712	− .2551
60°	− .5323	− .5305	− .5253	− .5156	− .5012	− .4805	− .4508	− .4075	− .3415	− .2254
70°	− .4890	− .4872	− .4820	− .4723	− .4579	− .4372	− .4075	− .3642	− .2982	− .1821
80°	− .4230	− .4212	− .4160	− .4063	− .3919	− .3712	− .3415	− .2982	− .2322	− .1161
90°	−0.3069	−0.3051	−0.2999	−0.2902	−0.2758	−0.2551	−0.2254	−0.1821	−0.1161	−0.0000

TABLE IVb Coefficients $c_1 = [\frac{1}{2}(\cos i + \cos\varepsilon) - (\cos^2 i + \cos^2\varepsilon) - \cos^3 i \ln(1 + \sec i) + \cos^3\varepsilon \ln(1 + \sec\varepsilon)]$ of eq. (12) on p. 48

0°	0.3862	0.3851	0.3811	0.3747	0.3648	0.3505	0.3304	0.3018	0.2598	0.1931
10°	.3851	.3840	.3801	.3736	.3637	.3494	.3293	.3007	.2587	.1920
20°	.3811	.3801	.3761	.3696	.3597	.3455	.3253	.2967	.2548	.1880
30°	.3747	.3736	.3696	.3632	.3533	.3391	.3189	.2903	.2483	.1816
40°	.3648	.3637	.3597	.3533	.3434	.3291	.3090	.2804	.2384	.1717
50°	.3505	.3494	.3455	.3390	.3291	.3148	.2947	.2661	.2242	.1574
60°	.3304	.3293	.3253	.3189	.3090	.2946	.2748	.2460	.2040	.1373
70°	.3018	.3007	.2967	.2903	.2804	.2661	.2461	.2174	.1754	.1087
80°	.2598	.2587	.2548	.2483	.2384	.2241	.2040	.1754	.1334	.0667
90°	0.1931	0.1920	0.1880	0.1816	0.1717	0.1574	0.1373	0.1087	0.0667	0.0000

TABLE IVb Coefficients $d_1 = [\frac{1}{3}(\cos i + \cos\varepsilon) - \frac{1}{2}(\cos^2 i + \cos^2\varepsilon) + \cos^3 i + \cos^3\varepsilon - \cos^4 i \ln(1 + \sec i) - \cos^4\varepsilon \ln(1 + \sec\varepsilon)]$ of eq. (12) on p. 48

0°	0.2804	0.2775	0.2767	0.2716	0.2640	0.2533	0.2382	0.2170	0.1866	0.1402
10°	.2775	.2746	.2738	.2687	.2611	.2504	.2353	.2141	.1837	.1373
20°	.2767	.2738	.2730	.2679	.2603	.2496	.2345	.2133	.1829	.1365
30°	.2716	.2687	.2679	.2628	.2552	.2445	.2294	.2082	.1778	.1314
40°	.2640	.2611	.2603	.2552	.2476	.2369	.2218	.2006	.1702	.1238
50°	.2533	.2504	.2496	.2445	.2369	.2262	.2111	.1899	.1595	.1131
60°	.2382	.2353	.2345	.2294	.2218	.2111	.1960	.1748	.1444	.0980
70°	.2170	.2141	.2133	.2082	.2006	.1899	.1748	.1536	.1232	.0768
80°	.1866	.1837	.1829	.1778	.1702	.1595	.1444	.1232	.0928	.0464
90°	0.1402	0.1373	0.1365	0.1314	0.1238	0.1131	0.0980	0.0768	0.0464	0.0000

TABLE IVb Coefficients $e_1 = [\frac{1}{4}(\cos i + \cos\varepsilon) - \frac{1}{3}(\cos^2 i + \cos^2\varepsilon) + \frac{1}{2}(\cos^3 i + \cos^3\varepsilon) - (\cos^4 i + \cos^4\varepsilon) + \cos^5 i \ln(1 + \sec i) + \cos^5\varepsilon \ln(1 + \sec\varepsilon)]$ of eq. (12) on p. 48

0°	0.2195	0.2189	0.2163	0.2125	0.2064	0.1977	0.1857	0.1699	0.1481	0.1098
10°	.2189	.2182	.2159	.2118	.2057	.1951	.1850	.1683	.1474	.1091
20°	.2163	.2159	.2133	.2094	.2033	.1946	.1826	.1659	.1450	.1067
30°	.2125	.2118	.2094	.2055	.1994	.1908	.1788	.1619	.1411	.1028
40°	.2064	.2057	.2033	.1994	.1933	.1847	.1727	.1558	.1350	.0966
50°	.1977	.1951	.1946	.1908	.1847	.1759	.1639	.1472	.1264	.0880
60°	.1857	.1850	.1826	.1788	.1727	.1639	.1509	.1352	.1143	.0760
70°	.1699	.1683	.1659	.1619	.1558	.1472	.1352	.1184	.0976	.0592
80°	.1481	.1474	.1450	.1411	.1350	.1264	.1143	.0976	.0767	.0383
90°	0.1098	0.1091	0.1067	0.1028	0.0966	0.0880	0.0760	0.0592	0.0383	0.0000

TABLE Va

BRIGHTNESSES OF AN AREA WITH PLANE BOUNDARIES, CALCULATED ACCORDING TO EQ.(13) ON p.48

$$h = \frac{\cos i}{\cos i + \cos \varepsilon}\left[1 + \cos^2\alpha + \frac{3}{16}\left(A'_1 a_1 + C'_1 c_1 + E'_1 e_1\right)\right].$$

ε	A	0°	10°	20°	30°	40°	50°	60°	70°	80°	90°
	0	1.446	1.418	1.339	1.215	1.057	0.875	0.679	0.473	0.248	0.000
	45	1.446	1.418	1.339	1.215	1.057	0.875	0.679	0.473	0.248	0.000
	60	1.446	1.418	1.339	1.215	1.057	0.875	0.679	0.473	0.248	0.000
0	75	1.446	1.418	1.339	1.215	1.057	0.875	0.679	0.473	0.248	0.000
	90	1.446	1.418	1.339	1.215	1.057	0.875	0.679	0.473	0.248	0.000
	105	1.446	1.418	1.339	1.215	1.057	0.875	0.679	0.473	0.248	0.000
	120	1.446	1.418	1.339	1.215	1.057	0.875	0.679	0.473	0.248	0.000
	135	1.446	1.418	1.339	1.215	1.057	0.875	0.679	0.473	0.248	0.000
	180	1.446	1.418	1.339	1.215	1.057	0.875	0.679	0.473	0.248	0.000
	0	1.440	1.447	1.395	1.291	1.141	0.956	0.743	0.513	0.265	0.000
	45	1.440	1.438	1.377	1.268	1.116	0.931	0.724	0.501	0.260	0.000
	60	1.440	1.431	1.365	1.251	1.098	0.915	0.711	0.493	0.257	0.000
10	75	1.440	1.423	1.351	1.233	1.078	0.896	0.697	0.484	0.254	0.000
	90	1.440	1.415	1.336	1.214	1.057	0.878	0.683	0.476	0.251	0.000
	105	1.440	1.407	1.321	1.195	1.037	0.860	0.670	0.469	0.249	0.000
	120	1.440	1.400	1.308	1.178	1.020	0.845	0.659	0.463	0.248	0.000
	135	1.440	1.394	1.296	1.164	1.005	0.831	0.650	0.458	0.247	0.000
	180	1.440	1.385	1.281	1.144	0.985	0.815	0.638	0.453	0.247	0.000
	0	1.425	1.461	1.443	1.366	1.234	1.053	0.830	0.577	0.292	0.000
	45	1.425	1.444	1.408	1.317	1.178	0.998	0.784	0.544	0.278	0.000
	60	1.425	1.430	1.382	1.284	1.141	0.962	0.755	0.525	0.270	0.000
20	75	1.425	1.415	1.355	1.247	1.101	0.924	0.724	0.506	0.262	0.000
	90	1.425	1.399	1.326	1.210	1.060	0.887	0.696	0.489	0.256	0.000
	105	1.425	1.385	1.298	1.174	1.023	0.854	0.672	0.476	0.253	0.000
	120	1.425	1.370	1.273	1.143	0.991	0.827	0.654	0.467	0.252	0.000
	135	1.425	1.359	1.253	1.117	0.966	0.805	0.640	0.462	0.253	0.000
	180	1.425	1.342	1.224	1.083	0.933	0.781	0.627	0.461	0.257	0.000
	0	1.404	1.469	1.483	1.439	1.331	1.163	0.938	0.663	0.347	0.000
	45	1.404	1.441	1.430	1.364	1.243	1.073	0.858	0.606	0.317	0.000
	60	1.404	1.423	1.394	1.314	1.187	1.017	0.810	0.572	0.301	0.000
30	75	1.404	1.402	1.354	1.260	1.126	0.958	0.762	0.540	0.287	0.000
	90	1.404	1.380	1.313	1.207	1.068	0.904	0.720	0.514	0.278	0.000
	105	1.404	1.358	1.274	1.158	1.016	0.858	0.687	0.497	0.274	0.000
	120	1.404	1.339	1.240	1.116	0.975	0.825	0.665	0.489	0.276	0.000
	135	1.404	1.323	1.212	1.083	0.944	0.802	0.654	0.489	0.281	0.000
	180	1.404	1.301	1.176	1.042	0.909	0.779	0.648	0.498	0.295	0.000
	0	1.380	1.468	1.514	1.505	1.434	1.284	1.064	0.774	0.416	0.000
	45	1.380	1.435	1.446	1.406	1.310	1.157	0.947	0.684	0.367	0.000
	60	1.380	1.412	1.400	1.341	1.234	1.079	0.878	0.633	0.341	0.000
40	75	1.380	1.387	1.350	1.273	1.155	1.001	0.811	0.587	0.319	0.000
	90	1.380	1.360	1.301	1.207	1.083	0.933	0.757	0.552	0.305	0.000
	105	1.380	1.334	1.254	1.149	1.023	0.880	0.720	0.533	0.302	0.000
	120	1.380	1.312	1.216	1.102	0.978	0.846	0.701	0.531	0.309	0.000
	135	1.380	1.293	1.185	1.067	0.948	0.827	0.697	0.540	0.322	0.000
	180	1.380	1.267	1.145	1.027	0.918	0.818	0.711	0.570	0.351	0.000
	0	1.361	1.464	1.539	1.566	1.531	1.416	1.213	0.915	0.512	0.000
	45	1.361	1.427	1.459	1.446	1.378	1.249	1.054	0.786	0.437	0.000
	60	1.361	1.402	1.406	1.370	1.285	1.150	0.961	0.714	0.398	0.000
50	75	1.361	1.374	1.350	1.291	1.192	1.055	0.877	0.652	0.365	0.000
	90	1.361	1.345	1.297	1.218	1.111	0.977	0.812	0.609	0.347	0.000
	105	1.361	1.318	1.248	1.157	1.048	0.923	0.775	0.592	0.346	0.000
	120	1.361	1.294	1.208	1.111	1.007	0.895	0.766	0.599	0.361	0.000
	135	1.361	1.274	1.178	1.080	0.985	0.889	0.777	0.624	0.385	0.000
	180	1.361	1.248	1.141	1.050	0.974	0.906	0.822	0.686	0.438	0.000

TABLE Va (continued)

/250

ε	A \ i	0°	10°	20°	30°	40°	50°	60°	70°	80°	90°
60	0	1.358	1.465	1.561	1.624	1.631	1.560	1.390	1.098	0.650	0.000
	45	1.358	1.427	1.474	1.487	1.451	1.355	1.183	0.920	0.540	0.000
	60	1.358	1.401	1.420	1.404	1.345	1.236	1.068	0.825	0.482	0.000
	75	1.358	1.373	1.362	1.320	1.243	1.127	0.965	0.744	0.438	0.000
	90	1.358	1.346	1.308	1.247	1.159	1.044	0.895	0.694	0.413	0.000
	105	1.358	1.320	1.263	1.190	1.102	0.997	0.864	0.683	0.417	0.000
	120	1.358	1.297	1.228	1.153	1.074	0.984	0.872	0.707	0.443	0.000
	135	1.358	1.280	1.204	1.133	1.067	0.999	0.906	0.754	0.484	0.000
	180	1.358	1.258	1.178	1.123	1.090	1.057	0.998	0.862	0.572	0.000
70	0	1.383	1.477	1.584	1.678	1.734	1.721	1.604	1.344	0.865	0.000
	45	1.383	1.442	1.495	1.533	1.533	1.476	1.345	1.107	0.702	0.000
	60	1.383	1.418	1.442	1.448	1.418	1.343	1.205	0.981	0.618	0.000
	75	1.383	1.394	1.389	1.366	1.313	1.224	1.087	0.879	0.553	0.000
	90	1.383	1.370	1.342	1.301	1.237	1.144	1.015	0.824	0.523	0.000
	105	1.383	1.349	1.307	1.259	1.195	1.113	0.999	0.824	0.533	0.000
	120	1.383	1.332	1.283	1.239	1.189	1.127	1.033	0.874	0.580	0.000
	135	1.383	1.320	1.271	1.237	1.208	1.172	1.102	0.955	0.648	0.000
	180	1.383	1.306	1.267	1.260	1.276	1.288	1.260	1.130	0.788	0.000
80	0	1.428	1.502	1.608	1.727	1.834	1.897	1.873	1.702	1.255	0.000
	45	1.428	1.473	1.529	1.582	1.620	1.619	1.556	1.382	1.001	0.000
	60	1.428	1.456	1.484	1.503	1.503	1.472	1.389	1.218	0.871	0.000
	75	1.428	1.439	1.442	1.433	1.406	1.352	1.261	1.090	0.774	0.000
	90	1.428	1.424	1.410	1.385	1.347	1.286	1.190	1.031	0.734	0.000
	105	1.428	1.412	1.392	1.367	1.332	1.282	1.200	1.051	0.759	0.000
	120	1.428	1.404	1.388	1.374	1.361	1.335	1.275	1.142	0.842	0.000
	135	1.428	1.401	1.393	1.402	1.418	1.425	1.395	1.276	0.958	0.000
	180	1.428	1.399	1.415	1.471	1.550	1.622	1.645	1.552	1.191	0.000
90	0	1.441	1.471	1.558	1.689	1.846	2.006	2.144	2.229	2.229	1.000
	45	1.441	1.456	1.498	1.559	1.632	1.702	1.757	1.776	1.732	0.750
	60	1.441	1.449	1.467	1.495	1.525	1.551	1.563	1.548	1.485	0.625
	75	1.441	1.443	1.445	1.447	1.447	1.439	1.421	1.380	1.302	0.534
	90	1.441	1.441	1.437	1.430	1.417	1.399	1.369	1.321	1.236	0.500
	105	1.441	1.443	1.445	1.447	1.447	1.439	1.421	1.380	1.302	0.534
	120	1.441	1.449	1.467	1.495	1.525	1.551	1.563	1.548	1.485	0.625
	135	1.441	1.456	1.498	1.559	1.632	1.702	1.757	1.776	1.732	0.750
	180	1.441	1.471	1.558	1.689	1.846	2.006	2.144	2.229	2.229	1.000

TABLE Vb

/251

FIRST TERM OF EQ.(13) ON p.48

$$1 + \cos^2\alpha = 1 + (\cos i \cos\varepsilon + \sin i \sin\varepsilon \cos A)^2.$$

ε	A \ i	0°	10°	20°	30°	40°	50°	60°	70°	80°	90°
	0	2.0000	1.9698	1.8830	1.7500	1.5868	1.4132	1.2500	1.1170	1.0302	1.0000
	45	2.0000	1.9698	1.8830	1.7500	1.5868	1.4132	1.2500	1.1170	1.0302	1.0000
	60	2.0000	1.9698	1.8830	1.7500	1.5868	1.4132	1.2500	1.1170	1.0302	1.0000
	75	2.0000	1.9698	1.8830	1.7500	1.5868	1.4132	1.2500	1.1170	1.0302	1.0000
0°	90	2.0000	1.9698	1.8830	1.7500	1.5868	1.4132	1.2500	1.1170	1.0302	1.0000
	105	2.0000	1.9698	1.8830	1.7500	1.5868	1.4132	1.2500	1.1170	1.0302	1.0000
	120	2.0000	1.9698	1.8830	1.7500	1.5868	1.4132	1.2500	1.1170	1.0302	1.0000
	135	2.0000	1.9698	1.8830	1.7500	1.5868	1.4132	1.2500	1.1170	1.0302	1.0000
	180	2.0000	1.9698	1.8830	1.7500	1.5868	1.4132	1.2500	1.1170	1.0302	1.0000
	0		2.0000	1.9698	1.8830	1.7500	1.5868	1.4132	1.2500	1.1170	1.0302
	45		1.9825	1.9359	1.8358	1.6946	1.5287	1.3584	1.2045	1.0853	1.0151
	60		1.9700	1.9122	1.8034	1.6566	1.4894	1.3222	1.1751	1.0659	1.0076
	75		1.9557	1.8851	1.7662	1.6136	1.4454	1.2823	1.1436	1.0464	1.0020
10°	90		1.9405	1.8564	1.7273	1.5691	1.4007	1.2425	1.1134	1.0293	1.0000
	105		1.9254	1.8281	1.6894	1.5264	1.3583	1.2057	1.0868	1.0161	1.0020
	120		1.9115	1.8023	1.6550	1.4879	1.3208	1.1741	1.0651	1.0073	1.0076
	135		1.8995	1.7804	1.6263	1.4562	1.2904	1.1491	1.0490	1.0025	1.0151
	180		1.8830	1.7500	1.5868	1.4132	1.2500	1.1170	1.0302	1.0000	1.0302
	0			2.0000	1.9698	1.8830	1.7500	1.5868	1.4132	1.2500	1.1170
	45			1.9326	1.8737	1.7660	1.6230	1.4614	1.3011	1.1611	1.0585
	60			1.8864	1.8087	1.6884	1.5402	1.3819	1.2324	1.1100	1.0292
	75			1.8341	1.7363	1.6033	1.4513	1.2988	1.1637	1.0627	1.0078
20°	90			1.7797	1.6623	1.5181	1.3648	1.2208	1.1033	1.0266	1.0000
	105			1.7271	1.5921	1.4394	1.2875	1.1546	1.0567	1.0058	1.0078
	120			1.6798	1.5304	1.3720	1.2237	1.1036	1.0258	1.0000	1.0292
	135			1.6405	1.4789	1.3185	1.1753	1.0679	1.0089	1.0056	1.0585
	180			1.5868	1.4132	1.2500	1.1170	1.0302	1.0000	1.0302	1.1170
	0				2.0000	1.9698	1.8830	1.7500	1.5868	1.4132	1.2500
	45				1.8590	1.7933	1.6848	1.5464	1.3950	1.2468	1.1250
	60				1.7656	1.6791	1.5598	1.4219	1.2822	1.1573	1.0625
	75				1.6637	1.5574	1.4301	1.2971	1.1746	1.0772	1.0167
30°	90				1.5625	1.4401	1.3099	1.1875	1.0879	1.0226	1.0000
	105				1.4696	1.3366	1.2094	1.1030	1.0305	1.0005	1.0167
	120				1.3906	1.2527	1.1334	1.0469	1.0037	1.0092	1.0625
	135				1.3286	1.1902	1.0817	1.0161	1.0013	1.0391	1.1250
	180				1.2500	1.1170	1.0302	1.0000	1.0302	1.1170	1.2500
	0					2.0000	1.9698	1.8830	1.7500	1.5868	1.4132
	45					1.7726	1.7066	1.6031	1.4749	1.3372	1.2066
	60					1.6287	1.5455	1.4374	1.3181	1.2021	1.1033
	75					1.4812	1.3842	1.2778	1.1750	1.0881	1.0277
40°	90					1.3443	1.2425	1.1467	1.0686	1.0177	1.0000
	105					1.2303	1.1332	1.0571	1.0112	1.0009	1.0277
	120					1.1449	1.0606	1.0109	1.0016	1.0336	1.1033
	135					1.0868	1.0208	1.0001	1.0273	1.0989	1.2066
	180					1.0302	1.0000	1.0302	1.1170	1.2500	1.4132
	0						2.0000	1.9698	1.8830	1.7500	1.5868
	45						1.6857	1.6250	1.5311	1.4162	1.2933
	60						1.4993	1.4265	1.3361	1.2390	1.1467
	75						1.3193	1.2431	1.1649	1.0942	1.0393
50°	90						1.1707	1.1033	1.0483	1.0125	1.0000
	105						1.0683	1.0224	1.0011	1.0070	1.0393
	120						1.0144	1.0001	1.0196	1.0705	1.1467
	135						1.0000	1.0218	1.0836	1.1778	1.2933
	180						1.0302	1.1170	1.2500	1.4132	1.5868

TABLE Vb (continued)

ε	λ \ ϑ	0°	10°	20°	30°	40°	50°	60°	70°	80°	90°
	0							2.0000	1.9698	1.8830	1.7500
	45							1.6089	1.5571	1.4760	1.3749
	60							1.3906	1.3340	1.2635	1.1875
	75							1.1972	1.1456	1.1002	1.0502
60°	90							1.0625	1.0292	1.0076	1.0000
	105							1.0031	1.0016	1.0204	1.0502
	120							1.0156	1.0556	1.1153	1.1875
	135							1.0786	1.1635	1.2664	1.3749
	180							1.2500	1.4132	1.5868	1.7500
	0								2.0000	1.9698	1.8830
	45								1.5497	1.5095	1.4416
	60								1.3119	1.2726	1.2208
	75								1.1194	1.0893	1.0591
70°	90								1.0137	1.0035	1.0000
	105								1.0124	1.0324	1.0591
	120								1.1053	1.1627	1.2208
	135								1.2575	1.3540	1.4416
	180								1.5868	1.7500	1.8830
	0									2.0000	1.9698
	45									1.5125	1.4850
	60									1.2653	1.2425
	75									1.0791	1.0650
80°	90									1.0009	1.0000
	105									1.0488	1.0650
	120									1.2068	1.2425
	135									1.4297	1.4850
	180									1.8830	1.9698
	0										2.0000
	45										1.5000
	60										1.2500
	75										1.0670
90°	90										1.0000
	105										1.0670
	120										1.2500
	135										1.5000
	180										2.0000

TABLE Vc

SECOND TERM OF EQ.(13) ON p.48 FOR THE MAXIMUM VALUE $\frac{3}{16}$ OF THE COEFFICIENT $\frac{\pi\mu}{k}$

$$\frac{3}{16}(A_1'a_1 + C_1'c_1 + E_1'c_1).$$

ε	A \ i	0°	10°	20°	30°	40°	50°	60°	70°	80°	90°
0°		0.892	0.889	0.881	0.869	0.850	0.823	0.787	0.739	0.646	0.441
	0		0.894	0.886	0.877	0.859	0.833	0.795	0.740	0.650	0.441
	45		0.892	0.885	0.873	0.856	0.829	0.793	0.738	0.648	0.441
	60		0.891	0.883	0.871	0.853	0.828	0.790	0.736	0.647	0.441
	75		0.890	0.881	0.869	0.851	0.825	0.788	0.734	0.647	0.441
10°	90		0.889	0.879	0.867	0.848	0.822	0.786	0.733	0.646	0.441
	105		0.888	0.878	0.864	0.845	0.820	0.784	0.731	0.645	0.441
	120		0.887	0.876	0.862	0.844	0.818	0.782	0.730	0.645	0.441
	135		0.887	0.875	0.861	0.842	0.815	0.781	0.729	0.645	0.441
	180		0.886	0.873	0.858	0.839	0.813	0.779	0.729	0.646	0.441
	0			0.886	0.879	0.865	0.842	0.804	0.748	0.655	0.441
	45			0.882	0.873	0.858	0.834	0.797	0.738	0.651	0.439
	60			0.878	0.869	0.853	0.828	0.793	0.735	0.648	0.438
	75			0.876	0.865	0.848	0.823	0.787	0.731	0.646	0.437
20°	90			0.872	0.861	0.843	0.819	0.783	0.728	0.644	0.437
	105			0.869	0.856	0.838	0.814	0.780	0.726	0.643	0.437
	120			0.866	0.853	0.835	0.811	0.778	0.724	0.644	0.438
	135			0.864	0.850	0.832	0.808	0.776	0.724	0.644	0.439
	180			0.861	0.846	0.828	0.805	0.775	0.728	0.646	0.441
	0				0.878	0.867	0.846	0.812	0.754	0.661	0.439
	45				0.869	0.856	0.834	0.799	0.744	0.652	0.434
	60				0.862	0.849	0.827	0.792	0.738	0.647	0.432
	75				0.856	0.842	0.819	0.785	0.731	0.643	0.430
30°	90				0.850	0.835	0.812	0.779	0.727	0.640	0.430
	105				0.845	0.828	0.806	0.774	0.725	0.640	0.430
	120				0.840	0.824	0.803	0.771	0.724	0.641	0.432
	135				0.837	0.821	0.800	0.771	0.725	0.644	0.434
	180				0.833	0.819	0.799	0.771	0.728	0.649	0.439
	0					0.867	0.845	0.812	0.758	0.663	0.433
	45					0.846	0.828	0.795	0.742	0.650	0.425
	60					0.838	0.818	0.786	0.733	0.642	0.422
	75					0.829	0.809	0.776	0.725	0.637	0.419
40°	90					0.821	0.801	0.769	0.720	0.634	0.417
	105					0.815	0.795	0.765	0.717	0.633	0.419
	120					0.811	0.792	0.764	0.718	0.636	0.422
	135					0.808	0.791	0.764	0.721	0.648	0.425
	180					0.806	0.792	0.769	0.729	0.651	0.433
	0						0.832	0.803	0.753	0.659	0.419
	45						0.812	0.783	0.731	0.640	0.409
	60						0.801	0.770	0.721	0.631	0.404
	75						0.790	0.761	0.711	0.623	0.400
50°	90						0.782	0.753	0.705	0.620	0.399
	105						0.777	0.750	0.704	0.621	0.400
	120						0.776	0.750	0.706	0.625	0.404
	135						0.777	0.754	0.712	0.632	0.409
	180						0.781	0.762	0.724	0.647	0.419
	0							0.780	0.732	0.640	0.394
	45							0.756	0.708	0.620	0.382
	60							0.744	0.696	0.607	0.375
	75							0.733	0.685	0.599	0.371
60°	90							0.726	0.680	0.595	0.369
	105							0.724	0.680	0.597	0.371
	120							0.727	0.684	0.603	0.375
	135							0.732	0.692	0.613	0.382
	180							0.746	0.709	0.630	0.394

TABLE Vc (continued)

/254

ε	A \ i	0°	10°	20°	30°	40°	50°	60°	70°	80°	90°
	0								0.688	0.597	0.346
	45								0.663	0.574	0.334
	60								0.649	0.563	0.327
	75								0.639	0.554	0.321
70°	90								0.634	0.550	0.321
	105								0.635	0.552	0.321
	120								0.642	0.559	0.327
	135								0.652	0.570	0.334
	180								0.672	0.590	0.346
	0									0.509	0.259
	45									0.488	0.247
	60									0.477	0.242
	75									0.469	0.237
80°	90									0.466	0.236
	105									0.468	0.237
	120									0.476	0.242
	135									0.486	0.247
	180									0.499	0.259
	0										0.000
	45										0.000
	60										0.000
	75										0.000
90°	90										0.000
	105										0.000
	120										0.000
	135										0.000
	180										0.000

TABLE VIa

PHASE CURVES φ_1 AND φ_2 IN EQ.(7) ON p.72 AND EQ.(12) ON p.73

$q_1 = q_1^0 \varphi_1(\alpha)$ accd. to Lambert

$q_2 = q_2^0 \varphi_2(\alpha)$ accd. to Seeliger

Phase Angle α	$\varphi_1(\alpha) = \frac{1}{\pi}[\sin\alpha + (\pi-\alpha)\cos\alpha]$		$\varphi_2(\alpha) = 1 - \sin\frac{\alpha}{2}\tan\frac{\alpha}{2}\ln\cot\frac{\alpha}{4}$		Phase Angle α	$\varphi_1(\alpha) = \frac{1}{\pi}[\sin\alpha + (\pi-\alpha)\cos\alpha]$		$\varphi_2(\alpha) = 1 - \sin\frac{\alpha}{2}\tan\frac{\alpha}{2}\ln\cot\frac{\alpha}{4}$	
	Log-arithms	Magn. Classes	Log-arithms	Magn. Classes		Log-arithms	Magn. Classes	Log-arithms	Magn. Classes
0°	0.0000	0.000	0.0000	0.000	84°	9.5709	1.073	9.6265	0.934
2	9.9997	0.001	9.9994	0.002	86	9.5490	1.128	9.6101	0.975
4	9.9990	0.003	9.9979	0.005	88	9.5263	1.184	9.5933	1.017
6	9.9977	0.006	9.9957	0.011	90	9.5029	1.243	9.5760	1.060
8	9.9959	0.010	9.9928	0.018	92	9.4787	1.303	9.5583	1.104
10	9.9936	0.016	9.9895	0.026	94	9.4537	1.366	9.5401	1.150
12	9.9908	0.023	9.9857	0.036	96	9.4278	1.431	9.5213	1.197
14	9.9876	0.031	9.9815	0.046	98	9.4011	1.497	9.5020	1.245
16	9.9839	0.040	9.9768	0.058	100	9.3735	1.566	9.4822	1.295
18	9.9797	0.051	9.9717	0.071	102	9.3449	1.638	9.4617	1.346
20	9.9750	0.063	9.9663	0.084	104	9.3154	1.712	9.4406	1.399
22	9.9699	0.075	9.9606	0.099	106	9.2848	1.788	9.4189	1.453
24	9.9644	0.089	9.9545	0.114	108	9.2532	1.869	9.3965	1.509
26	9.9583	0.104	9.9481	0.130	110	9.2204	1.949	9.3734	1.567
28	9.9518	0.121	9.9413	0.147	112	9.1864	2.034	9.3495	1.626
30	9.9449	0.138	9.9342	0.165	114	9.1512	2.122	9.3248	1.688
32	9.9375	0.156	9.9268	0.183	116	9.1147	2.213	9.2993	1.752
34	9.9296	0.176	9.9191	0.202	118	9.0768	2.308	9.2729	1.818
36	9.9213	0.197	9.9111	0.222	120	9.0374	2.407	9.2456	1.886
38	9.9125	0.219	9.9028	0.243	122	8.9964	2.509	9.2172	1.957
40	9.9033	0.242	9.8943	0.264	124	8.9538	2.616	9.1877	2.031
42	9.8936	0.266	9.8854	0.287	126	8.9095	2.726	9.1571	2.107
44	9.8834	0.292	9.8763	0.309	128	8.8632	2.842	9.1254	2.187
46	9.8728	0.318	9.8668	0.333	130	8.8149	2.963	9.0923	2.269
48	9.8617	0.346	9.8571	0.357	132	8.7643	3.089	9.0578	2.356
50	9.8501	0.375	9.8470	0.383	134	8.7114	3.222	9.0216	2.446
52	9.8380	0.405	9.8367	0.408	136	8.6559	3.360	8.9838	2.541
54	9.8254	0.437	9.8260	0.435	138	8.5976	3.506	8.9442	2.640
56	9.8123	0.469	9.8151	0.462	140	8.5362	3.659	8.9026	2.744
58	9.7987	0.503	9.8038	0.491	142	8.4715	3.821	8.8588	2.553
60	9.7846	0.539	9.7923	0.519	144	8.4030	3.993	8.8124	2.969
62	9.7700	0.575	9.7804	0.549	146	8.3304	4.174	8.7632	3.092
64	9.7548	0.613	9.7682	0.580	148	8.2532	4.367	8.7110	3.223
66	9.7391	0.652	9.7556	0.611	150	8.1707	4.573	8.6558	3.361
68	9.7228	0.693	9.7427	0.643	152	8.0824	4.794	8.5965	3.509
70	9.7059	0.735	9.7295	0.676	154	7.9873	5.032	8.5325	3.669
72	9.6885	0.779	9.7159	0.710	156	7.8843	5.289	8.4635	3.841
74	9.6705	0.824	9.7020	0.745	158	7.7722	5.570	8.3882	4.030
76	9.6519	0.870	9.6877	0.781	160	7.6492	5.877	8.3059	4.235
78	9.6326	0.919	9.6730	0.818	162	7.5129	6.218	8.2147	4.463
80	9.6127	0.968	9.6579	0.855	164	7.3603	6.599	8.1128	4.718
82	9.5921	1.020	9.6424	0.894					

TABLE VIb

AUXILIARY QUANTITIES P AND R OF SEELIGER'S FORMULA [EQ.(22)], p.76
FOR ILLUMINATION OF AN ELLIPSOID OF REVOLUTION

$$Q_1 = 2\pi J A_1 \sin^2 s \sin^2 \sigma \cos\alpha \,(P\cos^2 A + R\sin^2 A)$$

FOR THE AXIAL RATIO a/b OCCURRING IN THE SOLAR SYSTEM

a/b	$\log P$	P	$\log R$	R
1.04	9.5023 − 10	0.3179	9.5296 − 10	0.3385
	50	−36	16	+13
1.05	9.4973	0.3143	9.5312	0.3398
	49	−36	16	+12
1.06	9.4924	0.3107	9.5328	0.3410
	50	−35	16	+12
1.07	9.4874	0.3074	9.5344	0.3423
	49	−36	15	+12
1.08	9.4825	0.3038	9.5359	0.3435
	48	−34	15	+12
1.09	9.4777	0.3004	9.5374	0.3447
	49	−34	15	+12
1.10	9.4728	0.2970	9.5389	0.3459
	48	−32	15	+11
1.11	9.4680	0.2938	9.5404	0.3470
	47	−32	14	+12
1.12	9.4633	0.2906	9.5418	0.3482
	47	−31	14	+11
1.13	9.4586	0.2875	9.5432	0.3493
	47	−31	14	+11
1.14	9.4539	0.2844	9.5446	0.3504

TABLE VIc

REDUCTION OF THE BRIGHTNESS OF THE PLANET SATURN (WITHOUT RING)
AT A = 0 AND $\alpha = 0$ TO THE BRIGHTNESS AT A AND $\alpha \neq 0$

The table contains the values of $Z = P\cos^2 A + R\sin^2 A$; $Z(A) = \frac{Z}{P} = \cos^2 A + \frac{R}{P}\sin^2 A$ and $X(A) = \sqrt{1 + \frac{a^2 - b^2}{b^2}\sin^2 A}$ in eqs.(25) on p.77; for a/b, a value of 1.1222 is assumed.

A	$\log Z$	Z	$\log Z(A)$	$Z(A)$	$\log\sqrt{1+\frac{a^2-b^2}{b^2}\sin^2 A}$	$\sqrt{1+\frac{a^2-b^2}{b^2}\sin^2 A}$
0°	9.4623 − 10	0.2899	0.0000	1.0000	0.0000	1.0000
2	9.4624	0.2900	0.0001	1.0002	0.0001	1.0002
4	9.4627	0.2902	0.0004	1.0009	0.0003	1.0007
6	9.4632	0.2905	0.0009	1.0021	0.0006	1.0014
8	9.4640	0.2911	0.0017	1.0039	0.0011	1.0025
10	9.4649	0.2917	0.0026	1.0060	0.0017	1.0039
12	9.4661	0.2925	0.0038	1.0088	0.0024	1.0055
14	9.4674	0.2934	0.0051	1.0118	0.0033	1.0076
16	9.4689	0.2944	0.0066	1.0153	0.0042	1.0097
18	9.4706	0.2955	0.0083	1.0193	0.0053	1.0123
20	9.4724	0.2968	0.0101	1.0235	0.0065	1.0151
22	9.4744	0.2981	0.0121	1.0283	0.0078	1.0181
24	9.4766	0.2996	0.0143	1.0335	0.0091	1.0212
26	9.4788	0.3012	0.0165	1.0387	0.0106	1.0247
28	9.4812	0.3028	0.0189	1.0445	0.0121	1.0283
30	9.4837	0.3046	0.0214	1.0505	0.0136	1.0318

TABLE VIIa

SEELIGER'S DENSITY FUNCTION

$$\mathfrak{C} = \xi \int_0^{\pi/2} e^{-\xi\Phi} \cos\varphi \, d\varphi + \frac{8}{3} e^{-\xi\frac{3\pi-2}{8\pi}}$$

OF THE THEORY OF THE SATURN RING [EQ.(15), p.159]

The table contains

$$\log M = \log \frac{\mathfrak{C}(\infty)}{\mathfrak{C}(\xi)}, \text{ where } \mathfrak{C}(\infty) = \frac{16}{3} \quad \text{and} \quad \xi = \frac{N\vartheta}{\sin\alpha}.$$

ξ	$\log M$	ξ	$\log M$	ξ	$\log M$	ξ	$\log M$	ξ	$\log M$
0.0	0.3010	10.0	0.1389	20	0.0910	80	0.0311	200	0.0136
	163		37		29		16		43
0.5	0.2847	10.5	0.1352	21	0.0881	85	0.0295	300	0.0093
	147		35		28		15		22
1.0	0.2700	11.0	0.1317	22	0.0853	90	0.0280	400	0.0071
	134		32		25		13		14
1.5	0.2566	11.5	0.1285	23	0.0828	95	0.0267	500	0.0057
	121		30		25		11		9
2.0	0.2445	12.0	0.1255	24	0.0803	100	0.0256	600	0.0048
	111		29		23		20		7
2.5	0.2334	12.5	0.1226	25	0.0780	110	0.0236	700	0.0041
	101		28		22		18		5
3.0	0.2233	13.0	0.1198	26	0.0758	120	0.0218	800	0.0036
	93		27		20		15		4
3.5	0.2140	13.5	0.1171	27	0.0738	130	0.0203	900	0.0032
	85		26		19		13		3
4.0	0.2055	14.0	0.1145	28	0.0719	140	0.0190	1000	0.0029
	79		24		19		12		14
4.5	0.1976	14.5	0.1121	29	0.0700	150	0.0178	2000	0.0015
	74		23		17		10		8
5.0	0.1902	15.0	0.1098	30	0.0683	160	0.0168	4000	0.0007
	68		22		74		8		2
5.5	0.1834	15.5	0.1076	35	0.0609	170	0.0160	6000	0.0005
	63		22		60		8		1
6.0	0.1771	16.0	0.1054	40	0.0549	180	0.0152	8000	0.0004
	59		21		49		8		1
6.5	0.1712	16.5	0.1033	45	0.0500	190	0.0144	10000	0.0003
	55		19		40		8		
7.0	0.1657	17.0	0.1014	50	0.0460	200	0.0136		
	62		19		34				
7.5	0.1605	17.5	0.0995	55	0.0426				
	49		18		30				
8.0	0.1556	18.0	0.0977	60	0.0396				
	45		17		25				
8.5	0.1511	18.5	0.0960	65	0.0371				
	43		17		22				
9.0	0.1468	19.0	0.0943	70	0.0349				
	40		17		20				
9.5	0.1428	19.5	0.0926	75	0.0329				
	39		16		18				
10.0	0.1389	20.0	0.0910	80	0.0311				

TABLE VIIb

FUNCTION

$$\log M = \log \frac{\mathfrak{C}(\infty)}{\mathfrak{C}(\alpha)}$$

ACCORDING TO THE ARGUMENTS:

PHASE ANGLES α AND $\xi = \frac{N\delta}{\sin \alpha} = \frac{D}{\sin \alpha}$ WHERE D IS THE VOLUME DENSITY OF THE RING

α \ ξ	0.02	0.04	0.06	0.08	0.1	0.2	0.3	0.4	0.5	0.8
0.0	0.0000	0.0000	0.0000	0.0000	0.0000	0.0000	0.0000	0.0000	0.0000	0.0000
.1	.1288	.0830	.0618	.0493	.0412	.0228	.0158	.0123	.0099	.0063
.2	.1805	.1288	.1007	.0830	.0707	.0412	.0292	.0228	.0186	.0123
.3	.2084	.1591	.1288	.1086	.0940	.0571	.0412	.0325	.0266	.0175
.4	.2260	.1805	.1502	.1287	.1129	.0707	.0520	.0412	.0343	.0228
.5	.2381	.1964	.1670	.1455	.1288	.0830	.0618	.0493	.0412	.0277
.6	.2466	.2084	.1805	.1591	.1424	.0940	.0707	.0571	.0478	.0324
.7	.2533	.2183	.1915	.1706	.1539	.1038	.0790	.0643	.0540	.0369
.8	.2584	.2260	.2008	.1805	.1640	.1130	.0867	.0707	.0599	.0412
.9	.2626	.2324	.2084	.1889	.1728	.1213	.0940	.0770	.0656	.0454
1.0	.2661	.2381	.2151	.1964	.1805	.1288	.1007	.0830	.0707	.0493
1.5	.2769	.2559	.2380	.2222	.2086	.1591	.1288	.1086	.0944	.0675
2.0	.2825	.2660	.2513	.2381	.2260	.1805	.1502	.1288	.1129	.0830
2.5	.2860	.2724	.2598	.2486	.2380	.1964	.1670	.1454	.1288	.0965
3.0	.2885	.2769	.2661	.2559	.2467	.2086	.1805	.1591	.1424	.1086
3.5	.2906	.2798	.2706	.2617	.2533	.2183	.1915	.1706	.1539	.1192
4.0	.2917	.2825	.2741	.2660	.2584	.2260	.2008	.1805	.1640	.1288
4.5	.2927	.2843	.2769	.2695	.2626	.2324	.2086	.1888	.1727	.1374
5.0	.2936	.2860	.2791	.2724	.2661	.2381	.2151	.1963	.1804	.1454
5.5	.2942	.2873	.2811	.2749	.2688	.2426	.2209	.2028	.1872	.1525
6.0	.2948	.2885	.2825	.2769	.2713	.2466	.2259	.2084	.1935	.1591
6.5	.2953	.2895	.2836	.2786	.2734	.2501	.2304	.2135	.1989	.1650

TABLE VIIc

OBSERVED PHASE CURVE FOR THE MEAN SURFACE BRIGHTNESS OF THE RING, IN UNITS OF BRIGHTNESS OF THE PLANETARY CENTER IN OPPOSITION

α	In Magnitude Classes	In Absolute Units	α	In Magnitude Classes	In Absolute Units
0.0°	0.000	1.000	3.0°	0.270	0.780
0.2°	0.065	0.942	3.5°	0.290	0.766
0.4°	0.095	0.916	4.0°	0.310	0.752
0.6°	0.115	0.900	4.5°	0.330	0.738
0.8°	0.130	0.887	5.0°	0.345	0.728
1.0°	0.145	0.875	5.5°	0.360	0.718
1.5°	0.180	0.847	6.0°	0.370	0.711
2.0°	0.210	0.824	6.5°	0.380	0.705
2.5°	0.240	0.802			

TABLE VIIIa

VALUES FOR THE UNOCCULTED PORTION X OF THE RING AND THE SATURN DISK PORTION Y UNOCCULTED BY THE RING, IN EQ.(36) ON p.170, IN UNITS OF THE UNOCCULTED SATURN DISK

A	$\log X$	X		$\log Y$	Y	
0°	$-\infty$	0.000	47	0.0000	1.000	44
1	8.6694	0.047	46	9.9956	0.990	43
2	8.9705	0.093	47	9.9913	0.980	43
3	9.1469	0.140	47	9.9870	0.970	43
4	9.2719	0.187	47	9.9827	0.961	42
5	9.3691	0.234	47	9.9785	0.952	42
6	9.4486	0.281	47	9.9743	0.943	40
7	9.5160	0.328	48	9.9703	0.934	39
8	9.5745	0.376	47	9.9664	0.926	37
9	9.6262	0.423	48	9.9627	0.918	36
10	9.6726	0.471	48	9.9591	0.910	34
11	9.7147	0.519	48	9.9557	0.903	31
12	9.7533	0.567	48	9.9526	0.897	29
13	9.7890	0.615	49	9.9497	0.891	25
14	9.8223	0.664	49	9.9472	0.885	23
15	9.8533	0.713	50	9.9449	0.881	18
16	9.8827	0.763	51	9.9431	0.877	13
17	9.9105	0.814	51	9.9418	0.875	9
18	9.9469	0.865	52	9.9409	0.873	2
19	9.9623	0.917	53	9.9407	0.872	4
20	9.9866	0.970	54	9.9411	0.873	12
21	0.0102	1.024	56	9.9423	0.876	22
22	0.0332	1.080	58	9.9445	0.880	37
23	0.0560	1.138	63	9.9482	0.887	62
24	0.0796	1.201	64	9.9544	0.900	69
25	0.1022	1.265	64	9.9613	0.915	65
26	0.1234	1.329	62	9.9678	0.928	62
27	0.1433	1.391	61	9.9740	0.942	60
28	0.1621	1.452	61	9.9800	0.955	56
29	0.1799	1.513	60	9.9856	0.968	54
30	0.1966	1.573		9.9910	0.980	12

Reduction for Phase		
α	D	$\log D$
0°	1.0000	0.0000
1	0.9996	9.9998
2	0.9986	9.9994
3	0.9970	9.9987
4	0.9951	9.9979
5	0.9927	9.9968
6	0.9900	9.9956
7	0.9870	9.9943

TABLE VIIIb

REDUCTION OF SATURN BRIGHTNESSES TO THE VANISHED RING ACCORDING TO EQ.(36) ON p.170, UNDER ASSUMPTION OF LAMBERT'S LIGHT DISTRIBUTION OVER THE SATURN DISK

A	$\log X_L$	X_L	$\log Y_L$	Y_L
0°	$-\infty$	0.0000	0.0000	1.000
		72	52	12
1	8.8560	0.072	9.9948	0.988
		72	51	11
2	9.1571	0.144	9.9897	0.977
		72	51	12
3	9.3335	0.216	9.9846	0.965
		71	50	11
4	9.4585	0.287	9.9796	0.954
		72	47	10
5	9.5557	0.359	9.9749	0.944
		73	46	10
6	9.6352	0.432	9.9703	0.934
		72	43	9
7	9.7026	0.504	9.9660	0.925
		73	39	9
8	9.7611	0,577	9.9621	0,916
		73	36	7
9	9.8128	0.650	9.9585	0.909
		73	32	7
10	9.8592	0.723	9.9553	0.902
		74	26	5
11	9.9013	0.797	9.9527	0.897
		74	21	5
12	9.9399	0.871	9.9506	0.892
		74	17	3
13	9.9756	0.945	9.9489	0.889
		76	9	2
14	0.0089	1.021	9.9480	0.887
		75	5	1
15	0.0399	1.096	9.9475	0.886
		77	3	1
16	0.0693	1.173	9.9478	0.887
		78	11	2
17	0.0971	1.251	9.9489	0.889
		78	19	4
18	0.1235	1.329	9.9508	0.893
		80	26	5
19	0.1489	1.409	9.9534	0.898
		81	33	7
20	0.1732	1.490	9.9567	0.905
		83	43	9
21	0.1968	1.573	9.9610	0.914
		86	50	11
22	0,2199	1.659	9.9660	0.925
		89	60	13
23	0.2426	1.748	9.9720	0.938
		98	66	14
24	0.2662	1.846	9.9786	0.952
		98	61	13
25	0.2888	1.944	9.9847	0.965
		98	58	13
26	0.3100	2.042	9.9905	0.978
		95	54	12
27	0.3299	2.137	9.9959	0.990
		95	51	12
28	0.3487	2,232	0.0010	1.002
		93	48	11
29	0.3665	2.325	0.0058	1.013
		92	43	10
30	0,3832	2.417	0.0101	1.023

Reduction for Phase

α	$\log\cos\alpha$	$\cos\alpha$
0°	0.0000	1.0000
1	9.9999	0.9999
2	9.9997	0.9994
3	9.9994	0.9986
4	9.9989	0.9976
5	9.9983	0.9962
6	9.9976	0.9945
7	9.9968	0.9926

TABLE IXa

AUXILIARY QUANTITIES FOR CALCULATING THE SHADOW-CASTING OF THE RING ONTO SATURN AND OF THE PLANET ONTO THE RING

A	$\log b'$	$\varphi = v_{III}$	v_0	$\varphi' = v_{IV}$	v_0'	$\log c = \log\left(\frac{\sin A}{a\,b \cdot 180}\right)$	A
0°	9.9499	64° 1.′4	0° 0.′0	48°55.′6	0° 0.′0	$-\infty$	0°
		0° 1.4	2° 3.2	0.8	1° 8.9		
1	9.9499	64 2.8	2 3.2	48 56.4	1 8.9	6.0367	1
		0 4.0	2 3.6	2.4	1 8.9		
2	9.9500	64 6.8	4 6.8	48 58.6	2 17.8	6.3376	2
		0 6.9	2 4.4	3.8	1 9.2		
3	9.9501	64 13.7	6 11.2	49 2.4	3 27.0	6.5136	3
		0 9.6	2 5.6	5.4	1 9.5		
4	9.9502	64 23.3	8 16.8	49 7.8	4 36.5	6.6384	4
		0 12.4	2 7.1	6.8	1 10.0		
5	9.9504	64 35.7	10 23.9	49 14.6	5 46.5	6.7351	5
		0 15.4	2 9.2	8.5	1 10.5		
6	9.9505	64 51.1	12 33.1	49 23.1	6 57.0	6.8140	6
		0 18.4	2 11.8	10.0	1 11.1		
7	9.9508	65 9.5	14 44.9	49 33.1	8 8.1	6.8807	7
		0 21.6	2 14.8	11.7	1 11.9		
8	9.9510	65 31.1	16 59.7	49 44.8	9 20.0	6.9383	8
		0 24.9	2 18.5	13.3	1 12.9		
9	9.9513	65 56.0	19 18.2	49 58.1	10 32.9	6.9891	9
		0 28.4	2 22.8	15.0	1 13.9		
10	9.9516	66 24.4	21 41.0	50 13.1	11 46.8	7.0345	10
		0 32.2	2 27.7	16.8	1 15.1		
11	9.9520	66 56.6	24 8.7	50 29.9	13 1.9	7.0754	11
		0 36.3	2 33.8	18.5	1 16.4		
12	9.9524	67 32.9	26 42.5	50 48.4	14 18.3	7.1127	12
		0 40.7	2 40.7	20.4	1 17.9		
13	9.9528	68 13.6	29 23.2	51 8.8	15 36.2	7.1469	13
		0 45.7	2 49.0	22.4	1 19.5		
14	9.9532	68 59.3	32 12.2	51 31.2	16 55.7	7.1785	14
		0 51.2	2 58.8	24.4	1 21.3		
15	9.9537	69 50.5	35 11.0	51 55.6	18 17.0	7.2078	15
		0 57.5	3 10.7	26.4	1 23.3		
16	9.9542	70 48.0	38 21.7	52 22.0	19 40.3	7.2351	16
		1 4.9	3 25.2	28.7	1 25.6		
17	9.9547	71 52.9	41 46.9	52 50.7	21 5.9	7.2607	17
		1 13.8	3 43.5	31.0	1 27.9		
18	9.9552	73 6.7	45 30.4	53 21.7	22 33.8	7.2848	18
		1 24.9	4 7.2	33.5	1 30.7		
19	9.9558	74 31.6	49 37.6	53 55.2	24 4.5	7.3074	19
		1 39.5	4 39.6	36.1	1 33.6		
20	9.9564	76 11.1	54 17.2	54 31.3	25 38.1	7.3288	20
		2 0.4	5 27.4	38.9	1 36.9		
21	9.9570	78 11.8	59 44.6	55 10.2	27 15.0	7.3491	21
		2 34.9	6 48.9	41.9	1 40.5		
22	9.9577	80 46.4	66 33.5	55 52.1	28 55.5	7.3684	22
		3 56.8	10 8.2	45.1	1 44.6		
23	9.9584	84 43.2	76 41.7	56 37.2	30 40.1	7.3867	23
				48.6	1 49.1		
24	9.9591	90 0.0	90 0.0	57 25.8	32 29.2	7.4041	24
				52.5	1 54.1		
25	9.9598	90 0.0	90 0.0	58 18.3	34 23.3	7.4207	25
				56.7	1 59.7		
26	9.9605	90 0.0	90 0.0	59 15.0	36 23.0	7.4366	26
				61.5	2 6.3		
27	9.9612	90 0.0	90 0.0	60 16.5	38 29.3	7.4518	27
				66.7	2 13.6		
28	9.9620	90 0.0	90 0.0	61 23.2	40 42.9	7.4664	28
				72.9	2 22.3		
29	9.9628	90 0.0	90 0.0	62 36.1	45 5.2	7.4804	29
				79.8	2 32.3		
30	9.9636	90 0.0	90 0.0	63 55.9	45 37.5	7.4938	30

$\log \frac{\alpha^2}{2} = 0.41603$ $\log \frac{\alpha'^2}{2} = 0.06381$ $\log \frac{\alpha^2 - \alpha'^2}{2} = 0.16079$ $\log b = 9.94993$ $a = 1$

TABLE IXb

AUXILIARY QUANTITIES FOR CALCULATING THE SHADOW-CASTING OF THE SATURN RING ON THE PLANET, ACCORDING TO EQ.(40) ON p.172

A	$\log \Sigma_0$	$\log \Sigma_1$	$\log \Sigma$	$\log V$
0°	8.0704 − 10	8.5943 − 10	8.4398 − 10	$-\infty$
	3	2	5	
1	8.0707	8.5941	8.4393	5.735 − 10
	9	6	11	391
2	8.0716	8.5935	8.4382	6.036
	15	10	21	175
3	8.0731	8.5925	8.4361	6.211
	21	14	29	124
4	8.0752	8.5911	8.4332	6.335
	27	18	39	95
5	8.0779	8.5893	8.4293	6.430
	34	23	47	77
6	8.0813	8.5870	8.4246	6.507
	40	27	58	65
7	8.0853	8.5843	8.4188	6.572
	46	31	68	55
8	8.0899	8.5812	8.4120	6.627
	54	36	79	48
9	8.0953	8.5776	8.4041	6.675
	60	42	93	42
10	8.1013	8.5734	8.3948	6.717
	69	46	106	38
11	8.1082	8.5688	8.3842	6.755
	76	53	124	33
12	8.1158	8.5635	8.3718	6.788
	84	59	140	30
13	8.1242	8.5576	8.3578	6.818
	95	67	163	27
14	8.1337	8.5509	8.3415	6.845
	104	74	189	25
15	8.1441	8.5435	8.3226	6.870
	115	84	221	22
16	8.1556	8.5351	8.3005	6.892
	129	95	262	20
17	8.1685	8.5256	8.2743	6.912
	144	107	316	19
18	8.1829	8.5149	8.2427	6.931
	163	125	391	16
19	8.1992	8.5024	8.2036	6.947
	187	146	504	15
20	8.2179	8.4878	8.1532	6.962
	221	179	702	13
21	8.2400	8.4699	8.0830	6.975
	277	232	1076	12
22	8.2677	8.4467	7.9754	6.987
	407	361	2432	11
23	8.3084	8.4106	7.7322	6.998
	502	520		32
24	8.3586	8.3586	$-\infty$	7.030
	42	42		48
25	8.3544	8.3544	$-\infty$	7.078
	44	44		48
26	8.3500	8.3500	$-\infty$	7.126
	45	45		45
27	8.3455	8.3455	$-\infty$	7.171
	47	47		43
28	8.3408	8.3408	$-\infty$	7.214
	49	49		41
29	8.3359	8.3359	$-\infty$	7.255
	51	51		39
30	8.3308	8.3308	$-\infty$	7.294

TABLE IXc

AUXILIARY QUANTITIES λ(a), λ(b), AND λ(c) FOR CALCULATING THE SHADOW-CASTING OF SATURN ON THE RING, ACCORDING TO SEELIGER [EQ.(51)], p.175]

A	λ(a)	log λ(a)	λ(b)	log λ(b)	λ(c)	log λ(c)	A
0°	−0.0000		−0.0000	−	+	∞	0°
1	0	4.21_n-10	0	4.60_n-10	+0.4999	9.6989 − 10	1
2	0	4.66	0	5.34	0.2498	9.3976	2
3	0	5.00	1	5.72	0.1663	9.2200	3
4	0	5.29	1	5.97	0.1245	9.0952	4
5	0	5.48	1	6.16	0.0993	8.997	5
6	0	5.64	2	6.32	0.0825	8.916	6
7	1	5.78	3	6.46	0.0703	8.847	7
8	1	5.90	4	6.58	0.0611	8.786	8
9	1	6.00	5	6.69	0.0538	8.731	9
10	1	6.09	6	6.79	0.0480	8.681	10
11	2	6.18	8	6.88	0.0430	8.634	11
12	2	6.26	9	6.96	0.0388	8.589	12
13	2	6.33	11	7.043	0.0351	8.546	13
14	3	6.40	13	7.118	0.0319	8.503	14
15	3	6.46	16	7.191	0.0289	8.460	15
16	3	6.53	18	7.262	0.0262	8.417	16
17	4	6.58	21	7.331	0.0236	8.372	17
18	4	6.64	25	7.400	0.0211	8.324	18
19	5	6.69	30	7.470	0.0186	8.270	19
20	6	6.74	35	7.542	0.0161	8.207	20
21	6	6.79	42	7.619	0.0134	8.128	21
22	7	6.84	51	7.706	0.0104	8.015	22
23	8	6.89	66	7.822	0.0061	7.787	23
24	9	6.93	87	7.941	0.0009	6.935	24
25	10	6.98	82	7.914	0.0010	6.982	25
26	11	7.02	77	7.885	0.0011	7.025	26
27	12	7.07	72	7.856	0.0012	7.072	27
28	13	7.12	67	7.824	0.0013	7.117	28
29	14	7.16	62	7.793	0.0014	7.155	29
30	0.0016	7.20	0.0057	7.758	0.0016	7.201	30

TABLE Xa

MEAN EXTINCTION TABLES FOR POTSDAM (ELEVATION, 100 m) AND FOR THE SUMMIT OF SÄNTIS (2500 m); ACCORDING TO G.MÜLLER

True Zenith Distance	Potsdam		Säntis		True Zenith Distance	Potsdam		Säntis	
	Logarithms	Magn.	Logarithms	Magn.		Logarithms	Magn.	Logarithms	Magn.
11°	0.0006	0.00	0.0010	0.00	50°	0.0482	0.12	0.0310	0.08
12	0.0008	0.00	0.0012	0.00	51	0.0514	0.13	0.0328	0.08
13	0.0010	0.00	0.0014	0.00	52	0.0549	0.14	0.0348	0.09
14	0.0013	0.00	0.0017	0.00	53	0.0586	0.15	0.0369	0.09
15	0.0016	0.00	0.0019	0.00	54	0.0625	0.16	0.0391	0.10
16	0.0019	0.00	0.0022	0.01	55	0.0667	0.17	0.0415	0.10
17	0.0023	0.01	0.0025	0.01	56	0.0711	0.18	0.0440	0.11
18	0.0027	0.01	0.0029	0.01	57	0.0758	0.19	0.0466	0.12
19	0.0032	0.01	0.0032	0.01	58	0.0808	0.20	0.0494	0.12
20	0.0037	0.01	0.0036	0.01	59	0.0862	0.22	0.0524	0.13
21	0.0042	0.01	0.0040	0.01	60	0.0920	0.23	0.0556	0.14
22	0.0048	0.01	0.0044	0.01	61	0.0982	0.25	0.0590	0.15
23	0.0054	0.01	0.0048	0.01	62	0.1048	0.26	0.0627	0.16
24	0.0061	0.02	0.0053	0.01	63	0.1118	0.28	0.0667	0.17
25	0.0068	0.02	0.0058	0.01	64	0.1194	0.30	0.0710	0.18
26	0.0076	0.02	0.0063	0.02	65	0.1276	0.32	0.0757	0.19
27	0.0084	0.02	0.0068	0.02	66	0.1364	0.34	0.0808	0.20
28	0.0093	0.02	0.0074	0.02	67	0.1460	0.36	0.0863	0.22
29	0.0102	0.03	0.0080	0.02	68	0.1564	0.39	0.0922	0.23
30	0.0112	0.03	0.0086	0.02	69	0.1676	0.42	0.0987	0.25
31	0.0122	0.03	0.0093	0.02	70	0.1798	0.45	0.1059	0.26
32	0.0133	0.03	0.0100	0.03	71	0.1931	0.48	0.1139	0.28
33	0.0144	0.04	0.0107	0.03	72	0.2075	0.52	0.1228	0.31
34	0.0156	0.04	0.0115	0.03	73	0.2232	0.56	0.1327	0.33
35	0.0169	0.04	0.0123	0.03	74	0.2405	0.60	0.1438	0.36
36	0.0182	0.05	0.0132	0.03	75	0.2596	0.65	0.1563	0.39
37	0.0196	0.05	0.0141	0.04	76	0.2807	0.70	0.1705	0.43
38	0.0211	0.05	0.0150	0.04	77	0.3040	0.76	0.1868	0.47
39	0.0227	0.06	0.0160	0.04	78	0.3298	0.82	0.2057	0.51
40	0.0244	0.06	0.0170	0.04	79	0.3585	0.90	0.2277	0.57
41	0.0262	0.07	0.0181	0.05	80	0.3908	0.98	0.2536	0.63
42	0.0281	0.07	0.0192	0.05	81	0.4279	1.07	0.2845	0.71
43	0.0301	0.08	0.0204	0.05	82	0.4718	1.18	0.3221	0.81
44	0.0323	0.08	0.0217	0.05	83	0.5260	1.32	0.3688	0.92
45	0.0346	0.09	0.0231	0.06	84	0.5959	1.49	0.4277	1.07
46	0.0370	0.09	0.0245	0.06	85	0.6892	1.72	0.5034	1.26
47	0.0396	0.10	0.0260	0.06	86	0.8164	2.04	0.6035	1.51
48	0.0423	0.11	0.0276	0.07	87	0.9929	2.48	0.7408	1.85
49	0.0452	0.11	0.0293	0.07	88	1.2409	3.10	0.9358	2.34

The second column, under "logarithms", contains the values of $0.4(m_z - m_0)$, while the third column, under "magnitudes" gives the reductions of the brightnesses to the zenith $m_z - m_0$.

TABLE Xb

MEAN EXTINCTION TABLE FOR POTSDAM, BETWEEN 50° AND 88° ZENITH DISTANCE, FROM TENTH TO TENTH DEGREE IN BRIGHTNESS LOGARITHMS (ACCORDING TO G.MÜLLER)

True Zenith Distance	0.0	0.1	0.2	0.3	0.4	0.5	0.6	0.7	0.8	0.9
50°	0.0482	0.0485	0.0488	0.0491	0.0495	0.0498	0.0501	0.0504	0.0507	0.0511
51	514	517	521	524	528	531	535	538	542	545
52	549	553	556	560	564	567	571	575	578	582
53	586	590	594	597	601	605	609	613	617	621
54	625	629	633	637	642	646	650	654	658	663
55	667	671	676	680	684	689	693	698	702	706
56	711	716	720	725	729	734	739	744	748	753
57	758	763	768	773	778	783	788	793	798	803
58	808	813	818	824	829	835	840	845	851	856
59	862	868	873	879	885	891	896	902	908	914
60	920	926	932	938	944	951	957	963	969	976
61	982	988	995	1002	1008	1015	1021	1028	1035	1041
62	1048	1055	1062	1069	1076	1083	1090	1097	1104	1111
63	1118	1125	1133	1140	1148	1155	1163	1171	1178	1186
64	1194	1202	1210	1218	1226	1234	1242	1251	1259	1267
65	1276	1285	1293	1302	1310	1319	1328	1337	1346	1355
66	1364	1373	1383	1392	1401	1411	1421	1430	1440	1450
67	1460	1470	1480	1490	1501	1511	1521	1532	1543	1553
68	1564	1575	1586	1597	1608	1619	1630	1642	1653	1664
69	1676	1688	1700	1712	1724	1736	1748	1760	1773	1785
70	1798	1811	1824	1837	1850	1863	1876	1890	1904	1917
71	1931	1945	1959	1973	1987	2002	2016	2031	2045	2060
72	2075	2090	2106	2121	2137	2152	2168	2184	2200	2216
73	2232	2249	2265	2282	2299	2316	2334	2352	2369	2387
74	2405	2423	2442	2460	2479	2498	2517	2537	2556	2576
75	2596	2616	2637	2657	2678	2699	2720	2742	2763	2785
76	2807	2829	2852	2875	2898	2921	2944	2968	2992	3016
77	3040	3065	3090	3115	3140	3166	3192	3218	3244	3271
78	3298	3325	3353	3381	3409	3438	3467	3496	3525	3555
79	3585	3616	3647	3678	3710	3742	3775	3808	3841	3874
80	3908	3943	3978	4014	4050	4087	4124	4162	4200	4239
81	4279	4319	4360	4402	4444	4488	4532	4577	4623	4670
82	4718	4767	4817	4868	4920	4973	5028	5084	5141	5200
83	5260	5322	5385	5450	5517	5586	5656	5728	5803	5880
84	5959	6040	6124	6210	6299	6391	6485	6582	6682	6785
85	6892	7002	7115	7232	7353	7477	7606	7739	7876	8018
86	8164	0.8315	0.8471	0.8632	0.8799	0.8971	0.9150	0.9335	0.9526	0.9724
87	0.9929	1.0141	1.0360	1.0586	1.0821	1.1063	1.1314	1.1573	1.1842	1.2120

TABLE XIa

BEMPORAD'S MEAN EXTINCTION TABLE (FOR 0°C, 760 mm, AND SEA LEVEL)
Argument: apparent zenith distance z; transmission coefficient: p = 0.835.

z	Ext. in Magn. Classes		z	Ext. in Magn. Classes		z	Ext. in Magn. Classes		z	Ext. in Magn. Classes	
0°	0m.000	1	69°	0m.347	26	81°.8	1m.122	15	84°.7	1m.743	31
5	0.001	2	70	0.373	28	81.9	1.137	15	84.8	1.774	32
10	0.003	5	71	0.401	31	82.0	1.152	16	84.9	1.806	33
15	0.007	6	72	0.432	36	82.1	1.168	16	85.0	1.839	35
20	0.013	7	73	0.468	39	82.2	1.184	16	85.1	1.874	35
25	0.020	10	74	0.507	44	82.3	1.200	17	85.2	1.909	37
30	0.030	13	75	0.551	51	82.4	1.217	17	85.3	1.946	38
35	0.043	17	76	0.602	58	82.5	1.234	17	85.4	1.984	40
40	0.060	21	77	0.660	68	82.6	1.251	18	85.5	2.024	40
45	0.081	27	78	0.728	79	82.7	1.269	18	85.6	2.064	42
50	0.108	7	79	0.807	98	82.8	1.287	19	85.7	2.106	43
51	0.115	7	80.0	0.901	10	82.9	1.306	19	85.8	2.149	45
52	0.122	7	80.1	0.911	11	83.0	1.325	20	85.9	2.194	46
53	0.129	8	80.2	0.922	11	83.1	1.345	20	86.0	2.240	48
54	0.137	8	80.3	0.933	10	83.2	1.365	21	86.1	2.288	50
55	0.145	8	80.4	0.943	11	83.3	1.386	21	86.2	2.338	51
56	0.153	10	80.5	0.954	12	83.4	1.407	22	86.3	2.389	54
57	0.163	10	80.6	0.966	11	83.5	1.429	22	86.4	2.443	56
58	0.173	10	80.7	0.977	12	83.6	1.451	23	86.5	2.499	58
59	0.183	12	80.8	0.989	12	83.7	1.474	24	86.6	2.557	60
60	0.195	12	80.9	1.001	13	83.8	1.498	24	86.7	2.617	63
61	0.207	13	81.0	1.014	12	83.9	1.522	25	86.8	2.680	65
62	0.220	14	81.1	1.026	13	84.0	1.547	26	86.9	2.745	68
63	0.234	15	81.2	1.039	13	84.1	1.573	26	87.0	2.813	71
64	0.249	17	81.3	1.052	14	84.2	1.599	27	87.1	2.884	73
65	0.266	17	81.4	1.066	13	84.3	1.536	28	87.2	2.957	76
66	0.283	20	81.5	1.079	14	84.4	1.654	29	87.3	3.033	80
67	0.303	21	81.6	1.093	14	84.5	1.683	29	87.4	3.113	84
68	0.324	23	81.7	1.107	15	84.6	1.712	31	87.5	3.197	87

TABLE XIa (continued)

z	Ext. in Magn. Classes		z	Ext. in Magn. Classes		z	Ext. in Magn. Classes		z	Ext. in Magn. Classes	
87°.6	3m.284		88°.0	3m.678		88°.4	4m.154		88°.8	4m.739	
		92			110			135			167
87.7	3.376		88.1	3.788		88.5	4.289		88.9	4.906	
		96			116			142			176
87.8	3.472		88.2	3.904		88.6	4.431		89.0	5.082	
		101			122			150			
87.9	3.573		88.3	4.026		88.7	4.581				
		105			128			158			

TABLE XIb

CORRECTIONS OF EXTINCTION FOR PRESSURE AND TEMPERATURE
(ACCORDING TO BEMPORAD)
(units, 0.01 magnitude class)

$z = 87°.$

t \ B	720mm	730	740	750	760	770	780	790
−20°	−11	− 7	− 3	+ 1	+5	+9	+13	+17
−10	−13	− 9	− 5	− 1	+3	+6	+10	+14
0	−15	−11	− 7	− 4	0	+4	+ 8	+12
+10	−17	−13	− 9	− 6	−2	+2	+ 6	+ 9
+20	−19	−15	−11	− 8	−4	0	+ 3	+ 7
+30	−21	−17	−13	−10	−6	−2	+ 1	+ 5

$z = 88°.$

−20°	−12	− 7	− 2	+ 3	+ 9	+14	+19	+24
−10	−16	−11	− 6	− 1	+ 4	+ 9	+14	+20
0	−20	−15	−10	− 5	− 0	+ 5	+10	+15
+10	−24	−19	−14	− 9	− 4	+ 1	+ 6	+11
+20	−28	−23	−18	−13	− 8	− 3	+ 2	+ 7
+30	−31	−26	−21	−16	−12	− 7	− 2	+ 3

$z = 89°.$

−20°	−11	− 3	+ 4	+11	+19	+26	+34	+41
−10	−20	−12	− 5	+ 2	+ 9	+16	+24	+31
0	−28	−21	−14	− 7	0	+ 7	+15	+22
+10	−36	−29	−22	−15	− 8	− 1	+ 6	+13
+20	−43	−36	−29	−23	−16	− 9	− 2	+ 5
+30	−51	−44	−37	−31	−24	−17	−11	− 4

TABLE XIIa

TRAVERSED AIR MASSES ACCORDING TO BEMPORAD, FOR VARIOUS APPARENT ZENITH DISTANCES OF THE CELESTIAL BODY

z	F(z)	z	F(z)	z	F(z)	z	F(z)
0°	1.000	30°	1.154	60°	1.995	63.0	2.195
			12		6		8
1	1.000	31	1.166	60.1	2.001	63.1	2.203
			12		6		8
2	1.001	32	1.178	60.2	2.007	63.2	2.211
			13		6		7
3	1.002	33	1.191	60.3	2.013	63.3	2.218
			14		6		8
4	1.002	34	1.205	60.4	2.019	63.4	2.226
			15		6		8
5	1.004	35	1.220	60.5	2.025	63.5	2.234
			15		6		8
6	1.005	36	1.235	60.6	2.031	63.6	2.242
			16		6		8
7	1.007	37	1.251	60.7	2.037	63.7	2.250
			16		7		8
8	1.010	38	1.267	60.8	2.044	63.8	2.258
			18		6		8
9	1.012	39	1.285	60.9	2.050	63.9	2.266
			19		6		8
10	1.015	40	1.304	61.0	2.056	64.0	2.274
			20		6		8
11	1.018	41	1.324	61.1	2.062	64.1	2.282
			20		7		8
12	1.022	42	1.344	61.2	2.069	64.2	2.290
			22		7		8
13	1.026	43	1.366	61.3	2.076	64.3	2.298
			23		7		8
14	1.030	44	1.389	61.4	2.083	64.4	2.306
			24		6		8
15	1.035	45	1.413	61.5	2.089	64.5	2.314
			25		7		8
16	1.040	46	1.438	61.6	2.096	64.6	2.322
			26		6		8
17	1.046	47	1.464	61.7	2.102	64.7	2.330
			28		7		9
18	1.052	48	1.492	61.8	2.109	64.8	2.339
			30		7		9
19	1.058	49	1.522	61.9	2.116	64.9	2.348
			31		7		9
20	1.064	50	1.553	62.0	2.123	65.0	2.357
			33		7		8
21	1.071	51	1.586	62.1	2.130	65.1	2.365
			35		7		9
22	1.078	52	1.621	62.2	2.137	65.2	2.374
			37		7		9
23	1.086	53	1.658	62.3	2.144	65.3	2.383
			40		7		9
24	1.094	54	1.698	62.4	2.151	65.4	2.392
			42		7		9
25	1.103	55	1.740	62.5	2.158	65.5	2.401
			44		7		9
26	1.112	56	1.784	62.6	2.165	65.6	2.410
	10		47		7		9
27	1.122	57	1.831	62.7	2.172	65.7	2.419
	10		51		8		9
28	1.132	58	1.882	62.8	2.180	65.8	2.428
	11		55		7		9
29	1.143	59	1.937	62.9	2.187	65.9	2.437
	11		58		8		10

TABLE XIIa (continued)

z	F(z)	z	F(z)	z	F(z)	z	F(z)
66°.0	2.447	69°.1	2.785	72°.2	3.243	75°.3	3.890
	9		13		17		
66.1	2.456	69.2	2.798	72.3	3.260	75.4	3.915
	10		13		18		
66.2	2.466	69.3	2.811	72.4	3.278	75.5	3.941
	10		13		18		
66.3	2.476	69.4	2.824	72.5	3.296	75.6	3.967
	10		13		18		
66.4	2.486	69.5	2.837	72.6	3.314	75.7	3.993
	10		13		18		
66.5	2.496	69.6	2.850	72.7	3.332	75.8	4.020
	10		13		18		
66.6	2.506	69.7	2.863	72.8	3.340	75.9	4.047
	10		14		19		
66.7	2.516	69.8	2.877	72.9	3.369	76.0	4.075
	10		13		19		
66.8	2.526	69.9	2.880	73.0	3.388	76.1	4.103
	10		14		19		
66.9	2.536	70.0	2.904	73.1	3.407	76.2	4.131
	10		14		19		
67.0	2.546	70.1	2.918	73.2	3.426	76.3	4.159
	10		14		19		
67.1	2.556	70.2	2.932	73.3	3.445	76.4	4.188
	11		14		20		
67.2	2.567	70.3	2.946	73.4	3.465	76.5	4.218
	10		14		20		
67.3	2.577	70.4	2.960	73.5	3.485	76.6	4.248
	11		15		20		
67.4	2.588	70.5	2.975	73.6	3.505	76.7	4.278
	11		14		21		
67.5	2.599	70.6	2.989	73.7	3.526	76.8	4.309
	11		15		20		
67.6	2.610	70.7	3.004	73.8	3.546	76.9	4.340
	11		15		21		
67.7	2.621	70.8	3.019	73.9	3.567	77.0	4.372
	11		15		21		
67.8	2.632	70.9	3.034	74.0	3.588	77.1	4.404
	11		15				
67.9	2.643	71.0	3.049	74.1	3.610	77.2	4.436
	11		15				
68.0	2.654	71.1	3.064	74.2	3.632	77.3	4.469
	11		15				
68.1	2.665	71.2	3.079	74.3	3.654	77.4	4.503
	12		16				
68.2	2.677	71.3	3.095	74.4	3.676	77.5	4.537
	11		15				
68.3	2.688	71.4	3.110	74.5	3.699	77.6	4.572
	12		16				
68.4	2.700	71.5	3.126	74.6	3.722	77.7	4.607
	12		16				
68.5	2.712	71.6	3.142	74.7	3.745	77.8	4.643
	12		17				
68.6	2.724	71.7	3.159	74.8	3.768	77.9	4.679
	12		16				
68.7	2.736	71.8	3.175	74.9	3.792	78.0	4.716
	12		17				37
68.8	2.748	71.9	3.192	75.0	3.816	78.1	4.753
	12		17				39
68.9	2.760	72.0	3.209	75.1	3.840	78.2	4.792
	13		17				39
69.0	2.773	72.1	3.226	75.2	3.865	78.3	4.831
	12		17				39

TABLE XIIa (continued)

z	F(z)		z	F(z)		z	F(z)		z	F(z)	
78°.4	4.870	40	81°.5	6.512	71	84° 6′	9.032	22	84° 37′	9.770	26
78.5	4.910	40	81.6	6.583	73	84 7	9.054	22	84 38	9.796	26
78.6	4.950	42	81.7	6.656	74	84 8	9.076	22	84 39	9.822	26
78.7	4.992	42	81.8	6.730	76	84 9	9.098	23	84 40	9.848	26
78.8	5.034	43	81.9	6.806	78	84 10	9.121	23	84 41	9.874	26
78.9	5.077	43	82.0	6.884	80	84 11	9.143	23	84 42	9.900	26
79.0	5.120	44	82.1	6.964	81	84 12	9.166	23	84 43	9.926	27
79.1	5.164	46	82.2	7.045	83	84 13	9.189	23	84 44	9.953	26
79.2	5.210	46	82.3	7.128	85	84 14	9.212	23	84 45	9.979	27
79.3	5.256	47	82.4	7.213	87	84 15	9.235	23	84 46	10.006	27
79.4	5.303	48	82.5	7.300	89	84 16	9.258	23	84 47	10.033	27
79.5	5.351	48	82.6	7.389	92	84 17	9.281	23	84 48	10.060	27
79.6	5.399	49	82.7	7.481	93	84 18	9.304	24	84 49	10.087	27
79.7	5.448	50	82.8	7.574	96	84 19	9.328	23	84 50	10.114	28
79.8	5.498	51	82.9	7.670	98	84 20	9.351	24	84 51	10.142	27
79.9	5.549	51	83.0	7.768	101	84 21	9.375	24	84 52	10.169	28
80.0	5.600	52	83.1	7.869	103	84 22	9.399	24	84 53	10.197	28
80.1	5.652	53	83.2	7.972	106	84 23	9.423	24	84 54	10.225	28
80.2	5.705	55	83.3	8.078	108	84 24	9.447	24	84 55	10.253	28
80.3	5.760	56	83.4	8.186	112	84 25	9.471	24	84 56	10.281	29
80.4	5.816	57	83.5	8.298	114	84 26	9.495	25	84 57	10.310	28
80.5	5.873	59	83.6	8.412	117	84 27	9.520	24	84 58	10.338	29
80.6	5.932	60	83.7	8.529	121	84 28	9.544	25	84 59	10.367	28
80.7	5.992	61	83.8	8.650	123	84 29	9.569	24	85 0	10.395	29
80.8	6.053	61	83.9	8.773	127	84 30	9.593	25	85 1	10.424	29
80.9	6.114	63	84.0	8.900	22	84 31	9.618	25	85 2	10.453	30
81.0	6.177	64	84° 1′	8.922	22	84 32	9.643	25	85 3	10.483	29
81.1	6.241	65	84 2	8.944	22	84 33	9.668	26	85 4	10.512	30
81.2	6.306	67	84 3	8.966	22	84 34	9.694	25	85 5	10.542	29
81.3	6.373	69	84 4	8.988	22	84 35	9.719	25	85 6	10.571	30
81.4	6.442	70	84 5	9.010	22	84 36	9.744	26	85 7	10.601	30

TABLE XIIa (continued)

z	F(z)	z	F(z)	z	F(z)	z	F(z)
85° 8′	10.631	85° 39′	11.645	86° 10′	12.854	86° 41′	14.314
	30		36		43		52
85 9	10.661	85 40	11.681	86 11	12.897	86 42	14.366
	30		36		43		53
85 10	10.691	85 41	11.717	86 12	12.940	86 43	14.419
	31		36		43		52
85 11	10.722	85 42	11.753	86 13	12.983	86 44	14.471
	30		37		44		53
85 12	10.752	85 43	11.790	86 14	13.027	86 45	14.524
	31		36		44		54
85 13	10.783	85 44	11.826	86 15	13.071	86 46	14.578
	31		37		44		54
85 14	10.814	85 45	11.863	86 16	13.115	86 47	14.632
	31		37		45		54
85 15	10.845	85 46	11.900	86 17	13.160	86 48	14.686
	31		37		44		54
85 16	10.876	85 47	11.937	86 18	13.204	86 49	14.740
	32		37		45		55
85 17	10.908	85 48	11.974	86 19	13.249	86 50	14.795
	31		38		45		55
85 18	10.939	85 49	12.012	86 20	13.294	86 51	14.850
	32		38		46		56
85 19	10.971	85 50	12.050	86 21	13.340	86 52	14.906
	32		38		46		56
85 20	11.003	85 51	12.088	86 22	13.386	86 53	14.962
	32		38		46		56
85 21	11.035	85 52	12.126	86 23	13.432	86 54	15.018
	33		38		46		57
85 22	11.068	85 53	12.164	86 24	13.478	86 55	15.075
	32		38		47		57
85 23	11.100	85 54	12.202	86 25	13.525	86 56	15.132
	33		39		47		58
85 24	11.133	85 55	12.241	86 26	13.572	86 57	15.190
	33		39		47		58
85 25	11.166	85 56	12.280	86 27	13.619	86 58	15.248
	33		40		48		58
85 26	11.199	85 57	12.320	86 28	13.667	86 59	15.306
	33		39		48		59
85 27	11.232	85 58	12.359	86 29	13.715	87 0	15.365
	34		40		48		59
85 28	11.266	85 59	12.399	86 30	13.763	87 1	15.424
	33		40		49		59
85 29	11.299	86 0	12.439	86 31	13.812	87 2	15.483
	34		41		48		60
85 30	11.333	86 1	12.480	86 32	13.860	87 3	15.543
	34		40		49		60
85 31	11.367	86 2	12.520	86 33	13.909	87 4	15.603
	34		41		50		61
85 32	11.401	86 3	12.561	86 34	13.959	87 5	15.664
	34		41		50		61
85 33	11.435	86 4	12.602	86 35	14.009	87 6	15.725
	35		41		50		62
85 34	11.470	86 5	12.643	86 36	14.059	87 7	15.787
	35		42		50		62
85 35	11.505	86 6	12.685	86 37	14.109	87 8	15.849
	35		42		51		63
85 36	11.540	86 7	12.727	86 38	14.160	87 9	15.912
	35		42		51		63
85 37	11.575	86 8	12.769	86 39	14.211	87 10	15.975
	35		42		51		63
85 38	11.610	86 9	12.811	86 40	14.262	87 11	16.038
	35		43		52		64

TABLE XIIa (continued)

z	F(z)	z	F(z)	z	F(z)	z	F(z)
87° 12′	16.102	87° 39′	18.010	88° 6′	20.351	88° 33′	23.266
	64		78		97		121
87 13	16.166	87 40	18.088	88 7	20.448	88 34	23.387
	65		79		97		123
87 14	16.231	87 41	18.167	88 8	20.545	88 35	23.510
	65		80		98		123
87 15	16.296	87 42	18.247	88 9	20.643	88 36	23.633
	66		80		99		125
87 16	16.362	87 43	18.327	88 10	20.742	88 37	23.758
	66		81		100		126
87 17	16.428	87 44	18.408	88 11	20.842	88 38	23.884
	66		81		101		127
87 18	16.494	87 45	18.489	88 12	20.943	88 39	24.011
	67		82		102		128
87 19	16.561	87 46	18.571	88 13	21.045	88 40	24.139
	68		82		102		129
87 20	16.629	87 47	18.653	88 14	21.147	88 41	24.268
	68		83		103		130
87 21	16.697	87 48	18.736	88 15	21.250	88 42	24.398
	68		84		105		131
87 22	16.765	87 49	18.820	88 16	21.355	88 43	24.529
	69		85		105		133
87 23	16.834	87 50	18.905	88 17	21.460	88 44	24.662
	69		85		106		134
87 24	16.903	87 51	18.990	88 18	21.566	88 45	24.796
	70		86		106		137
87 25	16.973	87 52	19.076	88 19	21.672	88 46	24.931
	71		86		107		137
87 26	17.044	87 53	19.162	88 20	21.779	88 47	25.068
	71		87		109		137
87 27	17.115	87 54	19.249	88 21	21.888	88 48	25.205
	72		88		109		138
87 28	17.187	87 55	19.337	88 22	21.997	88 49	25.343
	72		89		111		140
87 29	17.259	87 56	19.426	88 23	22.108	88 50	25.483
	72		89		111		142
87 30	17.331	87 57	19.515	88 24	22.219	88 51	25.625
	73		90		112		142
87 31	17.404	87 58	19.605	88 25	22.331	88 52	25.767
	74		91		114		144
87 32	17.478	88 59	19.696	88 26	22.445	88 53	25.911
	74		91		114		146
87 33	17.552	88 0	19.787	88 27	22.559	88 54	26.057
	75		92		115		146
87 34	17.627	88 1	19.879	88 28	22.674	88 55	26.203
	75		92		116		148
87 35	17.702	88 2	19.971	88 29	22.790	88 56	26.351
	76		94		118		150
87 36	17.778	88 3	20.065	88 30	22.908	88 57	26.501
	77		95		118		151
87 37	17.855	88 4	20.160	88 31	23.026	88 58	26.652
	77		95		120		153
87 38	17.932	88 5	20.255	88 32	23.146	88 59	26.805
	78		96		120		154
						89 0	26.959

TABLE XIIb

CORRECTIONS OF THE AIR MASSES $[F_1(z) - F(z)]$ FOR PRESSURE AND TEMPERATURE, IN UNITS OF THE THIRD SIGNIFICANT FIGURE (ACCORDING TO BEMPORAD)

$z = 87°$.

B \ t	-20°	-10°	0°	+10°	+20°	+30°
720mm	+216	+ 96	−20	−131	−238	−342
730	+222	+101	−15	−126	−234	−338
740	+227	+107	−10	−122	−229	−333
750	+233	+112	− 5	−117	−225	−329
760	+239	+117	0	−112	−221	−325
770	+244	+123	+ 5	−108	−216	−321
780	+250	+128	+10	−103	−212	−317
790	+256	+133	+15	− 98	−207	−313

$z = 88°$.

B \ t	-20°	-10°	0°	+10°	+20°	+30°
720mm	+406	+178	−39	−246	−443	−632
730	+417	+188	−30	−237	−434	−624
740	+428	+198	−20	−228	−426	−616
750	+439	+209	−10	−219	−418	−608
760	+451	+219	0	−210	−410	−601
770	+462	+229	+10	−201	−401	−593
780	+473	+240	+19	−192	−393	−585
790	+484	+250	+28	−183	−385	−577

$z = 89°$.

B \ t	-20°	-10°	0°	+10°	+20°	+30°
720mm	+844	+365	−84	−504	−901	−1275
730	+869	+387	−63	−485	−883	−1259
740	+894	+410	−42	−466	−866	−1243
750	+920	+433	−21	−447	−848	−1226
760	+945	+456	0	−428	−831	−1210
770	+970	+479	+21	−409	−813	−1194
780	+996	+502	+42	−389	−795	−1177
790	+1021	+525	+63	−370	−778	−1161

TABLE XIIc

$\frac{\log p_1}{\log p}$ FOR VARIOUS VALUES OF PRESSURE AND TEMPERATURE (IN CELSIUS) ACCORDING TO BEMPORAD

B \ t	-20°	-10°	0°	+10°	+20°	+30°
720mm	9.97645	9.97648	9.97652	9.97655	9.97659	9.97662
730	9.98244	9.98247	9.98251	9.98254	9.98258	9.98261
740	9.98835	9.98838	9.98842	9.98845	9.98849	9.98852
750	9.99418	9.99421	9.99425	9.99428	9.99432	9.99435
760	9.99993	9.99997	0.00000	0.00003	0.00007	0.00010
770	0.00561	0.00564	0.00568	0.00571	0.00574	0.00579
780	0.01121	0.01125	0.01128	0.01131	0.01135	0.01138
790	0.01675	0.01678	0.01681	0.01685	0.01688	0.01691

TABLE XIIIa

THE FUNCTION $Ce^{-C}G\{c(\sec\zeta - 1)\}$ (ACCD. TO L. V. KING)

C \ ζ	0°	20°	40°	60°	70°	80°
0.00	0.0000	0.0000	0.0000	0.0000	0.0000	0.0000
.05	.0476	.0475	.0472	.0464	.0443	.0424
.10	.0905	.0902	.0891	.0861	.0813	.0720
.14	.1217	.1212	.1191	.1133	.1072	.0889
.18	.1502	.1492	.1461	.1377	.1270	.1009
.22	.1766	.1753	.1708	.1583	.1439	.1093
.26	.2002	.1985	.1927	.1761	.1575	.1150
.30	.2220	.2200	.2136	.1953	.1749	.1174
.34	.2420	.2395	.2298	.2052	.1776	.1198
.38	.2600	.2568	.2450	.2163	.1844	.1206
.50	.303	.298	.280	.238	.1964	.1154
.60	.329	.323	.301	.248	.1950	.1090
.70	.348	.340	.313	.250	.1930	.1006
.80	.359	.350	.318	.247	.1850	.0923
0.90	0.366	0.356	0.320	0.241	0.1740	0.0856

TABLE XIIIb

THE FUNCTION $G(C\sec\zeta) = \dfrac{1 - e^{-C\sec\zeta}}{C\sec\zeta}$ (ACCD. TO L. V. KING)

C \ ζ	0°	20°	40°	60°	70°	80°	85°
0.00	1.0000	1.0000	1.0000	1.0000	1.0000	1.0000	1.0000
.05	0.975	0.974	0.968	0.952	0.930	0.869	0.761
.10	.952	.949	.937	.906	.867	.760	.595
.14	.933	.929	.914	.872	.821	.686	.498
.18	.915	.910	.891	.840	.777	.623	.423
.22	.898	.892	.869	.809	.738	.567	.364
.26	.881	.874	.848	.780	.700	.518	.318
.30	.864	.856	.827	.752	.666	.476	.281
.34	.848	.839	.808	.726	.634	.439	.251
.38	.832	.823	.788	.700	.604	.406	.226
.50	.787	.775	.734	.632	.525	.328	.174
.60	.752	.739	.693	.583	.471	.280	.145
.70	.719	.705	.656	.538	.425	.244	.124
.80	.688	.673	.621	.499	.386	.215	.109
0.90	0.659	0.643	0.588	0.464	0.353	0.192	0.097

TABLE XIIIc

THE FUNCTIONS $\Phi(C, 0) = (1 - e^{-C})[1 - f(C)] + B(C) - B(2C) + e^{-C}[B(C) - \gamma]$,

$G(C) = \dfrac{1 - e^{-C}}{C}$ and $f(C) = e^{-C} + C\,\mathrm{li}(e^{-C})$,

(ACCD. TO L. V. KING)

C	$\Phi(C, 0)$	$G(C)$	$f(C)$
0.00	0.0000	1.0000	1.0000
.05	.0095	0.9754	0.828
.10	.0311	.9516	.722
.14	.0536	.933	.656
.18	.0801	.915	.600
.22	.1081	.898	.550
.26	.1403	.881	.508
.30	.1723	.864	.469
.34	.2065	.848	.435
.38	.2414	.832	.404
.50	.349	.787	.327
.60	.438	.752	.276
.70	.525	.719	.235
.80	.612	.688	.201
0.90	0.686	0.659	0.172

TABLE XIVa

THE FUNCTION $E(C, i) = \frac{G(C \sec i)}{\frac{1}{2}\{f(C) + G(C)\}}$, CORRESPONDING TO THE MEAN SOLUTION OF THE DIFFUSION INTEGRAL EQUATION [EQ.(29) ON p.247] AT AN ABSORPTION COEFFICIENT $\gamma = 0$ AND $C = c$

C \ i	0°	20°	40°	60°	70°	80°	90°
0.00	1.000	1.000	1.000	1.000	1.000	1.000	0.000
0.05	1.082	1.080	1.074	1.055	1.032	0.964	0.000
0.10	1.137	1.134	1.120	1.083	1.036	0.908	0.000
0.14	1.174	1.169	1.150	1.098	1.033	0.864	0.000
0.18	1.208	1.201	1.176	1.109	1.026	0.822	0.000
0.22	1.240	1.232	1.201	1.118	1.019	0.783	0.000
0.26	1.268	1.259	1.221	1.123	1.009	0.747	0.000
0.30	1.296	1.285	1.242	1.128	0.999	0.714	0.000
0.34	1.322	1.308	1.259	1.131	0.988	0.684	0.000
0.38	1.346	1.331	1.276	1.133	0.977	0.657	0.000
0.50	1.413	1.392	1.319	1.135	0.943	0.589	0.000
0.60	1.463	1.438	1.349	1.135	0.917	0.545	0.000
0.70	1.507	1.478	1.374	1.128	0.892	0.511	0.000
0.80	1.548	1.514	1.396	1.122	0.869	0.483	0.000
0.90	1.586	1.548	1.415	1.115	0.848	0.462	0.000

TABLE XIVb

THE FUNCTION

$$\Phi(C, \varepsilon) = (1 - e^{-C \sec \varepsilon}) \cdot (1 - f(C)) + \cos \varepsilon \left[B(C) - B(C(1 + \sec \varepsilon)) + e^{-C \sec \varepsilon}\{B(C) - B(-C(\sec \varepsilon - 1))\}\right]$$

[EQ.(35) ON p.249]

C \ ε	0°	20°	40°	60°	70°	80°	90°
0.00	0.000	0.000	0.000	0.000	0.000	0.000	0.000
0.05	0.008	0.010	0.013	0.019	0.025	0.049	0.172
0.10	0.031	0.036	0.041	0.060	0.083	0.144	0.278
0.14	0.054	0.057	0.067	0.102	0.137	0.227	0.344
0.18	0.080	0.085	0.099	0.147	0.198	0.312	0.400
0.22	0.110	0.116	0.137	0.196	0.262	0.395	0.450
0.26	0.140	0.148	0.176	0.248	0.325	0.471	0.492
0.30	0.172	0.182	0.216	0.301	0.388	0.545	0.531
0.34	0.206	0.217	0.257	0.355	0.450	0.609	0.565
0.38	0.241	0.253	0.300	0.405	0.509	0.669	0.596
0.50	0.348	0.364	0.420	0.560	0.675	0.818	0.673
0.60	0.437	0.456	0.526	0.676	0.795	0.911	0.724
0.70	0.526	0.549	0.625	0.783	0.899	0.984	0.765
0.80	0.609	0.634	0.717	0.879	0.985	1.042	0.799
0.90	0.692	0.719	0.803	0.969	1.060	1.088	0.828

TABLE XIVc

THE FUNCTION $R'(C, \epsilon, i) = C \sec \epsilon \; G(C(\sec \epsilon + \sec i))$ [EQ.(52) ON p.254] FOR VARIOUS VALUES OF C, ϵ, AND i

$R'(C, \epsilon, 0)$

C \ ε	0°	20°	40°	60°	70°	80°	90°
0.00	0.000	0.000	0.000	0.000	0.000	0.000	1.000
0.05	0.048	0.050	0.061	0.093	0.133	0.244	1.000
0.10	0.090	0.096	0.117	0.173	0.241	0.418	1.000
0.14	0.122	0.129	0.156	0.228	0.315	0.521	1.000
0.18	0.151	0.160	0.192	0.278	0.377	0.599	1.000
0.22	0.178	0.188	0.226	0.321	0.431	0.660	1.000
0.26	0.203	0.213	0.256	0.361	0.477	0.707	1.000
0.30	0.225	0.238	0.283	0.396	0.515	0.740	1.000
0.34	0.247	0.260	0.308	0.426	0.548	0.767	1.000
0.38	0.266	0.280	0.330	0.453	0.577	0.787	1.000
0.50	0.317	0.332	0.388	0.518	0.639	0.824	1.000
0.60	0.349	0.366	0.424	0.556	0.674	0.836	1.000
0.70	0.375	0.394	0.453	0.585	0.698	0.845	1.000
0.80	0.399	0.416	0.475	0.606	0.713	0.848	1.000
0.90	0.417	0.435	0.496	0.623	0.724	0.849	1.000

$R'(C, \epsilon, 20°)$

C \ ε	0°	20°	40°	60°	70°	80°	90°
0.00	0.000	0.000	0.000	0.000	0.000	0.000	1.000
0.05	0.048	0.050	0.061	0.093	0.132	0.244	1.000
0.10	0.090	0.096	0.117	0.172	0.241	0.417	1.000
0.14	0.121	0.129	0.156	0.227	0.314	0.519	1.000
0.18	0.150	0.160	0.191	0.276	0.375	0.597	1.000
0.22	0.177	0.187	0.223	0.319	0.429	0.655	1.000
0.26	0.201	0.212	0.252	0.358	0.473	0.699	1.000
0.30	0.224	0.236	0.280	0.392	0.511	0.734	1.000
0.34	0.244	0.257	0.305	0.423	0.543	0.760	1.000
0.38	0.263	0.277	0.327	0.448	0.572	0.781	1.000
0.50	0.312	0.328	0.382	0.512	0.632	0.815	1.000
0.60	0.344	0.360	0.417	0.548	0.667	0.829	1.000
0.70	0.370	0.387	0.447	0.577	0.687	0.838	1.000
0.80	0.391	0.408	0.467	0.597	0.702	0.840	1.000
0.90	0.409	0.426	0.485	0.612	0.715	0.841	1.000

$R'(C, \epsilon, 40°)$

C \ ε	0°	20°	40°	60°	70°	80°	90°
0.00	0.000	0.000	0.000	0.000	0.000	0.000	1.000
0.05	0.047	0.050	0.061	0.092	0.132	0.242	1.000
0.10	0.089	0.094	0.115	0.170	0.238	0.412	1.000
0.14	0.120	0.127	0.153	0.224	0.309	0.512	1.000
0.18	0.147	0.156	0.187	0.271	0.368	0.587	1.000
0.22	0.173	0.183	0.218	0.313	0.420	0.642	1.000
0.26	0.195	0.206	0.246	0.349	0.461	0.687	1.000
0.30	0.216	0.228	0.272	0.380	0.496	0.717	1.000
0.34	0.236	0.248	0.294	0.409	0.526	0.740	1.000
0.38	0.253	0.266	0.314	0.432	0.552	0.759	1.000
0.50	0.297	0.312	0.364	0.489	0.607	0.792	1.000
0.60	0.325	0.340	0.395	0.522	0.636	0.805	1.000
0.70	0.347	0.364	0.420	0.545	0.655	0.810	1.000
0.80	0.365	0.381	0.438	0.562	0.669	0.813	1.000
0.90	0.380	0.396	0.452	0.574	0.676	0.814	1.000

$R'(C, \epsilon, 60°)$

C \ ε	0°	20°	40°	60°	70°	80°	90°
0.00	0.000	0.000	0.000	0.000	0.000	0.000	1.000
0.05	0.046	0.049	0.060	0.091	0.129	0.238	1.000
0.10	0.086	0.091	0.112	0.164	0.230	0.401	1.000
0.14	0.114	0.121	0.146	0.214	0.296	0.491	1.000
0.18	0.139	0.147	0.177	0.256	0.349	0.558	1.000
0.22	0.161	0.170	0.204	0.293	0.393	0.607	1.000
0.26	0.181	0.190	0.227	0.325	0.429	0.644	1.000
0.30	0.198	0.208	0.248	0.350	0.457	0.671	1.000
0.34	0.213	0.224	0.267	0.371	0.482	0.689	1.000
0.38	0.226	0.238	0.282	0.391	0.502	0.705	1.000
0.50	0.259	0.272	0.319	0.432	0.543	0.726	1.000
0.60	0.278	0.292	0.341	0.455	0.563	0.737	1.000
0.70	0.293	0.307	0.356	0.469	0.575	0.740	1.000
0.80	0.303	0.317	0.366	0.480	0.582	0.741	1.000
0.90	0.311	0.326	0.375	0.486	0.587	0.741	1.000

$R'(C, \epsilon, 70°)$

C \ ε	0°	20°	40°	60°	70°	80°	90°
0.00	0.000	0.000	0.000	0.000	0.000	0.000	1.000
0.05	0.045	0.048	0.059	0.089	0.127	0.234	1.000
0.10	0.082	0.087	0.107	0.158	0.221	0.385	1.000
0.14	0.108	0.114	0.138	0.202	0.279	0.467	1.000
0.18	0.129	0.137	0.164	0.239	0.325	0.525	1.000
0.22	0.147	0.156	0.187	0.268	0.363	0.565	1.000
0.26	0.163	0.172	0.208	0.293	0.391	0.595	1.000
0.30	0.176	0.186	0.222	0.313	0.413	0.614	1.000
0.34	0.188	0.198	0.235	0.330	0.431	0.629	1.000
0.38	0.198	0.208	0.247	0.344	0.445	0.639	1.000
0.50	0.219	0.230	0.272	0.372	0.473	0.654	1.000
0.60	0.230	0.242	0.284	0.385	0.486	0.659	1.000
0.70	0.239	0.250	0.292	0.395	0.491	0.662	1.000
0.80	0.244	0.256	0.298	0.398	0.495	0.662	1.000
0.90	0.248	0.260	0.302	0.402	0.498	0.663	1.000

$R'(C, \epsilon, 80°)$

C \ ε	0°	20°	40°	60°	70°	80°	90°
0.00	0.000	0.000	0.000	0.000	0.000	0.000	1.000
0.05	0.042	0.045	0.055	0.083	0.118	0.219	1.000
0.10	0.073	0.077	0.094	0.140	0.195	0.342	1.000
0.14	0.091	0.096	0.116	0.171	0.237	0.400	1.000
0.18	0.104	0.111	0.133	0.194	0.266	0.437	1.000
0.22	0.115	0.121	0.146	0.211	0.287	0.460	1.000
0.26	0.122	0.129	0.155	0.224	0.302	0.475	1.000
0.30	0.128	0.136	0.163	0.233	0.311	0.483	1.000
0.34	0.133	0.140	0.168	0.239	0.319	0.490	1.000
0.38	0.136	0.144	0.172	0.245	0.324	0.494	1.000
0.50	0.143	0.150	0.180	0.252	0.331	0.499	1.000
0.60	0.145	0.153	0.182	0.256	0.335	0.500	1.000
0.70	0.147	0.155	0.183	0.257	0.336	0.500	1.000
0.80	0.147	0.155	0.184	0.257	0.337	0.501	1.000
0.90	0.148	0.156	0.185	0.258	0.337	0.501	1.000

$$R'(C, \epsilon, 90°) \begin{cases} = 0.000 \text{ for } \epsilon \neq 90° \\ = 0.500 \;\; ,, \;\; \epsilon = 90° \end{cases}$$

TABLE XIVd

THE FUNCTION $\frac{1}{2}\Phi(C, \epsilon)E(C, i)$ FOR VARIOUS VALUES OF C, ϵ, AND i

$\frac{1}{2}\Phi(C, \epsilon)\,E(C, 0)$

C \ ε	0°	20°	40°	60°	70°	80°	90°
0.00	0.000	0.000	0.000	0.000	0.000	0.000	0.000
0.05	0.004	0.005	0.007	0.010	0.014	0.027	0.093
0.10	0.018	0.020	0.023	0.034	0.047	0.082	0.158
0.14	0.032	0.033	0.039	0.060	0.080	0.133	0.202
0.18	0.048	0.051	0.060	0.089	0.120	0.188	0.242
0.22	0.068	0.072	0.085	0.122	0.162	0.245	0.279
0.26	0.089	0.094	0.112	0.157	0.206	0.299	0.312
0.30	0.111	0.118	0.140	0.195	0.251	0.353	0.344
0.34	0.136	0.143	0.170	0.235	0.297	0.403	0.373
0.38	0.162	0.170	0.202	0.273	0.343	0.450	0.401
0.50	0.246	0.257	0.297	0.396	0.478	0.578	0.475
0.60	0.320	0.334	0.385	0.494	0.582	0.666	0.530
0.70	0.396	0.414	0.471	0.590	0.677	0.741	0.576
0.80	0.471	0.491	0.555	0.680	0.761	0.807	0.618
0.90	0.549	0.570	0.637	0.768	0.841	0.863	0.657

$\frac{1}{2}\Phi(C, \epsilon)\,E(C, 20°)$

C \ ε	0°	20°	40°	60°	70°	80°	90°
0.00	0.000	0.000	0.000	0.000	0.000	0.000	0.000
0.05	0.004	0.005	0.007	0.010	0.014	0.026	0.093
0.10	0.018	0.020	0.023	0.034	0.047	0.082	0.158
0.14	0.032	0.033	0.039	0.060	0.080	0.133	0.201
0.18	0.048	0.051	0.059	0.088	0.119	0.187	0.240
0.22	0.068	0.071	0.084	0.121	0.161	0.243	0.277
0.26	0.088	0.093	0.111	0.156	0.205	0.296	0.310
0.30	0.111	0.117	0.139	0.193	0.249	0.350	0.341
0.34	0.135	0.142	0.168	0.232	0.294	0.398	0.370
0.38	0.160	0.168	0.200	0.270	0.339	0.445	0.397
0.50	0.242	0.253	0.292	0.390	0.470	0.569	0.468
0.60	0.314	0.328	0.378	0.486	0.572	0.655	0.521
0.70	0.389	0.406	0.462	0.579	0.664	0.727	0.565
0.80	0.461	0.480	0.543	0.665	0.746	0.789	0.605
0.90	0.536	0.557	0.622	0.750	0.820	0.842	0.642

$\frac{1}{2}\Phi(C, \epsilon)\,E(C, 40°)$

C \ ε	0°	20°	40°	60°	70°	80°	90°
0.00	0.000	0.000	0.000	0.000	0.000	0.000	0.000
0.05	0.004	0.005	0.007	0.010	0.013	0.026	0.092
0.10	0.017	0.020	0.023	0.034	0.046	0.081	0.156
0.14	0.031	0.033	0.039	0.059	0.079	0.131	0.198
0.18	0.047	0.050	0.058	0.086	0.116	0.183	0.235
0.22	0.066	0.070	0.082	0.118	0.157	0.237	0.270
0.26	0.085	0.090	0.107	0.151	0.198	0.288	0.300
0.30	0.107	0.113	0.134	0.187	0.241	0.338	0.330
0.34	0.130	0.137	0.162	0.223	0.283	0.383	0.356
0.38	0.154	0.161	0.191	0.258	0.325	0.427	0.380
0.50	0.229	0.240	0.277	0.369	0.445	0.539	0.444
0.60	0.295	0.308	0.355	0.456	0.536	0.614	0.488
0.70	0.361	0.377	0.429	0.538	0.618	0.676	0.526
0.80	0.425	0.443	0.500	0.614	0.688	0.727	0.558
0.90	0.490	0.509	0.568	0.686	0.750	0.770	0.586

$\frac{1}{2}\Phi(C, \epsilon)\,E(C, 60°)$

C \ ε	0°	20°	40°	60°	70°	80°	90°
0.00	0.000	0.000	0.000	0.000	0.000	0.000	0.000
0.05	0.004	0.005	0.007	0.010	0.013	0.026	0.091
0.10	0.017	0.019	0.022	0.032	0.045	0.078	0.151
0.14	0.030	0.031	0.037	0.056	0.075	0.125	0.189
0.18	0.044	0.047	0.055	0.082	0.110	0.173	0.222
0.22	0.061	0.065	0.077	0.110	0.146	0.221	0.252
0.26	0.079	0.083	0.099	0.139	0.182	0.264	0.276
0.30	0.097	0.103	0.122	0.170	0.219	0.307	0.299
0.34	0.116	0.123	0.145	0.201	0.254	0.344	0.320
0.38	0.137	0.143	0.170	0.229	0.288	0.379	0.338
0.50	0.197	0.207	0.238	0.318	0.383	0.464	0.382
0.60	0.248	0.259	0.299	0.384	0.451	0.517	0.411
0.70	0.297	0.310	0.352	0.442	0.507	0.555	0.431
0.80	0.342	0.356	0.402	0.493	0.553	0.585	0.448
0.90	0.386	0.401	0.448	0.540	0.591	0.607	0.462

$\frac{1}{2}\Phi(C, \epsilon)\,E(C, 70°)$

C \ ε	0°	20°	40°	60°	70°	80°	90°
0.00	0.000	0.000	0.000	0.000	0.000	0.000	0.000
0.05	0.004	0.005	0.007	0.010	0.013	0.025	0.089
0.10	0.016	0.019	0.021	0.031	0.043	0.075	0.144
0.14	0.028	0.029	0.035	0.053	0.071	0.117	0.178
0.18	0.041	0.044	0.051	0.075	0.102	0.160	0.205
0.22	0.056	0.059	0.070	0.100	0.133	0.201	0.229
0.26	0.071	0.075	0.089	0.125	0.164	0.238	0.248
0.30	0.086	0.092	0.108	0.150	0.194	0.272	0.265
0.34	0.102	0.107	0.127	0.175	0.222	0.301	0.279
0.38	0.118	0.124	0.147	0.198	0.249	0.327	0.291
0.50	0.164	0.172	0.198	0.264	0.318	0.386	0.317
0.60	0.200	0.209	0.241	0.310	0.365	0.418	0.332
0.70	0.235	0.245	0.279	0.349	0.401	0.439	0.341
0.80	0.265	0.275	0.312	0.382	0.428	0.453	0.347
0.90	0.293	0.305	0.340	0.411	0.449	0.461	0.351

TABLE XIVd (continued)

$\frac{1}{2}\Phi(C, \varepsilon)\, E(C, 80°)$.

C \ ε	0°	20°	40°	60°	70°	80°	90°
0.00	0.000	0.000	0.000	0.000	0.000	0.000	0.000
0.05	0.004	0.005	0.006	0.009	0.012	0.024	0.083
0.10	0.014	0.016	0.019	0.027	0.039	0.065	0.126
0.14	0.023	0.025	0.029	0.044	0.059	0.098	0.149
0.18	0.033	0.035	0.041	0.060	0.081	0.128	0.164
0.22	0.043	0.045	0.054	0.077	0.103	0.155	0.176
0.26	0.052	0.055	0.066	0.093	0.121	0.176	0.184
0.30	0.061	0.065	0.077	0.107	0.139	0.195	0.190
0.34	0.070	0.074	0.088	0.121	0.154	0.208	0.193
0.38	0.079	0.083	0.099	0.133	0.167	0.220	0.196
0.50	0.102	0.107	0.124	0.165	0.199	0.241	0.198
0.60	0.119	0.124	0.143	0.184	0.217	0.248	0.197
0.70	0.134	0.140	0.160	0.200	0.230	0.251	0.195
0.80	0.147	0.153	0.173	0.212	0.238	0.252	0.193
0.90	0.160	0.166	0.185	0.224	0.245	0.251	0.191

TABLE XIVe

THE FUNCTION $R'(C, \varepsilon, i) + \frac{1}{2}\Phi(C, \varepsilon)E(C, i)$ FOR VARIOUS VALUES OF C, ε, AND i

$R'(C, \varepsilon, 0) + \frac{1}{2}\Phi(C, \varepsilon)\, E(C, 0)$.

C \ ε	0°	20°	40°	60°	70°	80°	90°
0.00	0.000	0.000	0.000	0.000	0.000	0.000	1.000
0.05	0.052	0.055	0.068	0.103	0.147	0.271	1.093
0.10	0.108	0.116	0.140	0.207	0.288	0.500	1.158
0.14	0.154	0.162	0.195	0.288	0.395	0.654	1.202
0.18	0.199	0.211	0.252	0.367	0.497	0.787	1.242
0.22	0.246	0.260	0.311	0.443	0.593	0.905	1.279
0.26	0.292	0.307	0.368	0.518	0.683	1.006	1.312
0.30	0.336	0.356	0.423	0.591	0.765	1.093	1.344
0.34	0.383	0.403	0.478	0.661	0.846	1.170	1.373
0.38	0.428	0.450	0.532	0.726	0.920	1.237	1.401
0.50	0.563	0.589	0.685	0.914	1.117	1.402	1.475
0.60	0.669	0.700	0.809	1.050	1.256	1.502	1.530
0.70	0.771	0.808	0.924	1.175	1.375	1.586	1.576
0.80	0.870	0.907	1.030	1.286	1.474	1.655	1.618
0.90	0.966	1.005	1.133	1.391	1.565	1.712	1.657

$R'(C, \varepsilon, 20°) + \frac{1}{2}\Phi(C, \varepsilon)\, E(C, 20°)$.

C \ ε	0°	20°	40°	60°	70°	80°	90°
0.00	0.000	0.000	0.000	0.000	0.000	0.000	1.000
0.05	0.052	0.055	0.068	0.103	0.146	0.270	1.093
0.10	0.108	0.116	0.140	0.206	0.288	0.499	1.158
0.14	0.153	0.162	0.195	0.287	0.394	0.652	1.201
0.18	0.198	0.211	0.250	0.364	0.494	0.784	1.241
0.22	0.245	0.258	0.307	0.440	0.590	0.898	1.277
0.26	0.289	0.305	0.363	0.514	0.678	0.995	1.310
0.30	0.335	0.353	0.419	0.585	0.760	1.084	1.341
0.34	0.379	0.399	0.473	0.655	0.837	1.158	1.370
0.38	0.423	0.445	0.527	0.718	0.911	1.226	1.397
0.50	0.554	0.581	0.674	0.902	1.102	1.384	1.468
0.60	0.658	0.688	0.795	1.034	1.239	1.484	1.521
0.70	0.759	0.793	0.909	1.156	1.351	1.565	1.565
0.80	0.852	0.888	1.010	1.262	1.448	1.629	1.605
0.90	0.945	0.983	1.107	1.362	1.535	1.683	1.642

TABLE XIVe (continued)

$R'(C, \varepsilon, 40°) + \frac{1}{2}\Phi(C, \varepsilon)\, E(C, 40°)$

C \ ε	0°	20°	40°	60°	70°	80°	90°
0.00	0.000	0.000	0.000	0.000	0.000	0.000	1.000
0.05	0.051	0.055	0.068	0.102	0.145	0.268	1.092
0.10	0.106	0.114	0.138	0.204	0.284	0.493	1.156
0.14	0.151	0.160	0.192	0.283	0.388	0.643	1.198
0.18	0.194	0.206	0.245	0.357	0.484	0.770	1.235
0.22	0.239	0.253	0.300	0.431	0.577	0.879	1.270
0.26	0.280	0.296	0.353	0.500	0.659	0.975	1.300
0.30	0.323	0.341	0.406	0.567	0.737	1.055	1.330
0.34	0.366	0.385	0.456	0.632	0.809	1.123	1.356
0.38	0.407	0.427	0.505	0.690	0.877	1.186	1.380
0.50	0.526	0.552	0.641	0.858	1.052	1.331	1.444
0.60	0.620	0.648	0.750	0.978	1.172	1.419	1.488
0.70	0.708	0.741	0.849	1.083	1.273	1.486	1.526
0.80	0.790	0.824	0.938	1.176	1.357	1.540	1.558
0.90	0.870	0.905	1.020	1.260	1.426	1.584	1.586

$R'(C, \varepsilon, 60°) + \frac{1}{2}\Phi(C, \varepsilon)\, E(C, 60°)$

C \ ε	0°	20°	40°	60°	70°	80°	90°
0.00	0.000	0.000	0.000	0.000	0.000	0.000	1.000
0.05	0.050	0.054	0.067	0.101	0.142	0.264	1.091
0.10	0.103	0.110	0.134	0.196	0.275	0.479	1.151
0.14	0.144	0.152	0.183	0.270	0.371	0.616	1.189
0.18	0.183	0.194	0.232	0.338	0.459	0.731	1.222
0.22	0.222	0.235	0.281	0.403	0.539	0.828	1.252
0.26	0.260	0.273	0.326	0.462	0.611	0.908	1.276
0.30	0.295	0.311	0.370	0.520	0.676	0.978	1.299
0.34	0.329	0.347	0.412	0.572	0.736	1.033	1.320
0.38	0.363	0.381	0.452	0.620	0.790	1.084	1.338
0.50	0.456	0.479	0.557	0.750	0.926	1.190	1.382
0.60	0.526	0.551	0.640	0.839	1.014	1.254	1.411
0.70	0.590	0.617	0.708	0.911	1.082	1.295	1.431
0.80	0.645	0.673	0.768	0.973	1.135	1.326	1.448
0.90	0.697	0.727	0.823	1.026	1.178	1.348	1.462

$R'(C, \varepsilon, 70°) + \frac{1}{2}\Phi(C, \varepsilon)\, E(C, 70°)$

C \ ε	0°	20°	40°	60°	70°	80°	90°
0.00	0.000	0.000	0.000	0.000	0.000	0.000	1.000
0.05	0.049	0.053	0.066	0.099	0.140	0.259	1.089
0.10	0.098	0.106	0.128	0.189	0.264	0.460	1.144
0.14	0.136	0.143	0.173	0.255	0.350	0.584	1.178
0.18	0.170	0.181	0.215	0.314	0.427	0.685	1.205
0.22	0.203	0.215	0.257	0.368	0.496	0.766	1.229
0.26	0.234	0.247	0.297	0.418	0.555	0.833	1.248
0.30	0.262	0.278	0.330	0.463	0.607	0.886	1.265
0.34	0.290	0.305	0.362	0.505	0.653	0.930	1.279
0.38	0.316	0.332	0.394	0.542	0.694	0.966	1.291
0.50	0.383	0.402	0.470	0.636	0.791	1.040	1.317
0.60	0.430	0.451	0.525	0.695	0.851	1.077	1.332
0.70	0.474	0.495	0.571	0.744	0.892	1.101	1.341
0.80	0.509	0.531	0.610	0.780	0.923	1.115	1.347
0.90	0.541	0.565	0.642	0.813	0.947	1.124	1.351

TABLE XIVe (continued)

$R'(C, \epsilon, 80°) + \frac{1}{2}\Psi(C, \epsilon)\, E(C, 80°)$

C \ ϵ'	0°	20°	40°	60°	70°	80°	90°
0.00	0.000	0.000	0.000	0.000	0.000	0.000	1.000
0.05	0.046	0.050	0.061	0.092	0.130	0.243	1.083
0.10	0.087	0.093	0.113	0.167	0.233	0.407	1.126
0.14	0.114	0.121	0.145	0.215	0.296	0.498	1.149
0.18	0.137	0.146	0.174	0.254	0.347	0.565	1.164
0.22	0.158	0.166	0.200	0.288	0.390	0.615	1.176
0.26	0.174	0.184	0.221	0.317	0.423	0.651	1.184
0.30	0.189	0.201	0.240	0.340	0.450	0.678	1.190
0.34	0.203	0.214	0.256	0.360	0.473	0.698	1.193
0.38	0.215	0.227	0.271	0.378	0.491	0.714	1.196
0.50	0.245	0.257	0.304	0.417	0.530	0.740	1.198
0.60	0.264	0.277	0.325	0.440	0.552	0.748	1.197
0.70	0.281	0.295	0.343	0.457	0.566	0.751	1.195
0.80	0.294	0.308	0.357	0.469	0.575	0.753	1.193
0.90	0.308	0.322	0.370	0.482	0.582	0.752	1.191

$R'(C, \epsilon, 90°) + \frac{1}{2}\Psi(C, \epsilon)E(C, 90°)$ is zero for $\epsilon \neq 90°$ and 0.500 for $\epsilon = 90°$.

Tables XIII and XIV are accurate to within one unit of the last significant figure.

REFERENCES

1. Huygens: Hugenii Cosmotheoros, sive de terris coelestibus earumque ornatu conjecturae. Hagae-Comitum Ed., Vol.II, p.136, 1699.
2. Celsius: History of the Academy of Sciences (Histoire de l'Académie des Sciences). p.5, Paris, 1735.
3. Buffon: Memoires of the Academy of Sciences (Mémoires de l'Académie des Sciences). p.84, Paris, 1747.
4. Bouguer, Pierre: Optical Essay on the Gradation of Light (Essai d'optique sur la gradation de la lumière). Paris, 1729.
5. Bouguer, Pierre: Optical Treatise on the Gradation of Light; Posthumous Paper Published by the Abbé of Lacaille (Traité d'optique sur la gradation de la lumière. Ouvrage posthume, publié par l'abbé de Lacaille). Paris, 1760.
6. Lambert, J.H.: Photometria sive de mensura et gradibus luminis, colorum et umbrae. Augustae Vindelicorum, 1760; German Translation by E.Anding in: Ostwalds Klassiker der exakten Wissensch., No.31-33, Leipzig, 1892.
7. Euler: Reflections on the Various Degrees of Light of the Sun and other Celestial Bodies (Réflexions sur les divers degrés de lumière du soleil et des autres corps célestes). Hist. et Mém. de l'Acad. R. de Berlin, p.280, 1750.
8. Kies: On the Greatest Brightness of Venus, etc. (Sur le plus grand éclat de Vénus etc.). Histoire et Mémoires de l'Académie de Berlin, p.218, 1750.
9. Smith, R.: A Complete System of Optics. Cambridge, 1728.
10. Laplace, P.S.: Celestial Mechanics (Mécanique céleste). Part 4, Chapt.3.
11. Arago, F.: The Law of the Cosine Square for the Intensity of Polarized Light Transmitted by Birefringent Crystals (Über das Gesetz des Kosinusquadrats für die Intensität des polarisierten Lichts, welches von doppelbrechenden Kristallen durchgelassen wird). Pogg. Ann., Vol.35, p.444, 1835.
12. Neumann, F.E.: Photometric Method for Determining the Intensity of Ordinary and Extraordinary Rays and of the Reflected Light (Photometrisches Verfahren, die Intensität der ordentlichen und ausserordentlichen Strahlen sowie die des reflektierten Lichtes zu bestimmen). Pogg. Ann., Vol.40, p.497, 1837.
13. Seidel, L.: Investigations on Luminous Intensity of the Planets Mars, Venus, Jupiter, and Saturn Compared with Stars, and the Relative Albedo of their Surfaces (Untersuchungen über die Lichtstärke der Planeten Mars, Venus, Jupiter und Saturn, verglichen mit Sternen, und über die relative Weisse ihrer Oberflächen). Monumenta saecularia der Münchner Akad., II.Kl., 1859.
14. Steinheil: Elements of Brightness Measurements in the Starry Sky (Elemente der Helligkeitsmessungen am Sternenhimmel). Denkschr. der Münchner Akad., II.Kl., Vol.2, 1837; Improved Design of a Prism Photometer (Verbesserte Form eines Prismenphotometers). Münch. Gelehrte Anzeigen, Vol.15, p.9; Contributions to Stellar Photometry (Beiträge zur Photometrie des Himmels). Astron. Nachr., Vol.48, p.369, 1858.
15. Seidel and Arago: Seven Treatises on Photometry (Sieben Abhandlungen zur Photometrie). German Translation by Hankel, Vol.10, 1859.
16. Schwerd: Diffraction Phenomena (Beugungserscheinungen). Mannheim, 1835.

17. Airy: Cambridge Transactions, Vol.6, 1838.
18. Beer, A.: Four Photometric Problems (Vier photometrische Probleme). Pogg. Ann., Vol.88, p.114, 1853; Fundamentals of Photometric Calculus (Grundriss des photometrischen Calcüls). Braunschweig, 1854.
19. Recknagel, G.: Lambert's Photometry and its Relation to the Present State of the Art in Science (Lamberts Photometrie und ihre Beziehung zum gegenwärtigen Standpunkt der Wissenschaft). Awarded Competition Prize (Gekrönte Preisschrift), Munich, 1861.
20. Rheinauer, J.: Fundamentals of Photometry (Grundzüge der Photometrie). Halle, 1862.
21. Herschel, J.: Account of some Attempts to Compare the Intensities of Light of Stars one with another by the Intervention of the Moon by the Aid of an Astrometer Adapted to that Purpose. Results of Astr. Obs. Made during 1834 to 1838 at the Cape of Good Hope. p.353, London, 1847.
22. Zöllner, Fr.: Photometric Investigations (Photometrische Untersuchungen). Pogg. Ann., Vol.100, pp.381, 474, 651, 1857; Vol.109, p.244, 1860; Fundamentals of General Stellar Photometry (Grundzüge einer allgemeinen Photometrie des Himmels). Berlin, 1861; Photometric Investigations with Special Consideration of the Physical Consistency of Celestial Bodies (Photometrische Untersuchungen mit besonderer Rücksicht auf die physische Beschaffenheit der Himmelskörper). Leipzig, 1865; Some Theorems from Theoretical Photometry (Einige Sätze aus der theoretischen Photometrie). Pogg. Ann., Vol.128, p.46, 1866; Results of Photometric Observations on Celestial Bodies (Resultate photometrischer Beobachtungen an Himmelskörpern). Pogg. Ann., Vol.128, p.260, 1866; Astron. Nachr., Vol.66, p.225, 1866.
23. Wild, H.: On a New Photometer and Polarimeter, with some Observational Findings (Über ein neues Photometer und Polarimeter nebst einigen angestellten Beobachtungen). Pogg. Ann., Vol.118, p.235, 1856; On the Conversion of my Photometer into a Spectrophotometer (Über die Umwandlung meines Photometers in ein Spektrophotometer). Bull. Acad. St.Petersb., Vol.28, p.392, 1883.
24. Bond, G.P.: On the Results of Photometric Experiments upon the Light of the Moon and the Planet Jupiter, Made at the Observatory of the Harvard College. Mem. Am. Acad., New Ser., Vol.8, p.221, 1861; Comparison of the Light of the Sun and Moon. Mem. Am. Acad., New Ser., Vol.8, p.287, 1861; On the Light of the Sun, Moon, Jupiter and Venus. Monthly Notices Roy. Astron. Soc., Vol.21, p.197, 1861.
25. Cornu, A.: On the Possibility of Greatly Increasing the Accuracy of Observations of Jupiter Satellite Eclipses (Sur la possibilité d'accroître dans une grande proportion la précision des observations des éclipses des satellites de Jupiter). Compt. Rend., Vol.96, p.1609, 1883; On Photometric Observation Methods of Jupiter's Satellites (Sur les méthodes photométriques d'observations des satellites de Jupiter). Astron. Nachr., Vol.114, p.239, 1886.
26. Obrecht, A.: Studies on Eclipses of Jupiter's Satellites (Études sur les éclipses des satellites de Jupiter). Ann. Obs. Paris, Vol.18, 1885.
27. v.Seeliger, Hugo: Photometry of the Saturn Ring (Zur Photometrie des Saturnringes). Astron. Nachr., Vol.109, p.305, 1884; Remarks on Zöllner's "Photometric Investigations" (Bemerkungen zu Zöllners "Photometrische Untersuchungen"). V J S, Vol.21, p.216, 1886; On the Theory of Illumination of the Superior Planets, Especially of Saturn (Zur Theorie der

Beleuchtung der grossen Planeten, insbesondere des Saturn). Abhandl. Münch. Akad., II.Kl., Vol.16, p.405, 1888; On the Photometry of Diffusely Reflecting Substances (Zur Photometrie zerstreut reflektierender Substanzen). Sitz.ber. Münch. Akad., II.Kl., Vol.18, p.201, 1888; Theory of Illumination of Dust-Like Cosmic Masses, Especially of the Saturn Ring (Theorie der Beleuchtung staubförmiger kosmischer Massen, insbesondere des Saturnringes). Abhandl. Münch. Akad., II.Kl., Vol.18, p.1, 1893; On the Shadow of a Planet (Über den Schatten eines Planeten). Sitz.ber. Münch. Akad., II.Kl., Vol.24, p.423, 1894; On Cosmic Dust Formations and the Zodiacal Light (Über kosmische Staubmassen und das Zodiakallicht). Sitz.-ber. Münch. Akad., II.Kl., Vol.31, No.3; Apparent Enlargement of the Earth's Shadow during Lunar Eclipses (Die scheinbare Vergrösserung des Erdschattens bei Mondfinsternissen). Abhandl. Bayer. Akad. Wiss., II.Abt., Vol.19, 1899.

28. v.Seeliger, H. and Lommel, E.: On Fluorescence. Chapt.I: Principles of Photometry (Über Fluorescenz. Abschnitt I: Über die Grundsätze der Photometrie). Wied. Ann., Vol.10, p.449, 1880; Photometry of Diffuse Reflection (Die Photometrie der diffusen Zurückwerfung). Sitz.ber. Münch. Akad., II.Kl., Vol.17, p.95, 1887.
29. Anding, E.: Photometric Investigations on Eclipses of Jupiter's Satellites (Photometrische Untersuchungen über die Verfinsterungen der Jupiterstrabanten). Preisschr. Univ. München, 1889; On the Light Distribution over an Incompletely Illuminated Planetary Disk (Über die Lichtverteilung auf einer unvollständig beleuchteten Planetenscheibe). Astron. Nachr., Vol.129, p.377, 1892.
30. Wellmann, V.: On the Photometry of Jupiter's Satellites (Zur Photometrie der Jupiterstrabanten). Berlin, 1887.
31. Schwend, K.: On the Problem of Zodiacal Light (Zur Zodiakallichtfrage). Munich, 1904.
32. Müller, G.: Stellar Photometry (Die Photometrie der Gestirne). Leipzig, 1897.
33. Helmholtz: Handbook of Physiological Optics (Handbuch der physiologischen Optik). 1856-1866.
34. Aschkinass: Wied. Ann., Vol.55, p.401, 1895.
35. Widmark: In: R.Tigerstedt: Textbook of Physiology of Man (Lehrbuch der Physiologie des Menschen). Vol.II, p.254, Leipzig, 1920.
36. Arago: Collected Works (Sämtliche Werke). German Translation by Hankel, Vol.10, p.210.
37. Masson: Ann. Chim. Phys., Ser.3, Vol.14, p.150, 1845.
38. Fechner: On a Phychophysical Fundamental Law, etc. (Über ein psychophysisches Grundgesetz etc.). Abhandl. Kgl. Sächs. Ges. Wiss., Vol.4, p.455, 1859.
39. Schoenberg, E.: A Special Class of Variable Stars (Eine Sonderklasse veränderlicher Sterne). Soc. Sci. Fennica, Commentationes Phys.-Math., Vol.I, p.30, 1923.
40. Tigerstedt, R.: Textbook of Physiology of Man (Lehrbuch der Physiologie des Menschen). Vol.II, p.273, 1920.
41. Brodhun: Inaugural Dissertation. Berlin, 1887.
42. König, A.: Collected Treatises on Physiological Optics (Gesammelte Abhandlungen zur Physiologischen Optik). p.144, Leipzig, 1903.
43. Müller: Stellar Photometry (Photometrie der Gestirne). p.457, Leipzig, 1897.

44. Osthoff: Publ. Spec. Vatic., Vol.VIII, 1916.
45. v.Seeliger: Astron. Nachr., Vol.132, p.209, 1893.
46. Lambert: Photometria sive de mensura et gradibus luminis, colorum et umbrae, 1760. German Translation by Anding, Leipzig, 1892.
47. Zöllner: Photometric Investigations, with Special Consideration of the Physical Consistency of Celestial Bodies (Photometrische Untersuchungen mit besonderer Rücksicht auf die physische Beschaffenheit der Himmelskörper). p.12, Leipzig, 1865.
48. Beer: Fundamentals of Photometric Calculus (Grundriss des photometrischen Calcüls). p.6, Braunschweig, 1854.
49. Rheinauer: Fundamentals of Photometry (Grundzüge der Photometrie). p.2, Halle, 1862.
50. Lommel: Wied. Ann., Vol.10, p.449, 1880.
51. Smoluchowski de Smolan: J. Phys., Ser.3, Vol.5, p.488, 1896.
52. Lummer and Reiche: Ann. Phys., Vol.33, p.857, 1910.
53. Gross: Thesis, Breslau, 1911.
53a. v.Helmholtz, H.: Lectures on Theoretical Physics (Vorlesungen über theoretische Physik), Vol.6.
53b. Uljanin: Wied. Ann., Vol.62, p.528, 1897.
53c. Jentzsch, F.: Studies on Emission and Diffuse Reflection (Studien über Emission und diffuse Reflexion). Thesis, Giessen, 1912; Ann. Phys., Vol.39, p.997, 1912.
54. Emden: Problems of Astronomy (Probleme der Astronomie). Seeliger Jubilee Volume (Seeliger-Festschrift), p.347, 1924.
55. Witting: On Radiation from Various Parts of the Solar Disk (Om strålningen från olika delar af solskifvan). Jubilee Volume for A.Donner's 60th Anniversary, Helsinki, 1915.
56. Russell, H.N. and Shapley, H.: Astrophys. J., Vol.36, p.239, 1912.
57. Harzer, P.: Brightness Reduction of Occultation Variables (Über die Helligkeitsabnahme von Bedeckungsveränderlichen). Publik. Sternwarte in Kiel, Vol.16, 1927.
58. Lommel: Sitz.ber. Münch. Akad., II.Kl., Vol.17, p.95, 1887; Wied. Ann., Vol.36, p.473, 1889.
59. v.Seeliger: Vierteljahrschr. Astr. Ges., Vol.20, p.267, 1885; Vol.21, p.216, 1886; Sitz.ber. Münch. Akad., II.Kl., Vol.18, p.201, 1888.
60. Rayleigh: Phil. Mag., Vol.41, p.107, 1871; Collected Works, Vol.I, p.87.
61. Kelvin: Baltimore Lectures, p.311, 1904.
62. Schuster: Theory of Optics. p.325, 1909.
63. Mie: Ann. Phys., Vol.25, p.428, 1908.
64. Blumer, H.: Z. Physik, Vol.32, p.119, 1925; Vol.38, p.920, 1926.
65. Fessenkov: Diffusion of Light over Dull Surfaces (Sur la diffusion de la lumière par les surfaces mates). Bull. Soc. Astron. Russie, May 1916.
66. Rayleigh: Proc. Roy. Soc. (London), Vol.41, p.275, 1886.
67. Melloni: Ann. Chim. Phys., Vol.75, p.387, 1840.
68. Dessain: Pogg. Ann., Vol.84, p.147, 1848; Compt. Rend., Vol.24, p.60, 1847; Vol.33, p.444, 1851.
69. Macquenne: Thesis Presented at the Faculty of Sciences Paris, 1880.
70. Ångström, Knut: Wied. Ann., Vol.26, p.253, 1885.
71. Godard, L.: Ann. Chim. Phys., Ser.6, Vol.10, p.354, 1887.
72. Messerschmitt, J.B.: Wied. Ann., Vol.34, p.867, 1888.
73. Wiener: Wied. Ann., Vol.47, p.638, 1892.
74. Wright, H.: Ann. Phys., Vol.1, p.17, 1900.

75. Pegram: Science, Vol.13, p.148, 1906.
76. Matthews: Trans. Am. Inst. Electr. Eng., Vol.20, p.59, 1902.
77. Thaler: Diffuse Reflection on Dull Surfaces (Die diffuse Reflexion an matten Oberflächen). Thesis, Kiel, 1903; Ann. Phys., Vol.11, p.996, 1903.
78. Hutchins: Am. J. Sci., Nov. 1898.
79. Lehmann, H.: Verhandl. Deut. Phys. Ges., Vol.11, p.123, 1909.
80. Umow, N.: Phys. Z., Vol.6, p.674, 1905.
81. Chmyrow, D. and Slatowratzki: Phys. Z., Vol.7, p.533, 1906.
82. Návrat, Viktor: Ber. K. Akad. Wiss. Wien, Vol.120, No.2a, p.1229, 1911.
83. Woronkoff and Pokrowski: Z. Physik, Vol.20, p.358, 1923.
84. Pokrowski: Z. Physik, Vol.32, p.563, 1925.
85. Berry, E.M.: J. Opt. Soc. Am., Vol.7, p.627, 1923.
86. Schulz, H.: Z. Physik, Vol.31, p.496, 1925.
87. Woronkoff and Pokrowski: Z. Physik, Vol.30, p.139, 1924.
88. Woronkoff and Pokrowski: Z. Physik, Vol.33, p.860, 1925.
89. Pokrowski: Z. Physik, Vol.31, p.14, 1925; Vol.31, p.514, 1925.
90. Pokrowski: Z. Physik, Vol.32, p.713, 1925; Vol.36, p.548, 1926.
91. Pokrowski: Z. Physik, Vol.34, p.496, 1926.
92. Wild: Bull. Acad. Sci. St.Petersbourg, Vol.21, p.312, 1876; Vol.23, p.290, 1877.
93. Schramm: Thesis, Kiel, 1901.
94. Wiener, Chr.: Abhandl. Kais. Leop.-Car. Acad. Nova Acta, Vol.73.
95. Maissinger, C. LeRoy: Science, New Ser., Vol.55, p.20, 1922.
96. Brückmann, W.: Meteor. Z., Vol.39, p.107, 1922.
97. Wood, R.W.: Phil. Mag., Vol.39, p.423, 1920.
98. Fowle, F.E.: J. Opt. Soc. Am., Vol.6, p.99, 1922.
99. Gruner, P.: Beitr. Phys. Freien Atmosph., Vol.8, p.120, 1919.
100. Pokrowski, G.: Z. Physik, Vol.34, p.49, 1925; Vol.35, p.464, 1926.
101. Karrer and Smith: J. Opt. Soc. Am., Vol.7, p.1211, 1923.
102. Pokrowski: Z. Physik, Vol.34, p.55, 1925.
103. Mie: Ann. Phys., Vol.25, p.428, 1908.
104. Wiener, Chr.: Abhandl. Kais. Leop.-Car. Acad. Nova Acta, Vol.73.
105. v.Seeliger: Abhandl. K. Bayer. Akad. Wiss., II.Kl., Vol.16, p.430, 1887.
106. Wilsing, J. and Scheiner, J.: Spectral Photometric Observations on the Moon, Minerals, etc. (Spektralphotometrische Beobachtungen am Monde und an Gesteinen usw.). Publ. Astrophys. Obs. Potsdam, No.61, 1909.
107. Wilsing, J. and Scheiner, J.: Spectral Photometric Measurements on Minerals, Moon, Mars, and Jupiter (Spektralphotometrische Messungen an Gesteinen, am Monde, Mars und Jupiter). Publ. Astrophys. Obs. Potsdam, No.77, 1921.
108. Fessenkov: Publ. Obs. Central Astroph. Russie, Vol.II, p.97, 1923.
109. Kononowitsch: Fortschr. Physik, Vol.35, p.430, 1879; Vol.37, p.481, 1881.
110. Henning, F. and Heuse, W.: Z. Physik, Vol.10, p.111, 1922.
111. Coblentz: Bull. Bur. Std. (U.S.), Vol.9, p.283, 1913.
112. Abbot and Fowle: Smiths. Ann., Vol.2, p.136, 1908.
113. Aldrich, L.B.: Smiths. Ann., Vol.4, p.375, 1922.
114. Stuchtey, K. and Wegener, A.: The Albedo of Clouds and Earth (Die Albedo der Wolken und der Erde). Nachr. K. Ges. Wiss. Göttingen, 1911.
115. Luckiesh, M.: Astrophys. J., Vol.49, p.119, 1919.
116. v.Seeliger: Abhandl. K. Bayer. Akad. Wiss., II.Kl., Vol.16, p.405, 1887.
117. Bond: Proc. Am. Acad. Arts Sci., New Ser., Vol.8, p.232, 1861.
118. Russell, H.N.: Astrophys. J., Vol.43, p.175, 1916.

119. Russell: Astrophys. J., Vol.43, p.190, 1916.
120. Öpik, E.: Publ. Obs. Astron. Univ. Tartu (Dorpat), Vol.26, No.1, 1924.
121. Anding: Astron. Nachr., Vol.129, p.377, 1892.
122. v.Seeliger, H.: Vierteljahrsschr. Astron. Ges., Vol.21, p.216, 1886.
123. Searle, A.: Proc. Am. Acad. Sci., Vol.19, p.310, 1884.
124. Wislicenus, W.F.: Astron. Nachr., Vol.201, p.290, 1915.
125. Barabaschew: Astron. Nachr., Vol.217, p.445, 1923.
126. Markow: Astron. Nachr., Vol.221, p.65, 1924.
127. Barabaschew: Astron. Nachr., Vol.221, p.289, 1924.
128. Wilsing, J.: On the Developmental History of the Moon (Zur Entwicklungsgeschichte des Mondes). Publ. Astrophys. Obs. Potsdam, No.77, 1921.
129. Öpik, E.: Publ. Obs. Astron. Tartu, Vol.26, No.1, 1924.
130. Schoenberg, E.: Investigations on the Theory of Illumination of the Moon, etc. (Untersuchungen zur Theorie der Beleuchtung des Mondes usw.). Acta Soc. Sci. Fennicae, Vol.50, No.9, 1925.
131. Guthnick, P.: Astron. Nachr., Vol.206, p.157, 1918; Vol.212, p.39, 1920.
132. Schoenberg: Photometric Investigations on Jupiter and the Saturn System (Photometrische Untersuchungen über Jupiter und das Saturnsystem). Ann. Acad. Sci. Fennicae, Ser.A, Vol.16, p.33, Helsinki, 1921.
133. Schoenberg, E.: On the Illumination of Planets. Publ. Obs. Astron. Dorpat, Vol.24, 1917.
134. Fessenkov: Determination of the Earth's Albedo (Détermination de l'albedo de la terre). Publ. Obs. Astron. Univ. Kharkov, No.7, 1915.
135. Pickering: Annual Report of the Director of the Harvard College Observ. for the Year 1878; Harv. Ann., Vol.52, Part II, 1909.
136. Sampson, R.A.: A Discussion of the Eclipses of Jupiter's Satellites. 1878-1903.
137. Cornu: Compt. Rend., Vol.96, pp.1690, 1815, 1883.
138. Obrecht: Studies on Eclipses of Jupiter's Satellites (Études sur les éclipses des satellites de Jupiter). Paris, 1884.
139. Wellmann, V.: On the Photometry of Jupiter's Satellites (Zur Photometrie der Jupiterstrabanten). Thesis, Erlangen, 1887.
140. Anding, E.: Photometric Investigations on Jupiter's Satellites (Photometrische Untersuchungen über die Jupiterstrabanten). Competitive Thesis (Preisschrift), Munich, 1889.
141. v.Seeliger, H.: Vierteljahrsschr. Astron. Ges., Vol.27, p.197, 1892.
142. Schoenberg, E.: Photometric Investigations on Jupiter and the Saturn System (Photometrische Untersuchungen über Jupiter und das Saturnsystem). Acta Acad. Sci. Fennicae, Vol.16, 1921.
143. Sampson, R.: Harv. Ann., Vol.52, 1907.
144. Brosinsky, A.: Enlargement of the Earth's Shadow during Lunar Eclipses (Über die Vergrösserung des Erdschattens bei Mondfinsternissen). Göttingen, 1889.
145. Hartmann, J.: Enlargement of the Earth's Shadow during Lunar Eclipses (Die Vergrösserung des Erdschattens bei Mondfinsternissen). Abhandl. K. Sächs. Ges. Wiss., Vol.17, No.6, 1891.
146. v.Seeliger, H.: Vierteljahrsschr. Astron. Ges., Vol.27, p.186, 1892.
147. v.Seeliger, H.: Apparent Enlargement of the Earth's Shadow during Lunar Eclipses (Die scheinbare Vergrösserung des Erdschattens bei Mondfinsternissen). Abhandl. K. Bayer. Akad. Wiss., II.Kl., Vol.19, 1899.
148. v.Hepperger, J.: On the Brightness of the Eclipsed Moon, etc. (Über die Helligkeit des verfinsterten Mondes usw.). Sitz.ber. K. Akad. Wiss. Wien,

Math.-Naturw. Kl., Vol.104, p.189, Abt.IIa, 1895.
149. Airy: Trans. Phil. Soc. Cambridge, Vol.6, 1838.
150. Schwerd: Diffraction Phenomena (Die Beugungserscheinungen). Mannheim, 1835.
151. André: Study of Diffraction in Optical Instruments (Étude de la diffraction dans les instruments d'optique). Ann. Ecole Normale, 1876.
152. Struve, H.: On the Influence of Diffraction in Telescopes on Luminous Disks (Über den Einfluss der Diffraktion an Fernrohren auf Lichtscheiben). Mem. Acad. Imper. Sci. St.Petersbourg, Ser.7, Vol.30, No.8, 1882.
153. Lommel: Abhandl. K. Bayer. Akad., Vol.15, 1884; Vol.19, 1897.
154. Nagaoka, H.: Astrophys. J., Vol.51, p.73, 1920.
155. Fessenkov: R A J, Vol.2, p.171, 1925.
156. André: Origin of the Black Band (Origine du ligament noir). Ann. Ecole Normale, 1881; Study of Diffraction (Étude de la diffraction). Ann. Ecole Normale, 1876.
157. v.Seeliger, H.: On the Theory of Illumination of the Superior Planets, Especially of Saturn (Zur Theorie der Beleuchtung der grossen Planeten, insbesondere des Saturn). Abhandl. K. Bayer. Akad. Wiss., II.Kl., Vol.16, p.405, 1887; Theory of Illumination of Dust-Like Cosmic Masses, etc. (Theorie der Beleuchtung staubförmiger kosmischer Massen usw.). Abhandl. K. Bayer. Akad. Wiss., II.Kl., Vol.18, p.1, 1893.
158. Schoenberg, E.: Photometric Investigations on Jupiter and the Saturn System (Photometrische Untersuchungen über Jupiter und das Saturnsystem). Acta Acad. Sci. Fennicae, Vol.16, p.55, 1921.
159. Hepburn: Monthly Notices Roy. Astron. Soc., Vol.74, p.721, 1914.
160. Ainslie: Monthly Notices Roy. Astron. Soc., Vol.77, p.456, 1917.
161. v.Seeliger, H.: Abhandl. K. Bayer. Akad. Wiss., II.Kl., Vol.16, p.405, 1887.
162. Müller, G.: Publ. Astrophys. Obs. Potsdam, Vol.8, No.30, 1893.
163. Hertzsprung: Astron. Nachr., Vol.208, p.81, 1919.
164. Guthnick, P.: Astron. Nachr., Vol.206, p.157, 1918; Vol.212, p.39, 1920.
165. Wood: Astrophys. J., Vol.43, p.310, 1916.
166. Bell, L.: Astrophys. J., Vol.50, p.1, 1919.
167. Schoenberg, E.: On the Radiation of Planets (Über die Strahlung der Planeten). Ergeb. Exakt. Naturw., Vol.5, 1926.
168. v.Seeliger, H.: Astron. Nachr., Vol.137, p.129, 1895.
169. Schwend, K.: On the Zodiacal Light Problem (Zur Zodiakallichtfrage). Thesis, Munich, 1904.
170. Fessenkov: The Zodiacal Light (La lumière zodiacale). Paris, 1914.
171. van Rhijn: On the Brightness of the Sky, etc. Publ. Astron. Lab. Groningen, Vol.31, 1921.
172. v.Seeliger, H.: On Cosmic Dust Formations and the Zodiacal Light (Über kosmische Staubmassen und das Zodiacallicht). Sitz.ber. K. Bayer. Akad. Wiss., Vol.31, p.265, 1901.
173. Searle, A.: Researches on the Zodiacal Light. Harv. Ann., Vol.19, Part II, 1893.
174. Hertzsprung, E.: Astron. Nachr., Vol.195, p.449, 1913.
175. Holetschek: Investigations of the Size and Brightness of Comets and their Tails (Untersuchungen über die Grösse und Helligkeit der Kometen und ihrer Schweife). Denkschr. Kais. Akad. Wiss. Wien, Math.-Phys. Kl., Vol.63, 1896; Vol.78, 1905.
176. Berberich: Astron. Nachr., Vol.119, p.49, 1888.

177. Bosler: Compt. Rend., Vol.148, p.1738, 1909.
178. Orlov, S.V.: Astron. Nachr., Vol.189, p.1, 1911; Vol.190, p.157, 1912.
179. Kritzinger: Astron. Nachr., Vol.199, p.121, 1914.
180. Vsechsviatsky, S.: R A J, Vol.2, No.2, p.68, 1925.
181. Schwarzschild and Kron: Astrophys. J., Vol.34, p.342, 1911.
182. Bemporad: On the Theory of Extinction of Light, etc. (Zur Theorie der Extinktion des Lichts etc.). Mitt. Grossherz. Sternwarte Heidelberg. Astron. Inst., Vol.4, 1904.
183. Bemporad: Mem. Soc. Spettroscop. Ital., Vol.30, p.217, 1901.
184. Müller: Stellar Photometry (Photometrie der Gestirne). p.116.
185. Bemporad: Mem. Soc. Spettroscop. Ital., Vol.31, p.171, 1902.
186. Laplace: Celestial Mechanics (Mécanique céleste). Vol.4, Chapt.3.
187. Bemporad: Special Treatment of the Influence of the Atmosphere (Besondere Behandlung des Einflusses der Atmosphäre). Encyklopädie d. math. Wiss., Vol.6, Part 2, p.319, 1907.
188. Forbes: On the Transparency of the Atmosphere and the Law of Extinction etc. Phil. Trans. Roy. Soc. London, Vol.132, p.225, 1842.
189. Trépied: On Stellar Photometry and Transparency of the Air (Sur la photométrie des étoiles et la transparence de l'air). Compt. Rend., Vol.82, 1876.
190. Maurer: Extinction of the Light of Fixed Stars in the Earth's Atmosphere, etc. (Die Extinktion des Fixsternlichtes in der Erdatmosphäre usw.). Inaugural Thesis, Zürich, 1882.
191. v.Seeliger, H.: On the Extinction of Light in the Atmosphere (Über die Extinktion des Lichts in der Atmosphäre). Sitz.ber. K. Bayer. Akad., II.Kl., Vol.21, p.247, 1891.
192. Hausdorff: On the Absorption of Light in the Atmosphere (Über die Absorption des Lichtes in der Atmosphäre). Sitz.ber. Sächs. Ges. Wiss., 1895.
193. Kempf: Vierteljahrsschr. Astron. Ges., Vol.31, p.2, 1896.
194. Müller: Publ. Astrophys. Obs. Potsdam, Vol.8, No.27, 1891.
195. Müller and Kempf: Publ. Astrophys. Obs. Potsdam, Vol.11, No.38, 1898.
196. Bemporad: Mem. Soc. Spettroscop. Ital., Vol.31, p.171, 1902.
197. Bruns: On the Theory of Astronomic Refraction (Zur Theorie der astronomischen Strahlenbrechung). Sitz.ber. Sächs. Ges. Wiss., 1891.
198. Bemporad: On the Theory of Extinction of Light in the Earth's Atmosphere (Zur Theorie der Extinktion des Lichts in der Erdatmosphäre). Mitt. Grossherz. Sternwarte Heidelberg. Astron. Inst., No.4, 1904.
199. Bemporad: Mitt. Grossherz. Sternwarte Heidelberg. Astron. Inst., No.4, 1904.
200. Assmann and Berson: Scientific Flights (Wissenschaftliche Luftfahrten). Vol.III.
201. Langley, S.P.: Am. J. Sci., Ser.3, Vol.28, p.163, 1884.
202. Forbes: Phil. Trans. Roy. Soc. London, p.225, 1842.
203. Crova: Ann. Chim. Phys., Ser.5, Vol.11, p.433, 1877; Vol.19, p.167, 1880.
204. v.Seeliger, H.: Sitz.ber. K. Bayer. Akad. Wiss., Math.-Phys. Kl., Vol.21, p.247, 1891.
205. Wilsing, J.: Publ. Astrophys. Obs. Potsdam, Vol.24, No.76, p.16, 1920.
206. Bemporad: Mem. Soc. Spettroscop. Ital., Vol.31, p.171, 1902.
207. Müller: Publ. Astrophys. Obs. Potsdam, Vol.8, No.27, 1891.
208. Wolff, H.G.: Contributions to the Extinction of the Light of Fixed Stars in the Earth's Atmosphere (Beiträge z. Ext. d. Fixsternlichts in der Erdatmosphäre). Thesis, Breslau, 1911.

209. Zipler: Veröffentl. Univ. Sternwarte Berlin-Babelsberg, Vol.3, No.2, 1921.
210. Wilsing: Publ. Astrophys. Obs. Potsdam, Vol.25, No.80, 1924.
211. Abbot and Fowle: Ann. Astrophys. Obs. Smiths. Inst., Vol.2, p.109, 1908.
212. Bemporad: Selective Absorption, etc. (L'assorbimento selettivo etc.). Reale Accademia dei Lincei, Rome, 1908.
213. Langley: Professional Papers of the Signal Service U.S.A., No.15, 1884.
214. Müller and Kempf: Publ. Astrophys. Obs. Potsdam, Vol.11, No.38, 1898.
215. Bemporad: Boll. Accad. Gioenia Sci. Nat. Catania, 1904.
216. Müller and Kron: Publ. Astrophys. Obs. Potsdam, Vol.22, No.64, 1912.
217. Bemporad: V J S, Vol.47, p.325, 1913.
218. Ångström, K.: Nova Acta R. Soc. Upsal., Ser.3a, Vol.20, 1900.
219. Wilsing: Publ. Astrophys. Obs. Potsdam, Vol.25, No.80, 1924.
220. Bemporad: Selective Absorption of Solar Radiation, etc. (L'assorbimento selettivo della radiazione solare etc.). Reale Accad. Lincei, Vol.CCCV, p.99, 1908.
221. Bemporad: Theory of Atmospheric Absorption (La teoria dell'assorbimento atmosferico). R. Osserv. Astron. Capodimonte, Contr. Astron., No.6, 1913.
222. Wild: Pogg. Ann., Vol.134, p.312, 1868.
223. Wild: Pogg. Ann., Vol.135, p.99, 1868.
224. Haecker: Determination of the Transparency Coefficient of Fog and Pertaining Visibility, etc. (Bestimmung d. Transparenzkoeff. d. Nebels und d. zugehörigen Sichtweite usw.). Thesis, Kiel, 1905.
225. Oddone, E.: Rend. R. Ist. Lombardo Sci. Lettere, Ser.2, Vol.34, p.511, 1901.
226. Bemporad: Mem. Soc. Spettroscop. Ital., Vol.32, p.105, 1903; Mem. R. Ist. Lombardo Sci. Lettere, Cl. Sci. Mat., Vol.20, p.137.
227. Müller and Kron: Publ. Astrophys. Obs. Potsdam, Vol.22, No.64, p.71, 1912.
228. Abney: Phil. Trans. Roy. Soc. London, Vol.178, p.251, 1887.
228a. Mascart: Treatise on Optics (Traité d'Optique). Vol.III, p.372.
229. Langley: Professional Papers of the Signal Service U.S.A., No.15, p.151.
230. Wilsing: Publ. Astrophys. Obs. Potsdam, Vol.25, No.80, 1924.
231. Abbot: Astrophys. J., Vol.34, p.203, 1911.
232. Fowle, F.E.: Astrophys. J., Vol.38, p.392, 1913.
233. Rayleigh: Phil. Mag., Ser.4, Vol.41, p.107, 1871; Collected Works, Vol.I, p.87.
234. Schuster: Theory of Optics. Second Edition, p.325, 1909.
235. King, L.V.: On the Scattering and Absorption of Light, etc. Phil. Trans. Roy. Soc. London, Ser.A, Vol.212, 1913.
236. Fowle: Astrophys. J., Vol.40, p.435, 1914.
237. Boutaric, A.: Contribution to the Study of the Absorbtivity of the Terrestrial Atmosphere (Contribution à l'étude du pouvoir absorbant de l'atmosphère terrestre). Ann. Chim. Phys., Ser.9, Vol.9, p.113, 1918; Vol.10, p.5, 1918.
238. Wilsing: Publ. Astrophys. Obs. Potsdam, Vol.25, No.80, 1924.
239. Bemporad: Rend. R. Accad. Lincei, Cl. Sci. Fis. Mat. Nat., Ser.5, Vol.16, 1907.
240. Ångström, K.: Nova Acta R. Soc. Upsal., Ser.4, Vol.1, No.7, 1907.
241. Linke, F.: Beitr. Phys. Freien Atmosphäre, Vol.10, p.91, 1922.
242. Fowle, F.E.: Astrophys. J., Vol.35, p.149, 1912; Vol.37, p.359, 1913; Vol.38, p.392, 1913; Vol.42, p.394, 1915.
243. v.Bahr, Eva: The Effect of Pressure on the Absorption of Infrared Radiation

by Gases (Über die Einwirkung des Druckes auf die Absorption ultraroter Strahlung durch Gase). Upsala, 1908.
244. Humphrey: Bull. Mount Weather Obs., Vol.4, p.121, 1911.
245. Fowle: Astrophys. J., Vol.37, p.369, 1913.
246. Fessenkov, V. and Piaskovskiy, Ye.: R A J, Vol.2, No.3, p.37, 1925.
247. Rayleigh: Phil. Mag., Ser.4, Vol.41, pp.107, 274, 447, 1871; Ser.5, Vol.12, p.81, 1881; Ser.5, Vol.47, p.375, 1899.
248. King, L.V.: On the Scattering and Absorption of Light in Gaseous Media, etc. Phil. Trans. Roy. Soc. London, Ser.A, Vol.212, 1913.
249. Schuster: Astrophys. J., Vol.21, p.1, 1905.
250. Kelvin: Baltimore Lectures. p.311, 1904.
251. Schuster: Theory of Optics. Second Edition, p.315, 1909.
252. Wright, W.H.: Lick Obs. Bull., Vol.12, p.48, 1925; Vol.13, p.50, 1927.
253. Trümpler, R.J.: Lick Obs. Bull., Vol.13, p.32, 1927.
254. Ross, Frank E.: Astrophys. J., Vol.68, p.57, 1928.
255. Wood, R.: Astrophys. J., Vol.43, p.310, 1916.
256. Fessenkov, V.: Astron. Nachr., Vol.228, p.25, 1926.
257. Menzel, D.H.: Astrophys. J., Vol.63, p.48, 1926.

Translated for the National Aeronautics and Space Administration by the O.W.Leibiger Research Laboratories, Inc.